

Swampland Constraints and Non-perturbative String Theory

Towards the boundaries of moduli space in M- and F-theory

Rafael Álvarez García

Hamburg
2024

Swampland Constraints and Non-perturbative String Theory

Towards the boundaries of moduli space in M- and F-theory

Dissertation
zur Erlangung des Doktorgrades
an der Fakultät für Mathematik, Informatik und Naturwissenschaften
Fachbereich Physik
der Universität Hamburg

vorgelegt von

Rafael Álvarez García

Hamburg
2024

Gutachter/innen der Dissertation:

Prof. Dr. Timo Weigand
Dr. Alexander Westphal

Zusammensetzung der Prüfungskommission:

Prof. Dr. Gregor Kasieczka
Prof. Dr. Jan Louis
Prof. Dr. Günter Sigl
Prof. Dr. Timo Weigand
Dr. Alexander Westphal

Vorsitzende/r der Prüfungskommission:

Prof. Dr. Günter Sigl

Datum der Disputation:

06.05.2024

Vorsitzender des Fach-Promotionsausschusses PHYSIK:

Prof. Dr. Markus Drescher

Leiter des Fachbereichs PHYSIK:

Prof. Dr. Wolfgang J. Parak

Dekan der Fakultät MIN:

Prof. Dr.-Ing. Norbert Ritter

*A mis abuelos,
quienes no habiendo disfrutado
no del lujo, sino de su derecho
a la educación,
me enseñaron a contar.*



Abstract

In this thesis we analyse general criteria which consistent theories of quantum gravity must obey according to the so-called Swampland Conjectures, and their interplay with the quantum geometry of non-perturbative string compactifications.

The Swampland Distance Conjecture predicts that infinite-distance limits in the moduli space of a gravitational EFT that can be consistently completed to a theory of quantum gravity are accompanied by an infinite tower of asymptotically massless states, with an exponentially decreasing mass scale in the geodesic distance. The Emergent String Conjecture (ESC) refines this claim by stating that said towers are furnished either by Kaluza-Klein states, signalling a decompactification along the trajectory, or by the excitations of a unique, weakly coupled, asymptotically tensionless critical string, determining the equidimensional duality frame to which we transition at the endpoint of the limit.

We commence by studying the consistency conditions imposed by the ESC on the asymptotic behaviour of quantum gravity under dimensional reduction. Consider an infinite-distance limit in which a $(1+2)$ -dimensional membrane becomes asymptotically tensionless. If its circle reduction leads to a critical string, we show that such a membrane must parametrically decouple from the Kaluza-Klein scale in the original theory. We confirm this censorship against emergent membrane limits, i.e. trajectories in which the membrane sits at the Kaluza-Klein scale, in the hypermultiplet moduli space of Calabi-Yau threefold compactifications of M-theory. While it is possible to find putative membrane limits at the classical level, the quantum corrections to the hypermultiplet moduli space metric arising from M2-instantons obstruct such infinite-distance trajectories, turning them instead into decompactification limits to eleven dimensions.

Next, we turn our attention to the infinite-distance limits in the complex structure moduli space of elliptic Calabi-Yau threefolds. In the context of six-dimensional F-theory, these include infinite-distance trajectories in the non-perturbative open string moduli space. Geometrically, such limits are described as degenerations of elliptic threefolds whose central element exhibits non-minimal elliptic fibers, which do not admit a crepant resolution in the fiber. For this reason, F-theory models presenting codimension-one non-minimal singular elliptic fibers are usually discarded. We set out to understand the geometry and physics of the infinite-distance non-minimal singularities of Calabi-Yau threefolds. Our analysis shows how these non-crepant singularities can be removed by a systematic sequence of blow-ups of the base, leading to a union of log Calabi-Yau spaces glued together along their boundaries. We identify criteria for the blow-ups to give rise to open chains or more complicated trees of components, characterise the base geometry of the resulting log Calabi-Yau spaces, determine the line bundles defined over them and explain how to extract the gauge algebra for F-theory probing such reducible spaces. Focusing on those limits associated with the appearance of non-minimal singularities in the elliptic fiber over genus-zero curves in a Hirzebruch surface base, we determine the asymptotic physics that they lead to. As our main result, we interpret the central fiber of a subclass of these degenerations as endpoints of decompactification limits to theories with six-dimensional

defects. The genus-zero single infinite-distance limit degenerations of Hirzebruch models also give rise to emergent string limits, whose endpoints are at global weak coupling. We analyse the geometrical conditions that must be met in order for such global weak coupling to be possible. Our results rely on an adiabatic limit to gain information on the asymptotically massless states from the structure of vanishing cycles. Whenever possible, we employ F-theory/heterotic duality to compare our analysis to the heterotic dual description. Our findings provide further evidence for the Emergent String Conjecture, aligning with general expectations from quantum gravity.

Zusammenfassung

In der vorliegenden Arbeit untersuchen wir allgemeine Kriterien, die konsistente Quantengravitationstheorien gemäß der sogenannten Swampland Vermutungen erfüllen müssen, und ihr Wechselspiel mit der Quantengeometrie nicht-perturbativer Stringkompaktifizierungen.

Die Swampland Distance Vermutung ist eine Aussage über das Verhalten einer gravitativen effektiven Feldtheorie (EFT), die zu einer konsistenten Quantengravitationstheorie vervollständigt werden kann: Nahe den Rändern ihres Moduliraums, die unendlich weit von jedem anderen Punkt im Moduliraum entfernt sind, wird ein unendlicher Turm von Zuständen asymptotisch masselos. Hierbei nimmt die Massenskala exponentiell mit dem geodätischen Abstand der Region vom Zentrum des Moduliraums ab. Die sogenannte Emergent String Vermutung (ESC) schränkt die Natur der masselosen Zustände weiter ein: Sie entsprechen entweder Kaluza-Klein-Zuständen, deren Auftreten eine Dekompaktifizierung entlang der Trajektorie im Moduliraum signalisiert, oder den Anregungen eines eindeutig definierten, schwach gekoppelten, asymptotisch spannungslosen kritischen String; dieser legt dann das Dualitätsframe, welches die asymptotische Theorie definiert, fest.

Im ersten Teil der Arbeit untersuchen wir zunächst die Konsistenzbedingungen, die die ESC an das asymptotische Verhalten einer Quantengravitationstheorie stellt, wenn man die Theorie auf einem Kreis dimensionale reduziert. Gegeben sei ein unendlicher Limes im Moduliraum, in dem eine $(1+2)$ -dimensionale Membran asymptotisch masselos wird. Falls diese Membran unter dimensionaler Reduktion auf einem Kreis zu einem kritischen masselosen String wird, sprechen wir von einer kritischen Membran. Wir zeigen wir, dass die Masse einer solchen kritischen Membran in der ursprünglichen Theorie parametrisch stets oberhalb der Kaluza-Klein-Skala liegen muss. Dies verbietet sogenannte emergente Membran-Limites, d.h. Trajektorien, bei denen die Masse einer kritischen Membran an der Kaluza-Klein-Skala liegt und leicht wird. Wir bestätigen diese Schlussfolgerung für Trajektorien im Hypermultiplett-Moduliraum von M-Theorie-Kompaktifizierungen auf Calabi-Yau-Dreifalten. Obwohl es auf klassischer Ebene möglich ist, emergente Membran-Limites zu finden, obstruieren die von M2-Instantonen induzierten Quantenkorrekturen zur Metrik auf dem Hypermultiplett-Modulraum solche asymptotischen Trajektorien und verwandeln sie stattdessen in Dekompaktifizierungslimites nach elf Dimensionen.

Als Nächstes analysieren wir Limites im Komplexen-Struktur-Raum elliptischer Calabi-Yau-Dreifalten. Im Kontext von Kompaktifizierungen der F-Theorie nach sechs Dimensionen beschreiben diese unendlich langen Trajektorien bestimmte Limites im nicht-perturbativen Modulraum offener Strings. Aus geometrischer Sicht führen solche Limites zu Degenerierungen elliptischer Dreifalten, wobei die degenerierte Dreifalt nicht-minimale elliptische Fasern aufweist, die in der Faser nicht krepant aufgelöst werden können. Aus diesem Grund wurden in der bisherigen Literatur F-Theorie-Modelle mit Singularitäten nicht-minimaler elliptischer Fasern in Kodimension eins in der Regel verworfen. Wir versuchen, die Geometrie und Physik dieser Art von nicht-minimalen Singularitäten von Calabi-Yau-Dreifalten zu verstehen. Unsere Analyse zeigt, wie die nicht-krepanten Singularitäten durch eine systematische Abfolge von Blow-ups in der

Basis überwunden werden können. Dies führt zu einer Vereinigung glatter Log-Calabi-Yau-Räume, die entlang ihrer Ränder miteinander verklebt sind. Wir identifizieren Kriterien dafür, dass die Blow-ups zu offenen Ketten oder komplizierteren Bäumen von Komponenten führen, charakterisieren die Geometrie der Basen der resultierenden Log-Calabi-Yau-Räume, bestimmen die über ihnen definierten Liniensystemen und erklären, wie man die Eichalgebra von F-Theorie-Kompaktifizierungen auf solch reduzierbaren Räumen abliest. Wir konzentrieren uns auf diejenigen Limites, die zu nicht-minimalen Singularitäten in der elliptischen Faser über Kurven von Geschlecht null in einer Hirzebruch-Fläche als Basis führen, und bestimmen die asymptotische Physik im Limes. Als unser Hauptergebnis interpretieren wir die zentrale Faser einer Unterkategorie dieser Degenerationen als Endpunkte von Dekompaktifizierungslimes hin zu höherdimensionalen Theorien mit sechsdimensionalen Defekten. Darüberhinaus können die obige Klasse von Limites auch emergente String-Limes entsprechen, die zu asymptotisch globaler schwacher Kopplung führen. Wir analysieren die geometrischen Bedingungen, die erfüllt sein müssen, damit eine solche globale schwache Kopplung möglich ist. Unsere Ergebnisse beruhen auf einem adiabatischen Limes, um Informationen über die asymptotisch masselosen Zustände aus der Struktur verschwindender Zyklen zu gewinnen. Wo immer möglich, verwenden wir die F-Theorie/heterotische Dualität, um unsere Analyse mit der heterotischen dualen Beschreibung zu vergleichen. Unsere Erkenntnisse liefern neue Untermauerung für die Emergent String Vermutung und stimmen mit den allgemeinen Erwartungen der Quantengravitation überein.

Eidesstattliche Versicherung

Hiermit erkläre ich an Eides statt, dass ich die vorliegende Dissertationsschrift selbst verfasst und keine anderen als die angegebenen Quellen und Hilfsmittel benutzt habe.

Hamburg, den 12.03.2024

A handwritten signature in black ink, appearing to read "Rafał".

Unterschrift des Doktoranden

This thesis is based on the following publications:

- [1] R. Álvarez-García, D. Kläwer and T. Weigand,
Membrane limits in quantum gravity,
Phys. Rev. D **105** (2022) 066024 [2112.09136]
- [2] R. Álvarez-García, S.-J. Lee and T. Weigand,
Non-minimal Elliptic Threefolds at Infinite Distance I: Log Calabi-Yau Resolutions,
2310.07761
- [3] R. Álvarez-García, S.-J. Lee and T. Weigand,
Non-minimal Elliptic Threefolds at Infinite Distance II: Asymptotic Physics,
2312.11611

During his doctoral studies, the author has also contributed to the subsequent papers:

- [4] R. Álvarez-García, R. Blumenhagen, C. Kneissl, A. Makridou and L. Schlechter,
Swampland conjectures for an almost topological gravity theory,
Phys. Lett. B **825** (2022) 136861 [2107.07546]
- [5] R. Álvarez-García and L. Schlechter,
Analytic periods via twisted symmetric squares,
JHEP **07** (2022) 024 [2110.02962]

Contents

Abstract	v
Zusammenfassung	vii
I Exordium	1
1 Quantum Gravity and the Swampland	3
1.1 Quantum gravity	4
1.1.1 Quantum gravity: Unification in physics	5
1.1.2 Quantum gravity: An ineluctable development	7
1.1.3 Obstacles to the quantization of gravity	9
1.1.4 Semiclassical gravity	11
1.1.5 Gravity and effective field theories	12
1.1.6 Empirical challenges	13
1.2 String theory	14
1.2.1 Properties of the theory	14
1.2.2 A serendipitous discovery	17
1.2.3 Not (only) a theory of strings	19
1.3 The Landscape and the Swampland	21
1.3.1 The Landscape: A unique theory, a plethora of solutions	21
1.3.2 The swampland: An ocean surrounding an island	23
1.4 Motivation and summary	25
1.5 Outline	27
II Fundamenta	31
2 Basics of F-theory	33
2.1 String theory preliminaries	33
2.1.1 From the worldsheet to spacetime	34
2.1.2 String compactifications	37
2.1.2.1 Five-dimensional massless scalar	37
2.1.2.2 Five-dimensional Einstein gravity	38
2.1.2.3 Calabi-Yau compactifications	39
2.1.3 The string duality web	41
2.1.3.1 T-duality	42
2.1.3.2 Mirror symmetry	44

2.1.3.3	S-duality	47
2.1.4	D7-branes and $SL(2, \mathbb{Z})$ -duality	48
2.1.5	Geometrizing $SL(2, \mathbb{Z})$ -duality	50
2.2	F-theory	51
2.2.1	$[p, q]$ 7-branes and general monodromy action	52
2.2.2	Elliptic fibrations and Weierstrass models	53
2.2.3	F-theory from M-theory	55
2.2.4	Beyond non-abelian gauge algebras	60
3	The Swampland Program	63
3.1	The Swampland: Terra incognita	63
3.1.1	The Swampland	64
3.1.2	The Swampland Program	65
3.2	Swampland Conjectures	66
3.2.1	No Global Symmetries Conjecture	67
3.2.2	Weak Gravity Conjecture	68
3.2.3	The Species Scale	70
3.3	Swampland Distance Conjecture	71
3.4	Emergent String Conjecture	75
III	Membranes at Infinite Distance	79
4	Membrane Limits in Quantum Gravity	81
4.1	Introduction	81
4.2	Consistency under dimensional reduction	83
4.3	Classical membrane limits in M-theory	84
4.3.1	The moduli space of M-theory on Calabi-Yau threefolds	85
4.3.2	Classical membrane limits	85
4.4	Review: Type IIB hypermultiplet limits	86
4.4.1	Type II hypermultiplet moduli spaces	87
4.4.2	Classical string limits	88
4.4.3	Quantum corrections	89
4.4.4	Other possible limits	90
4.5	Type IIA hypermultiplet limits and relation to M-theory	92
4.5.1	Mirror map	92
4.5.2	Identification of the moduli spaces	96
4.6	Quantum obstructions to membrane limits	97
4.6.1	M5-limit	97
4.6.2	M2-limit	99
4.6.3	Decompactification process	100
4.7	Summary	101
IV	Non-minimal Elliptic Threefolds at Infinite Distance	103
5	Log Calabi-Yau Resolutions	105
5.1	Introduction and summary	105

5.2	Geometric description of 6D F-theory limits	109
5.2.1	Semi-stable degenerations of Calabi-Yau threefolds	110
5.2.2	Modifications of an infinite-distance degeneration	113
5.2.2.1	Base blow-ups	114
5.2.2.2	Family and component orders of vanishing	119
5.2.2.3	Class 1–5 models	121
5.2.3	Single infinite-distance limits and their open-chain resolutions	124
5.2.4	Geometry of the components in a single infinite-distance limit	127
5.2.5	Weierstrass models and log Calabi-Yau structure	131
5.2.6	General degenerations and their resolution trees	136
5.2.7	Comments on genus-one degenerations	137
5.3	Degenerations of Hirzebruch models	138
5.3.1	Single infinite-distance limits in Hirzebruch models	139
5.3.2	Horizontal models	142
5.3.3	Vertical models	145
5.3.4	Mixed genus-zero degenerations	147
5.3.4.1	Restriction of Cases C and D	147
5.3.4.2	Study of Case C	148
5.3.4.3	Study of Case D	149
5.4	Extracting the codimension-one information	150
5.4.1	Locally coincident discriminant components	151
5.4.2	Locally reducible discriminant components	155
5.4.3	Physical discriminant for the multi-component central fiber	157
5.4.4	Monodromy cover	163
5.4.5	Algorithm to read off the codimension-one gauge algebra	164
5.4.6	Special fibers at the intersection of components	164
5.5	Summary and future work	165
6	Asymptotic Physics	167
6.1	Introduction and summary	167
6.2	Review: Complex structure degenerations in F-theory	170
6.2.1	Degenerations of elliptic K3 surfaces	171
6.2.2	Degenerations of elliptic Calabi-Yau threefolds	174
6.3	General properties of horizontal models	176
6.3.1	Classification of horizontal models	176
6.3.2	Restrictions on components at strong and weak coupling	179
6.3.2.1	Effectiveness bounds	179
6.3.2.2	Tighter bounds on $ n_p - n_{p+1} $	180
6.3.2.3	Restrictions on global weak coupling limits	181
6.3.3	Types of global divisors	185
6.3.4	Restrictions on the local and global 7-brane content	188
6.3.4.1	Models with no components at weak coupling	188
6.3.4.2	Models with the intermediate components at weak coupling	188
6.3.4.3	Models with the end-components at weak coupling	189
6.3.5	Physical interpretation of the constraints	191
6.3.6	Bounds on the vertical gauge rank	192
6.4	Type II.a models as decompactifications with defects	195

6.4.1	F-theory/heterotic duality	196
6.4.2	Horizontal Type II.a models: generic vertical slices	200
6.4.3	Horizontal Type II.a models over $\hat{B} = \mathbb{F}_0$	201
6.4.3.1	Adiabatic regime: Decompactification with defects	202
6.4.3.2	Allowing for mixed enhancements	207
6.4.3.3	Away from the adiabatic regime	209
6.4.4	Horizontal Type II.a models over $\hat{B} = \mathbb{F}_n$	211
6.4.5	Non-minimal singularities of the heterotic K3 surface	213
6.5	Partial decompactification and weak coupling limits	214
6.5.1	Horizontal Type II.b models	214
6.5.2	Horizontal Type III.a models	214
6.5.2.1	Generic vertical slices	216
6.5.2.2	Asymptotic physics in the adiabatic regime	218
6.5.3	Horizontal Type III.b models	221
6.5.3.1	Type IIB orientifold picture	222
6.5.3.2	Generic vertical slices	223
6.5.3.3	Asymptotic physics in the adiabatic regime	223
6.6	Discussion and future directions	224
V	Peroratio	227
7	Conclusions	229
Appendices		233
A	Addenda to Part III	235
A.1	KK scale in A-F1-limits	235
B	Addenda to Part IV	237
B.1	Six-dimensional F-theory bases	237
B.1.1	\mathbb{P}^2 and \mathbb{F}_n	237
B.1.2	Blow-ups of algebraic surfaces	240
B.1.3	Arbitrary blow-ups of \mathbb{P}^2 and \mathbb{F}_n	241
B.1.3.1	Basis and notation for $\text{Bl}(\mathbb{P}^2)$ and $\text{Bl}(\mathbb{F}_n)$	242
B.1.3.2	Anticanonical class after an arbitrary blow-up	244
B.1.3.3	Intersection ring after an arbitrary blow-up	246
B.2	Restricting the genus of non-minimal curves	248
B.3	Obscured infinite-distance limits	256
B.4	Resolution trees	263
B.4.1	Geometry of the components	263
B.4.2	Line bundles	270
B.5	Single infinite-distance limits and their resolutions	273
B.6	Restricting star degenerations	277
B.6.1	Models constructed over \mathbb{P}^2 or \mathbb{F}_n	278
B.6.2	Models constructed over $\text{Bl}(\mathbb{F}_n)$ of type (A)	279
B.6.3	Models constructed over the remaining $\text{Bl}(\mathbb{F}_n)$	295

B.6.3.1	Type (B) blow-ups	295
B.6.3.2	Type (C) and (D) blow-ups	298
B.7	Blowing down vertical components	300
B.8	Polynomial factorization in rings with zero divisors	303
B.9	Discriminant in the weakly coupled components	304
B.10	Bounds on $ n_p - n_{p+1} $	306
B.10.1	Horizontal models	307
B.10.2	Vertical models	310
B.11	Bounds on the vertical gauge rank	310
B.11.1	$\hat{B} = \mathbb{F}_8$ with no components at weak coupling	311
B.11.2	$\hat{B} = \mathbb{F}_7$ with components at weak coupling	315
B.12	Defect algebras in the heterotic dual	319
B.12.1	Unbroken horizontal $E_8 \times E_8$ gauge algebra	321
B.12.2	Broken horizontal $E_8 \times E_8$ gauge algebra	326
B.13	Type IIB orientifold picture of Type III.b models	328
B.13.1	Sen limit in six-dimensional F-theory models	329
B.13.2	K3 double covers and horizontal Type III.b limits	334
B.13.3	K3 double covers and vertical Type III.b limits	335
B.14	Vertical and mixed (bi)section degenerations	335
B.14.1	Vertical models (Case B)	335
B.14.1.1	Effectiveness bounds	336
B.14.1.2	Restrictions on global weak coupling limits	336
B.14.1.3	Generic horizontal slices	338
B.14.2	Mixed section models (Case C)	339
B.14.2.1	Effectiveness bounds	339
B.14.2.2	Restrictions on global weak coupling limits	340
B.14.2.3	Generic vertical slices	341
B.14.2.4	Fiberwise analysis in the adiabatic regime	342
B.14.3	Mixed bisection models (Case D)	342
B.14.3.1	Effectiveness bounds	342
B.14.3.2	Restrictions on global weak coupling limits	343
B.14.3.3	Generic vertical slices	343
B.14.3.4	Fiberwise analysis in the adiabatic regime	344
Acknowledgements		345

Part I

Exordium

Chapter 1

Quantum Gravity and the Swampland

Gravity, both the subject of our early scientific explorations of nature and the most mysterious of forces, remains at the centre of modern research. The other known fundamental interactions are electromagnetism, its basic manifestations familiar to humanity since antiquity, and the weak and strong nuclear forces, whose discovery during the twentieth century provided profound insights into the inner workings of the cosmos. The latter three interactions have found a common description within quantum field theory in the form of the Standard Model, the most accurately verified theory in the natural sciences. However, naive attempts to describe gravity on the same footing—to formulate a theory of quantum gravity—are plagued with severe problems.

In a remarkable concatenation of breakthroughs, physicists began to realize in the 1970s that a theory, originally developed from the empirical study of hadronic resonances a decade earlier, not only unavoidably contained a realization of the elusive quantum description of gravity, but it also merged it with Yang-Mills theory. This theoretical construct, known as string theory, still stands today as our most promising candidate for a unified description of nature. It has not only grown into a vast—but still very much incomplete—tightly interconnected and consistent framework, but also reshaped our understanding of quantum field theories and inspired new mathematics, making it an integral part of modern theoretical physics.

The ultimate objective of any realistic theory of nature is to make contact with empirical observations. This is no different for string theory, and while many features of nature can be understood in isolation using its language, an all-encompassing, realistic model of our universe has not been extracted from string theory yet. Unlike in partial descriptions of nature, a realistic string model must describe all aspects of high-energy physics and cosmology at once; this is a problem as subtle and challenging as it is exciting. It is fair to say that the main obstacle seems to be our ignorance of the underlying principles of the theory, rather than the theory itself. Despite our ignorance being only relative—in absolute terms, a tremendous amount has been learnt about string theory in the past decades—it is reasonable to humbly take a step back and try to better understand the inner workings of the framework through some old and new questions: How are its different descriptions interconnected? What are the generic predictions of string theory? What does string theory forbid altogether? Which expectations does it set for the behaviour of any consistent theory of gravity? This line of inquiry finds a natural place within the Swampland Program, an effort to establish what is allowed and prohibited in a theory of quantum gravity and how this constrains low-energy physics.

One of the many features that sets string theory apart from other theoretical constructions, is that its internal consistency requirements are so stringent that they fix the dimensionality of spacetime. More concretely, the field content of the worldsheet theory must have a precise

central charge to cancel the conformal anomaly. While there is room to incorporate linear dilaton backgrounds allowing for the construction of non-critical string theories or CFT sectors without a spacetime interpretation, the most common way to cancel the conformal anomaly is by including a suitable number of free boson CFTs (and their supersymmetric partners if appropriate), each identified with a dimension of the flat spacetime vacuum of critical string theory. This yields, in the case of the five supersymmetric tachyon-free string theories, a ten-dimensional spacetime. Making some of these dimensions small, in a process known as compactification, renders them inaccessible at low energies. This leads to lower-dimensional effective field theories whose ultraviolet cut-off and physics are determined by the size and shape of the compact dimensions. Other than the string length, all parameters are dynamical in string theory, and the geometry of said dimensions is no exception: Its deformations are parametrized by the vacuum expectation values of a set of scalar fields known as moduli. These serve as coordinates on the moduli space, an auxiliary geometric space that is equipped with a natural metric and whose points correspond to all possible deformations of the theory. Making the compact dimensions subject to particularly extreme deformations corresponds to traversing paths of infinite distance in the moduli space. Since the low-energy, lower-dimensional physics depends on the internal geometry, such a drastic process should lead to equally radical consequences for the effective field theory describing it.

More concretely, one expects the effective field theory description to break due to an infinite tower of states becoming asymptotically massless as the infinite-distance boundaries of the moduli space are approached. Moreover, the decrease in the mass scale of this tower should be exponential in the distance measured using the moduli space metric. This behaviour is believed to be a property of any gravitational effective field theory that can be consistently UV completed to a theory of quantum gravity, an expectation that has crystallized in the form of the Swampland Distance Conjecture. One of its refinements, known as the Emergence String Conjecture, posits that the states furnishing the infinite tower are either Kaluza-Klein replicas or the excitations of a unique, weakly coupled and asymptotically tensionless critical string.

In the bulk of this thesis, after some preliminary material is reviewed, we will explore the validity of these two conjectures in the hypermultiplet moduli spaces of five-dimensional M-theory and six-dimensional F-theory, finding agreement with the expected behaviour. Before we delve into the more technical material, let us situate these problems in the broader context of the quest for a theory of quantum gravity. The reader eager to learn about the specific motivations for this work can safely jump to Section 1.4, where we also provide a concise summary of results. This is followed by a detailed outline of the thesis in Section 1.5.

1.1 Quantum gravity

Finding a theory of quantum gravity entails the reconciliation of the principles of general relativity and quantum mechanics. Harmonizing these two tremendously successful physical frameworks represents one of the great, if not the greatest, challenges in theoretical physics. Strictly speaking, in order to obtain a theory of quantum gravity, it is enough to consistently quantize the gravitational field. Many direct approaches to the problem limit their scope to first obtaining a theory of quantum gravity, leaving the question of how to accommodate the remaining fundamental interactions for a later stage in their development.

However, gravity is special in the sense that it couples to everything that has energy. This feature distinguishes it from the other fundamental interactions, which can be studied as isolated sectors from a theoretical point of view. The objects participating in an interaction contribute to

the quantum corrections of the theory; for quantum gravity, this includes the non-gravitational sector in its totality. One could then argue that a true theory of quantum gravity has not been achieved until all interactions are treated within a common framework and matter has been successfully coupled. In other words, that the quest for a theory of quantum gravity is intrinsically tied to a unification of quantum field theory and general relativity, and that the two problems cannot be disentangled. This is the dominant perspective among string theorists, and the fact that the framework makes such a unification inevitable is seen as one of the signs that string theory points in the right direction.

The need for a theory of quantum gravity manifests itself from various perspectives. After briefly discussing why such a quantum description of gravitation would be desirable, we review some of the unique challenges associated with finding one.

1.1.1 Quantum gravity: Unification in physics

The history of physics is long and complex; a fair account and analysis of it would require a specialized treatise. But even when told in broad strokes, it is largely a history of unification.

The first substantial unifications in physics occurred in the seventeenth century when Newton developed a framework capable of describing, through his laws of motion and his law of universal gravitation, both the terrestrial experiments of Galileo and the laws of planetary motion found by Kepler. This leap in our conception of the universe, capturing such disparate and distant phenomena under the same set of physical laws, implies that the gravitational constant G_N that Cavendish measured (much later) in a laboratory on Earth can be used to infer the motion of a celestial object in the confines of our Solar System.

The next major unification took place during the nineteenth century when, building on previous experimental and theoretical breakthroughs in the study of electricity and magnetism, Maxwell synthesized them into electromagnetism. Famously, this required modifying Ampère's law by introducing the displacement current term, motivated exclusively on theoretical grounds with the purpose of harmonizing the two theories. This addition enabled Maxwell to derive the equations describing the propagation of electromagnetic waves, and to compute the speed of light in terms of the permeability and permittivity of vacuum. Hertz discovered radio waves shortly after, in a spectacular confirmation of Maxwell's predictions.

At the turn of the twentieth century, the tension between Maxwell's equations of electromagnetism and Newtonian mechanics led Einstein to formulate special relativity, expanding upon earlier work by Lorentz and Poincaré. The theory acquired its modern form when Minkowski introduced the notion of spacetime, unifying space and time into a common substrate. A decade later, Einstein completed the general theory of relativity, to which Grossmann and Hilbert also had some contributions. It describes gravity as a geometrical property of spacetime, itself a dynamical entity whose curvature is determined by the matter and radiation content of the universe. Modern cosmology rests on this unification, which allows us to accurately describe the cosmos at scales as large as the observable universe, whose radius is roughly 10^{26} m.

The other great development of the twentieth century, ignited by the work of Planck and advanced by too many physicists to individually name, is quantum mechanics, necessary to describe nature at atomic and subatomic scales. Newtonian mechanics arises as an averaged picture for macroscopic objects with a sharply defined location. Early in the history of the subject, the first attempts to quantize the electromagnetic field were made, giving birth to quantum electrodynamics. To do so consistently requires putting together special relativity and quantum mechanics. Out of these considerations, the general framework of quantum field

theory was born. Within it, a further unification of fundamental interactions was achieved when Glashow, Salam and Weinberg successfully described electromagnetism and weak interactions as two facets of a more fundamental force, the electroweak interaction. To cite but one consequence of this unification, we know thanks to it that at some point in history, as the universe cools down, there needs to occur an electroweak phase transition triggered by the Higgs mechanism in which electromagnetism and weak interactions become distinct in appearance; depending on the details of this transition a gravitational wave background could be generated in the process, which could eventually be observed thanks to the advent of gravitational-wave astronomy in the past decade. The strong interaction can also be described as a quantum field theory, leading to quantum chromodynamics. The theory describing the known elementary particles and how they couple to the electroweak, strong and Higgs sectors is a quantum field theory known as the Standard Model. The experimental success of the Standard Model cannot be understated; it is able to accurately account for the observations at the Large Hadron Collider (LHC), which probes distances of 10^{-19} m.

Hence, taking the experimentally confirmed theories of the Standard Model and general relativity, we can describe phenomena with characteristic length scales spanning from 10^{-19} m to 10^{26} m. Arriving at this remarkable description of nature has *required* us to unify seemingly disparate sectors of physics. However, this is not the end of the road, as there is no lack of open problems, some of which we will review below. It is therefore the duty of physicists to inquire further, and given the past role that unification has played in deepening our understanding of nature, it would be wise to take it very seriously.

The electroweak and strong sectors are both an integral part of the Standard Model, but are not unified into a single fundamental interaction in it. A theory describing how such merging should occur at high enough energies is termed a Grand Unified Theory (GUT). This would be theoretically desirable, as such a theory would, for example, predict the assignment of quantized charges for the elementary particles and the relative strengths of the interactions measured at low energies, thereby reducing the number of free parameters present in the Standard Model. Indeed, running the observed couplings to high energies under the renormalization group approximately points towards a GUT scale $M_{\text{GUT}} \sim 10^{16}$ GeV (corresponding to lengths of 10^{-30} m) at which the unification would occur, far above the energy scales $M_{\text{LHC}} \sim 10^4$ GeV currently accessible at the LHC. For this reason, new particles predicted by concrete GUT models are unlikely to be observed in the near future, but we can still gather evidence in favour or against such models through their indirect consequences. For example, a GUT model predicting proton decay can be ruled out if the lower bounds on its lifetime are improved beyond what the model allows for. Future experiments like the Hyper-Kamiokande are expected to improve our current bounds on the proton lifetime. GUTs find a natural place in the low-energy limit of string theory, see [6] for a textbook account and [7] for a recent review. However, string theory does not necessarily enforce a quantum field theory unification of the forces; it can occur instead directly at the string level.

According to our present understanding of nature, the final frontier for unification is to merge the Standard Model and general relativity into a single theory, i.e. to find a framework describing both Yang-Mills theories and quantum gravity. This requires a greater theoretical leap than the unification achieved by GUTs: The quantization techniques so successful in the realm of quantum field theory lead to perturbatively non-renormalizable theories when applied to gravity, due to the presence of irrelevant operators. At the Planck scale $M_{\text{Pl}} \sim 10^{19}$ GeV (corresponding to lengths of 10^{-35} m) the effects of quantum gravity are strong enough that any gravitational EFT description will break, meaning that the unification of the interaction must occur before

this energy is reached. Given the high characteristic mass scale associated with quantum gravity effects, direct verification of any theory of quantum gravity is extremely difficult with current technology, leaving only indirect signatures as a hopeful avenue. This type of unification has only been successfully accomplished in string theory, making it the single framework from which we can draw both an intuitive and quantitative understanding of quantum gravity, and hence of invaluable importance to its study.

1.1.2 Quantum gravity: An ineluctable development

Above, we have argued that the unification of the Standard Model and general relativity would be a natural and desirable development, judging by how physics has evolved in the past. However, while the historical successes of unification motivate its appeal, they are not sufficient to establish its necessity: The trend need not extrapolate into the future. This objection is concerned with the necessary nature of a true unification of Yang-Mills theories and general relativity into a single entity, like the one achieved (and imposed) by string theory. Likewise, one could go even further, and question the need for a quantized description of the gravity.

It seems challenging to argue against the need for a theory of quantum gravity *sensu stricto*, i.e. merely a quantized version of general relativity. The alternative would be to live with incompatible theories, adhering to quantum and classical principles each, and whose domain of applicability is disjoint. In such a scenario, the need for quantum gravity would not arise, but a theoretical construction of this sort does not seem suitable for describing nature: We are aware of phenomena where both quantum and gravitational effects are relevant, and no successful and complete explanation of them should therefore be possible without a theory of quantum gravity. Moreover, there exists evidence suggesting that quantum gravity consistency considerations can constrain non-gravitational systems, as we will see when we review the ideas behind the Swampland Program. This points towards deep connections between all physical sectors, that would be more natural if gravity is not only quantized, but also unified with the other fundamental interactions.

To give an example of a system hinting at the need for quantum gravity, let us consider the characteristic length scales at which the effects of general relativity and quantum mechanics become relevant. Given an object of mass m , its Schwarzschild radius is given by $R_S = 2G_N m/c^2$. Concentrating the mass m to a smaller size than R_S results in the formation of a black hole. On the other hand, we can also associate a (reduced) Compton wavelength $\lambda = \hbar/mc$ to the mass m . Concentrating the mass m to a smaller size than λ requires enough energy that pair-production becomes possible. The two length scales equate close to the Planck mass $M_{\text{Pl}} = \sqrt{\hbar G_N/c} \sim 10^{19} \text{ GeV}$, at which point Planck-sized black hole pair production would be possible. To describe such a process, a quantized description of gravity should be necessary.

Continuing with black holes, we know thanks to Bekenstein [8, 9] and Hawking [10, 11] that they possess an entropy $S_{\text{BH}} = A/4$, where A is the event horizon area measured in Planck units. Restoring the units explicitly shows that this formula is at first order in \hbar . To derive this formula, one uses the temperature associated with Hawking radiation as computed within the framework of QFT in curved spacetime and then obtains the entropy through the use of thermodynamic relations [10, 11]. In this approximation, the black hole does not evaporate, but this can be improved by treating it in semiclassical gravity, where the metric is classical but dynamical. The no-hair theorem establishes that black holes in general relativity are completely characterized by their mass, charge and spin; in this description, black holes have a single microstate and hence no entropy. Explaining the Bekenstein-Hawking entropy formula in statistical mechanical

terms requires a microscopic theory of gravity capable of computing the microstate degeneracy of black holes. Moreover, S_{BH} is expected to receive higher order quantum corrections, whose computation would also require going beyond semiclassical gravity and considering a full theory of quantum gravity.

Semiclassical gravity not only offers black hole entropy as a quantum puzzle, but is also a fertile area for thought experiments attempting to prove the definite need for a quantized description of the gravitational field. The arguments usually proceed by considering a quantum system coupled to a classical gravitational sector and concluding that, if the gravitational sector is to remain classical, well-established quantum properties of the quantum system must be violated. Such a line of thought can already be seen in the discussions of the 1957 Chapel Hill conference [12], where Feynman gave an argument later collected in his famous lectures on gravitation [13]: Consider an electron subject to the double-slit experiment. The position of the electron corresponds to an amplitude that is evenly split between the two slits. But if gravity interacts through a field it must also have an amplitude, half of which corresponds to the gravity field of an electron going through the first slit, and half corresponding to the electron going through the second slit. In other words, the gravitational field behaves like a quantum field. A modified version of this argument due to Aharonov and Rohrlich can be found in [14]. The thought experiment of Eppley and Hannah [15] is a highly influential work in this area. It argues that a classical gravitational field would allow for a violation of either momentum conservation or the uncertainty principle for the quantum system to which it is coupled, or result in the superluminal transmission of signals. This conclusion has been criticised on the basis that the experimental device envisioned by Eppley and Hannah would be within its own Schwarzschild radius [16] if physically realized. A much simpler setup, to which the previous criticism does not apply, was proposed by Unruh [17]: The idea is to consider a Schrödinger's cat experiment in which the position of two masses within the sealed box is determined by the occurrence of a radioactive decay; the masses are separated if the decay does not take place, and next to each other if it does. A Cavendish balance is placed next to the box, its equilibrium position depending on that of the hidden masses. Computing in semiclassical gravity leads one to the conclusion that the external observer will see the Cavendish balance slowly and continuously shifting between its two equilibrium positions. Unruh argues that this is at odds with our expectations, and that the semiclassical prediction cannot be correct. Unruh's thought experiment is concisely reviewed in [18], alongside further commentary on this type of thought experiments. Using semiclassical inconsistency arguments to conclude the need for a quantized gravitational field is more subtle than it seems, and a careful analysis of hidden assumptions might put the simplest arguments at risk. Here we have only tried to give an intuition for the type of logic involved in these discussions, leaving a rigorous review of the subject for the specialized literature.

Let us now consider puzzles also involving particle physics. One of the central open questions in contemporary physics is the discrepancy between the observed value of the cosmological constant and the vacuum energy density computed from the Standard Model, see [19] for a detailed review on the subject. Following the discovery of the accelerated expansion of the universe [20, 21], the nature of dark energy is at the heart of cosmological research. The data gathered by the Planck collaboration [22] points towards a constant dark energy contribution, with equation of state $w = -1.03 \pm 0.03$, and a minuscule value of the cosmological constant $\Lambda = (2.846 \pm 0.076) \times 10^{-122} M_{\text{Pl}}^2$. In the context of QFT, the renormalized zero-point energy associated with the Standard Model is 54 orders of magnitude larger than the observed one, according to the analysis of [19]. A resolution to this puzzle requires a better understanding

of the gravitational properties of the quantum vacuum, and constitutes one instance in which some aspects of quantum gravity mix with large-scale effects like the curvature of space-time induced by the gravitational constant, a general phenomenon in gravitational theories known as UV/IR mixing. Given that the discrepancy occurs between the Standard Model prediction and the cosmological consequences of general relativity, a unified theory of the two might shed light on the problem.

Another related, but distinct, area in which quantum gravity effects become sizable is that of inflation. The quantum mechanical treatment of inflation at the semiclassical level, see [23, 24] for textbook treatments, naturally leads to density fluctuations stemming from the different local expansion histories triggered by the quantum fluctuations of the inflaton field. These seed the large-scale structure formation of the universe and are imprinted in the Cosmic Microwave Background anisotropies. This empirically successful theory must find its natural place, if we take the objections against the self-consistency of semiclassical gravity reviewed earlier seriously, within a theory of quantum gravity; the higher quantum corrections provided by such a completion might eventually be measurable in cosmological observations.

Numerous additional unsolved problems suggest that both the Standard Model and general relativity are by no means complete: the tiny neutrino masses inferred from neutrino oscillations, the electroweak hierarchy problem, the strong CP problem, the anomalous magnetic dipole moment of muons and the composition of dark matter are a few salient examples. While not all of these puzzles may in the end necessitate of a unified theory of interactions to be satisfactorily resolved, they may still benefit from developing such a picture: The task of reconciling the Standard Model and general relativity is highly non-trivial, and hence also constraining. Learning more about quantum gravity may lead to restrictions applicable to problems naively disconnected from it.

Altogether, the development of a consistent and unified theory of quantum gravity alongside the other fundamental interactions is bound to, once we sufficiently understand it, dramatically improve our description of nature. This is exemplified by string theory, our prime candidate for such a theoretical construct, which has already offered substantial insights in both physics and mathematics, despite our lack of a non-perturbative formulation.

1.1.3 Obstacles to the quantization of gravity

The need for a theory of quantum gravity was appreciated immediately after the initial successes of quantum mechanics and the formulation of general relativity, see [25] for a detailed exploration of the early history of the subject. As far back as 1916, Einstein wrote [26, p. 696]:

Gleichwohl müßten die Atome zufolge der inneratomischen Elektronenbewegung nicht nur electromagnetische, sondern auch Gravitationsenergie ausstrahlen, wenn auch in winzigem Betrage. Da dies in Wahrheit in der Natur nicht zutreffen dürfte, so scheint es, daß die Quantentheorie nicht nur die Maxwellsche Elektrodynamik, sondern auch die neue Gravitationstheorie wird modifizieren müssen.

His motivation for this statement is based in an analogy with the classical instability of atoms due to the emission of electromagnetic waves, but ultimately not solid, since the collapse time due to the emission of gravitational waves obtained for an electron “orbiting” a nucleus is much larger than the age of the universe [27]. In any case, it is clear that Einstein reflected on possible friction points between quantum and gravitational considerations.

The fact that the quantization of the gravitational field would turn out to be such a subtle problem was not appreciated at first. Physicists expected that the formalism so successful in

the quantum treatment of the electromagnetic field would apply as well to the gravitational one without much modification. While presenting the first field quantization in 1929, Heisenberg and Pauli express [28, p. 3]:

Erwähnt sei noch, daß auch eine Quantelung des Gravitationsfeldes, die aus physikalischen Gründen notwendig zu sein scheint, mittels eines zu dem hier verwendeten völlig analogen Formalismus ohne neue Schwierigkeiten durchführbar sein dürfte.

As is well known today, this early viewpoint is too optimistic: Applying the conventional quantization procedures of quantum field theory to general relativity leads to a non-predictive theory (when regarded as a fundamental description of nature, which does not detract from its usefulness as an effective theory, see Section 1.1.5), due to the presence of irrelevant operators that render it non-renormalizable.

With our modern understanding of quantum field theories, this is easy to see. One way of doing so is to start from the Einstein-Hilbert Lagrangian of general relativity

$$\mathcal{L}_{\text{EH}} = \frac{M_{\text{Pl}}^2}{2} \sqrt{-g} R. \quad (1.1.1)$$

In order to use the machinery of quantum field theory, we split the metric into

$$g_{\mu\nu} = \eta_{\mu\nu} + \frac{1}{M_{\text{Pl}}} h_{\mu\nu}, \quad (1.1.2)$$

where $\eta_{\mu\nu}$ acts as the background against which quantization is defined and $h_{\mu\nu}$ is the dynamical field, whose quantization we aim to study, acting as a perturbation of the background metric. The Planck mass M_{Pl} appears in the above expression in order to make the kinetic term for $h_{\mu\nu}$ canonically normalized once we perturbatively expand the Einstein-Hilbert Lagrangian. Such computation (schematically) yields

$$\mathcal{L}_{\text{EH}} = \frac{1}{2} (\partial h)^2 + \frac{1}{M_{\text{Pl}}} h (\partial h)^2 + \frac{1}{M_{\text{Pl}}^2} h^2 (\partial h)^2 + \dots \quad (1.1.3)$$

Given the mass dimensions $[M_{\text{Pl}}] = [h_{\mu\nu}] = 1$, we observe that the interacting part of the Lagrangian contains irrelevant operators, making the theory non-renormalizable.

Alternatively, one can ignore the Einstein-Hilbert Lagrangian and simply construct a consistent theory of interacting massless spin-2 particles. Doing so while including the minimal set of interactions simply leads to (1.1.1) with $g_{\mu\nu}$ in the expanded form (1.1.2), and the same conclusions therefore follow [13, 29].

It is worth noting that pure four-dimensional general relativity is renormalizable at one loop, although this property is spoiled if one couples it to scalar particles [30]. It has been shown that at two loops not even pure four-dimensional general relativity is renormalizable [31].

This is not a consistency problem, but one of predictive power: The infinite number of counterterms necessary to cure the divergencies lead to an infinite number of free parameters that need to be fixed by measurement. At low enough energies this does not constitute a practical problem, as exemplified by many useful non-renormalizable effective field theories like the 4-Fermi theory, but it indicates that a UV completion is necessary if we want to employ the theory at energies for which the higher-order terms in the Lagrangian become important. Once we concern ourselves not only with pure gravity, but also include other fields in the theory, this can even occur below the Planck scale M_{Pl} , see Section 3.2.3.

1.1.4 Semiclassical gravity

Earlier, we reviewed some arguments that point towards self-inconsistencies in the semiclassical treatment of gravity, i.e. in coupling classical gravity to quantum matter fields. This does not mean that semiclassical gravity is purposeless, quite the contrary: Hawking radiation and quantum fluctuations during cosmological inflation are presently understood thanks to this framework. The first of these is a well-established theoretical result, and the second shows excellent phenomenological success.

The lessons on black holes learnt from semiclassical gravity capture universal low-energy properties of the physics of these objects, and hence sustain the bottom-up rationale for some of the conjectured features that any theory of quantum gravity should have. These expectations are captured in the form of Swampland Conjectures, a notion that we will touch upon in Section 1.3.2 and explain in some detail in Chapter 3. Hence, it is worth spending a few moments recalling what semiclassical gravity precisely is.

The first step towards constructing semiclassical gravity consists of understanding quantum field theory in curved spacetime, i.e. to substitute the Minkowski spacetime background of conventional quantum field theory for a general spacetime. This classical spacetime geometry acts as a background, and the backreaction resulting from the quantum fields propagating through it is ignored at this level of approximation. Additionally, we must replace ordinary derivatives for their covariant counterparts and employ the covariant volume element in integrals. It is also possible to then add direct couplings of the quantum fields to the curvature tensor. These are known as non-minimal couplings, and they violate the strong equivalence principle, which states that all local effects of gravity must disappear in the local inertial frame. One of the most important facts about quantum field theory in curved spacetime is that, unless the background metric has a global timelike Killing vector, it is not possible to canonically define a vacuum. The path traversed in spacetime by an observer affects the notion of the vacuum, a phenomenon that lies at the heart of the Unruh effect and Hawking radiation. For introductions to quantum field theory in curved spacetime, see [32, 33].

Treating spacetime as a fixed background by neglecting the backreaction of the quantum fields limits the effects that can be captured at the above level of approximation. For example, it allows for the study of Hawking radiation, but is blind to the black hole mass loss that should be associated with it. The next level of refinement is semiclassical gravity, in which the dynamical nature of spacetime is incorporated while maintaining its classical description. Accounting for the backreaction of the quantum fields results in the modified Einstein equations

$$R_{\mu\nu} - \frac{1}{2}Rg_{\mu\nu} = \frac{8\pi G_N}{c^4}\langle T_{\mu\nu} \rangle_\psi, \quad (1.1.4)$$

where ψ is the state of the quantum fields. A derivation can be found in [33], but the result is intuitively clear: The l.h.s. of the equation is kept classical, and hence the best classical approximation of the r.h.s. needs to be used, which is the vacuum expectation value around which quantum fluctuations occur (which are assumed to be small).

Note that this treatment is analogous to considering a quantum electron in a classical electromagnetic field and then refining the picture by taking into account that the electron current produces an electromagnetic field itself. At no point is the electromagnetic field quantized, and hence this is a very crude approximation to quantum electrodynamics. Nonetheless, the early studies of quantum physics were entrenched in this regime, and led to invaluable insight without which quantum field theory may not have been developed. We would therefore do well to take the lessons learnt from semiclassical gravity seriously in our exploration of quantum

gravity; as mentioned, these are precisely the foundations on which the bottom-up side of the Swampland Program rests upon.

1.1.5 Gravity and effective field theories

Natural phenomena can be organized hierarchically according to their characteristic energy scale. If we look at the history of particle physics, or its predecessors nuclear and atomic physics, we observe that we have understood nature by describing phenomena at increasingly high energies, but while remaining ignorant about what lies ahead. In other words, we understood the atomic nucleus in spite of our ignorance of quarks.

This has crystallized in the notion of decoupling, the expectation that small-distance physics will not significantly affect the details of large-distance phenomena if the separation of scales is high enough. Decoupling lies behind the tremendously successful concept of Wilsonian effective field theories (EFTs). Starting from a quantum field theory that grants a more complete description of nature, we can integrate out those degrees of freedom above a certain energy scale to obtain an EFT. At low energies, the EFT will constitute a perfectly valid description of the relevant phenomena, but it will break as we increase the energy, at which point it must be UV completed. Conversely, if we do not know what the UV completion of a theory is, we can build an EFT by writing the Lagrangian containing the most general collection of operators consistent with known symmetries and constraints, and hiding our ignorance of high-energy physics in the Wilson coefficients of the expansion. A recent specialized textbook on the subject is [34].

Denoting the cut-off scale by Λ , the systematic expansion of the effective Lagrangian of a d -dimensional EFT is

$$\mathcal{L}_{\text{eff}}[\phi] = \mathcal{L}_0[\phi] + \sum_n c_n[\Phi] \frac{\mathcal{O}_n[\phi]}{\Lambda^{\delta_n-d}}, \quad (1.1.5)$$

where ϕ collectively denotes the field content of the theory and δ_n is the dimension of the local operator $\mathcal{O}_n[\phi]$. $\mathcal{L}_0[\phi]$ contains the renormalizable part of the Lagrangian, while the remainder of \mathcal{L}_{eff} is a sum of non-renormalizable corrections. The Wilson coefficients $c_n[\Phi]$ depend on the UV information that we ignore from the IR point of view, collectively represented here as the heavy fields Φ . A commonly used guiding principle to choose their value is that of naturalness, of which there are two notions: Dirac naturalness [35, 36], which prescribes that physical quantities should be of order one in units of the characteristic length scale Λ , and technical naturalness [37], which allows for a Wilson coefficient to have much smaller values than the Dirac natural ones as long as additional symmetries arise when said coefficient is set to zero.

To give an example, general relativity is expected to be the leading part of a Wilsonian effective action, meaning that the gravitational sector of the EFT can be written as

$$\mathcal{L}_{\text{grav}} = \frac{M_{\text{Pl}}^{D-2}}{2} \sqrt{-g} \left(R + \sum_n c_n[\Phi] \frac{\mathcal{O}_{2n}[R]}{M_{\text{Pl}}^{2n-2}} \right). \quad (1.1.6)$$

The higher-derivative terms encode the effects of quantum gravity, and lead to corrections affecting the predictions of general relativity. For instance, taking the four-dimensional Lagrangian

$$\mathcal{L}_{\text{grav}} = \sqrt{-g} (M_{\text{Pl}}^2 R + a R^2 + b R_{\mu\nu} R^{\mu\nu} + \dots) \quad (1.1.7)$$

one can compute the corrected gravitational potential of the Sun [29, 38, 39]

$$V(r) = \frac{M_{\odot}}{M_{\text{Pl}}} \frac{1}{r} \left(1 - \frac{M_{\odot}}{M_{\text{Pl}}^2 r} - \frac{127}{30\pi^2} \frac{1}{M_{\text{Pl}}^2 r^2} - 128\pi^2 \frac{a+b}{M_{\text{Pl}}^2} \delta^3(\vec{r}) + \dots \right). \quad (1.1.8)$$

The principle of decoupling to which we have alluded earlier serves us well in most quantum field theory contexts.¹ However, the situation is more subtle once gravity is considered. This is due to a phenomenon known as UV/IR mixing, i.e. the emergence of interrelations between UV and IR physics. We can heuristically understand how gravity enables UV/IR mixing through a simple example: In a non-gravitational EFT, describing a scattering process at energies higher than the cut-off would require the UV completion of the theory. Once we couple gravity, processes at energies higher than the Planck scale will result in black hole formation. If the energy is much larger than the Planck scale, the scattering process will lead to the creation of a large black hole, whose behaviour is well captured by general relativity or semiclassical gravity. Attempting to excite the theory in the deep UV results in probing IR physics.

Gravity leads to UV/IR mixing and, consequently, quantum gravity can impose non-trivial constraints in the IR. The conventional notions of naturalness, which are based on the idea of decoupling, might need to be reconsidered due to gravity. This can prompt us to revisit the electroweak and cosmological constant hierarchy problems under a new light [41]. The idea that quantum gravity can constrain the space of those EFTs coupled to gravity enjoying a consistent UV completion to a theory of quantum gravity lies at the heart of the Swampland Program.

1.1.6 Empirical challenges

Quantum gravity theories, like string theory, can be used to make definite predictions that can in principle be tested. For example, we could use string theory to compute the Wilson coefficients a and b in the effective Lagrangian (1.1.7). The first corrections to the gravitational potential of the Sun (1.1.8) are independent of the UV completion of general relativity, but the last term explicitly shown depends on these two Wilson coefficients. However, we immediately see the problem: While *a priori* we could indeed attempt to measure the effects of these corrections and contrast them with the predictions, the enterprise is hopeless in practice due to the huge suppression provided by the higher powers of M_{Pl} , even for an object as massive as the Sun. This can be counteracted by probing Planck sized distances, which currently is not experimentally viable either. The problem just described is faced by any theory of quantum gravity.

To get a feel for how far away the Planck scale is experimentally, note that the energies probed at the LHC are $M_{\text{LHC}}/M_{\text{Pl}} \sim 10^{-15}$. Turning our attention to the sky, ultra-high-energy cosmic rays like the Oh-My-God particle detected in 1991 [42] or the Amaterasu particle detected in 2021 [43] have an energy of $M_{\text{UHECR}}/M_{\text{Pl}} \sim 10^{-8}$. Directly measuring the quantum properties of the gravitational field is therefore notoriously difficult. The absence of empirical data resulting from this experimental challenge is one of the obstacles encountered by quantum gravity researchers.

One way to approach the problem, and the one adopted in the remainder of this work, is to exploit what we already know about nature: A theory of quantum gravity should be both internally consistent and compatible with our most well-established background knowledge, theoretical and experimental. These two requirements are then, hopefully, constraining enough to allow us to make progress. String theory exemplifies that this is indeed possible.

Nevertheless, empirical confirmation is still the gold standard in physics, and the progress achieved theoretically should be eventually ratified by observation. If the direct detection of individual gravitons is out of reach [44–46], we should instead turn our attention to the indirect detection of quantum gravitational effects. Previous experimental barriers have been crossed in this fashion, most notably with the indirect detection of gravitational waves by Hulse and Taylor,

¹An exception are non-commutative field theories, for which the phenomenon of UV/IR mixing arises [40].

almost 40 years before their direct detection was technologically possible. Let us review some of the possible tests that are being considered. Suffice it to say that pure theoretical progress will inevitably allow us to envision new viable empirical tests, thanks to a better understanding of the generic predictions and indirect effects associated with quantum gravity.

There are two possible avenues to overcome the difficulty of detecting quantum gravitational effects. The first of them is to find instances in which the history of the universe has led to an amplification of the Planck-sized effects characteristic of quantum gravity. In this direction, there have been proposals for tests relying on the measurement of CMB tensor modes with superhorizon correlations [47], on techniques to distinguish if CMB anisotropies are of quantum-mechanical origin [48], or on the detection of quantum field induced noise in gravitational wave detectors whose statistical properties depend on the quantum state of the gravitational field [49]. Another possibility is for the dynamics during inflation to perform a cosmological Bell-type experiment, such that through higher-point observables one could infer a violation of Bell's inequalities [50, 51].

The second idea is to exploit the fact that the strength of gravitational effects can be increased just by adding more mass to the experimental system. If the coupling of a small mass to the gravitational field is small, simply consider large aggregates of matter. The technical problem is to achieve masses large enough for gravitational effects to be accurately measured while maintaining control on quantum coherence. If this is realized, one can experimentally check whether the gravitational field is in a quantum superposition. Progress in tabletop experiments of this kind seems plausible, see [52] for a review of this approach.

1.2 String theory

Having discussed the importance of developing a theory of quantum gravity and the multifaceted difficulties arising in the enterprise, we now turn our attention to string theory, the leading candidate not only for a quantum description of the gravitational force, but for a unified theory of the fundamental interactions.

String theory is a vast and interconnected subject grown out of a strikingly simple idea: Instead of employing zero-dimensional particles as the fundamental degrees of freedom, consider a theory built from fundamental one-dimensional strings. These can be open or closed, leading to different spectra of oscillation modes each. The open string spectrum contains a massless spin-1 field, the hallmark of Yang-Mills theory. Remarkably, the closed string spectrum contains a massless spin-2 field, the mediator of the gravitational force. This makes the unification of fundamental interactions not an option in string theory, but an unavoidable consequence of the self-consistency of the framework.

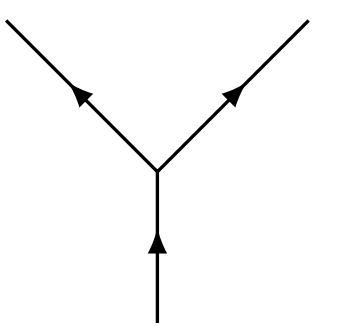
Various formulations of string theory exist, among which the five supersymmetric tachyon-free ten-dimensional string theories play a central role. These naively disparate constructions are, in fact, related to each other through a web of dualities, and represent but different perturbative incarnations of an underlying, presently unknown theory that also counts eleven-dimensional supergravity among its perturbative limits.

1.2.1 Properties of the theory

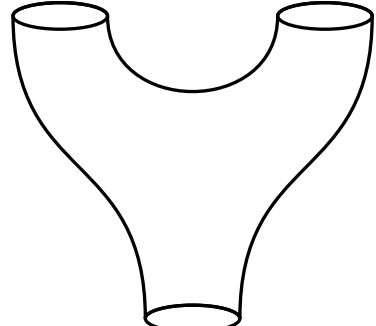
The humble assumption that the fundamental degrees of freedom of (perturbative) string theory should be one-dimensional strings, sweeping out a $(1+1)$ -dimensional worldsheet in spacetime, leads to a very constraining theory that automatically resolves a variety of problems. In Section 2.1

we will very concisely recall some core facts about string theory subjacent to the discussions in the bulk of this work, leaving a comprehensive treatment of the subject for the canonical textbooks [53–57]. Here we discuss some of the noteworthy properties that make string theory attractive and give a brief overview of its different manifestations.

In point particle theories, the divergencies in the computation of amplitudes can be traced back to the localized nature of the interactions; there is a well-defined Lorentz invariant point in spacetime at which an interaction occurs, see Figure 1.1a. One can cure this problem by smearing out the interaction point, but this is not straightforward to do while preserving the consistency of the theory. Smearing it in space spreads it in time as well (due to Lorentz invariance, which we know holds in nature to a high degree of accuracy), potentially leading to causality or unitarity loss. Substituting particles for strings precisely accomplishes the desired smearing consistently; Figure 1.1b shows that there is no well-defined point in spacetime at which the splitting or joining of strings takes place. The reason why strings are special is that they are the simplest generalization of the point particle with this property. Objects of higher dimensionality than strings have more degrees of freedom in their worldvolume, which complicates their quantization. They do play, however, a prominent role in string theory, as we will later discuss.



(a) QFT cubic interaction vertex.



(b) Pair of pants string diagram.

Figure 1.1: The interactions occur at a well-defined Lorentz invariant spacetime point in quantum field theories, but are smeared out in string theory.

Another benefit of string diagrams is that they do not give rise to the plethora of choices appearing in quantum field theory. In a theory of particles we would need to define the n -valent vertices independently of the cubic one, but in string theory this is not necessary because we can perform a pants decomposition of those string diagrams with more external legs, see Figure 1.2. The pair of pants diagram looks locally like the propagation of free strings at all times; everything is fixed once the propagation of free strings has been understood.

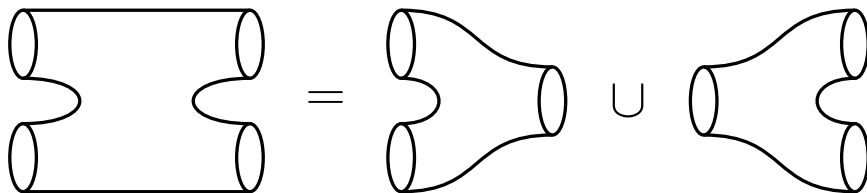


Figure 1.2: Pants decomposition of the four-point tree-level closed-string diagram.

Additionally, while at a given loop order many Feynman diagrams can contribute, there is a single string diagram at each order in perturbation theory, given by the Riemann surface of the

appropriate genus, see Figure 1.3. The previous statements are valid for closed-string diagrams, but similar considerations apply once the open sector is taken into account.

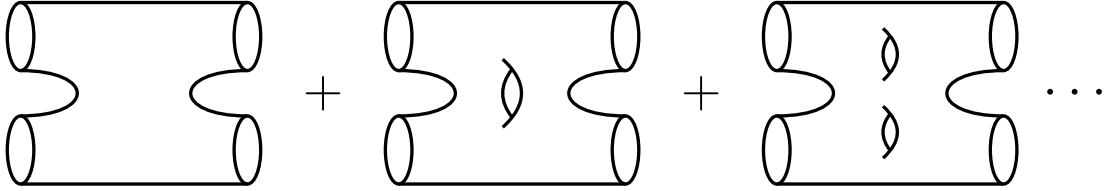


Figure 1.3: The perturbative expansion for the four-point amplitude of closed strings.

Quantizing the fundamental string leads to very strong consistency constraints which fix, among other properties, the dimensionality of the spacetime that the strings propagate through. In the path integral quantization, the number of dimensions is fixed by demanding the conformal anomaly of the worldsheet theory to vanish, leading to a critical dimension of $D = 10$ or 26 for the flat spacetime vacuum, depending on the precise formulation of the theory. This shows how restrictive consistency conditions can be in string theory as opposed to classical gravity, which can be formulated in an arbitrary number of dimensions.

The prediction of extra dimensions can naively appear as a shortcoming of the framework, but it is actually a blessing in disguise: Extra dimensions are not incompatible with our present understanding of the universe. If we consider a compactification of string theory with a small internal volume, the excitation modes associated with the additional dimensions are too massive to be observed at low energies. Moreover, the intricate shapes that these compact dimensions can take determine the lower-dimensional physics, and hence allow us to translate physical problems into geometrical ones, to which we can then apply sophisticated mathematical machinery.

To give just one example in which the extra dimensions have provided us with new insight, recall the tension between the no-hair theorem for black holes and the fact that they have a non-vanishing Bekenstein-Hawking entropy $S_{\text{BH}} = A/4$. In what constitutes one of the most celebrated results of string theory, Strominger and Vafa [58] gave a microscopic derivation of the Bekenstein-Hawking entropy formula for five-dimensional extremal black holes by relating it to the degeneracy of BPS D-brane systems in the internal dimensions.

Perturbative string theory is formulated as a double expansion in the following parameters: the string coupling g_s and the ratio α'/R_c^2 , involving the string length $\sqrt{\alpha'} = \ell_s/2\pi$ and the characteristic curvature radius R_c of spacetime. The expansion in g_s corresponds to a loop expansion from the spacetime point of view, and it is the one we have alluded to earlier when we discussed closed-string diagrams. It is analogous to the perturbative expansion in powers of the coupling constant in quantum field theory. However, one must note that string theory has no dimensionless parameters; the theory cannot be deformed arbitrarily. The string coupling g_s is not an exception, and it is, in fact, dynamically determined by the vacuum expectation value of a scalar field known as the dilaton. Conversely, the expansion in α'/R_c^2 corresponds to a loop expansion from the worldsheet point of view, with R_c set dynamically by the moduli fields. The worldsheet theory is free when the strings propagate through flat spacetime, but becomes an interacting non-linear σ -model once curvature is considered. Higher-order corrections in this expansion account for the deviations in how a string probes spacetime compared to a point particle, becoming more significant as its characteristic curvature radius approaches the string length. One of the main differences between the propagation of point particles and strings is that the latter can be well-defined on singular backgrounds.

Depending on the details involved in the construction of the worldsheet theory, one can obtain a variety of string theories. The simplest of them is bosonic string theory, living in $D = 26$ dimensions, but it presents a closed-string tachyon signalling a vacuum instability and exhibits no fermions in its spectrum. For these reasons, bosonic string theory does not play a prominent role in the search for realistic string models. Nonetheless, it is still a useful testing ground to understand how string theory behaves, for example in the study of D-brane decay via tachyon condensation [59, 60].

The most frequently considered incarnations of string theory are the five supersymmetric tachyon-free ones: Type IIA, Type IIB, Type I, Spin(32)/ \mathbb{Z}_2 heterotic and $E_8 \times E_8$ heterotic string theory. These contain fermions in their spectrum, can lead to chiral theories and are able to realize the Standard Model features, making them a natural ground for the exploration of realistic string models. The five string theories just enumerated have unbroken supersymmetry in ten-dimensional Minkowski spacetime; once a compactification is considered, the amount of supersymmetry preserved in the lower-dimensional theory depends on the properties of the internal space. In particular, while it is possible to construct string models with low-scale supersymmetry breaking, this is in no way enforced by string theory. Supersymmetry at the TeV scale is an attractive possibility from the perspective of particle physics naturalness, in relation with the electroweak hierarchy problems, but not a prediction of quantum gravity.

It is also possible to construct non-supersymmetric string theories with fermions in their spectrum, like the tachyonic E_8 heterotic string theory [61–63]. However, most of these present closed-string tachyons. Exceptions to this are the three ten-dimensional non-supersymmetric tachyon-free string theories: the $SO(16) \times SO(16)$ heterotic string theory [61, 64], the Sugimoto string [65] and the Sagnotti string [66, 67]. While these theories are non-supersymmetric, due to modular invariance and the absence of physical tachyons they present a property known as misaligned supersymmetry [68, 69], due to which there is an almost exact cancellation of bosons and fermions in the asymptotic density of states of the worldsheet theory, but one that is not realized level by level. Understanding the phenomenological implications of non-supersymmetric string theories is an interesting but largely unexplored possibility [70]. They present challenges like large cosmological constant contributions at the string scale arising from the vacuum energy density at one loop in g_s and, relatedly, dilaton tadpoles signalling an instability of the chosen perturbative vacuum. Recently, there has been some revived interest in these theories, see [71, 72] and references therein.

1.2.2 A serendipitous discovery

Earlier we characterized string theory as the framework resulting from replacing point particles by strings as the fundamental degrees of freedom of a theory of quantum gravity, with the idea of smearing out the interaction points and thereby removing the divergencies appearing in the computation of amplitudes. This is a perfectly valid starting point for a conceptual introduction to the subject, but it does not capture the intricate way in which physicists arrived at this hypothesis.

The early history of string theory reveals a fact that is not intrinsic to the framework itself, but simply an observation on the way it was discovered: While most proposed methods for quantizing gravity are purposefully constructed to address said problem, string theory was originally born from an attempt to understand hadronic resonances, without any reference to gravitation. The stringent consistency constraints arising in its study made the presence of an unwanted massless spin-2 particle in the spectrum unavoidable. Eventually, after the rise

of quantum chromodynamics, string theory was reinterpreted as a unified theory of quantum gravity and the other fundamental interactions. That string theory was a serendipitous discovery leading to a quantum description of the gravitational field only due to its rigidness, yet the most successful theory of quantum gravity to date, makes a compelling case for its careful study.

A brief exposition of the early history of string theory intertwined with a description of some of its basic properties can be found in the introduction of [53]. The succinct (and incomplete) summary that we attempt below is based on [73], a comprehensive recent study of the history of the subject, from which we also take the proposed division in epochs.

- 1. Dual models and early string theory (1968–1973):** Veneziano publishes the 4-point dual resonance model for hadrons [74]. The model is quickly generalized to N -point amplitudes and represented in terms of an infinite set of oscillators that are then formally interpreted as strings. The need for a critical dimension $D = 26$ is appreciated, and the Nambu-Goto action is proposed. Models with fermions, leading to a lower critical dimension of $D = 10$, are constructed. A self-consistent theory of quantum strings is shown to reproduce the physics of dual models. The limit of zero slope (low energy) of the dual models is found to correspond to Yang-Mills theory [75].
- 2. Theoretical exaptation (1974–1984):** The limit of zero slope is proved to yield general relativity [76]. An interacting string picture is developed. The GSO projection allows for the introduction of spacetime supersymmetric tachyon-free string theory, and the Type I, Type IIA and Type IIB nomenclature is adopted. The Polyakov action is put forward and used to reformulate the quantization of the theory. String field theory is constructed. Type I string theory is found to have a hexagon chiral gauge anomaly.
- 3. Early string phenomenology (1984–1994):** String theory is found to be anomaly free thanks to the Green-Schwarz mechanism [77]. Following this, the theory starts to be taken more seriously as a unified description of nature. Heterotic string theory is first constructed [78, 79], completing the set of five superstring theories. Compactifications of heterotic string theory on Calabi-Yau varieties leading to GUT groups are introduced [80]. These developments lead to the birth of heterotic string phenomenology. T-duality [81], S-duality [82] and mirror symmetry [83–86] are discovered. The notion of D-brane appears various times in the literature, but their true importance is not yet appreciated.
- 4. Dualities and modern string theory (1995–present):** D-branes are understood to be electric and magnetic sources of Ramond-Ramond charge [87]. Further work devoted to charting the string duality web is carried out. Low-energy Type IIA string theory at strong coupling is argued to lead to eleven-dimensional supergravity [88], giving rise to the idea that all string theories are limits of a more fundamental theory, termed M-theory. The Bekenstein-Hawking entropy formula is reproduced from microstate counting [58]. F-theory is introduced as a geometrization of non-perturbative Type IIB string theory [89]. The AdS/CFT conjecture is proposed [90], opening a new window into the study of string theory via conformal field theory and vice versa. Flux compactifications and moduli stabilization are developed [91–93]. The idea of statistically studying the string theory Landscape is pioneered [94]. Some influential proposals for dS vacua are presented [95–97]. Realistic models of inflation benefit from the discovery of D-branes. F-theory GUTs acquire a prominent role in string phenomenology [98–101]. The Swampland Program [102] rises in popularity, prompting a shift in perspective within string phenomenology.

The origins of string theory as a description of hadronic resonances can still be seen in some vestigial signs, like the term *Regge slope* used to refer to α' , the square of the string length. It appears in the relation $J = \alpha' M^2$ between the spin and mass of excited string states, which realize a *Regge trajectory*.

1.2.3 Not (only) a theory of strings

As suggested by both its name and the brief conceptual introduction to the subject given above, strings occupy a central place in string theory. The reasons underlying this were mentioned earlier: strings generalize the point particle, leading to the removal of pathological divergences, while at the same time having a worldvolume theory that is simple enough to be tractable. However, a look at the brief history of string theory charted in the preceding section reveals that our modern conception of the framework cannot be conceived without mentioning dualities and higher-dimensional objects like D- and M-branes.

When the five supersymmetric tachyon-free string theories were constructed, it was not immediately clear that they were equivalent to each other. Moreover, it was not precisely known how eleven-dimensional supergravity—a distinguished member of the family of supergravity theories that were being developed in parallel to string theory—fit into the picture, although there was evidence of the importance of M-branes and their connections to string theory [103–107]. This fragmented panorama, undesirable for a unified description of nature, turned out to be tightly interconnected through the string duality web, a simplified version of which is depicted in Figure 1.4. Perturbative string theory, in which the fundamental degrees of freedom are strings, is just one corner of the duality web; other limits of the theory do not even contain strings. At the core of the duality web sits the conjectured M-theory, of which the different corners are just perturbative descriptions, and whose fundamental degrees of freedom are not yet known. Furthermore, the dimensionality of spacetime varies among the different regimes of the theory, showing that it is not absolute, but dependent instead on the limit of M-theory used to describe the physics.

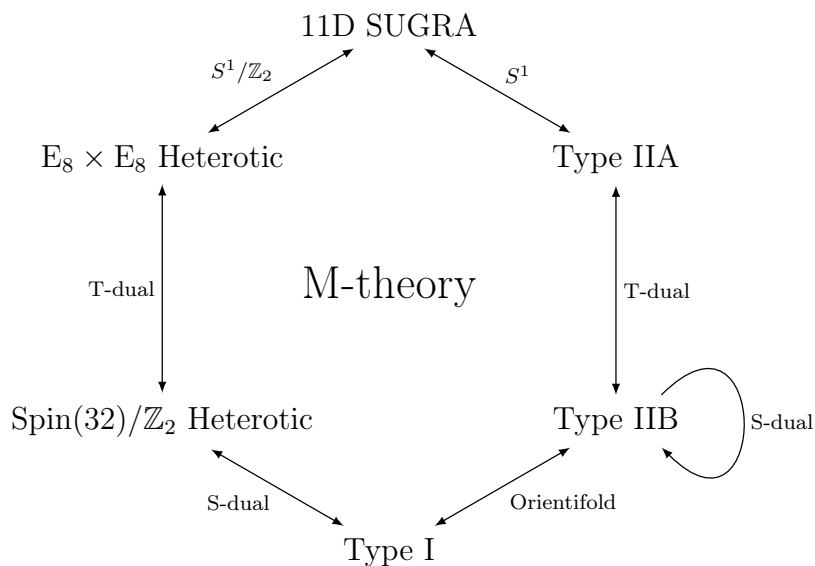


Figure 1.4: The string duality web, at the centre of which sits M-theory.

The best point of view to answer a question depends on the nature of the concrete question being asked: The duality web connects classical and quantum effects, and relates perturbative and non-perturbative phenomena. This offers a window into the non-perturbative physics of string theory through the familiar grounds of its perturbative formulation. Hence, dualities do not only provide a conceptual unification of the framework, but also constitute a very powerful computational tool. The calculation of the number of rational curves in a Calabi-Yau threefold (its Gromov-Witten invariants) through the period integrals of its mirror dual variety [86] is a triumphant example of this; a complicated problem in enumerative geometry was solved by relating quantum corrections to classical effects in string theory via mirror symmetry. This not only illustrates the paramount importance of dualities, but also the fruitful exchange that exists between string theory and mathematics.

D-branes and M-branes are arguably as important as strings for modern understanding of the subject. The identification of D-branes as electric and magnetic sources of Ramond-Ramond charge [87] not only gave rise to a long series of formal developments, but also reshaped the landscape of realistic string models. They allow for the appearance of localised gauge sectors, enabling the construction of realistic intersecting D-brane models [108] on which the Standard Model can live. Additionally, they are a crucial ingredient of flux compactifications, the backbone of much of contemporary string phenomenology [109, 110]. D_p- and M_p-branes fully wrapped on shrinking ($p+1$)-cycles lead to D- and M-instanton corrections, respectively, that can significantly modify the classical behaviour of the theory; we will have more to say about this in Chapter 4.

In this work, we focus on the geometrical regime of string theory and the part of the duality web depicted in Figure 1.4, completed by F-theory. Painting a complete picture of the framework would be an arduous task even for a dedicated monograph; we will just attempt to mention a few alternative angles from which one can approach the subject, while omitting many more. One of them is non-supersymmetric tachyon-free string theories, to which we already devoted some lines to above, and do not repeat here.

The AdS/CFT correspondence is possibly the most important one. It is a strong-weak duality between quantum gravity in the bulk of an AdS spacetime as described by string theory and a CFT defined on its boundary. The prime example is given by the relation between Type IIB string theory on $\text{AdS}_5 \times S^5$ and the $\mathcal{N} = 4$ super Yang-Mills theory on a stack of D3-branes in the decoupling limit. It offers new ways to study strongly coupled quantum field theories and non-perturbative quantum gravity. A textbook account of the AdS/CFT correspondence can be found in [111].

String theory can be compactified on non-geometric backgrounds, meaning that the internal space cannot be described purely in terms of geometry or that T-duality transformations are needed to make the background well-defined. Non-geometric fluxes can be useful in the context of string phenomenology, where they may be employed for moduli stabilization. In some instances, of which Gepner models are an example, a description in terms of a metric and background fields is not possible at all; CFT tools need then to be used in order to understand the background, which is, however, well-defined in string theory. See [112] for a review.

Beyond the well-known duality web discussed above, different string theories can also be connected dynamically through tachyon condensation. By considering non-critical string theories in various dimensions with a non-zero tachyon expectation value, one can construct dimension quenching solutions that connect these less commonly considered string theories to the familiar supersymmetric tachyon free string theories, and even to the bosonic formulation [113].

The bosonic string is the $\mathcal{N} = 0$ worldsheet theory, while the superstring corresponds to its $\mathcal{N} = 1$ counterpart. A natural generalization is to consider strings with an $\mathcal{N} = 2$ worldsheet

theory; these lead to a four-dimensional spacetime with signature $(2, 2)$ or $(4, 0)$, and therefore cannot be directly relevant for nature. As a consequence, after some interesting initial work on them, they have been largely ignored. See [114] for a review.

String field theory is a second-quantized formalism allowing for the computation of off-shell string amplitudes. The framework enabled the description of tachyon condensation in the open string sector for unstable D-branes. A modern introduction is [115].

A different second-quantized formulation of M-theory is given by the BFSS matrix model. This development arises from the BFSS conjecture [116], claiming that the infinite-momentum frame of M-theory can be captured by the matrix quantum mechanics describing the worldvolume theory of $N \rightarrow \infty$ Type IIA D0-branes, with the finite N theory conjectured to describe the discrete light-front quantized sector of M-theory [117]. This offers yet another departure from the geometric regime of string theory, since spacetime is only an emergent notion in this approach. See [118] for an exposition of the topic. There also exist matrix model descriptions of string theory, like the DVV matrix model for Type IIA string theory [119] or the matrix models for two-dimensional string theories [120].

1.3 The Landscape and the Swampland

Having discussed the most basic properties of string theory, let us now turn our attention to its vacuum structure. String theory has no adjustable parameters, it is unique in the UV as corresponds to a fundamental theory of nature. Its ability to describe very diverse physics in the IR comes from its rich vacuum structure. The collection of gravitational EFTs descending from string theory is known as the Landscape, a notion that can be more widely applied to any theory of quantum gravity. The Swampland is, by contrast, the set of gravitational EFTs that seem naively consistent, but hide some obstruction preventing their UV completion to a theory of quantum gravity. Understanding where the Landscape ends and the Swampland begins will teach us about the general properties that any theory of quantum gravity must possess.

1.3.1 The Landscape: A unique theory, a plethora of solutions

String theory contains the ingredients needed to describe the sectors of nature that we currently know. These ingredients need to be judiciously combined in order to produce the phenomenological features expected from a realistic string model, a nice checklist of which can be found in [121]. Most of these properties have been achieved in concrete models, but this is not enough: In a framework that unifies all fundamental interactions, a successful model cannot partially describe nature; rather, it is imperative for all phenomenological features of our universe to be simultaneously realized. This is no small task.

Due to the extra dimensions predicted by string theory, the first step in the construction of any realistic string model is to make six of the spacetime dimensions—we think of superstring theory for concreteness—unobservable at low energies. This is usually achieved by taking them to be a compact variety, leading to the notion of string compactification. While at energies low enough a four-dimensional observer will not be able to probe these additional dimensions, their geometry still has palpable consequences, since it determines the physics of the resulting low-energy four-dimensional EFTs. Hence, obtaining a realistic string compactification crucially depends on finding an appropriate internal geometry.

It is important to emphasize at this point that, while we customarily use the expression *constructing a string model*, this process involves no arbitrary choices. String theory has no

adjustable parameters and, as a consequence, the allowed internal geometries are dynamically determined. We start from a unique theory—conceptually M-theory, in practice one of its various perturbative corners—containing only a single (dimensionful) parameter, the string length ℓ_s , and we check if the proposed configuration is part of the space of solutions of its equations of motion. In that sense, we are not *constructing* a model, but simply checking the viability of a particular combination of internal geometry and content as a compactification. And, while the theory is uniquely determined in the UV, it gives rise to a rich vacuum structure.

For reasons of technical control and phenomenological interest, commonly considered string compactifications preserve some amount of supersymmetry (to be fully broken at a later stage). This selects a class of internal spaces known as Calabi-Yau varieties, of great mathematical interest in their own right. In 1985, at the time of the pioneering work [80] providing the first heterotic compactification leading to a four-dimensional E_6 GUT, the number of known (strict) Calabi-Yau threefolds was 6 simply connected varieties and 1 additional non-simply connected example obtained by taking a quotient of one of the previous geometries by a freely acting symmetry group. As a consequence of their interest for string phenomenology, many more Calabi-Yau threefolds were constructed in the years that followed. By 1987 (although published in 1988) a total of 7890 complete intersection Calabi-Yau threefolds were classified [122]. More than 3×10^4 topologically distinct Calabi-Yau threefolds were known by the year 2000 [123, 124].

The set of string vacuum configurations receives the name of Landscape, a notion which more generally applies to the set of vacua of any theory of quantum gravity. Lower estimates for its size following from the preceding discussion pale in comparison with the numbers arising from flux compactifications [109, 110]. These are compactifications of Type II string theory with non-trivial vacuum expectation values for the Neveu-Schwarz or Ramond-Ramond field strengths. Turning on the fluxes breaks the four-dimensional $\mathcal{N} = 2$ supersymmetry preserved by compactifying Type II string theory on a Calabi-Yau variety to $\mathcal{N} = 1$ supersymmetry. Additionally, they source a potential fixing the vacuum expectation values of (at least part of) the moduli, a collection of scalars parametrizing the deformations of the internal geometry. One can conclude that fluxes are quantized through an argument analogous to the Dirac quantization condition. Their choice is limited to an integral lattice, and they must satisfy the tadpole cancellation condition (the net charge in the compact internal space must vanish). The immensity of the Landscape was realized after the GKP class of vacua was constructed [125]. Estimates for the number of flux vacua for a typical Calabi-Yau threefold are $\mathcal{O}(10^{500})$ [126], while the number of inequivalent compactification geometries for F-theory has been estimated to be $\mathcal{O}(10^{755})$ [127]. The total size of the Landscape could be as large as $\mathcal{O}(10^{272,000})$ [128].

Among this plethora of possibilities, huge numbers of them can be immediately discarded if one is only concerned with the search for phenomenologically viable solutions. Nonetheless, searching the Landscape for vacua compatible with the known features of our universe requires solving problems that are generically NP-complete, NP-hard or even undecidable, all while scanning over a colossal data set. This makes the exploration of the Landscape a fertile area of application for machine learning and data science techniques [129].

The vast size of the Landscape raises the question of why, among all the possible string vacua, we live precisely in the one corresponding to our universe. One logical possibility is the existence of a vacuum selection mechanism, dynamically explaining the evolution path taken by the universe until it reached our vacuum. Beyond some attempts at understanding the number of large dimensions that we observe [130], not much progress has so far been made in this direction. The opposite approach is to treat all vacua of the Landscape as dynamically possible, with different regions of the universe realizing different vacua. The fact that we live in an observable

universe with the properties of ours would then be explained by invoking the anthropic principle. This is similar to the ideas put forward in the context of chaotic inflation [131]. A statistical study of ensembles of string theory vacua was initiated in [94].

Either way, if no vacua within the Landscape could explain the features of our universe, string theory would be ruled out. Hence, it is important to find vacua that at least qualitatively reproduce part of the properties that we observe in nature; a fundamental obstruction to even one of them would be a significant finding. The progress made in constructing string models with the gauge group, chiral matter content and Yukawa couplings of the Standard Model has been recently reviewed in [7], while the monograph [132] treats inflationary models in string theory. The existence of dS string vacua is disputed: The two prominent proposals for the construction of dS vacua, KKLT [95] and LVS [96, 97], are not complete top-down models, but rather string inspired constructions, i.e. recipes for combining stringy ingredients in a supergravity setting. While they are appealing proposals, their lack of a fully fledged string-theoretic realization calls into question whether they are in fact part of the Landscape or not [133–136]; a conclusive answer requires either achieving fully explicit models of either of these proposals, or encountering a fundamental obstruction to doing so in the attempt.

1.3.2 The swampland: An ocean surrounding an island

The size of the String Theory Landscape or, more generally, the Quantum Gravity Landscape is unfathomable. Faced with this situation, one may be tempted to take the following leap: Finding the string vacuum corresponding to our universe from top-down considerations is an arduous task. Given the sheer size of the Landscape, any consistent gravitational EFT one can think of will surely arise as the low-energy limit of some string compactification. Hence, it might be more productive to focus on the construction of phenomenologically attractive EFTs from the bottom-up perspective and then couple them to gravity.

While its importance for UV physics would remain unaffected, the arguments given above would greatly diminish the IR constraining power of string theory—or quantum gravity in a more general sense—if true. In his seminal paper [102], Cumrun Vafa argued that, in fact, almost the contrary holds: The Landscape of string vacua is but a minute subset of the collection of apparently consistent EFTs coupled to gravity. The remainder of these, not allowing for a consistent UV completion to a theory of quantum gravity, are said to be in the Swampland.

The Swampland Program, see [137–141] for reviews, aims to delineate the boundary between the Landscape and the Swampland. This is done through a series of Swampland Constraints, which are of general scope but conjectural in nature, and hence more commonly referred to as Swampland Conjectures. These should be criteria applicable directly at the level of the gravitational EFT, allowing us to discern if it may originate from a theory of quantum gravity or not. The constraints should become trivial when the Planck mass is sent to infinity, showing that they are truly related to the nature of gravity.

Gathering evidence in favour of (or against) the Swampland Conjectures can be done both from a bottom-up and from a top-down perspective. From the bottom-up point of view, one tries to exploit those low-energy aspects of quantum gravity that are believed to be universal features. A fruitful arena for this line of argumentation is provided by black holes physics; we already highlighted this in Section 1.1.4 as one of the reasons why semiclassical gravity offers an important stepping stone in the search for a theory of quantum gravity. Ideally, one would like to develop top-down derivations for the Swampland Constraints, obtained directly from microscopic physics. This requires a theory of quantum gravity that enables the study of the Swampland

Conjectures within a well-controlled framework, with string theory currently standing as the sole viable option. While desirable, a complete proof of a Swampland Conjecture is not within our current technical reach, unless we restrict ourselves to concrete corners of the moduli space. Nonetheless, some conjectures have been proven in perturbative string theory or by assuming the AdS/CFT correspondence. A complementary way in which string theory is helpful in the exploration of the Swampland, is not in gathering proof, but evidence for the validity of the conjectures. Testing them against all known string vacua allows us to examine how they hold and under what conditions.

The notion of the Swampland is defined independently of string theory, although the two are connected in practice due to the lack of alternative avenues for a top-down analysis of the conjectures. Nonetheless, it is worth maintaining the discussion general by distinguishing between a String Theory Swampland and a broader Quantum Gravity Swampland: The former consists of those naively consistent EFTs coupled to gravity that do not descend from string theory, while the latter is the subset of these not admitting a UV completion to any theory of quantum gravity. If string theory turns out to be the only possible theory of quantum gravity, a concept known as string universality and for which some evidence exists in higher dimensions [142–144], the String Theory Swampland and the Quantum Gravity Swampland would coincide. This splitting of concepts also applies to the Landscape, but with the inclusion relation inverted.

Two core conjectures of the Swampland Program are the Weak Gravity Conjecture [145] and the Swampland Distance Conjecture [146]. The Weak Gravity Conjecture roughly states that gravity must be the weakest force in any consistent theory of quantum gravity; it can be regarded as a generalization of the No Global Symmetries Conjecture [147, 148], which predates the Swampland Program and is the conjecture most firmly established. The Swampland Distance Conjecture and its refinement, the Emergent String Conjecture [149], make predictions about the precise way in which an EFT must break as we traverse an infinite distance in the moduli space of the theory. The bulk of this work is concerned with analysing the validity of these last two Swampland Conjectures in the hypermultiplet moduli space of five-dimensional M-theory and six-dimensional F-theory.

The change in perspective advocated by the Swampland Program—placing an emphasis on understanding, on general grounds, what is allowed in quantum gravity, in addition to the continued study of the Landscape and of bottom-up constructions—did not take effect immediately after the publication of [102, 145, 146]. Instead, interest grew after some apparent discrepancies with empirical data: The results from the BICEP2 experiment showing B-mode polarization in the CMB [150] pointed towards large field inflation, implying super-Planckian displacements in the inflaton field [151], and were therefore in tension with the Swampland Distance Conjecture. When the signal was found to actually correspond to dust [152], the Swampland Program gained a considerable impetus.

A more detailed discussion of the Swampland Program will be the subject of Chapter 3. Establishing the Swampland Conjectures on firmer grounds and finding connections among them is an exciting and effervescent direction in the study of quantum gravity. The efforts spent in refining the conjectures, gathering evidence in favour or against them, and in reexamining how solid older constructions are in view of these new constraints is bound to expand our understanding of string theory and quantum gravity, and, perhaps, even point in the direction that they are one and the same thing.

1.4 Motivation and summary

Following our examination of the importance of studying quantum gravity, of string theory as our prime example of it, and of the Landscape and the Swampland, we are prepared to consider the concrete questions with which the rest of this work is concerned. These revolve around the non-trivial ways in which the Emergent String Conjecture is satisfied.

The Swampland Distance Conjecture states that as we traverse an infinite distance in the moduli space of a gravitational EFT, an infinite tower of states must become asymptotically massless, thereby breaking the effective description of the theory. Moreover, the decrease in the mass scale of the tower must be exponential. The Emergent String Conjecture refines this statement by addressing the origin of the infinite tower of states: it must be furnished by either Kaluza-Klein replicas or by the excitations of a unique, weakly coupled and asymptotically tensionless critical string.

These two conjectures encapsulate, presuming they are correct, rather deep truths about the nature of quantum gravity. They are, in a sense, statements about the emergence of duality frames at the asymptotic corners of the moduli space. The infinite tower of states predicted to become massless in said asymptotic regions provides the appropriate set of light and weakly coupled fundamental degrees of freedom for the dual description. This can be illustrated by thinking about the T-dual Kaluza-Klein and winding modes of a string circle compactification. The refinement provided by the Emergent String Conjecture predicts that infinite-distance limits always bring us back to one of the corners of the moduli space that we are already familiar with, either by decompactifying to higher dimensions, or by going to the duality frame determined by the unique, weakly coupled and asymptotically tensionless string. Both conjectures have survived a wealth of tests, and are considered to be among the most robustly established Swampland Conjectures.

The Emergent String Conjecture is a non-trivial modification of the Swampland Distance Conjecture: We could, in principle, have infinite-distance limits in which the parametrically leading asymptotically massless object is instead higher-dimensional, for example a membrane. In most situations, membranes turn out to be parametrically heavier than particles or strings along infinite-distance trajectories, just on dimensional grounds. One can find, however, setups in which this is not the case at the classical moduli space level, like for some infinite-distance limits in the hypermultiplet moduli space of five-dimensional M-theory. This leads to a couple of natural questions.

First, are the aforementioned classical *membrane limits* in the hypermultiplet moduli space of five-dimensional M-theory removed once quantum corrections are considered? There have been previous instances in which carefully taking quantum corrections into account was crucial to find agreement with the Swampland Conjectures [153–155]; the putative membrane limits might simply be another classical mirage.

Second, if indeed the Emergent String Conjecture holds after quantum corrections are taken into account, can one understand why membrane limits should be forbidden in a heuristic way?

Both of these questions will be addressed in Chapter 4, where we report on our work [1], finding agreement with the Emergent String Conjecture. Our analysis shows that if the conjecture is consistent under dimensional reduction, a *critical membrane*—a membrane leading to a critical string upon circle reduction—cannot be the parametrically lightest object along an infinite-distance limit. As an explicit check of this fact, and without assuming the Emergent String Conjecture, we study the putative membrane limits in the classical hypermultiplet moduli space of five-dimensional M-theory. Once the M2-instanton corrections arising from M2-branes

wrapped along shrinking 3-cycles are taken into account, we find that these trajectories are deflected into decompactification limits.

The hypermultiplet moduli space of six-dimensional F-theory is where the other motivating questions for this thesis arise. The internal space of six-dimensional F-theory is an elliptic Calabi-Yau threefold, the complex structure deformations of which correspond to trajectories in the hypermultiplet moduli space. The loci of the base of this threefold over which the elliptic fiber becomes singular correspond to the location of stacks of $[p, q]$ 7-branes, which give rise to non-abelian gauge algebras. Moving a collection of 7-branes on top of each other in order to produce such non-abelian gauge algebra factors entails performing a finite-distance complex structure deformation of the internal space, enforcing the appropriate structure of minimal singular elliptic fibers. Along said trajectory in the hypermultiplet moduli space, a finite number of states become light; these are the states furnishing the algebra. The precise non-abelian gauge algebra arising from such a procedure can be read off from the type of codimension-one minimal singular elliptic fiber associated to the stack of 7-branes, as classified by Kodaira and Néron. This class of fibral singularities admits a crepant resolution in the fiber, i.e. the singularity can be removed by inserting a series of exceptional curves without spoiling the Calabi-Yau property of the threefold. Considering the resolved geometry takes us from F-theory to M-theory, with the F-theory limit corresponding to sending the volume of the elliptic fiber to zero at fixed complex structure. This shrinks the collection of exceptional curves as well. The massless states furnishing the non-abelian gauge algebra can then be understood as M2-branes wrapping the exceptional curves. Since the deformations discussed correspond to moving 7-branes within the internal space, we can regard them as trajectories in the open moduli space of string theory.

Naively, one could think that no infinite-distance trajectories in moduli space can arise through deformations of this fashion: The location of the 7-branes is varied within the base of the internal space of the F-theory compactification. Since we are concerned with the study of quantum gravity, the lower-dimensional Planck scale must be finite, which implies that the internal space must be compact and have finite volume. Hence, the 7-branes cannot be transported an infinite distance.

In fact, the above conclusion is wrong: Non-compact directions in the open string moduli space do occur at the non-perturbative level. This was argued in the context of eight-dimensional F-theory in [156, 157]. Along such trajectories, a suitable configuration of mutually non-local $[p, q]$ 7-branes coalesces, which in geometrical terms results in the appearance of codimension-one non-minimal singular elliptic fibers of the internal Calabi-Yau threefold. Unlike their minimal counterparts, this class of singularities does not admit a crepant resolution in the fiber. Models exhibiting them are, as a consequence, usually discarded in F-theory analyses.

It is precisely to the study of these singularities that we will devote Chapters 5 and 6 to. Understanding infinite-distance non-minimal singularities of elliptic Calabi-Yau threefolds in the context of F-theory is both of physical and mathematical interest. We will report on our detailed analysis of the two aspects, presented in [2, 3]. First, we perform systematic mathematical study of the complex structure degenerations of elliptic Calabi-Yau threefolds corresponding to infinite-distance limits. These can be put in semi-stable form through a sequence of base blow-ups, making the endpoint of the limits a union of log Calabi-Yau spaces glued together along their boundaries. We fully characterize the base geometry of these log Calabi-Yau spaces, as well as the line bundles defined over them. We also explain how to extract the non-abelian gauge algebra for F-theory probing such reducible asymptotic geometries, employing a physical discriminant that we define. Second, we concentrate on genus-zero single infinite-distance limit degenerations of Hirzebruch models and extract their asymptotic physics. As a novel feature

with respect to the eight-dimensional situation, we interpret the central fibers of (part of) these degenerations as the endpoints of decompactification limits to theories with six-dimensional defects. Emergent string limits, whose endpoints are at global weak coupling, can also arise within this class of degenerations; the geometrical conditions that must be realized for them to be possible are carefully analysed. We contrast our results in F-theory with the heterotic dual description where available. The expectations from the Emergent String Conjecture are also met in the hypermultiplet moduli space of six-dimensional F-theory.

1.5 Outline

In this section we provide an overview of the content treated in the remainder of the thesis. This is complemented by more detailed summaries at the beginning of each chapter.

Part II provides the necessary background to understand the subsequent developments. Chapter 2 is devoted to introducing F-theory, the language in which the bulk of this dissertation, namely Part IV, is formulated. Doing so entails revisiting the core string theory notions on which F-theory rests, an occasion that we employ to also review those concepts important for Part III. In Chapter 3 we introduce the notions of the Landscape and the Swampland; as explained earlier, understanding the boundary between the two is one of the motivations for this work.

We commence Chapter 2 discussing the string theory preliminaries in Section 2.1, focusing on the relation between the worldsheet theory of strings and the spacetime quantum gravity theory to which they give rise to. Continuing in this direction, we review the notions of string compactification and moduli space of a Calabi-Yau threefold, as well as the string duality web connecting the different formulations of the theory. The added complications emerging in the study of D7-brane solutions in Type IIB string theory, as compared to those associated to higher-codimension objects, are discussed next, alongside the $SL(2, \mathbb{Z})$ -duality so crucial to their understanding. To gain a more geometrical perspective on it, we revisit said $SL(2, \mathbb{Z})$ -duality from an M-theory perspective, by using the string duality web. From this fertile soil emerges F-theory, the topic of Section 2.2. We first approach the subject from Type IIB string theory, regarding it as a convenient way to geometrically describe non-perturbative Type IIB compactifications in the presence of general $[p, q]$ 7-branes through the properties of elliptically fibered Calabi-Yau spaces. After reviewing the most important facts about these geometries, we use the string duality web to approach F-theory from M-theory, which enables a direct identification of the states furnishing the non-perturbative gauge algebras localised on the 7-branes. We conclude with a concise overview of further entries in the geometry-physics dictionary provided by F-theory.

Chapter 3 opens by defining the two notions upon which it revolves, the Landscape and the Swampland, in Section 3.1. This is followed by an exploration of the Swampland Program, the endeavour that aims to establish criteria enabling us to discern which gravitational EFTs belong to the Landscape and which to the Swampland. In Section 3.2 we examine two core Swampland Conjectures in some detail, namely the No Global Symmetries Conjecture and the Weak Gravity Conjecture, ending with some comments on the species scale. We conclude the chapter by discussing the Swampland Distance Conjecture and the Emergent String Conjecture in Sections 3.3 and 3.4, respectively, in preparation for their study in subsequent chapters.

In Part III, consisting only of Chapter 4, based on [1], we challenge the Emergent String Conjecture by studying the possibility of realising emergent membrane limits, a putative type of limit in which a membrane would sit at the parametrically lightest scale, together with a suitable

Kaluza-Klein tower, along an infinite-distance trajectory in the moduli space. After introducing the problem in Section 4.1, we conclude in Section 4.2 that, if the membrane gives rise to a critical string upon circle reduction, consistency under dimensional reduction of the Emergent String Conjecture forces the membrane to parametrically decouple from the lightest Kaluza-Klein tower. This means that emergent membrane limits would be incompatible with the consistency of the Emergent String Conjecture under dimensional reduction. To test that these expectations from the Emergent String Conjecture are indeed realised, we turn our attention to the hypermultiplet moduli space of five-dimensional M-theory. In Section 4.3 we construct putative membrane limits in the classical hypermultiplet moduli space, which violate the Emergent String Conjecture at this level of approximation. However, the infinite-distance trajectories considered receive significant quantum corrections from M2-instantons. We devote Section 4.4 to the review of an analogous situation in the hypermultiplet moduli space of four-dimensional Type IIB string theory, where one can find classical pathological string limits that are obstructed once the quantum corrections arising from D-instantons are taken into account. Conveniently, we can relate the classical membrane limits under consideration to the aforementioned classical pathological string limits. This is done by noting that the hypermultiplet moduli spaces of five-dimensional M-theory and four-dimensional Type IIA string theory are identical, which allows us to formally identify the infinite-distance trajectories, and then using mirror symmetry to go to Type IIB; this chain of equivalences is explained in Section 4.5. In this way, we can incorporate the M2-instanton corrections to the putative membrane limits, finding that their effect is to turn the aforementioned classical membrane limits into decompactification limits in the quantum-corrected hypermultiplet moduli space. We offer some final conclusions in Section 4.7. Appendix A.1 contains some remarks regarding the Kaluza-Klein towers relevant for a subclass of the infinite-distance trajectories discussed.

Part IV is composed of Chapters 5 and 6, based on [2, 3], respectively. In this part of the thesis, we study the geometry and the physics of the infinite-distance non-minimal singularities of elliptic Calabi-Yau threefolds. Interpreted in the context of six-dimensional F-theory, the degenerations of elliptic threefolds giving rise to these singularities correspond to infinite-distance limits in the open string moduli space, and are therefore of interest in view of the Emergent String Conjecture. Chapter 5 contains a systematic mathematical analysis of the relevant geometry, which serves as the foundation for the interpretation of the asymptotic physics associated with these trajectories in Chapter 6.

Chapter 5 begins with an introduction and a detailed summary of its contents in Section 5.1. We describe the infinite-distance limits in the complex structure moduli space of six-dimensional F-theory that we are interested in by using the algebro-geometric language of degenerations; Section 5.2 explains in detail how to explicitly work with degenerations of Weierstrass models of elliptic Calabi-Yau varieties. The central fiber of these degenerations corresponds to the endpoint of the limit taken in the moduli space. Hence, our interest lies in those degenerations whose central fiber exhibits infinite-distance non-minimal singularities. We explain how to resolve the resulting geometries in order to put them in semi-stable form, which entails performing a series of base changes and modifications as suggested by the Semi-stable Reduction Theorem. The presentation of infinite-distance limits as semi-stable degenerations allows us to unambiguously extract the asymptotic physics, and is therefore of great importance for Chapter 6. This resolution process transforms the geometrical representative of the asymptotic spacetime, i.e. the central fiber of the degeneration, into a union of log Calabi-Yau spaces glued together along their boundaries. We determine criteria for the resolved central fiber to have the structure of an open chain or

a more complicated tree of components. Focusing on those infinite-distance limits associated to the appearance of non-minimal elliptic fibers over genus-one curves in the base, which we show are the most abundant class with only a few genus-one outliers, we completely characterise the base geometry of their log Calabi-Yau components, as well as the line bundles defined over them. In Section 5.3 we focus on genus-zero infinite-distance limit degenerations of Hirzebruch models, applying the machinery developed earlier to very explicitly study them. This analysis not only illustrates the discussion preceding it, but also provides the mathematical results on top of which Chapter 6 is built. Section 5.4 details how to extract the gauge algebra for F-theory probing such reducible asymptotic spacetimes from the physical discriminant that we introduce. Section 5.5 summarises the conclusions reached during Chapter 5 and comments on future work. The appendices collect a series of technical discussions that complement the material contained in the body of the chapter. Appendix B.1 reviews the geometry of those surfaces that can act as six-dimensional F-theory bases as well as the properties of their blow-ups, fixing notation in the process. In Appendix B.2 we prove that the curves supporting non-minimal singular elliptic fibers in a six-dimensional F-theory model must have either genus zero or genus one. Appendix B.3 discusses obscured infinite-distance limits; these correspond to degenerations in which the family variety does not exhibit non-minimal elliptic fibers even though its central fiber does, a discrepancy that can be remedied through an appropriate base change. Appendices B.4 to B.6 expand the analysis of the resolution process initiated in the body of the chapter to include the most general cases and to restrict the form of the resolved central fiber. We end the chapter with some comments on the process of blowing down so-called vertical components in Appendix B.7 and a brief review of the factorization properties of polynomials in rings with zero divisors in Appendix B.8.

Chapter 6 introduces and summarizes its contents in Section 6.1. We review previous works on the semi-stable degenerations of eight-dimensional F-theory models and concisely recall the most relevant aspects of the six-dimensional analysis of Chapter 5 in Section 6.2. The study of the asymptotic physics of genus-zero single infinite-distance limits of Hirzebruch models starts in Section 6.3, where we analyse the general properties of horizontal models. After providing a refined subclassification of them, by inheriting the Kulikov classification of their generic fiber, we study the patterns of codimension-zero singular elliptic fibers that can appear in their resolved central fibers. Global weak coupling limits correspond to particular patterns of codimension-zero singular elliptic fibers and are therefore fairly constrained; we study the geometric conditions that must be met for their realisation to be possible. We also explain how the pattern of codimension-zero singular elliptic fibers constrains the local and global 7-brane content of a model. The section concludes by studying bounds for the vertical gauge rank. Section 6.4 focuses on interpreting the asymptotic physics associated with horizontal Type II.a models, concluding that, in the adiabatic regime, they lead to a decompactified ten-dimensional theory containing six-dimensional defects. We also analyse the enhancements suffered by the non-abelian gauge algebras along these infinite-distance trajectories. Using F-theory/heterotic duality, we reinterpret these models from the heterotic dual description to gain further intuition about their physics. This duality also allows us to address the role of non-minimal singular elliptic fibers in the heterotic K3 surface, concluding that they are dual to (possibly obscured) infinite-distance limits on the F-theory side. In Section 6.5.3 we analyse the remaining horizontal models: horizontal Type II.b models, which correspond to the familiar Sen limit; horizontal Type III.a models, which lead to a partial decompactification limit combining components at local strong and weak coupling; and horizontal Type III.b models, corresponding to emergent string limits whose endpoint is at global weak coupling. We discuss our results and comment on

future work in Section 6.6. Once again, we use the appendices to collect technical results and complementary discussions, starting in Appendix B.9 with an analysis of the special structure of the discriminant in those components at local weak coupling. In Appendices B.10 and B.11 we derive bounds for the pattern of codimension-zero singular elliptic fibers and for the vertical gauge rank, respectively. We review and clarify some aspects regarding the heterotic dual interpretation of the defect algebras in Appendix B.12. Appendix B.13 reviews the geometry associated with the perturbative Type IIB orientifold picture for the Sen limit, i.e. for horizontal Type II.b models, and analyses its features when considering blown-down horizontal and vertical Type III.b models. Finally, Appendix B.14 extends the analysis developed in the body of the chapter to the remaining genus-zero single infinite-distance limit degenerations of Hirzebruch models: we provide partial results for vertical models and explain the difficulties arising due to their lack of an adiabatic limit, and carry out a more complete treatment of mixed section and mixed bisection models.

Part V, including only Chapter 7, summarises the motivations and results of the thesis.

Part II

Fundamenta

Chapter 2

Basics of F-theory

F-theory offers a powerful description of string theory in its geometric, large radius regime that incorporates non-perturbative effects in the string coupling g_s . This formulation of the theory originates from Type IIB, but is connected via dualities to M-theory and heterotic string theory too. All these corners of the string duality web, which we concisely introduce below, will be relevant in subsequent chapters.

We commence by reviewing some basic facts about string theory and its compactifications. The string duality web, which will feature prominently during the rest of this work, is discussed next, focusing on T-duality, mirror symmetry and S-duality. We then explain some of the difficulties arising in the treatment of D7-branes within perturbative Type IIB string theory, due to the strong backreaction associated to codimension-two objects. In preparation for the discussion of F-theory, we geometrize the S-duality of Type IIB by reviewing its M-theory origin.

Next, we introduce F-theory as a class of non-perturbative Type IIB compactifications in the presence of general $[p, q]$ 7-branes in which the $SL(2, \mathbb{Z})$ -duality is used to patch up the physical fields. This naturally leads to the appearance of elliptically fibered Calabi-Yau varieties, whose Weierstrass model description we then review. After these preliminaries, we approach F-theory from the M-theory perspective, focusing on identifying the origin and types of non-abelian gauge groups localised on $[p, q]$ 7-branes. We conclude by listing some additional correspondences between geometry and physics provided by F-theory, without expanding on them.

This material serves as a primer for the more technical discussions of Chapter 4, featuring five-dimensional M-theory and four-dimensional Type II string theory, and Chapters 5 and 6, framed in the context of six-dimensional F-theory, its M-theory formulation and its duality to heterotic string theory.

2.1 String theory preliminaries

F-theory is a corner of the string duality web indirectly defined through Type IIB string theory and M-theory. Before we can motivate the benefits of using its language, it is therefore convenient to recall some familiar facts about string theory. The condensed presentation that follows cannot do justice to the beauty and nuance of the subject, to which a more complete introduction can be found in the canonical textbooks [53–57].

2.1.1 From the worldsheet to spacetime

Perturbative string theory starts with the assumption that, rather than particles, the fundamental degrees of freedom should be one-dimensional strings sweeping out a (1+1)-dimensional worldsheet in spacetime. As already discussed in Section 1.2.1, this leads to a series of immediate benefits: the localised interaction points of particle theories, responsible for the divergencies in the computation of amplitudes, are smeared out, and the topological nature of the perturbative string expansion removes the combinatorial growth of the number of Feynman diagrams with the loop order.

The way in which the worldsheet theory leads to a unified quantum theory of gravity in spacetime can be most succinctly illustrated using the bosonic string. Consider a worldsheet Σ and a collection $\{X^\mu(\tau, \sigma)\}_{0 \leq \mu \leq D-1}$ of scalar fields defined on it. The $\mathcal{N} = 0$ worldsheet theory given by the Polyakov action

$$S = -\frac{1}{4\pi\alpha'} \int_{\Sigma} d^2\sigma \sqrt{-h} h^{\alpha\beta} \partial_\alpha X^\mu \partial_\beta X^\nu \eta_{\mu\nu} \quad (2.1.1)$$

describes two-dimensional gravity with metric $h_{\alpha\beta}$ coupled to the scalar fields, which can be interpreted as the components of the embedding map $X : \Sigma \rightarrow \mathbb{R}^{1,D-1}$ from the worldsheet into D -dimensional flat spacetime. Using the Weyl invariance of the worldsheet theory in the process, the bosonic string can be quantized in the path integral formalism by introducing Faddeev-Popov ghosts. The Weyl symmetry has an anomaly proportional to the central charge of the theory, which demands $D_{\text{crit}} = 26$ free bosons to cancel the contribution from the ghost system. One can also consider non-critical string theories in which the Weyl anomaly is cancelled through fields that cannot be interpreted as spacetime coordinates, but we will ignore this possibility and work in the critical dimension only. Depending on whether we take the fields $\{X^\mu(\tau, \sigma)\}_{0 \leq \mu \leq 25}$ to be periodic in σ or not, we obtain closed strings or open strings. Part of their spectra is given in Tables 2.1.1 and 2.1.2, respectively, where we observe that the closed string gives rise to the graviton, while the open string leads to gauge degrees of freedom.

Level	$\alpha'M^2$	Little group	Representation	26D field
0	-4	SO(25)	1	T
1	0	SO(24)	$\square\square + \square + \mathbf{1}$	$G_{\mu\nu}, B_{\mu\nu}, \phi$

Table 2.1.1: Lowest-lying states for the closed bosonic string.

Level	$\alpha'M^2$	Little group	Representation	26D field
0	-1	SO(25)	1	T
1	0	SO(24)	\square	A_μ

Table 2.1.2: Lowest-lying states for the open bosonic string.

Open strings can have Neumann boundary conditions (meaning freely moving endpoints) or Dirichlet boundary conditions (corresponding to fixed endpoints). An open string with $(p+1)$ Neumann boundary conditions and $(25-p)$ Dirichlet boundary conditions ends on

a Dp -brane, whose worldvolume contains a vector gauge boson arising from the open string spectrum. Stacking N D-branes one obtains a $U(N)$ Yang-Mills theory on their worldvolume. In this way, one can generate non-abelian gauge groups localized on D-branes. Separating the branes breaks the gauge group to its Cartan subgroup, realizing a form of Higgs mechanism. We are implicitly considering oriented strings, but their unoriented counterparts give rise to $O(N)$ and $Sp(2N)$ gauge theories in the worldvolume of D-brane stacks instead.

Considering the propagation of a bosonic string in a background field generated by the closed string massless spectrum leads to the non-linear σ -model

$$\begin{aligned} S = & -\frac{1}{4\pi\alpha'} \int_{\Sigma} d^2\sigma \sqrt{-h} h^{\alpha\beta} \partial_{\alpha} X^{\mu} \partial_{\beta} X^{\nu} G_{\mu\nu}(X^{\rho}) \\ & - \frac{1}{4\pi\alpha'} \int_{\Sigma} d^2\sigma \epsilon^{\alpha\beta} \partial_{\alpha} X^{\mu} \partial_{\beta} X^{\nu} B_{\mu\nu}(X^{\rho}) \\ & + \frac{1}{4\pi} \int_{\Sigma} d^2\sigma \sqrt{h} \phi(X^{\rho}) R. \end{aligned} \quad (2.1.2)$$

In order for this action to define a two-dimensional conformal field theory the Weyl invariance conditions must be fulfilled. They amount to the vanishing of the β -functions

$$\beta_{\mu\nu}^G = \beta_{\mu\nu}^B = \beta^{\phi} = 0, \quad (2.1.3)$$

an identity that results in a set of equations of motion for the spacetime fields. These can be seen to be equivalent to the Euler-Lagrange equations of the spacetime action

$$S = -\frac{1}{2\kappa^2} \int d^{26}x \sqrt{-G} e^{-2\phi} \left(R + \frac{1}{12} H_{\mu\nu\rho} H^{\mu\nu\rho} - 4D_{\mu}\phi D^{\mu}\phi \right) + \mathcal{O}\left(\frac{\alpha'}{R_c^2}\right), \quad (2.1.4)$$

where we have used the field strength $H = dB$ and R_c is the characteristic curvature radius of spacetime. In this way, we have recovered the Einstein-Hilbert action of general relativity and its stringy corrections from the worldsheet theory.

To obtain superstring theory we need to consider the $\mathcal{N} = 1$ worldsheet theory, obtained by substituting two-dimensional gravity for two-dimensional supergravity. This introduces a system of Majorana-Weyl spinors in the worldsheet acting as the supersymmetric partners of the scalar fields associated to the spacetime embedding. The worldsheet fermions can be given periodic boundary conditions, known as Ramond (R) boundary conditions, or antiperiodic boundary conditions, called Neveu-Schwarz (NS) boundary conditions. These can be chosen independently for the two spinor components, leading to four different spin structures corresponding to the possible combinations of boundary conditions.

The one-loop contribution to the closed string perturbative expansion in the string coupling g_s corresponds to a genus-one Riemann surface. Demanding for the associated torus partition function to be modular invariant, and closure of the OPEs and locality for the vertex operator algebra in the worldsheet results in the GSO projection, giving two tachyon-free consistent combinations of the right- and left-moving sectors, which lead to Type IIA and Type IIB string theory. It is also possible to take the quotient by the worldsheet parity transformation to obtain a theory of unoriented strings, which is known as Type I string theory. Finally, one can construct hybrid string theories in which the right-moving sector corresponds to the superstring, while the left-moving sector is given by the bosonic string with the 16 additional dimensions compactified on a torus. The internal bosons lead to spacetime bulk gauge symmetries, which due to modular invariance are limited to the gauge groups $Spin(32)/\mathbb{Z}_2$ and $E_8 \times E_8$ if one demands spacetime

Sector	SO(8) representation	Little group	Representation	10D field
NS-NS	$\mathbf{8}_V \otimes \mathbf{8}_V$	SO(8)	$\mathbf{1} + \mathbf{28}_V + \mathbf{35}_V$	$G_{\mu\nu}, B_{\mu\nu}, \phi$
NS-R	$\mathbf{8}_V \otimes \mathbf{8}_C$	SO(8)	$\mathbf{8}_S + \mathbf{56}_S$	$\lambda_\alpha^1, \psi_{\mu\alpha}^1$
R-NS	$\mathbf{8}_C \otimes \mathbf{8}_V$	SO(8)	$\mathbf{8}_S + \mathbf{56}_S$	$\lambda_\alpha^2, \psi_{\mu\alpha}^2$
R-R	$\mathbf{8}_C \otimes \mathbf{8}_C$	SO(8)	$\mathbf{1} + \mathbf{28}_C + \mathbf{35}_C$	$C_0, C_{\mu\nu}, C_{\mu\nu\rho\sigma}$

Table 2.1.3: Massless spectrum of Type IIB string theory.

supersymmetry. Altogether, one obtains from this mixed construction the $\text{Spin}(32)/\mathbb{Z}_2$ and $E_8 \times E_8$ heterotic string theories. These are the celebrated five supersymmetric tachyon-free string theories. In addition, the GSO projection allows for the construction a few non-supersymmetric string theories, see the comments in Section 1.2.1.

As for the bosonic string, it is possible to derive spacetime actions associated to strings moving in the background fields generated by the massless spectrum of the superstring theories. For concreteness, let us use Type IIB string theory as an example. Its massless spectrum is presented in Table 2.1.3, where we observe the C_0 , C_2 and C_4 forms to which the BPS D1-, D3-, and D5-branes electrically couple, respectively. The magnetic duals of these objects, not explicitly shown here, are also part of the spectrum. The bosonic part of the Type IIB spacetime action in string frame is given by

$$S_{\text{IIB}} = \frac{1}{(2\pi)^7 \alpha'^4} \left[\int d^{10}x \sqrt{-G} \left[e^{-2\phi} \left(R + 4\partial_\mu \phi \partial^\mu \phi - \frac{1}{2} |H_3|^2 \right) \right. \right. \\ \left. \left. - \frac{1}{2} |F_1|^2 - \frac{1}{2} |\tilde{F}_3| - \frac{1}{4} |\tilde{F}_5|^2 \right] - \frac{1}{2} \int C_4 \wedge H_3 \wedge F_3 \right], \quad (2.1.5)$$

with the definitions

$$\tilde{F}_3 = F_3 - C_0 \wedge H_3, \quad \tilde{F}_5 = F_5 - \frac{1}{2} C_2 \wedge H_3 + \frac{1}{2} B_2 \wedge F_3. \quad (2.1.6)$$

More precisely, the above expression is a pseudoaction for Type IIB string theory; it must be complemented by the self-duality constraint

$$\tilde{F}_5 = \star \tilde{F}_5 \quad (2.1.7)$$

for the \tilde{F}_5 field strength, which is imposed on the solutions. It will be convenient for later purposes to rewrite this action in Einstein frame, which results in

$$S_{\text{IIB}} = \frac{1}{2\kappa^2} \int d^{10}x \sqrt{-G_E} \left(R_E - \frac{\partial_\mu \bar{\tau} \partial^\mu \tau}{2(\text{Im } \tau)^2} - \frac{1}{2} |F_1|^2 - \frac{|G_2|^2}{2 \text{Im } \tau} - \frac{1}{4} |\tilde{F}_5|^2 \right) \\ + \frac{1}{2\kappa^2} \int C_4 \wedge \frac{G_3 \wedge \bar{G}_3}{4i \text{Im } \tau}. \quad (2.1.8)$$

Here we have introduced the Type IIB axio-dilaton τ and the complex 3-form G_3 , defined as

$$\tau = C_0 + ie^{-\phi} = C_0 + i/g_s, \quad G_3 = F_3 - \tau H_3. \quad (2.1.9)$$

The actions displayed above include no corrections; they correspond to the classical low-energy effective action of Type IIB string theory. In fact, the theory obtained is Type IIB supergravity, showing that it arises as the classical low-energy approximation of string theory.

Besides the terms shown above, one can add a piece to the action taking into account the local sources of the ten-dimensional supergravity fields, like D-branes and O-planes. BPS D-branes were already discussed earlier; they are the sources of R-R charge and have positive tension. O-planes correspond to the fixed locus of the \mathbb{Z}_2 -involution of an orientifold (the combination of the aforementioned involution with orientation reversal on the worldsheet). O-planes have negative tension and are also sources of R-R charge. It is negative in O^- -planes, the more commonly discussed type of orientifold plane, and positive in O^+ -planes. Unlike D-branes, O-planes are non-dynamical objects in perturbative string theory. They do not specify loci where open string endpoints can live; hence, they carry no gauge fields in their worldvolume, nor are there scalars parametrizing their fluctuations. In F-theory, which includes non-perturbative effects in the string coupling, O-planes are, in fact, dynamical at finite values of g_s , see the comments in Section 2.2.4.

It is also possible to derive a $(p+1)$ -dimensional effective action for the worldvolume theory of Dp -branes, corresponding to the dynamics of massless open string modes. The D-brane action consists of two pieces: a Dirac-Born-Infeld term describing its coupling to NS-NS fields, like the graviton and the Kalb-Ramond field, and a Chern-Simons term describing its topological couplings to the Ramond-Ramond fields.

D-branes are non-perturbative states in string theory that should be describable, at a classical level, as a collective excitation of the spacetime fields, like solitons in quantum field theory. The low-energy supergravity approximation of string theory has black brane solutions, some of which provide an approximation to D-branes. For BPS D-branes this identification can be trusted thanks to the existing protection against corrections, with the corresponding black brane solutions describing the backreacted spacetime in the presence of a stack of BPS D-branes.

2.1.2 String compactifications

Requiring the absence of conformal anomalies forces critical superstrings to live in $D = 10$ dimensions. A common way to make contact with d -dimensional physics is by compactifying the additional dimensions in an internal space X of $\dim_{\mathbb{R}}(X) = D - d$. The idea of compactifying extra dimensions is not new to string theory; it was introduced by Kaluza and Klein [158, 159] in an attempt to unify electromagnetism and general relativity into a common geometrical framework.

For brevity, we will content ourselves with illustrating some basic aspects of compactified theories through two simple five-dimensional examples, devoting only a few words to proper string compactifications at the end of the section. Beyond the material covered in standard textbooks [53–57], good resources providing a comprehensive treatment of (flux) compactifications are the reviews [109, 110, 160]. The two five-dimensional examples that we review are covered in [6].

2.1.2.1 Five-dimensional massless scalar

In flat five-dimensional Minkowski space $\mathbb{R}^{1,4}$ with coordinates $\{x^M\}_{M=0,\dots,4}$ a massless scalar field $\Phi(X^M)$ has an action

$$S_\Phi = \int_{\mathbb{R}^{1,4}} d^5x \left(-\frac{1}{2} \partial_M \Phi \partial^M \Phi \right). \quad (2.1.10)$$

Compactifying one of the dimensions on a circle S^1 of radius R amounts to considering instead the product manifold $\mathbb{R}^{1,3} \times S^1$. We use the coordinates $\{x^\mu\}_{\mu=0,\dots,3}$ for the external Minkowski space and x^4 for the internal circle. Performing a Fourier expansion we find

$$\Phi(x^\mu, x^4) \sim \Phi(x^\mu, x^4 + 2\pi R) \Rightarrow \Phi(x^\mu, x^4) = \sum_{k \in \mathbb{Z}} \phi_k(x^\mu) e^{\frac{ikx^4}{R}}. \quad (2.1.11)$$

Inserting this in S_Φ and performing the integral in x^4 we obtain the four-dimensional theory

$$S_{\phi_k} = (2\pi R) \int_{\mathbb{R}^{1,3}} d^4x \left(-\frac{1}{2} \partial_\mu \phi_0 \partial^\mu \phi_0 \right) - (2\pi R) \sum_{k=1}^{\infty} \int_{\mathbb{R}^{1,3}} d^4x \left(\partial_\mu \phi_k \partial^\mu \phi_{-k} + \frac{k^2}{R^2} \phi_k \phi_{-k} \right). \quad (2.1.12)$$

It corresponds to an infinite tower of scalar particles, known as Kaluza-Klein (KK) states, with masses

$$m_k^2 = \frac{k^2}{R^2}, \quad k \in \mathbb{Z}_{\geq 0}. \quad (2.1.13)$$

At energies $E \ll 1/R$ only the massless zero mode ϕ_0 is observable, making the extra dimension inaccessible at low-energies. Analogously, the additional dimensions of string theory might be unobservable if the volume of the internal space is small enough.

2.1.2.2 Five-dimensional Einstein gravity

Let us now examine the original Kaluza-Klein theory aimed at geometrizing electromagnetism. We start by considering the Einstein-Hilbert action in five-dimensions, given by

$$S_{5D} = \frac{M_{\text{Pl},5D}^3}{2} \int d^5x \sqrt{-G} R_{5D}. \quad (2.1.14)$$

Using the same notation as before, we compactify the theory on a circle. This leads to an expansion of the metric

$$G_{MN}(x^\mu, x^4) \sim G_{MN}(x^\mu, x^4 + 2\pi R) \Rightarrow G_{MN}(x^\mu, x^4) = \sum_{k \in \mathbb{Z}} G_{MN}^k(x^\mu) e^{\frac{ikx^4}{R}}. \quad (2.1.15)$$

At low energies, only the massless zero mode G_{MN}^0 will be observable. It can be written in the suggestive form

$$G_{MN}^0(x^\mu) = e^{\frac{\sigma}{3}} \left(\begin{array}{c|c} g_{\mu\nu}(x^\mu) + e^{-\sigma} A_\mu(x^\mu) A_\nu(x^\mu) & e^{-\sigma} A_\mu(x^\mu) \\ \hline e^{-\sigma} A_\mu(x^\mu) & e^{-\sigma} \end{array} \right), \quad (2.1.16)$$

leading to the four-dimensional action

$$S_{4D}^0 = M_{\text{Pl},5D}^3 \pi R \int d^4x \sqrt{-g} \left(R_{4D} - \frac{1}{6} \partial_\mu \sigma \partial^\mu \sigma - \frac{1}{4e^\sigma} F_{\mu\nu}^2 \right). \quad (2.1.17)$$

It contains a four-dimensional metric $g_{\mu\nu}$, a vector boson A_μ whose gauge transformations arise from the local reparametrizations of S^1 in the higher-dimensional theory, and a scalar field σ known as the radion.

The gauge coupling of the $U(1)$ gauge theory depends on σ , whose vacuum expectation value also sets the radius of the S^1 , as can be seen from the G_{44} component of the higher-dimensional metric. Hence, the radion is an example of a modulus field, i.e. a scalar field whose vacuum expectation value controls the lower-dimensional physics by parametrizing a deformation of the internal geometry. Finding mechanisms giving rise to a potential that fixes the vacuum expectation value of moduli, in a process known as moduli stabilization, is an important part of realistic string model building. The moduli space of this theory contains two infinite-distance limits, namely the decompactification limit $R \rightarrow \infty$ and the small volume limit $R \rightarrow 0$.

Finally, note that the lower-dimensional Planck mass is given by

$$M_{\text{Pl},4\text{D}}^2 = 16\pi^2 M_{\text{Pl},5\text{D}}^3 R, \quad (2.1.18)$$

showing that its value depends on the volume of the internal dimensions. If $R \rightarrow \infty$, then $M_{\text{Pl},4\text{D}} \rightarrow \infty$, illustrating the general fact that the internal space needs to be compact and of finite volume in order for gravity to not decouple in the lower-dimensional theory.

2.1.2.3 Calabi-Yau compactifications

The previous models, despite their simplicity, exemplify many features also present in the lower-dimensional theories arising from string compactifications: infinite-towers of Kaluza-Klein states (and winding towers in the presence of extended objects), moduli whose vacuum expectation values control details of the theory and must be fixed through moduli stabilization in realistic models, and a lower-dimensional Planck mass that can be different from the fundamental one.

Once we compactify supersymmetric theories, we also need to consider the amount of supersymmetry that is preserved in lower dimensions. Calabi-Yau varieties lead to lower-dimensional theories with the same number of copies of the supersymmetric algebra that were unbroken in the higher-dimensional Minkowski vacuum, making them a core element in the study of superstring theory.

Let us use the same conventions for the higher-dimensional, lower-dimensional, external and internal indices as above. Consider a compactification in which the only non-trivial background comes from the metric.¹ One can then check that the supersymmetric variations with parameter ϵ of a boson Φ , a gravitino ψ_M and a dilatino λ are

$$\langle \delta_\epsilon \Phi \rangle = 0, \quad (2.1.19)$$

$$\langle \delta_\epsilon \psi_M \rangle = \langle \nabla_M \epsilon + \dots \rangle = \langle \nabla_M \epsilon \rangle =: \bar{\nabla}_M \epsilon, \quad (2.1.20)$$

$$\langle \delta_\epsilon \lambda \rangle = 0. \quad (2.1.21)$$

Demanding for the supersymmetric variations to vanish leads to

$$\bar{\nabla}_M \epsilon = 0 \Rightarrow \bar{\nabla}_m \epsilon = 0 \quad \text{and} \quad \bar{\nabla}_\mu \epsilon = 0. \quad (2.1.22)$$

In other words, for some supersymmetry to be preserved in the lower-dimensional theory the internal manifold must have covariantly constant (Killing) spinors, which are singlets under its holonomy group \mathcal{H} .

For concreteness, let us examine how this restricts the internal geometry in four-dimensional compactifications of superstring theory. Six-dimensional oriented manifolds have holonomy

¹In compactifications of Type I and heterotic string theory, the Bianchi identities may enforce a non-trivial gauge background, see Section 6.4.1. The supersymmetric variations of the gaugini must then also be taken into account. Here, we neglect this aspect in order to maintain the discussion concise.

groups $\mathcal{H} \leq \mathrm{SO}(6)$, and no covariantly constant spinor exists for the generic case $\mathcal{H} = \mathrm{SO}(6)$. However, for manifolds with restricted holonomy group $\mathcal{H} = \mathrm{SU}(3) \leq \mathrm{SO}(6)$ the decomposition of the ten-dimensional spinors is

$$\begin{array}{ccccccc} \mathrm{SO}(10) & \longrightarrow & \mathrm{SO}(1,3) \times \mathrm{SO}(6) & \longrightarrow & \mathrm{SO}(1,3) \times \mathrm{SU}(3) \\ \mathbf{16} & & (\mathbf{2}, \mathbf{4}) + (\mathbf{2}', \overline{\mathbf{4}}) & & (\mathbf{2}, \mathbf{1}) + (\mathbf{2}', \mathbf{1}) + (\mathbf{2}, \mathbf{3}) + (\mathbf{2}', \overline{\mathbf{3}}) . \end{array} \quad (2.1.23)$$

This leads to the same number of gravitini in lower dimensions as there were originally in the higher-dimensional Minkowski vacuum. In other words, if we start from an $\mathcal{N} = 1$ or 2 theory in ten dimensions, the four-dimensional theory will have $\mathcal{N} = 1$ or 2 supersymmetry. This holds more generally for compactifications on internal spaces X of dimension $\dim_{\mathbb{C}}(X) = N$ and special holonomy $\mathcal{H} = \mathrm{SU}(N) \leq \mathrm{SO}(2N)$. If X has holonomy group $\mathcal{H} < \mathrm{SU}(N)$, the lower-dimensional theory has increased supersymmetry, e.g. Type II string theory compactified on $X = \mathrm{K3} \times T^2$, for which $\mathcal{H} = \mathrm{SU}(2)$, leads to $\mathcal{N} = 4$ supersymmetry in four dimensions.

The above considerations lead us to Calabi-Yau manifolds, see [161] for the bestiary.

Definition 2.1.1. A Calabi-Yau manifold X is a compact Kähler manifold with $c_1(X) = 0$.

An important result is Yau's theorem, which proves the Calabi conjecture.

Theorem 2.1.2 (Yau's theorem). *Let X be a compact Kähler manifold, J its Kähler form and $c_1(X)$ its first Chern class. Any closed real 2-form of type $(1,1)$ belonging to $2\pi c_1(X)$ is the Ricci form of one and only one Kähler metric in the class of J .*

This result is particularly relevant for Calabi-Yau manifolds — hence their name — for which it asserts that each Kähler class contains exactly one Ricci-flat metric. The theorem only establishes the existence of such a Ricci-flat metric, but is not constructive. In fact, for $\dim_{\mathbb{C}}(X) \geq 3$ not even a single example of the Ricci-flat metric of a strict Calabi-Yau manifold is known.² This is a major obstacle in string phenomenology: While a great deal can be learnt about the lower-dimensional theory simply from the topological properties of the internal Calabi-Yau space, complete knowledge of it requires the metric. However, one can employ numerical and machine learning methods to approximate the Ricci-flat metric [164].

Kähler manifolds X with $\dim_{\mathbb{C}}(X) = N$ have special holonomy $\mathcal{H} \leq \mathrm{U}(N)$. Additionally, the Ricci-flatness of Calabi-Yau manifolds implies the vanishing of the trace part of the connection, leading to $\mathcal{H} \leq \mathrm{SU}(N)$. Those Calabi-Yau manifolds with $\mathcal{H} = \mathrm{SU}(N)$ are called strict Calabi-Yau manifolds; we will often refer to these simply as Calabi-Yau manifolds, unless we specify otherwise.

One can prove that the following statements are equivalent for a compact Ricci-flat Kähler manifold X with $\dim_{\mathbb{C}}(X) = N$:

- There exists a unique holomorphic $(N,0)$ -form Ω .
- There exists a unique covariantly constant $(N,0)$ -form Ω .
- The canonical line bundle K_X is trivial.
- It has special holonomy $\mathcal{H} \leq \mathrm{SU}(N)$.

²For the case of K3 surfaces there was recent progress in [162, 163].

The Hodge numbers of simply connected Calabi-Yau manifolds are fairly constrained. Since we are considering manifolds with a single connected piece, we have $h^{3,3} = 1$. For any compact Kähler manifold the relations $h^{p,q} = h^{N-p,N-q}$ and $h^{p,q} = h^{q,p}$ hold, corresponding to Hodge star duality and complex conjugation, respectively. Considering simply connected manifolds leads, in turn, to $h^{1,0} = h^{0,1} = 0$. From the properties of Calabi-Yau manifolds enumerated above we read that $h^{3,0} = 1$. Finally, using Serre duality and Dolbeault's theorem it follows that $h^{p,0} = h^{N-p,0}$ and $h^{0,q} = h^{0,N-q}$.

Using all of these relations for Calabi-Yau threefolds leads to the Hodge diamond

$$\begin{array}{cccccccccc}
 & & h^{0,0} & & & & & & & 1 \\
 & h^{1,0} & & h^{0,1} & & & & & 0 & 0 \\
 h^{2,0} & & h^{1,1} & & h^{0,2} & & & 0 & h^{1,1} & 0 \\
 h^{3,0} & & h^{2,1} & & h^{1,2} & & h^{0,3} & \longrightarrow & 1 & h^{2,1} & h^{2,1} & 1 \\
 h^{3,1} & & h^{2,2} & & h^{1,3} & & & 0 & h^{1,1} & 0 \\
 h^{3,2} & & h^{2,3} & & & & & 0 & & 0 \\
 h^{3,3} & & & & & & & & & 1
 \end{array} \tag{2.1.24}$$

showing the two independent Hodge numbers $h^{1,1}$ and $h^{2,1}$. Consider the Kähler form J of a Calabi-Yau threefold. It can be expanded in a basis $\{\omega_a\}_{a=1,\dots,h^{1,1}}$ of $(1,1)$ -forms as

$$J = \sum_{a=1}^{h^{1,1}} v^a \omega_a. \tag{2.1.25}$$

Hence, $h^{1,1}$ counts the number of real parameters involved in the choice of Kähler class, which are known as Kähler moduli. If we are working in string theory, we can consider instead the complexified Kähler moduli by expanding the combination $B + iJ$, involving the Kalb-Ramond field B_2 , in the basis of $(1,1)$ -forms. The choice of complex structure I_k^l relates to the choice of a $(2,1)$ -form through the contraction $L_{ij\bar{k}} = \Omega_{ijl} I_k^l$ with the unique holomorphic $(3,0)$ -form Ω of the Calabi-Yau threefold. L can be expanded in a basis $\{\sigma_a\}_{a=1,\dots,h^{2,1}}$ of $(2,1)$ -forms

$$L = \sum_{a=1}^{h^{2,1}} z^a \sigma_a. \tag{2.1.26}$$

These $h^{2,1}$ complex parameters involved in the choice of complex structure are known as complex structure moduli. The moduli space \mathcal{M} of the Calabi-Yau threefold has $\dim_{\mathbb{R}}(X) = h^{1,1} + 2h^{2,1}$.

The Kähler and complex structure moduli of a Calabi-Yau threefold appear in the lower-dimensional theories arising from string compactifications as the scalar components of certain supergravity multiplets. The precise type of supermultiplet to which each of these types of moduli belongs depends on the theory under consideration and can change, e.g., upon going to the mirror dual frame, see Section 2.1.3.2.

2.1.3 The string duality web

The five superstring theories have fairly different properties in spacetime, stemming from their different worldsheet constructions. For example, Type IIA string theory is non-chiral, while

Type IIB is a chiral theory. Another dissimilarity is that $E_8 \times E_8$ heterotic string theory has an exceptional bulk gauge group, while exceptional gauge groups cannot be constructed in perturbative Type II string theories by stacking D-branes. Many more discrepancies can be found between the five superstrings.

Nonetheless, as emphasized already in Section 1.2.3, the five supersymmetric string theories are intimately connected to each other through a series of dualities. These form the string duality web, at the centre of which sits the conjectured M-theory, arising as the strong coupling limit of Type IIA string theory. The low-energy limit of M-theory is eleven-dimensional supergravity.³ A partial depiction of the string duality web connecting these theories was presented in Figure 1.4, with the relations to other string theories omitted for simplicity.

In what follows, we give a focused review of three links between string theories: T-duality, connecting Type IIA and Type IIB string theories compactified on tori; mirror symmetry, connecting their compactifications on Calabi-Yau threefolds; and the self-duality of Type IIB string theory, known as S-duality. These connections will play an important role in the remainder of this work, especially in Chapter 4.

2.1.3.1 T-duality

T-duality is short for target-space duality. It relates strings propagating through two different spacetimes which, however, describe the same physics. We will consider T-duality transformations connecting Type IIA and Type IIB string theory only, but it relates other corners of the string duality web too.

The simplest example of T-duality is obtained by compactifying string theory on a circle S^1 with radius R along its D -th dimension. Consider the CFT of the free boson X^{D-1} compactified on S^1 . Its torus partition function reads

$$\mathcal{Z}_{S^1}(\tau, \bar{\tau}) = \frac{1}{|\eta(\tau)|^2} \sum_{n,w \in \mathbb{Z}} q^{\frac{\alpha'}{4} \left(\frac{n}{R} + \frac{wR}{\alpha'} \right)^2} \bar{q}^{\frac{\alpha'}{4} \left(\frac{n}{R} - \frac{wR}{\alpha'} \right)^2}. \quad (2.1.27)$$

This expression fulfils

$$\mathcal{Z}_{S^1}(\tau, \bar{\tau}; R) = \mathcal{Z}_{S^1}(\tau, \bar{\tau}; \alpha'/R). \quad (2.1.28)$$

Hence, a closed string propagating on a circle cannot distinguish if its size is R or α'/R : they are T-dual to each other. In the torus partition function we sum over the KK and winding numbers; at the level of individual states (and including the contributions of the rest of the worldsheet CFT to the mass formula) we have instead

$$M^2 = \left(\frac{n}{R} \right)^2 + \left(\frac{wR}{\alpha'} \right)^2 + \frac{2}{\alpha'} (N_L + N_R - 2). \quad (2.1.29)$$

Hence, we must complement the radius transformation with an exchange of n and w , meaning that T-duality acts like

$$R \longleftrightarrow \frac{\alpha'}{R}, \quad n \longleftrightarrow w. \quad (2.1.30)$$

³Eleven-dimensional supergravity is sometimes also referred to as M-theory. Context usually makes it clear if the full all-encompassing theory or just its low-energy limit is meant by the term.

From the spacetime perspective, the T-duality transformation is a parity operation acting on the right-moving sector of the string, i.e.

$$X_L^{D-1} \mapsto X_L'^{D-1} = X_L^{D-1}, \quad (2.1.31a)$$

$$X_R^{D-1} \mapsto X_R'^{D-1} = -X_R^{D-1}, \quad (2.1.31b)$$

$$p_L^{D-1} \mapsto p_L'^{D-1} = p_L^{D-1}, \quad (2.1.31c)$$

$$p_R^{D-1} \mapsto p_R'^{D-1} = -p_R^{D-1}. \quad (2.1.31d)$$

This defines a new coordinate field

$$X'^{D-1} = X_L^{D-1} - X_R^{D-1} \quad (2.1.32)$$

with the same OPEs and energy momentum tensor as X^{D-1} , leading to the same physics written in terms of different fields. The relation between X^{D-1} and X'^{D-1} is non-local on the worldsheet.

In Type II string theory, we also need to consider how T-duality acts on the worldsheet fermions. By superconformal invariance, it is immediate to conclude that only the right moving fermion transformation

$$\psi_R^{D-1} \mapsto \psi_R'^{D-1} = -\psi_R^{D-1} \quad (2.1.33)$$

occurs. This changes the chirality of the right-moving R sector ground state, meaning that T-duality transforms Type IIA string theory into Type IIB and vice versa.

It is immediate to see that the coordinate transformations (2.1.31) exchange Neumann and Dirichlet boundary conditions

$$\partial_\sigma X^{D-1} = \partial_+ X_L^{D-1} - \partial_- X_R^{D-1} \mapsto \partial_+ X_L'^{D-1} + \partial_- X_R'^{D-1} = \partial_\tau X'^{D-1}, \quad (2.1.34)$$

turning a Dp -brane into a $D(p-1)$ -brane, if T-duality acts along a direction parallel to the brane, or into a $D(p+1)$ -brane, if the direction is transverse. The R-R forms change accordingly, giving the right set of BPS D-branes when going from Type IIA to Type IIB and in reverse.

Importantly, the string coupling also transforms under T-duality, such that measurements performed in the Planck units of the compactified theory remain invariant after the target space reinterpretation. The necessary change amounts to

$$g_s \mapsto g'_s = g_s \frac{\sqrt{\alpha'}}{R}. \quad (2.1.35)$$

The features just discussed generalize in the natural way to toroidal compactifications of string theory, where we can consider the torus to be a direct product of circles and employ the above rules for each internal direction separately. More generally, T-duality applies to string compactifications on a background with continuous isometries. For example, if we are considering an abelian isometry with Killing vector k^μ , we will have T-duality transformations as long as the non-linear σ -model for the chosen background is invariant under the diffeomorphism $X^\mu \mapsto X^\mu + k^\mu$. In this way, one can derive the general T-duality transformations for the string frame metric and the Kalb-Ramond field, which are known as Buscher rules.

The generalization to the relative case, i.e. to fiberwise T-duality, is more subtle. Consider for example a fiberwise T-duality along an elliptic fibration from Type IIB string theory on X to Type IIB on the T-dual space \tilde{X} . In this context, a BPS D-brane is a Π -stable object in the bounded derived category $D^b(X)$, or $D^b(\tilde{X})$, of the internal space. The fiberwise T-duality can be understood as a relative Fourier-Mukai transform between these categories. A review can be found in [165].

2.1.3.2 Mirror symmetry

The worldsheet theory of the bosonic string in conformal gauge is a CFT, with its conformal symmetry arising as a remnant of its reparametrization invariance. Similarly, the worldsheet theory of the superstring in superconformal gauge is an SCFT, with its superconformal invariance appearing as a leftover of the local supersymmetry. In compactifications of superstring theory, one can prove that the amount of surviving spacetime supersymmetry corresponds to the type of extended superconformal algebra in the worldsheet. In our specific case of interest, the four-dimensional $\mathcal{N} = 2$ supersymmetry preserved by compactifications of Type II string theory on Calabi-Yau threefolds implies that their worldsheet SCFT has $\mathcal{N} = (2, 2)$ superconformal symmetry [56].

An $\mathcal{N} = 1$ superconformal algebra has one fermionic partner $G(z)$ to the energy-momentum tensor $T(z)$. The action of $G_{-\frac{1}{2}}$ combines various primary fields⁴ into a super primary field, with two components. The extended $\mathcal{N} = 2$ superconformal algebra has instead two fermionic partners $G^\pm(z)$ to the energy-momentum tensor $T(z)$, leading through the action of $G_{-\frac{1}{2}}^\pm$ to super primary fields with four components. However, a new feature of the $\mathcal{N} = 2$ case is that there are also short supermultiplets consisting of super primary fields with only two components, arising from primary fields annihilated by either $G_{-\frac{1}{2}}^+$ or $G_{-\frac{1}{2}}^-$; these are called chiral and anti-chiral primary fields, respectively. They can be regarded as operator analogues of BPS states. One can prove that the OPE of two (anti-)chiral primary fields has no singular terms, allowing for the definition of a chiral and an anti-chiral ring per $\mathcal{N} = 2$ superconformal algebra [166].

The worldsheet $\mathcal{N} = (2, 2)$ superconformal symmetry of Type II string compactifications on Calabi-Yau threefolds means that, between the holomorphic and anti-holomorphic sectors of the theory (right- and left-moving sectors), we have a total of four chiral rings

$$(c, c), \quad (a, a), \quad (a, c), \quad (c, a). \quad (2.1.36)$$

The rings (c, c) and (a, a) , as well as (a, c) and (c, a) , are complex conjugate and isomorphic pairs. This leaves us with only two independent chiral rings, which can be taken to be (c, c) and (a, c) . From the perspective of the SCFT, the choice of which states we call (c, c) and which (a, c) is arbitrary, corresponding to the choice of relative sign between the right- and left-moving U(1) currents of the $\mathcal{N} = 2$ superconformal algebra. Altering the choice amounts to applying an outer automorphism of the algebra.

Chiral primary fields comprise the internal part of the vertex operators of massless NS-NS scalars in Type II string theory. Applying spacetime supersymmetry transformation to them, they can be completed into supermultiplets of the four-dimensional $\mathcal{N} = 2$ supersymmetry. The vertex operators corresponding to the components of these spacetime supermultiplets involve, in addition, NS-R, R-NS and R-R fields, which at the level of the SCFT arise through spectral flow from the NS-NS chiral primary fields. The analysis leads to the identification

$$\begin{aligned} \text{Type IIA} \left\{ \begin{array}{l} \text{K\"ahler moduli} \subset \text{vector multiplets} \longleftrightarrow (a, c) + (c, a) \text{ chiral ring,} \\ \text{complex structure moduli} \subset \text{hypermultiplets} \longleftrightarrow (c, c) + (a, a) \text{ chiral ring,} \end{array} \right. \\ \text{Type IIB} \left\{ \begin{array}{l} \text{K\"ahler moduli} \subset \text{hypermultiplets} \longleftrightarrow (a, c) + (c, a) \text{ chiral ring,} \\ \text{complex structure moduli} \subset \text{vector multiplets} \longleftrightarrow (c, c) + (a, a) \text{ chiral ring.} \end{array} \right. \end{aligned}$$

⁴We employ the operator-state correspondence and do not carefully distinguish between the two notions.

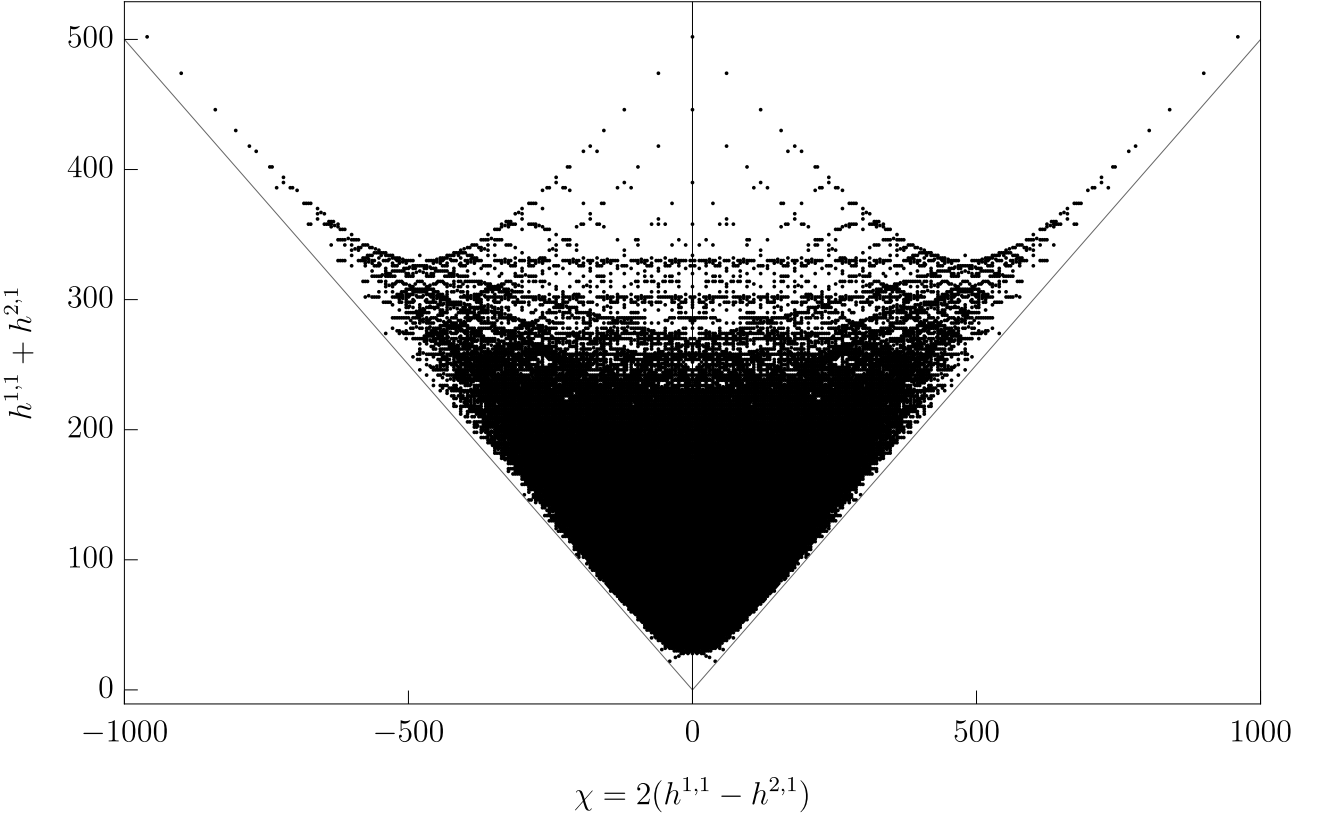


Figure 2.1: Plot produced using the distinct Hodge pairs $(h^{1,1}, h^{2,1})$ from the Kreuzer-Skarke list of four-dimensional reflexive polyhedra [124].

The outer automorphism of the superconformal algebra exchanging which fields are labelled as (c, c) and which as (a, c) may be trivial from the worldsheet SCFT point of view, but has radical consequences for the spacetime interpretation of the theory. It swaps a four-dimensional Type IIA compactification on a Calabi-Yau threefold for a Type IIB one, exchanging the Kähler and complex structure moduli in the process. This suggests that Calabi-Yau threefolds might exist in mirror pairs X and Y with

$$(h^{1,1}, h^{2,1})_X = (h^{2,1}, h^{1,1})_Y. \quad (2.1.37)$$

A compactification of Type IIA string theory on X is said to be mirror dual to Type IIB on Y , both leading to the same worldsheet SCFT and four-dimensional physics.

Constructing large sets of Calabi-Yau threefolds and plotting their Hodge numbers shows that, indeed, they do come in mirror pairs. In Figure 2.1 we plot the 30,108 different Hodge pairs $(h^{1,1}, h^{2,1})$ arising from the classification of four-dimensional reflexive polyhedra carried out by Kreuzer and Skarke [124]. The symmetry along the central vertical line, corresponding to the exchange $h^{1,1} \leftrightarrow h^{2,1}$, is immediately obvious. For an account of mirror symmetry from both a physics and mathematics perspective see [167].

As long as the four-dimensional $\mathcal{N} = 2$ supersymmetry of Type II compactifications on Calabi-Yau threefolds is not broken by the addition of further objects, the moduli have no potential and the kinetic terms of vector multiplets and hypermultiplets do not mix. Hence, the moduli space $\mathcal{M}_{\text{IIA/B}}$ is a direct product of these two moduli spaces, i.e.

$$\mathcal{M}_{\text{IIA/B}} = \mathcal{M}_{\text{VM}}^{\text{IIA/B}} \times \mathcal{M}_{\text{HM}}^{\text{IIA/B}}. \quad (2.1.38)$$

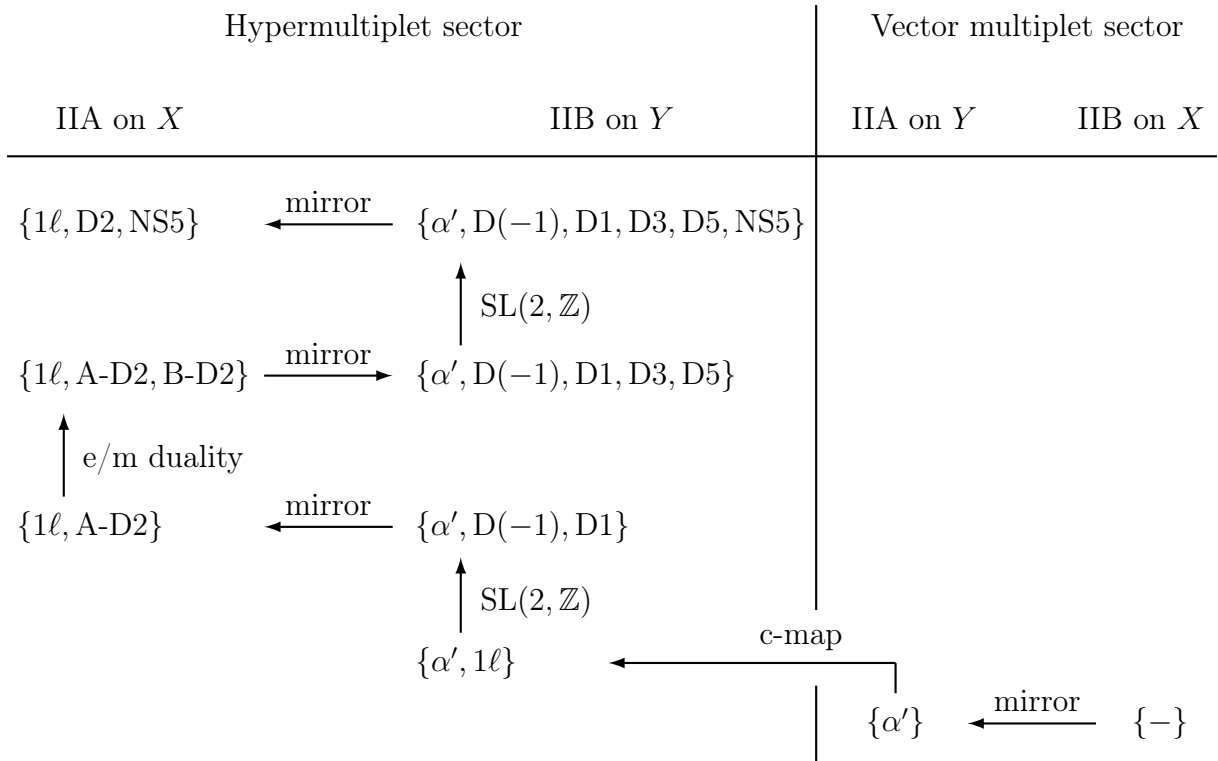


Figure 2.2: Prospective chain of dualities for determining the full quantum-corrected low-energy effective actions of a four-dimensional Type II mirror pair. Figure adapted from [170].

$\mathcal{M}_{\text{VM}}^{\text{IIA/B}}$ is a special Kähler manifold, while $\mathcal{M}_{\text{HM}}^{\text{IIA/B}}$ is a quaternion-Kähler manifold. The hypermultiplet moduli space is not affected by circle reduction, which allows one to formally identify the hypermultiplet moduli spaces of four-dimensional Type IIA/B string theory, five-dimensional M-theory and six-dimensional F-theory, a fact that we will exploit in Chapter 4.

Importantly, the types of quantum corrections received by $\mathcal{M}_{\text{VM}}^{\text{IIA}}$, $\mathcal{M}_{\text{VM}}^{\text{IIB}}$, $\mathcal{M}_{\text{HM}}^{\text{IIA}}$ and $\mathcal{M}_{\text{HM}}^{\text{IIB}}$ differ from each other. This means that, if we know the mirror map, i.e. the map allowing us to identify objects between two mirror pairs, we can translate some quantum corrections into another. The celebrated counting of rational curves for the quintic (the computation of its Gromov-Witten invariants) [86], exploited this fact: $\mathcal{M}_{\text{VM}}^{\text{IIB}}$ is classically exact, while $\mathcal{M}_{\text{VM}}^{\text{IIA}}$ does receive α' -corrections from worldsheet instantons. Mirror symmetry allows us to obtain quantum corrected volumes on the Type IIA side from the computation of period integrals on the Type IIB side. The number of rational curves can be then extracted from the sum over worldsheet instanton corrections. Understanding the quantum corrections to the hypermultiplet moduli space is much more complicated, see [168, 169] for reviews. The prospective chain of dualities from which the full set of corrections could be extracted is shown in Figure 2.2. The quantum-corrected hypermultiplet moduli space metric can be explicitly obtained in those situations in which only mutually local D-instantons contribute, see Section 4.4.3.

Strominger, Yau, and Zaslow proposed a way to understand mirror symmetry as a form of T-duality, in what is now known as the SYZ conjecture [171]. Following [172], the SYZ conjecture claims that for any mirror pair of compact simply connected Calabi-Yau threefolds X and Y there exist T^3 -fibrations of X and Y such that their non-singular fibers are special Lagrangian submanifolds and in the large volume/complex structure limit of X/Y the two fibrations are

T-dual to each other. The mathematical study of the SYZ conjecture is a rich topic of research, see, e.g., the review [173]. We will make use of this approach to mirror symmetry in Chapter 4.

2.1.3.3 S-duality

The classical low-energy effective action of Type IIB string theory corresponds to Type IIB supergravity. Written in Einstein frame, see (2.1.8) above, it is manifestly invariant under an $\text{SL}(2, \mathbb{R})$ symmetry acting on the fields like

$$G_E \mapsto G_E, \quad \tau \mapsto \frac{a\tau + b}{c\tau + d}, \quad \begin{pmatrix} C_2 \\ B_2 \end{pmatrix} \mapsto M \begin{pmatrix} C_2 \\ B_2 \end{pmatrix}, \quad C_4 \mapsto C_4, \quad (2.1.39)$$

for a group element

$$M = \begin{pmatrix} a & b \\ c & d \end{pmatrix} \in \text{SL}(2, \mathbb{R}). \quad (2.1.40)$$

Going beyond supergravity to string theory, the above $\text{SL}(2, \mathbb{R})$ symmetry must be broken into a subgroup; $\text{SL}(2, \mathbb{R})$ contains transformations that violate charge quantization for B_2 and C_2 , an example of which is

$$M = \begin{pmatrix} 1 & 0 \\ 0 & d \end{pmatrix}, \quad d \in \mathbb{R} \setminus \mathbb{Z}. \quad (2.1.41)$$

The maximal subgroup of $\text{SL}(2, \mathbb{R})$ avoiding this issue is $\text{SL}(2, \mathbb{Z})$, which is conjectured to be preserved in full non-perturbative Type IIB. Another way to see that the supergravity $\text{SL}(2, \mathbb{R})$ symmetry needs to be reduced to a subgroup in string theory involves the D-instantons. Their classical action is $S_{D(-1)} = 2\pi\tau$, meaning that their contribution to the path integral breaks the shift symmetry of τ down to integer shifts.

$\text{SL}(2, \mathbb{Z})$ is a reasonable proposal for the symmetry group of non-perturbative Type IIB string theory; as mentioned, it is the part of the classical symmetry surviving all known non-perturbative effects. However, due to the strong-weak coupling nature of some of its transformations, it is difficult to prove this from the perspective of perturbative Type IIB. A perturbative analysis only reveals the T generator of $\text{SL}(2, \mathbb{Z})$: C_0 enters physical quantities through its field strength $F_1 = dC_1$, invariant under a continuous shift symmetry that is broken down to the T transformation by D-instantons, as explained above. This makes sense from the point of view of the non-perturbative symmetry: We are performing an analysis at weak coupling, and hence can only see those elements of $\text{SL}(2, \mathbb{Z})$ that fix the cusp at infinity in the fundamental domain \mathcal{F} of τ . This corresponds to the parabolic subgroup $P_{i\infty} \subset \text{SL}(2, \mathbb{Z})$ of the full duality group, consisting of the elements

$$P_{i\infty} := \left\{ \pm \begin{pmatrix} 1 & b \\ 0 & 1 \end{pmatrix} \mid b \in \mathbb{Z} \right\}. \quad (2.1.42)$$

The T transformation is contained in $P_{i\infty}$, hence appearing already in perturbative Type IIB string theory. We will motivate the full $\text{SL}(2, \mathbb{Z})$ duality group from M-theory in Section 2.1.5.

It is worth mentioning that we have only focused on the bosonic sector of Type IIB string theory. If the fermions are also taken into account, the duality corresponds to the metaplectic group $\text{Mp}(2, \mathbb{Z})$ instead, arising as the metaplectic cover of $\text{SL}(2, \mathbb{Z})$ [174, 175]. Furthermore, including also the Type IIB worldsheet orientation reversal operation and the left-moving spacetime fermion parity transformations, the full duality group is $\text{Pin}^+(\text{GL}(2, \mathbb{Z}))$ [175]. In what follows we will only be concerned with the $\text{SL}(2, \mathbb{Z})$ -duality of Type IIB, but considering

the full duality group in conjunction with the Cobordism Conjecture (see Section 3.2.1), has led to the prediction of novel objects in string theory [176–178].

The term S-duality is sometimes used in a more restricted sense, referring exclusively to the strong-weak coupling transformation

$$S = \begin{pmatrix} 0 & 1 \\ -1 & 0 \end{pmatrix} \in \mathrm{SL}(2, \mathbb{Z}). \quad (2.1.43)$$

The existence of this element within the duality group of Type IIB makes its strong coupling behaviour very distinct from the one of Type IIA: Type IIB goes back to itself in the strong coupling limit (emergent string limit), while Type IIA grows an additional dimension at strong coupling (decompactification limit). These are the two types of infinite-distance limits in moduli space allowed by the Emergent String Conjecture, see Section 3.4. That these two strong coupling regimes are so diametrically opposed to each other does not subtract from the equivalence of the theories under T-duality. In fact, it is perfectly consistent with it, as we will see in Section 2.1.5.

2.1.4 D7-branes and $\mathrm{SL}(2, \mathbb{Z})$ -duality

Low-codimension objects produce strong backreactions in the spacetime in which they live, modifying the asymptotic structure of the vacuum. This can be heuristically motivated with an analogy to electromagnetism. The electric field is given by the solutions to Gauss's law

$$\nabla \cdot \vec{E} = \rho, \quad (2.1.44)$$

which leads to Poisson's equation for the electric potential V . Solving for the electric field of a point particle with charge q located at the origin of spacetime in $D = 1 + d$ dimensions leads to

$$E(r) = \frac{\Gamma\left(\frac{d}{2}\right)}{2\pi^{d/2}} \frac{q}{r^{d-1}}. \quad (2.1.45)$$

The radial dependence stems from the dimensionality of the sphere necessary to enclose the point particle and measure its flux, which depends on the codimension of the particle in the chosen spacetime. When $d = 2$ we have

$$E(r) \sim \frac{1}{r} \Rightarrow V(r) \sim -\log(r), \quad (2.1.46)$$

meaning that the potential does not decay at infinity. The same analysis applies in the transverse space to higher-dimensional objects, meaning that codimension-two objects lead to logarithmic potentials for any field profile dependent on the flux measured by an enclosing volume, their gravitational field being an example.

This also holds for D-branes in Type II string theory, and can already be seen working at the level of supergravity. BPS Dp -branes correspond in the classical low-energy approximation to supergravity black brane solutions. Denoting by r_\perp the radial direction in the transverse space to a stack of N Dp -branes, one can check that when $p \leq 6$ the corresponding supergravity solution develops a throat for $r_\perp \ll 1$, but asymptotes to Minkowski spacetime $\mathbb{R}^{1,9}$ for $r_\perp \gg 1$. Considering D7-branes instead, which are codimension-two BPS objects present in Type IIB, leads to a supergravity description with no asymptotically flat spacetime. This means that their effects on the geometry cannot be approximately ignored far away from their location, unlike for higher-codimension D-branes.

The special nature of D7-brane solutions in Type IIB string theory motivates the introduction of F-theory, and is therefore worth discussing in some detail; we do so following [57]. A D7-brane has a $(1+7)$ -dimensional worldvolume, leaving a transverse plane on which we define the complex coordinate z centred at the location of the D7-brane. Since the brane has a tension, it sources a gravitational field. From the point of view of the z -plane, the problem corresponds to that of a particle of mass m located at the origin of an otherwise empty $(1+2)$ -dimensional spacetime. Einstein's equations away from the D7-brane are $R_{\mu\nu} = 0$, leading to a flat conical spacetime that notices the presence of the D7-brane globally through a deficit angle $\Delta\varphi = m\kappa^2$, where κ is the three-dimensional gravitational coupling constant. Moreover, the D7-brane is a magnetic source for C_0 , which from the preceding discussion we expect to asymptotically vary like $C_0 \sim \frac{1}{2\pi i} \log(z)$ for $|z| \ll 1$. Note that the D7-brane preserves 16 supercharges, which constrains the axio-dilaton $\tau = C_0 + ie^{-\phi}$ to be holomorphic, i.e. $\bar{\partial}\tau(z, \bar{z}) = 0$ away from the location of the brane.

The above discussion motivates the Ansatz metric

$$ds^2 = -dt^2 + \sum_{i=1}^7 dx_i^2 + e^{B(z, \bar{z})} dz d\bar{z}. \quad (2.1.47)$$

The equation of motion for τ is derived from the low-energy effective action for Type IIB in Einstein frame (2.1.8), yielding

$$\partial\bar{\partial}\tau + \frac{2\partial\tau\bar{\partial}\tau}{\bar{\tau} - \tau} = 0, \quad (2.1.48)$$

which is indeed solved by holomorphic functions $\bar{\partial}\tau(z, \bar{z}) = 0$. Using the holomorphicity of τ , one can compute the energy density associated to its kinetic term in (2.1.8). This naively results in an infinite value, but is actually finite if one invokes the $SL(2, \mathbb{Z})$ symmetry of Type IIB string theory, which has a compatible $PSL(2, \mathbb{Z})$ action on τ , allowing us to restrict the integration domain to the fundamental domain \mathcal{F} of τ . Making sense of the D7-brane solution therefore requires the use of the non-perturbative $SL(2, \mathbb{Z})$ duality of the theory.

Since τ has branch cuts and is not single valued, its relation with z is more conveniently captured through an injective holomorphic function mapping $\tau \in \mathcal{F}$ to $z \in \mathbb{C} \cup \infty \simeq \mathbb{P}^1$ and automorphic under $SL(2, \mathbb{Z})$, such that it can lead to well-defined expressions [179]

$$j(\tau(z)) = g(z), \quad (2.1.49)$$

where $g(z)$ is a quotient of polynomials. This singles out the j -function

$$\begin{aligned} j : \mathcal{F} &\longrightarrow \mathbb{P}^1 \\ \tau &\longmapsto j(\tau), \end{aligned} \quad (2.1.50)$$

which is the unique modular form of weight zero. It has an expansion

$$j(\tau) = e^{-2\pi i\tau} + 744 + 196884e^{2\pi i\tau} + \dots. \quad (2.1.51)$$

The solution

$$j(\tau) = z \quad (2.1.52)$$

leads to

$$\tau(z) \sim \frac{1}{2\pi i} \log(z) \quad (2.1.53)$$

for $|z| \ll 1$, which is the expected logarithmic behaviour for a single D7-brane at the origin of the z -plane. By, in addition, solving for $B(z, \bar{z})$ and performing a change of variables, the metric in the transverse space can be brought to the form

$$ds^2 = d\rho^2 + \rho^2 d\theta^2, \quad \theta \in \left[0, 2\pi - \frac{\pi}{6}\right]. \quad (2.1.54)$$

Summarizing the preceding discussion, a single D7-brane in Type IIB string theory produces a deficit angle of $\pi/6$ in the transverse space and gives rise to a monodromy $\tau \mapsto \tau + 1$ upon circling once around its position. This is an $SL(2, \mathbb{Z})$ transformation contained in the parabolic subgroup $P_{i\infty}$, as we would expect for the 7-branes on which the perturbative fundamental string ends. Placing 24 parallel D7-branes leads to a deficit angle of 4π , corresponding to a sphere; the transverse space acquires compact \mathbb{P}^1 topology. This will be generalized and clarified in F-theory, the subject of Section 2.2.

2.1.5 Geometrizing $SL(2, \mathbb{Z})$ -duality

Before we move on to F-theory, it will be useful to revisit the $SL(2, \mathbb{Z})$ -duality of Type IIB, discussed in Section 2.1.3.3. As we have just seen, using this self-duality is crucial in the analysis of D7-brane solutions.

From the point of view of perturbative Type IIB string theory we can only access the T generator of $SL(2, \mathbb{Z})$. The full duality group is motivated by the fact that it is the biggest subgroup of the $SL(2, \mathbb{R})$ symmetry of the Type IIB supergravity action compatible with charge quantization and the coupling with D-instantons. This self-duality is much less mysterious if one arrives at it from an indirect route, namely starting from M-theory.

M-theory arises as the strong coupling limit of Type IIA string theory, with the eleventh dimension corresponding to a circle S_A^1 of radius

$$R_A = g_{\text{IIA}} \sqrt{\alpha'}, \quad (2.1.55)$$

which decompactifies when $g_{\text{IIA}} \rightarrow \infty$.

We also know from Section 2.1.3.1 that the result of compactifying Type IIA on a circle S_B^1 with radius R_B is T-dual to Type IIB, with the string couplings related by the Buscher rules

$$g_{\text{IIB}} = g_{\text{IIA}} \frac{\sqrt{\alpha'}}{R_B} = \frac{R_A}{R_B}. \quad (2.1.56)$$

Ten-dimensional Type IIB arises from the Type IIA perspective in the limit $R_B \rightarrow 0$. To keep the Type IIB coupling fixed, we also need to maintain $R_A/R_B \sim \text{const.}$ along the limit.

Putting these two facts together, we start from M-theory compactified on $T^2 = S_A^1 \times S_B^1$. In the absence of a twist angle $\theta = 2\pi \text{Re}(\tau)$, the modular parameter of the M-theory torus is simply $\tau = iR_B/R_A$. The ten-dimensional Type IIB limit corresponds to

$$\mathcal{V}_{T^2} = R_A R_B \rightarrow 0, \quad \text{Im}(\tau) = 1/g_{\text{IIB}} \sim \text{const.} \quad (2.1.57)$$

This duality can also be established for non-rectangular tori, in which case the Type IIB axion is identified with $\text{Re}(\tau) = C_0$. Altogether, ten-dimensional Type IIB string theory arises as the vanishing volume limit of M-theory on T^2 at fixed complex structure; the modular parameter τ of the M-theory torus is identified with the Type IIB axio-dilaton.

This explains the observed non-perturbative $SL(2, \mathbb{Z})$ -duality of Type IIB. The modular parameter τ of the M-theory torus is defined in the (compactified) upper half-plane $\overline{\mathcal{H}}$, on

which the modular group⁵ $\text{PSL}(2, \mathbb{Z})$ acts connecting those values of τ that lead to the same complex structure. This action is compatible with the one of $\text{SL}(2, \mathbb{Z})$ on the torus lattice, which is the one giving the non-perturbative duality group of Type IIB. In other words, the $\text{SL}(2, \mathbb{Z})$ -duality of Type IIB is simply the invariance of the T^2 -compactification of M-theory under the transformations given by the mapping class group of T^2 , defined as the quotient of all its orientation-preserving diffeomorphisms by the group of diffeomorphisms isotopic to the identity [180]

$$\text{MCG}(T^2) := \text{Diff}^+(T^2)/\text{Diff}_0(T^2) \cong \text{SL}(2, \mathbb{Z}). \quad (2.1.58)$$

In the M-theory/Type IIB duality, the F1-string arises from the M2-brane wrapped on S_A^1 and the D1-string from the M2-brane wrapped on S_B^1 , with the B_2 and C_2 R-R forms stemming from the corresponding circle reductions of the C_3 form of M-theory. Even though the difference between the modular and the mapping class groups of the torus cannot be seen at the level of the axio-dilaton, the additional element of the mapping class group

$$M = \begin{pmatrix} -1 & 0 \\ 0 & -1 \end{pmatrix} \quad (2.1.59)$$

has the physical effect of flipping the charges of the F1- and D1-string. In M-theory, this corresponds to flipping the orientation of the two 1-cycles of the torus T^2 , which preserves its overall orientation. This additional element is important for F-theory to describe all relevant 7-branes, see Section 2.2.2.

The strong-weak coupling transformation $S \in \text{SL}(2, \mathbb{Z})$ acquires a very natural meaning in this geometrized understanding of S-duality: It amounts to a reinterpretation of which S^1 factor of T^2 we regard as the Type IIA circle S_A^1 and which one as the Type IIB circle S_B^1 , exchanging the F1- and D1-strings accordingly.

2.2 F-theory

F-theory is the most powerful approach to the study of the geometric, large radius regime of string theory to date, incorporating non-perturbative effects in the string coupling g_s . Through the dictionary between geometry and physics that it establishes, it allows for the geometrization of physical problems. In this way, questions about physics can be formulated as precise mathematical statements, which can then be understood in the context of algebraic geometry. Similarly, physical insight can result in mathematical conjectures. F-theory combines features characteristic of different perturbative corners of string theory, e.g., gauge groups localized on stacks of 7-branes (as in Type II) that can be of exceptional type (like in heterotic). This makes F-theory fertile soil for studies of string phenomenology too.

Primed by the brief discussion of S-duality and D7-branes carried out in Section 2.1, we review below the basic concepts of F-theory. The aim is only to illustrate the core notions that will be subjacent to the analyses of Chapters 5 and 6, offering a glimpse into the nature of the subject in the process. More thorough treatments of F-theory can be found in the reviews [181–183], while a very focused introduction to the subject is given in [184]. The most recent and comprehensive review of F-theory is [185], which is the main source for our exposition below. F-theory was originally proposed in [89] and further refined in [186, 187].

⁵The nomenclature *modular group* can refer to $\text{PSL}(2, \mathbb{Z})$ or $\text{SL}(2, \mathbb{Z})$, depending on the source.

2.2.1 $[p, q]$ 7-branes and general monodromy action

D7-branes arise in perturbative Type IIB string theory as the 7-branes on which the F1-strings can end. Circling around a D7-brane induces, as we saw in Section 2.1.4, the monodromy action $\tau \mapsto \tau + 1$. For consistency, it must also affect the B_2 and C_2 forms in the way specified by the $\text{SL}(2, \mathbb{Z})$ -duality transformation (2.1.40). In other words, circling around the D7-brane has the same effect as performing the $\text{SL}(2, \mathbb{Z})$ -duality transformation

$$M_{[1,0]} = \begin{pmatrix} 1 & 1 \\ 0 & 1 \end{pmatrix} \in \text{SL}(2, \mathbb{Z}). \quad (2.2.1)$$

Let us refer to the F1-string as $(1, 0)$ string and to the D7-brane as $[1, 0]$ 7-brane. In Type IIB we also have D1-strings, which in this notation would correspond to $(0, 1)$ strings. For p and q coprime, there exist supersymmetric bound states of p F1-strings and q D1-strings, which are denoted (p, q) strings and couple to $pB_2 + qC_2$. Their tension in string frame is

$$\tau_{(p,q)} = |p + \tau q| \frac{1}{2\pi\alpha'}, \quad (2.2.2)$$

picking up a factor of $1/g_{\text{IIB}}$ in Einstein frame. These are heavy objects in perturbative Type IIB string theory, with their endpoints living in $[p, q]$ 7-branes. Starting from a $(1, 0)$ string and computing the transformation $g_{[p,q]} \in \text{SL}(2, \mathbb{Z})$ taking us to the duality frame in which it maps to the (p, q) string, we also obtain the monodromy induced by $[p, q]$ 7-branes⁶

$$M_{[p,q]} = g_{[p,q]} M_{[1,0]} g_{[p,q]}^{-1} = \begin{pmatrix} 1 + pq & p^2 \\ -q^2 & 1 - pq \end{pmatrix} \in \text{SL}(2, \mathbb{Z}). \quad (2.2.3)$$

This goes beyond perturbative Type IIB, since it includes transformations not contained in the parabolic subgroup $P_{i\infty} \leq \text{SL}(2, \mathbb{Z})$.

An isolated $[p, q]$ 7-brane is not truly different from a D7-brane, since we can always perform an $\text{SL}(2, \mathbb{Z})$ transformation to a duality frame in which it corresponds to the $[1, 0]$ 7-brane. This is no longer true once we have a collection of $[p, q]$ 7-branes of different types. While any individual 7-brane can be locally regarded as a D7-brane, it may occur that this cannot be done simultaneously for the whole set of 7-branes, in which case they are said to be *mutually non-local*; it is these configurations of 7-branes that go beyond perturbative Type IIB.

Let us consider a Type IIB compactification in the presence of 7-branes on an internal space that we will denote B_n , with $\dim_{\mathbb{C}}(B_n) = n$, preserving the maximal possible amount of supersymmetry. The Type IIB axio-dilaton τ holomorphically varies over B_n due to the profile sourced by the 7-branes. However, as seen above, it is not well-defined globally; rather, one must use the $\text{SL}(2, \mathbb{Z})$ -duality in order to patch the local definitions. This is true for the Type IIB fields more generally: They can be defined as local functions in an open cover $\{U_\alpha\}_{\alpha \in A}$, with each U_α corresponding to a particular $\text{SL}(2, \mathbb{Z})$ duality frame. On the overlaps $U_\alpha \cap U_\beta$, the fields are transformed from one frame to another by the action of an element of $\text{SL}(2, \mathbb{Z})$. The transition functions can then be used to define a holomorphic line bundle \mathcal{L} over B_n . A choice of sections of \mathcal{L}^4 and \mathcal{L}^6 uniquely determines an elliptic fibration $\pi_{\text{ell}} : Y_{n+1} \rightarrow B_n$, as we will soon motivate. Furthermore, one can check that the Type IIB equations of motion imply that the aforementioned elliptic variety must be Calabi-Yau.

The picture that arises is that of a twelve-dimensional theory compactified on an elliptic fibration over B_n , with the varying complex structure τ of the elliptic fiber corresponding to

⁶The form of $M_{[p,q]}$ depends on the chosen conventions; here we follow the ones in [185].

the Type IIB axio-dilaton profile and the rest of Type IIB fields defined in a compatible way: this is the celebrated F-theory. Note, however, that the two additional dimensions are not to be thought of as conventional spacetime dimensions. In the ten-dimensional theory there is no scalar field associated with the volume of the elliptic fiber, nor is there a limit of its parameters in which the spectrum becomes that of a theory in twelve non-compact dimensions. From the Type IIB perspective, F-theory is better regarded as a convenient way to package the information describing non-perturbative strongly backreacted Type IIB ten-dimensional solutions in terms of auxiliary twelve-dimensional geometries, thereby making them amenable to analysis in the powerful language of algebraic geometry.

2.2.2 Elliptic fibrations and Weierstrass models

It is clear at this point that elliptic fibrations play a central role in F-theory. Let us devote a few paragraphs to the review of Weierstrass models, a useful form of explicitly describing elliptic fibrations, and the way in which they encapsulate information about the $[p, q]$ 7-branes of F-theory compactifications.

An elliptic curve is a genus-one curve with a marked point. Analogously, an elliptic fibration is a genus-one fibration with a rational section, meaning that the marked point of the fibers can be consistently chosen. F-theory can be studied on genus-one fibrations without a rational section [188], which will make a brief appearance in Appendix B.13, but we will mostly be concerned with F-theory compactifications on elliptic fibrations. All elliptic fibrations are birationally equivalent to a Weierstrass model, which is the presentation on which we therefore focus.

Consider the weighted projective space \mathbb{P}_{231} with homogeneous coordinates $[x : y : z]$. Since genus-one curves are the only compact Calabi-Yau curves, they must correspond to the hypersurfaces $\mathbb{P}_{231}[6]$. The most generic hypersurface of this type is given by

$$\{y^2 + a_1xyz + a_3yz^3 = x^3 + a_2x^2z^2 + a_4xz^4 + a_6z^6\}_{\mathbb{P}_{231}}, \quad a_i \in \mathbb{C}, \quad (2.2.4)$$

where the coefficients of y^2 and x^3 have been rescaled to one. This is the long Weierstrass form. Since the field $K = \mathbb{C}$ over which we are working has $\text{char}(K) \neq 2, 3$ the square on y and the cube on x can be completed to yield the Weierstrass form

$$\{y^2 = x^3 + fxz^4 + gz^6\}_{\mathbb{P}_{231}}, \quad f, g \in \mathbb{C}. \quad (2.2.5)$$

Altering the parameters f and g deforms the elliptic curve. In order to obtain an elliptic fibration over a base B_n , we need to allow f and g to vary over it.

Choose a holomorphic line bundle \mathcal{L} over B_n and construct the ambient \mathbb{P}_{231} -bundle over B_n given by

$$\mathbb{P}_{231}(\mathcal{E}) := \mathbb{P}_{231}(\mathcal{L}^2 \oplus \mathcal{L}^3 \oplus \mathcal{O}). \quad (2.2.6)$$

Assume that \mathcal{L} is effective and pick two global holomorphic sections

$$f \in \Gamma(B_n, \mathcal{L}^4), \quad g \in \Gamma(B_n, \mathcal{L}^6). \quad (2.2.7)$$

The hypersurface

$$Y_{n+1} := \{y^2 = x^3 + fxz^4 + gz^6\}_{\mathbb{P}_{231}(\mathcal{E})} \quad (2.2.8)$$

is a Weierstrass model describing the elliptic fibration

$$\begin{array}{ccc} \mathcal{E} & \longrightarrow & Y_{n+1} \\ & & \downarrow \pi_{\text{ell}} \\ & & B_n. \end{array} \quad (2.2.9)$$

It has a holomorphic section given by the divisor

$$S_0 := \{z = 0\}_{\mathbb{P}_{231}(\mathcal{E})} \cap Y_{n+1}. \quad (2.2.10)$$

Computing the first Chern class of Y_{n+1} leads to the Calabi-Yau condition

$$c_1(Y_{n+1}) = c_1(B_n) - c_1(\mathcal{L}) = 0 \Rightarrow c_1(\mathcal{L}) = c_1(B_n). \quad (2.2.11)$$

The map⁷

$$c_1 : \text{Pic}(B_n) \cong H^1(B_n, \mathcal{O}^*) \longrightarrow H^2(B_n, \mathbb{Z}) \quad (2.2.12)$$

is injective when $h^{0,1}(B_n) = 0$, which is the case for the simply connected spaces that we consider. Hence, we conclude that the Calabi-Yau condition implies

$$c_1(\mathcal{L}) = c_1(B_n) = c_1(\overline{K}_{B_n}) \Rightarrow \mathcal{L} = \overline{K}_{B_n}, \quad (2.2.13)$$

where \overline{K}_{B_n} denotes the anticanonical class of B_n .

The elliptic curve (2.2.5) becomes singular when the discriminant

$$\Delta := 4f^3 + 27g^2 \quad (2.2.14)$$

vanishes. This applies to the Weierstrass model (2.2.8) too, with

$$\Delta \in \Gamma(B_n, \mathcal{L}^{12}) \quad (2.2.15)$$

defining the discriminant divisor in B_n , which hence corresponds to the locus over which the elliptic fiber becomes singular. The relation between the defining polynomials f and g of a Weierstrass model and the complex structure of the fiber over a given point is

$$j(\tau) = 4 \frac{24^3 f(\tau)^3}{4f(\tau)^3 + 27g(\tau)^2}. \quad (2.2.16)$$

The expression for the discriminant (2.2.14) enters the above identity, meaning that the denominator vanishes for singular elliptic fibers. If this occurs in such a way that the quotient on the r.h.s. diverges, then

$$j(\tau) \longrightarrow \infty \Rightarrow \tau \longrightarrow i\infty. \quad (2.2.17)$$

In F-theory the complex structure τ of the elliptic fiber over a point in B_n is identified with the Type IIB axio-dilaton, meaning that the subset of singular elliptic fibers just discussed are associated to local weak coupling $g_s \rightarrow 0$. Therefore, degenerations of the internal space

⁷The map printed above corresponds to the topological definition of c_1 . In the context of algebraic geometry, c_1 usually refers to the natural map from Cartier to Weil divisors $c_1 : \text{Pic}(B_n) \rightarrow \text{Cl}(B_n)$. By composing it with the cycle map $\text{cl}_{B_n} : \text{Cl}(B_n) \rightarrow H_{2n-2}^{\text{BM}}(B_n, \mathbb{Z})$ and invoking Poincaré duality $H_{2n-2}^{\text{BM}}(B_n, \mathbb{Z}) \cong H^2(B_n, \mathbb{Z})$ the topological map is recovered.

producing this type of singular elliptic fibers in codimension-zero are global weak coupling limits, see the comments in Section 2.2.4.

The discriminant divisor Δ is particularly relevant in F-theory, since it corresponds to the location of the 7-branes in the Type IIB internal space B_n . To see this, recall the content of the Picard-Lefshetz theorem [57, 180, 185]: The middle-dimensional (co)homology of a complex variety is subject to a monodromy action upon circling around a point in the complex structure moduli space over which it contains a vanishing cycle. For the elliptic fibrations under consideration this means that, for a fixed $x_0 \in B_n$ and the fiber \mathcal{E}_{x_0} over it, we have a map⁸

$$\mu : \pi_1(B_n \setminus \Delta, x_0) \longrightarrow \text{MCG}(\mathcal{E}_{x_0}) \cong \text{Aut}(H^1(\mathcal{E}_{x_0}, \mathbb{Z})) \cong \text{Sp}(2, \mathbb{Z}) \cong \text{SL}(2, \mathbb{Z}). \quad (2.2.18)$$

For a loop γ_i encircling a single irreducible component Δ_i of Δ , corresponding to just one $[p, q]$ 7-brane, the concrete monodromy action can be computed based on the vanishing combination of one-cycles associated to the singular locus, according to the Picard-Lefshetz formula. The conjugacy class of $\mu(\gamma_i) = M_{[p, q]} \in \text{SL}(2, \mathbb{Z})$ completely determines the intrinsic properties of the 7-brane. Note, however, that the j -invariant of the associated singular elliptic fiber does not uniquely determine the type of $[p, q]$ 7-brane, since the j -function is only sensitive to the projective representation in $\text{PSL}(2, \mathbb{Z})$, cf. Section 2.1.5. This has important physical consequences: Consider, e.g., an F-theory model at global weak coupling, meaning that the j -invariant of all elliptic fibers diverges. The fact that we can still distinguish various types of $[p, q]$ 7-branes with $j(\tau) \rightarrow \infty$ based on their monodromy conjugacy class is what allows for all perturbative Type IIB gauge groups—these are $\text{SU}(N)$, $\text{SO}(N)$ and $\text{Sp}(2N)$ —to be realized in the appropriate F-theory limit.

Kodaira, Néron and Tate classified the types of singular elliptic fibers, local monodromies and j -invariants that can appear in codimension-one in the base of a holomorphic elliptic fibration. We reproduce part of this data in Table 2.2.1, using which the type of generic singular elliptic fiber over a discriminant component can be read off directly from the defining polynomials of the Weierstrass model.

To illustrate the preceding discussion, let us consider an eight-dimensional F-theory model. The elliptic Calabi-Yau twofold $\pi_{\text{ell}} : Y_2 \rightarrow B_1$ can only be an elliptic K3 surface with $B_1 = \mathbb{P}^1$. Denoting by H the hyperplane class of \mathbb{P}^1 , the anticanonical class of the base is $\bar{K}_{B_1} = 2H$. This leads to $\Delta = 12\bar{K}_{B_1} = 24H$, which generically corresponds to 24 points in B_1 supporting a Kodaira type I₁ fiber associated to a D7-brane. In this way, we recover the conclusion we had reached by analysing the D7-brane supergravity solution in Section 2.1.4.

2.2.3 F-theory from M-theory

Finding the M-theory origin of the $\text{SL}(2, \mathbb{Z})$ -duality of Type IIB string theory demystified it by presenting it in a geometrical way: M-theory compactified on T^2 is dual to Type IIB in the limit of $\mathcal{V}_{T^2} \rightarrow 0$ at fixed complex structure and S-duality simply corresponds to the mapping class group of the M-theory torus, see the discussion in Section 2.1.5.

The Type IIB approach to F-theory leads to a twelve-dimensional theory compactified on an elliptic fibration $\pi : Y_{n+1} \rightarrow B_n$ whose base corresponds to the physical spacetime. The elliptic fiber is an auxiliary object keeping track of how the non-perturbative $\text{SL}(2, \mathbb{Z})$ -duality acts on the physical fields when moving in between patches. As discussed in Section 2.2.2, the

⁸The mapping class group of a Riemann surface and the group of symplectic automorphisms of its first cohomology group are not always isomorphic. The former group is generally bigger, with the difference between the two measured by the Torelli subgroup, which is trivial for genus-one curves.

Type	$\text{ord}(f)$	$\text{ord}(g)$	$\text{ord}(\Delta)$	Sing.	Monodromy cover	Lie algebra	Split	$j(\tau)$
I ₀	≥ 0	≥ 0	0	—	—	—	—	\mathbb{C}
I ₁	0	0	1	—	—	—	—	∞
II	≥ 1	1	2	—	—	—	—	0
III	1	≥ 2	3	A ₁	—	$\mathfrak{su}(2)$	—	1728
IV	≥ 2	2	4	A ₂	$\psi^2 - \frac{g}{w^2} _{w=0}$	1-comp: $\mathfrak{sp}(1)$ 2-comp: $\mathfrak{su}(3)$	IV ^{ns} IV ^s	0
I_m $m \geq 2$	0	0	m	A _{$m-1$}	$\psi^2 + \frac{9g}{2f} _{w=0}$	1-comp: $\mathfrak{sp}([\frac{m}{2}])$ 2-comp: $\mathfrak{su}(m)$	I _{m} ^{ns} I _{m} ^s	∞
I ₀ [*]	≥ 2	≥ 3	6	D ₄	$\psi^3 + \psi \frac{f}{w^2} _{w=0} + \frac{g}{w^3} _{w=0}$	1-comp: \mathfrak{g}_2 2-comp: $\mathfrak{so}(7)$ 3-comp: $\mathfrak{so}(8)$	I ₀ ^{* ns} I ₀ ^{* ss} I ₀ ^{* s}	\mathbb{C}
I_{2m-5}^* $m \geq 3$	2	3	$2m+1$	D _{$2m-1$}	$\psi^2 + \frac{1}{4} \left(\frac{\Delta}{w^{2m+1}} \right) \left(\frac{2wf}{9g} \right)^3 _{w=0}$	1-comp: $\mathfrak{so}(4m-3)$ 2-comp: $\mathfrak{so}(4m-2)$	I _{$2m-5$} ^{* ns} I _{$2m-5$} ^s	∞
I_{2m-4}^* $m \geq 3$	2	3	$2m+2$	D _{$2m$}	$\psi^2 + \left(\frac{\Delta}{w^{2m+2}} \right) \left(\frac{2wf}{9g} \right)^2 _{w=0}$	1-comp: $\mathfrak{so}(4m-1)$ 2-comp: $\mathfrak{so}(4m)$	I _{$2m-4$} ^{* ns} I _{$2m-4$} ^s	∞
IV [*]	≥ 3	4	8	E ₆	$\psi^2 - \frac{g}{w^4} _{w=0}$	1-comp: \mathfrak{f}_4 2-comp: \mathfrak{e}_6	IV ^{* ns} IV ^{* s}	0
III [*]	3	≥ 5	9	E ₇	—	\mathfrak{e}_7	—	1728
II [*]	≥ 4	5	10	E ₈	—	\mathfrak{e}_8	—	0
non-min.	≥ 4	≥ 6	≥ 12	non-can.	—	—	—	—

Table 2.2.1: Classification of singular elliptic fibers by Kodaira, Néron and Tate in terms of the Weierstrass data, reproduced from [185]. The vanishing orders displayed refer to a divisor $D \subset B_n$ locally defined by the equation $D := \{w = 0\}_{B_n}$, i.e. we use the abridged notation $\text{ord}(\cdot)$ for $\text{ord}_{Y_{n+1}}(\cdot)_D$.

monodromy action associated to $[p, q]$ 7-branes corresponds to the Picard-Lefshetz monodromy on the elliptic fibers when transporting them around their singular loci.

Mimicking the strategy employed in the analysis of ten-dimensional Type IIB, we consider M-theory as a starting point. Since M-theory geometrizes the $\text{SL}(2, \mathbb{Z})$ -duality of Type IIB, the auxiliary part of the F-theory geometry becomes part of spacetime in M-theory, which we must therefore consider compactified on the elliptic fibration $\pi : Y_{n+1} \rightarrow B_n$. F-theory is recovered in the limit in which the volume of the elliptic fiber is sent to zero $\mathcal{V}_\mathcal{E} \rightarrow 0$.

Taking this perspective facilitates some derivations. For example, analysing the amount of supersymmetry preserved by a strongly backreacted Type IIB compactification containing $[p, q]$ 7-branes is not that direct, but can be done, leading to the Calabi-Yau condition for Y_{n+1} . In M-theory the internal spacetime corresponds to the whole elliptic fibration $\pi_{\text{ell}} : Y_{n+1} \rightarrow B_n$, and the Calabi-Yau condition hence follows immediately. From our discussion in Section 2.1.2.3 we know exactly how these geometries affect the supersymmetry algebra, leading to a total of $32/(n+1)$ preserved supercharges in the lower-dimensional theory, where $n = 1, 2, 3$ or 4 .

In perturbative string theory, the gauge bosons present in the open string spectrum lead to non-abelian gauge groups localized in the worldvolume of the D-branes on which the open strings end. Similarly, in non-perturbative Type IIB $[p, q]$ 7-branes have (p, q) strings ending on them, which also lead to non-abelian gauge algebras. Determining these is most immediate from the M-theory point of view, as we now explain.

The bosonic content of the low-energy limit of M-theory (eleven-dimensional supergravity) is given by the metric $G_{\mu\nu}$ and the 3-form gauge potential C_3 . Expanding C_3 in a basis of

2-forms of the internal space will lead to a collection of external U(1) gauge fields observable in the dimensionally reduced theory; at least a subset of these should correspond to the Cartan subgroups of the non-abelian gauge groups associated with $[p, q]$ 7-branes.

The singular elliptic fibers associated with $[p, q]$ 7-branes can make the total space Y_{n+1} of the elliptic fibration singular itself. As we explain below, it is these singular elliptic fibers that are associated with the appearance of non-abelian gauge algebras. The resulting types of singularities for Y_{n+1} are listed in Table 2.2.1, where we see that (for Weierstrass models) only the fibers of Kodaira type I₀, I₁ and II do not lead to a singular Y_{n+1} . To explicitly see the origin of the states furnishing the non-abelian gauge factors⁹ of the F-theory model, we consider the resolved internal space

$$\pi : \hat{Y}_{n+1} \longrightarrow Y_{n+1}. \quad (2.2.19)$$

Minimal singular elliptic fibers admit a crepant fibral resolution, meaning that the singularity can be removed by introducing exceptional curves in the fiber while

$$\overline{K}_{\hat{Y}_{n+1}} = \pi^* (\overline{K}_{Y_{n+1}}) = 0, \quad (2.2.20)$$

such that the Calabi-Yau condition is preserved. In Table 2.2.1 we observe that there also exist non-minimal singular elliptic fibers, which in a Weierstrass model $\pi_{\text{ell}} : Y_{n+1} \rightarrow B_n$ appear over a locus $D \subset B_n$ when the vanishing orders are

$$\text{ord}_{Y_{n+1}}(f, g, \Delta)_D \geq (4, 6, 12). \quad (2.2.21)$$

These do not admit a crepant fibral resolution, making their analysis much more subtle. Those degenerations of the internal space that give rise to non-minimal singular elliptic fibers can correspond to infinite-distance limits in the complex structure moduli space, and are therefore of interest in view of the Swampland Distance Conjecture and the Emergent String Conjecture, see Sections 3.3 and 3.4. The mathematics and physics of infinite-distance non-minimal singularities is the subject of Chapters 5 and 6; we hence postpone their study for now, assuming that they are absent from the geometries considered in the remainder of this section.

Denote by $\{\Delta_I\}_{I=0, \dots, N}$ the irreducible components of the discriminant divisor Δ . These are codimension-one loci in B_n over which the elliptic fiber becomes singular, with its Kodaira type determined by the vanishing orders¹⁰

$$\text{ord}_{Y_{n+1}}(f, g, \Delta)_{\Delta_I} = (\alpha, \beta, \gamma). \quad (2.2.22)$$

Let us fix a discriminant component Δ_I . Using Table 2.2.1, we can read off how the singular elliptic fibers over it fit into the ADE classification, let us call their type $\tilde{\mathfrak{g}}_I$. The nomenclature responds to the fact that the crepant resolution of the fiber introduces a collection of exceptional curves $\{\mathbb{P}_{r_I}^1\}_{r_I=1, \dots, \text{rank}(\tilde{\mathfrak{g}}_I)}$ which, together with the strict transform \mathbb{P}_0^1 of the original fiber (distinguished by its intersection with the holomorphic section S_0), make the resolved elliptic fiber

$$\mathcal{E} = \sum_{r_I=0}^{\text{rank } \tilde{\mathfrak{g}}_I} a_{r_I} \mathbb{P}_{r_I}^1 \quad (2.2.23)$$

⁹The type of non-abelian gauge algebras associated to the singular elliptic fibers can be determined directly in the singular model from the Picard-Lefschetz monodromy that they induce. The benefit of working with the resolved geometry is that it allows us to identify the states furnishing the algebras in the F-theory limit in terms of M2-branes wrapping vanishing 2-cycles in M-theory.

¹⁰See Section 5.2.2.2 for more precise statements on the relation between the vanishing orders of the defining polynomials of the Weierstrass model over a given locus in the base and the type of singular elliptic fibers that it supports.

take the form of the (extended) Dynkin diagram associated with $\tilde{\mathfrak{g}}_I$.¹¹

In compactifications on an internal space $\pi_{\text{ell}} : Y_{n+1} \rightarrow B_n$ with $n \geq 2$, the components $\{P_{r_I}^1\}_{r_I=0,\dots,\text{rank}(\tilde{\mathfrak{g}}_I)}$ of the resolved fiber may undergo monodromies when moving along Δ_I . This monodromy action will organize the fiber components into invariant orbits $\{C_{i_I}\}_{i_I=0,\dots,\text{rank}(\mathfrak{g}_I)}$, out of which a set of independent rational curves $\{\mathbb{P}_{i_I}^1\}_{i_I=0,\dots,\text{rank}(\mathfrak{g}_I)}$ can be selected. Here, \mathfrak{g}_I is the Lie algebra obtained by dividing the covering algebra $\tilde{\mathfrak{g}}_I$ by the outer automorphism to which this monodromy action corresponds. If the monodromy action is non-trivial, this results in a non-simply-laced Lie algebra \mathfrak{g}_I , i.e. the monodromy folds the Dynkin diagram associated to $\tilde{\mathfrak{g}}_I$. The divisors $\{E_{i_I}\}_{i_I=0,\dots,\text{rank}(\mathfrak{g}_I)}$ obtained by fibering the invariant orbits $\{C_{i_I}\}_{i_I=0,\dots,\text{rank}(\mathfrak{g}_I)}$ over the discriminant component Δ_I are called resolution or Cartan divisors.

The original classification of Kodaira and Néron applied to elliptic surfaces, for which $n = 1$ and the monodromy effects just discussed do not arise. Tate refined it by taking into account the monodromies, thereby extending the validity of the classification to the generic fibers found over base divisors also when $n \geq 2$. This resulted in Tate's algorithm [189], explained in the F-theory literature in [190–192]. The only simple Lie algebras \mathfrak{g} with non-trivial outer automorphisms are

$$\text{Aut}(\text{A}_{n \geq 2}) / \text{Aut}^0(\text{A}_{n \geq 2}) \cong \text{Aut}(\text{D}_{n \neq 4}) / \text{Aut}^0(\text{D}_{n \neq 4}) \cong \text{Aut}(\text{E}_6) / \text{Aut}^0(\text{E}_6) \cong \mathbb{Z}_2 \quad (2.2.24)$$

and

$$\text{Aut}(\text{D}_4) / \text{Aut}^0(\text{D}_4) \cong \mathbb{Z}_3. \quad (2.2.25)$$

Those discriminant components Δ_I supporting singular elliptic fibers of one of these types may exhibit a non-trivial monodromy acting on the components of the resolved fiber. It can be efficiently described by means of a *monodromy cover* of Δ_I , which leads to polynomials in an auxiliary variable ψ corresponding to a meromorphic section of an appropriate line bundle over Δ_I . These polynomials are printed in Table 2.2.1, reproducing the list in [192]. The number of irreducible components of the monodromy cover determines whether the relevant Dynkin diagram is folded or not, with more components leading to larger gauge algebras \mathfrak{g}_I .

We have discussed two types of divisors¹² of \hat{Y}_{n+1} : the holomorphic section¹³ S_0 and the resolution divisors $\{E_{i_I}\}_{i_I=0,\dots,\text{rank}(\mathfrak{g}_I)}^{I=0,\dots,N}$. In addition to these, we also have the pullbacks of the base divisors $\{\pi_{\text{ell}}^*(D_\alpha^b)\}_{\alpha=1,\dots,h^{1,1}(B_n)}$. Moreover, the elliptic fibration may have extra rational sections $\{S_A\}_{A=1,\dots,\text{rank}(\text{MW}(\pi_{\text{ell}}))}$, which are the generators of the free part of the Mordell-Weil group $\text{MW}(\pi_{\text{ell}})$ of $\pi_{\text{ell}} : Y_{n+1} \rightarrow B_n$. The Shioda-Tate-Wazir theorem [194–197] implies that these are all the generators of the Néron-Severi group

$$\text{NS}(\hat{Y}_{n+1}) = \langle S_0, S_A, E_{i_I}, \pi_{\text{ell}}^*(D_\alpha^b) \rangle_{\mathbb{Z}} \cong H^{1,1}(\hat{Y}_{n+1}) \cap H^2(\hat{Y}_{n+1}, \mathbb{Z}). \quad (2.2.27)$$

The lower-dimensional U(1) gauge factors of the M-theory compactification arise from the decomposition of C_3 in terms of these (1, 1)-forms. However, what we are actually interested in

¹¹Except for the Kodaira types III and IV, which lead to somewhat degenerate presentations of the diagrams.

¹²We are working with a smooth simply connected variety $X = \hat{Y}_{n+1}$. Since $h^{0,1}(X) = 0$, the first Chern class $c_1 : \text{Pic}(X) \cong H^1(X, \mathcal{O}^*) \rightarrow H^2(X, \mathbb{Z})$ is injective, see also Footnote 7. This implies that $\text{NS}(X) \cong \text{Pic}(X)$. Moreover, the Lefschetz theorem on (1, 1)-classes states that for a compact Kähler manifold the restriction $c_1 : \text{Pic}(X) \rightarrow H^{1,1}(X) \cap H^2(X, \mathbb{Z})$ is surjective [193]. Altogether,

$$\text{NS}(X) \cong \text{Pic}(X) \cong H^{1,1}(X) \cap H^2(X, \mathbb{Z}) \quad (2.2.26)$$

for the smooth simply connected compact Kähler manifolds under consideration. Hence, we will denote the elements of these groups identically, in a slight abuse of notation.

¹³We denote the divisors of Y_{n+1} and their strict transforms in \hat{Y}_{n+1} by the same symbol.

is the F-theory limit, which corresponds to $\mathcal{V}_{\mathcal{E}} \rightarrow 0$. Some $U(1)$ factors found in M-theory do not remain gauge vectors in F-theory, and hence cannot form part of the Cartan subgroups of the non-abelian gauge factors localized on $[p, q]$ 7-branes. One can prove that the $U(1)$ factor arising from the term of the expansion of C_3 featuring the holomorphic section is associated with the Kaluza-Klein $U(1)$ arising from the circle reduction of F-theory to M-theory, with the KK tower of charged states corresponding to M2-branes wrapping $n\mathcal{E}$. It can also be proven that the $U(1)$ factors associated with the $\{\pi_{\text{ell}}^*(D_{\alpha}^b)\}_{\alpha=1,\dots,h^{1,1}(B_n)}$ divisors stem from the reduction on the aforementioned circle of the 2-forms appearing in Type IIB/F-theory from the expansion of C_4 on $\{D_{\alpha}^b\}_{\alpha=1,\dots,h^{1,1}(B_n)}$. This leaves us only with the $U(1)$ factors associated with $\{S_A\}_{A=1,\dots,\text{rank}(\text{MW}(\pi_{\text{ell}}))}$ and $\{E_{i_I}\}_{i_I=0,\dots,\text{rank}(\mathfrak{g}_I)}^{I=0,\dots,N}$.

The $U(1)$ factors arising from those terms in C_3 including the $\{S_A\}_{A=1,\dots,\text{rank}(\text{MW}(\pi_{\text{ell}}))}$ do survive the F-theory limit. These cannot, however, correspond to the Cartan subgroups of the $[p, q]$ 7-brane gauge groups: They are associated with the generators of the free part of the Mordell-Weil group, and therefore related to global features of the internal geometry, while the $[p, q]$ 7-branes give rise to localised gauge groups. It can be proven that these gauge vectors furnish an abelian $U(1)^{\text{rank}(\text{MW}(\pi_{\text{ell}}))}$ gauge algebra instead [187, 198–200]. The torsional part of the Mordell-Weil group is also relevant for the physics, determining the global structure of the non-abelian F-theory gauge groups [199, 201].

The remaining $U(1)$ factors, associated with the resolution divisors $\{E_{i_I}\}_{i_I=0,\dots,\text{rank}(\mathfrak{g}_I)}^{I=0,\dots,N}$, do correspond to the Cartan subgroups of the localised non-abelian gauge groups of F-theory. This makes sense intuitively: On the F-theory side, we expect the non-abelian gauge factors to arise from the dynamics of (p, q) strings ending on $[p, q]$ 7-branes. These correspond to the irreducible components of the discriminant divisor Δ in B_n . The monodromy action induced by circling around a $[p, q]$ 7-brane is understood as the Picard-Lefshetz monodromy arising from circling around singular elliptic fibers, which do indeed appear over Δ . On the resolved M-theory side, it is the resolution of these fibral singularities that gives rise to the $\{E_{i_I}\}_{i_I=0,\dots,\text{rank}(\mathfrak{g}_I)}^{I=0,\dots,N}$, which are hence intrinsically tied to the 7-branes. The type of non-abelian gauge algebra associated to a collection of $[p, q]$ 7-branes corresponds to the Lie algebra whose (extended) Dynkin diagram is reproduced by the resolved elliptic fibers (after taking the monodromy cover into account), which can be read off from the Kodaira-Néron-Tate classification Table 2.2.1.

This can be made more precise by noting that we have the intersection products

$$E_{i_I} \cdot E_{j_J} \cdot \pi^*(\omega_{2n-2}) = -\delta_{IJ} \mathfrak{C}_{i_I j_J}^{\mathfrak{g}_I} \Delta_I \cdot_{B_n} \omega_{2n-2}, \quad \forall \omega_{2n-2} \in H^{2n-2}(B_n), \quad (2.2.28a)$$

$$E_{i_I} \cdot \mathbb{P}_{j_J}^1 = -\delta_{IJ} C_{i_I j_J}^{\mathfrak{g}_I}, \quad (2.2.28b)$$

$$S_0 \cdot \mathbb{P}_{i_I}^1 = 0, \quad (2.2.28c)$$

where $C^{\mathfrak{g}_I}$ is the Cartan matrix of \mathfrak{g}_I and $\mathfrak{C}^{\mathfrak{g}_I}$ is a related matrix that can be computed from $C^{\mathfrak{g}_I}$. For a fixed discriminant component Δ_I , this identifies the resolution divisors $\{E_{i_I}\}_{i_I=0,\dots,\text{rank}(\mathfrak{g}_I)}$ with the coroots of \mathfrak{g}_I , while the fibral curves $\{\mathbb{P}_{i_I}^1\}_{i_I=0,\dots,\text{rank}(\mathfrak{g}_I)}$ are associated with the negative of its simple roots. Hence, taking combinations of the $\{\mathbb{P}_{i_I}^1\}_{i_I=0,\dots,\text{rank}(\mathfrak{g}_I)}$, the whole root lattice is generated. The states obtained from wrapping M2-branes on these combinations of fibral curves, together with the generators of the Cartan subalgebra $\mathfrak{h}_I := \mathfrak{u}(1)^{\text{rank}(\mathfrak{g}_I)}$, furnish the full adjoint representation¹⁴ of \mathfrak{g}_I .

M2-branes wrapped on combinations of the $\{\mathbb{P}_{i_I}^1\}_{i_I=0,\dots,\text{rank}(\mathfrak{g}_I)}$ yield particles non-trivially charged under the Cartan subalgebra \mathfrak{h}_I . Their masses are proportional to the volume of the

¹⁴When \mathfrak{g}_I is non-simply-laced, there can occur additional representations stemming from the decomposition of the adjoint representation of the covering algebra $\tilde{\mathfrak{g}}_I$ into irreducible representations of \mathfrak{g}_I .

curve that they wrap, meaning that in the resolved M-theory model the gauge algebra \mathfrak{g}_I is broken down to \mathfrak{h}_I , i.e. resolving the fibral singularities corresponds to moving in the Coulomb branch of the theory. The F-theory limit entails sending the volume of all fibral curves to zero, leading to the full restoration of the non-abelian gauge algebra \mathfrak{g}_I ; F-theory sits at the origin of the Coulomb branch of the M-theory model.

2.2.4 Beyond non-abelian gauge algebras

Our focus has been on the correspondence between the codimension-one minimal singular elliptic fibers of the F-theory internal elliptic Calabi-Yau variety and the non-abelian gauge factors localised on $[p, q]$ 7-branes. We have also mentioned how the Mordell-Weil group relates to the abelian gauge algebra and to the global structure of the gauge groups. The dictionary between geometry and physics provided by F-theory is, however, much richer than this. Below, we mention without explanation a few more of its entries, directing the reader to the reviews [181–183, 185] for further details.

Some singular elliptic fibers have a divergent $j(\tau) \rightarrow \infty$, which implies, after their complex structure τ is identified with the Type IIB axio-dilaton, that the locus that supports them is at local weak string coupling $g_s \rightarrow \infty$. These are the A and D type singular elliptic fibers, see Table 2.2.1. Consistent with this fact, these are the 7-branes whose induced monodromies belong to the parabolic subgroup $P_{i\infty} \leq \mathrm{SL}(2, \mathbb{Z})$, cf. Section 2.1.3.3. Hence, tuning an F-theory model such that A type singularities arise in codimension-zero over the base corresponds to a global weak coupling limit, known as the Sen limit [202, 203]. It is an infinite-distance trajectory in the complex structure moduli space, which is better understood using the algebro-geometric language of degenerations; the Type II.b degenerations that we analyse in Chapters 5 and 6 are Sen limits expressed in this formalism. Due to the global weak coupling, their endpoints can be understood as a perturbative Type IIB orientifold compactification. Indeed, the geometry of a Calabi-Yau double cover of the F-theory base naturally arises in the context of the Sen limit, as we review in Appendix B.13. The branching locus of this double cover corresponds, from the Type IIB point of view, to the location of the O7-planes. As mentioned in Section 2.1.1, O-planes are non-dynamical objects in perturbative string theory; their analysis in F-theory reveals that at finite g_s coupling they split into a particular collection of $[p, q]$ 7-branes and are, therefore, on an equal footing with the rest of 7-branes.

The intersection locus of two $[p, q]$ 7-branes leads to localized matter transforming under charged representations of the associated gauge groups. The representations arising in this way can be read off from the type of codimension-two singular elliptic fibers appearing at the intersection locus [192, 204, 205]. Localised uncharged matter corresponds instead to \mathbb{Q} -factorial terminal singularities in codimension-two [206, 207]. If the internal space of the F-theory model is of high enough dimensionality, namely in compactifications to four and two dimensions, the codimension-two loci supporting the matter can themselves intersect in higher codimension, giving rise to Yukawa interactions, see the references in [185].

Weierstrass models always have a holomorphic section, hence describing an elliptic fibration. More generally, F-theory can be studied on genus-one fibrations without rational sections [188]. It is possible to associate to any genus-one fibration $\pi : Y \rightarrow B$ an elliptic fibration $\pi_J : J(Y) \rightarrow B$ known as the Jacobian. The set of all genus-one fibrations leading to the same Jacobian is known as the Tate–Shafarevich group $\mathrm{III}_B(J(Y))$. The various elements of the Tate–Shafarevich group correspond to different M-theory vacua with the same F-theory uplift, which can be seen to

exhibit a discrete gauge symmetry given by $\text{III}_B(J(Y))$. Discrete gauge symmetries in F-theory can also be understood in terms of torsional cohomology, see the reviews [185, 208].

The F-theory models that we have considered have, from the Type IIB perspective, trivial B_2 and C_2 background values, and so do the gauge fields along the 7-branes. These Type IIB features are all unified into the background value of $G_4 = dC_3$ in M-theory. However, choosing a G_4 background in a supersymmetry preserving way is only compatible with F-theory compactifications to four and two dimensions. G_4 -flux can be used, for example, to break the non-abelian gauge groups of an F-theory models not by deforming the relevant singular elliptic fibers, but by turning gauge flux along the associated 7-brane. Four-dimensional F-theory compactifications can make use of these features for the construction of phenomenologically appealing models, see the references in [183, 185].

We have approached F-theory from Type IIB string theory, to motivate its definition, and from M-theory, to learn more about the details of its non-perturbative gauge algebras. If the internal elliptic Calabi-Yau variety of an F-theory model exhibits, in addition, a compatible K3-fibration, it is also possible to establish a duality with heterotic string theory. We review the details of F-theory/heterotic duality in Section 6.4.1.

Chapter 3

The Swampland Program

The study of string theory has revealed the existence of an immense space of low-energy EFTs coupled to gravity that correspond to string vacua. Generalizing this concept to any theory of quantum gravity, we arrive at the notion of the Landscape. However vast the Landscape may be, it is surrounded by an even larger set of EFTs coupled to gravity that cannot be consistently UV completed to a theory of quantum gravity, known as the Swampland.

Delineating the boundary between the Landscape and the Swampland is the main objective of the Swampland Program. The idea is to find a series of very general Swampland Constraints that gravitational EFTs must satisfy in order to form part of the Landscape. In this chapter, we start by reviewing the concept of the Swampland and the way in which the Swampland Program operates. After examining three core Swampland Conjectures and reviewing some of the evidence supporting them, we centre our attention on the Swampland Distance Conjecture and the Emergent String Conjecture, in preparation for Chapters 4 to 6.

3.1 The Swampland: Terra incognita

The String Theory Landscape is the set of low-energy gravitational EFTs that descend from string theory, i.e. those that stem from string vacua. As we briefly reviewed in Section 1.3.1, it is unfathomably large: While even just the number of known topologically distinct Calabi-Yau threefolds is vast, the size of the Landscape of flux vacua is estimated to be $\mathcal{O}(10^{272,000})$ [128]. More generally, one could think of the set of consistent gravitational EFTs that have a UV completion to a theory of quantum gravity as the Quantum Gravity Landscape, of which the String Theory Landscape would be a subset.

Since the size of the Landscape is astronomically large, one could argue that it might be more pragmatic to prioritize a bottom-up approach to phenomenological questions. After all, the characteristic energy scale of quantum gravity is so large that the details of low-energy physics will not be too sensitive to it; this is the principle of decoupling that has served us so well in our progressive understanding of quantum field theories. Once a phenomenologically viable low-energy theory has been found, only coupling it to gravity remains: The Landscape contains such a plethora of gravitational EFTs that the ones we construct from bottom-up arguments must be very likely to have a UV completion to a theory of quantum gravity.

The shift in perspective central to the Swampland Program is to highlight that the preceding conclusion is not valid. Gravity escapes, in this regard, conventional effective field theory thinking. In spite of the high-energy scales at which its quantum effects become explicitly relevant, it indirectly constrains the space of low-energy theories.

3.1.1 The Swampland

The notion of the Swampland was introduced in [102] to explicitly address the misconception that no IR constraints for gravitational EFTs arise from the UV nature of quantum gravity. It can be defined in the following way:

The Swampland and the Landscape

The set of gravitational EFTs that do not have a consistent UV completion to a theory of quantum gravity is the *Swampland*, while those that do have such a completion belong to the *Landscape*.

A consistent non-gravitational EFT must be anomaly free; even then, coupling it to gravity may give rise to gravitational anomalies, that must also vanish for the theory to be consistent at the effective level. From the bottom-up perspective, one would then be forgiven to think that such an EFT is always free of problems. These are the theories that we call naively consistent.

The fact that the details of IR physics are largely insensitive to the properties of its UV completion is known as decoupling. This concept, alongside the one of naturalness, plays a major role in the framework of EFTs. However, as we discussed in Section 1.1.5, gravity behaves differently: Scattering processes at energies much higher than the Planck scale lead to the creation of large black holes, whose properties are well approximated at the semiclassical level. This is one instance of a phenomenon known as UV/IR mixing, which is pervasive to quantum gravity. The notion of locality, also central to quantum field theory, acquires a less univocal nature once quantum gravity is considered. For example, in a circle compactification of string theory the local KK excitations are T-dual to the topological winding states, showing that the notion depends on the duality frame. These departures from the expected quantum field theoretic behaviour may also mean that our notion of naturalness needs to be modified to take quantum gravity into account.

What is important to our present discussion is that quantum gravity affects IR physics, and that naively consistent EFTs need to satisfy additional criteria if they are to have a UV completion to a theory of quantum gravity; these are known as *Swampland Constraints*.

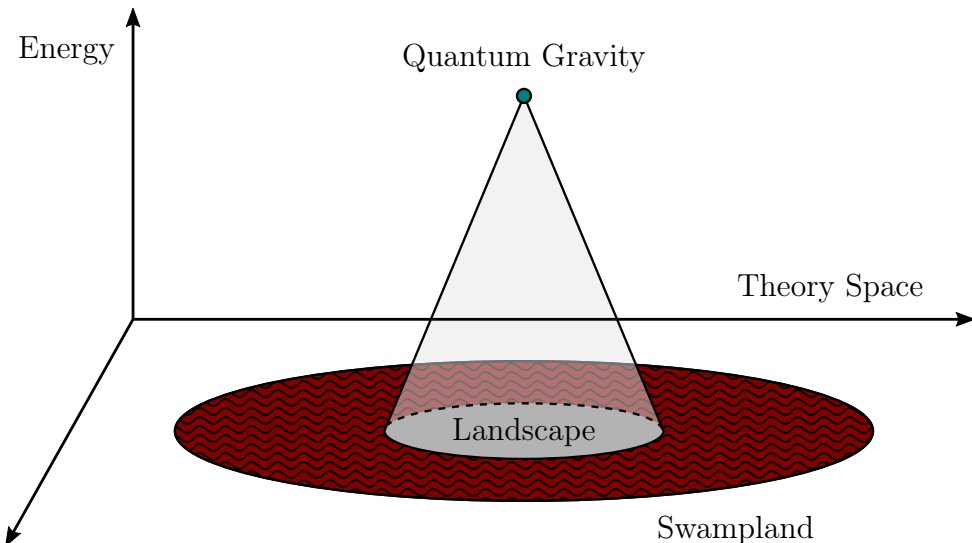


Figure 3.1: The Landscape and the Swampland.

Consider a concrete EFT together with its cut-off scale Λ_{EFT} . Once we consider processes whose characteristic energy scale is close to Λ_{EFT} the EFT stops being unitary, and requires integrating in new states in order to consistently describe the higher energy scales. The EFT resulting from this modification has a higher cut-off Λ_{EFT} , at which the process needs to be repeated. This is the usual way of operating purely within the context of EFT reasoning. Once quantum gravity is taken into consideration, the notion of quantum gravity cut-off Λ_{QG} arises, in coexistence with the conventional cut-off Λ_{EFT} . The scale Λ_{QG} is the one in which the EFT can no longer be amended in the conventional way, and a radical departure is necessary in order to fix it. This can entail, for example, changing the dimensionality of the spacetime considered, or changing the description of the fundamental degrees of freedom by abandoning the framework of quantum field theory and going to string theory. If $\Lambda_{\text{QG}} < \Lambda_{\text{EFT}}$, the EFT is in the Swampland; note that, since Λ_{EFT} increases as we conventionally modify the theory within the framework of EFTs, the statement that an EFT belongs to the Swampland or to the Landscape is energy-dependent. This gives rise to the common depiction of these two spaces of theories, a rendition of which is provided in Figure 3.1. Below, we will see specific instances in which Λ_{QG} can be predicted from Swampland considerations.

3.1.2 The Swampland Program

Defining the notions of the Landscape and the Swampland might have taken us just a few paragraphs, but tracing the boundary between the two is a much harder task. The ongoing effort to establish on firm grounds what conditions a naively consistent gravitational EFT must fulfil in order to not be part of the Swampland, and hence to belong to the Landscape, is known as the Swampland Program. Our exposition draws from the many excellent reviews on the subject [137–141], to which we direct the reader for a more comprehensive treatment.

Swampland Constraints are the criteria used to delineate this boundary. Due to their tentative nature, they are commonly referred to as Swampland Conjectures; the ultimate objective of the Swampland Program is to make the latter nomenclature obsolete. Different Swampland Conjectures are supported by varying degrees of evidence, and the aim is to either strengthen the case for them, or to find compelling arguments as to why they should be modified or abandoned altogether. This problem can be approached from a bottom-up or from a top-down perspective. The best-established Swampland Conjectures are sustained by both classes of arguments, which, reassuringly, agree in the forbidden regions of theory space that they predict.

Bottom-up evidence in favour of the Swampland Conjectures is usually gathered from the domain of black-hole physics. Since our knowledge of them is mostly semiclassical, we cannot prove conjectures in this fashion, but we can still offer strong heuristic arguments pointing in their direction. Consistency of the S-matrix or positivity constraints can also be fruitful ways to tackle the problem. The bottom-up approach has the benefit of providing us with insight into the aspects that would go wrong were the Swampland Constraints to be violated by a theory. Additionally, these types of arguments are based on quantum gravity features that are believed to be universal, hence motivating the conjectures without reference to a particular UV completion like string theory.

Top-down corroboration of the Swampland Conjectures is more robust, but must be procured by a concrete theory of quantum gravity. This makes string theory an invaluable tool for the cartographers of the Swampland: It offers a self-consistent theory of quantum gravity from which we can extract quantitative conclusions under good technical control. The ideal scenario would be to obtain a proof for the Swampland Conjectures starting from string theory. Such

a direction proves challenging due to our lack of a complete, non-perturbative formulation of the theory. Nevertheless, notable progress can be made in the asymptotic regions of the moduli space; understanding its deep interior is of great interest both from the Swampland Program and purely string theoretic points of view. Another way in which string theory enables us to assess the validity of the Swampland Conjectures is by acting as a theoretical laboratory. Once we have a hypothesis about the general behaviour of quantum gravity, we can compare it against all the known string vacua, or even try to find new ones tailored to testing a particular aspect of the conjecture. If the hypothesis survives the experiment, we can learn something non-trivial about how string theory makes sure that it is realized; if we instead find evidence against it, we can discard it or make an informed modification of the original proposal. One possible danger of using known string constructions to test the conjectures is that we know the theory much better in some corners of the moduli space than others, and hence need to be careful to not suffer from a lamppost effect.

The notions of the Landscape and the Swampland can be defined for any theory of quantum gravity or, more restrictively, focusing only on string theory. This leads to the inclusions

$$\begin{aligned} \text{String Theory Landscape} &\subseteq \text{Quantum Gravity Landscape} , \\ \text{String Theory Swampland} &\supseteq \text{Quantum Gravity Swampland} . \end{aligned}$$

If string theory is proven to be the unique theory of quantum gravity, this distinction would disappear. The idea that this might be indeed the case is known as *String Universality* or *String Lamppost Principle*. Evidence in favour of it exists in higher dimensions [142–144].

Our universe corresponds, by definition, to a point in the Landscape. As the Swampland Program evolves and our understanding of the Swampland Constraints is refined, we will have a clearer picture of where the Landscape sits within the theory space. This might lead to general quantum gravity predictions about our universe. Well-established Swampland Conjectures can also serve as guiding principles for physics beyond the Standard Model or cosmology. Interestingly, quantum gravity might constrain systems that, *a priori*, have no relation with it. To give one example, the Completeness Hypothesis states that all allowed charged states of a gauge field coupled to gravity must be realized as physical states in a theory of quantum gravity [56]; conventionally, we would not think of the existence of the photon demanding the presence of the electron.

In most Swampland discussions it is assumed that the gravitational EFTs considered contain Einstein gravity in dimensions equal or bigger than four, such that the gravitational field has propagating degrees of freedom. Nonetheless, some Swampland Conjectures have been explored in AdS_3 , where gravity is topological but allows for non-trivial solutions like the BTZ black hole [209]. Similarly, it would be interesting to understand whether non-standard gravitational EFTs can be compatible with known Swampland Criteria or if they will all ultimately lie in the Swampland [4].

3.2 Swampland Conjectures

The general notions discussed above have crystallized in the form of a growing collection of Swampland Conjectures. These are not isolated statements about quantum gravity, but are organized instead in a connected network. Finding relations between the different conjectures constitutes by no means proof or evidence in favour of them, but at least shows a degree of internal consistency. A benefit of further exploring how these connections are configured is that,

if understood well enough, one might be able to translate evidence in favour of one conjecture into substantiation for another. The hope is for these interdependences to hint at something deeper, i.e. to be different facets of a more fundamental quantum gravity principle that we have not understood yet, but that we might eventually unveil.

The degree of supporting evidence in favour of the various Swampland Conjectures is not uniform, and a careful exposition of the case for each of them is better left for more panoramic reviews of the Swampland Program, like [137–141]. Here we will mainly concentrate on three Swampland Conjectures: the No Global Symmetries Conjecture [147, 148], the Weak Gravity Conjecture [145] and the Swampland Distance Conjecture [146]. These conjectures are well-established, and are usually regarded as the core conjectures of the Swampland Program. Our treatment of the Swampland Distance Conjecture and its refinement, the Emergent String Conjecture, will prime us for the discussion in Chapters 4 to 6, while the other two will serve us to illustrate the general Swampland notions explained above. We also briefly comment on the species scale.

3.2.1 No Global Symmetries Conjecture

The No Global Symmetries Conjecture—certainly a Swampland Conjecture in spirit and commonly listed as one—actually predates the Swampland Program. Its statement is the following:

No Global Symmetries Conjecture [147, 148]

Quantum gravity theories coupled to a finite number of degrees of freedom cannot exhibit exact global symmetries.

In the case of continuous global symmetries, this conjecture can be motivated, as we do below, from bottom-up considerations thanks to the universal low-energy properties of black holes. Alternative lines of argumentation generalize it to include discrete and generalized global symmetries as well [210–212].

Assume that a gravitational EFT has a non-abelian continuous global symmetry G . For this statement to not be vacuous, at least one state in the theory must be charged under a non-trivial representation of G . Using a sufficient number of such states, one can create a black hole that will therefore transform in a large representation of G . Since the symmetry is global, Hawking radiation will not discharge the black hole. As the black hole evaporates, its mass, and hence its area, decreases. Eventually, the dimension of the Hilbert space of the black hole, which can be estimated from the exponential of its entropy, will be too small to fit the representation of G under which it transforms, leading to a contradiction.

If we consider instead an abelian continuous symmetry G , a similar argument can be made. An outside observer cannot determine the global charge of a black hole (this assumes the no-hair theorem), which can therefore be in an infinite number of microstates, associated to the different choices of charge. This uncertainty should lead to an infinite entropy, but a finite value for it is predicted by the Bekenstein-Hawking entropy formula (we can take the black hole to be large, such that no subtleties associated with Planck-sized objects arise). Alternatively, one can argue that black hole evaporation would lead to an infinite number of remnants, classified by their global charge, in a finite mass range, which has been argued to make the renormalized Planck mass diverge [213]. This is difficult to establish on firm grounds, since the semiclassical

treatment breaks down for the Planck-sized remnants. The argument can also be reformulated in terms of a violation of the covariant entropy bound [148].

The absence of global symmetries in a theory of quantum gravity is also supported from top-down considerations. Namely, perturbative string theory makes global symmetries of the worldsheet theory correspond to gauge symmetries from the target space point of view [147]. Using the machinery of holography, the conjecture has been validated for quantum gravity in AdS spacetimes within the context of the AdS/CFT correspondence [214, 215].

The Standard Model has a non-anomalous global symmetry, commonly denoted $U(1)_{B-L}$, that corresponds to the difference between the baryon and lepton numbers. According to the No Global Symmetries Conjecture, $U(1)_{B-L}$ cannot be an exact global symmetry of nature, and hence must be broken or gauged at sufficiently high energies. While this is among the most robust predictions of the Swampland Program, the energy scale at which this could occur might be high enough that its implications may not be of immediate phenomenological interest.

The No Global Symmetries Conjecture has been generalized to include topological global charges in the following way:

Cobordism Conjecture [216]

Consider a D -dimensional theory of quantum gravity compactified on any k -dimensional internal space. The cobordism class of the compactification space must be trivial, i.e.

$$\Omega_k^{\text{QG}} = 0. \quad (3.2.1)$$

This means that no exact superselection sectors exist in quantum gravity. We will not be able to explore the consequences of this interesting generalization of the conjecture here.

3.2.2 Weak Gravity Conjecture

The Weak Gravity Conjecture (WGC), originally proposed in [145], is one of the best studied Swampland Conjectures. The literature just on the WGC is sizable; our treatment here will be partial, but different aspects of the ongoing discussion about its refinements and a more representative list of references can be found in the general reviews on the Swampland Program [137–141], as well as in the reviews [217, 218], specialized on the WGC.

The statement of the WGC conjecture acquires various forms depending on the details of the objects to which it is applied. Broadly, one can distinguish between electric and magnetic formulations of the claim. Let us start by considering the electric formulation of the WGC conjecture for $U(1)$ gauge symmetries. All masses are measured in Planck units.

Electric Weak Gravity Conjecture [145]

Consider a $U(1)$ gauge theory with gauge coupling g that is weakly coupled to Einstein gravity. Then, there exists an electrically charged object whose charge-to-mass ratio fulfills

$$\frac{g^2 q^2}{m^2} \geq \left. \frac{g^2 Q^2}{M^2} \right|_{\text{ext.}} = \mathcal{O}(1), \quad (3.2.2)$$

where Q and M are the charge and mass of an extremal black hole.

This statement can be generalized to p -form symmetries by substituting the black holes for black branes and the masses for the tensions of the higher-dimensional objects [219]. It is also possible to apply it to non-abelian gauge groups G by decomposing its irreducible representations into charges under the $U(1)^{\text{rank}(G)}$ Cartan subgroup of G and demanding the ordinary WGC to hold for each $U(1)$ gauge factor [218].

To motivate the Electric WGC from a bottom-up perspective, we resort again to arguments based on black hole physics. The Weak Cosmic Censorship Conjecture posits that black hole singularities must be shielded by an event horizon, which for charged black holes occurs if the extremality bound

$$M^2 \geq \alpha^2 g^2 Q^2, \quad \alpha \sim \mathcal{O}(1) \quad (3.2.3)$$

is satisfied. The concrete value of α depends on the theory, e.g. $\alpha = 2$ for Einstein-Maxwell theory in four dimensions. The statement of the Electric WGC then follows from requiring extremal black holes to be kinematically allowed to decay. The need for the black holes to decay can be justified asymptotically in the weak coupling limit: If extremal black holes were unable to decay, we would end up with a collection of $N \sim 1/g$ black hole remnants whose masses only differ by $\Delta M \sim g$. In the limit $g \rightarrow 0$, this reduces to the pathological situation used in the heuristic argument against exact global symmetries.

As occurred for the No Global Symmetries Conjecture, its bottom-up justification is an indication as to why the conjecture should be true, but not a rigorous proof; it could not be any different, since it stems from semiclassical considerations. The best evidence for the validity of the Electric WGC is that it is satisfied in all string vacua known to date [218].

The extremality bound for black holes entering the inequality (3.2.2) is affected by quantum corrections, which become non-negligible for smaller black holes. As a consequence, the extremality curve may deviate from its classical counterpart in such a way as to allow small black holes to be both extremal and kinematically allowed decay products of larger black holes. The available evidence seems to indeed point in this direction [218]. Such a possibility was already foreseen in the original proposal of the conjecture [145].

Stronger versions of the Electric WGC demand for extremal black holes to be able to decay by emitting charged particles, which means that the object satisfying (3.2.2) should be one. Possible strong forms of the Electric WGC [145] are to demand the lightest particle in the theory to be superextremal, or the particle of smallest charge to be superextremal, but these are violated in examples from heterotic string theory [220]. Exploring the stronger form of the Electric WGC in string theory has led to various refinements of it that address its consistency under dimensional reduction. As enunciated in [221], these are:

- **Tower Weak Gravity Conjecture [222]:** For every site in the charge lattice, $\vec{q} \in \Gamma$, there exists a positive integer n such that there is a superextremal particle of charge $n\vec{q}$.
- **Sublattice Weak Gravity Conjecture [209, 220]:** There exists a positive integer n such that for any site in the charge lattice, $\vec{q} \in \Gamma$, there is a superextremal particle of charge $n\vec{q}$.

The Sublattice WGC is a milder version of the Lattice WGC proposed in [219] by the same authors, but found to be in contradiction with some string theory examples [220]. This illustrates the use of string theory as a theoretical laboratory for the exploration of the Swampland, as alluded to in Section 3.1.2. A careful analysis of weak coupling limits in F-theory [223] and M-theory [224] has revealed that towers of (super)extremal particles are not needed for consistency under dimensional reduction of the conjecture in those asymptotic directions along which the notion of circle compactification breaks down, leading to another refined form of the WGC:

- **Minimal Weak Gravity Conjecture [225]:** Towers of (super)extremal particle states below the black hole threshold exist if and only if they are required by consistency of the WGC under dimensional reduction. This is the case for either emergent string limits, Kaluza–Klein reductions with KK gauge bosons, or strongly coupled limits with exactly extremal states.

The magnetic version of the WGC restricts weak coupling limits by establishing how the cut-off of the EFT should decrease along such a deformation of the theory.

Magnetic Weak Gravity Conjecture [145]

Consider a U(1) gauge theory with gauge coupling g that is weakly coupled to Einstein gravity in d dimensions. The EFT cut-off is bounded by

$$\Lambda \leq g M_{\text{Pl}}^{(d-2)/2}. \quad (3.2.4)$$

This form of the conjecture can be obtained by applying the Electric WGC to the magnetic dual field as a constraint on the mass of the magnetic monopole, or by demanding the theory to have some monopole that is not a black hole. The Magnetic WGC conjecture becomes more constraining as we increase the desired regime of validity of the EFT description, i.e. the characteristic energy of the processes that we wish to describe, since it demands for the gauge coupling to grow accordingly.

The WGC could have consequences for large field inflation [226–228], although its weakest form is not enough to rule it out [229]. Additionally, some recent examples violating the Weak Cosmic Censorship Conjecture are ruled out if one accepts the consequences of the WGC [230]. The constraining power of the WGC for low-energy EFTs may be diminished if clockwork-like mechanisms are not constrained [231, 232].

3.2.3 The Species Scale

In Section 1.1.5 we briefly discussed gravitational EFTs, whose natural cut-off scale corresponds to the Planck scale M_{Pl} . Interestingly, when gravity is coupled to a large number N of species of light fields the cut-off corresponds instead to the *species scale* $\Lambda_s \leq M_{\text{Pl}}$, first introduced in [233–236]. One way to derive this is by demanding the smallest black hole that the d -dimensional gravitational EFT can describe to have an entropy capable of accounting for all the light species, which leads to the expression

$$\Lambda_s = M_{\text{Pl}} N^{\frac{-1}{d-2}}. \quad (3.2.5)$$

Hence, the true cut-off of the gravitational EFT can be much lower than the Planck scale if the number of light species is sufficiently high. Since the species scale directly depends on the number of light species, and said number varies as we move in the moduli space of the theory, it must be a moduli dependent quantity itself. A bound for the gradient of Λ_s was obtained in [237] by working in two steps: First, integrating out the massive modes above Λ_s yields an effective gravitational action whose expansion is in inverse powers of Λ_s . Second, integrating out the UV modes of the light species up to a distance $1/\Lambda_s$ generates higher-dimension smeared operators that correct the action. Requiring the expansion to be under control leads to the constraint

$$\frac{|\nabla \Lambda_s|^2}{\Lambda_s^2} \leq \frac{c}{M_{\text{Pl}}^{d-2}}, \quad c \sim \mathcal{O}(1). \quad (3.2.6)$$

The coefficient c is not fixed by this argument alone, but invoking the Emergent String Conjecture, to be discussed in Section 3.4, it can be seen to be [237, 238]

$$c = \frac{1}{d-2}. \quad (3.2.7)$$

The close connection between Λ_s and black holes has motivated a thermodynamic approach to the study of its moduli dependence [239–242].

3.3 Swampland Distance Conjecture

Having discussed the general notion of the Swampland and illustrated the types of constraints for gravitational EFTs that arise from its study, we are ready to review the conjecture whose exploration motivates the remainder of this work: the Swampland Distance Conjecture (SDC).

Central to any discussion of the SDC is the concept of moduli space. In a mathematical context, a moduli space is a geometric space whose points represent (possibly isomorphism classes of) some geometric object of a fixed class; hence, moving along the moduli space captures deformations within said class of objects. The moduli are the coordinates on the moduli space parametrizing the deformations. In physics, the term moduli space usually refers to the geometric space of vacuum expectation values of a set of scalar fields, e.g. the scalar components of the vector multiplets or the hypermultiplets of a theory. The two notions are naturally linked in string theory, where the deformations of the internal geometry of a string compactification are parametrized by the vacuum expectation values of a set of scalars in the resulting low-energy effective description.

The moduli spaces of physical theories come equipped with a natural metric of Euclidean signature, which can be extracted from their action. Consider a d -dimensional gravitational EFT coupled to a set $\{\phi^i\}_{i=1,\dots,I}$ of scalar fields whose vacuum expectation values parametrize a moduli space \mathcal{M} . The metric $g_{ij}^{\mathcal{M}}$ on \mathcal{M} can be read from the kinetic terms of the scalar fields, i.e. it appears as

$$S = \frac{M_{\text{Pl}}^{d-2}}{2} \int d^d x \sqrt{-g} (R - g_{ij}^{\mathcal{M}} \partial_\mu \phi^i \partial^\mu \phi^j). \quad (3.3.1)$$

Using the moduli space metric one can compute the distance $d(P, Q)$ between two vacuum configurations $P, Q \in \mathcal{M}$ as

$$d(P, Q) := \int_{\gamma} \left(g_{ij}^{\mathcal{M}} \frac{\partial \phi^i}{\partial s} \frac{\partial \phi^j}{\partial s} ds \right)^{\frac{1}{2}}, \quad (3.3.2)$$

where γ is the shortest geodesic connecting the two points in the moduli space.

The Swampland Distance Conjecture, originally proposed in [146], is concerned with the way in which gravitational EFTs break down as we traverse an infinite distance in the moduli space. Such infinite-distance directions are conjectured to arise in all gravitational EFTs with a non-trivial moduli space, i.e. as long as \mathcal{M} is not a point. More precisely, the conjecture can be stated in the following way:

Swampland Distance Conjecture [146]

Consider a gravitational EFT with a non-trivial moduli space \mathcal{M} , two points $P, Q \in \mathcal{M}$ with P fixed, and their distance $\Delta\phi := d(P, Q)$. Then Q can be varied such that $\Delta\phi \rightarrow \infty$. Moreover, as we traverse an infinite distance in \mathcal{M} , an infinite tower of states with mass scale M becomes asymptotically massless at an exponential rate, i.e.

$$M(Q) \sim M(P)e^{-\alpha\Delta\phi}, \quad \Delta\phi \rightarrow \infty, \quad \alpha \sim \mathcal{O}(1). \quad (3.3.3)$$

The SDC is closely related to the appearance of dual descriptions at infinite distance in the moduli space, whose fundamental light degrees of freedom are dictated by the asymptotically massless infinite towers. This aspect will become more apparent when we discuss the Emergent String Conjecture, a refinement of the SDC treated in Section 3.4.

Some infinite-distance directions in the moduli space can lead to towers of instantons with asymptotically vanishing action; the metric corrections stemming from such instanton contributions may significantly modify the metric on the moduli space. In particular, a classically infinite-distance point may be rendered a finite-distance point by the effect of the instanton corrections [154, 155]. This theme will be one of the topics of Chapter 4. To give one simple example of this phenomenon, consider the pair given by Type IIA string theory compactified on the quintic and its Type IIB mirror dual. On the Type IIA side, starting from an interior point of the Kähler moduli space close to the large volume regime and going to zero classical volume looks like an infinite-distance trajectory from a classical point of view, but is at finite-distance once the quantum corrections from worldsheet instantons are considered; from the Type IIB side, this simply corresponds to a trajectory from near the large complex structure regime to the conifold point.

The SDC is satisfied in all infinite-distance limits in which it has been tested to date, constituting one of the most robustly established Swampland Conjectures. A rather simple, but nonetheless illustrative, example is given by the circle compactifications of string theory. Such a compactification gives rise to an infinite tower of Kaluza-Klein states and an infinite tower of winding modes, whose radius-dependent masses are given by

$$M_n^2 = \left(\frac{n}{R}\right)^2, \quad M_w^2 = \left(\frac{wR}{\alpha'}\right)^2, \quad n, w \in \mathbb{Z}, \quad (3.3.4)$$

respectively. By explicitly performing the dimensional reduction and going to the Einstein frame in order to extract the moduli space metric, one can check that in the large radius limit $R \rightarrow \infty$ the mass of the Kaluza-Klein states $m_n \rightarrow 0$ at an exponential rate, while in the small radius limit $R \rightarrow 0$ the same occurs for the mass of the winding modes $m_w \rightarrow 0$, in agreement with the expectations from the SDC. Repeating the experiment with Einstein gravity coupled to a massless scalar field, the compactification process only leads to the Kaluza-Klein tower of states. Hence, the small radius limit is not accompanied by an infinite tower of states, indicating that such a gravitational EFT is in the Swampland. The extended nature of strings, allowing them to wind along the internal circle, is what makes the string theory example well-behaved from the SDC point of view. In the small radius limit the local Kaluza-Klein excitations become massive, while the topological winding states become light; this indicates that the theory would be better described by a new set of fundamental degrees of freedom, i.e. that the well-known T-dual frame arises in the $R \rightarrow 0$ infinite distance corner of the moduli space.

In the standard formulation of the SDC, the exponential decay of the mass scale of the relevant tower occurs asymptotically along the infinite-distance trajectory. Hence, it does not

forbid for a large super-Planckian field displacement to occur in the interior of the moduli space, before its asymptotic regions are approached and the exponential decay of the mass scale of the tower is triggered. The Refined Swampland Distance Conjecture (RSDC) was proposed in [243, 244] to precisely address this aspect.

Refined Swampland Distance Conjecture [243, 244]

Consider a gravitational EFT with a non-trivial moduli space \mathcal{M} , two points $P, Q \in \mathcal{M}$ with P fixed, and their distance $\Delta\phi := d(P, Q)$. There exists an infinite tower of states with mass scale M such that

$$M(Q) < M(P)e^{-\alpha\Delta\phi}, \quad \alpha \sim \mathcal{O}(1), \quad (3.3.5)$$

if $\Delta\phi \gtrsim 1$ in Planck units. Moreover, the above statement not only applies for exact moduli, but also for fields with a potential, where the moduli space is replaced with the field space in the effective theory.

Testing that, indeed, the exponential decay in the mass scale of the infinite tower of states sets in after $\Delta\phi \gtrsim 1$ requires accurately computing distances away from the large volume/large complex structure regimes. This has been done for various Type IIA compactifications on one-parameter and two-parameter Calabi-Yau threefolds [5, 245–248], finding agreement with the prediction from the RSDC. While the evidence gathered thus far supports this aspect of the RSDC, further research is needed to establish it on firmer grounds, given the important cosmological implications of forbidding super-Planckian displacements in the inflaton field.

The last part of this refined version of the conjecture claims that its domain of applicability should not only be that of exact moduli spaces, but rather the space of vacua of the theory, which includes the case in which the scalars are subject to a potential. Materializing this claim in the context of four-dimensional compactifications of Type II string theory, this means that the RSDC applies not only to those compactifications preserving $\mathcal{N} = 2$ supersymmetry, but also to the ones exhibiting $\mathcal{N} = 1$ supersymmetry, like the flux compactifications so prevalent in the construction of realistic string models. One way in which the RSDC can be useful in the presence of potentials is by restricting the shape that these can take [249]: The potential of the IR moduli space restricts the pseudo-moduli to move along its valleys. These will generically not correspond to geodesic trajectories of the UV moduli space. If the RSDC is to apply at any energy scale, the valleys of the potential should only allow for trajectories whose deviation from a geodesic of the UV moduli space is small enough that no contradiction with the predicted exponential decay of the mass scale of the infinite tower in terms of the geodesic field displacement arises.

Studying the SDC entails the computation of the moduli space metric, which is non-trivial to obtain beyond the simplest cases. For example, in compactifications of Type IIA string theory on Calabi-Yau threefolds the Kähler moduli space metric expanded around the large volume point can be obtained by computing the periods of the mirror dual around the large complex structure point and then using the mirror map [250, 251]. The resulting expressions need then to be analytically continued to other phases of the Kähler moduli space [245, 246]. An efficient method to extract the Kähler moduli space metric is to exploit the sphere partition function of the gauged linear sigma model [245, 247]. Powerful techniques from asymptotic Hodge theory can be employed to study the periods in a lot of generality; their use in the context of string theory was initiated in [252–254]. The exact diameter of some phases of the Kähler moduli space can be computed by exploiting dualities and modular properties [248], or by making use of

the twisted symmetric square of Picard-Fuchs operators [5]. Infinite-distance limits can also be treated through the theory of semi-stable degenerations as done in [2, 3, 156, 157], an approach that we will develop in plenty of detail in Chapters 5 and 6.

The constant α appearing in the formulation of the SDC is not fixed, but only estimated to be $\alpha \sim \mathcal{O}(1)$. If an example with $\alpha \ll 1$ could be found in contradiction with this expectation, the decrease in the mass scale of the infinite tower could be functionally exponential, while still negligible for a large $\Delta\phi$ range due to the linearization resulting from the small value of α . In every test of the SDC carried out to date this does not occur, and in fact

$$\alpha \geq \frac{1}{\sqrt{d-2}} \quad (3.3.6)$$

in all d -dimensional examples. Hence, $\alpha \sim \mathcal{O}(1)$ seems to be a fair assumption indeed. The proposal that (3.3.6) is the precise lower bound for α , motivated by the fact that it is preserved under dimensional reduction and from example-based evidence, is known as the *Sharpened Distance Conjecture* [255]. In fact, it seems that (3.3.6) is saturated if and only if the infinite-distance limit is an emergent string limit, more on this in Section 3.4.

Weak coupling limits correspond to infinite-distance limits in all known examples; this is expected to be a general feature, but no proof of it exists yet. Nonetheless, this would provide a clear link between the SDC and the WGC: Taking a weak coupling limit implies an infinite-distance limit, which by the SDC is accompanied by an asymptotically massless infinite tower of states. In string theory examples, one can identify a sub-tower of superextremal states of the SDC tower as the one predicted by the Tower and Sublattice WGCs. While the SDC and the WGC are two distinct conjectures, it would be interesting to understand to which extent they are related to each other. There are proposals that go in the opposite direction, claiming that every infinite-distance limit results in a global symmetry being restored due to a p -form gauge coupling going to zero [256], but it is not clear how this is realized in those infinite-distance limits in which the SDC tower is not charged, e.g. in the strong coupling limit of $E_8 \times E_8$ heterotic string theory.

A rich scenario for the exploration of the SDC is that of theories with an AdS background. One can deform such a theory by varying the value of the cosmological constant, or by maintaining it fixed. The first possibility is the one with which the *AdS Distance Conjecture* is concerned [257]. It generalizes the core idea of the SDC by claiming that the limit of vanishing cosmological constant in discrete families of vacua, which is at infinite distance in the metric configuration space, is also accompanied by an asymptotically massless infinite tower of states. In its strongest forms, it forbids AdS vacua with scale separation. This is in agreement with known examples except for the DGKT class of vacua [258], whose validity is presently under discussion [259–263]. The second possibility has been analysed using holography, leading to the *CFT Distance Conjecture* [264, 265], which posits that there is an equivalence between higher-spin and infinite-distance points in the conformal manifold. That the former imply the latter has been proven in [266].

The (R)SDC can have phenomenological implications for particle physics and cosmology. For example, photons could have a technically natural small mass not originating from the Higgs mechanism and consistent with current experimental bounds. Such a mass term can be written in Stückelberg form and, since it is allowed by current observations, a careful EFT model should include it. However, the massless photon point would then lie at infinite-distance in field space, and the phenomenological constraints imply that the infinite tower of states predicted by the SDC would decrease the cut-off scale of the EFT beyond what is empirically allowed. As a consequence, the photon of the Standard Model must be exactly massless, and the

mass of dark photons is constrained to stem mostly from Higgs, rather than S \ddot{u} ckelberg, mass terms [267]. In cosmology, the (R)SDC can constrain inflationary models, since big values of the tensor-to-scalar ratio imply large field excursions due to the Lyth bound, in tension with the constraint pointing in the opposite direction obtained from the (R)SDC [268, 269].

3.4 Emergent String Conjecture

The SDC predicts that an infinite tower of states becomes asymptotically massless at an exponential rate as we traverse an infinite-distance trajectory in the moduli space, but it does not predict the nature of the states that furnish said tower. As illustrated above through the circle compactification example, the SDC tower seems to correspond to the light fundamental degrees of freedom of a dual frame arising in the relevant asymptotic region of the moduli space. Hence, knowing the types of states that form the infinite tower is relevant in order to determine the nature of the theories that we encounter at infinite distance.

In infinite-distance limits, more than one infinite tower of states can become asymptotically massless. The theories found in the asymptotic regions of the moduli space are determined by the parametrically lightest tower along the corresponding infinite-distance limit; these are the towers that we need to characterize in order to answer the questions raised above. The simplest of examples in string theory already exhibit two very different types of SDC towers.

Deccompactification limits: Consider a circle compactification of string theory and take the large radius limit $R \rightarrow \infty$. The parametrically lightest tower along this infinite-distance limit is the one furnished by the Kaluza-Klein modes. Their mass, printed in (3.3.4) as a dimensionful quantity, must be compared to the lower-dimensional Planck scale, which leads to

$$\frac{M_n^2}{M_{\text{Pl},d}^2} = \left(\frac{1}{2\pi R} \right)^{\frac{2}{7}} \left(\frac{n}{R} \right)^2. \quad (3.4.1)$$

In the limit considered, the KK tower becomes massless and the circle direction decompactifies. Analysing the small radius limit $R \rightarrow 0$ leads to analogous conclusions for the infinite tower of states populated by the winding modes; the trajectory in moduli space still corresponds to a decompactification limit, but this interpretation becomes transparent only after applying T-duality, which transforms the winding tower into a KK tower.

Hence, decompactification limits are those in which the parametrically leading asymptotically massless tower is furnished by Kaluza-Klein modes, possibly in a dual sense, presenting linearly spaced masses

$$M_n \sim |n| M_0. \quad (3.4.2)$$

These limits result in higher-dimensional theories.

Emergent String Limits: Consider superstring theory in ten dimensions. The relation between the Planck mass M_{Pl} and the string scale M_s is

$$M_s = g_s^{1/4} M_{\text{Pl}}, \quad (3.4.3)$$

where g_s is the string coupling. The mass of the excited string states in Planck units is then

$$\frac{M_N^2}{M_{\text{Pl}}^2} \sim N g_s^{1/2}, \quad (3.4.4)$$

where N is the level of the state. In the weak string coupling limit $g_s \rightarrow 0$, the asymptotically massless infinite tower is given by the excitations of the fundamental string. Particularizing the example to Type IIB string theory, it is clear that we can use S-duality to translate this into a limit in which the SDC tower is given by the excitations of the D1-string instead. The term *critical string* refers, in the context of infinite-distance limits, to any string that can be regarded as the fundamental string in some appropriate duality frame, even if this is usually left implicit.

Emergent string limits are those in which the parametrically leading asymptotically massless tower is furnished by the excitations of a unique, weakly coupled, asymptotically tensionless critical string, which leads to masses spaced like

$$M_N \sim \sqrt{N} M_0. \quad (3.4.5)$$

In $d \leq D_{\text{crit}}$ dimensions, where D_{crit} stands for the critical dimension appropriate to the type of critical string characterizing the limit under consideration, the tower of string excitations is accompanied by a Kaluza-Klein tower at the same parametric scale, but exhibiting the coarser spacing (3.4.2). These limits are equidimensional, leading to a duality frame determined by the critical string whose excitations populate the parametrically leading tower.

The Emergent String Conjecture (ESC), proposed in [149], claims that the two types of infinite-distance limits just discussed are the only allowed possibilities in a gravitational EFT that can be consistently UV completed to a theory of quantum gravity.

Emergent String Conjecture [149]

Consider a gravitational EFT with a non-trivial moduli space \mathcal{M} . All infinite-distance limits in \mathcal{M} are either decompactification or emergent string limits.

This is a non-trivial refinement of the SDC: The ESC could fail in a variety of ways while not endangering the validity of the SDC, as we now review.

One conceivable violation of the ESC remaining compatible with the SDC would occur if an infinite-distance limit is not dominated by Kaluza-Klein replicas or a tensionless string, e.g. if we have asymptotically tensionless membranes. The possibility of having *membrane limits* was investigated in [1], and will be the subject of Chapter 4. We concluded that, after quantum corrections are properly taken into account, membranes parametrically decouple from the Kaluza-Klein scale.

A different possibility would be for the tensionless string characterizing the infinite-distance limit to not be weakly coupled and critical. These types of limits can occur in the moduli space, but are always found at finite distance. The tensionless E-strings associated with the 6D SCFTs arising as finite-distance non-minimal codimension-two singularities in six-dimensional F-theory are one such example [270].

The ESC also posits that in an emergent string limit there cannot be two or more weakly coupled, critical strings becoming tensionless at leading parametric scale. This has been explicitly addressed in the Kähler moduli space of five-dimensional M-theory [149]: The choice of M-theory was motivated by the fact that it is not a theory of strings, making the tests of the ESC as non-trivial as possible. In this context, equidimensional infinite-distance limits arise if the internal Calabi-Yau threefold has a fibration structure, allowing for the fiber to shrink and the base to grow at fixed overall volume. The weakly coupled, asymptotically tensionless critical string corresponds to extended objects wrapped on the shrinking fiber. The only possibilities are proven to be Type T^2 , Type K3 and Type T^4 emergent string limits, the nomenclature

reflecting the type of fiber shrinking along the infinite-distance trajectory. Having two such strings competing along an infinite-distance limit would geometrically correspond to the existence of two incompatible fibration structures whose fibers shrink at the same rate. This was proven to not occur through a very non-trivial uniqueness result; when one tries to force the situation, the geometry singles out a different, unique fibration shrinking at the fastest rate. The fact that the emergent string is unique makes the duality frame that it determines well-defined, showing that the ESC captures something non-trivial about the appearance of dual descriptions in the asymptotic corners of the moduli space.

Emergent string limits in $d < D_{\text{crit}}$ must present an asymptotically massless KK tower at the same parametric scale as the emergent string. Putative infinite-distance limits in which this does not occur, such that the emergent string parametrically decouples from the lightest KK tower, are known as *pathological string limits*. They are expected to be forbidden, since otherwise their endpoint would be a lower-dimensional critical string theory. However, the way in which they are prevented can be subtle. For example, one can find pathological string limits in the classical hypermultiplet moduli space of four-dimensional Type IIB string theory. These are only removed once worldsheet and D-instanton quantum corrections to the metric of the hypermultiplet moduli space are properly taken into account [154, 155]. Section 4.4 is devoted to the review of this class of naively pathological string limits.

The ESC has been subjected to non-trivial tests in various corners of the moduli space, always finding agreement with its postulates. This includes in the Kähler moduli space of F/M/IIA-theory in 6D/5D/4D in [149, 271–273], in the hypermultiplet moduli space of F-theory in 8D in [156, 157], in the 4D $\mathcal{N} = 2$ hypermultiplet moduli space of Type IIB in [154, 155], in M-theory on G_2 manifolds in [274], in 4D $\mathcal{N} = 1$ F-theory in [153, 275], in toroidal compactifications of the heterotic and CHL strings [276, 277], and in the context of non-supersymmetric string theories [278]. We studied the ESC in the hypermultiplet moduli space of six-dimensional F-theory in [2, 3], an analysis to which Chapters 5 and 6 are devoted.

The nature of the asymptotically massless towers has consequences for the coefficient α appearing in the (R)SDC [279, 280]. In fact, there are arguments motivating the precise bound (3.3.6) on α proposed by the Sharpened SDC by assuming the ESC [141]. First, one notes that, since emergent string limits are characterized by a unique, weakly coupled, asymptotically tensionless critical string, they are described in the appropriate duality frame by a fixed worldsheet theory with a coupling that goes to zero. Writing the corresponding effective d -dimensional spacetime action in string frame and comparing it with its Einstein frame counterpart, one can deduce that the mass of the excitations of the critical string measured in d -dimensional Planck units decreases exponentially with $\alpha = 1/\sqrt{d-2}$, and that this is universal for all emergent string limits. Second, the decompactification limit corresponding to only varying the overall volume modulus of a $(D-d)$ -dimensional internal space has $\alpha = \sqrt{(D-2)/[(D-d)(d-2)]}$. This value is always bigger than the one found for an emergent string limit. Moreover, in the asymptotic region of the moduli space associated with the decompactification to the D -dimensional theory, the limit in which only the overall volume modulus is varied is the most efficient, since it avoids any changes to the moduli that do not affect the relevant KK tower; hence, the associated value of α is the biggest one in that asymptotic direction of the moduli space. The smallest value for α in that chamber of the moduli space must be at the boundary of the region in which the asymptotics correspond to the D -dimensional theory, but according to the ESC this must be either an emergent string limit or a decompactification limit to a theory in more than D dimensions. Iterating the argument, one arrives at either a rigid decompactification limit

corresponding to an overall volume modulus, in which case $\alpha > 1/\sqrt{d-2}$, or at an emergent string limit, in which case $\alpha = 1/\sqrt{d-2}$.

This has, in turn, consequences for the slope of the species scale Λ_s . The asymptotically massless infinite tower of states predicted by the SDC along an infinite-distance limit contributes light-species that lower the quantum gravity cut-off. This occurs at an exponential rate as we approach the boundaries of the moduli space. Assuming the ESC, and using the previous arguments to constrain α , one concludes that the slope of the species scale is bounded from above by the slope corresponding to emergent string limits, i.e. [237, 238]

$$\frac{|\nabla \Lambda_s|^2}{\Lambda_s^2} \leq \frac{1}{d-2} \frac{1}{M_{\text{Pl}}^{d-2}}. \quad (3.4.6)$$

Part III

Membranes at Infinite Distance

Chapter 4

Membrane Limits in Quantum Gravity

The Emergent String Conjecture was introduced in Section 3.4. It predicts that infinite-distance limits in the moduli space of quantum gravity are accompanied by a tower of light states that either induce a decompactification or correspond to the emergence of a unique, weakly coupled, asymptotically tensionless critical string. In this chapter, we study the consistency conditions implied by this conjecture on the asymptotic behaviour of quantum gravity under dimensional reduction. If the emergent string descends from a $(1+2)$ -dimensional membrane in a higher-dimensional theory, we find that such a membrane must parametrically decouple from the Kaluza-Klein scale. We verify this censorship against emergent membrane limits, where the membrane would sit at the Kaluza-Klein scale, in the hypermultiplet moduli space of Calabi-Yau threefold compactifications of string/M-theory. At the classical level, a putative membrane limit arises, up to duality, from an M5-brane wrapping the asymptotically shrinking special Lagrangian 3-cycle corresponding to the Strominger-Yau-Zaslow fiber of the Calabi-Yau. We show how quantum corrections in the moduli space obstruct such a limit and instead lead to a decompactification to eleven dimensions, where the role of the M5- and M2-branes are interchanged. These results are further evidence that infinite-distance trajectories in the moduli space can only correspond to decompactification or emergent string limits.

4.1 Introduction

As reviewed in Section 3.1, the Swampland Program [102] aims to delineate the boundary between the landscape (the set of those gravitational EFTs that can be consistently completed to a theory of quantum gravity) and the swampland (the set of those that cannot). One of the theorised Swampland Constraints that should allow us to distinguish between these two regions of theory space is the Emergent String Conjecture [149], discussed in Section 3.4. This conjecture is a refinement of the Swampland Distance Conjecture, see Section 3.3, proposing that infinite-distance limits in moduli space either are pure decompactification limits or signal a transition to a duality frame determined by a unique emergent critical weakly coupled string such that $T_{\text{str}} \sim M_{\text{KK}}^2$. Here, we concern ourselves with the constraints that the ESC imposes on the asymptotic behaviour of quantum gravity under dimensional reduction, its validity in the hypermultiplet moduli space of five-dimensional M-theory, and the (im)possibility of realising infinite-distance membrane limits.

Carefully including quantum corrections in concrete string theory and M-theory models can be crucial to find not only quantitative, but qualitative, agreement with the Swampland Conjectures. In the context of the ESC, their effect, both in the vector multiplet and hypermultiplet moduli

spaces, is to remove pathological string limits in which $T_{\text{str}} \prec M_{\text{KK}}^2$.¹ Such limits are expected to be impossible in the landscape, as otherwise one could decouple the Kaluza-Klein (KK) scale and obtain genuinely lower-dimensional critical string theories. The quantum obstruction to pathological string limits in the hypermultiplet moduli space of four-dimensional Type IIB was studied in [154, 155]. Similarly, quantum corrections will prove to be essential too in our analysis of the ESC below.

In the present chapter we analyse infinite-distance limits in the hypermultiplet moduli space of M-theory on a Calabi-Yau threefold X in which, classically, a distinguished membrane becomes light at the same rate as the KK scale. Such putative limits will be called (emergent) membrane limits. We find that quantum corrections forbid these limits, deflecting them into trajectories in which the membrane always sits at a scale parametrically higher than the KK scale, as is characteristic for a decompactification of the theory.

Our motivation for this study is twofold. The first motivation is to challenge the Emergent String Conjecture by trying to construct limits in which an object different from a critical string becomes equally light as the KK scale. The natural candidate for such an object would indeed be a membrane which is as close to being “critical” as possible, in the sense that at least under dimensional reduction it becomes a critical string. What we have in mind is a situation similar to the one for the M2-brane in eleven-dimensional M-theory. Even if realisable, emergent membrane limits would presumably still qualify as decompactification limits since, unlike a critical string, the membrane is not expected to give rise to a dense tower of particle excitations. However, if they existed, we could start in the interior of the moduli space, where the KK scale and the tension of the M2-brane are comparable, and move to an infinite-distance point, where again a (dual) membrane sits at the same scale as the effective KK scale. In this sense, we would encounter essentially the same theory at infinite distance—analogous to what happens for emergent string limits in the hypermultiplet moduli space of Type II string theory [155]. We find it intriguing that gravity censors the appearance of such emergent membrane limits in the quantum moduli space.

The second motivation is to investigate the implications of the Emergent String Conjecture upon dimensional reduction. As it turns out, the observed quantum obstruction against a membrane limit is a consequence of the Emergent String Conjecture in the theory obtained by dimensional reduction. More precisely, emergent membrane limits would lead, under further compactification on an M-theory circle, to pathological string limits in which $T_{\text{str}} \prec M_{\text{KK}}^2$. The quantum obstruction to these limits must therefore already be at work for the membranes in the five-dimensional M-theory setting. In this sense, the Emergent String Conjecture acts as a censor against emergent membrane limits in one dimension higher.

To provide a realisation of this quantum obstruction to membrane limits we exploit a useful fact: The hypermultiplet moduli space of M-theory on $\mathbb{R}^{1,4} \times X$ is identical to that of Type IIA string theory on $\mathbb{R}^{1,3} \times X$. This implies, after mirror symmetry, an identification of the emergent string limits of [154, 155] with the trajectories of the membrane limits under consideration, allowing us to translate the effect of the quantum corrections from one setting to the other. This leads to the conclusion that the putative membrane limits are quantum obstructed and the five-dimensional M-theory undergoes a decompactification limit instead. The situation is depicted in Figure 4.1.

The structure of the chapter is the following. In Section 4.2 we discuss how consistency under dimensional reduction for the Emergent String Conjecture forbids the existence of limits

¹By writing $A \precsim B$, we mean that $\lim(A/B) < \infty$, i.e. the two quantities either scale in the same way with respect to a limiting parameter or B is parametrically dominating A ; similarly, $A \prec B$ means $\lim(A/B) = 0$.

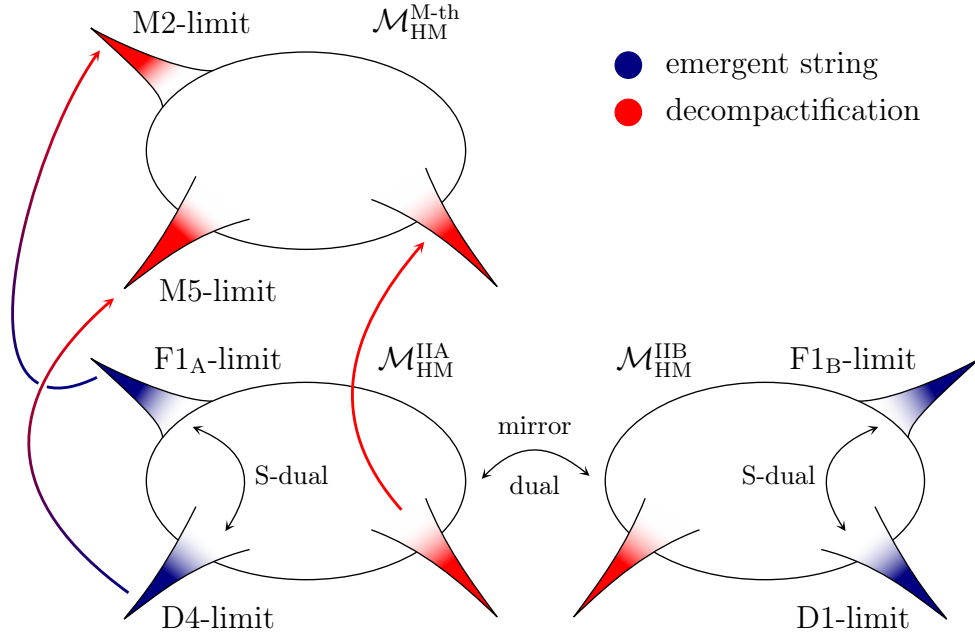


Figure 4.1: Under the identification of the 5D M-theory and 4D Type IIA hypermultiplet moduli spaces, the quantum corrected emergent string limits of [154, 155] correspond to decompactification limits in M-theory.

in which a “critical” membrane becomes light at the same rate as the KK scale. Section 4.3 gives a review of the hypermultiplet moduli space of five-dimensional M-theory and analyses the type of scalings needed in said moduli space to give rise to a classical membrane limit. In Section 4.4 we review the Type IIB hypermultiplet moduli space limits of [154, 155]. In Section 4.5 we translate these limits to the Type IIA setting via mirror symmetry and make contact with the five-dimensional M-theory limits through the identification of the corresponding hypermultiplet moduli spaces. Section 4.6 analyses how quantum corrections obstruct the classical membrane limits and instead lead to a decompactification of the theory. We conclude with a summary in Section 4.7.

4.2 Consistency under dimensional reduction

Consistency under dimensional reduction has served as a fruitful guiding principle for formulating swampland conjectures, most prominently in the context of the Weak Gravity Conjecture [138, 219–222, 281–283]. Here we would like to address the following question:

Is the Emergent String Conjecture consistent under dimensional reduction?

Suppose we have a theory in D dimensions and fix an infinite-distance limit in its moduli space. Denote by $M_{\text{KK}}^{(D)}$ the mass scale of the lightest KK tower in the limit and assume that $M_{\text{KK}}^{(D)}/M_{\text{Pl}}^{(D)} \rightarrow 0$ asymptotically. Denote furthermore by $T_{\text{str}}^{(D)}$ the tension of the lightest *critical* string in the limit. The Emergent String Conjecture predicts that $T_{\text{str}}^{(D)} \gtrsim (M_{\text{KK}}^{(D)})^2$ asymptotically. Under compactification on a circle of constant radius, as measured in units of the D -dimensional Planck scale, this relation will be preserved. In addition, the string will generate a tower of winding states on the circle. These will however not lead to any inconsistency.

The situation is different if, instead of a critical string, we consider a membrane with a (1+2)-dimensional worldvolume in the D -dimensional theory. Let us denote the tension of the lightest such brane by $T_{\text{brane}}^{(D)}$. Assuming the existence of such a brane in the D -dimensional theory, its infinite-distance limits will be characterised by the dimensionless parameter

$$\mu = \frac{T_{\text{brane}}^{(D)}}{(M_{\text{KK}}^{(D)})^3}. \quad (4.2.1)$$

After compactification, the membrane will lead to a new string of tension $T_{\text{str}}^{(D-1)} = R_{S^1} \cdot T_{\text{brane}}^{(D)}$ from wrapping the brane on the S^1 of radius R_{S^1} . In the sequel it is always understood that the membrane under consideration has the special property that the string obtained in this way is a critical string. We will sometimes call such objects *critical membranes*.

The special case $\mu = \text{const.}$ could be called an “emergent membrane” limit. The reader will object that, unlike a critical string, a membrane is not expected to give rise to an infinite tower of particle-like excitations and hence the special nature of such a regime might be dubious. Thus, such a limit should be classified as a decompactification limit in view of the Emergent String Conjecture. We will see, however, that the existence of an emergent membrane limit can potentially lead to trouble with the Emergent String Conjecture in lower dimensions.

In the dimensionally reduced theory, the Emergent String Conjecture imposes the scaling $T_{\text{str}}^{(D-1)} \gtrsim (M_{\text{KK}}^{(D-1)})^2$. For a circle of constant radius of order one in units of $M_{\text{Pl}}^{(D)}$, $M_{\text{KK}}^{(D-1)} \sim M_{\text{KK}}^{(D)}$. This gives rise to a non-trivial constraint on admissible limits in the D -dimensional theory:²

$$\begin{aligned} \frac{T_{\text{str}}^{(D-1)}}{(M_{\text{KK}}^{(D-1)})^2} &\sim \frac{T_{\text{brane}}^{(D)} \cdot R_{S^1}}{(M_{\text{KK}}^{(D)})^2} = \frac{T_{\text{brane}}^{(D)}}{(M_{\text{KK}}^{(D)})^3} \cdot \frac{M_{\text{KK}}^{(D)}}{M_{\text{KK}}^{S^1}} \\ &\sim \mu \cdot \frac{M_{\text{KK}}^{(D)}}{M_{\text{KK}}^{S^1}} = \mu \cdot \frac{M_{\text{KK}}^{(D)}}{M_{\text{Pl}}^{(D)}} \cdot \frac{M_{\text{Pl}}^{(D)}}{M_{\text{KK}}^{S^1}} \sim \mu \cdot \frac{M_{\text{KK}}^{(D)}}{M_{\text{Pl}}^{(D)}} \gtrsim 1. \end{aligned} \quad (4.2.2)$$

Since the KK scale is assumed to approach zero in the D -dimensional theory, it is necessary that $\mu \rightarrow \infty$ in the limit. Hence, we find that the Emergent String Conjecture predicts a censorship of infinite-distance limits in a higher-dimensional theory where a critical membrane sits at the same scale as (or below) the KK tower.

In the saturated case of an emergent string limit in the dimensionally reduced theory, $T_{\text{str}}^{(D-1)} \sim (M_{\text{KK}}^{(D)})^2$, we can extract the following scaling in the D -dimensional theory from (4.2.2):

$$\left(\frac{M_{\text{KK}}^{(D)}}{M_{\text{Pl}}^{(D)}} \right)^3 \sim \frac{1}{\mu^3}, \quad \frac{T_{\text{brane}}^{(D)}}{(M_{\text{Pl}}^{(D)})^3} \sim \frac{1}{\mu^2}. \quad (4.2.3)$$

In the remainder of this article, we will explore how this censorship is realized quantitatively in the five-dimensional setting of M-theory compactified on a Calabi-Yau threefold.

4.3 Classical membrane limits in M-theory

In this section we briefly review the moduli space of M-theory compactified on a Calabi-Yau threefold and we analyse the conditions that need to be met to engineer classical membrane limits.

²Clearly, one can also consider limits in which the circle radius scales with respect to $M_{\text{Pl}}^{(D)}$, but the fact that we run into a constraint for the current limit is already enough for our argument.

4.3.1 The moduli space of M-theory on Calabi-Yau threefolds

M-theory compactified on a Calabi-Yau threefold gives rise to a five-dimensional $\mathcal{N} = 2$ supergravity theory containing a number of hypermultiplets and vector multiplets whose scalar fields parametrise the deformations of the internal space. Such a dimensional reduction of eleven-dimensional supergravity was carried out in [284].

In $D = 11$ the bosonic field content is given by the metric $G_{\hat{\mu}\hat{\nu}}$ and a 3-form gauge field $C_{\hat{\mu}\hat{\nu}\hat{\rho}}$. Upon dimensional reduction on a Calabi-Yau threefold X with Hodge numbers $(h^{1,1}, h^{2,1})$ we obtain $h^{1,1} - 1$ vector multiplets and $h^{2,1} + 1$ hypermultiplets. In the following we denote the splitting of indices by $\hat{\mu} = (\mu, i, \bar{i})$ ($\mu = 1, \dots, 5$, $i, \bar{i} = 1, 2, 3$).

The scalar components of the vector multiplets parametrising the moduli space are accounted for by the (real) scalars $G_{i\bar{j}}$ except for the overall volume of X , which in five-dimensional M-theory decouples from the vector multiplets. If we denote by M_Λ the Kähler coordinates in the decomposition of the Kähler form, the vector multiplet moduli space coordinates would be given by $t_\Lambda = M_\Lambda / \mathcal{V}^{\frac{1}{3}}$ subject to the constraint $\mathcal{V}(t_\Lambda) = 1$, i.e. the vector multiplet moduli space of five-dimensional M-theory is a hypersurface cut from the real projection of that of Type IIA string theory.

The volume scalar \mathcal{V} , the real scalar $C_{\mu\nu\rho}$ and the complex scalar $C_{ijk} = \epsilon_{ijk}D$ conform the four scalar degrees of freedom of the universal hypermultiplet $(\mathcal{V}, C_{\mu\nu\rho}, D)$. The remaining $h^{2,1}$ hypermultiplets are accounted for by the complex scalars $(G_{ij}, C_{i\bar{j}})$.

4.3.2 Classical membrane limits

We would like to investigate if it is possible to engineer infinite-distance limits in the hypermultiplet moduli space of five-dimensional M-theory along which a critical membrane in the sense defined in Section 4.2 becomes exponentially light at the same rate as the KK scale. In analogy with [149, 153] we would call them emergent membrane limits.

We will consider trajectories involving only the volume scalar \mathcal{V} and the complex structure moduli z^a , $a = 1, \dots, h^{2,1}$, of X . Varying z^a will affect the volume of certain 3-cycles. We denote the 3-cycles with the slowest and fastest scaling along the limit by \mathcal{A} and \mathcal{B} , respectively. Then, the mass scales of the membranes and KK modes in the theory compare to the five-dimensional Planck scale as

$$\frac{T_{M2}}{(M_{\text{Pl}}^{5D})^3} \sim \frac{1}{\mathcal{V}_X^{11D}} \sim \left(\frac{T_{M5}}{(M_{\text{Pl}}^{5D})^6} \right)^{\frac{1}{2}}, \quad (4.3.1a)$$

$$\frac{T_{M5|_{\mathcal{A}}}}{(M_{\text{Pl}}^{5D})^3} \sim \mathcal{V}_{\mathcal{A}}^{11D} \frac{1}{\mathcal{V}_X^{11D}}, \quad (4.3.1b)$$

$$\left(\frac{M_{\text{KK}}}{M_{\text{Pl}}^{5D}} \right)^3 \sim \min \left(\frac{1}{\mathcal{V}_{\mathcal{B}}^{11D}}, \left(\frac{1}{\mathcal{V}_X^{11D}} \right)^{\frac{1}{2}} \right) \frac{1}{\mathcal{V}_X^{11D}}, \quad (4.3.1c)$$

where all the volumes are measured in eleven-dimensional units. At the classical level, we can distinguish two scenarios:

- **M2-limit:** The unwrapped M2-brane becomes light at the same rate as the KK modes, which happens if³

$$\mathcal{V}_{\mathcal{B}}^{11D} \sim \text{constant}. \quad (4.3.2)$$

³This condition follows straightforwardly from (4.3.1c) if the minimal KK scale comes from \mathcal{B} . If the minimal KK scale instead comes from X , it follows that $\mathcal{V}_X^{11D} \sim 1$ and hence $\mathcal{V}_{\mathcal{B}}^{11D} \asymp 1$. If \mathcal{B} is shrinking, so must be all

- **M5-limit:** The M5-brane wrapped on the \mathcal{A} -cycle becomes light at the same rate as the KK modes, which requires that

$$\mathcal{V}_{\mathcal{A}}^{11D} \sim \frac{1}{\mathcal{V}_{\mathcal{B}}^{11D}} \quad \text{or} \quad \mathcal{V}_{\mathcal{A}}^{11D} \sim \left(\frac{1}{\mathcal{V}_X^{11D}} \right)^{\frac{1}{2}}. \quad (4.3.3)$$

In order for the membrane obtained by wrapping the M5-brane on the \mathcal{A} -cycle to correspond to a critical membrane (i.e. one which gives rise to a critical string once wrapped on a circle), the \mathcal{A} -cycle must be a special Lagrangian three-torus [285]. This will become particularly clear from the perspective of the dual Type IIA string theory in Section 4.5.

Obtaining membrane limits is therefore classically possible. However, the hypermultiplet moduli space of five-dimensional M-theory receives quantum corrections that could deflect the chosen trajectories, modifying their properties such that the membrane no longer becomes light at the same rate as the KK modes.

A similar phenomenon was observed for infinite-distance limits in the hypermultiplet moduli space of Type IIB string theory in [154, 155]. There, the D1-limit presented an infinite-distance trajectory along which classically a D1-string became tensionless faster than the KK scale. Such behaviour is expected to be forbidden after taking quantum corrections into account, as otherwise we would be able to decouple both scales and obtain critical four-dimensional strings with an infinite number of oscillation modes. Indeed, the authors found that including the relevant effects due to D(-1)- and D1-instantons modified the trajectory in such a way that both scales became light at the same rate, yielding an emergent string limit. Similar quantum obstructions to pathological string limits in the vector multiplet moduli space of Type II theories were analysed in [149] and for 4D $\mathcal{N} = 1$ theories in [153].

Given the above, we need a way to take into account the quantum corrections to the hypermultiplet moduli space of five-dimensional M-theory. Our strategy will be to first study the problem in the hypermultiplet moduli space of Type IIA string theory and to then translate the results to the M-theory setup.

4.4 Review: Type IIB hypermultiplet limits

The quantum corrections to the hypermultiplet moduli space of Type II string theories compactified on Calabi-Yau threefolds have been extensively studied in the literature; see [168, 169] and references therein. In the settings in which only mutually local D-instantons contribute, the quantum-corrected metric for the hypermultiplet moduli space can be given explicitly.⁴ This fact was exploited in [154, 155], where all the limits fall in this category.

We are investigating limits in the hypermultiplet moduli space of M-theory on $\mathbb{R}^{1,4} \times X$. Since the radius of the M-theory circle, measured in five-dimensional Planck units, sits in a vector multiplet from the point of view of the dimensionally reduced theory, this moduli space coincides with the hypermultiplet moduli space of Type IIA string theory on $\mathbb{R}^{1,3} \times X$ [288]. By then exploiting mirror symmetry to Type IIB on $\mathbb{R}^{1,3} \times Y$ we will be able to translate the quantum corrections computed in [154, 155] to the membrane limits under consideration.

other 3-cycles since by assumption \mathcal{B} has the fastest scaling. In order to avoid a contradiction with $\mathcal{V}_X^{11D} \sim 1$, we should therefore again require $\mathcal{V}_{\mathcal{B}}^{11D} \sim 1$.

⁴This metric was first computed in [286]. See also [287] for a recent mathematical treatment of quaternionic Kähler metrics including the case of the hypermultiplet metric with mutually local D-instanton corrections.

We would like to stress that the relation between the limits is at the level of the trajectories in the respective hypermultiplet moduli spaces, once viewed as hypermultiplets of the four-dimensional Type IIA compactification on X and once as those of the five-dimensional M-theory compactification. In the first case, the trajectories describe emergent string limits, while the nature of the limit in the second case is the subject of our investigation. We will elaborate on this point more in Section 4.5.2.

In this section we review the results of [154, 155] on emergent string limits in the hypermultiplet moduli space of Type IIB string theory and the quantum corrections they receive. At the end we also comment on the reasons behind focusing on the class of limits under consideration here.

4.4.1 Type II hypermultiplet moduli spaces

To fix notation, let us list the scalars parametrising the hypermultiplet moduli space of Type II string theories. Excellent reviews on said moduli spaces and the quantum corrections that they receive can be found in [168, 169].

For Type IIB string theory on a Calabi-Yau threefold Y we have $h^{1,1}(Y) + 1$ hypermultiplets with the following bosonic content:

$$\text{universal hypermultiplet: } (\tau_{\text{IIB}}, b^0, c^0), \quad (4.4.1a)$$

$$h^{1,1}(Y) \text{ hypermultiplets: } (z_{\text{IIB}}^a, c^a, d^a). \quad (4.4.1b)$$

Here $\tau_{\text{IIB}} = C_0 + ie^{-\phi_{\text{IIB}}} = \tau_1^{\text{IIB}} + i\tau_2^{\text{IIB}}$ is the ten-dimensional Type IIB axio-dilaton and b^0 and c^0 are the axions dual to the four-dimensional components of the B_2 and C_2 2-forms respectively. Furthermore, $z_{\text{IIB}}^a = b^a + it^a$ are the complexified Kähler moduli for the decomposition of the Kähler form over a basis $\{\gamma_{\text{IIB}}^a\}$ of 2-cycles and c^a and d^a are two axions related to the integrals of the C_2 and C_4 forms over the same basis of 2-cycles.

Defining the four-dimensional dilaton by

$$(M_{\text{Pl}}^{\text{4D}})^2 = 4\pi e^{-2\varphi_4} M_s^2 = 2\pi(\tau_2^{\text{IIB}})^2 \mathcal{V}_Y(t^a) M_s^2 \quad (4.4.2)$$

we have appropriate coordinates to express the classical hypermultiplet moduli space metric as

$$ds_{\mathcal{M}_{\text{HM}}^{\text{IIB}}}^2 = \frac{1}{2} (\varphi_4)^2 + g_{a\bar{b}} dz_{\text{IIB}}^a d\bar{z}_{\text{IIB}}^b + (\text{axions}). \quad (4.4.3)$$

Corresponding to the membrane limits with which we would like to make contact, and as in the trajectories considered in [154, 155], we will keep the axions set to zero.

Type IIA string theory compactified on a Calabi-Yau threefold X presents $h^{2,1}(X) + 1$ hypermultiplets, whose bosonic content is as follows:

$$\text{universal hypermultiplet: } (\phi_{\text{IIA}}, \sigma, \zeta^0, \tilde{\zeta}_0), \quad (4.4.4a)$$

$$h^{2,1}(X) \text{ hypermultiplets: } (z_{\text{IIA}}^a, \zeta^a, \tilde{\zeta}_a). \quad (4.4.4b)$$

Here ϕ_{IIA} is the ten-dimensional Type IIA dilaton, σ is the Neveu-Schwarz axion dual to the four-dimensional 2-form B_2 and ζ^0 and $\tilde{\zeta}_0$ are obtained by integrating the 3-form C_3 over the 3-cycle γ^0 dual to the unique holomorphic $(3,0)$ -form Ω_X of X and its symplectic pair γ_0 respectively. The remaining $h^{2,1}(X)$ hypermultiplets involve the complex structure moduli $z_{\text{IIA}}^a = X^a/X^0$, where (X^0, X^a) are the Ω_X periods of X . Finally, ζ^a and $\tilde{\zeta}_a$ are obtained by integrating C_3 over the A- and B-cycles conforming the $\{\gamma_{\text{IIA}}^a, \gamma_a^{\text{IIA}}\}$ basis of $(1,2)$ - and $(2,1)$ -cycles.

The four-dimensional dilaton is defined by

$$(M_{\text{Pl}}^{\text{4D}})^2 = 4\pi e^{-2\varphi_4} M_s^2 = \pi \mathcal{R}^2 K(z_{\text{IIA}}^a, \bar{z}_{\text{IIA}}^a) M_s^2, \quad (4.4.5)$$

where \mathcal{R} is related to the ten-dimensional Type IIA string coupling as displayed in (4.5.1). The classical hypermultiplet moduli space metric is *mutatis mutandis* the same as (4.4.3). Again, the axions will be set to zero in the following. Throughout the text we will denote the string coupling by $g_{\text{IIA(B)}} = 1/\tau_2^{\text{IIA(B)}}$.

4.4.2 Classical string limits

Out of the limits in the hypermultiplet moduli space of Type IIB string theory discussed in [154, 155] we are interested in recalling the properties of the D1- and F1-limits, which we will later identify with the M5- and M2-limits, respectively.

D1-limit: The classical D1-limit corresponds to a strong coupling, large volume limit in which the 2-cycles of Y are uniformly scaled.⁵ More concretely, the scaling along the trajectory is given by

$$\text{D1: } g_{\text{IIB}} \sim \lambda^{\frac{3}{2}}, \quad t^a \sim \lambda, \quad \lambda \rightarrow \infty. \quad (4.4.6)$$

The object becoming massless at the fastest rate, in the classical limit, is the D1-string with tension

$$\frac{T_{\text{D1}}}{(M_{\text{Pl}}^{\text{4D}})^2} = \frac{1}{g_{\text{IIB}}} \left(\frac{M_s}{M_{\text{Pl}}^{\text{4D}}} \right)^2 \sim \frac{1}{\lambda^{\frac{3}{2}}}. \quad (4.4.7)$$

The KK scale is set by the overall volume of the manifold Y as

$$\left(\frac{M_{\text{KK}}}{M_{\text{Pl}}^{\text{4D}}} \right)^2 = \frac{1}{\mathcal{V}_Y^{\frac{1}{3}}} \left(\frac{M_s}{M_{\text{Pl}}^{\text{4D}}} \right)^2 \sim \frac{1}{\lambda}. \quad (4.4.8)$$

F1-limit: The F1-limit is the S-dual of the D1-limit. Taking into account the action of S-duality,

$$\tau'_{\text{IIB}} = -\frac{1}{\tau_{\text{IIB}}}, \quad t'^a = |\tau_{\text{IIB}}| t^a, \quad e^{-2\varphi'_4} = g_{\text{IIB}} e^{-2\varphi_4}, \quad (4.4.9)$$

we obtain the trajectory of the weak coupling, small volume limit

$$\text{F1: } g'_{\text{IIB}} \sim \frac{1}{\lambda^{\frac{3}{2}}}, \quad t'^a \sim \frac{1}{\lambda^{\frac{1}{2}}}, \quad \lambda \rightarrow \infty. \quad (4.4.10)$$

As expected from S-duality, it is now the F1-string that classically becomes the lightest,

$$\frac{T_{\text{F1}}}{(M_{\text{Pl}}^{\text{4D}})^2} = \left(\frac{M'_s}{M_{\text{Pl}}^{\text{4D}}} \right)^2 \sim \frac{1}{\lambda^{\frac{3}{2}}}, \quad (4.4.11)$$

with the KK scale falling once again behind as

$$\left(\frac{M_{\text{KK}}}{M_{\text{Pl}}^{\text{4D}}} \right)^2 = \frac{1}{\mathcal{V}_Y^{\frac{1}{3}}} \left(\frac{M'_s}{M_{\text{Pl}}^{\text{4D}}} \right)^2 \sim \frac{1}{\lambda}. \quad (4.4.12)$$

Both of these classical limits, in which a critical string becomes parametrically lighter than the KK scale, get deflected by quantum corrections [154, 155].

⁵See Section 4.4.4 for a discussion on the systematics behind the infinite-distance limits.

4.4.3 Quantum corrections

Along the F1-limit, the relevant quantum corrections are the α' -corrections and the worldsheet instanton contributions. For the D1-limit it is the D (-1) - and D1-instantons that will give the relevant corrections, which constitute a mutually local configuration of instantons. The two sets of quantum corrections are S-dual to each other, as one would have expected.

When only D (-1) - and D1-instantons contribute, enough continuous shift symmetries in the Ramond-Ramond sector remain unbroken so that the hypermultiplet moduli space simplifies and can be described in terms of tensor multiplets. The quantum corrections can then be captured in an object known as the contact potential χ , which is a quantum-corrected version of the four-dimensional dilaton,

$$\left(\frac{M_s}{M_{\text{Pl}}^{\text{4D}}}\right)^2 \sim e^{2\varphi_4} \xrightarrow{\text{QC}} \frac{1}{\chi}, \quad \chi' = \frac{\chi}{|\tau_{\text{IIB}}|} \xleftrightarrow{\text{S-dual}} \chi. \quad (4.4.13)$$

It was argued in [154] that this quantity determines a metric that asymptotically approximates the one on the hypermultiplet space in the relevant limits. In particular, it acts as an approximate Kähler potential

$$K = -\log \chi \quad (4.4.14)$$

for the metric $g_{a\bar{b}}$ on the space of complexified Kähler moduli. The explicit expression for χ was found in [289] by exploiting the c-map and considerations of $\text{SL}(2, \mathbb{Z})$ invariance, and recast in a new form by Poisson resummation in [170] to make the role of the D (-1) - and D1-instantons manifest.

This was used in [154, 155] to analyse exactly which contributions need to be taken into account along the F1- and D1-limits, and how they modify the classical trajectory. The pathological behaviour classically found for the string limits is thereby removed.

F1-limit: For the F1-limit, in which classically the volume of the manifold shrinks to zero, it was argued in [155] that instead one eventually reaches a minimal quantum-corrected volume such that the Kähler coordinates freeze but one still encounters an infinite-distance limit along the quantum-corrected four-dimensional dilaton. This was supported by analysing a similar trajectory in the vector multiplet moduli space of Type IIA string theory on Y , which was then embedded into the hypermultiplet moduli space of Type IIB string theory on Y via the c-map. The effect of this is that the contribution of the worldsheet instantons freezes deep enough into the trajectory, i.e. once the quantum volume has been reached, the quantum-corrected quantities contain a constant piece corresponding to the worldsheet instantons that no longer affects the functional dependence on the parameter λ . The scaling of the four-dimensional dilaton is quantum corrected to

$$\left(\frac{M'_s}{M_{\text{Pl}}^{\text{4D}}}\right)^2 \sim \frac{1}{\lambda^{\frac{3}{2}}} \xrightarrow{\text{QC}} \frac{1}{\chi'} \sim \frac{1}{\lambda^3}, \quad (4.4.15)$$

which results in the F1-string tension

$$\frac{T_{\text{F1}}}{(M_{\text{Pl}}^{\text{4D}})^2} = \frac{1}{\chi'} \sim \frac{1}{\lambda^3} \quad (4.4.16)$$

and the KK scale

$$\left(\frac{M_{\text{KK}}}{M_{\text{Pl}}^{\text{4D}}}\right)^2 = \frac{1}{(\mathcal{V}_Y^{\text{QC}})^{\frac{1}{3}}} \frac{1}{\chi'} \sim \frac{1}{\lambda^3} \quad (4.4.17)$$

decreasing at the same rate. In other words, the quantum corrections deflect the pathological string limit in the necessary way to obtain an emergent string limit.

D1-limit: The results for the F1-limit were then translated to the D1-limit setting by S-duality. Under S-duality, freezing of the worldsheet instantons is translated into freezing of the D1-instanton contributions deep enough along the trajectory. For a classical D1-type trajectory the relative scaling of the Kähler coordinates and the string coupling is such that

$$\frac{t^a}{g_{\text{IIB}}} \xrightarrow{\lambda \rightarrow \infty} 0 \quad (4.4.18)$$

(note that if the quotient goes to ∞ we have a decompactification limit, see below). This corresponds under S-duality to an F1-type limit in which the classical volume of the manifold is shrinking. Now, in order for the contribution of the D1-instantons to freeze, we need the scaling of the Kähler moduli to get quantum accelerated deep enough along the trajectory to obtain

$$\frac{t_{\text{QC}}^a}{g_{\text{IIB}}} \xrightarrow{\lambda \rightarrow \infty} 1. \quad (4.4.19)$$

This yields a quantum-corrected trajectory for the four-dimensional dilaton

$$\left(\frac{M_s}{M_{\text{Pl}}^{\text{4D}}} \right)^2 \sim 1 \xrightarrow{\text{QC}} \frac{1}{\chi} \sim \frac{1}{\lambda^{\frac{3}{2}}}, \quad (4.4.20)$$

which is compatible with (4.4.15) under S-duality. As a result, the D1-string tension,

$$\frac{T_{\text{D1}}}{(M_{\text{Pl}}^{\text{4D}})^2} = \frac{1}{g_{\text{IIB}}} \frac{1}{\chi} \sim \frac{1}{\lambda^3}, \quad (4.4.21)$$

and the KK mass,

$$\left(\frac{M_{\text{KK}}}{M_{\text{Pl}}^{\text{4D}}} \right)^2 = \frac{1}{\left(\mathcal{V}_Y^{\text{QC}} \right)^{\frac{1}{3}}} \frac{1}{\chi} \sim \frac{1}{\lambda^3}, \quad (4.4.22)$$

scale in the same way. Once again, the quantum corrections modify the classical trajectory so as to remove the pathological behaviour and to yield an emergent string limit.

4.4.4 Other possible limits

We have just reviewed the physics of the D1-limit and its S-dual, the F1-limit. Throughout the text we will only consider limits that are related, after an appropriate chain of identifications, to these two limits. This restriction, present already in [154, 155], stems from the inherent difficulty of performing explicit computations for the quantum corrections to trajectories in the hypermultiplet moduli space of Type II string theories. Therefore, we have to content ourselves with configurations in which only mutually local D-instantons contribute, for which the problem is tractable.

Consider a homogeneously scaling manifold with

$$t^a \sim \lambda^\mu, \quad g_{\text{IIB}} \sim \lambda^\nu. \quad (4.4.23)$$

As long as we are in the classical large volume regime, the non-perturbative contributions then scale like

$$S_{\text{WS}} \sim \mathcal{V}_{\text{2-cycle}} \sim t^a \sim \lambda^\mu, \quad (4.4.24\text{a})$$

$$S_{\text{D}(-1)} \sim \frac{\mathcal{V}_{\text{0-cycle}}}{g_{\text{IIB}}} \sim \frac{1}{g_{\text{IIB}}} \sim \lambda^{-\nu}, \quad (4.4.24\text{b})$$

$$S_{\text{D}1} \sim \frac{\mathcal{V}_{\text{2-cycle}}}{g_{\text{IIB}}} \sim \frac{t^a}{g_{\text{IIB}}} \sim \lambda^{\mu-\nu}, \quad (4.4.24\text{c})$$

$$S_{\text{D}3} \sim \frac{\mathcal{V}_{\text{4-cycle}}}{g_{\text{IIB}}} \sim \frac{(t^a)^2}{g_{\text{IIB}}} \sim \lambda^{2\mu-\nu}, \quad (4.4.24\text{d})$$

$$S_{\text{D}5} \sim \frac{\mathcal{V}_{\text{6-cycle}}}{g_{\text{IIB}}} \sim \frac{(t^a)^3}{g_{\text{IIB}}} \sim \lambda^{3\mu-\nu}, \quad (4.4.24\text{e})$$

$$S_{\text{NS}5} \sim \frac{\mathcal{V}_{\text{6-cycle}}}{g_{\text{IIB}}^2} \sim \frac{(t^a)^3}{g_{\text{IIB}}^2} \sim \lambda^{3\mu-2\nu}. \quad (4.4.24\text{f})$$

Demanding that D3-, D5- and NS5-instantons do not give relevant contributions along the limit⁶ constrains μ and ν to either fulfil the inequality

$$\mu > 0 \quad \text{and} \quad \nu \leq \frac{3\mu}{2} \quad (4.4.25)$$

or the inequality

$$\mu \leq 0 \quad \text{and} \quad \nu \leq 3\mu. \quad (4.4.26)$$

Trajectories fulfilling condition (4.4.25) are related by S-duality to trajectories that satisfy condition (4.4.26), and vice versa. The D1-limit saturates condition (4.4.25) and, as a consequence, the F1-limit lies in the regime of condition (4.4.26). For $\lambda \rightarrow \infty$ the latter of course leaves the regime of validity of the large volume approximation and quantum corrections to the volume formulae become important, as discussed.

Looking closer at (4.4.25) we see that it also includes trajectories that classically lead to decompactification limits and are therefore not of our interest. Computing the classical tension of the different object and imposing that the KK scale sits below all of them amounts to the condition $\mu > \nu$. To exclude the classical decompactification limits we therefore also impose $\mu \leq \nu$, obtaining

$$0 < \mu \leq \nu \leq \frac{3\mu}{2}. \quad (4.4.27)$$

The classical D1-limit trajectory saturates $\nu \leq 3\mu/2$, while the quantum-corrected trajectory, after taking (4.4.19) into account, saturates $\mu \leq \nu$.

Within the class of limits in which the manifold is homogeneously growing or shrinking, this explains the choice of limits. We could ask ourselves if inhomogeneous limits could lead to other situations in which the problem is also tractable and that present different physics.

Beyond an overall scaling of the manifold, the large distance finite volume limits in the classical Kähler moduli space of a Calabi-Yau threefold were classified in [149]. There are three possibilities: Type T^2 , K3 and T^4 limits. The nomenclature refers to the type of fiber that

⁶Mutually local instanton configurations in which D3- and D5-instantons contribute do exist. However, after mirror symmetry to the Type IIA side, a symplectic transformation and mirror symmetry back to the IIB side, they can be written as a configuration in which the only D-instantons whose action decreases are the D(-1)- and D1-instantons. We therefore consider only this mutually local type of configuration.

shrinks along the limit, given by a genus-one curve T^2 , a K3 surface or an Abelian surface T^4 , respectively.

A particular realisation of a Type T^2 limit was considered in [155], termed D3-limit in reference to the leading tensionless string obtained from wrapping D3-branes on the shrinking elliptic fiber. The D3-limit is obtained as a Fourier-Mukai transform of the D1-limit. This means that, in spite of D3-instantons contributing to the D3-limit, the quantum corrections can still be extracted from the results for the D1-limit. It also means that the physics of the two limits is equivalent, and therefore there is no need to discuss the D3-limit separately.

The same discussion should in principle go through for a Type T^4 limit. After translating such a limit to a D1-limit via a Fourier-Mukai transform we can essentially repeat the analysis. Such limits are expected to be physically equivalent to those D1-limits with tractable instanton contributions, and we therefore do not pursue this direction further. By contrast, a Type IIB 5-brane on a shrinking K3-fiber does not give rise to a critical string⁷ and hence such degenerations do not lead to an emergent string limit. This is a notable difference to the emergent heterotic string limits in Type IIA string theory/M-theory associated with a shrinking K3-fiber wrapped by an NS5/M5-brane [149].

4.5 Type IIA hypermultiplet limits and relation to M-theory

We now use mirror symmetry to translate the trajectories in the hypermultiplet moduli space of Type IIB string theory studied in the previous section to limits in the Type IIA setting. We also review the equivalence between the hypermultiplet moduli spaces necessary to make contact with five-dimensional M-theory. This section provides the technical foundation for the analysis in Section 4.6.

4.5.1 Mirror map

In the picture advocated by Strominger, Yau, and Zaslow (SYZ) [171], mirror symmetry is understood, near the large complex structure point of X , as T-duality along a special Lagrangian 3-cycle with T^3 topology by which X is fibered. We will refer to this cycle as the SYZ-cycle. See Figure 4.2 for an illustration.

The classical mirror map was found in [290], with the role of quantum corrections, such as instanton effects, discussed in [291–293]. The quantum-corrected mirror map for the fields we are interested in coincides with the classical one for D-instanton configurations with vanishing magnetic charge [286], such as the ones we are considering. Therefore, it will suffice for our purposes to take into account the relations

$$z_{\text{IIA}}^a = z_{\text{IIB}}^a, \quad \varphi_4^{\text{IIA}} = \varphi_4^{\text{IIB}} \Leftrightarrow \frac{g_{\text{IIA}}}{\mathcal{V}_{\text{SYZ}}^{\text{IIA}}} = g_{\text{IIB}} = \frac{1}{2\mathcal{R}}. \quad (4.5.1)$$

Here $\mathcal{V}_{\text{SYZ}}^{\text{IIA}}$ is the volume of the SYZ-cycle.

The D-instantons are accordingly mapped under mirror symmetry [170]. D (-1) -instantons wrapping a 0-cycle in Y are mapped to D2-instantons wrapping γ^0 in X , which we can identify with the SYZ-cycle, i.e.

$$\mathcal{V}_{\text{SYZ}} = \mathcal{V}_{\gamma^0}. \quad (4.5.2)$$

⁷For example, if the K3 fiber is also elliptically fibered, a Fourier-Mukai transform along the elliptic fiber transforms a D5-brane on the K3 fiber to a D3-brane wrapping the base of the K3, which yields a non-critical string. By S-duality similar conclusions hold for wrapped Type IIB NS5-branes.

D1-instantons wrapping a 2-cycle $k_a \gamma_{\text{IIB}}^a$ in Y with n units of D(-1)-charge are mapped to D2-instantons wrapping a special Lagrangian 3-cycle $k_a \gamma_{\text{IIA}}^a + n\gamma^0$ in X . Therefore, mirror symmetry identifies

$$\text{D}(-1)|_{0\text{-cycle}} \longleftrightarrow \text{D}2|_{\gamma^0=\text{SYZ-cycle}}, \quad (4.5.3a)$$

$$\text{D}1|_{k_a \gamma_{\text{IIB}}^a} \longleftrightarrow \text{D}2|_{k_a \gamma_{\text{IIA}}^a}. \quad (4.5.3b)$$

Strings coming from $\text{D}(p+2)$ -branes wrapping $(p+1)$ -cycles and $\text{D}p$ -instantons supported on the same cycles scale in the same way on both sides of the mirror map.

Volume of special Lagrangian 3-cycles: On the Type IIA side, knowing the scaling of the volume of some special Lagrangian 3-cycles will prove to be necessary in order to compute the tensions of the objects under scrutiny.

The volume of a special Lagrangian 3-cycle Γ in X is given by (see e.g. [149])

$$\mathcal{V}_{\Gamma}^{\text{IIA}} = \frac{(8\mathcal{V}_X^{\text{IIA}})^{\frac{1}{2}}}{(i \int_X \Omega_X \wedge \bar{\Omega}_X)^{\frac{1}{2}}} \text{Im} \int_{\Gamma} e^{-i\theta} \Omega_X, \quad (4.5.4)$$

where θ is related to the calibration and the superscript IIA indicates that the volume is measured in string units. The first thing we observe is that, since on the Type IIA side we are taking a complex structure limit, $\mathcal{V}_X^{\text{IIA}} = \int_X (J_X^{\text{IIA}})^3$ is constant. In order to make effective use of this formula we need to justify how the scaling of the rest of the quantities involved will be extracted via mirror symmetry from the Type IIB trajectories.

We start by looking at the classical D1- and F1-limits. We have seen that the corresponding trajectories are modified by taking into account the appropriate quantum corrections relevant deep into the limit, but at the initial stages of the trajectory we are still in a regime of reasonably large volume and moderate string coupling. This situation corresponds, under mirror symmetry, to the large complex structure (LCS) region in complex structure moduli space. As long as this approximation is valid, the denominator scales like

$$\left(i \int_X \Omega_X \wedge \bar{\Omega}_X \right)^{\frac{1}{2}} \sim \left(\int_Y J_Y^3 \right)^{\frac{1}{2}} \sim (t^a)^{\frac{3}{2}}. \quad (4.5.5)$$

The period vector, evaluated for the 3-cycles in $\{\gamma^0, \gamma_{\text{IIA}}^a, \gamma_a^{\text{IIA}}, \gamma_0\} = \{\gamma^\alpha\}$, scales as

$$\text{Im} \int_{\gamma^\alpha} e^{-i\theta} \Omega_X \sim \Pi^\alpha(t^a), \quad \Pi^\alpha(t^a) \sim (1, t^a, (t^a)^2, (t^a)^3), \quad (4.5.6)$$

where we have exploited the structure of the LCS periods.

Therefore, for the D1-limit the 3-cycle with the slowest scaling $\mathcal{V}_{\mathcal{A}}$ will be the SYZ-cycle with

$$\mathcal{V}_{\text{SYZ}}^{\text{IIA}} \sim \frac{1}{(t^a)^{\frac{3}{2}}}, \quad (4.5.7)$$

while its symplectic dual γ_0 will be the one with the fastest scaling $\mathcal{V}_{\mathcal{B}}$ with

$$\mathcal{V}_{\gamma_0}^{\text{IIA}} \sim (t^a)^{\frac{3}{2}}. \quad (4.5.8)$$

In the F1-limit, classically $t^a \rightarrow 0$ as $\lambda \rightarrow \infty$ and therefore the roles of the slowest and fastest scaling cycles are exchanged.

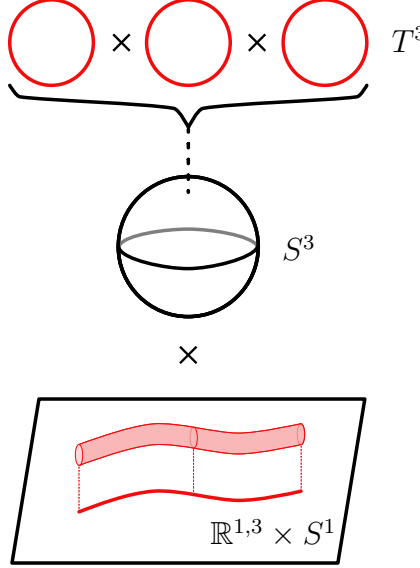


Figure 4.2: The SYZ fibration structure taken into consideration for the limits in the region of large volume/LCS.

The above reasoning is valid only in an appropriate region of moduli space. By definition, the classical limits are obtained by taking the scaling of certain quantities beyond their regime of applicability, already on the Type IIB side, i.e. ignoring the relevant quantum corrections. Therefore, it is implicit in the nomenclature that in order to obtain the classical Type IIA trajectories we can use the above formulae for both the D1- and F1-limits.

Of course, we are interested in the quantum-corrected limits deep along the trajectory, which are modified compared to the classical situation in such a way that the pathological string limits found by naively extrapolating the classical scalings are removed. Here we should be more careful, as for example the behaviour of the periods could change as we move in moduli space.

The D1-limit is a large volume limit that should correspond via mirror symmetry to an LCS limit in complex structure moduli space. Therefore, we can continue to trust both the SYZ fibration structure and the scaling of the periods, which we used to extract the dependence of the volume of the relevant 3-cycles on the mirror dual t^a variables. We then just need to take into consideration the quantum acceleration of the scaling discussed around (4.4.19) in order to account for the quantum corrections.

In the F1-limit the situation is more subtle, as we are moving away from the large volume region. Indeed, the naive vanishing of the volume along the classical trajectory arises from taking the large volume/LCS analysis too far. This was argued in [155] by analysing the analogous problem in the vector multiplet moduli space and embedding the trajectory into the hypermultiplet moduli space via the c-map. If we denote by y^a a set of coordinates in complex structure moduli space, the naive vanishing of the volume on the Kähler side would be found by employing the classical mirror map

$$z_{\text{IIA}}^a = z_{\text{IIB}}^a = \frac{1}{2\pi i} \log(y^a), \quad (4.5.9)$$

valid around the LCS point $y^a = 0$, also deep along the trajectory. The small volume point corresponding to $y^a \rightarrow 1$ is actually a constant volume point, as the periods, and consequently the quantum-corrected mirror map, tend to a constant value. For specific examples of this

phenomenon in the vector multiplet moduli space see [245, 246]. In this way, the Type IIB Kähler coordinates z_{IIB}^a freeze at late stages of the F1-limit and by mirror symmetry so do the Type IIA complex structure coordinates z_{IIA}^a . Since in the mirror dual to the F1-limit no D-instantons contribute significantly and the hypermultiplet moduli space is α' -exact,⁸ the fact that the z_{IIA}^a approach a constant value should also be seen directly from the structure of the periods in concrete examples. Ultimately, the important fact is that even when the formulae derived above stop being valid along the F1-limit and its mirror dual, deep enough along the trajectory we know that z_{IIA}^a will become constant. This is enough information to obtain the asymptotic behaviour for the mass scales appearing in the problem, and reproduces the results found after quantum corrections on the Type IIB side.

After these preliminaries, let us now analyse the mirror duals of the D1- and the F1-limits.

D4-limit: First, consider the D1-limit. We have tensionless D1-strings and D(-1)-instantons wrapping a 0-cycle in Y . Under mirror symmetry the lightest object must hence be a D4-string wrapping the SYZ-cycle. Therefore, we call this limit the D4-limit. Indeed, under the three T-dualities which define mirror symmetry in the SYZ picture, a D4-brane along the T^3 fiber maps to a D1-brane in Type IIB.

The Type IIA string coupling is given, taking into account (4.5.1), (4.5.7) and (4.4.19), by

$$g_{\text{IIA}} \sim \frac{g_{\text{IIB}}}{(t^a)^{\frac{3}{2}}} \sim 1 \xrightarrow{\text{QC}} \frac{1}{\lambda^{\frac{3}{4}}}. \quad (4.5.10)$$

The tension of the D4-brane wrapping the SYZ-cycle scales, using (4.5.1) and (4.4.20), like

$$\frac{T_{\text{D4|SYZ}}}{(M_{\text{Pl}}^{\text{4D}})^2} = \frac{\mathcal{V}_{\text{SYZ}}^{\text{IIA}}}{g_{\text{IIA}}} \left(\frac{M_s}{M_{\text{Pl}}^{\text{4D}}} \right)^2 \sim \frac{1}{\lambda^{\frac{3}{2}}} \xrightarrow{\text{QC}} \frac{1}{\lambda^3}. \quad (4.5.11)$$

In this complex structure limit the volume of X measured in string units remains unaltered, but the manifold becomes highly inhomogeneous, with the KK scale set by the γ_0 -cycle. From (4.5.8), (4.4.19) and (4.4.20) we see that

$$\left(\frac{M_{\text{KK}}}{M_{\text{Pl}}^{\text{4D}}} \right)^2 = \frac{1}{(\mathcal{V}_{\gamma_0}^{\text{IIA}})^{\frac{2}{3}}} \left(\frac{M_s}{M_{\text{Pl}}^{\text{4D}}} \right)^2 \sim \frac{1}{\lambda} \xrightarrow{\text{QC}} \frac{1}{\lambda^3}. \quad (4.5.12)$$

Along the D4-limit the only cycles whose volume varies are the 3-cycles. Since we only have even D-branes available, no other candidate tower except for that of D0-branes exists that could signal a decompactification to M-theory. Employing (4.5.10) and (4.4.20) we observe that their mass scales like

$$\left(\frac{M_{\text{D0}}}{M_{\text{Pl}}^{\text{4D}}} \right)^2 = \frac{1}{g_{\text{IIA}}^2} \left(\frac{M_s}{M_{\text{Pl}}^{\text{4D}}} \right)^2 \sim 1 \xrightarrow{\text{QC}} 1 \quad (4.5.13)$$

and hence we are safely within the realm of validity of Type IIA string theory. The mirror tower of particles in the D1-limit is given by D3-branes wrapping the mirror dual to the SYZ-cycle which, although Ω_Y is constant along the D1-limit, has a varying volume due to the factor of $\mathcal{V}_Y^{\text{IIB}}$ in the analogous expression to (4.5.4).

⁸From the point of view of the Type IIA mirror of the F1-limit taking the complete form of the periods as opposed to only considering the leading terms around the LCS is not a quantum correction, as both situations are classical. Therefore, the term “quantum corrections” for this limit refers to the splitting of the quantities that one would observe on the Kähler moduli space side.

A-F1-limit: In the mirror dual to the F1-limit, which we will refer to as the A-F1-limit, no D-instantons contribute significantly and the hypermultiplet moduli space is α' -exact. As discussed before, quantum corrections imply the freezing of the complex structure moduli. Taking this into account, as well as (4.5.1) and (4.5.7), we obtain

$$g'_{\text{IIA}} \sim \frac{g'_{\text{IIB}}}{(t'^a)^{\frac{3}{2}}} \sim \frac{1}{\lambda^{\frac{3}{4}}} \xrightarrow{\text{QC}} \frac{1}{\lambda^{\frac{3}{2}}}. \quad (4.5.14)$$

The lightest string is the fundamental Type IIA string, whose tension behaves, in view of (4.4.15), like

$$\frac{T_{\text{F1}}}{(M_{\text{Pl}}^{\text{4D}})^2} = \left(\frac{M'_s}{M_{\text{Pl}}^{\text{4D}}} \right)^2 \sim \frac{1}{\lambda^{\frac{3}{2}}} \xrightarrow{\text{QC}} \frac{1}{\lambda^3}. \quad (4.5.15)$$

In Appendix A.1 we argue that the KK scale is set by the shrinking S^3 . This scale tends to zero at the same rate as the fundamental string scale once the periods have approached their constant value

$$\left(\frac{M_{\text{KK}}}{M_{\text{Pl}}^{\text{4D}}} \right)^2 = \frac{1}{(\mathcal{V}_{\gamma_0}^{\text{IIA}})^{\frac{2}{3}}} \left(\frac{M'_s}{M_{\text{Pl}}^{\text{4D}}} \right)^2 \sim \frac{1}{\lambda} \xrightarrow{\text{QC}} \frac{1}{\lambda^3}, \quad (4.5.16)$$

where we have used (4.5.7) and (4.4.15). The mass scale of the D0-branes, obtained from (4.5.14) and (4.4.15), remains constant along the limit,

$$\left(\frac{M_{\text{D0}}}{M_{\text{Pl}}^{\text{4D}}} \right)^2 = \frac{1}{g'_{\text{IIA}}^2} \left(\frac{M'_s}{M_{\text{Pl}}^{\text{4D}}} \right)^2 \sim 1 \xrightarrow{\text{QC}} 1, \quad (4.5.17)$$

and therefore we are safely within the Type IIA framework.

To conclude, on the Type IIB side the self-similarity of the theory under strong coupling limits was instrumental in relating the D1- and F1-limits. Although ten-dimensional Type IIA string theory does not enjoy such an S-duality, and just decompactifies to M-theory under purely strong coupling limits, when compactified on a Calabi-Yau threefold it inherits the S-duality of Type IIB string theory through mirror symmetry. Therefore, the D4- and A-F1-limits are related to each other in this way, but the possibility to connect the two frames is a property of the compactified theory only.

4.5.2 Identification of the moduli spaces

As mentioned at the beginning of Section 4.4, the hypermultiplet moduli space of five-dimensional M-theory and that of four-dimensional Type IIA string theory can be identified. This owes to the fact that when compactifying five-dimensional M-theory on S^1 the M-theory circle is associated with a vector multiplet from the four-dimensional M-theory perspective. More precisely, the radius in five-dimensional Planck units is expressed in terms of the volume of X in string units via the standard relation

$$R M_{\text{Pl}}^{\text{5D}} = (\mathcal{V}_X^{\text{IIA}})^{\frac{1}{3}}. \quad (4.5.18)$$

Therefore, the hypermultiplet moduli space of M-theory on $\mathbb{R}^{1,4} \times X$ remains unaltered if we further compactify to obtain M-theory on $\mathbb{R}^{1,3} \times X \times S^1$, which can then be identified with Type IIA string theory on $\mathbb{R}^{1,3} \times X$.

The precise equivalence between the M-theory and Type IIA quantities can be seen explicitly from the dimensional reduction of eleven-dimensional supergravity. By comparison of the Lagrangian densities in [284], where the aforementioned reduction was explicitly carried out, one

infers that the complex structure moduli z_{IIA}^a remain the same on both sides, while the volume scalar in M-theory gets identified with

$$\mathcal{V}_X^{\text{11D}} = \frac{\mathcal{V}_X^{\text{IIA}}}{g_{\text{IIA}}^2}. \quad (4.5.19)$$

This is essentially the four-dimensional dilaton

$$\frac{\mathcal{V}_X^{\text{IIA}}}{g_{\text{IIA}}^2} = \frac{\mathcal{V}_X^{\text{IIA}}}{g_{\text{IIB}}^2} \frac{1}{(\mathcal{V}_{\text{SYZ}}^{\text{IIA}})^2} \sim \frac{\int_X \Omega_X \wedge \bar{\Omega}_X}{g_{\text{IIB}}^2} \sim \frac{\mathcal{V}_Y(t^a)}{g_{\text{IIB}}^2} \sim e^{-2\varphi_4}. \quad (4.5.20)$$

Therefore, the coordinates employed in all three hypermultiplet moduli spaces considered are equivalent after taking into account circle reduction and mirror symmetry, so that we can directly translate the results on quantum corrections from one setting to another. The volumes of the three-cycles are related, via (4.5.4), as

$$\mathcal{V}_{\text{3-cycle}}^{\text{11D}} = \frac{\mathcal{V}_{\text{3-cycle}}^{\text{IIA}}}{g_{\text{IIA}}}. \quad (4.5.21)$$

We have seen that the D4- and A-F1-limits are truly four-dimensional physical settings that do not undergo a decompactification to M-theory, where a rescaling of the Kähler forms like $J_{\text{M}} = J^{\text{IIA}}/g_{\text{IIA}}^{2/3}$ would be justified as exploited in [149]. Similarly, the classical membrane limits considered in Section 4.3.2 are five-dimensional scenarios in which the M-theory circle is not present. Nonetheless, the identifications just discussed allow us to formally express all the mass scales of the classical membrane limits in terms of the Type IIA variables and then, through mirror symmetry, in terms of the Type IIB quantities discussed in [154, 155]. For the latter the quantum corrections are known, a fact that we exploit in the next section.

4.6 Quantum obstructions to membrane limits

We are finally in a position to address the main question of this article, namely the fate of the classical membrane limits in five-dimensional M-theory, as introduced in Section 4.3.2. Recall that in these limits a “critical” membrane, either the M2-brane or the M5-brane wrapping a shrinking T^3 fiber, classically becomes light at the same rate as the KK modes. We refer to these two classical limits as the M2- and M5-limit, respectively. With the help of the results from Section 4.5 we will now show that quantum corrections obstruct such membrane limits, precisely as predicted on general grounds in Section 4.2.

4.6.1 M5-limit

The classical M5-limit occurs when either of the two conditions in (4.3.3) is fulfilled. The first of them, when expressed in Type IIA variables using (4.5.21), reads

$$\mathcal{V}_{\mathcal{A}}^{\text{IIA}} \sim \frac{g_{\text{IIA}}^2}{\mathcal{V}_{\mathcal{B}}^{\text{IIA}}}, \quad (4.6.1)$$

while the second one is

$$\mathcal{V}_{\mathcal{A}}^{\text{IIA}} \sim \frac{g_{\text{IIA}}^2}{(\mathcal{V}_X^{\text{IIA}})^{\frac{1}{2}}}. \quad (4.6.2)$$

Let us focus on (4.6.1) first. Consider a situation in which the mirror manifold Y is homogeneously growing (in string units), i.e. where along the trajectory in hypermultiplet moduli space, expressed in terms of the Type IIB variables, all Kähler coordinates scale like λ , with $\lambda \rightarrow \infty$. From the form of the periods of X under mirror symmetry it follows that the 3-cycles whose volume exhibits the slowest and fastest scaling are given by the SYZ-cycle γ^0 with the property (4.5.7) and its symplectic dual γ_0 scaling as in (4.5.8), as we saw in the D4-limit. This means that the condition (4.6.1) translates into

$$g_{\text{IIA}} \sim 1, \quad (4.6.3)$$

which is the behaviour classically found for (4.5.10). Therefore, under these conditions the M5-limit corresponds to the classical trajectory of the D4-limit, or its mirror dual, the D1-limit. After taking the quantum corrections into account, we find that the relevant scales now behave like

$$\frac{T_{\text{M2}}}{(M_{\text{Pl}}^{\text{5D}})^3} \sim \frac{g_{\text{IIA}}^2}{\mathcal{V}_X^{\text{IIA}}} \sim 1 \xrightarrow{\text{QC}} \frac{1}{\lambda^{\frac{3}{2}}} \sim \frac{1}{\tilde{\lambda}}, \quad (4.6.4a)$$

$$\frac{T_{\text{M5}|\mathcal{A}}}{(M_{\text{Pl}}^{\text{5D}})^3} \sim \frac{\mathcal{V}_{\mathcal{A}}^{\text{IIA}} g_{\text{IIA}}}{\mathcal{V}_X^{\text{IIA}}} \sim \frac{1}{\lambda^{\frac{3}{2}}} \xrightarrow{\text{QC}} \frac{1}{\lambda^3} \sim \frac{1}{\tilde{\lambda}^2}, \quad (4.6.4b)$$

$$\left(\frac{M_{\text{KK},\mathcal{B}}}{M_{\text{Pl}}^{\text{5D}}} \right)^3 \sim \frac{g_{\text{IIA}}^3}{\mathcal{V}_{\mathcal{B}}^{\text{IIA}} \mathcal{V}_X^{\text{IIA}}} \sim \frac{1}{\lambda^{\frac{3}{2}}} \xrightarrow{\text{QC}} \frac{1}{\lambda^{\frac{9}{2}}} \sim \frac{1}{\tilde{\lambda}^3}, \quad (4.6.4c)$$

$$\left(\frac{M_{\text{KK},\mathcal{V}}}{M_{\text{Pl}}^{\text{5D}}} \right)^3 \sim \left(\frac{g_{\text{IIA}}^2}{\mathcal{V}_X^{\text{IIA}}} \right)^{\frac{3}{2}} \sim 1 \xrightarrow{\text{QC}} \frac{1}{\lambda^{\frac{9}{4}}} \sim \frac{1}{\tilde{\lambda}^{\frac{3}{2}}}, \quad (4.6.4d)$$

with $\tilde{\lambda} \rightarrow \infty$. The impact of the quantum corrections was characterised in the Type IIB language as the freezing of the D1-instanton contributions. By (4.5.3b) this translates, on the Type IIA side, into the freezing of the D2-instanton contributions associated with (1,2)-cycles. In M-theory, finally, the quantum corrections hence freeze the volumes of said (1,2)-cycles measured in eleven-dimensional units. The classical membrane limit is deflected by the effect of quantum corrections coming from M2-brane instantons on the 3-cycles. The five-dimensional M-theory undergoes a decompactification limit along the trajectory and realises exactly the ratio (4.2.3) between the membrane tension and the KK scale which is predicted by requiring consistency under dimensional reduction. In Section 4.6.3 we will further analyse the decompactification limit induced by the quantum corrections

Let us briefly comment on the second putative realisation of an M5-limit, corresponding to (4.6.2). This condition results, for the mirror of a homogeneously growing manifold, in a scaling

$$g_{\text{IIA}} \sim \frac{1}{\lambda^{\frac{3}{4}}}. \quad (4.6.5)$$

At the classical level the tension of the wrapped M5-brane indeed sits at the KK scale set by the overall volume of the manifold, but the assumption that this was the lowest-lying KK scale was

unfounded:

$$\frac{T_{M2}}{(M_{Pl}^{5D})^3} \sim \frac{g_{IIA}^2}{\mathcal{V}_X^{IIA}} \sim \frac{1}{\lambda^{\frac{3}{2}}}, \quad (4.6.6a)$$

$$\frac{T_{M5|\mathcal{A}}}{(M_{Pl}^{5D})^3} \sim \frac{\mathcal{V}_{\mathcal{A}}^{IIA} g_{IIA}}{\mathcal{V}_X^{IIA}} \sim \frac{1}{\lambda^{\frac{9}{4}}}, \quad (4.6.6b)$$

$$\left(\frac{M_{KK,\mathcal{B}}}{M_{Pl}^{5D}}\right)^3 \sim \frac{g_{IIA}^3}{\mathcal{V}_{\mathcal{B}}^{IIA} \mathcal{V}_X^{IIA}} \sim \frac{1}{\lambda^{\frac{15}{4}}}, \quad (4.6.6c)$$

$$\left(\frac{M_{KK,\mathcal{V}}}{M_{Pl}^{5D}}\right)^3 \sim \left(\frac{g_{IIA}^2}{\mathcal{V}_X^{IIA}}\right)^{\frac{3}{2}} \sim \frac{1}{\lambda^{\frac{9}{4}}}. \quad (4.6.6d)$$

Already at the classical level do we therefore encounter a decompactification limit. This is, in fact, no different than in the analogous Type IIB limit: there the condition (4.6.5) would imply that

$$g_{IIB} = \frac{g_{IIA}}{\mathcal{V}_{SYZ}^{IIA}} \sim \lambda^{\frac{3}{4}} \lesssim \lambda \sim t^a, \quad (4.6.7)$$

and therefore we also face a classical decompactification limit from the point of view of the Type II theories.

4.6.2 M2-limit

The classical M2-limit corresponds to the condition (4.3.2), i.e. the KK tower becoming light at the fastest rate must be associated with a 3-cycle that is not scaling in eleven-dimensional Planck units. Naively, one might think that a classical M2-limit cannot be realised since as soon as (measured in eleven-dimensional units) a 3-cycle shrinks the wrapped M5-brane will be lighter, while if it grows the corresponding KK tower will be leading.

However, in view of the M5-limit discussed above, it is natural to expect the M2-limit to correspond to the A-F1-limit. This is indeed the case, and the KK towers that would naively lead to a decompactification in the M2-limit are precisely the ones argued to be absent in Appendix A.1. Taking therefore only the relevant scales into account⁹ and expressing the A-F1-limit in the M-theory language, we find the scaling behaviour

$$\frac{T_{M2}}{(M_{Pl}^{5D})^3} \sim \frac{g_{IIA}^2}{\mathcal{V}_X^{IIA}} \sim \frac{1}{\lambda^{\frac{3}{2}}} \xrightarrow{QC} \frac{1}{\lambda^3} \sim \frac{1}{\tilde{\lambda}^2}, \quad (4.6.8a)$$

$$\frac{T_{M5|\mathcal{B}}}{(M_{Pl}^{5D})^3} \sim \frac{\mathcal{V}_{\mathcal{B}}^{IIA} g_{IIA}}{\mathcal{V}_X^{IIA}} \sim 1 \xrightarrow{QC} \frac{1}{\lambda^{\frac{3}{2}}} \sim \frac{1}{\tilde{\lambda}}, \quad (4.6.8b)$$

$$\left(\frac{M_{KK,\mathcal{A}}}{M_{Pl}^{5D}}\right)^3 \sim \frac{g_{IIA}^3}{\mathcal{V}_{\mathcal{A}}^{IIA} \mathcal{V}_X^{IIA}} \sim \frac{1}{\lambda^{\frac{3}{2}}} \xrightarrow{QC} \frac{1}{\lambda^{\frac{9}{2}}} \sim \frac{1}{\tilde{\lambda}^3}, \quad (4.6.8c)$$

$$\left(\frac{M_{KK,\mathcal{V}}}{M_{Pl}^{5D}}\right)^3 \sim \left(\frac{g_{IIA}^2}{\mathcal{V}_X^{IIA}}\right)^{\frac{3}{2}} \sim \frac{1}{\lambda^{\frac{9}{4}}} \xrightarrow{QC} \frac{1}{\lambda^{\frac{9}{2}}} \sim \frac{1}{\tilde{\lambda}^3}, \quad (4.6.8d)$$

with $\tilde{\lambda} \rightarrow \infty$. Note that here the \mathcal{A} -cycle and \mathcal{B} -cycle are the S^3 and T^3 respectively, since the dependence of the volumes on λ is the inverse of that for the D4-limit. Once again, the classical

⁹The arguments after (A.1.2) also explain why there are no KK states in the classical theory associated with the scale of \mathcal{V}_X^{11D} , which would naively destroy the membrane limit already before quantum corrections come into play.

membrane limit is deflected by the quantum corrections and we observe the ratio (4.2.3) between the scalings, as expected from consistency under dimensional reduction.

We might wonder what is the fate of the membrane coming from wrapping an M5-brane on the shrinking S^3 . After taking the quantum corrections into account it falls behind,

$$\frac{T_{M5|_A}}{(M_{Pl}^{5D})^3} \sim \frac{\mathcal{V}_A^{IIA} g_{IIA}}{\mathcal{V}_X^{IIA}} \sim \frac{1}{\lambda^{\frac{3}{2}}} \xrightarrow{QC} \frac{1}{\lambda^{\frac{3}{2}}} \sim \frac{1}{\tilde{\lambda}}, \quad (4.6.9)$$

but in the classical limit we might be tempted to analyse its role as it sits at the same scale as the fundamental string. We could have asked this already for the D4-brane wrapping the same cycle in the A-F1-limit. The resulting object corresponds to a non-critical string and therefore does not lead to a competing critical string, even in the classical theory. This non-critical string has an analogue also in the D1-limit: indeed, the D4-brane wrapping the S^3 in the A-F1-limit dualises to a D7-brane wrapping the whole Calabi-Yau Y in the F1-limit, which in turn is S-dual to a $(0, 1)$ 7-brane wrapping the whole Calabi-Yau X in the D1-limit.

4.6.3 Decompactification process

We now analyse in more detail the process of decompactification characterising the quantum deflected membrane limits. For concreteness, the discussion is phrased in the framework of the M5-limit fulfilling condition (4.6.1).

With the quantum corrections taken into account, the KK tower from the S^3 base of the SYZ fibration becomes light at the fastest rate. The theory should therefore undergo a decompactification to eight-dimensional M-theory with the internal dimensions accounted for by the T^3 . As the volume of the base grows without bound all supersymmetry breaking defects, in particular the degeneration loci of the T^3 fibration, are driven to infinity, thereby restoring the appropriate amount of supersymmetry.

In the eight-dimensional theory we measure the mass scales in terms of M_{Pl}^{8D} , finding

$$\frac{T_{M2}}{(M_{Pl}^{8D})^3} \sim \left(\frac{1}{\mathcal{V}_A^{11D}} \right)^{\frac{1}{2}} \sim \lambda^{\frac{3}{4}}, \quad (4.6.10a)$$

$$\frac{T_{M5|_A}}{(M_{Pl}^{8D})^3} \sim (\mathcal{V}_A^{11D})^{\frac{1}{2}} \sim \frac{1}{\lambda^{\frac{3}{4}}}. \quad (4.6.10b)$$

If we now consider the tower of particles coming from M2-branes wrapped on $S^1 \times S^1 \subset T^3$ we see that they signal further decompactification to eleven dimensions, becoming light like

$$\frac{T_{M2|_{S^1 \times S^1}}}{M_{Pl}^{8D}} \sim (\mathcal{V}_A^{11D})^{\frac{3}{2}} \sim \frac{1}{\lambda^{\frac{9}{4}}}. \quad (4.6.11)$$

These set the KK scale

$$\tilde{M}_{KK} := T_{M2|_{S^1 \times S^1}} \quad (4.6.12)$$

for a dual torus \tilde{T}^3 with volume

$$\text{vol}(\tilde{T}^3) = \left(\frac{1}{\tilde{M}_{KK}} \right)^3 \sim \left(\frac{1}{(\mathcal{V}_A^{11D})^{\frac{2}{3}}} M_{Pl}^{11D} \right)^3. \quad (4.6.13)$$

Compactifying the dual eleven-dimensional theory on it, we obtain the relation

$$\left(\tilde{M}_{\text{Pl}}^{11\text{D}}\right)^3 = (M_{\text{Pl}}^{8\text{D}})^2 M_{\text{Pl}}^{11\text{D}} (\mathcal{V}_{\mathcal{A}}^{11\text{D}})^{\frac{2}{3}}, \quad (4.6.14)$$

from which one reads

$$\left(\frac{M_{\text{Pl}}^{8\text{D}}}{\tilde{M}_{\text{Pl}}^{11\text{D}}}\right)^3 \sim \left(\frac{1}{\mathcal{V}_{\mathcal{A}}^{11\text{D}}}\right)^{\frac{1}{2}} \sim \lambda^{\frac{3}{4}}. \quad (4.6.15)$$

Expressing the tensions in terms of $\tilde{M}_{\text{Pl}}^{11\text{D}}$ we find

$$\frac{T_{\text{M2}}}{\left(\tilde{M}_{\text{Pl}}^{11\text{D}}\right)^3} \sim \lambda^{\frac{3}{2}}, \quad \frac{T_{\text{M5}|_{\mathcal{A}}}}{\left(\tilde{M}_{\text{Pl}}^{11\text{D}}\right)^3} \sim 1. \quad (4.6.16)$$

We conclude that the wrapped M5-brane is the new M2-brane while the M2-brane orthogonal to the original torus becomes the M5-brane wrapping the dual torus.

4.7 Summary

In five-dimensional M-theory we were able to engineer classical infinite-distance limits in the hypermultiplet moduli space in which a critical membrane, in the terminology of Section 4.2, becomes parametrically light at the same rate as the KK scale. These trajectories are equivalent, under identification of the hypermultiplet moduli spaces of M-theory on $\mathbb{R}^{1,4} \times X$ and Type IIA string theory on $\mathbb{R}^{1,3} \times X$ and application of mirror symmetry, to the classical string limits discussed in [154, 155]. In these an emergent critical string becomes tensionless parametrically faster than the KK scale.

Taking quantum corrections into account modifies the string limits such that the tension of the critical string becoming parametrically light is bounded from below by the KK scale. Translating the corrections to the trajectories to the M-theory setting, we see that the membrane limits are deflected into a limit with scaling

$$\frac{T_{\text{heavy}}}{(M_{\text{Pl}}^{5\text{D}})^3} \sim \frac{1}{\tilde{\lambda}}, \quad (4.7.1a)$$

$$\frac{T_{\text{light}}}{(M_{\text{Pl}}^{5\text{D}})^3} \sim \frac{1}{\tilde{\lambda}^2}, \quad (4.7.1b)$$

$$\left(\frac{M_{\text{KK}}}{M_{\text{Pl}}^{5\text{D}}}\right)^3 \sim \frac{1}{\tilde{\lambda}^3}, \quad (4.7.1c)$$

with $\tilde{\lambda} \rightarrow \infty$. This explicitly reproduces the behaviour expected from consistency under dimensional reduction, as obtained in (4.2.3).

The identification of the moduli spaces relied on the fact that, from the point of view of five-dimensional M-theory compactified on S^1 , the M-theory circle is a vector multiplet. As a consequence, the hypermultiplet moduli space of M-theory on $\mathbb{R}^{1,4} \times X$ and M-theory on $\mathbb{R}^{1,3} \times X \times S^1$ are identical, the latter theory being equivalent to Type IIA string theory on $\mathbb{R}^{1,3} \times X$.

Both in five-dimensional M-theory and in Type IIA string theory we are considering pure hypermultiplet moduli space trajectories. The complex structure moduli are the same in

both theories, while the remaining coordinate is the volume scalar for M-theory and the four-dimensional dilaton for string theory. This four-dimensional dilaton involves the string coupling and the volume of X measured in string units, which from the Type IIA perspective is unchanged as no Kähler moduli are varied. Therefore, the scaling of the volume scalar measured in eleven-dimensional units directly determines the scaling of the Type IIA string coupling.

Type IIA hypermultiplet and vector multiplet moduli spaces locally factor, and the possible limits in the vector multiplet moduli space were studied in [149], where no membrane limit was found. The light membranes in the five-dimensional theory would become, upon wrapping this M-theory circle, the light strings in the Type IIA string theory, and their mass scale would appropriately pick up a factor of the M-theory circle radius. Therefore, we can interpret the fact that five-dimensional M-theory membrane limits turn into decompactification limits after quantum corrections are taken into account as a preventive measure against pathological string limits in the related, but not physically equivalent, four-dimensional string theory settings. In other words, the decoupling of membranes in the M-theory limits is necessary for the consistency under dimensional reduction of the Emergent String Conjecture.

Indeed, all compactifications of a consistent theory of quantum gravity must be consistent as well. Eleven-dimensional M-theory gives rise to both the five-dimensional M-theory and the four-dimensional Type IIA string theory as considered in this article. The spectra of light states along the hypermultiplet moduli space limits of these two descendant theories are connected so as to ensure the quantum consistency of both.

Without the hypermultiplet moduli space identification there is no obvious *a priori* reason for the separation of scales (4.2.3) between the KK modes and the lightest (critical) membrane in the theory, as observed in five-dimensional M-theory. The consistency of the Emergent String Conjecture under dimensional reduction provides a rationale for this relation and hence sheds new light also on the asymptotics of quantum gravity theories with no critical strings in their spectrum.

Part IV

Non-minimal Elliptic Threefolds at Infinite Distance

Chapter 5

Log Calabi-Yau Resolutions

In this chapter, we study infinite-distance limits in the complex structure moduli space of elliptic Calabi-Yau threefolds. In F-theory compactifications to six dimensions, such limits include infinite-distance trajectories in the non-perturbative open string moduli space. The limits are described as degenerations of elliptic threefolds whose central elements exhibit non-minimal elliptic fibers, in the Kodaira sense, over curves on the base. We show how these non-crepant singularities can be removed by a systematic sequence of blow-ups of the base, leading to a union of log Calabi-Yau spaces glued together along their boundaries. We identify criteria for the blow-ups to give rise to open chains or more complicated trees of components and analyse the blow-up geometry. While our results are general and applicable to all non-minimal degenerations of Calabi-Yau threefolds in codimension one, we exemplify them in particular for elliptic threefolds over Hirzebruch surface base spaces. We also explain how to extract the gauge algebra for F-theory probing such reducible asymptotic geometries. This analysis is the basis for a detailed F-theory interpretation of the associated infinite-distance limits that will be provided in Chapter 6.

5.1 Introduction and summary

The Swampland Distance Conjecture and the Emergent String Conjecture, introduced earlier in Sections 3.3 and 3.4 respectively, are concerned with the behaviour of quantum gravity theories along infinite-distance trajectories in their moduli space. In Chapter 6 we will continue with the study of these Swampland Conjectures, focusing on those infinite-distance limits in the non-perturbative open string moduli space, within the context of six-dimensional F-theory. This chapter develops the mathematical understanding necessary to carry out such a physical analysis; the concise summary of its contents provided in Sections 6.1 and 6.2.2 should make reading Chapter 6 possible without complete familiarity with the developments presented below.

Closed-moduli infinite-distance limits have been thoroughly explored across various contexts, providing substantial supporting evidence for the SDC—see [252–254] for works regarding the Type II/M-theory complex structure moduli—and the ESC; their open-moduli counterparts, by contrast, have remained relatively neglected in the existing literature. F-theory constitutes a natural setting in which to study this class of infinite-distance limits. In it, what one would naively call the open moduli is in fact part of the complex structure moduli space of an elliptic fibration; finite-distance complex structure deformations rendering the internal elliptic fibration singular over codimension-one loci can be physically interpreted as moving a collection of 7-branes on top of each other. The stack that they form supports a non-abelian gauge algebra given by a

finite number of states becoming light along the trajectory in the moduli space. Since we are concerned with the study of quantum gravity, the internal space in which the 7-branes move is compact. Interestingly, varying the location of 7-branes within this space can still correspond to an infinite-distance limit in the complex structure moduli space of F-theory, if the brane stack includes a suitable group of mutually non-local $[p, q]$ 7-branes [294–296].

These are the open-moduli infinite-distance limits that we analyse, extending previous work in eight-dimensional F-theory [156, 157] to the geometrically far richer framework of six-dimensional F-theory. Our first objective is to find a useful geometric description of the limiting points, which is the content of the present work. We exploit these results in Chapter 6 to provide a physical interpretation of the infinite-distance limits under scrutiny, with the assessment of the ESC threading the discussion. Our geometric approach is complementary to the analysis of complex structure degenerations using the formalism of asymptotic Hodge theory [252–254]. It would be extremely beneficial to connect these two approaches, which respectively take a more geometric or algebraic viewpoint, in the future.

While we have framed the discussion thus far from the perspective of the Swampland Program, the properties of these limits are also intriguing from an intrinsically F-theoretic standpoint. Above we alluded to the existing relation between stacks of 7-branes carrying a non-abelian gauge algebra and the singularities of the internal elliptic fibration in codimension-one. Increasing the number of $[p, q]$ 7-branes in the stack suitably until we reach an infinite-distance point in the complex structure moduli space also has a manifestation in the internal geometry, namely, the singular elliptic fibers over the locus become non-minimal. By this, we mean that the vanishing orders of the sections f and g which enter the Weierstrass equation

$$y^2 = x^3 + fxz^4 + gz^6 \quad (5.1.1)$$

of the elliptic fiber exceed the Kodaira bound that either $\text{ord}(f) < 4$ or $\text{ord}(g) < 6$. Such singularities behave radically different to their minimal analogues, since they do not admit a crepant resolution in the fiber. For this reason, F-theory models with codimension-one non-minimal fibers are usually discarded.

However, non-minimal singularities can still be resolved while preserving the flatness of the elliptic fibration through a sequence of base blow-ups. This turns the internal space at the endpoint of the infinite-distance limit into an arrangement of log Calabi-Yau components appropriately glued together. The study of log Calabi-Yau degenerations is a fascinating endeavour in its own right, constituting an active discipline in mathematics that has also percolated to the physics literature [297]. The stable degeneration limit sometimes taken in the F-theory literature [186, 187, 298, 299] is an example of this phenomenon.

The equivalent problem for F-theory compactifications to eight dimensions leads to the theory of degenerations of elliptic K3 surfaces. Their resolutions give rise to so-called Kulikov models, which for general K3 surfaces are classified into Type I, Type II and Type III [300–302]. Models of Type I correspond to finite-distance degenerations, while Type II and III models lie at infinite distance. For infinite-distance degenerations of elliptic K3 surfaces, a finer subdivision [156, 303–307] into models of Type II.a, II.b, III.a and III.b parallels the physics interpretation of the associated infinite-distance limits [157] as (possibly partial) decompactification or weak coupling limits.

Open-moduli infinite-distance limits in six-dimensional F-theory can not only be produced by stacking suitable branes together as explained above, a codimension-one effect, but also by forcing them to intersect with high enough multiplicity, a codimension-two effect. This leads to non-minimal elliptic fibers supported over points in the base of the internal elliptic fibration.

When this occurs at finite distance in the moduli space, the degenerations encode strongly coupled SCFTs in six dimensions. These have been understood in a major classification effort, see the review [270] and references therein. Their counterparts at infinite distance, by contrast, remain mysterious. Although we include occasional remarks in the text, our primary focus lies in comprehending non-minimal F-theory models in codimension one, deferring the exploration of codimension-two cases for future research.

Summary of Chapter 5

We now guide the reader through the results of the chapter.

The infinite-distance limits we are considering are most conveniently formulated in the language of semi-stable degenerations of elliptic Calabi-Yau threefolds. As we explain in Section 5.2.1, the idea is to consider a family of Weierstrass models Y_u parametrised by a complex parameter u ; then, for $u = 0$, non-minimal singularities in the elliptic fiber arise over curves in the base of the fibration. As noted above, these singularities are non-crepant and hence do not admit a Calabi-Yau resolution in the fiber. Our strategy is, instead, to blow up the base of the fibration in a suitable fashion. This can be achieved without compromising the Calabi-Yau condition, but at the cost of making the compactification space reducible: The original Calabi-Yau is replaced by a union of elliptic threefolds glued together over divisors. The general structure of these base blow-ups is described in Section 5.2.2, and made concrete in many examples thereafter. Upon performing a suitable number of blow-ups, the central element of the family is free of non-minimal singularities in codimension-one. The criterion for this is formulated in terms of the so-called family vanishing orders, introduced in Section 5.2.2.2, which compute the vanishing orders of defining polynomials of the Weierstrass model of the family of threefolds; these are to be distinguished from the component vanishing orders, which are defined by restriction to the components of the central element. The latter contain information on the 7-brane content of the Weierstrass model. If the family vanishing orders are minimal, but the component vanishing orders are not, we cannot read off this brane content, nor can we perform a base blow-up. However, as we explain in Appendix B.3, such obscured non-minimalities can be removed by first performing a base change $u \mapsto u^k$ for an appropriate integral $k > 1$ making both vanishing orders agree.

The key point of our analysis, and that of [156, 157] for elliptic K3 surfaces, is that the non-minimalities can be grouped into five classes according to their degree of non-minimality, which we display in Definition 5.2.5. If both f and g in (5.1.1) vanish to order higher than 4 and 6, respectively, we speak of a Class 5 non-minimality. Importantly, it turns out that such degenerations can always be transformed either into degenerations with only minimal Kodaira type vanishing orders, which arise at finite distance in the moduli space, or into the less extreme degenerations of Class 1–4, where either $\text{ord}(f) = 4$ or $\text{ord}(g) = 6$. The transformations we have in mind are combinations of base changes and the set of birational transformations given by blow-ups and blow-downs of the base. That such transformations must exist is, generally, a consequence of Mumford’s Semi-stable Reduction Theorem [308] because a resolution of Class 5 singularities would lead to degenerations which are not semi-stable. However, this proof is not constructive. We therefore go a substantial step beyond this general statement for at least a subclass of configurations, namely, codimension-one non-minimal fibers on Hirzebruch surfaces. For these, we are able to describe an explicit algorithm to transform the Class 5 singularities into milder ones. This technical discussion is the content of [309].

The importance of these considerations comes from the fact that the different components after the blow-up, as required for Class 1–4 non-minimalities, have a rather constrained form: The fiber over general points can only be of Kodaira type I_m , with $m > 0$ for Class 4 and $m = 0$ otherwise. Regions with generic $I_{m>0}$ fibers are interpreted as weakly coupled regions, where the string coupling $g_s \rightarrow 0$, while non-perturbative effects can only occur in those with generic I_0 fibers. This will be very relevant for the interpretation of the degenerations from a physics point of view in Chapter 6.

In Section 5.2.3 we establish two important results that further constrain the possible degenerations and the structure of the blow-ups. First, we show that non-minimal fibers can be tuned only over curves of genus zero or one, and in the second case only over an anti-canonical divisor of the base. This greatly restricts the possibilities. We explicitly show this for all possible types of base spaces, an analysis which we delegate to Appendix B.2.

Next, we study the resolutions in more detail. First, we define what one could call the simplest type of infinite-distance limit, namely one where essentially only a single curve supports codimension-one non-minimal fibers. As it turns out, this statement is well-defined only up to base change and birational transformations, but modulo these complications leads to a clear restriction on the types of curves over which non-minimal singularities can occur. Such so-called single infinite-distance limit degenerations, defined precisely in Definition 5.2.10, admit resolutions whose components form an open chain, as in Figure 5.1. The proof of this statement, which is our Proposition 5.2.11, requires again explicit checks for the possible base spaces and is performed in Appendix B.5. If we depart from these simple single infinite-distance limits, one instead finds trees of intersecting resolution components, see Section 5.2.6.

In Section 5.2.4 we analyse the components of the resolution, focusing only on degenerations over genus-zero curves. For single infinite-distance limits, the exceptional components of the base of the Weierstrass model are all Hirzebruch surfaces of type \mathbb{F}_n , where n is the self-intersection of the blow-up curve. The Weierstrass models over the individual base components give rise to elliptic fibrations which by themselves are not Calabi-Yau; they are, however, glued together to form a reducible Calabi-Yau space, which we should view as the resolved compactification space. The individual components are, in fact, log Calabi-Yau spaces, as we explain in detail in Section 5.2.5. In degenerations which are not of the single infinite-distance limit type, the individual base components are Hirzebruch surfaces and blow-ups thereof, which intersect in a more complicated tree structure. We highlight this phenomenon in Section 5.2.6, with derivations and examples contained in Appendix B.4. To conclude the general discussion, we also briefly comment in Section 5.2.7 on degenerations over curves of genus-one, whose in-depth study, however, is beyond the scope of this work.

All results so far have been obtained for elliptic fibrations over any of the allowed base spaces \mathbb{P}^2 , \mathbb{F}_n , and their blow-ups. Of particular interest for us are degenerations over Hirzebruch surfaces, due to the duality with the heterotic string. Indeed, in Chapter 6 we will focus on this class of models in proposing an interpretation of the infinite-distance degenerations from a physics point of view. For this reason, we devote Section 5.3 to an explicit investigation of the single infinite-distance limits over genus-zero curves on Hirzebruch surfaces. Apart from the relation to the heterotic string, this is also motivated by the fact that some of these degenerations admit toric resolutions, which serves as an independent check and illustration of our general results. First, we classify the possible genus-zero and genus-one curves which can support non-minimal degenerations of single infinite-distance limit type in Section 5.3.1. Focusing in the sequel on the much richer class of genus-zero degenerations, we can naturally group them into models with non-minimal fibers over the $(\pm n)$ -curves of the Hirzebruch surface (horizontal models), over a

fiber (vertical models), or over a mixed curve (mixed models), which we analyse in turn in the following subsections. The types of resolutions one obtains for the base space and the types of Weierstrass models over the blown up base are summarised concisely in Table 5.3.1.

As an immediate consequence of these geometric results, we conclude that the infinite-distance behaviour of F-theory is encoded in the way in which the theory probes the chain of log Calabi-Yau spaces, glued together along their boundaries. While this question is reserved for Chapter 6, there is one aspect which we analyse already in this chapter, and which concerns the structure of the discriminant of the Weierstrass model. In F-theory on elliptic Calabi-Yau spaces, the Kodaira types of singular fibers over the irreducible components of the discriminant determine the non-abelian gauge algebra. When the elliptic fibration factors into log Calabi-Yau spaces, there arise a number of subtleties that demand our attention. First, special care must be taken in determining the components of the discriminant which correspond to global divisors from the point of view of the resolved space. An analysis of the discriminant in each component of the base can be misleading, for two reasons: Two divisors may coincide in one component of the base while being clearly distinct in others. Or a single such global divisor may factor into various irreducible components in some of the base components. We illustrate these two phenomena, which are special to the factorisation of the resolution space, in Section 5.4.1 and Section 5.4.2, and explain how to read off the correct vanishing orders of the discriminant in both types of configurations. Armed with this intuition, we give the general prescription for reading off the components of the discriminant in Section 5.4.3. Technically, we must perform a suitable factorisation of the discriminant polynomial modulo the product of all exceptional coordinates. We also comment on the proper formulation of this intuitively clear concept in terms of ideal theory. When the dust settles, we can assign, as summarised in Section 5.4.5, to each discriminant component a non-abelian gauge algebra, for which one also has to take into account that monodromies in the fiber may act only locally over some of the base components, as stressed in Section 5.4.4. This gauge algebra, however, may enhance to a higher algebra as a consequence of a second effect not yet taken into account, namely the fact that the infinite-distance limits may describe partial decompactifications of the originally six-dimensional effective theory. The analogous effect was discussed in eight dimensions in [156, 157] for F-theory on non-minimal K3 surfaces. There, the enhanced gauge algebra after (possibly partial) decompactification combines with the Kaluza-Klein U(1) factors into a loop algebra (see [276, 310] for the dual heterotic effect). We leave a discussion of the analogous effect for F-theory on Calabi-Yau threefolds to the physics analysis in Chapter 6.

5.2 Geometric description of 6D F-theory limits

Infinite-distance limits in the complex structure moduli space of six-dimensional F-theory can be described geometrically in the language of degenerations of elliptically fibered threefolds, a notion that we review in Section 5.2.1. The elliptically fibered threefolds undergoing the degeneration must have as their base one of the allowed six-dimensional F-theory bases, whose geometry we recall in Appendix B.1.

The same infinite-distance limit may be represented by various degenerations, which differ in their geometrical representative of the endpoint of the limit. In Section 5.2.2 we discuss how to obtain the degenerations in which this geometrical representative has the most convenient form for our purposes, and which will be the one used throughout the rest of this chapter and in Chapter 6 to extract the physics.

The infinite-distance nature of the limits we study is associated with the presence of non-minimal fibers over certain curves in the central fiber of the degeneration. These curves can only be of genus zero or genus one, as we discuss in Section 5.2.3 and proof in Appendix B.2. We will furthermore introduce the notion of so-called single infinite-distance limits, and show that their resolution always takes the form of an open chain of log Calabi-Yau spaces, relegating most of the technicalities of the discussion to Appendix B.5.

Genus-one curves supporting non-minimal singularities only occur in highly tuned models, and we hence focus on the much more prevalent genus-zero degenerations for the rest of the chapter. Their geometrical properties are studied in great detail in Sections 5.2.4 to 5.2.6, with additional technical remarks contained in Appendices B.3 to B.7. We conclude the section with some comments on genus-one degenerations in Section 5.2.7, leaving their systematic study for future work. While the discussion is kept general throughout, we include numerous examples illustrating each of the features analysed.

5.2.1 Semi-stable degenerations of Calabi-Yau threefolds

Our goal is to study infinite-distance limits in the complex structure moduli space of F-theory compactified on elliptically fibered Calabi-Yau threefolds and the associated physics. Throughout the text, we will focus on those limits that can be described by one parameter, which we will denote by u . In order to formulate this mathematically, we will use the algebro-geometric language of degenerations.

Let $D := \{u \in \mathbb{C} : |u| < 1\}$ be the unit disk.¹ A one-parameter family of varieties is a variety² $\hat{\mathcal{Y}}$ together with a morphism

$$\hat{\rho} : \hat{\mathcal{Y}} \longrightarrow D. \quad (5.2.1)$$

The members of the family are given by the fibers $\hat{Y}_u := \rho^{-1}(u)$, with $u \in D$. We will often denote the family simply as $\hat{\mathcal{Y}}$. By distinguishing the central fiber \hat{Y}_0 , we can see this as a degeneration, in which the elements $\hat{Y}_{u \neq 0}$ of the family degenerate to \hat{Y}_0 . A degeneration is called semi-stable if $\hat{\mathcal{Y}}$ is smooth and the central fiber \hat{Y}_0 is reduced with local normal crossings.

Denote by D^* the punctured unit disk. A modification of $\rho : \hat{\mathcal{Y}} \rightarrow D$ is another family of varieties $\rho' : \hat{\mathcal{Y}}' \rightarrow D$ such that there exists a birational morphism $f : \hat{\mathcal{Y}} \rightarrow \hat{\mathcal{Y}}'$ that is compatible with the projections to D and an isomorphism over D^* .

Intuitively speaking, D is a small patch in the moduli space of the Calabi-Yau under consideration. A degeneration $\rho : \hat{\mathcal{Y}} \rightarrow D$ and its modifications and base changes all describe the same limit³ in D^* , approaching the boundary point at $u = 0$. They will present, however, different central fibers, which constitute equally valid geometrical representatives of the endpoint of the limit. To extract the physics of the infinite-distance limits, we will birationally transform the family, with the aim of finding a modification from which the physical information can be most directly read off.

For degenerations of K3 surfaces, there, in fact, exists a canonical model of the central fiber. The associated degenerations are the Kulikov degenerations, which we review in Section 6.2.1 and

¹More generally, in the context of the semi-stable reduction theorem [308] one can substitute D for a non-singular curve C with an origin, i.e. with a marked point $0 \in C$. In those concrete examples that we treat by toric methods, we will substitute D for \mathbb{C} ; this does not affect any of the properties relevant to us.

²By variety we will always mean an algebraic variety over the field \mathbb{C} .

³For a precise mathematical definition of equivalent degenerations (particularized for degenerations of elliptic K3 surfaces) see [299].

were studied in the context of F-theory in [156, 157]. For degenerations of Calabi-Yau threefolds, such a canonical geometrical representative for the endpoint of the limit is no longer available.

In the context of six-dimensional compactifications of F-theory, we are interested in (degenerations of) genus-one fibered Calabi-Yau threefolds. Throughout the text, we will assume the existence of a section, i.e. focus on elliptically fibered Calabi-Yau threefolds. A Calabi-Yau \hat{Y} within this class can be described as a Weierstrass model over a twofold base \hat{B} given by the hypersurface

$$\hat{Y} : \quad y^2 = x^3 + f x z^4 + g z^6, \quad (5.2.2)$$

with discriminant

$$\Delta := 4f^3 + 27g^2, \quad (5.2.3)$$

in the ambient \mathbb{P}_{231} -bundle over \hat{B}

$$\mathbb{P}_{231}(\mathcal{E}) := \mathbb{P}_{231}(\mathcal{L}^2 \oplus \mathcal{L}^3 \oplus \mathcal{O}). \quad (5.2.4)$$

Here, the holomorphic line bundle⁴ is $\mathcal{L} = \overline{K}_{\hat{B}}$, where $\overline{K}_{\hat{B}}$ denotes the anticanonical class of \hat{B} , such that the Calabi-Yau condition $c_1(\mathcal{L}) = c_1(\overline{K}_{\hat{B}})$ is fulfilled. The defining polynomials f and g of the Weierstrass model and the discriminant Δ are global holomorphic sections

$$f \in \Gamma\left(\hat{B}, \overline{K}_{\hat{B}}^{\otimes 4}\right), \quad g \in \Gamma\left(\hat{B}, \overline{K}_{\hat{B}}^{\otimes 6}\right), \quad \Delta \in \Gamma\left(\hat{B}, \overline{K}_{\hat{B}}^{\otimes 12}\right). \quad (5.2.5)$$

For these to exist, $\overline{K}_{\hat{B}}$ must be effective.

To construct a family of elliptically fibered Calabi-Yau threefolds, we consider a relative version of this Weierstrass model by taking the family base

$$\hat{\mathcal{B}} = \hat{B} \times D \quad (5.2.6)$$

and promoting f , g and Δ to global holomorphic sections of $\overline{K}_{\hat{\mathcal{B}}}^{\otimes m}$. We therefore consider the degeneration $\rho : \hat{\mathcal{Y}} \rightarrow D$ with fibers

$$\hat{Y}_u : \quad y^2 = x^3 + f_u x z^4 + g_u z^6, \quad (5.2.7)$$

and hence the elliptic fibration naturally extends to the family of Calabi-Yau threefolds. Note that $\hat{\mathcal{B}}$ is itself a (trivial) family of two-dimensional complex varieties with $\hat{B}_u = \hat{B}$ for all $u \in D$.

In practical terms, given a set of homogeneous coordinates $\{x_i\}_{i \in \mathcal{I}}$ describing the surface \hat{B} , a Weierstrass model over \hat{B} is fixed by choosing two defining polynomials $f = f(x_i)$ and $g = g(x_i)$, homogeneous under the \mathbb{C}^* -actions with degrees such that they are global holomorphic sections of the line bundles $F = 4\overline{K}_{\hat{B}}$ and $G = 6\overline{K}_{\hat{B}}$, respectively. In case a global description of \hat{B} in terms of homogeneous coordinates is not available, the same explicit construction can be done in patches using local coordinates. Then, in order to pass from a fixed Weierstrass model $\pi_{\text{ell}} : \hat{Y} \rightarrow \hat{B}$ to the elliptically fibered fourfold $\Pi_{\text{ell}} : \hat{\mathcal{Y}} \rightarrow \hat{\mathcal{B}}$, which represents the one-parameter family of threefolds \hat{Y}_u , we simply introduce a u dependence into the defining polynomials $f_u = f_u(x_i, u)$ and $g_u = g_u(x_i, u)$. As mentioned already, the base of the family variety is taken to be $\hat{\mathcal{B}} = \hat{B} \times D$. Since the class of the divisor $\mathcal{U} := \{u = 0\}_{\hat{\mathcal{B}}} = \pi_D^*(0)$ is trivial, we obtain $\overline{K}_{\hat{\mathcal{B}}} = \pi_{\hat{\mathcal{B}}}^*(\overline{K}_{\hat{B}})$, where the maps are the projections $\pi_{\hat{B}} : \hat{B} \times D \rightarrow \hat{B}$ and $\pi_D : \hat{B} \times D \rightarrow D$.

⁴We will often not distinguish between divisors and their associated line bundles, denoting both objects by the same symbol. It will also be implicit, but clear from context, if we are referring to a divisor class or to a concrete representative of it.

This means that u can appear with arbitrary degrees in f_u and g_u . The effect of varying u is to vary the monomial coefficients in f_u and g_u , and therefore u -trajectories correspond to complex structure deformations in the moduli space of six-dimensional F-theory. In what follows, we will denote by f , g and Δ the defining polynomials of the family of Weierstrass models, and only use the subscript when we want to highlight that we are working with a concrete fiber of the family associated to a set value of u , most commonly the central fiber \hat{Y}_0 .

Consider a fixed element \hat{Y}_u of the family $\hat{\mathcal{Y}}$. The elliptic fiber of such a threefold will be singular over the divisor of the base \hat{B}_u defined by the vanishing locus of the discriminant Δ_u . The type of fibral singularity over a given point in the base \hat{B}_u can be read off from the vanishing orders⁵ of the defining polynomials of the Weierstrass model at that locus. The non-minimal singularities that may lie at infinite distance in the moduli space are those with

$$\text{codimension-one: } \text{ord}_{\hat{Y}_u}(f_u, g_u, \Delta_u)_{\mathcal{D}} \geq (4, 6, 12), \quad (5.2.8a)$$

$$\text{codimension-two: } \text{ord}_{\hat{Y}_u}(f_u, g_u, \Delta_u)_p \geq (8, 12, 24). \quad (5.2.8b)$$

Here \mathcal{D} and p denote an irreducible divisor and a point of \hat{B}_u , respectively. We will refer to vanishing orders (5.2.8) as infinite-distance non-minimal vanishing orders.⁶ Note that over points, vanishing orders satisfying

$$(4, 6, 12) \leq \text{ord}_{\hat{Y}_u}(f_u, g_u, \Delta_u)_p < (8, 12, 24), \quad (5.2.9)$$

are not associated to infinite-distance points in the moduli space, even though they are non-minimal. Such vanishing orders will be called finite-distance non-minimal vanishing orders. We will assume that the generic elements $\hat{Y}_{u \neq 0}$ of the family do not present any infinite-distance non-minimal fibral singularities, while the central fiber \hat{Y}_0 does, corresponding to the fact that the degeneration $\hat{\mathcal{Y}}$ potentially represents an infinite-distance limit in complex structure moduli space.

The family $\hat{\mathcal{Y}}$ can be birationally transformed in such a way that the central fiber decomposes into a union of threefolds with normal crossings, as we discuss in detail in Section 5.2.2. This is achieved by performing a series of blow-ups along the base $\hat{\mathcal{B}}$ of the degeneration $\hat{\mathcal{Y}}$. The resulting modification \mathcal{Y} is free of infinite-distance non-minimal fibral singularities, with the geometrical representative of its central fiber taking the form

$$\pi_0 : Y_0 = \bigcup_{p=0}^P Y^p \longrightarrow B_0 = \bigcup_{p=0}^P B^p, \quad (5.2.10)$$

with components

$$\pi^p : Y^p \longrightarrow B^p, \quad p = 0, \dots, P. \quad (5.2.11)$$

Here, each Y^p is an elliptic threefold with base B^p . Performing then fibral blow-ups⁷ at every value of u leads to yet another modification \mathcal{X} , which corresponds to the Coulomb branch in the

⁵Various notions of vanishing order will be at play when analysing the geometry of infinite-distance complex structure limits. We will define what we exactly mean by each of them in Section 5.2.2.2.

⁶While infinite-distance complex structure degenerations are associated to infinite-distance non-minimal vanishing orders, the converse is not necessarily true. Some degenerations presenting loci with infinite-distance non-minimal vanishing orders can be seen to lie at finite distance, a phenomenon on which we comment in Section 5.2.2.3.

⁷Working with elliptic Calabi-Yau threefolds, we may encounter codimension-two terminal singularities that do not admit a crepant resolution, signalling the presence of localised matter uncharged under any continuous gauge group [206, 207]. These are kept unresolved in \mathcal{X} in order to preserve the Calabi-Yau condition.

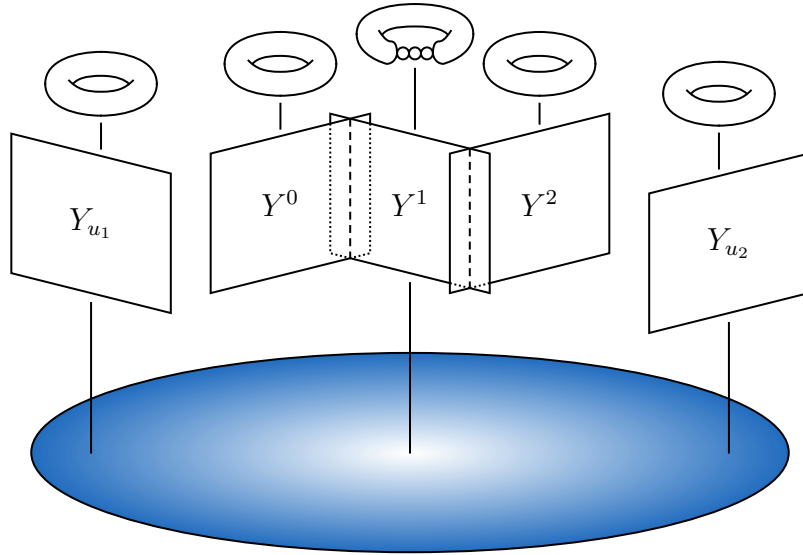


Figure 5.1: A representation of a semi-stable degeneration of elliptically fibered threefolds. The blue disk represents D , over which we have two generic fibers Y_{u_1} and Y_{u_2} , that degenerate to the multi-component central fiber Y_0 .

dual M-theory description. Altogether, we can schematically summarize the modifications of the degeneration of interest as

$$\begin{array}{ccccc}
 \mathcal{X} & \xrightleftharpoons[\text{fibral blow-up}]{\text{fibral blow-down}} & \mathcal{Y} & \xrightleftharpoons[\text{base blow-up}]{\text{base blow-down}} & \hat{\mathcal{Y}} \\
 \downarrow & & \downarrow & & \downarrow \\
 \mathcal{B} & \simeq & \mathcal{B} & \xrightleftharpoons{\quad} & \hat{\mathcal{B}}.
 \end{array} \tag{5.2.12}$$

We will often refer to the modification $\rho : \mathcal{Y} \rightarrow D$ as the resolved degeneration, even if the fibral singularities are kept unresolved in it. Along with a general discussion, we also provide some explicit examples of the degenerations just described and their modifications starting in Section 5.2.2.

Finally, recall that the set of allowed six-dimensional F-theory bases that can play the role of $\hat{\mathcal{B}}$ consists of the Enriques surface, the complex projective plane \mathbb{P}^2 , the Hirzebruch surfaces \mathbb{F}_n (with $0 \leq n \leq 12$) and their blow-ups $\text{Bl}(\mathbb{F}_n)$ [311]. The Enriques surface has trivial $\overline{K}_{\hat{\mathcal{B}}}$ (up to torsion), and we therefore discard it; the models constructed over it support no gauge group or matter content, and in particular cannot exhibit the fibral non-minimal singularities that we seek to study. In Appendix B.1 we briefly review the geometry of the other complex surfaces listed in order to set the notation used throughout the text.

5.2.2 Modifications of an infinite-distance degeneration

Given a starting degeneration $\hat{\rho} : \hat{\mathcal{Y}} \rightarrow D$, our task is now to find the equivalent resolved degeneration $\rho : \mathcal{Y} \rightarrow D$ and, eventually, to extract the physics in Chapter 6.

We describe, in Section 5.2.2.1, the resolution process that eliminates the infinite-distance non-minimal singularities of the family variety $\hat{\mathcal{Y}}$, both in general terms and in an explicit example. In Section 5.2.2.2 we clarify the different notions of vanishing orders that we employ in the description of the degeneration. A subtlety is explained in Appendix B.3: In the context of

the Semi-stable Reduction Theorem [308], it is well known that performing a base change may be necessary in order to make a modification to a semi-stable degeneration possible; we observe in Appendix B.3 how the need for base change is explicitly realised in our context through the appearance of non-minimal elliptic fibers of the central fiber of the degeneration that may be minimal for the family variety. We conclude by classifying the codimension-one infinite-distance degenerations of elliptically fibered Calabi-Yau threefolds into five classes, mirroring the classification performed in [156, 157] for the infinite-distance degenerations of elliptic K3 surfaces. As an important result of this discussion, we will explain that it suffices to restrict our attention to geometrical representatives of the central fiber in which the components only support Kodaira type I_m singularities in codimension-zero.

5.2.2.1 Base blow-ups

Let $\hat{\mathcal{Y}}$ be a degeneration of an elliptically fibered Calabi-Yau threefold. As argued in Section 5.2.1, we only allow infinite-distance non-minimal fibers to appear over the central fiber \hat{Y}_0 of the degeneration. Furthermore, we focus on infinite-distance limits related to codimension-one non-minimal fibers in \hat{Y}_0 , leaving codimension-two degenerations for future work. Let us denote the divisor of \hat{B}_0 over which we find the non-minimal fibers by C . We will assume that C is a smooth, irreducible curve. Then, the vanishing orders of the defining polynomials of the Weierstrass model will be

$$\text{ord}_{\hat{Y}_0}(f_0, g_0, \Delta_0)_C \geq (4, 6, 12). \quad (5.2.13)$$

Turning our attention to the family fourfold $\hat{\mathcal{Y}}$, and defining

$$\mathcal{U} := \{u = 0\}_{\hat{\mathcal{B}}}, \quad (5.2.14)$$

the curve $C \subset \hat{B}_0 \subset \hat{\mathcal{B}}$ can be written as $C = \mathcal{C} \cap \mathcal{U}$, where \mathcal{C} is the divisor of $\hat{\mathcal{B}}$ given by $\mathcal{C} = C \times D$. We will sometimes denote the curve by C when we want to regard it as a divisor in \hat{B}_0 , and by $\mathcal{C} \cap \mathcal{U}$ when we want to see it as a curve in $\hat{\mathcal{B}}$. The non-minimal nature of the locus will then manifest itself⁸ in the family variety through

$$\text{ord}_{\hat{\mathcal{Y}}}(f, g, \Delta)_{\mathcal{C} \cap \mathcal{U}} = (4 + \alpha, 6 + \beta, 12 + \gamma), \quad \alpha, \beta, \gamma \geq 0. \quad (5.2.15)$$

To arrive at the modification of the degeneration that we will use to extract the physics in Chapter 6, we blow up the fourfold $\hat{\mathcal{Y}}$ until we have removed all of its codimension-one⁹ non-minimal elliptic fibers, obtaining the equivalent degeneration \mathcal{Y} .

We first focus our attention on limits presenting a single non-minimal codimension-one locus. This corresponds to the naive notion of taking a single infinite-distance limit in complex structure moduli space instead of a superposition of several limits. We make this concept more precise in Section 5.2.3 and return to the general case in Section 5.2.6. The resolution process that we are about to discuss is no different in the presence of multiple codimension-one loci of non-minimal fibers; we simply apply the same procedure iteratively to each irreducible locus until all the non-minimal elliptic fibers of the family variety have been removed.

⁸This is not entirely precise; we discuss the interplay between family and component vanishing orders in Section 5.2.2.2, as well as the appearance of “obscured” infinite-distance limits (in which the former are minimal while the latter are not) in Appendix B.3. We can, however, always find an equivalent degeneration in which they mutually agree, and we therefore assume that this is the case during the remainder of this section.

⁹When we refer to the codimension of a locus supporting non-minimal fibers we always compute it in the central fiber \hat{Y}_0 , rather than in the family variety $\hat{\mathcal{Y}}$, unless explicitly stated. Hence, we say that $\mathcal{C} \cap \mathcal{U}$ is a codimension-one degeneration instead of a codimension-two one.

The resolution of a codimension-one non-minimal locus amounts to blowing up the intersection curve of the divisors \mathcal{C} and \mathcal{U} in $\hat{\mathcal{B}}$ and performing a line bundle shift in order to ensure that the Calabi-Yau condition still holds for the blown up Weierstrass model. Even if only a single codimension-one locus of non-minimal elliptic fibers is present in $\hat{\mathcal{Y}}$, multiple blow-ups may be needed before the non-minimal fibers are fully removed from the family fourfold, since we may encounter new curves of non-minimal fibers in the exceptional components of the blow-ups. Let us analyse how this resolution process affects the geometry of the central fiber.

The blow-up of $\hat{\mathcal{B}}$ at $\mathcal{C} \cap \mathcal{U}$ is the pair given by a threefold \mathcal{B} and a birational map

$$\pi : \mathcal{B} \longrightarrow \hat{\mathcal{B}}. \quad (5.2.16)$$

The exceptional set of the blow-up is the irreducible variety

$$E := \pi^{-1}(\mathcal{C} \cap \mathcal{U}). \quad (5.2.17)$$

Given an irreducible divisor \mathcal{D} of $\hat{\mathcal{B}}$ that intersects the blow-up locus, the strict transform of \mathcal{D} is the irreducible divisor of \mathcal{B} given by the closure of $\pi^{-1}(\mathcal{D} \setminus \mathcal{C} \cap \mathcal{U})$. It is equal to the reducible divisor $\pi^*(\mathcal{D})$, known as the proper or total transform of \mathcal{D} , up to copies of E . More concretely, for \mathcal{C} and \mathcal{U} we have

$$\tilde{\mathcal{C}} := \pi^*(\mathcal{C}) = \mathcal{C}' + E, \quad (5.2.18)$$

$$\tilde{\mathcal{U}} := \pi^*(\mathcal{U}) = \mathcal{U}' + E, \quad (5.2.19)$$

where we denote the strict transforms by the primes and the proper transforms by the tildes, for brevity. It is common to omit the primes and denote the original divisor and its strict transform by the same symbol, something that we will also do when the context makes clear what is meant.

The anticanonical classes of \mathcal{B} and $\hat{\mathcal{B}}$ are related by

$$\overline{K}_{\mathcal{B}} = \pi^*(\overline{K}_{\hat{\mathcal{B}}}) - E, \quad (5.2.20)$$

and therefore, after the blow-up, the Calabi-Yau condition is no longer satisfied in the resulting Weierstrass model unless we perform a line bundle shift, as we now explain. In view of (5.2.15), the strict transforms of the divisors associated to the global holomorphic sections given by the defining polynomials are related to their proper transforms by

$$\tilde{F} = F' + (4 + \alpha)E, \quad (5.2.21a)$$

$$\tilde{G} = G' + (6 + \beta)E, \quad (5.2.21b)$$

$$\tilde{\Delta} = \Delta' + (12 + \gamma)E. \quad (5.2.21c)$$

Let us denote the holomorphic line bundle defining the Weierstrass model over $\hat{\mathcal{B}}$ by $\mathcal{L}_{\hat{\mathcal{B}}}$, and the one defining it over \mathcal{B} by $\check{\mathcal{L}}_{\mathcal{B}}$. The total transforms (5.2.21) are in the class

$$m\check{\mathcal{L}}_{\mathcal{B}} = \pi^*(m\mathcal{L}_{\hat{\mathcal{B}}}) = \pi^*(m\overline{K}_{\hat{\mathcal{B}}}) = m\overline{K}_{\mathcal{B}} + mE, \quad (5.2.22)$$

where $m = 4, 6$ and 12 for \tilde{F} , \tilde{G} and $\tilde{\Delta}$, respectively. We can restore the Calabi-Yau condition by shifting the line bundles \tilde{F} , \tilde{G} and $\tilde{\Delta}$ such that the holomorphic line bundle $\mathcal{L}_{\mathcal{B}}$ defining the new Weierstrass model over \mathcal{B} fulfils

$$\mathcal{L}_{\mathcal{B}} = \check{\mathcal{L}}_{\mathcal{B}} - E = \overline{K}_{\mathcal{B}}. \quad (5.2.23)$$

In view of (5.2.22), the necessary shift leads to the divisors¹⁰

$$\begin{aligned} F &= \tilde{F} - 4E = F' + \alpha E, \\ G &= \tilde{G} - 6E = G' + \beta E, \\ \Delta &= \tilde{\Delta} - 12E = \Delta' + \gamma E, \end{aligned} \tag{5.2.24}$$

where we observe that, depending on the original vanishing orders, copies of E still appear factored out. Note that the line bundle shift restoring the Calabi-Yau condition yields effective divisors thanks to the starting non-minimal vanishing orders (5.2.15), without which the operation would not result in a consistent F-theory model. Non-minimal vanishing orders are therefore needed so that we can restore the Calabi-Yau condition by dividing f , g and Δ by the required powers of the blow-up coordinate without turning them into rational functions.

The blow-up operation is a local one, meaning that away from $\mathcal{C} \cap \mathcal{U} \subset \mathcal{U} \subset \mathcal{B}$ the geometry remains unaffected, as we expect for a modification of a degeneration. The geometrical representative of the central fiber has been, however, changed. Let us rename the divisors

$$E_0 := \mathcal{U}', \quad E_1 := E. \tag{5.2.25}$$

The total transform $\tilde{\mathcal{U}}$ of \mathcal{U} is the locus of the central fiber B_0 of the modified degeneration \mathcal{B} . It is now reducible and, in this case, given by

$$\tilde{\mathcal{U}} = E_0 + E_1. \tag{5.2.26}$$

In other words, blowing up the base once and shifting the line bundles to restore the Calabi-Yau condition has left us with a two-component model for the central fiber of the degeneration. The components of the base are given by

$$B_0 := \mathcal{B}|_{\tilde{\mathcal{U}}}, \quad B^p := \mathcal{B}|_{E_p}, \quad p = 0, 1, \tag{5.2.27}$$

and the holomorphic line bundles defined over them and pertaining to the elliptic fibrations Y_0 , Y^0 and Y^1 are

$$\begin{aligned} F_{B_0} &:= F|_{\tilde{\mathcal{U}}}, & F_p &:= F|_{E_p}, \\ G_{B_0} &:= G|_{\tilde{\mathcal{U}}}, & G_p &:= G|_{E_p}, \quad p = 0, 1. \\ \Delta_{B_0} &:= \Delta|_{\tilde{\mathcal{U}}}, & \Delta_p &:= \Delta|_{E_p}, \end{aligned} \tag{5.2.28}$$

From (5.2.24) we read off

$$\text{ord}_{\mathcal{Y}}(f, g, \Delta)_{E_1} = (\alpha, \beta, \gamma), \tag{5.2.29}$$

so that the elliptic fibers over B^1 could be singular in codimension-zero depending on the values of α , β and γ . The fibers over B^0 could also be singular in codimension-zero, depending on $\text{ord}_{\hat{\mathcal{Y}}}(f, g, \Delta)_{\mathcal{U}} = \text{ord}_{\mathcal{Y}}(f, g, \Delta)_{E_0}$.

Example 5.2.1. In order to make the above discussion more concrete, let us see how the blow-up process works in a particular example. We choose as the base \hat{B} of the degenerating six-dimensional F-theory models the Hirzebruch surface $\hat{B} = \mathbb{F}_7$. For details on the notation that we employ, we refer to Appendix B.1. In particular, we denote by $[s : t]$ and $[v : w]$ the homogenous coordinates on the fiber \mathbb{P}_f^1 and the base \mathbb{P}_b^1 of the Hirzebruch surface, respectively,

¹⁰We denote the (shifted) line bundles defining the elliptic fibration in \mathcal{Y} in the same way as those defining it in $\hat{\mathcal{Y}}$. For additional clarity, we will denote the defining polynomials of the blown up family Weierstrass model by f_b , g_b and Δ_b .

see (B.1.12). The (toric) divisors associated with their vanishing loci are referred to by a corresponding capital letter, as in (B.1.13).

An example of a Weierstrass model giving an elliptically fibered family variety $\hat{\mathcal{Y}}$ over the base $\hat{\mathcal{B}} = \mathbb{F}_7 \times D$ is

$$f = s^4 t^4 v^2 (uv^6 - 3v^4 w^2 + 6v^2 w^4 - 3w^6) , \quad (5.2.30a)$$

$$g = s^5 t^5 v^3 (s^2 v^{16} - 2stv^6 w^3 + 6stv^4 w^5 - 6stv^2 w^7 + 2stw^9 + t^2 u^2 w^2) , \quad (5.2.30b)$$

$$\Delta = s^{10} t^{10} v^6 p_{4,32} ([s : t], [v : w : t], u) , \quad (5.2.30c)$$

where the subscripts in the residual polynomial of Δ refer to its homogeneous degrees under the two \mathbb{C}^* -actions of \mathbb{F}_7 given in (B.1.12). One can see that the generic fibers $\hat{Y}_{u \neq 0}$ of the family only present minimal singular elliptic fibers. The central fiber \hat{Y}_0 , however, supports non-minimal singular elliptic fibers over the curve $\mathcal{S} \cap \mathcal{U} = \{s = u = 0\} \subset \hat{B}_0 \subset \hat{\mathcal{B}}$, as can be seen from the vanishing orders

$$\text{ord}_{\hat{\mathcal{Y}}}(f, g, \Delta)_{s=u=0} = (4, 6, 13) . \quad (5.2.31)$$

To perform a (toric) blow-up of $\hat{\mathcal{B}}$ along the curve $\mathcal{S} \cap \mathcal{U}$ and obtain \mathcal{B} , we introduce a new (exceptional) coordinate e_1 in the (total) coordinate ring of $\hat{\mathcal{B}}$, accompanied by a new \mathbb{C}^* -action

$$\begin{aligned} \mathbb{C}_{\mu_1}^* : \mathbb{C}_{(s', t, v, w, e'_0, e_1)}^* &\longrightarrow \mathbb{C}_{(s', t, v, w, e'_0, e_1)}^* \\ (s', t, v, w, e'_0, e_1) &\longmapsto (\mu_1 s', t, v, w, \mu_1 e'_0, \mu_1^{-1} e_1) . \end{aligned} \quad (5.2.32)$$

In the above expression, we have employed the coordinates s' and e'_0 , whose vanishing locus corresponds in \mathcal{B} to the strict transform of the vanishing locus of the coordinates s and e_0 in $\hat{\mathcal{B}}$, i.e. we have the relations

$$\pi^*(\mathcal{S}) = \pi^*(\{s = 0\}_{\hat{\mathcal{B}}}) = \{s' = 0\}_{\mathcal{B}} \cup \{e_1 = 0\}_{\mathcal{B}} = \mathcal{S}' + E_1 , \quad (5.2.33a)$$

$$\pi^*(\mathcal{U}) = \pi^*(\{e_0 = 0\}_{\hat{\mathcal{B}}}) = \{e'_0 = 0\}_{\mathcal{B}} \cup \{e_1 = 0\}_{\mathcal{B}} = E'_0 + E_1 . \quad (5.2.33b)$$

To simplify the notation, we now drop the primes for the strict transforms. The blow-up process prompts us to also modify the Stanley-Reisner ideal to

$$\mathcal{I}_{\hat{\mathcal{B}}} = \langle st, vw \rangle \longmapsto \mathcal{I}_{\mathcal{B}} = \langle st, vw, se_0, te_1 \rangle . \quad (5.2.34)$$

The total transforms of the divisors corresponding to the vanishing loci of the defining polynomials are obtained by performing the substitutions

$$s \longmapsto se_1 , \quad (5.2.35a)$$

$$u \longmapsto e_0 e_1 , \quad (5.2.35b)$$

in f , g and Δ , obtaining the polynomials

$$(f, g, \Delta) \longmapsto (\tilde{f}, \tilde{g}, \tilde{\Delta}) . \quad (5.2.36)$$

Since

$$e_1^4 \mid \tilde{f} , \quad e_1^6 \mid \tilde{g} , \quad e_1^{12} \mid \tilde{\Delta} , \quad (5.2.37)$$

we are allowed to perform the line bundle shift by prescribing the new defining polynomials

$$f_b := e_1^{-4} \tilde{f} , \quad g_b := e_1^{-6} \tilde{g} , \quad \Delta_b := e_1^{-12} \tilde{\Delta} . \quad (5.2.38)$$

The resulting expressions are

$$f_b = s^4 t^4 v^2 (e_0 e_1 v^6 - 3v^4 w^2 + 6v^2 w^4 - 3w^6) , \quad (5.2.39a)$$

$$g_b = s^5 t^5 v^3 (e_1 s^2 v^{16} + e_0^2 e_1 t^2 w^2 - 2s t v^6 w^3 + 6s t v^4 w^5 - 6s t v^2 w^7 + 2s t w^9) , \quad (5.2.39b)$$

$$\Delta_b = s^{10} t^{10} v^6 e_1 p_{4,32,3}([s:t], [v:w:t], [s:e_0:e_1]) . \quad (5.2.39c)$$

The generic fibers over the new base component $B^1 = \{e_1 = 0\}$ are singular of Kodaira type I_1 , as follows from the vanishing orders

$$\text{ord}_{\mathcal{Y}}(f_b, g_b, \Delta_b)_{E_1} = (0, 0, 1) . \quad (5.2.40)$$

In this concrete example, performing one blow-up is not enough to remove the non-minimal fibers of the family variety, since we have

$$\text{ord}_{\mathcal{Y}}(f_b, g_b, \Delta_b)_{s=e_1=0} = (4, 6, 12) . \quad (5.2.41)$$

Suppose that P successive blow-ups of the $\mathcal{C} \cap \mathcal{U}$ locus are necessary in order to fully remove the non-minimal fibers of the family variety $\hat{\mathcal{Y}}$ and arrive at \mathcal{Y} . Composing the blow-up maps, we find that the total transform of the locus of the original base central fiber \hat{B}_0 is reducible with $P + 1$ components, i.e.

$$\tilde{\mathcal{U}} = \sum_{p=0}^P E_p , \quad (5.2.42)$$

where the E_p represent the strict transforms of the exceptional divisors after the composition of all blow-up maps. The components of the base are given by

$$B_0 := \mathcal{B}|_{\tilde{\mathcal{U}}} , \quad B^p := \mathcal{B}|_{E_p} , \quad p = 0, \dots, P , \quad (5.2.43)$$

and the holomorphic line bundles defined over them and associated to the elliptic fibrations Y_0 and $\{Y^p\}_{0 \leq p \leq P}$ are

$$\begin{aligned} F_{B_0} &:= F|_{\tilde{\mathcal{U}}} , & F_p &:= F|_{E_p} , \\ G_{B_0} &:= G|_{\tilde{\mathcal{U}}} , & G_p &:= G|_{E_p} , \quad p = 0, \dots, P . \\ \Delta_{B_0} &:= \Delta|_{\tilde{\mathcal{U}}} , & \Delta_p &:= \Delta|_{E_p} , \end{aligned} \quad (5.2.44)$$

The geometry of the base components will be discussed in Sections B.4.1 and 5.2.4, and the line bundles over them detailed in Sections B.4.2 and 5.2.5. Each base component B^p together with the line bundles F_p , G_p and Δ_p defines a Weierstrass model

$$\pi^p : Y^p \longrightarrow B^p , \quad p = 0, \dots, P , \quad (5.2.45)$$

the collection of which gives the central fiber

$$\pi_0 : Y_0 = \bigcup_{p=0}^P Y^p \longrightarrow B_0 = \bigcup_{p=0}^P B^p \quad (5.2.46)$$

of the family variety \mathcal{Y} . The type of codimension-zero fibers in the component Y^p will be given by $\text{ord}_{\mathcal{Y}}(f, g, \Delta)_{E_p}$. As we could observe explicitly in Example 5.2.1, the type of these singularities over a component E_p depends on the vanishing orders $\text{ord}_{\mathcal{Y}}(f, g, \Delta)_{\mathcal{C} \cap E_{p-1}}$ over the curve whose blow-up gives rise to it. If the family variety $\hat{\mathcal{Y}}$ we start with presents various curves $\{\mathcal{C}_i \cap \mathcal{U}\}_{1 \leq i \leq r}$ supporting non-minimal singular fibers we simply repeat the process we just described for each of them until all non-minimal fibers have been removed from the family variety.

5.2.2.2 Family and component orders of vanishing

In the preceding sections, we have made use of the notion of the order of vanishing $\text{ord}_{\hat{\mathcal{Y}}}(f, g, \Delta)_{\mathcal{Z}}$ of the defining polynomials f , g and Δ of a Weierstrass model $\hat{\Pi}_{\text{ell}} : \hat{\mathcal{Y}} \rightarrow \hat{\mathcal{B}}$ along a given locus \mathcal{Z} in the base $\hat{\mathcal{B}}$ of the elliptic fibration. While it is intuitively clear what is meant by this notation, let us be fully explicit in order to set the stage for the discussions in the upcoming sections. The examples in Appendix B.3 illustrate the differences between the different orders of vanishing that we employ.

Assume first that \mathcal{Z} is an irreducible component of the discriminant Δ of $\hat{\Pi}_{\text{ell}} : \hat{\mathcal{Y}} \rightarrow \hat{\mathcal{B}}$, and hence a prime divisor of $\hat{\mathcal{B}}$. The order of vanishing of a rational function h on an algebraic variety $\hat{\mathcal{B}}$ along a prime divisor is well-defined,¹¹ and can be obtained working in a local patch $\mathcal{A} \subset \hat{\mathcal{B}}$. Choosing local coordinates $\{a_i\}_{1 \leq i \leq \dim(\hat{\mathcal{B}})}$ for $\mathcal{A} \subset \hat{\mathcal{B}}$ in which \mathcal{Z} is locally defined by an equation¹² $\{\mathcal{Z}(a_i) = 0\}_{\mathcal{A}}$, we simply count the factors of $\mathcal{Z}(a_i)$ in h . Tate's algorithm allows us then to determine the type of elliptic fiber in the Kodaira-Néron list¹³ found over the generic points of \mathcal{Z} using $\text{ord}_{\hat{\mathcal{Y}}}(f, g, \Delta)_{\mathcal{Z}}$. In practice, many of the examples we work with have toric bases in which this can be done using a global description, rather than locally in a patch.

When $\text{codim}_{\hat{\mathcal{B}}}(\mathcal{Z}) > 1$, e.g. for the intersection of various components of the discriminant, we work by restricting $\hat{\mathcal{B}}$ to a generic irreducible subvariety \mathcal{W} such that $\mathcal{Z} \subset \mathcal{W}$ and

$$\text{codim}_{\hat{\mathcal{B}}}(\mathcal{W}) = \text{codim}_{\hat{\mathcal{B}}}(\mathcal{Z}) - 1 \Rightarrow \text{codim}_{\mathcal{W}}(\mathcal{Z}) = 1. \quad (5.2.47)$$

The orders of vanishing are now again determined in codimension-one, and Tate's algorithm identifies the type of Kodaira singularity in the slice of $\hat{\Pi}_{\text{ell}} : \hat{\mathcal{Y}} \rightarrow \hat{\mathcal{B}}$ given by restricting the elliptic fibration to \mathcal{W} . It is important that the restriction is taken such that the slice is generic; in a non-generic slice we may find singularities that are worse than those found in the generic one, see Examples B.3.1 and B.3.2.

In codimension-two and higher, the Kodaira-Néron classification of singular fibers no longer is complete, and we can encounter non-Kodaira fibers even when the vanishing orders are minimal, see e.g. [205, 312–317]. At least for threefolds, the non-Kodaira fibers in crepant resolutions of Weierstrass models over codimension-two loci with minimal vanishing orders are contractions of the Kodaira fibers read off from Tate's algorithm for the generic surface slice of the model [317]. In the associated singular Weierstrass model, the generic slice passing through such a codimension-two point presents a Du Val singularity in the Kodaira-Néron list, while the threefold presents a compound Du Val singularity at that point; locally, the threefold can be seen as a deformation of a Du Val singularity. We are interested, however, in higher codimension loci over which we have non-minimal orders of vanishing. It has been proven for threefolds that a crepant resolution of such loci, over which the singularities are still rational Gorenstein but no longer compound Du Val, would yield a non-equidimensional elliptic fibration [317]. Hence, even in higher codimension, loci with non-minimal orders of vanishing behave very differently from their minimal counterparts. Working in F-theory, we want to preserve the equidimensional elliptic fibration structure, and therefore choose instead to resolve the codimension-two (from

¹¹The local ring of a prime divisor in a normal variety is a discrete valuation ring, allowing us to define the order of vanishing of a function in its field of fractions. Higher codimension irreducible subvarieties no longer have an associated discrete valuation.

¹²Let us recall that, since the bases we consider are smooth, there is a one-to-one correspondence between Cartier and Weil divisors; hence, we can assume the existence of such a local equation without any further considerations.

¹³Tate's algorithm [189] can also distinguish between split, semi-split and non-split fibers, see [190–192] for a discussion of it in the context of F-theory.

the point of view of $\hat{\mathcal{B}}$) non-minimal singularities in the family variety through a non-crepant base blow-up followed by a line bundle shift in order to restore the Calabi-Yau condition, as explained in Section 5.2.2.1.

We will refer to the orders of vanishing of f , g and Δ over loci in $\hat{\mathcal{B}}$ (respectively, for the resolved degeneration, f_b , g_b and Δ_b over loci in \mathcal{B}) computed in this way as family orders of vanishing, this being the notion used in most of Section 5.2.2.1.

Definition 5.2.2 (Family vanishing orders). Let $\hat{\mathcal{Y}}$ (or \mathcal{Y}) be the elliptically fibered family variety with base $\hat{\mathcal{B}}$ (or \mathcal{B}) of a (resolved) degeneration, and let \mathcal{Z} be an irreducible subvariety in $\hat{\mathcal{B}}$ (or \mathcal{B}). The family order of vanishing of a rational function h of $\hat{\mathcal{B}}$ (or of \mathcal{B}) at \mathcal{Z} is the order of vanishing computed directly through the discrete valuation associated to \mathcal{Z} when \mathcal{Z} is a prime divisor, and by reduction to the codimension-one problem through the generic slice passing through \mathcal{Z} in higher codimension. We denote it by $\text{ord}_{\hat{\mathcal{Y}}}(h)_{\mathcal{Z}}$ (or $\text{ord}_{\mathcal{Y}}(h)_{\mathcal{Z}}$).

The family orders of vanishing are important for the resolution of the degeneration in order to remove the non-minimal singularities of the family variety. When the subvariety \mathcal{Z} is taken as $E_p \subset \mathcal{B}$, they also define the relevant vanishing orders which determine the singular elliptic fibers over generic points in a component B^p of the central fiber; we refer to these as the codimension-zero singular fibers. On the other hand, for the interpretation of the model in F-theory, what matters are the individual fibers Y_u . Therefore, to later extract the physical information corresponding to the endpoint of the infinite-distance limit, we also need to consider what we will call component orders of vanishing.

Definition 5.2.3 (Component vanishing orders). Let $\hat{\mathcal{Y}}$ (or \mathcal{Y}) be the elliptically fibered family variety with base $\hat{\mathcal{B}}$ (or \mathcal{B}) of a (resolved) degeneration and pick (a component of) one of its fibers, denoting it by Y and its base by B . Let \mathcal{Z} be an irreducible subvariety $\mathcal{Z} \subset B \subset \hat{\mathcal{B}}$ (or $\mathcal{Z} \subset B \subset \mathcal{B}$). The component order of vanishing of a rational function h of $\hat{\mathcal{B}}$ (or \mathcal{B}) at \mathcal{Z} is the order of vanishing computed by reducing the problem to codimension-one through a slice contained in the restriction of the elliptic fibration $\hat{\mathcal{Y}}$ (or \mathcal{Y}) to the elliptic fibration $\pi_{\text{ell}} : Y \rightarrow B$. We denote it by $\text{ord}_Y(h|_B)_{\mathcal{Z}}$.

Note that, under the conditions of Definition 5.2.3, we always have

$$\text{ord}_{\hat{\mathcal{Y}}}(h)_{\mathcal{Z}} \leq \text{ord}_Y(h|_B)_{\mathcal{Z}}, \quad (5.2.48)$$

and similarly for \mathcal{Y} . This occurs because the definition of the component order of vanishing is the same as that of the family order of vanishing, but specifying a concrete slice that must be chosen to reduce to codimension-one, which may in particular be a non-generic slice.

Such a phenomenon gives rise to an important subtlety: It can happen that the component orders of vanishing of the defining polynomials of the Weierstrass model along a given locus are non-minimal, while the family orders of vanishing are minimal. We refer to such a situation as an obscured infinite-distance limit and analyse it in Appendix B.3. In particular, we will see that it is always possible to perform a base change to render the family and component vanishing orders identical. This is important to ensure that another sequence of blow-ups can be performed to remove all non-minimal elliptic fibers of the Weierstrass models \hat{Y}_u , which are the ones relevant for the F-theory interpretation, and not only those in the family variety $\hat{\mathcal{Y}}$.

Specifically for codimension-three points (from the point of view of \mathcal{B}) located on a curve $C_{p,q}$ along which two components B^p and B^q of the multi-component base central fiber B_0 intersect, it will be useful to also consider what we will call the interface order of vanishing, an even less generic specialization of the family vanishing order at the point.

Definition 5.2.4 (Interface vanishing orders). Under the hypotheses of Definition 5.2.3, let $C \subset B$ be a curve and \mathcal{Z} a point such that $\mathcal{Z} \subset C \subset B$. We call the interface order of vanishing of a rational function h of $\hat{\mathcal{B}}$ (or \mathcal{B}) the order of vanishing of h at \mathcal{Z} computed by reducing the problem to codimension-one by further restricting the elliptic fibration $\pi_{\text{ell}} : Y \rightarrow B$ to the elliptic fibration $\pi_{\text{ell}} : S \rightarrow C$. We denote it by $\text{ord}_S(h|_C)_{\mathcal{Z}}$.

Under the conditions of Definition 5.2.4 we have

$$\text{ord}_{\hat{\mathcal{Y}}}(h)_{\mathcal{Z}} \leq \text{ord}_Y(h|_B)_{\mathcal{Z}} \leq \text{ord}_S(h|_C)_{\mathcal{Z}}, \quad (5.2.49)$$

respectively for the resolved degeneration \mathcal{Y} .

Both for the component and interface orders of vanishing, if $\text{ord}_{\hat{\mathcal{Y}}}(h)_B \neq 0$, respectively $\text{ord}_Y(h|_B)_C \neq 0$, the restrictions of the rational function h that we need to consider in order to compute the non-generic orders of vanishing are zero. When this occurs, we assign infinite component, respectively interface, order of vanishing to h over that locus. Occasionally, we will define modified rational functions in which we remove the vanishing piece in order to obtain a finite result, see e.g. Definition 5.2.16.

Note that one can in practice compute the relevant interface orders of vanishing directly in the unresolved degeneration, as long as one is careful with how base components and curves contract through the pushforward of the blow-up map. This may be useful to extract information about how the resolved degeneration will behave before attempting the resolution process, as we showcase in Example B.3.2.

5.2.2.3 Class 1–5 models

In [156, 157] the infinite-distance degenerations of elliptic K3 surfaces were sorted into five different classes depending on how the vanishing orders over the non-minimal loci exceeded the non-minimal bound. It is useful to consider an analogous classification for the codimension-one infinite-distance degenerations of elliptically fibered threefolds.

Definition 5.2.5 (Degenerations of Class 1–5). Let $\hat{\mathcal{Y}}$ (or \mathcal{Y}) be the elliptically fibered family variety with base $\hat{\mathcal{B}}$ (or \mathcal{B}) of a (resolved) degeneration, and let $\mathcal{Z} \subset \hat{\mathcal{B}}_0$ be a curve with

$$\text{ord}_{\hat{\mathcal{Y}}}(f_{(b)}, g_{(b)}, \Delta_{(b)})_{\mathcal{Z}} = (4 + \alpha, 6 + \beta, 12 + \gamma), \quad \alpha, \beta, \gamma \geq 0. \quad (5.2.50)$$

We classify the family vanishing orders of the defining polynomials of the Weierstrass model over \mathcal{Z} into

$$\text{Class 1: } \alpha = 0, \beta = 0, \gamma = 0, \quad (5.2.51)$$

$$\text{Class 2: } \alpha > 0, \beta = 0, \gamma = 0, \quad (5.2.52)$$

$$\text{Class 3: } \alpha = 0, \beta > 0, \gamma = 0, \quad (5.2.53)$$

$$\text{Class 4: } \alpha = 0, \beta = 0, \gamma > 0, \quad (5.2.54)$$

$$\text{Class 5: } \alpha > 0, \beta > 0, \gamma > 0. \quad (5.2.55)$$

The degeneration $\hat{\rho} : \hat{\mathcal{Y}} \rightarrow D$ is then termed to be a Class 5 model if it presents any curves with Class 5 vanishing orders, a Class 1–4 model if it presents curves of non-minimal elliptic fibers all exhibiting Class 1–4 vanishing orders, and a finite-distance model otherwise.

Since in Definition 5.2.5 we are assuming that the family variety \mathcal{Y} supports non-minimal elliptic fibers over \mathcal{Z} , the degeneration is amenable to a resolution process like the one described in Section 5.2.2.1. Denoting by E the exceptional divisor arising from the blow-up $\pi : \mathcal{B} \rightarrow \hat{\mathcal{B}}$ with centre at \mathcal{Z} , the codimension-zero elliptic fibers over the base component E will be the ones read off from

$$\text{ord}_{\mathcal{Y}}(f_b, g_b, \Delta_b)_E = (\alpha, \beta, \gamma), \quad (5.2.56)$$

c.f. Example 5.2.1. Hence, we see that for Class 1–4 family vanishing orders the generic fiber over the exceptional base component is of Kodaira type I_m with $m = \gamma$, while Class 5 vanishing orders lead to the remaining fiber types in the Kodaira-Néron list.

The type of fibers found over a base component in codimension-zero will play an important role in the physical analysis of Chapter 6. Focusing on Class 4 vanishing orders first, we see that when the generic fiber in a component is of type $I_{m \geq 1}$, the complex structure τ of the elliptic fiber attains a value for which $j(\tau) \rightarrow \infty$, implying that $\tau \rightarrow i\infty$. In F-theory, the complex structure of the elliptic fiber is identified with the Type IIB axio-dilaton, meaning that these are components in which $g_s \rightarrow 0$, i.e. regions of weak string coupling. This affects the types of 7-branes that one can encounter in said region of spacetime, which must be compatible with this background value of the axio-dilaton. Class 1–3 vanishing orders lead to codimension-zero type I_0 fibers over the exceptional component; over such regions the string coupling becomes non-perturbative.

We now come to an important result: Class 5 vanishing orders can always be removed by a modification of the degeneration, possibly after a base change. This is a consequence of the classical result of Kempf, Knudsen, Mumford and Saint-Donat on semi-stable reduction that we have alluded to a few times above. In the remainder of this section, we recall this theorem and explain how it allows us to exclude Class 5 models, pointing out a few subtleties related to what we call obscured Class 5 models. As a conclusion, degenerations of Class 5 can always either be transformed into Class 1–4 degenerations, which lie at infinite distance in the moduli space, or to degenerations invoking only minimal singularities, which lie at finite distance.

Theorem 5.2.6 (Semi-stable Reduction Theorem [308]). *After a base change*

$$\begin{aligned} \delta_k : D &\longrightarrow D \\ u &\longmapsto u^k, \end{aligned} \quad (5.2.57)$$

*every degeneration admits a modification that is semi-stable.*¹⁴

For degenerations of K3 surfaces, this result can be improved. From the work of Kulikov [319] and Persson–Pinkham [320] we know that semi-stability can be achieved while making the canonical bundle $K_{\mathcal{Y}}$ trivial. Moreover, a very complete description of the possible types of central fiber is available [300–302], a fact that was exploited in [156, 157]. Once we venture into the degenerations of Calabi-Yau threefolds, we lack such strong results, but we can still invoke Theorem 5.2.6 to our advantage.

Components originating from the blow-up of a curve with Class 5 family vanishing orders lead to codimension-zero fibers of the types II, III, IV, I_m^* , IV^* , III^* and II^* , given (5.2.56) above.

¹⁴The Semi-stable Reduction Theorem is actually stronger than stated, leading to a central fiber of the degeneration that has strict normal crossings. Insisting on preserving the Calabi-Yau condition may spoil this property, vide [318]. In our case, we are happy to preserve some singularities unresolved in order to maintain a trivial canonical class, cf. Footnote 7.

A degeneration presenting a component with these types of generic fibers cannot be a semi-stable degeneration,¹⁵ since

- Kodaira fibers of types II, III and IV present singularities that are not of normal crossing type, and
- Kodaira fibers of types I_m^* , IV^* , III^* and II^* contain exceptional rational curves of multiplicity bigger than one, meaning that the components over which they are fibered appear with multiplicity bigger than one as well, violating reducedness.

We hence conclude that the Semi-stable Reduction Theorem ensures that, possibly after performing a base change, Class 5 family vanishing orders can be removed from any model under consideration. The theorem is, however, not constructive, and we therefore do not know a priori what combination of base changes and modifications of the degeneration must be taken in order to remove Class 5 vanishing orders. It is a logical possibility that, given a model presenting Class 5 vanishing orders, in the equivalent semi-stable degeneration the elliptic fibration does not extend to some components of the central fiber. We have not encountered such an example, and it may very well be that in the restricted class of degenerations that we consider this problem does not arise; were this to occur, we would interpret the model in the context of M-theory as having an obstructed F-theory limit.

While the discussion here is kept general, in Chapter 6 we mainly focus on degenerations of elliptic fibrations over Hirzebruch surfaces, both to make the discussion more explicit and to draw connections to the heterotic dual models to which some of these are related. In this explicit context, we can go substantially beyond the existence provided by the Semi-stable Reduction Theorem and determine the precise combination of base changes and modifications that transform a degeneration of Class 5 into a Class 1–4 or finite-distance model. This explicit analysis holds for degenerations on divisors of Hirzebruch surfaces and is presented in [309].

As we discuss at length in Appendix B.3, in some models a curve can exhibit minimal family vanishing orders, while having non-minimal component vanishing orders, leading to an obscured infinite-distance limit. A situation similar in spirit occurs when the curve exhibits non-minimal family vanishing orders of Class 1–4, but non-minimal component vanishing orders of Class 5. The exceptional component arising from a blow-up centred at such a curve would support codimension-zero I_m fibers, as their type is determined by the family vanishing orders of the curve. The (fibral resolution of) the resolved degeneration obtained from such a model as explained in Section 5.2.2.1 will not be semi-stable, however, and therefore these obscured Class 5 models can be discarded by invoking the Semi-stable Reduction Theorem as was done above.

To see that these are not semi-stable, note that two components arising from Class 1–4 loci Y^p and Y^q and supporting codimension-zero I_m and $I_{m'}$ fibers, respectively, intersect (either trivially or) on an elliptically fibered surface $Y^p \cap Y^q$ with codimension-zero $I_{m''}$ fibers. By contrast, if one of the two components stems from an obscured Class 5 curve the codimension-zero fibers of $Y^p \cap Y^q$ will be of type II, III, IV, I_m^* , IV^* , III^* or II^* . Denoting the components of the fibral resolution of the multi-component central fiber by $X_0 = \bigcup_{p=0}^P \bigcup_{i_p=1}^{l_p} X_{i_p}^p$, one can see that, although the arguments given above do not apply directly to each component, they do apply to the restrictions $(X_0 - X_{i_p}^p) \Big|_{X_{i_p}^p}$, meaning that the degeneration is not semi-stable.

¹⁵More precisely, we mean that the degeneration $\rho : \mathcal{X} \rightarrow D$ in which even the minimal fibral singularities have been resolved will not be semi-stable.

This implies, in particular, that in the resolution process of a semi-stable degeneration the curves over which the components intersect will not exhibit non-minimal component vanishing orders, as this would imply that we are facing at least an obscured Class 5 model.

In the context of the explicit removal of Class 5 loci through the methods presented in [309], we would first apply a base change to an obscured Class 5 model in order to make the Class 5 vanishing orders apparent at the family level, and then apply the combination of base changes and modifications required to remove the regular Class 5 models.

As we mentioned above, the modifications of the degeneration taken as part of the application of the Semi-stable Reduction Theorem can be assumed to preserve the elliptic fibration in F-theory. Hence, the modifications of $\hat{\rho} : \hat{\mathcal{Y}} \rightarrow D$ induce modifications of $\hat{\rho}|_{\hat{\mathcal{B}}} : \hat{\mathcal{B}} \rightarrow D$, over which the elliptic fibration is extended to obtain a Calabi-Yau variety. A modification of the base degeneration is a birational morphism that is an isomorphism over D^* , which is a Zariski open set. Hence, due to the Weak Factorization Theorem [321–323], it can be factored into a sequence of blow-ups and blow-downs at smooth centres contained in the central fiber. In other words, the modifications of the base can be obtained by applying the process discussed in Section 5.2.2.1. The modification of $\hat{\rho} : \hat{\mathcal{Y}} \rightarrow D$ is then obtained by taking the appropriate line bundles over the base degeneration, as explained in the same section. In some concrete examples, we will also consider flops connecting two different resolutions of the degeneration that, in agreement with the Weak Factorization Theorem, are equivalent to a sequence of blow-ups and blow-downs, cf. Remark B.4.1.

5.2.3 Single infinite-distance limits and their open-chain resolutions

We are now in a position to characterise the resolutions $\rho : \mathcal{Y} \rightarrow D$ of the infinite-distance degenerations $\hat{\rho} : \hat{\mathcal{Y}} \rightarrow D$ more precisely.

As a first result, we constrain the types of curves over which non-minimal singularities can arise. In a six-dimensional F-theory model, non-abelian gauge algebras are associated to minimal singular fibers over irreducible curves C , which we are assuming to be smooth, in the base B . With this assumption, C is a Riemann surface embedded in B , and its topology is completely classified by its genus $g(C)$. The choices for C within a fixed base B are numerous, and we can go up to very high genus. For example, in a model constructed over the base $B = \mathbb{P}^2$ it is easy to tune a Kodaira singularity of type III over a generic representative of $C = 9H$, for which the genus is $g(C) = 28$. The situation becomes more restrictive as the singular fibers that we try to tune over C become worse. Hence, the choices we have for C become the most constrained when we try to tune non-minimal singular fibers over it. In fact, smooth irreducible curves can only support non-minimal fibers if they have genus zero or one:

Proposition 5.2.7. *Let Y be an elliptically fibered Calabi-Yau threefold with base \hat{B} , where \hat{B} is one of the allowed six-dimensional F-theory bases. Let $C \subset \hat{B}$ be a smooth irreducible curve of genus $g(C)$ supporting non-minimal singular fibers. Then, $g(C) \leq 1$, and $g(C) = 1$ if and only if $C = \overline{K}_{\hat{B}}$.*

The proof of this result is technical, and we relegate the details to Appendix B.2. In fact, it is easy to see that non-minimal singularities are possible only over curves $C \leq \overline{K}_{\hat{B}}$, and the main work of Appendix B.2 consists in showing explicitly that smooth irreducible curves on the F-theory base spaces with this property behave as in the proposition.

With this restriction in place, we only need to analyse what we will call genus-zero and genus-one degenerations, depending on the genus of the curve that supports the non-minimal

fibers. Given Proposition 5.2.7, genus-one degenerations are only possible over those bases in which the anticanonical class has irreducible representatives, as otherwise tuning non-minimal singularities over the reducible curve $C = \overline{K}_B$ just amounts to tuning several simultaneous genus-zero degenerations over its irreducible components.

Corollary 5.2.8. *With the hypothesis of Proposition 5.2.7, $g(C) = 1$ is only possible if $B = \mathbb{P}^2$, $B = \mathbb{F}_n$ with $0 \leq n \leq 2$ or a blow-up of them that does not spoil the irreducibility of \overline{K}_B .*

There cannot occur genus-one degenerations over the Hirzebruch surfaces \mathbb{F}_n with $3 \leq n \leq 12$, since their anticanonical class is reducible, as has been exploited in the F-theory literature in the study of non-Higgsable clusters [324]. Their blow-ups $\text{Bl}(\mathbb{F}_n)$, with $3 \leq n \leq 12$, suffer the same fate. Therefore, as claimed above, we can only tune genus-one degenerations in models constructed over the bases \mathbb{P}^2 , \mathbb{F}_n with $0 \leq n \leq 2$, and those blow-ups of them that do not spoil the irreducibility of the anticanonical class (see Remark B.2.4 for an example). Moreover, once we blow up along a genus-zero curve the line bundles over the resulting components are strictly smaller than the anticanonical class, and therefore no longer allow for the tuning of non-minimal singular fibers over an irreducible genus-one curve, even if it is present in the geometry, as will become evident in Sections B.4.2 and 5.2.5. This means that further components can then only arise through genus-zero blow-ups. Hence, the possible genus-zero degenerations outnumber the genus-one degenerations by far, and they will for this reason constitute our primary focus in what follows. We briefly comment on genus-one degenerations in Section 5.2.7.

In the upcoming sections, we will geometrically characterize genus-zero degenerations in detail. Before we come to this, however, we introduce the notion of a “single infinite-distance limit.” This should correspond to the simplest type of limit, which we can then extend further. Naively, such limits should be characterised by a single irreducible curve supporting non-minimal singular fibers in the base $\hat{B}_0 \subset \hat{\mathcal{B}}$, as assumed to be the case in Section 5.2.2. As it turns out, however, this definition is not stable under base change and modifications, and the better way to define single infinite-distance limits is as follows.

Definition 5.2.9 (Single infinite-distance limits). Let $\hat{\rho} : \hat{\mathcal{Y}} \rightarrow D$ be a degeneration of the type described in Section 5.2.1 such that there is a collection of curves $\hat{\mathcal{C}}_r := \{\mathcal{C}_i \cap \mathcal{U}\}_{1 \leq i \leq r}$ in $\hat{\mathcal{B}}$ with non-minimal component vanishing orders. We call the degeneration a single infinite-distance limit if

- (i) $(\mathcal{C}_i \cap \mathcal{U}) \cdot_{\hat{\mathcal{B}}} (\mathcal{C}_j \cap \mathcal{U}) = 0$ for all $1 \leq i < j \leq r$,
- (ii) no point in the $\{\mathcal{C}_i \cap \mathcal{U}\}_{1 \leq i \leq r}$ curves has non-minimal interface vanishing orders, and
- (iii) no point in $\hat{\mathcal{B}} \setminus (\bigcup_{i=1}^r \mathcal{C}_i \cap \mathcal{U})$ presents infinite-distance non-minimal component vanishing orders.

Indeed, the limits falling under this definition can be birationally transformed to limits with a single curve of non-minimal degenerations, hence conforming with the general intuition of what a single infinite-distance limit should be. To see this, let us first define the related notion of an open-chain resolution.

Definition 5.2.10 (Open-chain resolution). Let $\hat{\rho} : \hat{\mathcal{Y}} \rightarrow D$ be a degeneration of the type described in Section 5.2.1 and let $\rho : \mathcal{Y} \rightarrow D$ be its modification removing the non-minimal singular fibers by repeated blow-ups and line bundle shifts as explained in Section 5.2.2, leading

to a multi-component central fiber $Y_0 = \bigcup_{p=0}^P Y^p$. We say that $\rho : \mathcal{Y} \rightarrow D$ is an open-chain resolution if the components of Y_0 form an open chain, i.e. they intersect in pairs

$$Y^{p-1} \cap Y^p \neq \emptyset, \quad Y^p \cap Y^{p+1} \neq \emptyset, \quad 0 < p < P, \quad (5.2.58)$$

over curves, with all the other intersections vanishing.

A key result of our work is that resolutions of single infinite-distance limits, in the sense of Definition 5.2.9, are always open-chain resolutions:

Single infinite-distance limit degenerations

Proposition 5.2.11. *Let $\hat{\rho} : \hat{\mathcal{Y}} \rightarrow D$ be a single infinite-distance limit degeneration. Its resolved modifications $\rho : \mathcal{Y} \rightarrow \mathcal{B}$, obtained as explained in Section 5.2.2, are open-chain resolutions.*

This result will be proven in Appendices B.5 and B.6, after we have explored the properties of the resolved central fiber in greater depth. As part of the proof, we will see that a resolution that deviates from the open-chain structure can be blown down to a model with non-minimal singularities over curves that fall out of the allowed class as per Definition 5.2.9. Showing this explicitly requires some knowledge of the structure of base spaces of elliptic Calabi-Yau threefolds, and in particular the $\text{Bl}(\mathbb{F}_n)$, to which we devote Section B.1.3.

As one aspect of these results, we can rule out star-shaped resolutions: Such a structure would occur if on a base surface one could tune non-minimal elliptic fibers exclusively over three or more mutually non-intersecting curves. This, however, is not possible, as we explicitly show in Appendix B.6. Tuning such non-minimal curves inevitably leads to non-minimalities over curves intersecting at least one element of the original set of curves, hence compromising the star shape of the resolution.

Now, apart from clarifying the structure of the resolutions of the degenerations falling under Definition 5.2.9, Proposition 5.2.11 also shows that we can birationally transform such a degeneration into one in which we only have one single irreducible curve supporting non-minimal fibers: This is possible simply by blowing down the open chain to one of its end-components. In this sense, Definition 5.2.9 does realise the “naive” definition of single infinite-distance limit, but in a way invariant under blow-ups and blow-downs (and also under base change). This type of degenerations is the one represented in Figure 5.1.

Let us now come back to Definition 5.2.9 and gain some intuition behind Conditions (ii) and (iii) in Definition 5.2.9 and why they are needed for the definition to make sense.

First, the existence of an open-chain resolution as such is not necessarily invariant under base change. To understand this, note first that if $\hat{\rho} : \hat{\mathcal{Y}} \rightarrow D$ is a degeneration whose resolution leads to an open-chain central fiber as in Definition 5.2.10, its modifications obtained by blow-ups and blow-downs of curves in $\hat{\mathcal{B}}$ will be as well. However, the existence of an open-chain resolution is no longer guaranteed after modifications involving base changes, depending on the type of obscured infinite-distance limits present in the model. Example B.3.2 showcases this behaviour, where the original resolution contains some obscured infinite-distance limits which, when made apparent for the family variety through a base change, spoil the open chain structure. As we will see in Appendix B.5, Condition (ii) of Definition 5.2.9 prevents this from happening for a single infinite-distance limit degeneration; base change does not spoil its open-chain resolution structure.

Furthermore, we remark that models containing codimension-two infinite-distance non-minimal points may also lead to open-chain resolutions as defined in Definition 5.2.10, but in which some of the non-trivial intersections among components occur over points instead of curves. Since our primary focus is on codimension-one degenerations, we have excluded such models from our definition of single infinite-distance limits through Condition (iii) in Definition 5.2.9, and from our definition of open-chain resolution by demanding that the components intersect over curves.

In Sections 5.2.4 and 5.2.5 we study the geometry of genus-zero single infinite-distance limits in detail. With this intuition at hand, we make the discussion more general in Sections B.4.1 and B.4.2, exploring the geometry of those degenerations that do not allow for a simple open-chain resolution; we briefly advance some of their features in Section 5.2.6.

5.2.4 Geometry of the components in a single infinite-distance limit

Focusing first on genus-zero single infinite-distance limit degenerations $\hat{\rho} : \hat{\mathcal{Y}} \rightarrow D$, we turn our attention to the geometry of the components of the blown up base family variety $\hat{\mathcal{B}}$. As just discussed, these degenerations have open-chain resolutions, and we therefore assume in this section that the degenerations considered have such a resolution structure, relegating the general case to Section B.4.1.

Since we will have to keep track of various successive blow-ups, let us denote the initial base variety and the one resulting from the p -th blow-up along a curve of non-minimal singular elliptic fibers by

$$\text{Bl}_0(\hat{\mathcal{B}}) := \hat{\mathcal{B}}, \quad \text{Bl}_p(\hat{\mathcal{B}}) := \pi_p^* \circ \cdots \circ \pi_1^*(\hat{\mathcal{B}}), \quad (5.2.59)$$

where $\pi_i : \text{Bl}_i(\hat{\mathcal{B}}) \rightarrow \text{Bl}_{i-1}(\hat{\mathcal{B}})$ denotes the i -th blow-up map. With this notation, the final base family variety after P blow-ups is

$$\text{Bl}_P(\hat{\mathcal{B}}) = \mathcal{B}. \quad (5.2.60)$$

At each step, the central fiber $\text{Bl}_p(\hat{\mathcal{B}})_0$ of the base family variety $\text{Bl}_p(\hat{\mathcal{B}})$ has $p+1$ irreducible components,

$$\text{Bl}_p(\hat{\mathcal{B}})_0 = \bigcup_{i=0}^p B^i = \bigcup_{i=0}^p E_i, \quad (5.2.61)$$

which we simply denote by $B^i = E_i$ in all cases, always taking their strict transforms in the next step of the blow-up process and, hence, without risk of confusion. The elliptically fibered varieties over the successive $\{\text{Bl}_p(\hat{\mathcal{B}})\}_{0 \leq p \leq P}$ bases will be denoted by $\{\text{Bl}_p(\hat{\mathcal{Y}})\}_{0 \leq p \leq P}$.

We start with a curve $C_1 = \mathcal{C}_1 \cap \mathcal{U} \subset B^0 \subset \text{Bl}_0(\hat{\mathcal{B}})$ with $g(C_1) = 0$ that is blown-up to produce a new component $B^1 = E_1 \subset \text{Bl}_1(\hat{\mathcal{B}})_0 \subset \text{Bl}_1(\hat{\mathcal{B}})$. The process may end here, or we may still have curves of non-minimal singular fibers. Because we are assuming to work with a degeneration whose resolution is an open-chain, we may encounter at most one such irreducible curve C_2 , that must be contained either in B^0 or in B^1 , and whose intersection with C_1 must be trivial

$$C_1 \cap C_2 = \emptyset. \quad (5.2.62)$$

Because one genus-zero blow-up has already been performed, the line bundles over the components B^0 and B^1 are such that they only allow for non-minimal singular fibers to be tuned over irreducible genus-zero curves, as we advanced above and discuss in Sections B.4.2 and 5.2.5. Hence, $g(C_2) = 0$. Blowing up along C_2 yields a new component $B^2 = E_2 \subset \text{Bl}_2(\hat{\mathcal{B}})_0 \subset \text{Bl}_2(\hat{\mathcal{B}})$. Continuing in this way, we finish after P blow-ups and have a central fiber $B_0 \subset \mathcal{B}$ whose

component B^p arose from a blow-up along an irreducible curve C_p with $g(C_p) = 0$ and trivial intersection with all other curves that were blown-up. Note that, because of the open-chain resolution that we are assuming, the new curves of non-minimal singular fibers at each step can only be found in the end-components of the chain.

Under the conditions described above, all components B^p are Hirzebruch surfaces. This is intuitively clear since the blow-up operation leading to the B^p component is placing a \mathbb{P}^1 factor on top of each point of the genus-zero curve $C_p \cong \mathbb{P}^1$, ultimately resulting in a \mathbb{P}^1 -fibration over \mathbb{P}^1 . Running this argument more carefully, we can see that it is, in fact, a \mathbb{P}^1 -bundle over \mathbb{P}^1 , and hence a Hirzebruch surface $B^p = F_{n_p}$.

Hirzebruch surfaces as components of open-chain resolutions

Proposition 5.2.12. *Let $\text{Bl}_{p-1}(\hat{B})$ be the result of blowing up $p-1$ times the base family variety \hat{B} of a genus-zero degeneration $\hat{\rho} : \hat{\mathcal{Y}} \rightarrow D$ with an open-chain resolution. Let C_p be an irreducible curve supporting non-minimal singular fibers and contained in the component B^i . Then, the exceptional component $B^p = E_p$ arising from the blow-up of $\text{Bl}_{p-1}(\hat{B})$ along C_p is the Hirzebruch surface $\mathbb{F}_{|C_p \cdot B^i C_p|}$.*

Proof. Denoting by $\mathcal{C}_{C_p/\text{Bl}_{p-1}(\hat{B})}$ the normal cone of C_p in $\text{Bl}_{p-1}(\hat{B})$ and by $\mathcal{N}_{C_p/\text{Bl}_{p-1}(\hat{B})}$ its normal bundle, the exceptional divisor of the blow-up along C_p is the projectivization

$$E_p = \mathbb{P} \left(\mathcal{C}_{C_p/\text{Bl}_{p-1}(\hat{B})} \right) = \mathbb{P} \left(\mathcal{N}_{C_p/\text{Bl}_{p-1}(\hat{B})} \right), \quad (5.2.63)$$

where the second equality is a consequence of the smoothness of C_p and $\text{Bl}_{p-1}(\hat{B})$. Altogether, E_p is therefore the projectivization of a rank 2 vector bundle over the genus-zero curve $C_p \cong \mathbb{P}^1$, which is by definition (as we reviewed in Appendix B.1) a Hirzebruch surface \mathbb{F}_{n_p} for some n_p .

Let us now determine the concrete Hirzebruch surface that we obtain. We start by noting that, due to the inclusions $C_p \subset B^i \subset \text{Bl}_{p-1}(\hat{B})$, we have the short exact sequence

$$0 \longrightarrow \mathcal{N}_{C_p/B^i} \longrightarrow \mathcal{N}_{C_p/\text{Bl}_{p-1}(\hat{B})} \longrightarrow \mathcal{N}_{B^i/\text{Bl}_{p-1}(\hat{B})} \Big|_{C_p} \longrightarrow 0. \quad (5.2.64)$$

These are all holomorphic vector bundles over $C_p \cong \mathbb{P}^1$, and due to Grothendieck's splitting theorem we can therefore conclude that

$$\mathcal{N}_{C_p/\text{Bl}_{p-1}(\hat{B})} = \mathcal{N}_{C_p/B^i} \oplus \mathcal{N}_{B^i/\text{Bl}_{p-1}(\hat{B})} \Big|_{C_p}. \quad (5.2.65)$$

Furthermore, due to the smoothness of the curve C_p , the component $B^i = E_i$ and $\text{Bl}_{p-1}(\hat{B})$,

$$\mathcal{N}_{C_p/B^i} = \mathcal{O}_{C_p}(C_p) := \mathcal{O}_{B^i}(C_p)|_{C_p} = \mathcal{O}_{\mathbb{P}^1}(C_p \cdot_{B^i} C_p), \quad (5.2.66a)$$

$$\mathcal{N}_{E_i/\text{Bl}_{p-1}(\hat{B})} = \mathcal{O}_{E_i}(E_i) := \mathcal{O}_{\text{Bl}_{p-1}(\hat{B})}(E_i)|_{E_i}. \quad (5.2.66b)$$

To evaluate the last expression, note that due to the open-chain resolution structure, the component B^i where C_p lies must be one of the end-components of the open chain, and hence

$$E_i \cdot_{\text{Bl}_{p-1}(\hat{B})} E_j = C_q \neq 0 \quad (5.2.67)$$

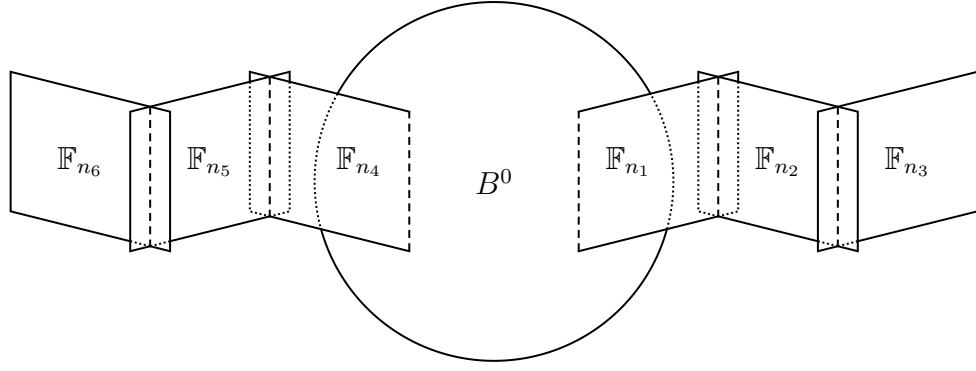


Figure 5.2: The open-chain of B^p components arising for the central fiber B_0 of the base family variety \mathcal{B} of the (open-chain) resolution of a single infinite-distance limit degeneration $\hat{\rho} : \hat{\mathcal{Y}} \rightarrow D$. The strict transform B^0 of the original base \hat{B} preserves its original geometry $B^0 \cong \hat{B}_0$, while the rest of the components B^p for $1 \leq p \leq P$ are Hirzebruch surfaces, as proved in Proposition 5.2.12.

for some particular value of j and q , with the intersections with the components $E_{k \neq i,j}$ vanishing. Then, we have

$$\mathcal{N}_{E_i/\text{Bl}_{p-1}(\hat{B})} = E_i \cdot_{\text{Bl}_{p-1}(\hat{B})} E_i = -E_i \cdot_{\text{Bl}_{p-1}(\hat{B})} E_j = -C_q, \quad (5.2.68)$$

and therefore

$$\mathcal{N}_{B^i/\text{Bl}_{p-1}(\hat{B})} \Big|_{C_p} = \mathcal{O}_{\mathbb{P}^1}(-C_q \cdot_{B^i} C_p) = \mathcal{O}_{\mathbb{P}^1}, \quad (5.2.69)$$

where the intersection is vanishing due to the open-chain resolution assumption. Altogether, this leads to

$$E_p = \mathbb{P}(\mathcal{O}_{\mathbb{P}^1} \oplus \mathcal{O}_{\mathbb{P}^1}(C_p \cdot_{B^i} C_p)). \quad (5.2.70)$$

Finally, due to the invariance of the projectivization of a bundle under twists by Abelian line bundles, we can always take

$$E_p = \mathbb{P}(\mathcal{O}_{\mathbb{P}^1} \oplus \mathcal{O}_{\mathbb{P}^1}(|C_p \cdot_{B^i} C_p|)) = \mathbb{F}_{|C_p \cdot_{B^i} C_p|}. \quad (5.2.71)$$

□

For smooth divisors D_1 , D_2 and D_3 in a smooth threefold X , the intersection product satisfies

$$D_1 \cdot_X D_2 \cdot_X D_3 = D_1|_{D_3} \cdot_{D_3} D_2|_{D_3}. \quad (5.2.72)$$

Applying this to E_i and E_p in $\text{Bl}_p(\hat{\mathcal{B}})$, we have

$$\begin{aligned} C_p \cdot_{B^i} C_p &= -E_i|_{E_i} \cdot_{E_i} E_p|_{E_i} = -E_i \cdot_{\text{Bl}_p(\hat{\mathcal{B}})} E_p \cdot_{\text{Bl}_p(\hat{\mathcal{B}})} E_i = E_i \cdot_{\text{Bl}_p(\hat{\mathcal{B}})} E_p \cdot_{\text{Bl}_p(\hat{\mathcal{B}})} E_p \\ &= E_i|_{E_p} \cdot_{E_p} E_p|_{E_p} = -C_p \cdot_{B^p} C_p. \end{aligned} \quad (5.2.73)$$

Hence, $C_p \subset B^p \cong \mathbb{F}_{|C_p \cdot_{B^i} C_p|}$ is the $(-C_p \cdot_{B^i} C_p)$ -curve of the Hirzebruch surface.

The geometry of the central fiber B_0 of the base variety \mathcal{B} of the open-chain resolution, as described in Proposition 5.2.12, is schematically represented in Figure 5.2. In the proof of Proposition 5.2.12, the fact that we are dealing with an open-chain resolution was only used to determine the fact that $(E_i \cdot_{\text{Bl}_{p-1}(\hat{\mathcal{B}})} E_j) \cap C_p = \emptyset$ for all $i \neq j \in \{0, \dots, p-1\}$. Hence, the same proof applies to the following rephrased proposition.

Proposition 5.2.13. *Let $\hat{\mathcal{B}}$ be the base family variety of a genus-zero degeneration $\hat{\rho} : \hat{\mathcal{Y}} \rightarrow D$ and $\text{Bl}_{p-1}(\hat{\mathcal{B}})$ be the result of $p-1$ blow-ups of $\hat{\mathcal{B}}$ with centres along the irreducible curves $\{C_q\}_{1 \leq q \leq p-1}$. Let C_p be a smooth irreducible curve over which $\text{Bl}_{p-1}(\hat{\mathcal{Y}})$ presents non-minimal singular fibers, contained in the component B^i and with trivial intersections $C_p \cdot_{\text{Bl}_{p-1}(\hat{\mathcal{B}})} C_q$ for all $1 \leq q \leq p-1$. Then, the exceptional component $B^p = E_p$ arising from the blow-up of $\text{Bl}_{p-1}(\hat{\mathcal{B}})$ along C_p is the Hirzebruch surface $\mathbb{F}_{|C_p \cdot_{B^i} C_p|}$.*

This slightly modified form of the proposition will be the one that we will generalize in Section B.4.1 when we go beyond the study of open-chain resolutions. It tells us that, if we keep blowing up along genus-zero curves that do not intersect each other, we only produce chains of Hirzebruch surfaces¹⁶ attached to the strict transform B^0 of the original component \hat{B}_0 . Each Hirzebruch surface \mathbb{F}_{n_p} intersects its predecessor in the chain along the $(\pm n_p)$ -curve, and hence its successor along the $(\mp n_p)$ -curve, if we are to avoid intersections among the blow-up centres. For the end-components of such chains of Hirzebruch surfaces, we will refer to the $(\pm n_p)$ -curves over which the end-component does not intersect its predecessor in the chain as the end-curves.

We conclude the section with an illustrative example making the above discussion concrete.

Example 5.2.14. Before concluding Example 5.2.1, we noticed that the single blow-up that we had performed did not completely remove the non-minimal singular fibers from the family variety $\text{Bl}_1(\hat{\mathcal{B}})$, since

$$\text{ord}_{\mathcal{Y}}(f_b, g_b, \Delta_b)_{s=e_1=0} = (4, 6, 12). \quad (5.2.74)$$

Let us finish the resolution process and analyse the geometry of the resulting components. We carry out a second and final (toric) blow-up leading to $\text{Bl}_2(\hat{\mathcal{B}}) = \mathcal{B}$, this time with centre $\mathcal{S} \cap E_1$. To this end, we add a new (exceptional) coordinate e_2 to the (total) coordinate ring of $\text{Bl}_1(\hat{\mathcal{B}})$, together with a new \mathbb{C}^* -action

$$\begin{aligned} \mathbb{C}_{\mu_2}^* : \mathbb{C}_{(s,t,v,w,e_0,e_1,e_2)}^* &\longrightarrow \mathbb{C}_{(s,t,v,w,e_0,e_1,e_2)}^* \\ (s, t, v, w, e_0, e_1, e_2) &\longmapsto (\mu_2 s, t, v, w, e_0, \mu_2 e_1, \mu_2^{-1} e_2), \end{aligned} \quad (5.2.75)$$

and we modify the Stanley-Reisner ideal to be

$$\mathcal{I}_{\mathcal{B}} = \langle st, vw, se_0, se_1, te_1, te_2, e_0 e_2 \rangle. \quad (5.2.76)$$

In the defining polynomials of the Weierstrass model we perform the substitutions

$$s \longmapsto se_2, \quad (5.2.77a)$$

$$e_1 \longmapsto e_1 e_2, \quad (5.2.77b)$$

and then divide them by the appropriate powers of e_2 . Altogether, we arrive at the Weierstrass model given by

$$f_b = s^4 t^4 v^2 (e_0 e_1 e_2 v^6 - 3v^4 w^2 + 6v^2 w^4 - 3w^6), \quad (5.2.78a)$$

$$g_b = s^5 t^5 v^3 (e_1 e_2^2 s^2 v^{16} + e_0^2 e_1 t^2 w^2 - 2s t v^6 w^3 + 6s t v^4 w^5 - 6s t v^2 w^7 + 2s t w^9), \quad (5.2.78b)$$

$$\Delta_b = s^{10} t^{10} v^6 e_1 p_{4,32,3,1}([s:t], [v:w:t], [s:e_0:e_1], [s:e_1:e_2]), \quad (5.2.78c)$$

¹⁶We can have at most two such chains of Hirzebruch surfaces attached to the strict transform of the original base component, see the discussion in Appendix B.6.

in which all non-minimal singular fibers have been removed.¹⁷

Since we have blown up a total of two times, the central fiber Y_0 of the resolved degeneration $\rho : \mathcal{Y} \rightarrow D$ consists of three components $\{Y^p\}_{0 \leq p \leq 2}$ with base $\{B^p\}_{0 \leq p \leq 2}$. The base of the central fiber of the original degeneration was $\hat{B}_0 = \mathbb{F}_7$, and therefore its strict transform is also $B^0 = \mathbb{F}_7$. Since this is an open-chain resolution (of, in this case, a single infinite-distance limit), we can now apply Proposition 5.2.12 to determine the geometry of the other components. The first blow-up was along the curve $C_1 = \mathcal{S} \cap \mathcal{U}$, which is the (-7) -curve of \hat{B}_0 . This makes the associated exceptional component $B^1 = \mathbb{F}_7$ again. The next blow-up occurs along the curve $C_2 = \mathcal{S} \cap E_1$, which is the (-7) -curve of B^1 , and therefore we also find $B^2 = \mathbb{F}_7$. Hence, we expect that all components are

$$B^0 \cong B^1 \cong B^2 \cong \mathbb{F}_7. \quad (5.2.79)$$

Let us check this explicitly only for B^1 , since the computation is totally analogous for B^2 . Given that $B^1 = \{e_1 = 0\}$, the Stanley-Reisner ideal (5.2.76) tells us that in this component s and t cannot vanish. We can then first use the $\mathcal{C}_{\lambda_1}^*$ -action of (B.1.12) with $\lambda_1 = 1/s$ and then the $\mathbb{C}_{\mu_1}^*$ -action of (5.2.32) with $\mu_1 = t/s$ to set the coordinates to

$$(s, t, v, w, e_0, 0, e_2) \mapsto (1, 1, v, w, e_0 t/s, 0, e_2). \quad (5.2.80)$$

Dropping the coordinates that are fixed, renaming $\tilde{e}_0 := e_0 t/s$, and relabelling the remaining \mathbb{C}^* -actions in (B.1.12) and (5.2.75) by defining $\eta_1 := \mu_2^{-1}$ and $\eta_2 := \lambda_2$, we have

$$\begin{aligned} \mathbb{C}_{\eta_2}^* : \mathbb{C}_{(v, w, \tilde{e}_0, e_2)}^* &\longrightarrow \mathbb{C}_{(v, w, \tilde{e}_0, e_2)}^* \\ (v, w, \tilde{e}_0, e_2) &\mapsto (v, w, \eta_1 \tilde{e}_0, \eta_1 e_2), \end{aligned} \quad (5.2.81a)$$

$$\begin{aligned} \mathbb{C}_{\eta_2}^* : \mathbb{C}_{(v, w, \tilde{e}_0, e_2)}^* &\longrightarrow \mathbb{C}_{(v, w, \tilde{e}_0, e_2)}^* \\ (\eta_2 v, \eta_2 w, \eta_2^7 \tilde{e}_0, e_2) &\mapsto (v, w, \tilde{e}_0, e_2). \end{aligned} \quad (5.2.81b)$$

Altogether, we find that, indeed

$$B^1 = (\mathbb{C}_{(v, w, \tilde{e}_0, e_2)} \setminus Z) / \mathbb{C}_{\eta_1}^* \times \mathbb{C}_{\eta_2}^* \cong \mathbb{F}_7, \quad (5.2.82a)$$

$$Z := \{v = w = 0\} \cup \{\tilde{e}_0 = e_2 = 0\}, \quad (5.2.82b)$$

as expected from Proposition 5.2.12. Moreover, we see that $C_1 = \{\tilde{e}_0 = 0\}_{B^1} = \{e_0 = e_1 = 0\}_{\mathcal{B}}$ is the $(+7)$ -curve of B^1 , as was explained after (5.2.72).

5.2.5 Weierstrass models and log Calabi-Yau structure

Having described the geometry of the base components of an open-chain resolution, we now turn to the Weierstrass model that is defined over them. In other words, we need to see how the holomorphic line bundle \mathcal{L} over \mathcal{B} defining the elliptic fibration for the family variety \mathcal{Y} restricts to the individual base components $\{B^p\}_{0 \leq p \leq P}$ to define the elliptic fibrations $\{Y^p\}_{0 \leq p \leq P}$. We recall that the analysis of this section will apply to single infinite-distance limits in particular, leaving the general case for Section B.4.2. As we will see, the individual components of the resolved central fiber give rise to a log Calabi-Yau structure.

Our starting point is given by the degenerations $\hat{\rho} : \hat{\mathcal{Y}} \rightarrow D$ of the type described in Section 5.2.1, where the base family variety is $\hat{\mathcal{B}} = \hat{B} \times D$. By construction, both every fiber \hat{Y}_u

¹⁷All infinite-distance non-minimal singularities have been removed, but there still exist non-minimal singular fibers in codimension-two corresponding to SCFT points, that we keep unresolved.

of the family and the family variety $\hat{\mathcal{Y}}$ itself are elliptically fibered Calabi-Yau varieties, since the holomorphic line bundle defining their respective Weierstrass models satisfies

$$\mathcal{L}_{B_u} = \overline{K}_{B_u} = \overline{K}_B, \quad \mathcal{L}_{\hat{\mathcal{B}}} = \overline{K}_{\hat{\mathcal{B}}}. \quad (5.2.83)$$

The resolution process described in Section 5.2.2 and leading to the modification of the degeneration $\rho : \mathcal{Y} \rightarrow D$ consists of a series of blow-ups, each of them followed by a line bundle shift that ensures that the Calabi-Yau condition is satisfied at each step. This means that at the end we also have a Calabi-Yau family variety, since

$$\mathcal{L}_B = \overline{K}_B. \quad (5.2.84)$$

The modification of the degeneration is an isomorphism over D^* , and we therefore do not need to worry about the generic fibers $Y_{u \neq 0}$. The geometrical representative of the endpoint of the limit is now, however, the multi-component central fiber $Y_0 = \bigcup_{p=0}^P Y^p$ with base $B_0 = \bigcup_{p=0}^P B^p$. The elliptic fibration $\pi_p : Y^p \rightarrow B^p$ is given by a Weierstrass model that is obtained as the restriction of the Weierstrass model of \mathcal{Y} to Y^p . Hence, and since the base component B^p is the exceptional divisor E_p , the defining holomorphic line bundle of $\pi_p : Y^p \rightarrow B^p$ is the restriction $\mathcal{L}_B|_{E_p}$.

In an open-chain resolution, shown in Figure 5.2, the base components only intersect the adjacent members of the chain, i.e. we have the non-trivial intersections

$$B^{p-1} \cap B^p \neq \emptyset, \quad B^p \cap B^{p+1} \neq \emptyset, \quad 0 < p < P, \quad (5.2.85)$$

with all the other intersections vanishing. Here, we have relabelled the components such that p runs in sequential order in the open chain. The intersections occur over the $\{C_p\}_{1 \leq p \leq P}$ curves that acted as the centres for the blow-ups, having

$$E_{p-1} \cdot_B E_p = C_p, \quad 1 \leq p \leq P. \quad (5.2.86)$$

With this in mind, let us compute the restriction $\mathcal{L}_B|_{E_p}$.

Weierstrass models over open-chain resolutions

Proposition 5.2.15. *Let $\{B^p\}_{0 \leq p \leq P}$ be the base components of the central fiber Y_0 of the modification $\rho : \mathcal{Y} \rightarrow D$ giving an open-chain resolution of a degeneration $\hat{\rho} : \hat{\mathcal{Y}} \rightarrow D$. Then, the holomorphic line bundles $\{\mathcal{L}_p\}_{0 \leq p \leq P} := \{\mathcal{L}_{B^p}\}_{0 \leq p \leq P}$ defining the Weierstrass models over the $\{B^p\}_{0 \leq p \leq P}$ are*

$$\mathcal{L}_0 = \overline{K}_{B^0} - C_1, \quad (5.2.87a)$$

$$\mathcal{L}_p = \overline{K}_{B^p} - C_{p-1} - C_{p+1}, \quad 1 \leq p \leq P-1, \quad (5.2.87b)$$

$$\mathcal{L}_P = \overline{K}_{B^P} - C_{P-1}. \quad (5.2.87c)$$

Proof. The line bundles are given by

$$\mathcal{L}_p := \mathcal{L}_{B^p} = \mathcal{L}_B|_{E_p}. \quad (5.2.88)$$

To compute this restriction let us recall the adjunction formula for the smooth divisors $\{E_p\}_{0 \leq p \leq P}$ in the smooth variety \mathcal{B} , which takes the form

$$K_{E_p} = (K_{\mathcal{B}} + E_p)|_{E_p}. \quad (5.2.89)$$

Using then the fact that the family variety \mathcal{Y} is Calabi-Yau, and therefore $\mathcal{L}_B = \overline{K}_B$, we obtain

$$\mathcal{L}_p = \overline{K}_{B^p} + E_p|_{E_p} . \quad (5.2.90)$$

From the relation

$$\tilde{\mathcal{U}} = \sum_{p=0}^P E_p , \quad (5.2.91)$$

the triviality of the $\tilde{\mathcal{U}}$ class and the intersections (5.2.86), the result follows. \square

We can be even more concrete if we remember that the components of B_0 , besides the strict transform of \hat{B}_0 , are Hirzebruch surfaces, see Proposition 5.2.12. As pointed out after (5.2.72), the blow-up centres, as seen from the Hirzebruch surfaces \mathbb{F}_{n_p} , are just the $(\pm n_p)$ -curves, and therefore the holomorphic line bundles over them are simply the anticanonical class of the Hirzebruch surface with some section classes subtracted. In particular, intermediate \mathbb{F}_{n_p} components of the chain have line bundles consisting only of vertical classes. Using the notation of (B.1.13), the holomorphic line bundles over the \mathbb{F}_{n_p} components are

$$\mathcal{L}_p = 2V_p , \quad \text{if } B^p \text{ is an intermediate component,} \quad (5.2.92a)$$

$$\mathcal{L}_p = S_p + 2V_p \quad \text{or} \quad \mathcal{L}_p = T_p + 2V_p , \quad \text{if } B^p \text{ is an end-component.} \quad (5.2.92b)$$

Since for all components we have that $\mathcal{L}_p \leq \overline{K}_{B^p}$, and given Proposition 5.2.7, tuning non-minimal elliptic fibers to appear over a genus-one curve is not possible.

From Proposition 5.2.15, we observe that the Weierstrass models $\pi_p : Y^p \rightarrow B^p$ are describing varieties that are not Calabi-Yau, since $\mathcal{L}_p \neq \overline{K}_{B^p}$. While each component of the central fiber Y_0 is not Calabi-Yau, the multi-component central fiber $Y_0 = \bigcup_{p=0}^P Y^p$ still is, as we can see from

$$\mathcal{L}_{B_0} = \mathcal{L}_B|_{\tilde{\mathcal{U}}} = \overline{K}_{\tilde{\mathcal{U}}} + \tilde{\mathcal{U}}|_{\tilde{\mathcal{U}}} = \overline{K}_{\tilde{\mathcal{U}}} = \sum_{p=0}^P \mathcal{L}_p . \quad (5.2.93)$$

Let us abuse notation and denote the pullback divisors $\pi_p^*(C_q)$ in Y^p also by C_q . Rephrasing the above discussion, the pairs

$$(Y^0, C_1) , \quad (Y^p, C_{p-1} + C_{p+1}) , \quad p = 1, \dots, P-1 , \quad (Y^P, C_{P-1}) \quad (5.2.94)$$

are log Calabi-Yau spaces,¹⁸ their union along the boundaries

$$Y_0 = Y^0 \cup_{C_1} Y^1 \cup_{C_2} \dots \cup_{C_{P-1}} Y^{P-1} \cup_{C_P} Y^P \quad (5.2.95)$$

giving a Calabi-Yau variety.

The divisors associated to the defining polynomials and discriminant

$$f_p := f_b|_{e_p=0} , \quad g_p := g_b|_{e_p=0} , \quad \Delta_p := \Delta_b|_{e_p=0} , \quad (5.2.96)$$

of the Weierstrass model of the component Y_p are in the classes

$$F_p := F|_{E_p} = 4\mathcal{L}_p , \quad (5.2.97a)$$

$$G_p := G|_{E_p} = 6\mathcal{L}_p , \quad (5.2.97b)$$

$$\Delta_p := \Delta|_{E_p} = 12\mathcal{L}_p . \quad (5.2.97c)$$

¹⁸A log Calabi-Yau space is a pair (X, D) , where X is a variety and D an effective divisor in X , called the boundary, such that $K_{(X,D)} = K_X + D$ is trivial. For some applications of this notion in the context of physics, and F-theory in particular, see [297].

Depending on the type of codimension-zero fibers over a given component, the restrictions (5.2.96) may vanish. In particular, exceptional components stemming from a blow-up along a curve with Class 5 family vanishing orders will yield trivial restrictions for all defining polynomials. However, we do not need to consider this case since, as discussed in Section 5.2.2.3, it can always be eliminated by a series of base changes and modifications of the degeneration. Focusing then on models with Class 1–4 family vanishing orders and an open-chain resolution, the information about the geometry of the base components and the type of codimension-zero elliptic fibers found over them can be encapsulated in a diagram

$$\begin{array}{ccccccc} I_{n_0} & - & \cdots & - & I_{n_p} & - & \cdots & - & I_{n_P} \\ | & & & & | & & & & | \\ B_0 & - & \cdots & - & B_p & - & \cdots & - & B_P. \end{array} \quad (5.2.98)$$

Out of the Class 1–4 family vanishing orders, Classes 2 and 3 will lead to vanishing f_p and g_p restrictions for the exceptional component of the blow-up, respectively, to which we assign infinite component vanishing orders, see the paragraph after (5.2.49). For Class 4 family vanishing orders, we obtain a vanishing Δ_p restriction for the exceptional component of the blow-up. In analogy with what was done in [156, 157] for the eight-dimensional F-theory analysis, it is convenient to define a modified discriminant divisor Δ' of the family variety \mathcal{Y} that restricts to the components Y^p non-trivially. We will use this divisor in Section 5.4 to read the physical 7-brane content of the components. With this application in mind, we define the modified discriminant Δ' to be the one in which we remove the discriminant components responsible for the codimension-zero singular fibers of the components Y^p , i.e. we “subtract the background value of the axio-dilaton” before reading the 7-brane content in said components.

Definition 5.2.16. Let $\{B^p\}_{0 \leq p \leq P}$ be the base components of the central fiber Y_0 of the open-chain resolution $\rho : \mathcal{Y} \rightarrow D$ of a degeneration $\hat{\rho} : \hat{\mathcal{Y}} \rightarrow D$, and let

$$\text{ord}_{\mathcal{Y}}(f_b, g_b, \Delta_b)_{E_p} = (0, 0, n_p), \quad 0 \leq p \leq P, \quad (5.2.99)$$

be the vanishing orders associated to the codimension-zero singular fibers in said components. We define the divisor class of the modified discriminant in \mathcal{B} to be

$$\Delta' := \Delta - \sum_{p=0}^P n_p E_p. \quad (5.2.100)$$

At the level of the defining polynomials of the Weierstrass model of \mathcal{Y} , the modified discriminant is defined by the equation

$$\Delta = e_0^{n_0} \cdots e_P^{n_P} \Delta', \quad (5.2.101)$$

and therefore it no longer restricts to zero in the components.

Whenever we analyse the endpoint of an infinite-distance limit component by component, we will always work in what follows with the set of polynomials $\{f_p, g_p, \Delta'_p\}_{0 \leq p \leq P}$. For future reference, we collect their associated divisor classes.

Proposition 5.2.17. Let $\{B^p\}_{0 \leq p \leq P}$ be the base components of the central fiber Y_0 of the open-chain resolution $\rho : \mathcal{Y} \rightarrow D$ of a degeneration $\hat{\rho} : \hat{\mathcal{Y}} \rightarrow D$, and let

$$\text{ord}_{\mathcal{Y}}(f_b, g_b, \Delta_b)_{E_p} = (0, 0, n_p), \quad 0 \leq p \leq P, \quad (5.2.102)$$

be the vanishing orders associated to the codimension-zero singular fibers in said components. The (modified) divisor classes associated to the Weierstrass models in the components are

$$F_p = 4\bar{K}_{B^p} - (1 - \delta_{p,0})4C_{p-1} - (1 - \delta_{p,P})4C_{p+1}, \quad (5.2.103a)$$

$$G_p = 6\bar{K}_{B^p} - (1 - \delta_{p,0})6C_{p-1} - (1 - \delta_{p,P})6C_{p+1}, \quad (5.2.103b)$$

$$\Delta'_p = 12\bar{K}_{B^p} + (1 - \delta_{p,0})(n_{p-1} - 12)C_{p-1} + (1 - \delta_{p,P})(n_{p+1} - 12)C_{p+1}, \quad (5.2.103c)$$

for $0 \leq p \leq P$.

Proof. It follows from Proposition 5.2.15 and Definition 5.2.16. \square

We illustrate these computations with an example.

Example 5.2.18. Continuing with Example 5.2.14, we see from the defining polynomials (5.2.78) that the codimension-zero singular fibers in the components $\{Y^p\}_{0 \leq p \leq 2}$ are associated to the vanishing orders

$$\text{ord}_Y(f_b, g_b, \Delta_b)_{E_0} = (0, 0, 0), \quad (5.2.104a)$$

$$\text{ord}_Y(f_b, g_b, \Delta_b)_{E_1} = (0, 0, 1), \quad (5.2.104b)$$

$$\text{ord}_Y(f_b, g_b, \Delta_b)_{E_2} = (0, 0, 0), \quad (5.2.104c)$$

i.e. the geometry of the model is

$$\begin{array}{ccc} I_0 & \text{---} & I_1 & \text{---} & I_0 \\ | & & | & & | \\ \mathbb{F}_7 & \text{---} & \mathbb{F}_7 & \text{---} & \mathbb{F}_7. \end{array} \quad (5.2.105)$$

Using Proposition 5.2.15 we can compute the defining holomorphic line bundle over each component to be

$$\mathcal{L}_0 = S_0 + 9V_0, \quad (5.2.106a)$$

$$\mathcal{L}_1 = 2V_1, \quad (5.2.106b)$$

$$\mathcal{L}_2 = S_2 + 2V_2, \quad (5.2.106c)$$

where we are using the notation of (B.1.13) with the added subscripts indicating the base component that we are referring to. The divisors associated to the defining polynomials of the component Weierstrass models, as well as the restrictions of the modified discriminant, are

$$F_0 = 4S_0 + 36V_0, \quad (5.2.107a)$$

$$G_0 = 6S_0 + 54V_0, \quad (5.2.107b)$$

$$\Delta'_0 = 11S_0 + 108V_0, \quad (5.2.107c)$$

in the B^0 component,

$$F_1 = 8V_1, \quad (5.2.108a)$$

$$G_1 = 12V_1, \quad (5.2.108b)$$

$$\Delta'_1 = 2S_1 + 31V_1, \quad (5.2.108c)$$

in the B^1 component, and

$$F_2 = 4S_2 + 8V_2, \quad (5.2.109a)$$

$$G_2 = 6S_2 + 12V_2, \quad (5.2.109b)$$

$$\Delta'_2 = 11S_2 + 17V_2, \quad (5.2.109c)$$

in the B^2 component. Computing the polynomials $\{f_p, g_p, \Delta'_p\}_{0 \leq p \leq 2}$ starting from (5.2.78) we find

$$f_0 = -3t^4v^2w^2(v-w)^2(v+w)^2, \quad (5.2.110a)$$

$$g_0 = t^5v^3(e_1v^{16} - 2tv^6w^3 + 6tv^4w^5 - 6tv^2w^7 + 2tw^9), \quad (5.2.110b)$$

$$\Delta'_0 = 27t^{10}v^{22}(e_1v^{16} - 4tv^6w^3 + 12tv^4w^5 - 12tv^2w^7 + 4tw^9), \quad (5.2.110c)$$

for the B^0 component,

$$f_1 = -3v^2w^2(v-w)^2(v+w)^2, \quad (5.2.111a)$$

$$g_1 = -2v^3w^3(v-w)^3(v+w)^3, \quad (5.2.111b)$$

$$\Delta'_1 = -108v^6w^3(v-w)^3(v+w)^3(e_2^2v^{16} - e_0e_2v^8w + e_0e_2v^6w^3 + e_0^2w^2), \quad (5.2.111c)$$

for the B^1 component, and

$$f_2 = -3s^4v^2w^2(v-w)^2(v+w)^2, \quad (5.2.112a)$$

$$g_2 = s^5v^3w^2(e_1 - 2sv^6w + 6sv^4w^3 - 6sv^2w^5 + 2sw^7), \quad (5.2.112b)$$

$$\Delta'_2 = 27s^{10}v^6w^4(e_1 - 4sv^6w + 12sv^4w^3 - 12sv^2w^5 + 4sw^7), \quad (5.2.112c)$$

for the B^2 component, where we have used the available \mathbb{C}^* -actions to set to one those coordinates that are not allowed to vanish in a given component in view of the Stanley-Reisner ideal (5.2.76). We see that, indeed, the zero loci of (5.2.110), (5.2.111) and (5.2.112) are in the divisor classes (5.2.107), (5.2.108) and (5.2.109), respectively.

5.2.6 General degenerations and their resolution trees

In Sections 5.2.4 and 5.2.5 we have analysed the geometry of the base components of an open-chain resolution $\rho : \mathcal{Y} \rightarrow D$ of a genus-zero degeneration $\hat{\rho} : \hat{\mathcal{Y}} \rightarrow D$, as well as the line bundles associated to the Weierstrass model describing the elliptic fibrations over them. Restricting our attention to open-chain resolutions meant that in the geometrical study we could assume that the centres of the successive blow-ups were non-intersecting. Under these conditions, we only produce Hirzebruch surfaces as exceptional base components, as explained in Proposition 5.2.13 and depicted in Figure 5.2, with the line bundles printed in Proposition 5.2.15 defined over them.

More generally, one can relax this condition by allowing the blow-up centres to intersect, which corresponds to the most general degenerations of the type we consider, see the discussions in Section 5.2.1 and Section 5.2.2. The central fiber B_0 of \mathcal{B} no longer has to be an open chain of surfaces, but can consist of a central component B^0 , stemming from the original component \hat{B}_0 , with ‘‘branches’’ of intersecting surfaces attached to it that can split, resembling a tree. Moreover, B^0 may be a blow-up of \hat{B}_0 at points, and not always the same type of surface as occurred for the open-chain resolutions. We depict this in Figure 5.3. Note that allowing the branches to split automatically implies that the blow-up centres must intersect, since in a Hirzebruch

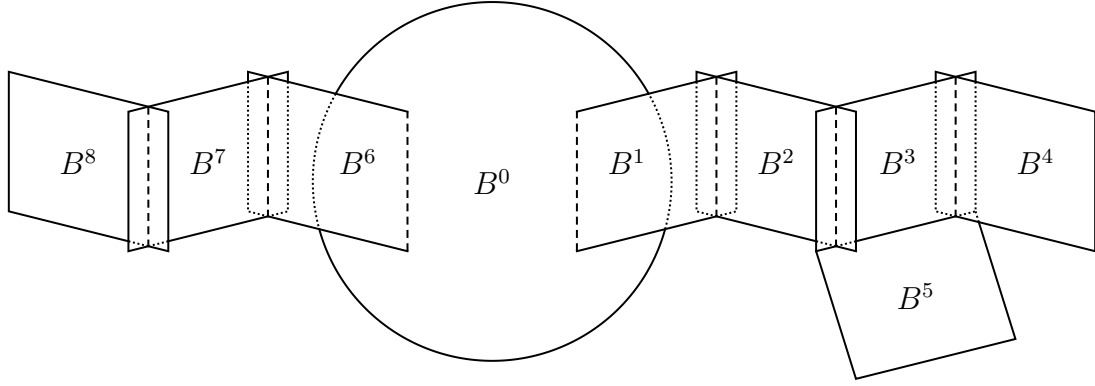


Figure 5.3: Central fiber B_0 of the base \mathcal{B} of the tree resolution of a general degeneration $\hat{\rho} : \hat{\mathcal{Y}} \rightarrow D$ not falling under the single infinite-distance limit category. Note that a resolution with the configuration of components depicted here will always present obscured infinite-distance limits, see the discussions in Appendices B.3 and B.5.

surface we cannot tune more than two non-intersecting curves of non-minimal singular fibers, see Proposition B.6.1.

We relegate a detailed description of the structure of such resolution trees and the Weierstrass models over them to Appendix B.4. As we will see, the study of the open-chain resolutions associated to single infinite-distance limit degenerations already allowed us to discuss most of the needed concepts, and only minor modifications of the analysis will be necessary in order to include the new cases. The structure of the more general resolution trees is, in fact, summarised in the following proposition.

Proposition 5.2.19. *Let $\hat{\mathcal{B}}$ be the base family variety of a genus-zero degeneration $\hat{\rho} : \hat{\mathcal{Y}} \rightarrow D$, and $\text{Bl}_{p-1}(\hat{\mathcal{B}})$ be the result of $p-1$ blow-ups of $\hat{\mathcal{B}}$. Let $C_p \subset B^i$ be a smooth irreducible curve over which $\text{Bl}_{p-1}(\hat{\mathcal{Y}})$ presents non-minimal singular fibers. Then, the exceptional component $B^p = E_p$ arising from the blow-up of $\text{Bl}_{p-1}(\hat{\mathcal{B}})$ along C_p is the Hirzebruch surface*

$$B^p = \mathbb{F}_{|n_p|}, \quad n_p := C_p \cdot_{B^i} C_p + \sum_{\substack{q=0 \\ q \neq i}}^{p-1} E_q|_{E_i} \cdot_{B^i} C_p. \quad (5.2.113)$$

Moreover, define the set of components $\{B^q\}_{q \in \mathcal{I}}$ to be comprised by those elements in $\{B^q\}_{0 \leq q \leq p-1}$ such that

$$\text{codim}_{B^i} (E_q|_{E_i} \cdot_{B^i} C_p) = 2. \quad (5.2.114)$$

After the blow-up along C_p , the old components $\{B^q\}_{q \in \mathcal{I}}$ must be substituted for their blow-ups $\{\text{Bl}_{E_q|_{E_i} \cdot_{B^i} C_p}(B^q)\}_{q \in \mathcal{I}}$.

With this understanding of the more general resolution trees, we can finally tackle the proof of Proposition 5.2.11, which guarantees that single infinite-distance limits only give rise to open-chain resolutions, rather than to resolutions trees. This analysis can be found in Appendix B.5.

5.2.7 Comments on genus-one degenerations

We saw in Section 5.2.3 that genus-one degenerations are much more constrained than their genus-zero counterparts. In fact, they can only occur if the curve C in the central fiber \hat{B}_0 of $\hat{\mathcal{B}}$

is in the anticanonical class $C = \overline{K}_{\hat{B}_0}$, see Proposition 5.2.7. We leave the study of these highly non-generic class of infinite-distance limits for future works, merely offering some comments on them before we conclude the section.

Let us look at the geometry of the base components of the resolved degeneration. A study analogous to the one carried out in Sections B.4.1 and 5.2.4 would show that the exceptional components of the base blow-ups would be the projectivization of rank 2 vector bundles over a genus one curve. This is the first non-trivial case of algebraic vector bundles over a curve, where Grothendieck's splitting theorem no longer applies. Algebraic vector bundles over an elliptic curve defined over an algebraically closed field have been classified by Atiyah [325].

Regarding the holomorphic line bundles defined over the components and associated to the Weierstrass models giving the elliptic fibrations of which they are the bases, one can perform an analysis similar to the one in Sections B.4.2 and 5.2.5. Considering a two-component model arising from a genus-one degeneration, this would lead us to conclude that the line bundle defined over the strict transform of the original base components is trivial, meaning in physical terms that it contains no local 7-brane content. Hence, the resolution of genus-one degenerations will present some spectator tails of the base geometry over which the elliptic fibration is trivial and the Type IIB axio-dilaton constant. This structure also implies that repeatedly blowing up along genus-one curves leads to open-chain resolutions.

5.3 Degenerations of Hirzebruch models

While the previous section analysed single infinite-distance limits for arbitrary base spaces, we now specialise the discussion to elliptic fibrations over Hirzebruch surfaces $\hat{B} = \mathbb{F}_n$, with $0 \leq n \leq 12$ (see Section B.1.1). These models are of particular interest because of heterotic duality. For this reason, we use this section to lay out the properties of this subclass of degenerations as explicitly as possible.

After briefly reviewing their relation to the heterotic string, we classify the possible genus-zero (and genus-one) curves over which non-minimal elliptic fibers can be supported in a single infinite-distance limit. We then explicitly describe the open-chain resolutions for the different single infinite-distance limits involving genus-zero non-minimal curves. This gives rise to so-called horizontal, vertical, or mixed degenerations (and their resolutions), where the terminology refers to the location of the non-minimal curve(s) with respect to the rational fibration of the Hirzebruch surface $\hat{B}_0 = \mathbb{F}_n$. The base blow-ups taken during the resolution process yield chains of intersecting Hirzebruch surfaces of special types acting as the base of the elliptic fibration of the central fiber of the degeneration; the log Calabi-Yau structure of the elliptic fibrations in its components can be made very explicit. These results are a direct application of the general discussion in Section 5.2. However, toric methods can be used in the analysis of some degenerations of Hirzebruch models, allowing us to rederive a subset of the results obtained in Section 5.2 in a succinct and alternative way and therefore serving as further examples for the general discussion.

To set the stage, recall that six-dimensional F-theory models over Hirzebruch surfaces have $n_T = 1$ tensors and are of particular interest due to their connection to perturbative heterotic dual models [186, 187, 190, 326]. This is reflected in the appearance of a compatible K3 fibration structure which extends to the degeneration $\hat{\rho} : \hat{\mathcal{Y}} \rightarrow D$ introduced in Section 5.2.1 in the following way. For $\hat{B} = \mathbb{F}_n$, the \mathbb{P}^1 -fibration in \mathbb{F}_n implies that a fixed member \hat{Y}_u of the family

$\hat{\mathcal{Y}}$ can be seen as an elliptic fibration over \mathbb{F}_n , or as a K3-fibration over the base \mathbb{P}_b^1 of \mathbb{F}_n , i.e.

$$\begin{array}{ccc} \mathcal{E} & \longrightarrow & \hat{Y}_u \\ & \downarrow \pi_{\text{ell}} & \text{and} \\ & \mathbb{F}_n & \\ & & \mathbb{P}_b^1. \end{array} \quad (5.3.1)$$

The two fibrations naturally extend to $\hat{\mathcal{Y}}$, where we have

$$\begin{array}{ccc} \mathcal{E} & \longrightarrow & \hat{\mathcal{Y}} \\ & \downarrow \Pi_{\text{ell}} & \text{and} \\ & \mathbb{F}_n \times D & \\ & & \mathbb{P}_b^1 \times D, \end{array} \quad (5.3.2)$$

with $\pi_{\text{ell}} = \hat{\rho} \circ \Pi_{\text{ell}}$ and $\pi_{\text{K3}} = \hat{\rho} \circ \Pi_{\text{K3}}$. The K3-fibration compatible with the elliptic fibration over $\hat{B} = \mathbb{F}_n$ yields a Kulikov degeneration of the K3 fibers that can be interpreted in the heterotic dual model as a (possibly infinite-distance) limit; this is the dual of the infinite-distance limit in the complex structure moduli space of six-dimensional F-theory represented by the degeneration $\hat{\rho} : \hat{\mathcal{Y}} \rightarrow D$. While this duality is expected to hold in general, the precise map between the theories is available only under certain conditions, which we recall in Section 6.4.1.

The heterotic interpretation for (at least some of) the degenerations of Hirzebruch models will prove most useful in Chapter 6 when we try to gain some intuition for the physics obtained at the endpoints of the infinite-distance limits under study. This motivates a detailed study of the underlying geometry.

5.3.1 Single infinite-distance limits in Hirzebruch models

The simplest kind of degenerations of Hirzebruch models are those in which a single curve supports non-minimal singular elliptic fibers, rather than a collection of them, meaning that we are facing a single infinite-distance limit instead of a simultaneous superposition of more of them. This intuition was more carefully encapsulated in the notion of a single infinite-distance limit degeneration, see Definition 5.2.9, which allows for slightly more general configurations that would nonetheless arise as equivalent degenerations to the ones just described.

We will mostly concern ourselves with this class of degenerations in Chapter 6, and it would therefore be useful to precisely determine over which curves they can occur. We already know from Proposition 5.2.7 that they must be curves of genus-zero or genus-one. Restricting our attention to Hirzebruch models, we can be more explicit and give a complete list of the curves that can support non-minimal elliptic fibers as part of a single infinite-distance limit. To derive such a list, we analyse below the non-minimal fibers over curves in a Weierstrass model $\pi : Y \rightarrow B$ with $B = \mathbb{F}_n$. This applies, in particular, to the non-minimal elliptic fibers in the central fiber of a degeneration of a Hirzebruch model, meaning that the list is relevant both for conventional and obscured single infinite-distance limits (as defined and discussed in Appendix B.3).

In the sequel, we denote by h and f the class of the exceptional section and the fiber of the Hirzebruch surface $B = \mathbb{F}_n$, respectively, with intersection products $h \cdot h = -n$, $h \cdot f = 1$ and $f \cdot f = 0$. For more details on the notation, we refer to Appendix B.1.

Proposition 5.3.1. *Let $\pi : Y \rightarrow B$ be a Calabi-Yau Weierstrass model over $B = \mathbb{F}_n$. The smooth, irreducible curves C that can support non-minimal fibers are the following:*

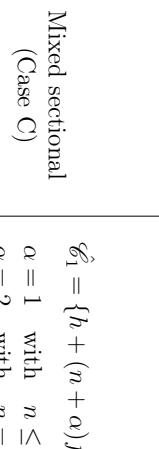
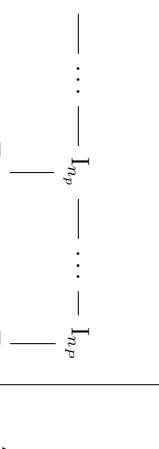
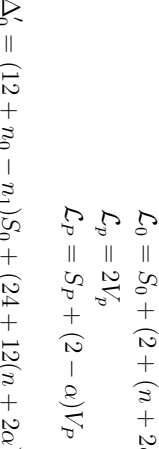
Non-minimal curves	Central component structure	Component line bundles and discriminants
Horizontal (Case A)	$\hat{\mathcal{C}}_1 = \{h\}$ $\hat{\mathcal{C}}_1 = \{h + nf\}$ $\hat{\mathcal{C}}_2 = \{h, h + nf\}$ 	$\mathcal{L}_0 = S_0 + (2 + n)V_0$ $\mathcal{L}_p = 2V_p$ $\mathcal{L}_P = S_P + 2V_P$ $\Delta'_0 = (12 + n_0 - n_1)S_0 + (24 + 12n)V_0$ $\Delta'_p = (2n_p - n_{p-1} - n_{p+1})S_p + (24 + n(n_p - n_{p-1}))V_p$ $\Delta'_P = (12 + n_P - n_{P-1})S_P + (24 + n(n_P - n_{P-1}))V_P$
Vertical (Case B)	$\hat{\mathcal{C}}_1 = \{f\}$ 	$\mathcal{L}_0 = 2S_0 + (1 + n)W_0$ $\mathcal{L}_p = 2S_p$ $\mathcal{L}_P = 2S_P + W_P$ $\Delta'_0 = 24S_0 + (12 + 12n + n_0 - n_1)W_0$ $\Delta'_p = 24S_p + (2n_p - n_{p-1} - n_{p+1})W_p$ $\Delta'_P = 24S_P + (12 + n_P - n_{P-1})W_P$
Mixed sectional (Case C)	$\hat{\mathcal{C}}_1 = \{h + (n + \alpha)f\}$ $\alpha = 1 \quad \text{with} \quad n \leq 6$ $\alpha = 2 \quad \text{with} \quad n = 0$ 	$\mathcal{L}_0 = S_0 + (2 + (n + 2\alpha))V_0$ $\mathcal{L}_p = 2V_p$ $\mathcal{L}_P = S_P + (2 - \alpha)V_P$ $\Delta'_0 = (12 + n_0 - n_1)S_0 + (24 + 12(n + 2\alpha))V_0$ $\Delta'_p = (2n_p - n_{p-1} - n_{p+1})S_p + (24 + (n + 2\alpha)(n_p - n_{p-1}))V_p$ $\Delta'_P = (12 + n_P - n_{P-1})S_P + ((24 - 12\alpha) + (n + \alpha)(n_P - n_{P-1}))V_P$
Mixed bisectional (Case D)	$\hat{\mathcal{C}}_1 = \{2h + bf\}$ $(n, b) = (0, 1)$ $(n, b) = (1, 2)$ 	$\mathcal{L}_0 = S_0 + (2 + 4)V_0$ $\mathcal{L}_p = 2V_p$ $\mathcal{L}_P = V_P$ $\Delta'_0 = (12 + n_0 - n_1)S_0 + (24 + 12 \cdot 4)V_0$ $\Delta'_p = (2n_p - n_{p-1} - n_{p+1})S_p + (24 + 4(n_p - n_{p-1}))V_p$ $\Delta'_P = 2(n_P - n_{P-1})S_P + (12 + (n + 1)(n_P - n_{P-1}))V_P$

Table 5.3.1: Genus-zero single infinite-distance limit degenerations of Hirzebruch models.

- $C = f$, with $g(C) = 0$;
- $C = h + bf$, with $b = 0, n, n+1, n+2$ and $g(C) = 0$;
- $C = 2h + bf$, with $(n, b) = (0, 1), (1, 2)$ and $g(C) = 0$; and
- $C = 2h + bf$, with $(n, b) = (0, 2), (1, 3), (2, 4)$ and $g(C) = 1$.

Proof. Let us express the divisor class of C as

$$C = ah + bf, \quad a, b \in \mathbb{Z}_{\geq 0}. \quad (5.3.3)$$

From the effectiveness constraint $C \leq \bar{K}_B$, see Proposition B.2.2, we find the bounds

$$a \leq 2, \quad b \leq 2 + n, \quad (5.3.4)$$

to which we add $a + b > 0$ to avoid the trivial case. We study the possible curves for the three allowed values of $a = 0, 1, 2$ separately.

- $a = 0$: For this case, the curves

$$C = bf, \quad 0 < b \leq 2 + n, \quad (5.3.5)$$

are generically reducible, unless $b = 1$. Hence, $C = f$, and from the Adjunction formula of Proposition B.1.3 we read $g(C) = 0$.

- $a = 1$: We have the curves

$$C = h + bf, \quad 0 \leq b \leq 2 + n. \quad (5.3.6)$$

From the intersection with h we see, applying Proposition B.1.2, that, for $b \neq 0$, C is generically irreducible when

$$C \cdot h \geq 0 \Leftrightarrow b \geq n. \quad (5.3.7)$$

Additionally, the curve $C = h$ is also irreducible. Altogether, we have the curves $C = h + bf$ with $b = 0, n, n+1, n+2$. From the Adjunction formula, we see that $g(C) = 0$ for all of them.

- $a = 2$: Computing the intersection product of the curves

$$C = 2h + bf, \quad 0 \leq b \leq 2 + n, \quad (5.3.8)$$

with h we see, applying Proposition B.1.2, that, for $b \neq 0$, C is generically irreducible when

$$C \cdot h \geq 0 \Leftrightarrow b \geq 2n. \quad (5.3.9)$$

Writing $b = 2n + \beta$, we observe that both inequalities can only be fulfilled in a handful of cases. These are listed in Table 5.3.2, with their genus computed through the Adjunction formula. The curves with $g(C) = 1$ are those in the anti-canonical class. When $b = 0$, which can only occur for $n = 0$, the curve $C = 2h$ is also reducible.

□

$\beta \backslash n$	0	1	2
0	$b = 0$	$g(C) = 0$	$g(C) = 1$
1	$g(C) = 0$	$g(C) = 1$	
2	$g(C) = 1$		

Table 5.3.2: Irreducible $C = 2h + (2n + \beta)f$ curves and their genus.

A degeneration $\hat{\rho} : \hat{\mathcal{Y}} \rightarrow D$ of Hirzebruch models in which the set curves $\hat{\mathcal{C}}_r$ in $\hat{\mathcal{B}}$ with non-minimal component vanishing orders is $\hat{\mathcal{C}}_1 = \{C\}$ with $C \subset \hat{B}_0$ in the list of Proposition 5.3.1 can be a single infinite-distance limit degeneration if the other conditions in Definition 5.2.9 are met. Beyond these candidates, the only other possible single infinite-distance limit degenerations of Hirzebruch models are those in which $\hat{\mathcal{C}}_2 = \{C_0, C_\infty\}$. All other choices of $\hat{\mathcal{C}}_r$ violate Condition (i) of Definition 5.2.9. We show this in Proposition B.6.1, to which we refer for details. In particular, one cannot engineer non-minimal fibers over two (unless $n = 0$) or more distinct representatives of f without tuning non-minimalities also over h .

Focusing on genus-zero degenerations of Hirzebruch models, we can classify them into four cases sharing similar properties, depending on which of the curves in Proposition 5.3.1 support the non-minimal elliptic fibers. We will use the following nomenclature.

Definition 5.3.2. Let $\hat{\rho} : \hat{\mathcal{Y}} \rightarrow D$ with $\hat{\mathcal{B}} = \mathbb{F}_n \times D$ and $0 \leq n \leq 12$ be a single (obscured) infinite-distance limit degeneration of Hirzebruch models. The curves in \hat{B}_0 that present non-minimal (component) vanishing orders can be classified as follows:

- Case A: $C = h$, or $C = h + nf$, or both (horizontal model).
- Case B: $C = f$ (vertical model).
- Case C: $C = h + (n + 1)f$, or $C = h + (n + 2)f$ (mixed section model).
- Case D: $C = 2h + bf$, with $(n, b) = (0, 1), (1, 2)$ (mixed bisection model).

For Cases A and B there are representatives of the divisor classes of the non-minimal curves that coincide with coordinate divisors of the toric description of $\hat{\mathcal{B}}$, which makes the blow-up process of the base very explicit thanks to its global coordinate description. This was already used in Examples 5.2.1 and 5.2.14, which refer to a Case A degeneration of Hirzebruch models, and will be exploited in Section 5.3.2 to rederive the results of Proposition 5.2.12 for this particular set of degenerations. Cases C and D, on the other hand, cannot be treated in such a convenient way, but may still be analysed following the general discussion of single infinite-distance limits of Sections 5.2.4 and 5.2.5.

5.3.2 Horizontal models

Consider a single infinite-distance limit degeneration $\hat{\rho} : \hat{\mathcal{Y}} \rightarrow D$ of Hirzebruch models corresponding to a horizontal model, i.e. in Case A. This means that the set of non-minimal curves in $\hat{B}_0 = \mathbb{F}_n \subset \hat{\mathcal{B}}$ is either $\hat{\mathcal{C}}_1 = \{h\}$, $\hat{\mathcal{C}}_1 = \{h + nf\}$ or $\hat{\mathcal{C}}_2 = \{h, h + nf\}$. Through a sequence of blow-ups and blow-downs, we may assume without loss of generality that it is $\hat{\mathcal{C}}_1 = \{h\}$, see Section 5.2.3. Let $\rho : \mathcal{Y} \rightarrow D$ be the open-chain resolution of $\hat{\rho} : \hat{\mathcal{Y}} \rightarrow D$. Since $\hat{B}_0 = \mathbb{F}_n$ and

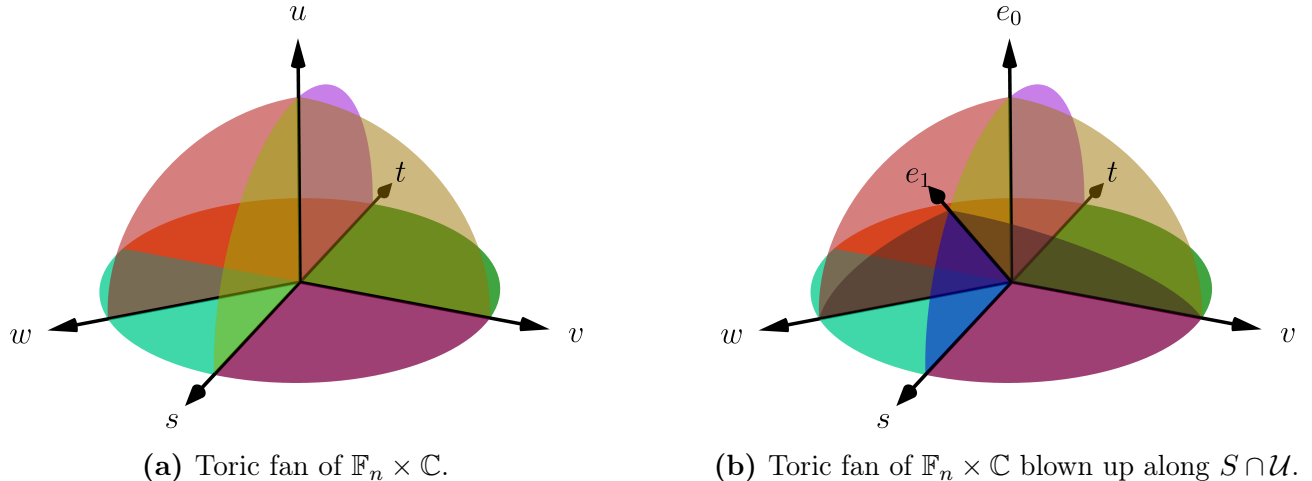


Figure 5.4: Toric fans associated to the family base of a horizontal model.

$\hat{\mathcal{C}}_1 = \{h\}$, we know from Proposition 5.2.12 that the components $\{B^p\}_{0 \leq p \leq P}$ of the base of the central fiber $Y_0 = \bigcup_{p=0}^P Y^p$ of the open chain resolution will be $B^p = \mathbb{F}_n$ for $0 \leq p \leq P$. Let us rederive this succinctly using toric methods.

The base $\hat{\mathcal{B}}$ of the original family $\hat{\mathcal{Y}}$ is $\hat{\mathcal{B}} = \mathbb{F}_n \times D \simeq \mathbb{F}_n \times \mathbb{C}$. As a toric variety, it can be described in the lattice

$$N := \langle (1, 0, 0), (0, 1, 0), (0, 0, 1) \rangle_{\mathbb{Z}} \quad (5.3.10)$$

using the fan $\Sigma_{\hat{\mathcal{B}}}$ given by the edges

$$v = (1, 0, 0), \quad t = (0, 1, 0), \quad w = (-1, -n, 0), \quad s = (0, -1, 0), \quad u = (0, 0, 1), \quad (5.3.11)$$

which we represent in Figure 5.4a. We use the notation for the coordinates introduced in Appendix B.1. Performing a toric blow-up with centre the curve $S \cap \mathcal{U} = \{s = u = 0\}_{\hat{\mathcal{B}}}$ subdivides the fan by adding a new edge and the appropriate 2-cones. The resulting fan $\Sigma_{\mathcal{B}}$ is given in Figure 5.4b. If P such blow-ups are necessary in order to arrive at the \mathcal{Y} family variety, the corresponding family base \mathcal{B} will be described by the fan with edges (5.3.11), in which we rename $e_0 := u$, and to which we add the set of edges

$$\{e_p = (0, -p, 1)\}_{1 \leq p \leq P}, \quad (5.3.12)$$

as well as the necessary 2-cones. The toric divisors associated to the edges v , t , w and s of the blown-up fan are the strict transforms under the composition of the blow-up maps of the original toric divisors. The different components $\{B^p\}_{0 \leq p \leq P}$ of the central fiber B_0 of \mathcal{B} correspond to the toric divisors given by the original u edge and the exceptional edges, i.e.

$$B^p = \{e_p = 0\}_{\mathcal{B}}, \quad p = 0, \dots, P. \quad (5.3.13)$$

The toric fan Σ_{B^p} of B^p can be computed using the orbit closure theorem for the e_p edge. The 2-cones that contain e_p as a face, and will therefore become the edges of the orbit closure fan, are

$$(v, e_p), \quad (e_{p-1}, e_p), \quad (w, e_p), \quad (e_{p+1}, e_p), \quad (5.3.14)$$

where we use the notation

$$e_{-1} := t, \quad e_{P+1} := s. \quad (5.3.15)$$

Taking then the quotient by $N_{e_p} := \langle (0, -p, 1) \rangle_{\mathbb{Z}}$, we obtain the lattice $N(e_p) := N/N_{e_p}$, in which we have the fan Σ_{B^p} is given by the edges

$$\begin{aligned} v &= (1, 0, 0) \sim v_p = (1, 0, 0) \pmod{(0, -p, 1)}, \\ e_{p-1} &= (0, -(p-1), 1) \sim t_p = (0, 1, 0) \pmod{(0, -p, 1)}, \\ w &= (-1, -n, 0) \sim w_p = (-1, -n, 0) \pmod{(0, -p, 1)}, \\ e_{p+1} &= (0, -(p+1), 1) \sim s_p = (0, -1, 0) \pmod{(0, -p, 1)}. \end{aligned} \quad (5.3.16)$$

This is the fan of the Hirzebruch surface \mathbb{F}_n , as we already knew from Proposition 5.2.12. With the embedding map implied above, we have the divisor restrictions

$$E_{p+1}|_{E_p} = S_p, \quad E_{p-1}|_{E_p} = T_p, \quad V|_{E_p} = V_p, \quad W|_{E_p} = W_p. \quad (5.3.17)$$

We now describe the Weierstrass models associated with the components $\{Y^p\}_{0 \leq p \leq P}$ of the central fiber Y_0 . The anti-canonical class of each of the P components of B_0 , which are \mathbb{F}_n surfaces by themselves, is

$$\bar{K}_{B^p} = 2S_p + (2+n)V_p, \quad p = 0, \dots, P. \quad (5.3.18)$$

We know from Section 5.2.5 that the total space of the elliptic fibration over each of these components is a log Calabi-Yau space, meaning that the holomorphic line bundle defining it differs from \bar{K}_{B^p} . Let us particularise, for future reference, the line bundle computations of that section to the case of horizontal models.

Performing the sequence of toric blow-ups necessary to arrive at the open-chain resolution of a Class 1–4 horizontal model, we will have at the p -th step of the blow-up process the family vanishing orders

$$\text{ord}_{\text{Bl}_p(\hat{\mathcal{Y}})}(\Delta)_{s=e_p=0} = 12 + n_{p+1}, \quad (5.3.19)$$

ultimately leading to a central fiber Y_0 with the structure

$$\begin{array}{ccccccc} I_{n_0} & - & \cdots & - & I_{n_p} & - & \cdots & - & I_{n_P} \\ | & & & & | & & & & | \\ \mathbb{F}_n & - & \cdots & - & \mathbb{F}_n & - & \cdots & - & \mathbb{F}_n. \end{array} \quad (5.3.20)$$

The relation between the total and strict transforms under the composition of blow-up maps of the toric divisors of $\hat{\mathcal{B}}$ is

$$\tilde{\mathcal{S}} = \mathcal{S} + \sum_{p=1}^P E_p, \quad \tilde{\mathcal{T}} = \mathcal{T}, \quad \tilde{\mathcal{V}} = \mathcal{V}, \quad \tilde{\mathcal{W}} = \mathcal{W}, \quad \tilde{\mathcal{U}} = \sum_{p=0}^P E_p, \quad (5.3.21)$$

where here and in what follows we denote the strict transforms without a prime.

The holomorphic line bundle defining the elliptic fibration $\Pi_{\text{ell}} : \mathcal{Y} \rightarrow \mathcal{B}$ is

$$\mathcal{L} = \bar{K}_{\mathcal{B}} = 2\mathcal{S} + (2+n)\mathcal{V} + \sum_{p=1}^P pE_p. \quad (5.3.22)$$

From its restrictions we obtain the holomorphic line bundles over the B^p components of B_0 defining the Weierstrass models $\pi^p : Y^p \rightarrow B^p$, which are

$$\mathcal{L}_0 := \mathcal{L}|_{E_0} = S_0 + (2+n)V_0, \quad (5.3.23a)$$

$$\mathcal{L}_p := \mathcal{L}|_{E_p} = 2V_p, \quad p = 1, \dots, P-1, \quad (5.3.23b)$$

$$\mathcal{L}_P := \mathcal{L}|_{E_P} = S_P + 2V_P, \quad (5.3.23c)$$

cf. (5.2.92). The divisors associated to the defining polynomials and the discriminant are obtained as appropriate powers of these line bundles, while the modified discriminant in each component is in the divisor class

$$\Delta'_0 = (12 + n_0 - n_1)S_0 + (24 + 12n)V_0, \quad (5.3.24a)$$

$$\Delta'_p = (2n_p - n_{p-1} - n_{p+1})S_p + (24 + n(n_p - n_{p-1}))V_p, \quad p = 1, \dots, P-1, \quad (5.3.24b)$$

$$\Delta'_P = (12 + n_P - n_{P-1})S_P + (24 + n(n_P - n_{P-1}))V_P. \quad (5.3.24c)$$

Horizontal models of this type are a relative version of the K3 degenerations discussed in [156, 157]. By taking the intersection of Δ'_p with the fiber class V_p of B^p we see that it indeed agrees with the distribution of 7-branes in components obtained for the complex structure infinite-distance limits of eight-dimensional F-theory computed in [156].

The Calabi-Yau nature of the central fiber Y_0 , obtained as the union of the log Calabi-Yau components Y^p along their boundaries, can be seen explicitly by using (5.2.93) and the relations between the divisors in Y_0 and those in the individual components Y^p . These are given by

$$\mathcal{S}|_{\tilde{\mathcal{U}}} = S_P, \quad \mathcal{T}|_{\tilde{\mathcal{U}}} = T_0, \quad \mathcal{V}|_{\tilde{\mathcal{U}}} = \sum_{p=0}^P V_p, \quad \mathcal{W}|_{\tilde{\mathcal{U}}} = \sum_{p=0}^P W_p, \quad (5.3.25)$$

$$E_0|_{\tilde{\mathcal{U}}} = T_1 - S_0, \quad E_p|_{\tilde{\mathcal{U}}} = (T_{p+1} - T_p) - (S_p - S_{p-1}), \quad E_P|_{\tilde{\mathcal{U}}} = -(T_P - S_{P-1}),$$

where $p = 1, \dots, P-1$.

5.3.3 Vertical models

Consider now a vertical single infinite-distance limit degeneration $\hat{\rho} : \hat{\mathcal{Y}} \rightarrow D$ of Hirzebruch models, i.e. a degeneration in Case B. The set of non-minimal curves in $\hat{B}_0 = \mathbb{F}_n \subset \hat{\mathcal{B}}$ is then $\hat{\mathcal{C}}_1 = \{f\}$. Without loss of generality, we can take the non-minimal curve to be the representative $\mathcal{V} \cap \mathcal{U}$ of f ; the resolution process leading to the open-chain resolution $\rho : \mathcal{Y} \rightarrow D$ then consists of toric blow-ups.

The starting point is the fan $\Sigma_{\hat{\mathcal{B}}}$, with the edges given in (5.3.11). To arrive at the fan $\Sigma_{\mathcal{B}}$ describing the resolved family base \mathcal{B} , we rename $e_0 := u$ and add to $\Sigma_{\hat{\mathcal{B}}}$ the set of edges

$$\{e_p = (p, 0, 1)\}_{1 \leq p \leq P} \quad (5.3.26)$$

and the necessary 2-cones to complete the fan.

The toric fan Σ_{B^p} of the component B^p can be obtained applying the orbit closure theorem to the edge e_p . The 2-cones that contain e_p as a face are

$$(e_{p+1}, e_p), \quad (t, e_p), \quad (e_{p-1}, e_p), \quad (s, e_p), \quad (5.3.27)$$

where we use the notation

$$e_{-1} := w, \quad e_{P+1} := v. \quad (5.3.28)$$

Let us apply this to the components B^p with $p = 1, \dots, P$. The quotient by $N_{e_p} := \langle (p, 0, 1) \rangle_{\mathbb{Z}}$ leads to the lattice $N(e_p) = N/N_{e_p}$, in which the fan Σ_{B^p} is given by the edges

$$\begin{aligned} e_{p+1} &= (p+1, 0, 1) \sim v_p = (1, 0, 0) \pmod{(p, 0, 1)}, \\ t &= (0, 1, 0) \sim t_p = (0, 1, 0) \pmod{(p, 0, 1)}, \\ e_{p-1} &= (p-1, 0, 1) \sim w_p = (-1, 0, 0) \pmod{(p, 0, 1)}, \\ s &= (0, -1, 0) \sim s_p = (0, -1, 0) \pmod{(p, 0, 1)}. \end{aligned} \quad (5.3.29)$$

This is the fan of the Hirzebruch surface \mathbb{F}_0 . If one computes the orbit closure of e_0 , the resulting fan is instead that of \mathbb{F}_n , i.e. B^0 is a Hirzebruch surface of the same type as \hat{B}_0 . These results agree with Proposition 5.2.12.

While blowing the open-chain resolution down to the B^0 component can be done directly, doing so to one of the components B^p , with $p = 1, \dots, P$, requires flopping some curves first. We comment on this fact in Appendix B.7.

Let us now collect the holomorphic line bundles associated to the Weierstrass models over vertical models. At the p -th step of the sequence of blow-ups necessary to arrive at the open-chain resolution of a Class 1–4 vertical model, we have the family vanishing orders

$$\text{ord}_{\text{Bl}_p}(\hat{\mathcal{Y}})(\Delta)_{v=e_p=0} = 12 + n_{p+1}. \quad (5.3.30)$$

This leads to a central fiber Y_0 with the structure

$$\begin{array}{ccccccc} \mathbb{I}_{n_0} & -\cdots- & \mathbb{I}_{n_p} & -\cdots- & \mathbb{I}_{n_P} & & \\ | & & | & & | & & \\ \mathbb{F}_n & -\cdots- & \mathbb{F}_0 & -\cdots- & \mathbb{F}_0 & . & \end{array} \quad (5.3.31)$$

The relation between the total and strict transforms under the composition of the blow-up maps of the toric divisors of $\hat{\mathcal{B}}$ is

$$\tilde{\mathcal{S}} = \mathcal{S}, \quad \tilde{\mathcal{T}} = \mathcal{T}, \quad \tilde{\mathcal{V}} = \mathcal{V} + \sum_{p=1}^P E_p, \quad \tilde{\mathcal{W}} = \mathcal{W}, \quad \tilde{\mathcal{U}} = \sum_{p=0}^P E'_p. \quad (5.3.32)$$

The holomorphic line bundle defining the elliptic fibration $\Pi_{\text{ell}} : \mathcal{Y} \rightarrow \mathcal{B}$ is, expressed in terms of the strict transforms,

$$\mathcal{L} = \overline{K}_{\mathcal{B}} = 2\mathcal{S} + (2+n)\mathcal{W} - \sum_{p=1}^P pE_p. \quad (5.3.33)$$

Taking the pertinent restrictions of it we obtain the holomorphic line bundles defining the Weierstrass models $\pi^p : Y^p \rightarrow B^p$, which are

$$\mathcal{L}_0 := \mathcal{L}|_{E_0} = 2S_0 + (1+n)W_0, \quad (5.3.34a)$$

$$\mathcal{L}_p := \mathcal{L}|_{E_p} = 2S_p, \quad p = 1, \dots, P-1, \quad (5.3.34b)$$

$$\mathcal{L}_P := \mathcal{L}|_{E_P} = 2S_P + W_P. \quad (5.3.34c)$$

Appropriate powers of these line bundles yield the divisor classes associated to the defining polynomials and the discriminant, while the modified discriminant in each component is in the divisor class

$$\Delta'_0 = 24S_0 + (12 + 12n + n_0 - n_1)W_0, \quad (5.3.35a)$$

$$\Delta'_p = 24S_p + (2n_p - n_{p-1} - n_{p+1})W_p, \quad p = 1, \dots, P-1, \quad (5.3.35b)$$

$$\Delta'_P = 24S_P + (12 + n_P - n_{P-1})W_P. \quad (5.3.35c)$$

As occurred for horizontal models, the fact that the log Calabi-Yau components Y^p give, when glued along their boundaries, a Calabi-Yau central fiber Y_0 can be seen explicitly by using

(5.2.93) and the relations between the divisors in Y_0 and those in the individual components Y^p , that now are given by

$$\mathcal{S}|_{\tilde{\mathcal{U}}} = \sum_{p=0}^P S_p, \quad \mathcal{T}|_{\tilde{\mathcal{U}}} = \sum_{p=0}^P T_p, \quad \mathcal{V}|_{\tilde{\mathcal{U}}} = V_P, \quad \mathcal{W}|_{\tilde{\mathcal{U}}} = W_0, \quad (5.3.36)$$

$$E_0|_{\tilde{\mathcal{U}}} = W_1 - V_0, \quad E_p|_{\tilde{\mathcal{U}}} = (W_{p+1} - W_p) - (V_p - V_{p-1}), \quad E_P|_{\tilde{\mathcal{U}}} = -(W_P - V_{P-1}),$$

where $p = 1, \dots, P-1$.

5.3.4 Mixed genus-zero degenerations

The remaining single infinite-distance limit genus-zero degenerations of Hirzebruch models are, according to the classification of Definition 5.3.2, those in the Cases C and D. We recall that the non-minimal curves for these two cases are:

- Case C: $C = h + (n+1)f$, or $C = h + (n+2)f$ (mixed section model).
- Case D: $C = 2h + bf$, with $(n, b) = (0, 1), (1, 2)$ (mixed bisection model).

While for Cases A and B we could choose toric divisors as the representatives of the curve class C , leading to a very explicit resolution process based on the description in terms of global homogeneous coordinates, the same is not true for Cases C and D. Nonetheless, we can proceed by employing the general machinery for single infinite-distance limits, discussed in Sections 5.2.4 and 5.2.5. Before we do so, let us further restrict the realization of Cases C and D.

5.3.4.1 Restriction of Cases C and D

In Proposition 5.3.1 we obtained a list of the smooth, irreducible curves that can support non-minimal elliptic fibers in a single infinite-distance limit degeneration of Hirzebruch models. We did this by demanding that $C \leq \bar{K}_{\hat{B}_0}$, see Proposition B.2.2, and checking which curves satisfying this condition were smooth and irreducible. We did not, however, check if tuning said curves would force a second curve C' to factorize with non-minimal vanishing orders and such that $C \cdot C' \neq 0$. This would violate Condition (i) of Definition 5.2.9, hence not corresponding to a single infinite-distance limit degeneration. We now study when this occurs, further constraining Cases C and D.

Focusing first on Case C, the two possible curve classes are

$$C = h + (n + \alpha)f, \quad \alpha = 1, 2, \quad (5.3.37)$$

leading to

$$F - 4C = 4[h + (2 - \alpha)f], \quad (5.3.38)$$

$$G - 6C = 6[h + (2 - \alpha)f]. \quad (5.3.39)$$

When $\alpha = 2$, this means that

$$F - 4C = 4h, \quad G - 6C = 6h. \quad (5.3.40)$$

If $n > 0$, the class h has the unique representative $S = \{s = 0\}_{\hat{B}_0}$, and therefore the above factorization implies

$$\text{ord}_{\hat{Y}_0}(f_0, g_0)_{s=0} = (4, 6). \quad (5.3.41)$$

Since $C \cdot h = 2$, the model does not correspond to a single infinite-distance limit. When $n = 0$, the classes $4h$ and $6h$ factorizing in F and G , respectively, yield a residual discriminant $12h$. Since h now moves in a linear system, this generically leads to 12 horizontal curves of type I_1 fibers, and we obtain a valid single infinite-distance limit degeneration.

For $\alpha = 1$ we find, instead,

$$F - 4C = 4h + 4f, \quad G - 6C = 6h + 6f. \quad (5.3.42)$$

As we increase the value of n , these classes will become generically reducible with components h , eventually forcing non-minimal fibers over this curve. This occurs when

$$(G - 6C - 5h) \cdot h = n + 6 < 0 \Leftrightarrow n \geq 7. \quad (5.3.43)$$

Since $C \cdot h = 1$, this means that the model is beyond the single infinite-distance limit case. In conclusion, Case C can be restricted to

$$\alpha = 1 \quad \text{with} \quad n \leq 6, \quad \text{or} \quad \alpha = 2 \quad \text{with} \quad n = 0. \quad (5.3.44)$$

Case D does not suffer from any additional restrictions. The divisors F and G are, after factoring out the appropriate number of copies of C ,

$$F - 4C = 4(2 + n - b)f = 4f, \quad (5.3.45a)$$

$$G - 6C = 6(2 + n - b)f = 6f. \quad (5.3.45b)$$

This means that the residual discriminant in such a model is purely vertical and reducible, generically leading to 12 vertical curves of type I_1 fibers.

5.3.4.2 Study of Case C

Let $\hat{\rho} : \hat{\mathcal{Y}} \rightarrow D$ be a single infinite-distance limit degeneration of Hirzebruch models in Case C, and let $\rho : \mathcal{Y} \rightarrow D$ be its open-chain resolution. To determine the geometry of the base components B^p of the central fiber B_0 of \mathcal{B} , we apply Proposition 5.2.12. To this end, note that the self-intersection of C is

$$C \cdot C = n + 2\alpha, \quad (5.3.46)$$

meaning that the first base blow-up produces an exceptional component $B^1 = \mathbb{F}_{n+2\alpha}$. The curve $E_0 \cap E_1$ over which the components B^0 and B^1 meet is the $(-(n+2\alpha))$ -curve of the B^1 component. Therefore, within the single infinite-distance limit class of degenerations, we can tune further non-minimal elliptic fibers along the $(+(n+2\alpha))$ -curve of B^1 , prompting us to perform a second blow-up giving rise to a new component $B^2 = \mathbb{F}_{n+2\alpha}$. We can continue iterating this until we tune a model with, say, $P + 1$ components. The central fiber of the open-chain resolution of a Class 1–4 single infinite-distance degeneration of Hirzebruch models in Case C has therefore the structure

$$\begin{array}{ccccccc} I_{n_0} & \text{---} & \cdots & \text{---} & I_{n_p} & \text{---} & \cdots & \text{---} & I_{n_P} \\ | & & & & | & & & & | \\ \mathbb{F}_{n+2\alpha} & \text{---} & \cdots & \text{---} & \mathbb{F}_{n+2\alpha} & \text{---} & \cdots & \text{---} & \mathbb{F}_n, \end{array} \quad (5.3.47)$$

where we have inverted the labelling of the components to more effectively draw comparisons with the results of Section 5.3.2. We see that the P first components are the same as in a

horizontal model constructed, not over the Hirzebruch surface \mathbb{F}_n , but of $\mathbb{F}_{n+2\alpha}$. The same is true for the holomorphic line bundles defining the Weierstrass models $\pi^p : Y^p \rightarrow B^p$, which are

$$\mathcal{L}_0 := S_0 + (2 + (n + 2\alpha))V_0, \quad (5.3.48a)$$

$$\mathcal{L}_p := 2V_p, \quad p = 1, \dots, P-1, \quad (5.3.48b)$$

$$\mathcal{L}_P := S_P + (2 - \alpha)V_P. \quad (5.3.48c)$$

The divisors associated to the defining polynomials and the discriminant are obtained as appropriate powers of these line bundles, while the modified discriminant in each component is in the divisor class

$$\Delta'_0 = (12 + n_0 - n_1)S_0 + (24 + 12(n + 2\alpha))V_0, \quad (5.3.49a)$$

$$\Delta'_p = (2n_p - n_{p-1} - n_{p+1})S_p + (24 + (n + 2\alpha)(n_p - n_{p-1}))V_p, \quad p = 1, \dots, P-1, \quad (5.3.49b)$$

$$\Delta'_P = (12 + n_P - n_{P-1})S_P + ((24 - 12\alpha) + (n + \alpha)(n_P - n_{P-1}))V_P. \quad (5.3.49c)$$

As in the other cases, each component Y^p of the central fiber Y_0 is a log Calabi-Yau space, while Y_0 is the Calabi-Yau space obtained by taking their union along the boundaries.

5.3.4.3 Study of Case D

Assume now instead that $\hat{\rho} : \hat{\mathcal{Y}} \rightarrow D$ is a single infinite-distance limit degeneration of Hirzebruch models in Case D. Since

$$C \cdot C = 4(b - n) = 4, \quad (5.3.50)$$

the exceptional component obtained after the first blow-up is $B^1 = \mathbb{F}_4$. Arguing as we did for Case C, and inverting the labelling of the components, a Class 1–4 single infinite-distance limit degeneration of Hirzebruch models in Case D leads to a central fiber with the structure

$$\begin{array}{ccccccc} I_{n_0} & - & \cdots & - & I_{n_p} & - & \cdots & - & I_{n_P} \\ | & & & & | & & & & | \\ \mathbb{F}_4 & - & \cdots & - & \mathbb{F}_4 & - & \cdots & - & \mathbb{F}_n. \end{array} \quad (5.3.51)$$

The holomorphic line bundles defining the Weierstrass models $\pi^p : Y^p \rightarrow B^p$ are

$$\mathcal{L}_0 := S_0 + (2 + 4)V_0, \quad (5.3.52a)$$

$$\mathcal{L}_p := 2V_p, \quad p = 1, \dots, P-1, \quad (5.3.52b)$$

$$\mathcal{L}_P := V_P. \quad (5.3.52c)$$

Adequate powers of these give the divisor classes associated to the defining polynomials and the discriminant, while the modified discriminant in each component is in the divisor class

$$\Delta'_0 = (12 + n_0 - n_1)S_0 + (24 + 12 \cdot 4)V_0, \quad (5.3.53a)$$

$$\Delta'_p = (2n_p - n_{p-1} - n_{p+1})S_p + (24 + 4(n_p - n_{p-1}))V_p, \quad p = 1, \dots, P-1, \quad (5.3.53b)$$

$$\Delta'_P = 2(n_P - n_{P-1})S_P + (12 + (n + 1)(n_P - n_{P-1}))V_P. \quad (5.3.53c)$$

In this case, the first P components behave like in a horizontal model constructed over \mathbb{F}_4 . As in the previous cases, the union of the Y^p log Calabi-Yau spaces along their boundary yields the Calabi-Yau central fiber Y_0 .

5.4 Extracting the codimension-one information

In this section, we analyse the discriminant structure of the central fiber of the semi-stable degeneration. This is required in order to read off the gauge algebra of the effective action in F-theory, prior to taking the decompactification limit, as we will explain.

According to the usual F-theory dictionary, the gauge algebras found in space-time are encoded in the types of singularities of the elliptic fiber of the internal Calabi-Yau space over codimension-one loci in the base; these loci are the spacetime regions wrapped by 7-branes, and the singularity in the elliptic fiber captures the singular nature of the Type IIB axio-dilaton profile on top of its sources.

Let \mathcal{D} be an irreducible divisor in the base of an elliptic Calabi-Yau n -fold Y . The gauge algebra¹⁹ supported on \mathcal{D} can be read off from the vanishing orders $\text{ord}_Y(f, g, \Delta)_{\mathcal{D}}$ with the help of the Kodaira-Néron classification of singular elliptic fibers. From the point of view of M-theory, the type of singular elliptic fibers over \mathcal{D} determines the pattern of exceptional curves that shrink as we take the F-theory limit (going to the origin of the Coulomb branch), with the gauge algebras furnished by the light states arising from M2-branes wrapped on these curves. The relation between the type of singular elliptic fibers over a certain locus and the vanishing orders of the defining polynomials over it was discussed in Section 5.2.2.2 (see also, e.g., [185] for a review on F-theory).

Given a degeneration $\hat{\rho} : \hat{\mathcal{Y}} \rightarrow D$ of the type described in Section 5.2.1, this is how we would determine the gauge algebras for the F-theory models described by the generic elements $\hat{Y}_{u \neq 0}$ of the family, which do not exhibit any infinite-distance non-minimal fibral singularities. The situation is more subtle for the central fiber \hat{Y}_0 of the degeneration due to the appearance of non-minimal elliptic fibers. To read off the gauge algebra, we therefore first have to apply the procedures explained in Section 5.2.2 to obtain the resolved degeneration $\rho : \mathcal{Y} \rightarrow D$ (which must be free of obscured infinite-distance limits, see Appendix B.3). Its central fiber Y_0 presents then no infinite-distance non-minimal singularities.

However, Y_0 factors into multiple log Calabi-Yau components $\{Y^p\}_{0 \leq p \leq P}$. This gives rise to interesting phenomena not occurring in conventional six-dimensional F-theory models. When the base of the fibration is an irreducible surface, the 7-branes correspond to irreducible curves in it. Two irreducible curves in an irreducible surface will either coincide, leading to a gauge enhancement, or intersect over points if they are distinct, resulting in localized matter. When the base of the elliptic fibration is instead a reducible surface, as occurs for Y_0 , two distinct 7-branes in a component may overlap in a different component, leading to what looks like a local gauge enhancement. This gives rise to subtleties in determining the gauge algebra content from the component vanishing orders, whose definition was given in Definition 5.2.3.

More precisely, there are two types of complications that obscure the interpretation of the vanishing orders of the Weierstrass model at first sight:

1. **Locally coincident discriminant components:** Certain components of the discriminant locus may coincide in some components of the base B_0 while being separated in others. An example is shown in Figure 5.5.
2. **Locally reducible discriminant components:** Two or more divisors in some component of B_0 may in fact be part of a single connected divisor extending over the entire base B_0 , as illustrated in Figure 5.6.

¹⁹In six dimensions or fewer, the unambiguous determination of the gauge algebra requires also analysing the monodromy cover. Obtaining the global form of the gauge group requires additional information as well.

In Sections 5.4.1 and 5.4.2, we analyse these two complications in turn. We first exhibit them in some examples, and then propose a way to unambiguously read off the global gauge algebra content of the F-theory model represented by Y_0 . A first step in this direction was the definition of the modified discriminant Δ' , see Definition 5.2.16, in which we subtract the background value of the axio-dilaton in the components. The general algorithm to unambiguously extract the vanishing orders of the Weierstrass model is then presented in Section 5.4.3. The gauge algebra assignment also needs to take into account possible local monodromies in the fiber over some components, as pointed out in Section 5.4.4. The final algorithm to determine the gauge algebra as encoded in the Weierstrass model is summarised in Section 5.4.5.

It is worth noting that the subsequent analysis maintains a six-dimensional standpoint; the gauge algebra extracted from Y_0 is that of a six-dimensional effective theory prior to partial decompactification. The partial decompactification may be a consequence of taking the infinite-distance limit, possibly leading to partial gauge enhancements as viewed from the point of view of the asymptotic, higher-dimensional gauge theory. When we refer to the ‘‘gauge algebra’’ in this section, this important effect has not been considered yet. It will be discussed in Chapter 6.

Some of the considerations below also apply to the study of open-moduli infinite-distance limits in eight-dimensional F-theory performed in [156, 157], but are not crucial for the correct identification of the codimension-one physics. The 7-branes in an eight-dimensional model correspond to points in the base, and they hence cannot extend between the components of the central fiber of the resolved degeneration as it occurs in six dimensions.

As emphasized in Section 5.2.2.2, the gauge algebras can be determined using a global description of the F-theory model, if available like in toric examples, or by working in local patches. In the remainder of the section, we frame the discussion using the global picture for ease of exposition, with analogous considerations following *mutatis mutandis* for a local analysis.

5.4.1 Locally coincident discriminant components

In this section, we illustrate the phenomenon where components of the discriminant may locally overlap in certain parts of the base B_0 , and how this, naively, leads to ambiguities in the vanishing orders of the components in the Weierstrass model.

Consider, for instance, a degeneration $\hat{\rho} : \hat{\mathcal{Y}} \rightarrow D$ with $\mathcal{B} = \mathbb{F}_n \times D$ and non-minimal family vanishing orders over the curve $\mathcal{S} \cap \mathcal{U}$,

$$\text{ord}_{\hat{\mathcal{Y}}}(f, g, \Delta)_{\mathcal{S} \cap \mathcal{U}} = (4, 6, 12). \quad (5.4.1)$$

This requires at least one base blow-up along $\mathcal{S} \cap \mathcal{U}$, followed by an appropriate line bundle shift, in order to arrive at the resolved degeneration $\rho : \mathcal{Y} \rightarrow D$. The curve of the central fiber $\mathcal{V} \cap \tilde{\mathcal{U}} = \{v = 0\}_{B_0}$ traverses both the B^0 and B^1 components. It may occur, however, that the component vanishing orders differ between the two components,

$$\text{ord}_{Y^0}(f_0, g_0, \Delta'_0)_{v=0} \neq \text{ord}_{Y^1}(f_1, g_1, \Delta'_1)_{v=0}. \quad (5.4.2)$$

This prompts us to question how they are related to the gauge algebra content and to each other. We can see this realised explicitly in the following degeneration.

Example 5.4.1. Consider the Weierstrass model

$$f = s^3 t^3 (sv + tu) (suv^8 + tuw^7 + tv^3 w^4 + tv^2 w^5 + tw^6), \quad (5.4.3a)$$

$$g = s^4 t^5 v w^5 (sv + tu)^2 (sw^5 + tv^4 + tv^3 w + tv^2 w^2 + tw^3), \quad (5.4.3b)$$

$$\Delta = s^8 t^9 (sv + tu)^3 p_{4,24}([s : t], [v : w], u), \quad (5.4.3c)$$

defining an elliptically fibered variety $\hat{\mathcal{Y}}$ over the base $\hat{\mathcal{B}} = \mathbb{F}_1 \times D$ with non-minimal singular elliptic fibers over $\mathcal{S} \cap \mathcal{U}$,

$$\text{ord}_{\hat{\mathcal{Y}}}(f, g, \Delta)_{s=u=0} = (4, 6, 12). \quad (5.4.4)$$

This is a single infinite-distance limit horizontal model according to the classification in Definition 5.3.2. After performing a (toric) blow-up along $\mathcal{S} \cap \mathcal{U}$ and the necessary line bundle shift, we arrive at the open-chain resolution

$$f = s^3 t^3 (e_0 t + sv) (e_0 e_1 s v^8 + e_0 e_1 t w^7 + t v^3 w^4 + t v^2 w^5 + t v w^6), \quad (5.4.5a)$$

$$g = s^4 t^5 v w^5 (e_0 t + sv)^2 (e_1 s w^5 + t v^4 + t v^3 w + t v^2 w^2 + t v w^3), \quad (5.4.5b)$$

$$\Delta = s^8 t^9 (s v + t e_0)^3 p_{4,24,1}([s : t], [v : w : t], [s : e_0 : e_1]), \quad (5.4.5c)$$

with Stanley-Reisner ideal

$$\mathcal{I}_{\mathcal{B}} = \langle st, vw, se_0, te_1 \rangle. \quad (5.4.6)$$

The central fiber of the resolved degeneration has the following pattern of codimension-zero singularities:

$$\begin{array}{ccc} \mathbb{I}_0 & \longrightarrow & \mathbb{I}_0 \\ | & & | \\ \mathbb{F}_1 & \longrightarrow & \mathbb{F}_1. \end{array} \quad (5.4.7)$$

Computing the restricted polynomials (5.2.96) and modified discriminant (5.2.101), we find for the B^0 component

$$f_0 = t^4 v^2 w^4 (v^2 + vw + w^2), \quad (5.4.8a)$$

$$g_0 = t^5 v^3 w^5 (e_1 w^5 + t v^4 + t v^3 w + t v^2 w^2 + t v w^3), \quad (5.4.8b)$$

$$\Delta'_0 = t^{10} v^6 w^{10} p_{2,10}([t : e_1], [v : w]), \quad (5.4.8c)$$

while for the B^1 component we obtain

$$f_1 = s^3 v w^4 (v^2 + vw + w^2) (e_0 + sv), \quad (5.4.9a)$$

$$g_1 = s^4 v^2 w^5 (v + w) (v^2 + w^2) (e_0 + sv)^2, \quad (5.4.9b)$$

$$\Delta'_1 = s^8 v^3 w^{10} (e_0 + sv)^3 p_{1,8}([e_0 : s], [v : w]). \quad (5.4.9c)$$

Here we have used the available \mathbb{C}^* -actions to set the redundant coordinates to one.

The model presents a discrepancy between the family and component vanishing orders

$$(1, 5, 3) = \text{ord}_{\mathcal{Y}}(f, g, \Delta)_{w=e_0=0} \leq \text{ord}_{Y^0}(f_0, g_0, \Delta'_0)_{w=0} = (4, 5, 10), \quad (5.4.10)$$

$$(2, 5, 6) = \text{ord}_{\mathcal{Y}}(f, g, \Delta)_{w=e_1=0} \leq \text{ord}_{Y^1}(f_1, g_1, \Delta'_1)_{w=0} = (4, 5, 10), \quad (5.4.11)$$

which is expected to occur, as discussed in Section 5.2.2.2. This is not a problem for determining the gauge algebra because, as is emphasized in Appendix B.3, it is the component vanishing orders that are expected to be of physical relevance for the codimension-one physics; the family vanishing orders, by contrast, play a role during the resolution process and for identifying the codimension-zero singular elliptic fibers over the components of the central fiber. More importantly, we observe a discrepancy between the component vanishing orders

$$(2, 3, 6) = \text{ord}_{Y^0}(f_0, g_0, \Delta'_0)_{v=0} \neq \text{ord}_{Y^1}(f_1, g_1, \Delta'_1)_{v=0} = (1, 2, 3). \quad (5.4.12)$$

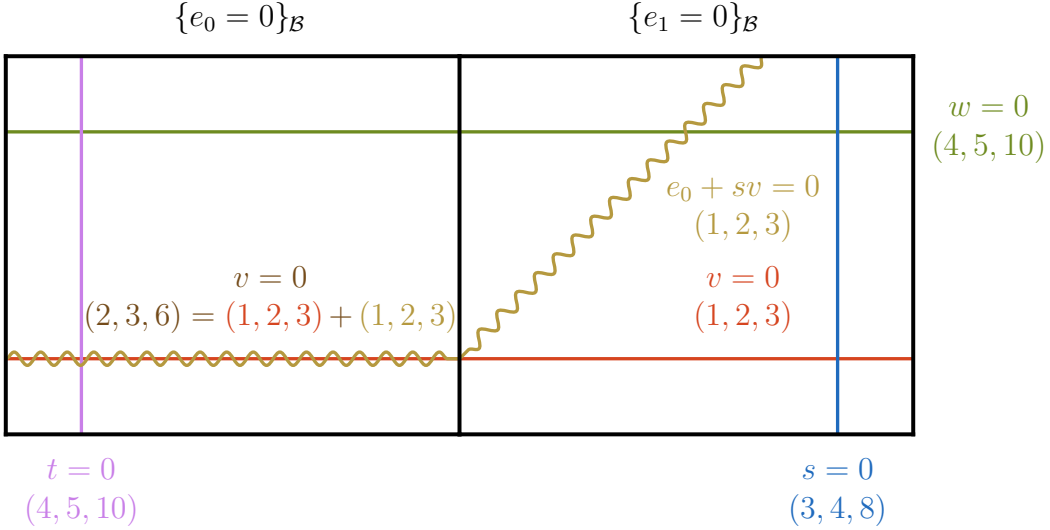


Figure 5.5: Restrictions Δ'_0 and Δ'_1 of the (modified) discriminant for Example 5.4.1, with the residual discriminant omitted for clarity. The printed vanishing orders correspond to the component vanishing orders in each component.

Hence reading off the gauge algebra supported on $\mathcal{V} \cap \tilde{\mathcal{U}} \subset B_0$ from the component vanishing orders in B^0 seemingly results in a bigger gauge factor than the one read in the B^1 component.

To resolve this puzzle, note that in the multi-component central fiber Y_0 of a resolved degeneration $\rho : \mathcal{Y} \rightarrow D$, the component vanishing orders $\text{ord}_{Y^p}(f_p, g_p, \Delta'_p)_{C_p}$ only reflect the information available in a given component Y^p . The physics associated with the endpoints of open-moduli infinite-distance limits in six-dimensional F-theory involves, however, the central fiber Y_0 taken as a whole.

To exploit this observation, a more revealing way to look at Example 5.4.1 is by graphically representing the restrictions Δ'_0 and Δ'_1 of its (modified) discriminant Δ' . We do so in Figure 5.5, omitting the residual discriminant in both components. We also print the component vanishing orders computed in Y^0 and Y^1 . From the point of view of the Y^1 component, a gauge enhancement occurs over four curves. In terms of their divisor classes within B^1 , these curves and their associated component vanishing orders are

$$S_1 : (3, 4, 8), \quad T_1 : (1, 2, 3), \quad V_1 : (1, 2, 3), \quad W_1 : (4, 5, 10). \quad (5.4.13)$$

From the perspective of the Y^0 component, we have instead three curves supporting a gauge enhancement, with vanishing orders

$$T_0 : (4, 5, 10), \quad V_0 : (2, 3, 6), \quad W_0 : (4, 5, 10). \quad (5.4.14)$$

From Figure 5.5, we observe that the additional enhancement over V_1 with respect to V_0 occurs because the representative $\{e_0 + sv = 0\}_{B^1}$ of the class T_1 intersects the curve $\{e_0 = 0\}_{B^1}$ at $\{e_0 = v = 0\}_{B^1}$ and extends to the component $B^0 = \{e_0 = 0\}_B$ in such a way that it overlaps the representative $\{v = 0\}_{B^0}$ of V_0 . This is the analysis of local gauge enhancements as read off from the component vanishing orders.

Let us now take a global perspective and express the same vanishing orders in terms of the restrictions of the divisors of the family variety \mathcal{Y} to $\tilde{\mathcal{U}}$. For a single infinite-distance limit horizontal model such as Example 5.4.1, these restrictions are given in (5.3.25). In this way, we

see that

$$\mathcal{T}|_{\tilde{\mathcal{U}}} = T_0 : (4, 5, 10), \quad (5.4.15)$$

$$\mathcal{S}|_{\tilde{\mathcal{U}}} = S_2 : (3, 4, 8), \quad (5.4.16)$$

$$(\mathcal{T} + E_0)|_{\tilde{\mathcal{U}}} = (\mathcal{S} + \mathcal{V})|_{\tilde{\mathcal{U}}} = V_0 + T_1 : (1, 2, 3), \quad (5.4.17)$$

$$\mathcal{V}|_{\tilde{\mathcal{U}}} = V_0 + V_1 : (1, 2, 3), \quad (5.4.18)$$

$$\mathcal{W}|_{\tilde{\mathcal{U}}} = W_0 + W_1 : (4, 5, 10). \quad (5.4.19)$$

From this point of view, there is no ambiguity in assigning a gauge factor to the divisor $\mathcal{V}|_{\tilde{\mathcal{U}}} = \{v = 0\}_{B_0}$: The vanishing orders are $(1, 2, 3)$, and the associated gauge algebra is $\mathfrak{su}(2)$.

This enhancement observed for the central fiber of Example 5.4.1 is not present at finite distance, as one can check for the base divisor $\{v = 0\}_{B_{\tilde{u}}}$ of the generic fibers $\hat{Y}_{u \neq 0} \simeq Y_{\tilde{u} \neq 0}$ of the degeneration. The tuning over $\{v = 0\}_{B_{\tilde{u}}}$ occurs at the same time as we take the infinite-distance limit. In contrast to this, the enhancement over $\pi^*(\{tu + sv = 0\}_{B_{\tilde{u}}}) = \{te_0 + sv = 0\}_{B_{\tilde{u}}}$ is present both at finite distance and once we reach the endpoint of the limit, appearing with vanishing orders $(1, 2, 3)$ throughout. The local enhancement over $\{v = 0\}_{B^0}$ in the B^0 component, as compared to the gauge algebra read for $\{v = 0\}_{B^1}$, is a consequence of the fact that the restrictions of $\{v = 0\}_{B_0}$ and $\{te_0 + sv = 0\}_{B_0}$ to B^0 coincide, needing the global picture to distinguish between the two.

Note that working with the resolved degeneration $\rho : \mathcal{Y} \rightarrow D$ is crucial to correctly read the gauge algebra content, from the global picture, at the endpoint of the limit. If we try to avoid the multi-component central fiber Y_0 of the resolved degeneration by working with the original degeneration $\hat{\rho} : \hat{\mathcal{Y}} \rightarrow D$ while ignoring the non-minimal elliptic fibers of \hat{Y}_0 , we potentially run into the same problems that can occur for Y_0 when only looking at the component vanishing orders without taking the global picture into account.

Let us use Example 5.4.1 to showcase such a behaviour explicitly. Denote by $\check{\rho} : \check{\mathcal{Y}} \rightarrow D$ the blow-down of $\rho : \mathcal{Y} \rightarrow D$ in which we contract the Y^0 component. Both $\hat{\rho} : \hat{\mathcal{Y}} \rightarrow D$ and $\check{\rho} : \check{\mathcal{Y}} \rightarrow D$ have $\rho : \mathcal{Y} \rightarrow D$ as their open-chain resolution, the process of reaching it involving the base blow-ups $\hat{\pi} : \mathcal{B} \rightarrow \hat{\mathcal{B}}$ with centre $\mathcal{S} \cap \mathcal{U}$ and $\check{\pi} : \mathcal{B} \rightarrow \check{\mathcal{B}}$ with centre $\mathcal{T} \cap \check{\mathcal{U}}$, respectively. These three degenerations are equivalent, and therefore represent the same infinite-distance limit in the complex structure moduli space of six-dimensional F-theory. Given the relations

$$\hat{\pi}_*(F_0) = F|_{\mathcal{U}} - 4(\mathcal{S} \cap \mathcal{U}), \quad (5.4.20a)$$

$$\hat{\pi}_*(G_0) = G|_{\mathcal{U}} - 6(\mathcal{S} \cap \mathcal{U}), \quad (5.4.20b)$$

$$\hat{\pi}_*(\Delta_0) = \Delta|_{\mathcal{U}} - 12(\mathcal{S} \cap \mathcal{U}), \quad (5.4.20c)$$

and

$$\check{\pi}_*(F_1) = F|_{\check{\mathcal{U}}} - 4(\mathcal{T} \cap \check{\mathcal{U}}), \quad (5.4.21a)$$

$$\check{\pi}_*(G_1) = G|_{\check{\mathcal{U}}} - 6(\mathcal{T} \cap \check{\mathcal{U}}), \quad (5.4.21b)$$

$$\check{\pi}_*(\Delta_1) = \Delta|_{\check{\mathcal{U}}} - 12(\mathcal{T} \cap \check{\mathcal{U}}), \quad (5.4.21c)$$

see (B.5.2), it is clear that

$$\text{ord}_{\hat{Y}_0}(f|_{u=0}, g|_{u=0}, \Delta'|_{u=0})_{v=0} = \text{ord}_{Y^0}(f_0, g_0, \Delta'_0)_{v=0} = (2, 3, 6), \quad (5.4.22)$$

$$\text{ord}_{\hat{Y}_0}(f|_{\check{u}=0}, g|_{\check{u}=0}, \Delta'|_{\check{u}=0})_{v=0} = \text{ord}_{Y^1}(f_1, g_1, \Delta'_1)_{v=0} = (1, 2, 3). \quad (5.4.23)$$

Hence, reading off the gauge algebra from the component vanishing orders found in the central fiber of $\hat{\rho} : \hat{\mathcal{Y}} \rightarrow D$ is equivalent to performing a local analysis of the resolved degeneration taking only into account the Y^0 component; it gives the wrong impression that the local enhancement occurring in this component is a global feature, and only the resolution process resolves the ambiguity. In this example, the vanishing orders over the curve $\mathcal{T} \cap \mathcal{U}$ of the central fiber of $\check{\rho} : \check{\mathcal{Y}} \rightarrow D$ happen to coincide with those read off from the resolved degeneration.

5.4.2 Locally reducible discriminant components

The preceding discussion showed how studying the multi-component central fiber of the resolved degeneration as a whole can reveal certain enhancements occurring over components to be a local phenomenon, which proved important in correctly identifying the types of gauge factors in the model, as illustrated using Example 5.4.1. We now focus on another phenomenon that also highlights the importance of studying the global picture. Namely, a single irreducible curve in one component may intersect the interface curve with an adjacent component more than once, extending to said component as a collection of irreducible curves. A local analysis in the adjacent component would prompt us then to overcount the gauge factors, while the global picture shows that these irreducible curves all join together as a single irreducible curve in the component originally considered, and should therefore be counted as a single gauge factor contribution. We showcase this behaviour in the following example.

Example 5.4.2. Consider the Weierstrass model of the family variety $\hat{\mathcal{Y}}$, elliptically fibered over the base $\hat{\mathcal{B}} = \mathbb{F}_1 \times D$, given by the defining polynomials

$$f = -s^3 t^4 v^4 w (u^2 t(v - 2w) + s(v + w)(v - w)) (4u^2 v + 3u^2 w + 2v + w) , \quad (5.4.24a)$$

$$g = s^4 t^5 v^5 w^2 (u^2 t(v - 2w) + s(v + w)(v - w))^2 (23sv^2 + 8svw + 7sw^2 + 6tv + 5tw) , \quad (5.4.24b)$$

$$\Delta = s^8 t^{10} v^{10} w^3 (u^2 t(v - 2w) + s(v + w)(v - w))^3 p_{3,7}([s : t], [v : w], u) . \quad (5.4.24c)$$

It is a single infinite-distance limit horizontal model presenting non-minimal elliptic fibers over the curve $\mathcal{S} \cap \mathcal{U}$ with

$$\text{ord}_{\hat{\mathcal{Y}}}(f, g, \Delta)_{\mathcal{S} \cap \mathcal{U}} = (4, 6, 12) . \quad (5.4.25)$$

The resolved degeneration $\rho : \mathcal{Y} \rightarrow D$, reached after $P = 2$ (toric) blow-ups, is the three-component model given by the defining polynomials

$$f = -s^3 t^4 v^4 w (e_0^2 e_1 t(v - 2w) + s(v + w)(v - w)) (e_0^2 e_1^2 e_2^2 (4v + 3w) + 2v + w) , \quad (5.4.26a)$$

$$g = s^4 t^5 v^5 w^2 (e_0^2 e_1 t(v - 2w) + s(v + w)(v - w))^2 \times (e_1 e_2^2 s (23v^2 + 8vw + 7w^2) + 6tv + 5tw) , \quad (5.4.26b)$$

$$\Delta = s^8 t^{10} v^{10} w^3 (e_0^2 e_1 t(v - 2w) + s(v + w)(v - w))^3 \times p_{3,7,1,1}([s : t], [v : w], [s : e_0 : e_1], [s : e_1 : e_2]) , \quad (5.4.26c)$$

with Stanley-Reisner ideal

$$\mathcal{I}_{\mathcal{B}} = \langle st, vw, se_0, se_1, te_1, te_2, e_0 e_2 \rangle . \quad (5.4.27)$$

The pattern of codimension-zero fibers over the components of the central fiber of the resolved degeneration is

$$\begin{array}{ccc} \mathbb{I}_0 & \longrightarrow & \mathbb{I}_0 & \longrightarrow & \mathbb{I}_0 \\ | & & | & & | \\ \mathbb{F}_1 & \longrightarrow & \mathbb{F}_1 & \longrightarrow & \mathbb{F}_1. \end{array} \quad (5.4.28)$$

Computing the restricted polynomials (5.2.96) and modified discriminant (5.2.101) we obtain for the B^0 component

$$f_0 = -t^4 v^4 w (v + w) (v - w) (2v + w), \quad (5.4.29a)$$

$$g_0 = t^5 v^5 w^2 (v + w)^2 (v - w)^2 (23e_1 v^2 + 8e_1 v w + 7e_1 w^2 + 6t v + 5t w), \quad (5.4.29b)$$

$$\Delta'_0 = t^{10} v^{10} w^3 (v + w)^3 (v - w)^3 p_{2,7}([t : e_1], [v : w]), \quad (5.4.29c)$$

for the B^1 component

$$f_1 = -v^4 w (v + w) (v - w) (2v + w), \quad (5.4.30a)$$

$$g_1 = v^5 w^2 (v + w)^2 (v - w)^2 (6v + 5w), \quad (5.4.30b)$$

$$\Delta'_1 = -v^{10} w^3 (v + w)^3 (v - w)^3 p_{0,5}([e_0, e_1], [v : w]), \quad (5.4.30c)$$

and for the B^2 component

$$f_2 = -s^3 v^4 w (e_1 (v - 2w) + s(v + w)(v - w)) (2v + w), \quad (5.4.31a)$$

$$g_2 = s^4 v^5 w^2 (e_1 (v - 2w) + s(v + w)(v - w))^2 (6v + 5w), \quad (5.4.31b)$$

$$\Delta'_2 = -s^8 v^{10} w^3 (e_1 (v - 2w) + s(v + w)(v - w))^3 p_{1,5}([e_1, s], [v : w]). \quad (5.4.31c)$$

From the point of view of the B^0 and B^1 components, we observe two local gauge enhancements along

$$\text{ord}_{Y^0}(f_0, g_0, \Delta'_0)_{v+w=0} = \text{ord}_{Y^1}(f_1, g_1, \Delta'_1)_{v+w=0} = (1, 2, 3), \quad (5.4.32)$$

$$\text{ord}_{Y^0}(f_0, g_0, \Delta'_0)_{v-w=0} = \text{ord}_{Y^1}(f_1, g_1, \Delta'_1)_{v-w=0} = (1, 2, 3), \quad (5.4.33)$$

which extend into the B^2 component as a single irreducible curve

$$\text{ord}_{Y^2}(f_2, g_2, \Delta'_2)_{e_1(v-2w)+s(v+w)(v-w)=0} = (1, 2, 3). \quad (5.4.34)$$

Performing the gauge assignment from the local information in the components B^0 or B^1 would lead to an overcounting of the gauge algebra factors. The global perspective clarifies that we have a single gauge algebra corresponding to vanishing orders $(1, 2, 3)$ over the divisor

$$\mathcal{D}_{\text{phys}} := \{e_0^2 e_1 t (v - 2w) + s(v + w)(v - w) = 0\}_{B_0} \quad (5.4.35)$$

of B_0 , which is in the class

$$\mathcal{D}_{\text{phys}} = (\mathcal{T} + 2E_0 + E_1 + \mathcal{V})|_{\tilde{\mathcal{U}}} = (\mathcal{S} + 2\mathcal{V})|_{\tilde{\mathcal{U}}} = (2V_0) + (2V_1) + (T_2 + V_2), \quad (5.4.36)$$

and restricts in the components to the curves listed above and portrayed in Figure 5.6.

In this example, it is particularly clear that a single gauge factor should be associated with the divisor $\mathcal{D}_{\text{phys}}$ extending through the multiple components of the reducible variety B_0 . The

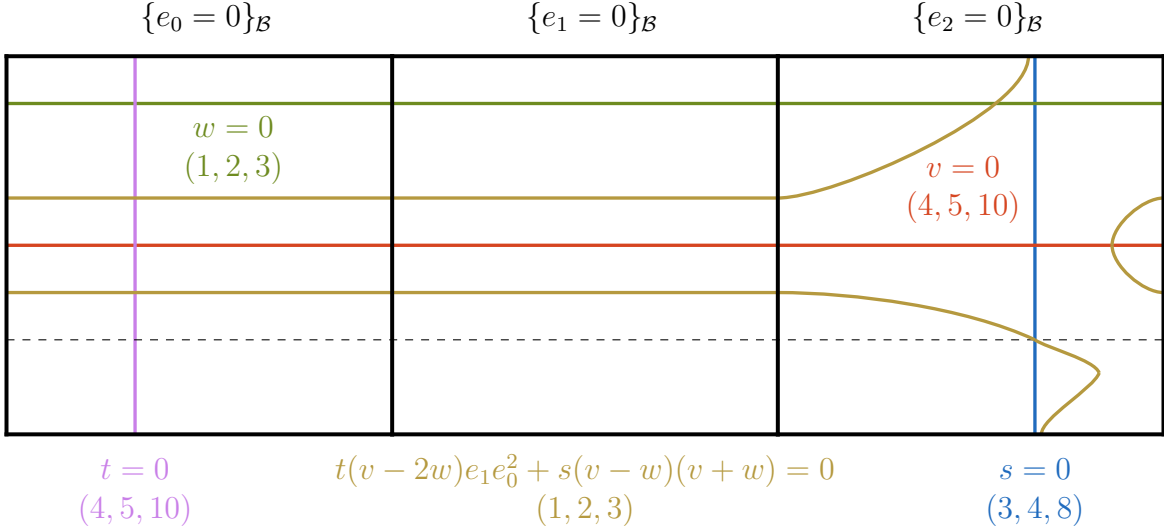


Figure 5.6: Restrictions Δ'_0 , Δ'_1 and Δ'_2 of the (modified) discriminant for Example 5.4.2, with the residual discriminant omitted for clarity. The printed vanishing orders correspond to the component vanishing orders in each component. Although the divisor $\mathcal{D}_{\text{phys}}$ restricts to two irreducible curves both in B^0 and B^1 , it restricts to a single irreducible curve in B^2 , corresponding therefore to a single gauge factor.

gauge algebra supported on it is already present in all models represented by the fibers at finite distance, since in any $Y_{\tilde{u} \neq 0}$ we have

$$\text{ord}_{Y_{\tilde{u} \neq 0}}(f|_{\tilde{u} \neq 0}, g|_{\tilde{u} \neq 0}, \Delta|_{\tilde{u} \neq 0})_{\tilde{u}^2 t(v-2w) + s(v+w)(v-w) = 0} = (1, 2, 3). \quad (5.4.37)$$

This enhancement is unaffected by the infinite-distance limit. Note that determining the gauge algebra from the central fiber \hat{Y}_0 of the unresolved degeneration $\hat{\rho} : \hat{\mathcal{Y}} \rightarrow D$ would lead to the same conclusions as the local analysis in the Y^0 component of the resolved degeneration, and therefore to an overcounting of the gauge factors; working with the global picture of Y_0 in $\rho : \mathcal{Y} \rightarrow D$ avoids this problem.

5.4.3 Physical discriminant for the multi-component central fiber

Having illustrated through Examples 5.4.1 and 5.4.2 the problems that can occur, let us now discuss how to extract in practice the codimension-one physics from the central fiber Y_0 of a resolved degeneration $\rho : \mathcal{Y} \rightarrow D$. We start with an informal, but operational explanation of the matter paired with an explicit example, concluding the section by concisely restating the information in a cleaner fashion.

As can be distilled from the examples above, we need to associate the gauge factors to divisors $\mathcal{D}_{\text{phys}}$ of the multi-component base B_0 of the resolved degeneration, rather than to the irreducible components of the restrictions $\{\Delta'_p\}_{0 \leq p \leq P}$ of the modified divisor Δ' . These components, however, must consistently glue together between components, as shown in Figures 5.5 and 5.6, to produce divisors defined in B_0 . Since the surface B_0 is itself reducible, so will be the divisors extending between components. We then assign a single gauge algebra factor to each divisor $\mathcal{D}_{\text{phys}}$ of B_0 obtained by consistently gluing together the irreducible components of $\{\Delta'_p\}_{0 \leq p \leq P}$ and such that it restricts to a single irreducible divisor in at least one of the components $\{B^p\}_{0 \leq p \leq P}$.

In practical terms, it would be useful to obtain these divisors by factorising a physical discriminant defined in B_0 . In the same way that the restricted polynomials $\{f_p\}_{0 \leq p \leq P}$, $\{g_p\}_{0 \leq p \leq P}$ and $\{\Delta'_p\}_{0 \leq p \leq P}$ associated to the individual components $\{B^p\}_{0 \leq p \leq P}$ are obtained by restricting their counterparts in \mathcal{B} to the vanishing locus of the appropriate e_p coordinate, we can define similar quantities for the multi-component surface $B_0 = \bigcup_{p=0}^P B^p$ as a whole. In light of the relation (5.2.42), we simply need to take the restriction of the defining polynomials to the vanishing locus of the coordinate $\tilde{u} = \prod_{p=0}^P e_p$. We will call these restrictions the physical defining polynomials, and denote them by f_{phys} , g_{phys} and Δ_{phys} . The divisors described in the previous paragraph, and to which the individual gauge algebra factors are associated, correspond to the vanishing loci of the factors of Δ_{phys} . In terms of divisor classes, the physical defining polynomials correspond to the restrictions $F|_{\tilde{\mathcal{U}}}$, $G|_{\tilde{\mathcal{U}}}$ and $\Delta'|_{\tilde{\mathcal{U}}}$.

For the polynomial Δ' or its restrictions $\{\Delta'_p\}_{0 \leq p \leq P}$, the factorization is performed in the standard way. When factorizing

$$\Delta_{\text{phys}} := \Delta'|_{\tilde{u}=0}, \quad \tilde{u} = \prod_{p=0}^P e_p, \quad (5.4.38)$$

to obtain the loci supporting the gauge algebra, however, we need to keep in mind that the product $\tilde{u} = \prod_{p=0}^P e_p$ is zero when evaluated over B_0 , and therefore the factorization is to be done up to terms proportional to \tilde{u} . That is, a divisor $\mathcal{D}_{\text{phys}} = \{p_{\mathcal{D}_{\text{phys}}} = 0\}_{B_0}$ is a component of $\Delta'|_{\tilde{\mathcal{U}}}$ if the remainder of the quotient Δ_{phys} by $p_{\mathcal{D}_{\text{phys}}}$ is proportional to \tilde{u} , i.e. when

$$\Delta_{\text{phys}} = p_{\mathcal{D}_{\text{phys}}} q + \tilde{u} r' \quad (5.4.39)$$

for some polynomials q and r' .

It may not always be needed to take this into account. For example, if a gauge enhancement is present at finite distance, i.e. for the generic fibers $Y_{\tilde{u} \neq 0}$ of the degeneration $\rho : \mathcal{Y} \rightarrow D$, the corresponding divisor will factorize in Δ' and hence appear factorized in Δ_{phys} . This is, in fact, what occurs in Examples 5.4.1 and 5.4.2. To give one instance of this, consider $\mathcal{D}_{\text{phys}}$ in Example 5.4.2. We have that the divisor

$$\mathcal{D} = \{e_0^2 e_1 t(v - 2w) + s(v + w)(v - w) = 0\}_{\mathcal{B}} \quad (5.4.40)$$

in \mathcal{B} restricts to the base $B_{\tilde{u}}$ of all elements of the degeneration such that $\mathcal{D}|_{B_{\tilde{u}}} \subset \Delta'|_{B_{\tilde{u}}}$, and in particular

$$\begin{aligned} \mathcal{D}_{\text{phys}} = \mathcal{D}|_{\tilde{\mathcal{U}}} &= \{e_0^2 e_1 t(v - 2w) + s(v + w)(v - w) = 0\}_{B_0} \\ &= (\{v + w = 0\}_{Y^0} \cup \{v - w = 0\}_{Y^0}) \\ &\quad \cup (\{v + w = 0\}_{Y^1} \cup \{v - w = 0\}_{Y^1}) \\ &\quad \cup (\{e_1(v - 2w) + s(v + w)(v - w) = 0\}_{Y^2}) = \mathcal{D}_0 \cup \mathcal{D}_1 \cup \mathcal{D}_2, \end{aligned} \quad (5.4.41)$$

with the factorization

$$\Delta_{\text{phys}} = \Delta'|_{\tilde{\mathcal{U}}} = 3\mathcal{D}|_{\tilde{\mathcal{U}}} + \Delta''|_{\tilde{\mathcal{U}}} = \sum_{p=0}^2 (3\mathcal{D}_p + \Delta''_p) = \sum_{p=0}^2 \Delta'_p. \quad (5.4.42)$$

When the finite-distance tuning necessary to produce a certain gauge enhancement takes place at the same time as the infinite-distance limit is taken, it may occur that the factorization of the corresponding $\mathcal{D}_{\text{phys}}$ divisor in Δ_{phys} is not immediately apparent unless we factorize up to terms proportional to \tilde{u} , see (5.4.39), as we now show in a concrete example.

Example 5.4.3. Consider the family variety $\hat{\mathcal{Y}}$ with base $\hat{\mathcal{B}} = \mathbb{F}_1 \times D$ given by the Weierstrass model with defining polynomials

$$f = s^3 t^3 v (s^2 u v^8 + s t w^4 (u w^3 + v^3 + v^2 w + v w^2) + t^2 u w^4 (v^2 + v w + w^2)) , \quad (5.4.43a)$$

$$g = s^4 t^5 v^2 w^5 (s^3 v w^5 + s^2 t v^2 (v + w) (v^2 + w^2) + 2 s t^2 u v (v + w) (v^2 + w^2) + t^3 u^2 (v + w) (v^2 + w^2)) , \quad (5.4.43b)$$

$$\Delta = s^8 t^9 v^3 p_{7,24}([s : t], [v : w], u) . \quad (5.4.43c)$$

This model is only a minor modification of Example 5.4.1, and we therefore do not analyse it fully. The difference between the two is that in the present model the finite-distance (1, 2, 3) enhancement over $\mathcal{D}_{\text{phys}} := \{t e_0 + s v = 0\}_{B_0}$ is not present for the generic fibers of the degeneration; it only occurs at the endpoint of the limit. The open-chain resolution is given by the defining polynomials

$$f = s^3 t^3 v (e_0 e_1^2 s^2 v^8 + t w^4 (v^2 + v w + w^2) (e_0 t + s v) + e_0 e_1 s t w^7) , \quad (5.4.44a)$$

$$g = s^4 t^5 v^2 w^5 (e_1 s^3 v w^5 + t (v + w) (v^2 + w^2) (e_0 t + s v)^2) , \quad (5.4.44b)$$

$$\Delta = s^8 t^9 v^3 p_{7,24,4}([s : t], [v : w], [s : e_0 : e_1]) . \quad (5.4.44c)$$

One thing that can be noted from this model and its cousin Example 5.4.1 is that their restrictions to the components $\{B^p\}_{0 \leq p \leq 3}$ coincide, showing that the finite-distance deviation from one another associated to the tuning over $\mathcal{D}_{\text{phys}}$ does not alter the endpoint of the limit.

Considering the local analysis performed in Example 5.4.1, we expect $\mathcal{D}_{\text{phys}}$ to factorize with multiplicities one and two in f_{phys} and g_{phys} , respectively. Computing the restriction

$$f|_{e_0 e_1 = 0} = s^3 t^4 v w^4 (t e_0 + s v) (v^2 + v w + w^2) , \quad (5.4.45)$$

the factorization of $p_{\mathcal{D}_{\text{phys}}}$ is indeed explicit. Computing the same restriction for g , however, leads to

$$g|_{e_0 e_1 = 0} = g , \quad (5.4.46)$$

for which the expected factorization of $p_{\mathcal{D}_{\text{phys}}}^2$ is not apparent. Note that to obtain the restriction $g|_{e_0 e_1 = 0}$ we only set to zero those monomials that contain powers of $\tilde{u} = e_0 e_1$, rather than just individual powers of e_0 or e_1 . The same is true for $\Delta'|_{e_0 e_1 = 0}$, where we do not observe $p_{\mathcal{D}_{\text{phys}}}^3$ factorizing. However, recalling that the factorization needs to occur up to terms proportional to $\tilde{u} = e_0 e_1$, we can perform the division of polynomials

$$g|_{e_0 e_1 = 0} = (t e_0 + s v)^2 q + r , \quad (5.4.47)$$

finding that

$$r = e_0^2 e_1 s^4 t^7 w^{10} (2 e_0 t + 3 s v) , \quad (5.4.48)$$

so that $r|_{e_0 e_1 = 0} = 0$ and indeed the factorization goes through.

After these considerations, we now define the objects f_{phys} , g_{phys} and Δ_{phys} more precisely. The reader only interested in the practical use of f_{phys} , g_{phys} and Δ_{phys} can safely skip to Section 5.4.4. Before we delve into the discussion, and since we are phrasing it in the context in which \mathcal{B} has a global description as a toric variety in terms of the homogeneous coordinates, let us recall the definition of the homogeneous coordinate ring of a toric variety (see, e.g., [327]).

Definition 5.4.4. The homogeneous coordinate ring of a toric variety X defined by the toric fan Σ_X is

$$S_X := \mathbb{C} [x_\rho \mid \rho \in \Sigma_X(1)] . \quad (5.4.49)$$

For each cone $\sigma \in \Sigma$, define the monomial

$$x^\sigma = \prod_{\rho \notin \sigma(1)} x_\rho . \quad (5.4.50)$$

The irrelevant ideal of X is defined to be

$$B_X := \langle x^\sigma \mid \sigma \in \Sigma_X \rangle = \langle x^\sigma \mid \sigma \in \Sigma_X^{\max} \rangle \subseteq S_X , \quad (5.4.51)$$

where Σ_X^{\max} is the set of maximal cones of Σ_X .

The vanishing locus of $V(B_X) \subseteq \mathbb{C}^{\Sigma_X(1)}$ is the exceptional set of the quotient construction of the toric variety.

The homogeneous coordinate ring of a toric variety, introduced by Cox in [328], is the analogue in the toric context of the homogeneous coordinate ring of projective varieties, which is the object we would need to use if we phrased the discussion in that language. Cox's notion has been generalized to that of the total coordinate ring, which applies more generally.

Definition 5.4.5. Let X be a normal projective variety with divisor class group $\text{Cl}(X)$, and assume that $\text{Cl}(X)$ is a finitely generated free abelian group. The total coordinate ring or Cox ring of X is

$$\text{TC}(X) := \bigoplus_D H^0(X, \mathcal{O}_X(D)) , \quad (5.4.52)$$

where the sum is over all Weil divisors contained in a fixed complete system of representatives of $\text{Cl}(X)$.

Note that nowadays, the homogeneous coordinate ring of a toric variety is usually called total coordinate ring, since it is a particular example of this notion.

The ideal-variety correspondence of affine and projective algebraic varieties goes through for toric varieties when we use the total coordinate ring.

Proposition 5.4.6. *Let X be a simplicial toric variety associated with the fan Σ_X . Then there is a bijective correspondence [327]*

$$\{ \text{closed subvarieties of } X \} \longleftrightarrow \{ \text{radical homogeneous ideals } I \subseteq B_X \subseteq S_X \} . \quad (5.4.53)$$

With this in mind, we see that the physical defining polynomials f_{phys} , g_{phys} and Δ_{phys} are defined in the following way.

Definition 5.4.7 (Physical defining polynomials). Let B_0 be the base central fiber of a resolved degeneration $\rho : \mathcal{Y} \rightarrow D$ in which \mathcal{B} has homogeneous coordinate ring $S_{\mathcal{B}}$. Consider the homogeneous ideal

$$I_{\tilde{\mathcal{U}}} := \langle e_0 \cdots e_P \rangle \trianglelefteq S_{\mathcal{B}} , \quad (5.4.54)$$

whose vanishing locus corresponds to B_0 . The physical defining polynomials f_{phys} , g_{phys} and Δ_{phys} , whose vanishing loci represent $F|_{\tilde{\mathcal{U}}}$, $G|_{\tilde{\mathcal{U}}}$ and $\Delta'|_{\tilde{\mathcal{U}}}$, respectively, are

$$f_{\text{phys}} := f + I_{\tilde{\mathcal{U}}} , \quad g_{\text{phys}} := g + I_{\tilde{\mathcal{U}}} , \quad \Delta_{\text{phys}} := \Delta' + I_{\tilde{\mathcal{U}}} , \quad (5.4.55)$$

where $f_{\text{phys}}, g_{\text{phys}}, \Delta_{\text{phys}} \in S_{\mathcal{B}}/I_{\tilde{\mathcal{U}}}$.

From these, we obtain the physical vanishing orders used above as the appropriate vanishing orders in the global analysis of the central fiber Y_0 .

Definition 5.4.8 (Physical vanishing orders). Let $C = \{p_C = 0\} \subset B_0$ be a curve in the central fiber of a resolved degeneration $\rho : \mathcal{Y} \rightarrow D$ with base components $\{B^p\}_{0 \leq p \leq P}$ and such that at least one of the restrictions $\{C|_{B^p}\}_{0 \leq p \leq P}$ is a single irreducible curve. Let α, β and γ be

$$\alpha := \max \{i \in \mathbb{Z}_{\geq 0} \mid \langle f_{\text{phys}} \rangle \trianglelefteq \langle p_C^i \rangle\}, \quad (5.4.56a)$$

$$\beta := \max \{j \in \mathbb{Z}_{\geq 0} \mid \langle g_{\text{phys}} \rangle \trianglelefteq \langle p_C^j \rangle\}, \quad (5.4.56b)$$

$$\gamma := \max \{k \in \mathbb{Z}_{\geq 0} \mid \langle \Delta_{\text{phys}} \rangle \trianglelefteq \langle p_C^k \rangle\}. \quad (5.4.56c)$$

We define the physical vanishing orders over C , denoted by $\text{ord}_{Y_0}(f_{\text{phys}}, g_{\text{phys}}, \Delta_{\text{phys}})_C$, to be

$$\text{ord}_{Y_0}(f_{\text{phys}}, g_{\text{phys}}, \Delta_{\text{phys}})_C := (\alpha, \beta, \gamma). \quad (5.4.57)$$

We can now see how the need to be more cautious during the factorization process, as in Example 5.4.3, arises when we consider the multi-component central fiber B_0 , but not when we consider the base family variety \mathcal{B} or the individual base components $\{B^p\}_{0 \leq p \leq P}$. Under the ideal-variety correspondence, irreducible subvarieties are associated with prime ideals. If the homogeneous coordinate ring of the variety is a GCD domain (hence, in particular, in a unique factorization domain), the notions of prime and irreducible element coincide. When we factorize the discriminant polynomial into irreducible polynomials to determine the prime divisors supporting the non-abelian gauge algebra, we are making use of this fact.²⁰ This works well for \mathcal{B} and $\{B^p\}_{0 \leq p \leq P}$ because their homogeneous coordinate rings are unique factorization domains, as can be deduced from the following result concerning the total coordinate ring [329].

Theorem 5.4.9. *The total coordinate ring of a connected normal Noetherian scheme whose divisor class group is a finitely generated free abelian group is a unique factorization domain.*

For a smooth, and hence locally factorial, variety X we have $\text{Pic}(X) \cong \text{Cl}(X)$, which applies to \mathcal{B} and $\{B^p\}_{0 \leq p \leq P}$. The $\{B^p\}_{0 \leq p \leq P}$ surfaces are either \mathbb{P}^2 , \mathbb{F}_n or a blow-ups thereof, for which $\text{Pic}(X)$ is a finitely generated free abelian group. \mathcal{B} is the blow-up of $\hat{\mathcal{B}} = B \times D$, with B one of the previously listed surfaces, and since $\text{Cl}(B \times \mathbb{A}^1) \cong \text{Cl}(B)$ the result applies as well.

Hence, when we use the restrictions $\{f_p, g_p, \Delta'_p\}_{0 \leq p \leq P}$ to compute the component vanishing orders, we are taking the image of the defining polynomials f, g and Δ' of the elliptic fibration over \mathcal{B} under the ring homomorphism

$$\begin{aligned} \phi_p : S_{\mathcal{B}} &\longrightarrow S_{B^p} \cong S_{\mathcal{B}}/\langle e_p \rangle \\ p &\longmapsto p + \langle e_p \rangle, \end{aligned} \quad (5.4.58)$$

choosing $p|_{e_p=0}$ as a concrete representative of $p + \langle e_p \rangle$. The homogeneous ideal $\langle e_p \rangle \trianglelefteq S_{\mathcal{B}}$, its vanishing locus corresponding to the irreducible subvariety B^p of \mathcal{B} , is a prime ideal, and S_{B^p} is a unique factorization domain. Hence, S_{B^p} is in particular an integral domain, where the notion of irreducible element is well-defined; the representative $p|_{e_p=0}$ is as good as any other to judge this property.

²⁰More precisely, we are performing the primary decomposition of the ideal generated by the discriminant polynomial. Primary ideals are powers of prime ideals, leading to the same vanishing locus but containing the multiplicity information necessary to determine the gauge algebra.

For the base central fiber B_0 the situation is different because it is a reducible surface, meaning that the homogeneous ideal $I_{\tilde{\mathcal{U}}} \trianglelefteq S_{\mathcal{B}}$ is not a prime ideal. In fact, its primary decomposition is

$$I_{\tilde{\mathcal{U}}} = \langle e_0 \cdots e_P \rangle = \langle e_0 \rangle \cap \cdots \cap \langle e_P \rangle. \quad (5.4.59)$$

The physical polynomials f_{phys} , g_{phys} and Δ_{phys} of Definition 5.4.7 are the images of f , g and Δ' under the ring homomorphism

$$\begin{aligned} \phi : S_{\mathcal{B}} &\longrightarrow S_{\mathcal{B}}/I_{\tilde{\mathcal{U}}} \\ p &\longmapsto p + I_{\tilde{\mathcal{U}}}. \end{aligned} \quad (5.4.60)$$

Since $I_{\tilde{\mathcal{U}}}$ is not a prime ideal, the quotient $S_{\mathcal{B}}/I_{\tilde{\mathcal{U}}}$ is not an integral domain. It is this ring in which the factorisation of the physical defining polynomials takes place. However, the behaviour of polynomial factorisation in rings with zero divisors is vastly different from the one in integral domains. In fact, there are four different notions of irreducible element that one can define, which all coincide for integral domains. We do not delve into this topic further, providing only a small collection of relevant facts alongside useful references in Appendix B.8. For our purposes, it suffices to note that the image of $\phi : S_{\mathcal{B}} \longrightarrow S_{\mathcal{B}}/I_{\tilde{\mathcal{U}}}$ captures the same information as taking the restrictions into all individual components into account together, i.e. consistently gluing together the irreducible components of the $\{\Delta'_p\}_{0 \leq p \leq P}$ as explained earlier in the section. This follows from the fact that the ring homomorphism

$$\begin{aligned} \psi : S_{\mathcal{B}} &\longrightarrow S_{B^0} \times \cdots \times S_{B^P} \\ p &\longmapsto (p + \langle e_0 \rangle, \dots, p + \langle e_P \rangle) \end{aligned} \quad (5.4.61)$$

is not surjective, since the ideals $\langle e_p \rangle$ and $\langle e_q \rangle$ are not coprime for all $p \neq q$. The First Isomorphism Theorem²¹ then establishes, since $\text{Ker}(\psi) = \bigcap_{p=0}^P \langle e_p \rangle$, that $\phi(S_{\mathcal{B}}) = S_{\mathcal{B}}/I_{\tilde{\mathcal{U}}} \cong \psi(S_{\mathcal{B}})$. One can, as a consequence, conclude that being able to factorise the defining polynomial of a curve $C = \{p_C = 0\}_{B_0}$ from Δ_{phys} is equivalent to being able to factorise its restrictions $\{p_C|_{e_p=0}\}_{0 \leq p \leq P}$ from all the $\{\Delta'_p\}_{0 \leq p \leq P}$, as one would intuitively expect.

Proposition 5.4.10. *With the notation used above, we have that*

$$p + I_{\tilde{\mathcal{U}}} \mid \Delta_{\text{phys}} \Leftrightarrow p + \langle e_p \rangle \mid \Delta' + \langle e_p \rangle, \quad \forall p = 0, \dots, P. \quad (5.4.62)$$

Proof. Consider the ring homomorphism

$$\begin{aligned} \tilde{\phi} : S_{\mathcal{B}}/I_{\tilde{\mathcal{U}}} &\longrightarrow (S_{\mathcal{B}}/I_{\tilde{\mathcal{U}}})/(\langle e_p \rangle/I_{\tilde{\mathcal{U}}}) \cong S_{B^p} \\ p + I_{\tilde{\mathcal{U}}} &\longmapsto p + \langle e_p \rangle, \end{aligned} \quad (5.4.63)$$

where we have used the Third Isomorphism Theorem. It is then clear that

$$p + I_{\tilde{\mathcal{U}}} \mid \Delta_{\text{phys}} \Rightarrow \tilde{\phi}(p + I_{\tilde{\mathcal{U}}}) \mid \tilde{\phi}(\Delta_{\text{phys}}) \Rightarrow p + \langle e_p \rangle \mid \Delta' + \langle e_p \rangle. \quad (5.4.64)$$

Conversely, consider that $p + \langle e_p \rangle \mid \Delta' + \langle e_p \rangle, \forall p = 0, \dots, P$. This implies that

$$\langle \Delta' + \langle e_p \rangle \rangle \trianglelefteq \langle p + \langle e_p \rangle \rangle, \quad \forall p = 0, \dots, P. \quad (5.4.65)$$

Then, in the product ring $S_{B^0} \times \cdots \times S_{B^P}$ we have

$$\langle \Delta' + \langle e_0 \rangle \rangle \times \cdots \times \langle \Delta' + \langle e_P \rangle \rangle \trianglelefteq \langle p + \langle e_0 \rangle \rangle \times \cdots \times \langle p + \langle e_P \rangle \rangle. \quad (5.4.66)$$

²¹We follow the numbering of [330] for the isomorphism theorems.

But note that these product ideals are in the image of $\psi : S_{\mathcal{B}} \longrightarrow S_{B^0} \times \cdots \times S_{B^P}$, and since $\phi(S_{\mathcal{B}}) = S_{\mathcal{B}}/I_{\tilde{\mathcal{U}}} \cong \psi(S_{\mathcal{B}})$ we have that

$$\psi(\Delta') \trianglelefteq \psi(p) \Leftrightarrow \langle \Delta_{\text{phys}} \rangle \trianglelefteq \langle p + I_{\tilde{\mathcal{U}}} \rangle \Leftrightarrow p + I_{\tilde{\mathcal{U}}} \mid \Delta_{\text{phys}}. \quad (5.4.67)$$

□

This also shows that the subtleties in the factorization process highlighted in Example 5.4.3 only arise for divisors that extend between components, while, e.g. the strict transform of the original $(-n)$ -curve in a single infinite-distance limit horizontal model is not subject to them. In particular, this is true for all divisors appearing in the study of infinite-distance limits in the complex structure moduli space of eight-dimensional F-theory [156, 157], which are all points completely contained in a component.

5.4.4 Monodromy cover

At the beginning of Section 5.4, we recalled how non-abelian gauge algebras in F-theory arise from M2-branes wrapping the exceptional curves of the resolved fiber supported over the generic points of a given divisor, see Section 5.2.2.2 for their determination. The intersection matrix of the exceptional curves reproduces the Cartan matrix of the associated simply-laced Lie algebra, and the exceptional curves themselves correspond to the nodes of the appropriate ADE Dynkin diagram.²² In eight-dimensional F-theory, this local analysis of the resolved elliptic fiber determines the gauge algebra associated to the divisor.

In F-theory models in six dimensions or fewer, global effects along the discriminant locus can modify this picture. Namely, the components of the resolved fiber may undergo monodromies that establish identifications among them; this corresponds to folding the ADE Dynkin diagram, meaning that non-simply-laced Lie algebras can arise as well. If this occurs or not can actually be determined directly in the singular Weierstrass model through Tate's algorithm [189], discussed in the context of F-theory in [190–192].

Following the explanation of Tate's algorithm in [192], the monodromy can be described by means of a monodromy cover of the discriminant component under study. In practical terms, one studies a degree two or three polynomial involving an auxiliary variable, which is a meromorphic section of an appropriate line bundle over the discriminant component; the factorization properties of this polynomial inform us about the number of irreducible components of the monodromy cover, with the irreducible case indicating a folding of the ADE Dynkin diagram. Said polynomials are tabulated in [192].

As we have seen above, the gauge algebra information contained in the central fiber Y_0 of a resolved degeneration $\rho : \mathcal{Y} \rightarrow D$ is extracted by studying the irreducible components of $\{\Delta'\}_{0 \leq p \leq P}$ consistently glued along the base components $\{B^p\}_{0 \leq p \leq P}$. One such consistent gluing supporting a non-abelian gauge algebra factor corresponds to the factorizations of (the defining polynomial of) a divisor $\mathcal{D}_{\text{phys}}$ in the physical discriminant Δ_{phys} . Since the gauge algebra is associated to $\mathcal{D}_{\text{phys}}$ taken as a whole, rather than to individual components that could suffer local gauge enhancements, a reduction of the gauge rank in a given component B^p affects the gauge algebra globally read for $\mathcal{D}_{\text{phys}}$. Hence, we study the monodromy cover in the conventional way for each of the irreducible components of $\{\mathcal{D}_{\text{phys}}|_{B^p}\}_{0 \leq p \leq P}$. If we find that it is irreducible in one component, we have a monodromy action locally folding the Dynkin diagram and the

²²More precisely, the components of the fiber correspond to an affine ADE Dynkin diagram, with the additional node given by the fibral component intersecting the section of the fibration.

gauge rank associated to $\mathcal{D}_{\text{phys}}$ is reduced. If, on the contrary, the monodromy cover is split in all components, then it is split globally, and we assign to $\mathcal{D}_{\text{phys}}$ the gauge algebra corresponding to the unfolded Dynkin diagram.

5.4.5 Algorithm to read off the codimension-one gauge algebra

Summarizing the discussion of this section, let us give a practical algorithm to read the gauge algebra associated to the central fiber of a degeneration $\hat{\rho} : \hat{\mathcal{Y}} \rightarrow D$.

1. Follow the procedures described in Section 5.2 to arrive at a resolved degeneration $\rho : \mathcal{Y} \rightarrow D$ free of obscured infinite-distance limits.
2. Compute the restrictions (f_p, g_p, Δ'_p) of the defining polynomials and the modified discriminant. List the irreducible components $\{\Delta'_{p,i_p}\}_{0 \leq i_p \leq I_p}$ for each of the component discriminants $\{\Delta'_p\}_{0 \leq p \leq P}$.
3. Consistently glue the $\{\Delta'_{p,i_p}\}_{0 \leq p \leq P}^{0 \leq i_p \leq I_p}$ together into global divisors Δ_{phys}^i of B_0 appearing as factors of Δ_{phys} . If a local irreducible divisor has $\Delta'_{p,i_p} \cdot E_q|_{E_p} = 0$ for all $p \neq q \in \{0, \dots, P\}$, it does not extend to the adjacent components and directly captures the global information.
4. Compute the physical vanishing orders $\text{ord}_{Y_0}(f_{\text{phys}}, g_{\text{phys}}, \Delta_{\text{phys}})_{\Delta_{\text{phys}}^i}$ to determine from the Kodaira-Néron classification the simply-laced covering gauge algebra $\tilde{\mathfrak{g}}_i$ supported on the global divisor Δ_{phys}^i .
5. Determine the splitting properties of the monodromy covers associated to the restrictions $\{\Delta_{\text{phys}}^i|_{B_p}\}_{0 \leq p \leq P}$, and assign to Δ_{phys}^i the subalgebra \mathfrak{g}_i of $\tilde{\mathfrak{g}}_i$ left invariant by the collection of inferred outer automorphisms.

We stress again that some of the gauge algebra factors enhance into a higher algebra in the infinite-distance limits which correspond to decompactification limits. The above algebra is hence the algebra prior to taking this effect into account, which will be the subject of Chapter 6.

5.4.6 Special fibers at the intersection of components

The resolved degeneration $\rho : \mathcal{Y} \rightarrow D$ associated with a Class 1–4 degeneration $\hat{\rho} : \hat{\mathcal{Y}} \rightarrow D$ has a central fiber Y_0 in which the generic fibers over the base components $\{B^p\}_{0 \leq p \leq P}$ can only be of Kodaira type I_m . Moreover, two components Y^p and Y^q presenting codimension-zero I_m and $I_{m'}$ fibers, respectively, intersect on an elliptically fibered surface $Y^p \cap Y^q$ with codimension-zero $I_{m''}$ fibers, since intersections of other types would mean that $B^p \cap B^q$ is an obscured Class 5 curve, as discussed in Section 5.2.2.3.

Still within Class 1–4 models, it may occur that $m'' > m + m'$. In this case, the component vanishing orders, computed in the Y^p or the Y^q component, indicate that the curve $B^p \cap B^q$ supports type $I_{m''-m-m'}$ fibers. These special fibers located at the intersection of components make it slightly more ambiguous to determine the gauge algebra content, since they actually do not correspond to gauge enhancements. Let us argue why this is the case and how they can be removed through a series of transformations.

First, the $I_{m''-m-m'}$ fibers over $B^p \cap B^q$ may be found at the level of the components $\{Y^p\}_{0 \leq p \leq P}$, while absent for the family variety. This mismatch between component and family vanishing orders is analysed in our discussion of obscured infinite-distance limits in Appendix B.3;

the two notions of vanishing orders can be made to agree by performing a base change with high enough branching degree.

Let us therefore assume that the family variety \mathcal{Y} also presents $I_{m''-m-m'}$ fibers over the curve $B^p \cap B^q$. By blowing the model down and performing a base change the resolution process demands additional base blow-ups. This gives rise to extra components in the central fiber Y_0 of the resolved degeneration, in which the former special fibers at the intersection of components are now the codimension-zero fibers. Hence, said special fibers did not correspond to information about gauge algebra enhancements, but about the background value of the axio-dilaton, which can be made explicit through an appropriate base change. This does not imply, however, that the new components may not present codimension-one enhancements. The analogous problem for degenerations of eight-dimensional F-theory models was analysed in [156, 157].

A base change with a high enough branching degree can both equate the component and family vanishing orders and remove all special fibers at the intersections of components, leading to a geometrical representative of the central fiber suitable to extract the physical information.

5.5 Summary and future work

In this first part of our analysis of non-minimal elliptic threefolds we have given a geometric account of the degenerations in which a family of Weierstrass fibrations specialises to a model exhibiting non-Kodaira singularities in codimension-one. Such degenerations are of interest because they encode a subclass of infinite-distance limits in the complex structure moduli space of the elliptic threefold. For instance, in F-theory they admit an interpretation as deformations in the non-perturbative open moduli space at infinite distance. The geometry of the degenerations studied in this chapter hence offers an entrance point to understanding the asymptotic physics along such trajectories in the moduli space. We will capitalise on this point of view in the second part of our analysis, see Chapter 6.

Our goal has been to establish a concrete geometric picture of the described complex structure degenerations. To this end, we have studied the resolutions of the infinite-distance degenerations. They give rise, at the endpoint of the limit, to a reducible elliptic threefold free of non-minimalities that consists of intersecting log Calabi-Yau components. More precisely, the central element of the resolved degeneration is an elliptic fibration whose base space factors into, generally, a tree of intersecting surfaces. As we have discussed in detail, for a subclass of non-minimal configurations, the blow-up geometry forms an open chain: This is guaranteed to occur for so-called single infinite-distance limits. In these there are no intersections between different curves supporting non-minimal elliptic fibers, and there are no infinite-distance non-minimal singularities over points in the base. Such degenerations are equivalent, up to base changes and modifications, to configurations with non-minimal fibers over a single curve, which explains their name.

The curves over which non-minimal elliptic fibers can occur are very constrained: They can either be of genus zero or of genus one, and in the latter case they must lie in the anti-canonical class of the base. We have focused in this chapter on the rich class of genus-zero non-minimal curves. For these, the blow-up of the base that removes the non-minimalities gives rise to Hirzebruch surfaces, whose types we have specified.

At a slightly technical level, a special role is played by non-Kodaira singularities which are over-non-minimal, in the sense that the sections f and g of the Weierstrass model both vanish to orders strictly larger than the boundary values 4 and 6, respectively. The blow-ups required to cure these so-called Class 5 singularities (in the terminology of Definition 5.2.5) give rise to degenerations that are not semi-stable. As we have discussed, the Semi-stable Reduction Theorem

hence guarantees that degenerations presenting such singularities can be modified, possibly after a base change, into ones only exhibiting either minimal singularities or non-minimal singularities of Class 1–4. However, finding the required sequence of transformations may be very non-trivial in concrete cases. In [309] we explicitly determine these for non-minimal degenerations of elliptic fibrations over Hirzebruch base spaces. These results are also interesting for the analogous classification of degenerations of elliptic K3 surfaces into Kulikov models: Our analysis in [309] shows that, in such cases, the models presenting Class 5 non-minimalities can always be transformed to give rise to Kulikov models of Kulikov Type I, which lie at finite distance, or their infinite-distance counterparts of Kulikov Type II.a in the notation of [299], but not of Type III. In particular, it is not true that all non-minimal singularities lie at infinite distance—some of the Class 5 singularities are, in fact, equivalent to standard Kodaira singularities, after performing these transformations.

We have seen in this chapter that the non-minimal singularities of elliptic threefolds enjoy a very rich systematics. In fact, there are a number of important questions left for future work: First, it would be desirable to understand non-minimalities over curves in the anti-canonical class in a similarly detailed fashion, expanding on the observations and remarks in this direction made in Section 5.2.7. Second, one should also methodically study degenerations enhancing over the intersection locus of two or several curves. Most interestingly, infinite-distance non-minimal fibers can also occur entirely in such codimension-two loci, i.e. over isolated points on the base. Studying the systematics of their blow-up resolutions is an obvious direction that we are planning to return to in the future.

But even the single infinite-distance limits associated with codimension-one non-minimalities lead to a rather intricate structure, especially once viewed through the lens of F-theory. We have already highlighted subtleties in determining the components of the discriminant locus, which is a prerequisite to identify the gauge algebra of the effective theory. As stressed several times, however, this is only the beginning of a more involved analysis of the asymptotic physics. This analysis is the subject of Chapter 6. Inspired by the analogous problem in [156, 157], we will interpret the factorisation of the compactification space (the central fiber of the resolved degeneration) as indicating that the effective theory generically undergoes a partial decompactification (at least in a dual frame). On top of this, there can occur regions of weak coupling, associated with those components of the base over which the generic elliptic fiber degenerates to a Kodaira type $I_{m>0}$ fiber. In combination, these two effects either result in decompactification or, possibly, global weak coupling limits. This intuition can be made particularly precise for the special subclass of models whose base geometries are Hirzebruch surfaces. The duality with the heterotic string then offers a welcome entrance point to the physics of the infinite-distance limits. Even in this class of models, however, we will find novel effects not present in eight dimensions [156, 157]: The asymptotic theory generally contains defects which break the higher-dimensional Poincaré symmetry. With the exception of those factors localised in the defects, the naive gauge algebra undergoes certain gauge enhancements in the partial decompactification process. The appearance of defects is a slight twist on, but generally in agreement with the Emergent String Conjecture. Similar effects have been observed recently in different setups in [280]. The geometric analysis of non-minimal degenerations hence sheds interesting light on how string theory probes geometry near the boundaries of the moduli space.

Chapter 6

Asymptotic Physics

In this chapter, we interpret infinite-distance limits in the complex structure moduli space of F-theory compactifications to six dimensions in the light of general ideas in quantum gravity. The limits we focus on, which were mathematically studied in Chapter 5, arise from non-minimal singularities in the elliptic fiber over curves in a Hirzebruch surface base, which do not admit a crepant resolution. Such degenerations take place along infinite directions in the non-perturbative brane moduli space in F-theory. A blow-up procedure, detailed generally in Chapter 5, gives rise to an internal space consisting of a union of log Calabi-Yau threefolds glued together along their boundaries. We geometrically classify the resulting configurations for genus-zero single infinite-distance limits. Special emphasis is put on the structure of singular fibers in codimension zero and one. As our main result, we interpret the central fiber of these degenerations as endpoints of a decompactification limit with six-dimensional defects. The conclusions rely on an adiabatic limit to gain information on the asymptotically massless states from the structure of vanishing cycles. We also compare our analysis to the heterotic dual description where available. Our findings are in agreement with general expectations from quantum gravity and provide further evidence for the Emergent String Conjecture. In order to make Chapter 6 accessible without familiarity with the finer details of Chapter 5, we provide a focused summary of the latter in Sections 6.1 and 6.2.2.

6.1 Introduction and summary

In this chapter, we continue the systematic analysis of a large class of infinite-distance degenerations of elliptic Calabi-Yau threefolds and their F-theory interpretation initiated in Chapter 5. The degenerations studied are those in which the threefold develops non-minimal, or non-Kodaira, singularities in the elliptic fiber over loci of complex codimension one in the base of the elliptic fibration. Our interest in these degenerations is largely motivated by the goal to understand asymptotic regions in the moduli spaces of string compactifications which lie at infinite distance. According to general ideas in the Swampland Program of quantum gravity [102, 137–141], near such asymptotic branches infinite towers of states should become light, and the theory should asymptote to a dual description [146]. The towers should furthermore admit an interpretation as Kaluza-Klein towers, possibly in some dual frame, or as excitations of a unique critical and asymptotically weakly coupled string [149]. If true, this Emergent String Conjecture would greatly constrain the moduli space dynamics, at least in all asymptotic regions.

These and related ideas have so far withstood numerous quantitative tests, mostly in the closed string moduli space of Calabi-Yau compactifications. This includes the complex structure

and Kähler moduli space probed by string and M-theory, see for instance [1, 5, 149, 155, 245–248, 252–254, 271, 272, 331]. In the present chapter, we aim to advance our understanding of infinite-distance limits in what to first approximation can be viewed as the open string moduli space. As argued in [156, 157] in the context of F-theory compactifications to eight dimensions, non-compact directions in the open string moduli space occur at the non-perturbative level. Along such non-compact directions, suitable mutually non-local $[p, q]$ 7-branes coalesce. In F-theory on elliptic K3 surfaces, the resulting brane configurations are encoded geometrically in non-Kodaira singularities over points on the rational base. Their study is interesting by itself, which furnishes an independent motivation for the present work.

More precisely, in the complex structure moduli space of elliptic K3 surfaces, any fibral degenerations at infinite distance involve such non-Kodaira fibers in codimension-one and/or minimal Kodaira singularities in codimension-zero. As such, they are classified as Type II and Type III Kulikov models [300, 301, 319, 320], with a more recent refinement as Type II.a, Type II.b, Type III.a and Type III.b [156] (see [303–307] for independent treatments). Furthermore, the physical interpretation of this refinement indeed confirmed the ideas of the Emergent String Conjecture in a non-trivial manner [156, 157], as illustrated in Figure 6.1.

In the first part of the current analysis, contained in Chapter 5, we have provided a classification of the analogous codimension-one non-Kodaira degenerations of elliptic Calabi-Yau threefolds, underlying F-theory compactifications to six dimensions. This geometric analysis is complementary to the Hodge theoretic approach to studying complex structure degenerations of Calabi-Yau varieties, explored in [252–254] in the context of string theory. A succinct summary of Chapter 5, focusing on so-called single infinite-distance limits, will be provided in Section 6.2.2. The goal of the present chapter is to interpret these geometric results from the physics point of view. As we will see, the situation is considerably richer compared with the degenerations of elliptic K3 surfaces. Our strategy will therefore be to focus on a favourable corner of the moduli space, where a particularly clear picture emerges.

Specifically, the main part of our analysis is devoted to what we call horizontal models. The base of the degenerating elliptic fibration is taken to be a Hirzebruch surface \mathbb{F}_n , which is, topologically, a fibration of a rational curve \mathbb{P}_f^1 over a rational base \mathbb{P}_b^1 . Consequently, the threefold admits a fibration by K3 surfaces over \mathbb{P}_b^1 . This allows us to leverage, in favourable cases, the insights gained in [156, 157] on the degenerations of K3 surfaces. Such favourable cases include the horizontal models, where the non-minimal fibers are engineered to appear over certain section divisors of the base \mathbb{F}_n . After performing a suitable chain of blow-ups and line bundle shifts in order to resolve the degeneration, as described generally in Chapter 5, the endpoint of the limit is described by a Calabi-Yau threefold free of non-minimal singularities in codimension one. Its base is an open chain of surfaces B^p , each of which has the topology of an \mathbb{F}_n surface. It is furthermore guaranteed that the elliptic fiber can degenerate at worst to a Kodaira type $I_{n_p \geq 0}$ fiber over the generic points of each base component B^p . Those components B^p for which $n_p > 0$ represent a local region of asymptotic weak coupling in F-theory, while in those for which $n_p = 0$ the physics remains strongly coupled. The infinite-distance limits that we take lead to consistent patchings of these so-called log Calabi-Yau spaces. The resulting asymptotic physics is encoded both in the nature of the codimension-zero fibers of the different log Calabi-Yau spaces, and in the way how the 7-branes extend through the intersection loci between them. The degeneration furthermore turns out to be responsible for the appearance of asymptotically massless particle towers.

Our first task is to classify the patterns of generic I_{n_p} fibers that can appear at the endpoints of the limits. The resulting models are found to fall into four classes, examples of which can also

be obtained by fibering the four types of refined Kulikov models for elliptic K3 surfaces over the base of the original \mathbb{F}_n surface. They are the following:

- **Type II.a model:** There are at least two components and all $n_p = 0$, such that the physics is globally at strong coupling.
- **Type II.b model:** There is a single component with $n_0 > 0$; the models of this type are a bit of an outlier and correspond to global Type IIB orientifold limits.
- **Type III.a model:** There are at least two components, with $n_p = 0$ for one or both end-components and $n_p > 0$ for the intermediate components, so that weak and strong coupling regions are mixed at the global level.
- **Type III.b model:** There are at least two components and all $n_p > 0$, such that the physics is globally at weak coupling; as we explain, such limits are only possible for models constructed over \mathbb{F}_n with $0 \leq n \leq 4$.

Apart from the structure of codimension-zero fibers over the base components, we must also account for the types of divisors wrapped by 7-branes in the open-chain formed by them. According to their position with respect to the rational fibration of the base, we distinguish between horizontal, vertical and mixed divisors. Horizontal branes are the direct analogue of the 7-branes in the eight-dimensional degenerations of [156, 157], while the most interesting new effects of the degenerations of threefolds are associated with the vertical branes. Before coming to their interpretation in the infinite-distance limits, we first find general constraints on the patterns of enhancements that can occur, and in particular establish bounds on the rank of the gauge algebra supported on the vertical divisors.

With this geometric understanding at our disposal, we approach the interpretation of the infinite-distance limits, beginning with the horizontal Type II.a models. To retain control, we first take an adiabatic limit, in which the base curve \mathbb{P}_b^1 is taken to be asymptotically large. This regime in the moduli space affords us a clear geometric picture of the degenerating cycles in the infinite-distance limit, and also allows us to compare our conclusions to the heterotic dual side. Over a generic point on \mathbb{P}_b^1 , one can locally define two vanishing 2-cycles of the topology of a torus, as in the eight-dimensional analysis of [156, 157]. In the M-theory picture, two towers of asymptotically massless states arise from M2-branes wrapped multiple times around these local 2-cycles. By comparison with the heterotic dual, we can identify these as Kaluza-Klein towers of a decompactification limit. More precisely, the heterotic dual is defined on an elliptic K3 surface which undergoes an adiabatic decompactification limit of large generic fiber with $\mathcal{V}_{\mathbb{P}_b^1} \gg \mathcal{V}_{T_{\text{het}}^2} \rightarrow \infty$. The two towers associated with the locally defined vanishing 2-cycles on the F-theory side map to the two Kaluza-Klein towers along the decompactifying heterotic torus. However, unlike for the simpler eight-dimensional models, these towers are not globally well-defined because the construction of the two-cycles breaks down over special points on \mathbb{P}_b^1 . These special points include, in particular, the location of vertical 7-branes. Our interpretation is that these vertical branes do not participate in the decompactification process, but remain as six-dimensional defects. In the adiabatic limit of large \mathbb{P}_b^1 , these defects can be thought of as being pushed to infinity so that we end up with a decompactification to ten dimensions with six-dimensional defects. As noted above, the total rank of the defect algebras is bounded, unlike in generic theories with lower-dimensional defects. This reflects the special status of the asymptotic theories as decompactification limits of lower-dimensional ones, which have to obey more stringent quantum gravity bounds on the ranks of the allowed gauge algebras.

On the dual heterotic side, the vertical branes map to non-perturbative gauge sectors which are localised at the geometric singularities of the heterotic K3 surface probed by point-like instantons with discrete holonomy. We explain this phenomenon, which is interesting by itself, in a separate appendix.

Away from the adiabatic regime, the two (dual) Kaluza-Klein towers associated with the locally defined 2-cycles reorganise in a complicated manner, which reflects the fact that the globally defined objects degenerating in the infinite-distance limits are 3-cycles. We argue that, on the heterotic side, departure from adiabaticity still leads to a decompactification limit to ten dimensions. While this constitutes no proof, we take it nonetheless as pointing towards a ten-dimensional decompactification also on the F-theory side. An independent identification of the towers away from the adiabatic regime remains as a challenge, but our analysis confirms that, at least modulo the assumption of adiabaticity, the towers indeed admit an interpretation as Kaluza-Klein towers, as postulated by the Emergent String Conjecture.

The analysis can be carried out in a very similar fashion for horizontal Type III.a models, which contain both weak and strong coupling regions. In the adiabatic regime, we propose a decompactification to nine dimensions, together with lower-dimensional defects. The remaining horizontal limits are found to be all weak coupling limits, possibly superimposed with a decompactification limit.

Finally, in addition to the horizontal models, there exist three more types of genus-zero single infinite-distance limit degenerations of Hirzebruch models, see Definition 5.3.2. Two of them admit a straightforward generalisation of the adiabatic analysis, with a corresponding physical interpretation.

The chapter is organised as follows. We begin, in Section 6.2, with a review of the four types of Kulikov models for elliptic K3 surfaces. We also briefly summarise the main results of the geometric analysis of the analogous non-minimal degenerations of elliptic Calabi-Yau threefolds carried out in Chapter 5. In Section 6.3, we then elaborate on the geometry of what we call horizontal models over Hirzebruch base spaces. This includes a derivation of rank bounds for the gauge algebras supported on vertical branes. Various technical details are relegated to Appendices B.9 to B.11. The interpretation of horizontal Type II.a models as decompactification limits and their dual heterotic interpretation is the subject of Section 6.4. As a spin-off of our analysis of the defects, we elaborate on the heterotic dual interpretation of vertical gauge algebras as non-perturbative heterotic gauge theories at the location of ADE singularities probed by point-like instantons with discrete holonomy. We include this analysis in Appendix B.12. In Section 6.5 we generalise our interpretation of the infinite-distance limits to horizontal Type III.a models, as well as the globally weakly coupled Type II.b models and Type III.b models. Their relation to perturbative Type IIB orientifold limits is analysed in Appendix B.13. Generalisations to genus-zero single infinite-distance limits that are not of horizontal type are the subject of Appendix B.14. Section 6.6 contains our conclusions and points out avenues for future studies.

6.2 Review: Complex structure degenerations in F-theory

Our study of open-moduli infinite-distance limits in six-dimensional F-theory will make frequent use of the results obtained in [156, 157] for the analogous problem in eight dimensions. We therefore briefly recall, in Section 6.2.1, the main conclusions of [156, 157]. This is followed, in Section 6.2.2, by a succinct summary of key results on the degenerations of elliptic Calabi-Yau threefolds in the language of Chapter 5.

To set notation, let us recall that an elliptic fibration $\pi : Y \rightarrow B$ can be described in terms of a Weierstrass model

$$y^2 = x^3 + fxz^4 + gz^6. \quad (6.2.1)$$

Here $[x : y : z]$ are homogenous coordinates in the weighted projective space \mathbb{P}_{231} , which is the ambient space of the elliptic fiber cut out by the hypersurface (6.2.1). Furthermore, the defining polynomials f and g depend on the coordinates on the base B of the fibration. When the vanishing orders of f, g and of the discriminant

$$\Delta = 4f^3 + 27g^2 \quad (6.2.2)$$

at a locus D exceed the Kodaira bound,

$$\text{ord}_Y(f, g, \Delta)_D \geq (4, 6, 12), \quad (6.2.3)$$

the resulting singularity in the elliptic fibers over D is called non-minimal. Below this bound, the singularities give rise to degenerate elliptic fibers classified, for surfaces, by Kodaira and Néron. In F-theory, the vanishing locus of the discriminant Δ on the base is interpreted as the location of 7-branes. The non-abelian gauge algebra can be read off from the Kodaira type of the degenerate fibers. For more details on elliptic fibrations and their appearance in F-theory we refer to the review [185] and references therein.

6.2.1 Degenerations of elliptic K3 surfaces

For F-theory compactified to eight dimensions, the elliptically fibered internal space is an elliptic K3 surface with base $B = \mathbb{P}^1$. The infinite-distance limits in the open string moduli space¹ of 7-branes are encoded in the complex structure deformations of the elliptic K3 surface at infinite distance. For simplicity, we focus on degenerations described by a single complex parameter $u \in D$, with $D \subset \mathbb{C}$ an open disk. Our starting point is a family of Weierstrass models $\hat{\mathcal{Y}}$, whose elements \hat{Y}_u are Weierstrass models over the base \mathbb{P}^1 . The central element \hat{Y}_0 of the family, located at $u = 0$, is a Weierstrass model with certain degenerations. These include, in particular, the non-minimal fibral singularities (6.2.3) over points on the base. Possibly after performing a base change $u \mapsto u^k$, with $k \in \mathbb{Z}_{\geq 1}$, one can find a birational transformation to a related² family of Weierstrass models, that we denote \mathcal{Y} , whose central element Y_0 is free of infinite-distance non-minimal singularities. After resolving the remaining Kodaira fibral singularities, one arrives at a family \mathcal{X} of smooth K3 surfaces X_u whose central element is reduced with local normal crossings,

$$X_0 = \bigcup_{p=0}^P X^p, \quad (6.2.4)$$

with a very complete description of the possible types of central fiber available [300–302]. The resulting so-called Kulikov models are classified into Type I, Type II and Type III. Models of Type I correspond to finite-distance degenerations, and their central fiber X_0 is a smooth, irreducible variety. Type II and III models constitute the complex structure infinite-distance limits studied in [156, 157].

¹Throughout this text we use this term despite the fact that in non-perturbative string theory the open and closed moduli spaces are, of course, not clearly distinguishable.

²More precisely, the original degeneration $\hat{\rho} : \hat{\mathcal{Y}} \rightarrow D$ and the resolved degeneration $\rho : \mathcal{Y} \rightarrow D$ are equivalent, representing the same limit of algebraic varieties but with different geometrical representatives for its endpoint, see Section 5.2.1.

We are mostly interested in the family \mathcal{Y} of Kulikov Weierstrass models Y_u , whose geometry and associated physics we describe below. By slight abuse of nomenclature, we refer to these as Kulikov models as well.

Before doing so, let us denote the two independent 1-cycles of an elliptic curve \mathcal{E} by $\sigma_i \in H_1(\mathcal{E}, \mathbb{Z})$, for $i = 1, 2$. If \mathcal{E} is the elliptic fiber of the central element Y_0 of a Kulikov Weierstrass model, σ_1 and σ_2 will be trivial in $H_1(Y_0, \mathbb{Z}) = 0$. However, in Y_0 the base of the elliptic K3 surface degenerates into an open chain³

$$B_0 = \bigcup_{p=0}^P B^p \quad (6.2.5)$$

of \mathbb{P}^1 curves intersecting at points. The presence of 7-branes in this chain allows us to define a 1-chain Σ on B_0 that cannot be slipped off into triviality. Fibering σ_i over Σ we obtain a non-trivial 2-cycle $\gamma_i \in H_2(Y_0, \mathbb{Z})$ of the topology of a torus that we will often reference in the remainder of the text.

The geometry and physics of Type II and Type III Kulikov models is reviewed below, and succinctly summarised in Figure 6.1.

Type II.a Kulikov models: These degenerations can be brought into a canonical form in which the central fiber Y_0 has two components intersecting over an elliptic curve \mathcal{E} over the intersection point $B^0 \cap B^1$ of the two base components, i.e. $Y_0 = Y^0 \cup_{\mathcal{E}} Y^1$. The components Y^0 and Y^1 have I_0 type fibers in codimension-zero. Each component has 12 7-branes of arbitrary ADE type located at points in the base components B^p . The 2-cycles γ_1 and γ_2 can be globally defined in Y_0 , and their calibrated volume vanishes in the limit. Since the γ_i have the topology of a torus, M2-branes can wrap arbitrarily often around them, leading to two towers of asymptotically massless BPS particles. These are, in a dual frame, understood as Kaluza-Klein towers signalling a decompactification from eight to ten dimensions. One can argue using string junctions that the towers lead to a double loop enhancement of the gauge algebras associated to the 7-branes of each Y^p component taken together (since their separation is an artefact of the resolution process). In the infinite-distance limit, this leads to the gauge algebra

$$G_\infty = \left(\hat{E}_9 \oplus \hat{E}_9 \right) / \sim, \quad (6.2.6)$$

where the quotient indicates that the imaginary roots are to be identified. The decompactified theory has a gauge algebra

$$G_{10D} = E_8 \oplus E_8. \quad (6.2.7)$$

These models can be understood in terms of a dual heterotic picture in which the $E_8 \times E_8$ heterotic string compactified on a torus T_{het}^2 undergoes a large volume limit in which the complexified Kähler modulus diverges, i.e. $T_{\text{het}} \rightarrow i\infty$.

Type II.b Kulikov models: In their canonical form, the central fiber Y_0 of these models also consists of two components $Y_0 = Y^0 \cup_E Y^1$ meeting over an elliptic curve E whose two 1-cycles we denote $\sigma_i^E \in H_1(E, \mathbb{Z})$, for $i = 1, 2$. However, the base B_0 consists of a single rational curve that acts as the base of both components. The elliptic curve $E = Y^0 \cap Y^1$ is a bisection of the fibration and gives a double cover of B_0 branched at four points. Y_0 has I_2 type fibers in codimension-zero,

³This picture applies to Type II.a and Type III models, with Type II.b models described below.

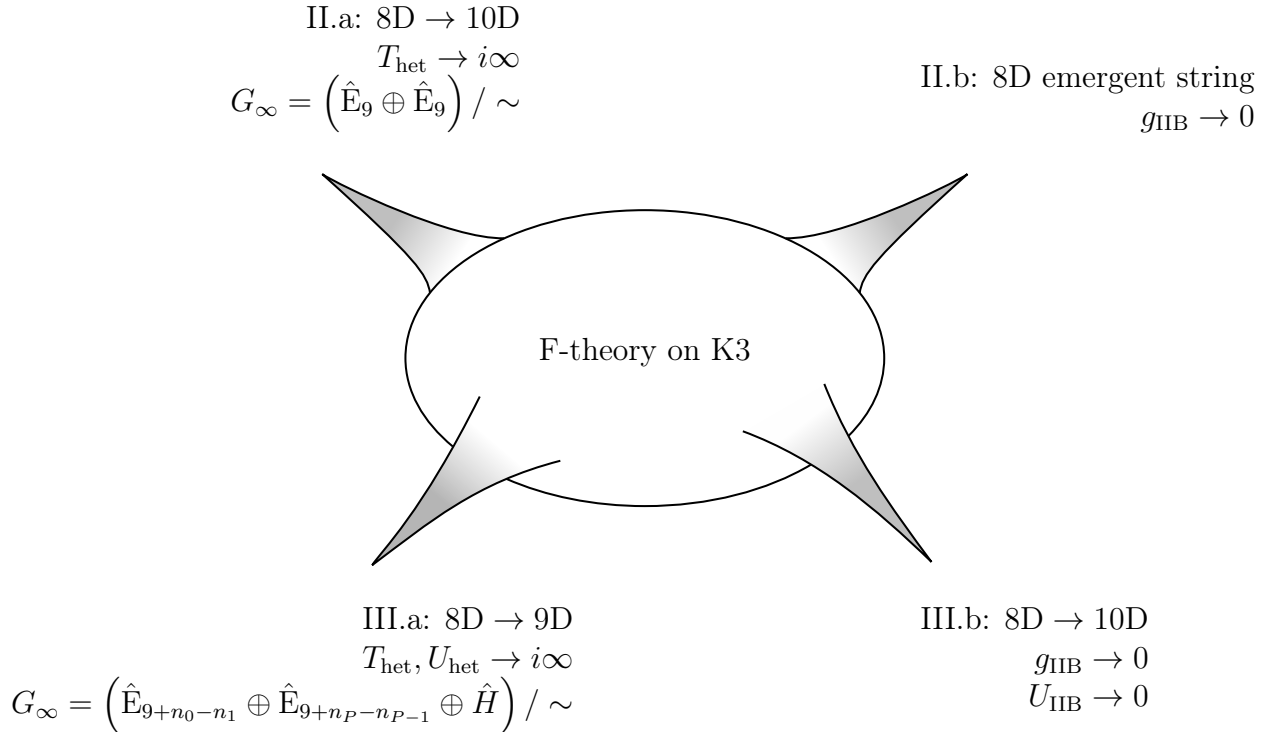


Figure 6.1: Infinite-distance complex structure degenerations for F-theory on an elliptic K3 surface and their associated physics. Figure adapted from [157].

signalling a global weak coupling limit. Due to the codimension-zero I_2 type singularities, only one of the $\{\sigma_i\}_{i=1,2}$ 1-cycles of the elliptic fiber \mathcal{E} is monodromy invariant, namely the collapsed one, say σ_1 . Combining the σ_i^E with σ_1 we still obtain two 2-cycles $\gamma_i \in H_2(Y_0, \mathbb{Z})$ with torus topology and vanishing calibrated volume in the limit. M2-branes multiply wrapping the γ_i lead again to two towers of asymptotically massless BPS particles that are dually interpreted as Kaluza-Klein towers. However, we can also wrap an M2-brane around σ_1 , leading to an asymptotically tensionless fundamental Type II string that is non-BPS due to the triviality of $\sigma_1 \in H_1(Y_0, \mathbb{Z}) = 0$. The excitations of this string are at the same parametric scale as the Kaluza-Klein towers, leading to the interpretation of these models as equidimensional weak coupling emergent string limits.

Type III.a Kulikov models: The central fiber Y_0 is a chain of surfaces $Y_0 = \bigcup_{p=0}^P Y^p$, with $P \geq 1$, in which the middle components and up to one of the end-components have $I_{n>0}$ type fibers in codimension-zero. The end-component(s) with I_0 type fibers in codimension-zero are rational elliptic surfaces. The middle components can only have I_n type fibers in codimension-one, while an end-component with codimension-zero singular fibers, if present, always has two I_n^* type, and possibly also additional I_n type, fibers in codimension-one. The presence of the codimension-zero singularities means that only one of the 1-cycles of the elliptic fiber \mathcal{E} is monodromy invariant, say σ_1 , and by fibering it over a base 1-chain Σ we obtain a single two-cycle $\gamma_1 \in H_2(Y_0, \mathbb{Z})$ with torus topology. This leads to a single tower of asymptotically massless BPS particles with a dual interpretation as a Kaluza-Klein tower. The theory partially decompactifies from eight to nine dimensions, with the gauge algebra undergoing a single loop

enhancement [157, 276, 310]. If $n_0 = n_P = 0$, the enhanced algebra takes the form,

$$G_\infty = \left(\hat{E}_{9-n_1} \oplus \hat{H} \oplus \hat{E}_{9-n_{P-1}} \right) / \sim, \quad (6.2.8)$$

where the H factor accounts for the A-type gauge algebras associated to the 7-branes located in the middle components; in this case, from the point of view of the decompactified theory in nine dimensions we have

$$G_{9D} = E_{9-n_1} \oplus H \oplus E_{9-n_{P-1}}. \quad (6.2.9)$$

If, instead, $n_p = 0$ and $n_q > 0$, for $p, q \in \{0, P\}$ and $p \neq q$, the enhanced algebra is

$$G_\infty = \left(\hat{E}_{9-n_p} \oplus \hat{H} \right) / \sim, \quad (6.2.10)$$

leading in the decompactified theory to

$$G_{9D} = E_{9-n_p} \oplus H. \quad (6.2.11)$$

These models correspond in the dual $E_8 \times E_8$ heterotic string compactified on T_{het}^2 to a large volume limit $T_{\text{het}} \rightarrow i\infty$ in which, simultaneously, the complex structure U_{het} scales such that $T_{\text{het}}/U_{\text{het}}$ remains finite.

Type III.b Kulikov models: The geometry and 7-brane content of the central fiber Y_0 is the one described above for Type III.a models, but with all components having $I_{n>0}$ type fibers in codimension-zero, including both end-components. This signals a global weak coupling limit, allowing us to reinterpret the endpoint of the limit as a perturbative Type IIB orientifold compactification on a torus T_{IIB}^2 . This torus undergoes a large complex structure limit at constant volume. There are two towers of asymptotically massless particles, one coming from the winding modes of the F1-string around the shrinking 1-cycle of T_{IIB}^2 , and an additional supergravity Kaluza-Klein tower from the dual 1-cycle of T_{IIB}^2 ; the volume of the latter is inversely proportional to that of the shrinking 1-cycle. Only the former tower can be seen in the F-theory picture, from M2-branes wrapping the single shrinking 2-cycle γ_1 obtained analogously as for Type III.a models. Altogether, this indicates a full decompactification to ten-dimensional weakly coupled Type IIB string theory.

6.2.2 Degenerations of elliptic Calabi-Yau threefolds

In analogy to the degenerations of elliptic K3 surfaces, one can consider degenerations $\hat{\rho} : \hat{\mathcal{Y}} \rightarrow D$ of Weierstrass models whose elements \hat{Y}_u are Calabi-Yau threefolds elliptically fibered over a base \hat{B}_u . The family degenerates to its central element \hat{Y}_0 , which, in particular, may present infinite-distance non-minimal singularities. The compositions of base changes and birational transformations required to turn this into an equivalent degeneration $\rho : \mathcal{Y} \rightarrow D$ whose central fiber Y_0 , again an elliptic fibration $\pi_0 : Y_0 \rightarrow B_0$, is free of infinite-distance non-minimal singularities is now considerably more involved, and was studied systematically in Chapter 5. Notice that the base spaces of these elliptic fibrations form themselves families $\hat{\mathcal{B}}$ and \mathcal{B} ; we will denote the divisor classes corresponding to \hat{B}_0 and B_0 in said family varieties by \mathcal{U} and $\tilde{\mathcal{U}}$, respectively.

Focusing on non-minimal fibers supported over a curve $C \subset \hat{B}_0$, an important technicality is the distinction between so-called Class 5 models, in which the vanishing orders of the defining polynomials f and g over C lie strictly above the minimality bound (6.2.3), i.e.

$$\text{ord}_{\hat{\mathcal{Y}}}(f)_C > 5 \quad \text{and} \quad \text{ord}_{\hat{\mathcal{Y}}}(g)_C > 7, \quad (6.2.12)$$

and those where at least one (Class 2 or 3) or both of them (Class 1 or 4) saturate the bound. Class 5 models can be turned, after a sequence of base changes and modifications, into an equivalent Class 1–4 model, or into one presenting only minimal degenerations [2, 309]. Focusing therefore on Class 1–4 degenerations, it was shown in Chapter 5 that, for so-called single infinite-distance limits, the central fiber Y_0 is again an open chain of intersecting components after suitable birational transformations. Single infinite-limits distance arise when, morally speaking, non-minimal singular elliptic fibers in \hat{Y}_0 are supported over non-intersecting curves. For the precise definitions and proofs, we refer to Section 5.2.3.

In this chapter, we will focus on single infinite-distance limit degenerations of Hirzebruch models, i.e. those in which the degenerating Calabi-Yau threefolds \hat{Y}_u are elliptic fibrations over Hirzebruch surfaces $\hat{B}_u = \mathbb{F}_n$

$$\begin{array}{ccc} \mathcal{E} & \longrightarrow & \hat{Y}_u \\ & & \downarrow \pi_{\text{ell}} \\ & & \mathbb{F}_n. \end{array} \quad (6.2.13)$$

Recall that a Hirzebruch surface \mathbb{F}_n is a rational fibration over the complex projective plane, whose fiber and base we denote by \mathbb{P}_f^1 and \mathbb{P}_b^1 , respectively. It has two distinguished sections: The $(-n)$ -curve, in the divisor class h , and the $(+n)$ -curve, in the divisor class $h + nf$, where f is the class of the fiber. Depending on the set of curves $\hat{\mathcal{C}}_r$ in $\hat{B}_0 = \mathbb{F}_n$ over which the non-minimal elliptic fibers are supported, the resulting models fall into four classes⁴ of degenerations, which are listed in Table 6.2.1 alongside their main properties.

After a suitable composition of base changes and blow-ups, the central fiber Y_0 of the resolved degeneration $\rho : \mathcal{Y} \rightarrow D$ is a union

$$Y_0 = \bigcup_{p=0}^P Y^p. \quad (6.2.14)$$

The components Y^p are themselves the total spaces of elliptic fibrations $\pi^p : Y^p \rightarrow B^p$, and the bases B^p are again Hirzebruch surfaces. Correspondingly, the base B_0 of the central fiber can be expressed as the union

$$B_0 = \bigcup_{p=0}^P B^p. \quad (6.2.15)$$

Each component B^p of the base corresponds to the divisor E_p associated to the vanishing locus of the exceptional coordinate e_p , introduced in the p -th blow-up during the resolutions process necessary to remove the non-minimal singularities. Renaming $e_0 := u$, the (strict transform of) the original base component \hat{B}_0 corresponds to B^0 , in the divisor class E_0 .

In Class 1–4 models, the generic elliptic fiber over each of the base components B^p can only be of Kodaira type I_{n_p} , for some value $n_p \geq 0$. Each component Y^p is not a Calabi-Yau variety by itself, but rather a log Calabi-Yau space; their union along specific divisors, however, makes Y_0 a reducible Calabi-Yau variety. To the Weierstrass model of each component $\pi^p : Y^p \rightarrow B^p$, there is an associated holomorphic line bundle \mathcal{L}_p over B^p , in the sense that its defining polynomials f_p and g_p are sections of $\mathcal{L}_p^{\otimes 4}$ and $\mathcal{L}_p^{\otimes 6}$, respectively. Furthermore, the discriminant Δ'_p is obtained, after factoring out all overall powers of the exceptional coordinates, by restriction of the discriminant of \mathcal{Y} . Since the base components B^p are all Hirzebruch surfaces, we distinguish

⁴In the present chapter, we focus on genus-zero single infinite-distance limit degenerations of Hirzebruch models. In addition, non-minimal singularities can arise over an anti-canonical divisor, which is a genus-one curve, see Section 5.2.7 for further comments.

the $(-n)$ -curve, $(+n)$ -curve and fiber divisor class of each of B^p denoting them by S_p , T_p and $V_p = W_p$, respectively. This is the notation employed in Table 6.2.1 while summarising the relevant line bundles for each class of models. The divisors of the base family \mathcal{B} that are the natural extension of the aforementioned classes will be denoted calligraphically, e.g. \mathcal{V} is the divisor of \mathcal{B} restricting to the fiber class in the elements $B_{\tilde{u}}$ of the family.

6.3 General properties of horizontal models

Horizontal models, as defined in Section 5.3.1, are single infinite-distance limit degenerations of Hirzebruch models $\hat{\rho} : \hat{\mathcal{Y}} \rightarrow D$ in which the non-minimal elliptic fibers are supported over either the $(-n)$ -curve in the base central fiber $\hat{B}_0 = \mathbb{F}_n$, a $(+n)$ -curve, or both. This class of degenerations is of particular interest because it has a well-controlled heterotic dual, which we explore in Section 6.4. Moreover, it is possible to interpret the degenerations fiberwise as the generalization of the Kulikov models reviewed in Section 6.2.1, a point of view that we exploit in Section 6.5. This makes horizontal models a natural starting point for the analysis of infinite-distance limits in the complex structure moduli space of six-dimensional F-theory.

Before we delve into the aforementioned aspects, we study some general properties of horizontal models in this section. The busy reader interested mostly in the physics interpretation of the infinite-distance limits is invited to skip these slightly more technical details in a first read and jump directly to Section 6.4 after Section 6.3.1.

The fine-grained classification of Kulikov models of [156, 157] attending to their physical interpretation is mirrored for horizontal models in Section 6.3.1. The Kodaira type of singular fibers in codimension-zero in the components $\{Y^p\}_{0 \leq p \leq P}$ of the central fiber Y_0 encodes important information about the background value of the axio-dilaton; in Section 6.3.2 we restrict the possible patterns of codimension-zero singular fibers that horizontal models can present. This results in constraints on the existence of horizontal models representing global weak-coupling limits. As emphasized in Section 5.4, the assignment of non-abelian gauge algebra factors to divisors (taking a six-dimensional standpoint prior to considering any enhancements to higher-dimensional algebras) should be carried out taking into account the global components of the physical discriminant, whose the possible types we list in Section 6.3.3. We then analyse in Section 6.3.4 the restrictions on the local and global 7-brane content. Out of the possible non-abelian gauge algebra factors that a horizontal model can present, the so-called vertical ones have a distinguished interpretation in the analyses of Sections 6.4 and 6.5; in Section 6.3.6 we derive some bounds on their gauge rank for later reference. A number of technical details are relegated to Appendices B.9 to B.11. Many aspects of this analysis carry over, *mutatis mutandis*, to the remaining three types of degenerations listed in Table 6.2.1, as we explain in Appendix B.14.

6.3.1 Classification of horizontal models

An elliptic fibration over a Hirzebruch surface can be equivalently seen as a K3-fibration over the complex projective line. Both fibrations naturally extend to the family variety $\hat{\mathcal{Y}}$ of a degeneration of Hirzebruch models $\hat{\rho} : \hat{\mathcal{Y}} \rightarrow D$. If we restrict to a point on the base \mathbb{P}_b^1 of the Hirzebruch surface, we arrive at a degeneration of elliptic K3 surfaces. Concretely, given a point $p_b := [v_0 : w_0] \in \mathbb{P}_b^1$, the degeneration of elliptic K3 surfaces is obtained by the restriction

$$\hat{\sigma}_{p_b} := \hat{\rho}|_{\hat{\mathcal{Z}}_{p_b}} : \hat{\mathcal{Z}}_{p_b} \longrightarrow D, \quad \hat{\mathcal{Z}}_{p_b} := \Pi_{\text{K3}}^{-1}(p_b \times D). \quad (6.3.1)$$

Non-minimal curves		Central component structure	Component line bundles and discriminants
Horizontal (Case A)	$\hat{\mathcal{C}}_1 = \{h\}$	$\mathbf{I}_{n_0} \dashrightarrow \cdots \dashrightarrow \mathbf{I}_{n_p} \dashrightarrow \cdots \dashrightarrow \mathbf{I}_{n_P}$	$\mathcal{L}_0 = S_0 + (2+n)V_0$ $\mathcal{L}_p = 2V_p$ $\mathcal{L}_P = S_P + 2V_P$
	$\hat{\mathcal{C}}_1 = \{h+nf\}$	$\mathbf{I}_{n_0} \dashrightarrow \cdots \dashrightarrow \mathbf{I}_{n_p} \dashrightarrow \cdots \dashrightarrow \mathbf{I}_{n_P}$	$\Delta'_0 = (12+n_0-n_1)S_0 + (24+12n)V_0$ $\Delta'_p = (2n_p-n_{p-1}-n_{p+1})S_p + (24+n(n_p-n_{p-1}))V_p$ $\Delta'_P = (12+n_P-n_{P-1})S_P + (24+n(n_P-n_{P-1}))V_P$
Vertical (Case B)	$\hat{\mathcal{C}}_1 = \{f\}$	$\mathbf{I}_{n_0} \dashrightarrow \cdots \dashrightarrow \mathbf{I}_{n_p} \dashrightarrow \cdots \dashrightarrow \mathbf{I}_{n_P}$	$\mathcal{L}_0 = 2S_0 + (1+n)W_0$ $\mathcal{L}_p = 2S_p$ $\mathcal{L}_P = 2S_P + W_P$
		$\mathbb{F}_n \dashrightarrow \cdots \dashrightarrow \mathbb{F}_0 \dashrightarrow \cdots \dashrightarrow \mathbb{F}_0$	$\Delta'_0 = 24S_0 + (12+12n+n_0-n_1)W_0$ $\Delta'_p = 24S_p + (2n_p-n_{p-1}-n_{p+1})W_p$ $\Delta'_P = 24S_P + (12+n_P-n_{P-1})W_P$
Mixed sectional (Case C)	$\hat{\mathcal{C}}_1 = \{h+(n+\alpha)f\}$	$\mathbf{I}_{n_0} \dashrightarrow \cdots \dashrightarrow \mathbf{I}_{n_p} \dashrightarrow \cdots \dashrightarrow \mathbf{I}_{n_P}$	$\mathcal{L}_0 = S_0 + (2+(n+2\alpha))V_0$ $\mathcal{L}_p = 2V_p$ $\mathcal{L}_P = S_P + (2-\alpha)V_P$
	$\begin{array}{ll} \alpha = 1 & \text{with } n \leq 6 \\ \alpha = 2 & \text{with } n = 0 \end{array}$	$\mathbb{F}_{n+2\alpha} \dashrightarrow \cdots \dashrightarrow \mathbb{F}_{n+2\alpha} \dashrightarrow \cdots \dashrightarrow \mathbb{F}_n$	$\Delta'_0 = (12+n_0-n_1)S_0 + (24+12(n+2\alpha))V_0$ $\Delta'_p = (2n_p-n_{p-1}-n_{p+1})S_p + (24+(n+2\alpha)(n_p-n_{p-1}))V_p$ $\Delta'_P = (12+n_P-n_{P-1})S_P + ((24-12\alpha)+(n+\alpha)(n_P-n_{P-1}))V_P$
Mixed bisectional (Case D)	$\hat{\mathcal{C}}_1 = \{2h+bf\}$	$\mathbf{I}_{n_0} \dashrightarrow \cdots \dashrightarrow \mathbf{I}_{n_p} \dashrightarrow \cdots \dashrightarrow \mathbf{I}_{n_P}$	$\mathcal{L}_0 = S_0 + (2+4)V_0$ $\mathcal{L}_p = 2V_p$ $\mathcal{L}_P = V_P$
	$\begin{array}{ll} (n, b) = (0, 1) \\ (n, b) = (1, 2) \end{array}$	$\mathbb{F}_4 \dashrightarrow \cdots \dashrightarrow \mathbb{F}_4 \dashrightarrow \cdots \dashrightarrow \mathbb{F}_n$	$\Delta'_0 = (12+n_0-n_1)S_0 + (24+12\cdot 4)V_0$ $\Delta'_p = (2n_p-n_{p-1}-n_{p+1})S_p + (24+4(n_p-n_{p-1}))V_p$ $\Delta'_P = 2(n_P-n_{P-1})S_P + (12+(n+1)(n_P-n_{P-1}))V_P$

Table 6.2.1: Genus-zero single infinite-distance limit degenerations of Hirzebruch models, see Section 5.3. The horizontal models are analysed in detail in the bulk of the present chapter. The remaining three classes are studied in Appendix B.14.

Here $\Pi_{K3} : \hat{\mathcal{Y}} \rightarrow \mathbb{P}_b^1 \times D$ is the K3-fibration of the family variety. For the reasons reviewed in Section 6.2.2, it suffices to only consider Class 1–4 horizontal models. Their induced degeneration of elliptic K3 surfaces $\hat{\sigma}_{p_b} : \hat{\mathcal{Z}}_{p_b} \rightarrow D$ obtained for a generic $p_b \in \mathbb{P}_b^1$ will then be a Class 1–4 Kulikov Weierstrass model, in the language of [156]. In what follows, we drop the p_b subscript, understanding that we always refer to the generic restriction unless stated otherwise.

We recall from Table 6.2.1 that the central fiber Y_0 of the open-chain resolution $\rho : \mathcal{Y} \rightarrow D$ of the horizontal model has the structure

$$\begin{array}{ccccccc} I_{n_0} & - & \cdots & - & I_{n_p} & - & \cdots & - & I_{n_P} \\ | & & & & | & & & & | \\ \mathbb{F}_n & - & \cdots & - & \mathbb{F}_n & - & \cdots & - & \mathbb{F}_n. \end{array} \quad (6.3.2)$$

Due to the way in which the resolution process works for horizontal models, the generic vertical slice $\sigma : \mathcal{Z} \rightarrow D$ of $\rho : \mathcal{Y} \rightarrow D$ corresponds to the resolution of the Kulikov Weierstrass model $\hat{\sigma} : \hat{\mathcal{Z}} \rightarrow D$ that we would have obtained following the steps described in [156]. Its central fiber Z_0 presents then the pattern of codimension-zero singular fibers

$$\begin{array}{ccccccc} I_{n_0} & - & \cdots & - & I_{n_p} & - & \cdots & - & I_{n_P} \\ | & & & & | & & & & | \\ \mathbb{P}^1 & - & \cdots & - & \mathbb{P}^1 & - & \cdots & - & \mathbb{P}^1, \end{array} \quad (6.3.3)$$

which can be readily classified into Type II.a, II.b, III.a or III.b, see Section 6.2.1. The same would be true for finite-distance degenerations of Hirzebruch surfaces, whose generic vertical restriction would be a Type I Kulikov model.

The classification of Kulikov models can therefore be inherited by the horizontal degenerations of Hirzebruch surfaces. That is, we say that a horizontal model $\hat{\rho} : \hat{\mathcal{Y}} \rightarrow D$ is of Type I, II.a, II.b, III.a or III.b if its generic vertical restriction $\sigma : \mathcal{Z} \rightarrow D$ is of the corresponding Kulikov type. Since the pattern of codimension-zero singular elliptic fibers is the same for both Y_0 and Z_0 , the criterion is equal to the one reviewed in Section 6.2.1, which we now write in a condensed form.

Let $\hat{\rho} : \hat{\mathcal{Y}} \rightarrow D$ be a Class 1–4 horizontal model and $\rho : \mathcal{Y} \rightarrow D$ its open-chain resolution, with codimension-zero $I_{n_0} - \cdots - I_{n_P}$ fibers in the components $\{Y^p\}_{0 \leq p \leq P}$ of its central fiber Y_0 . It can be classified into one of the following types:

- **Horizontal Type II.a model:** If $P \geq 1$ and $n_p = 0$ for all $p \in \{0, \dots, P\}$.
- **Horizontal Type II.b model:** If $P = 0$ and $n_0 > 0$.
- **Horizontal Type III.a model:** If $P \geq 1$, $n_p > 0$ for all $p \in \{1, \dots, P-1\}$, and $n_p = 0$ for $p = 0$ and/or $p = P$.⁵
- **Horizontal Type III.b model:** If $P \geq 1$ and $n_p > 0$ for all $p \in \{0, \dots, P\}$.

Note that the horizontal Type II.a model with $P = 1$ and $n_0 = n_1 = 0$ is the stable degeneration limit that is usually taken in the F-theory literature [186, 187, 190, 298, 299, 326] when considering the duality to the heterotic string.

As we will see in the subsequent sections, this classification of the geometry of the central fiber of the degeneration reflects the properties of the asymptotic physics, just like in the eight-dimensional scenario.

⁵A horizontal Type III.a model with $P = 1$ is not allowed to have both $n_0=0$ and $n_P=0$.

6.3.2 Restrictions on components at strong and weak coupling

The Kodaira type of codimension-zero elliptic fibers in the components $\{Y^p\}_{0 \leq p \leq P}$ of the central fiber Y_0 of a resolved horizontal model encodes important physical information. In F-theory, the base of the elliptic fibration is identified with the internal Type IIB spacetime. The complex structure τ of the elliptic curve over a given point corresponds to the value of the axio-dilaton and, hence, the string coupling g_s . The codimension-zero elliptic fibers therefore inform us about the generic (i.e. background) value of the axio-dilaton in a given spacetime component. Since we are considering Class 1–4 (horizontal) models, said fibers can only be of Kodaira type I_m , see Section 5.2.2.3. We need to distinguish the following cases:

- **Y^p with codimension-zero $I_{m>0}$ fibers:** In these components the complex structure τ of the generic elliptic fiber attains a value for which $j(\tau) \rightarrow \infty$, implying that $\tau \rightarrow i\infty$ and therefore $g_s \rightarrow 0$. This means that these components are at weak string coupling.
- **Y^p with codimension-zero I_0 fibers:** In these components the $j(\tau)$ associated to the generic elliptic fiber is finite, and hence so are τ and the string coupling g_s . These components present non-perturbative string coupling.

A global weak coupling limit is therefore one in which all components $\{Y^p\}_{0 \leq p \leq P}$ of Y_0 have codimension-zero $I_{n_p>0}$ fibers. These are either horizontal Type II.b or Type III.b models.

The background value of the axio-dilaton also affects the local types of 7-brane stacks that can exist in a given component, since their associated type of singular elliptic fiber must be compatible with the generic one; we explore this further in Section 6.3.4.

Given the importance of the pattern $I_{n_0} - \cdots - I_{n_P}$ of codimension-zero fibers of Y_0 for the asymptotic physics, we use the remainder of this section to constrain it in different ways. It will be useful to keep in mind from Section 6.2.2 and Table 6.2.1 that the holomorphic line bundles over the components $\{B^p\}_{0 \leq p \leq P}$ of B_0 are

$$\mathcal{L}_0 = S_0 + (2 + n)V_0, \quad (6.3.4a)$$

$$\mathcal{L}_p = 2V_p, \quad p = 1, \dots, P-1, \quad (6.3.4b)$$

$$\mathcal{L}_P = S_P + 2V_P, \quad (6.3.4c)$$

with the modified discriminant in each component lying in the divisor class

$$\Delta'_0 = (12 + n_0 - n_1)S_0 + (24 + 12n)V_0, \quad (6.3.5a)$$

$$\Delta'_p = (2n_p - n_{p-1} - n_{p+1})S_p + (24 + n(n_p - n_{p-1}))V_p, \quad p = 1, \dots, P-1, \quad (6.3.5b)$$

$$\Delta'_P = (12 + n_P - n_{P-1})S_P + (24 + n(n_P - n_{P-1}))V_P. \quad (6.3.5c)$$

The polynomial form of the restrictions $\{\Delta'_p\}_{0 \leq p \leq P}$ of the modified discriminant Δ' to those components at weak string coupling has a particular structure, as we detail in Appendix B.9.

6.3.2.1 Effectiveness bounds

An immediate constraint for the $I_{n_0} - \cdots - I_{n_P}$ pattern of codimension-zero fibers of Y_0 can be obtained by taking into account that the divisor classes (6.3.5) of the restrictions $\{\Delta'_p\}_{0 \leq p \leq P}$ of the modified discriminant Δ' must be effective.

From the horizontal part of (6.3.5) we then obtain the bounds

$$n_0 \geq n_1 - 12, \quad (6.3.6a)$$

$$n_p \geq \frac{n_{p-1} + n_{p+1}}{2}, \quad p = 1, \dots, P-1, \quad (6.3.6b)$$

$$n_P \geq n_{P-1} - 12, \quad (6.3.6c)$$

where $n_p \in \mathbb{Z}_{\geq 0}$ for all $p \in \{0, \dots, P\}$. These inequalities also apply to the eight-dimensional models studied in [156, 157]. One consequence of these constraints is that, if one component Y^p has codimension-zero $I_{n_p > 0}$ fibers, all the intermediate components Y_p with $p \in \{1, \dots, P-1\}$ must be at local weak coupling as well. Moreover, tuning a component to have higher codimension-zero singularities may force an enhancement in the adjacent components. For example, it is not possible to further tune the pattern $I_0 - I_1 - I_1 - I_1 - I_0$ to achieve the pattern $I_0 - I_2 - I_1 - I_1 - I_0$, since the latter does not satisfy the bounds; instead, the tuning will actually result in the pattern $I_0 - I_2 - I_2 - I_1 - I_0$. These constraints also imply that $n(p) := n_p$ is a concave function, as also discussed in [309].

A bound new to the six-dimensional models can be obtained considering the vertical part of (6.3.5), from which we infer that

$$n_{p-1} - n_p \leq \frac{24}{n}, \quad p = 1, \dots, P. \quad (6.3.7)$$

For example, a pattern of codimension-zero fibers $I_0 - I_3 - I_0$ cannot occur for a model constructed over $\hat{B} = \mathbb{F}_9$, even if it satisfies the constraints (6.3.6).

Satisfying the effectiveness constraints is a necessary condition to obtain a consistent model, but not a sufficient one. To illustrate this, consider a two-component model constructed over $\hat{B} = \mathbb{F}_{12}$, with codimension-zero fibers $I_1 - I_0$. Such a model fulfills the above inequalities. We could try to tune it further to obtain a model with the pattern $I_1 - I_1$, which also satisfies the effectiveness constraints. The result of this tuning is, however, a model with three components and codimension-zero fibers $I_1 - I_1 - I_0$.

This last example shows that when we try to construct a horizontal Type III.b model over $\hat{B} = \mathbb{F}_{12}$, the geometry has forced a new component with codimension-zero fibers of Kodaira type I_0 , preventing us from doing so. Indeed, models in which the asymptotic physics is at global weak coupling, like horizontal Type III.b models, cannot be constructed over arbitrary Hirzebruch surfaces. We revisit this aspect in Section 6.3.2.3.

6.3.2.2 Tighter bounds on $|n_p - n_{p+1}|$

While the effectiveness bounds (6.3.6) and (6.3.7) can be obtained rather directly from (6.3.5), they can be improved by exploiting our knowledge of the resolution process for horizontal models. Said class of models is amenable to toric methods, as was studied in Section 5.3. This leads to a global description in terms of homogeneous coordinates, both for the initial degeneration $\hat{\rho} : \hat{\mathcal{Y}} \rightarrow D$ and for its open-chain resolution $\rho : \mathcal{Y} \rightarrow D$. In this description, the exceptional coordinates $\{e_p\}_{0 \leq p \leq P}$ do not appear arbitrarily, but their powers follow specific patterns, a fact that threads the discussion in [309]. Studying this structure we can obtain tighter bounds for $|n_p - n_{p+1}|$, with $p \in \{0, \dots, P-1\}$.

Postponing the technical details to Section B.10.1, the inequalities that we find from the resolution structure are

$$n_p - n_{p+1} \leq \begin{cases} 8, & 0 \leq n \leq 2, \\ 4, & 3 \leq n \leq 4, \\ 2, & 5 \leq n \leq 8, \\ 1, & 9 \leq n \leq 12, \end{cases} \quad p = 0, \dots, P-1, \quad (6.3.8)$$

and

$$n_p - n_{p-1} \leq 8, \quad p = 1, \dots, P. \quad (6.3.9)$$

These bounds apply when the codimension-zero $I_{n_p > 0}$ fibers in the Y^p component arise from a single or double accidental cancellation structure, see Appendix B.9. It would be interesting to know if allowing for higher accidental cancellations would relax the inequalities to be fulfilled, equating them to the effectiveness bounds (6.3.6) and (6.3.7).

6.3.2.3 Restrictions on global weak coupling limits

As mentioned earlier, in a global weak coupling limit all components $\{Y^p\}_{0 \leq p \leq P}$ of Y_0 have codimension-zero $I_{n_p > 0}$ fibers. Within Class 1–4 horizontal models, this property corresponds to either horizontal Type II.b or Type III.b models. However, such models cannot be constructed over arbitrary Hirzebruch surfaces $\hat{B} = \mathbb{F}_n$. As we will now show, they cannot be engineered over Hirzebruch surfaces $\hat{B} = \mathbb{F}_n$ with $n \geq 5$, while for $n = 3$ and 4 they necessarily enforce a horizontal line of D type enhancements of rank at least 3 and 4, respectively. For $n = 0, 1, 2$, no restrictions arise.

In a Hirzebruch surface \mathbb{F}_n there is a single irreducible curve with negative self-intersection, the $(-n)$ -curve that is the unique representative of the h class. Given another curve C , the intersection product $C \cdot h$ is negative if and only if C contains h as a component.⁶ Considering the divisors F, G and Δ associated with a Weierstrass model over \mathbb{F}_n , one can see that

$$F \cdot h < 0, \quad G \cdot h < 0, \quad \Delta \cdot h < 0, \quad n \geq 3. \quad (6.3.10)$$

This inevitably leads to the presence of gauge algebra factors supported on h , the so-called non-Higgsable clusters [324]. We list the generic vanishing orders⁷ associated with the non-Higgsable clusters supported on h for the different Hirzebruch surfaces $\hat{B} = \mathbb{F}_n$ in Table 6.3.1.

Consider now how this applies to models with components at global weak coupling. First, take a horizontal Type III.b model $\hat{\rho} : \hat{\mathcal{Y}} \rightarrow D$, which we are considering, without loss of generality, to be one in which the non-minimal elliptic fibers are supported over $\hat{\mathcal{C}}_1 = \{h\}$. In the central fiber Y_0 of its open-chain resolution $\rho : \mathcal{Y} \rightarrow D$, the h class in the end-component B^P is the only one that can support non-abelian gauge enhancements, since the remaining $(-n)$ -curves in the $\{B^p\}_{0 \leq p \leq P-1}$ correspond to the interface curves between components.⁸ To achieve a global weak

⁶We review this and other useful facts about algebraic surfaces in Appendix B.1.

⁷To be more precise, we are printing the family vanishing orders for a degeneration $\rho : \hat{\mathcal{Y}} \rightarrow D$ of Hirzebruch models. In the variety $\hat{\mathcal{Y}}$, the base of the elliptic fibration is the threefold $\hat{B} = \mathbb{F}_n \times D$. Each Weierstrass model $\hat{\mathcal{Y}}_u$ presents a non-Higgsable cluster over $\{s = 0\}_{\hat{B}_u}$, with the component vanishing orders printed in Table 6.3.1; since this applies to all fibers of the degeneration, it results in the corresponding family vanishing orders being realised over $\{s = 0\}_B$ too. See Section 5.2.2.2 for the differences between the various notions of vanishing orders.

⁸The interface curves can be arranged to have trivial vanishing orders by a combination of base changes and modifications of the degeneration, see Section 5.4.6.

n	3	4	5	6	7
$\text{ord}_{\hat{\mathcal{Y}}}(f, g, \Delta)_{s=0}$	(2, 2, 4)	(2, 3, 6)	(3, 4, 8)	(3, 4, 8)	(3, 5, 9)

n	8	9	10	11	12
$\text{ord}_{\hat{\mathcal{Y}}}(f, g, \Delta)_{s=0}$	(3, 5, 9)	(4, 5, 10)	(4, 5, 10)	(4, 5, 10)	(4, 5, 10)

Table 6.3.1: Generic vanishing orders associated with the non-Higgsable clusters over the $(-n)$ -curve h of \mathbb{F}_n .

coupling limit, all components of Y_0 , and Y^P in particular, must support codimension-zero $\text{I}_{n_P > 0}$ fibers. This means that, at the very least, the single accidental cancellation structure

$$f_p = -3h_p^2, \quad g_p = 2h_p^3, \quad h_p \in H^0(B^p, \mathcal{L}_p^{\otimes 2}), \quad (6.3.11)$$

must be enforced. This restricts the modified discriminant to be of the form

$$\Delta'_p = h_p^k \Delta''_p, \quad k \geq 2. \quad (6.3.12)$$

For details see Appendix B.9. Denoting the divisor class associated to h_p by H_p , this means, in view of (6.3.4), that the relevant divisors are

$$F_p = 2H_p, \quad G_p = 3H_p, \quad H_p = 2\mathcal{L}_p = \begin{cases} 2S_0 + (4 + 2n)V_0, & p = 0, \\ 4V_p, & p = 1, \dots, P-1, \\ 2S_P + 4V_P, & p = P. \end{cases} \quad (6.3.13)$$

Note that tuning the components $\{Y^p\}_{0 \leq p \leq P-1}$ to be at local weak coupling does not lead to enhancements of type II, III, IV, I_m^* , IV^* , III^* or II^* at the interfaces $\{B^p \cap B^{p+1}\}_{0 \leq p \leq P-1}$ between components, which would turn the model into a (possibly obscured) Class 5 model. This is a consequence of

$$H_p \cdot h \geq 0, \quad p = 0, \dots, P-1, \quad (6.3.14)$$

which implies that no forced factorizations occur. The discriminant Δ'_p , which is not simply a multiple of H_p , does not lead to special fibers at the intersections with the adjacent components either: Indeed, (6.3.5a) and (6.3.5b) imply

$$\Delta'_p \cdot S_p = -n(n_p - n_{p+1}) + 24 \geq 0 \Leftrightarrow n_p - n_{p+1} \leq \frac{24}{n}, \quad p = 0, \dots, P-1, \quad (6.3.15)$$

and the last inequality is guaranteed by the effectiveness bounds, namely by (6.3.7). For the Y^P component, instead,

$$H_P \cdot S_P < 0 \Leftrightarrow n \geq 3, \quad (6.3.16)$$

$$(H_P - S_P) \cdot S_P < 0 \Leftrightarrow n \geq 5, \quad (6.3.17)$$

leading to

$$h_P \propto \begin{cases} s, & n = 3, 4, \\ s^2, & n \geq 5. \end{cases} \quad (6.3.18)$$

Given the structure of f_P , g_P and Δ'_P , we find that the minimal component vanishing orders over S_P are

$$\text{ord}_{Y^P}(f_P, g_P, \Delta'_P)_{s=0} \geq \begin{cases} (2, 3, k + \alpha), & n = 3, 4, \\ (4, 6, 2k + \alpha), & n \geq 5, \end{cases} \quad (6.3.19)$$

where α accounts for additional factorisations forced by the reducibility of

$$\Delta''_P := \Delta'_P - kH_P. \quad (6.3.20)$$

Its value can be explicitly computed by once again analysing the intersection numbers of the classes Δ''_P and S_P . The class $\Delta''_P - \alpha S_P$ will continue to contain S_P components as long as

$$(\Delta''_P - \alpha S_P) \cdot S_P < 0 \Leftrightarrow \alpha < \frac{4k - 24}{n} + 12 - 2k. \quad (6.3.21)$$

Therefore, the final value of α , taking all the mandatory factorizations into account, is

$$\alpha = \max \left\{ \left\lceil \frac{4k - 24}{n} + 12 - 2k \right\rceil, 0 \right\}. \quad (6.3.22)$$

A similar analysis can be performed for horizontal Type II.b models. Their central fiber Y_0 consists of a single component, whose Weierstrass model is associated to the line bundle

$$\mathcal{L}_{B_0} = h + 2f + (h + nf) = \mathcal{L}_P + (h + nf). \quad (6.3.23)$$

Since $(h + nf) \cdot h = 0$, the same conclusions follow. Hence, in the following paragraphs we write Y^P using the notation pertaining to the horizontal Type III.b case, but it is interchangeable with the Y_0 central fiber of the horizontal Type II.b model.

Let us summarize what the above considerations imply for the horizontal models constructed over the Hirzebruch surfaces $\hat{B} = \mathbb{F}_n$, with $0 \leq n \leq 12$.

Models with $5 \leq n \leq 12$ The horizontal models constructed over these Hirzebruch surfaces have component vanishing orders in the Y^P component

$$\text{ord}_{Y^P}(f_P, g_P)_{s=0} = (4, 6). \quad (6.3.24)$$

This means that after tuning the Y^P component to be at local weak coupling, one must perform at least one further base blow-up⁹ in order to arrive at the open-chain resolution of the degeneration.

As a consequence, global weak coupling limits cannot be realised in horizontal models constructed over $\hat{B} = \mathbb{F}_n$, with $5 \leq n \leq 12$. If we try to forcefully tune one, the geometry prevents this by shedding a new component for Y_0 that is at strong coupling, preventing us from constructing a horizontal Type II.b or Type III.b model. We schematically summarise the discussion in Figure 6.2.

From (6.3.19) and (6.3.22) we observe that $\{s = 0\}_{B^P}$ can present component vanishing orders

$$\text{ord}_{Y^P}(f_P, g_P, \Delta'_P)_{s=0} = (4, 6, < 12), \quad (6.3.25)$$

model and some generic representatives of a subset of the global divisor classes discussed in which seem pathological. These hold no physical significance, since the component vanishing orders should be used to read off the physics once the degeneration has been fully resolved as explained in Chapter 5, at which point these vanishing orders cannot appear. Nonetheless, one can arrange via an appropriate base change for the component vanishing orders to not present this pathological behaviour even for the intermediate steps of the resolution process.

⁹The need for a further base blow-up, accompanied by an appropriate line bundle shift, may only be apparent after a base change, see the comments on obscured infinite-distance limits in Appendix B.3.

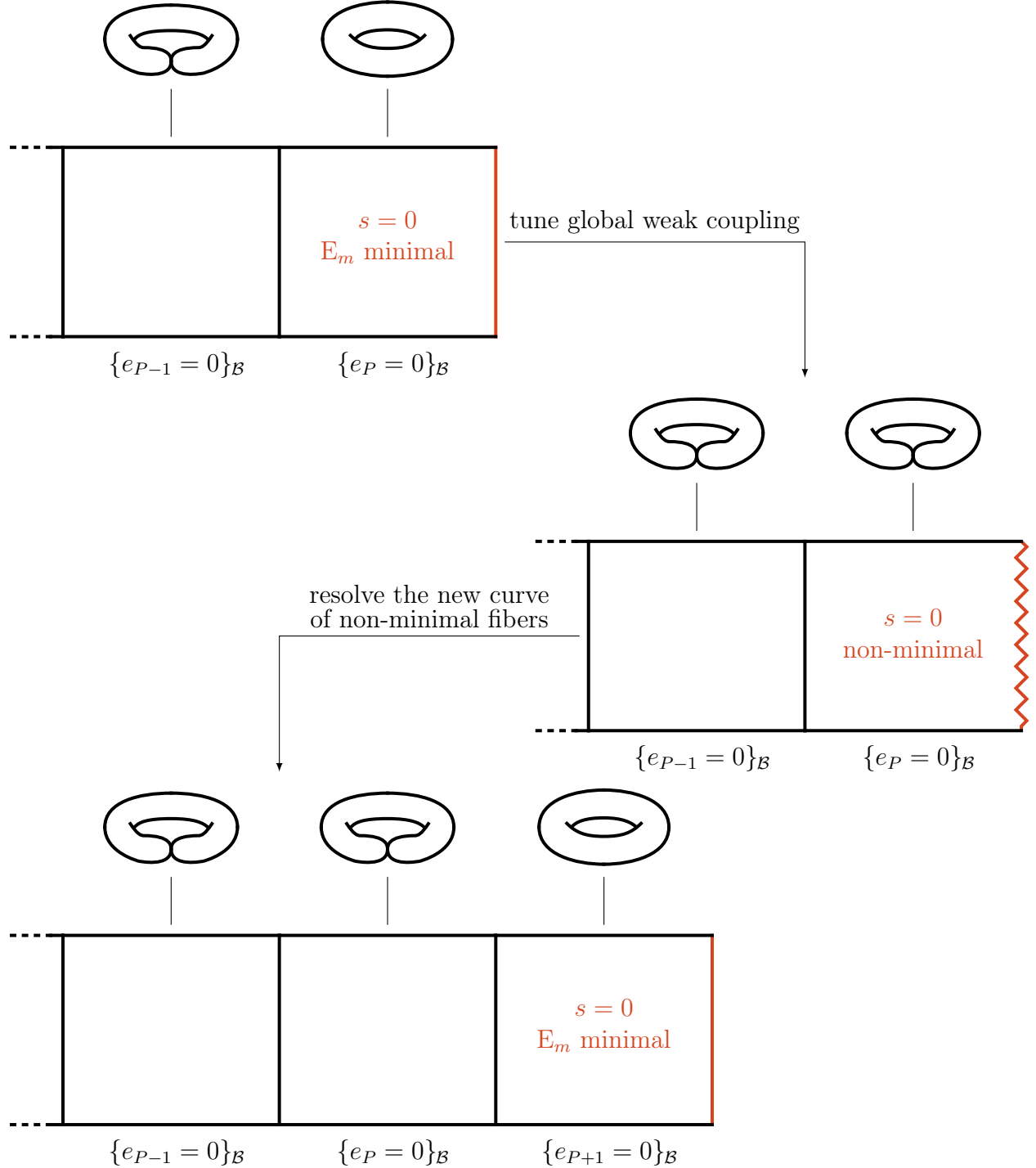


Figure 6.2: The open-chain resolutions of horizontal models constructed over the Hirzebruch surfaces $\hat{B} = \mathbb{F}_n$, with $5 \leq n \leq 12$, present a non-Higgsable cluster over the $(-n)$ -curve of the Y^P component of the central fiber Y^0 . It corresponds to an exceptional algebra \mathfrak{e}_m , with $m = 6, 7$ or 8 depending on the value of n , see Table 6.3.1. Forcing said component to be at weak coupling enhances the non-Higgsable cluster to be non-minimal. The resolution process demands then, possibly after a base change, at least a further base blow-up. In other words, the geometry prevents global weak coupling limits by shedding a new component at strong coupling.

Models with $3 \leq n \leq 4$ These Hirzebruch surfaces lead to horizontal models whose Y^P component exhibits component vanishing orders

$$\text{ord}_{Y^P}(f_P, g_P)_{s=0} = (2, 3). \quad (6.3.26)$$

When $n = 4$, (6.3.19) and (6.3.22) imply that

$$\text{ord}_{Y^P}(f_P, g_P, \Delta'_P)_{s=0} = (2, 3, \geq 6), \quad (6.3.27)$$

meaning that we either find the non-Higgsable cluster present at finite distance or an enhancement of it. For $n = 3$, we infer instead that

$$\text{ord}_{Y^P}(f_P, g_P, \Delta'_P)_{s=0} = (2, 3, \geq 5). \quad (6.3.28)$$

The non-Higgsable cluster associated to Kodaira type IV singularities present at finite distance is always enhanced to be of Kodaira type I_m^* , a fact that we comment on again in Section 6.3.4. While the $n = 4$ case starts off with D_4 singularities that may worsen in particular models, the $n = 3$ case allows for D_3 singularities over $\{s = 0\}_{B^P}$. Tuning horizontal Type II.b or Type III.b global weak coupling limits is therefore possible over these Hirzebruch surfaces.

Models with $0 \leq n \leq 2$ For these Hirzebruch surfaces no forced factorisation of S_P classes occurs, and we generically have

$$\text{ord}_{Y^P}(f_P, g_P, \Delta'_P)_{s=0} = (0, 0, 0). \quad (6.3.29)$$

Hence, constructing horizontal Type II.b or Type III.b global weak coupling limits is possible.

The same conclusions can be reached directly for horizontal Type II.a models by using the Sen limit [202, 203] in its formulation for Tate models [332, 333] and performing a similar analysis. However, the above treatment is more appropriate for horizontal Type III.b models, since their Sen limit presentation does not properly distinguish them from horizontal Type III.a models, as we discuss in Section 6.5.3.1. Moreover, the analysis carried out above generalises for the non-horizontal models listed in Table 6.2.1, as we exploit in Appendix B.14, for which the constraints can actually be stricter. The absence of horizontal Type II.a models constructed over $\hat{B} = \mathbb{F}_n$ with $5 \leq n \leq 12$ was also commented on in [334] from the consideration of Nikulin involutions [335–337].

6.3.3 Types of global divisors

To fix the notation that we will employ in subsequent sections, let us review the types of global divisors that can occur in the multi-component base B_0 of the central fiber Y_0 of the resolved degeneration $\rho : \mathcal{Y} \rightarrow D$ of a horizontal model.

Given a fibration $\pi : V \rightarrow W$, horizontal divisors D_{hor} of V are those fulfilling $\pi_*(D_{\text{hor}}) = W$, while vertical divisors D_{ver} of V map to a proper subvariety $\pi_*(D_{\text{ver}}) \neq W$ of W . Any effective divisor D in V can be decomposed as a sum $D = D_{\text{hor}} + D_{\text{ver}}$. We can classify the global divisors of B_0 into horizontal, vertical and mixed divisors using a similar nomenclature.

The discussion is illustrated in Figure 6.3, in which we depict generic representatives of a subset of the global divisor classes listed below.

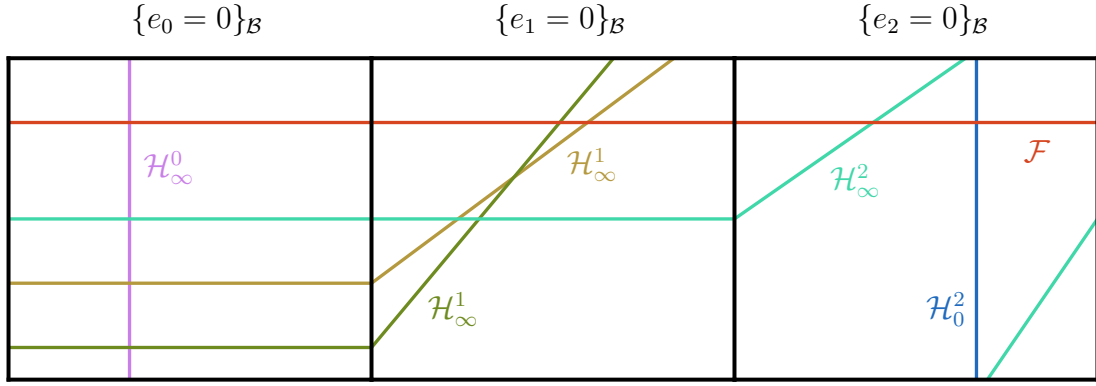


Figure 6.3: We schematically represent the base of the central fiber of a resolved horizontal model and some generic representatives of a subset of the global divisor classes discussed in Section 6.3.3. The depiction is based on models constructed over $\hat{B} = \mathbb{F}_1$.

Vertical divisors

These divisors project to points $p_b \in \mathbb{P}_b^1$, and correspond to the divisor class

$$\mathcal{F} := \sum_{p=0}^P V_p = \mathcal{V}|_{\tilde{\mathcal{U}}} . \quad (6.3.30)$$

Here and below we use the notation of Chapter 5, reviewed in Section 6.2.2.

They extend through the whole base B_0 of the multi-component central fiber Y_0 ,

$$\mathcal{F} \cdot E_p \neq 0, \quad p = 0, \dots, P . \quad (6.3.31)$$

Vertical divisors are $P+1$ copies of \mathbb{P}_f^1 intersecting in an open-chain, i.e. a collection of genus-zero curves; they conform the base of the central fiber Z_0 of the associated degeneration of K3 surfaces $\sigma_{p_b} : \mathcal{Z}_{p_b} \rightarrow D$, see Section 6.3.1. We will refer to the gauge enhancements supported on this class of divisors as the vertical gauge algebras.

Horizontal divisors

We call horizontal divisors those that restrict to a horizontal divisor in a single component B^p of B_0 , not extending to the adjacent ones. The interface curves given by the classes $\{S_p\}_{0 \leq p \leq P-1}$ are an edge case, but they are not relevant to the discussion, since they do not support gauge algebras in an open-chain resolution of the horizontal model, see Section 5.4.6. The possibilities are:

- The genus-zero curves in the class

$$\mathcal{H}_\infty^0 := T_0 = \mathcal{T}|_{\tilde{\mathcal{U}}} , \quad (6.3.32)$$

which have the intersections

$$\mathcal{H}_\infty^0 \cdot E_0 \neq 0, \quad \mathcal{H}_\infty^0 \cdot E_p = 0, \quad p = 1, \dots, P, \quad \mathcal{H}_\infty^0 \cdot \mathcal{F} = 1 . \quad (6.3.33)$$

- The genus-zero curve in the class

$$\mathcal{H}_0^P := S_P = \mathcal{S}|_{\tilde{\mathcal{U}}} , \quad (6.3.34)$$

with intersections

$$\mathcal{H}_0^P \cdot E_P \neq 0 , \quad \mathcal{H}_0^p \cdot E_p = 0 , \quad p = 0, \dots, P-1 , \quad \mathcal{H}_0^P \cdot \mathcal{F} = 1 . \quad (6.3.35)$$

- When the model has been constructed over $\hat{B}_0 = \mathbb{F}_0$, the definition also encompasses the genus-zero curves

$$\mathcal{H}_\infty^p := T_p = S_p = \left(T + \sum_{i=0}^{p-1} (p-i) E_i \right) \Big|_{\tilde{\mathcal{U}}} , \quad p = 1, \dots, P , \quad (6.3.36)$$

which intersect

$$\mathcal{H}_\infty^p \cdot E_p \neq 0 , \quad \mathcal{H}_\infty^p \cdot E_q = 0 , \quad p \neq q = 0, \dots, P , \quad \mathcal{H}_\infty^p \cdot \mathcal{F} = 1 . \quad (6.3.37)$$

- Multiples $\alpha \mathcal{H}_\infty^p$ of the above curve classes, whose genus can be computed via adjunction resulting in

$$g(\alpha \mathcal{H}_\infty^p) = \frac{1}{2}(\alpha - 1)(\alpha n - 2) . \quad (6.3.38)$$

Mixed divisors

The remaining divisors we call mixed divisors. Among these, we can highlight two classes:

- When the model has been constructed over $\hat{B}_0 = \mathbb{F}_n$ with $n \geq 1$, we have the curve classes

$$\mathcal{H}_\infty^p := \sum_{i=0}^{p-1} n V_i + T_p = \left(T + \sum_{i=0}^{p-1} (p-i) E_i \right) \Big|_{\tilde{\mathcal{U}}} , \quad p = 1, \dots, P , \quad (6.3.39)$$

with intersections

$$\mathcal{H}_\infty^p \cdot E_q \neq 0 , \quad q = 0, \dots, p , \quad \mathcal{H}_\infty^p \cdot E_q = 0 , \quad q = p+1, \dots, P , \quad \mathcal{H}_\infty^p \cdot \mathcal{F} = 1 . \quad (6.3.40)$$

They restrict to genus-zero curves in all the components that they intersect non-trivially.

- Divisors arising from a combination of all the previously listed classes. For example, the divisors in the classes $\mathcal{H}_\infty^p + \alpha \mathcal{F}$, that restrict in B^p to the sections $h + (n + \alpha)f$ and extend vertically to the left.

Mixed divisors can be split via a finite-distance complex structure deformation into horizontal and vertical divisors, and we will therefore interpret the gauge factors supported on the former as a Higgsing of the latter.

Exceptional divisors

In models presenting codimension-two finite-distance non-minimal points, we may also have exceptional curves arising from their resolution. These curves are completely contained within a component $\{B^p\}_{0 \leq p \leq P}$ and are therefore global divisors. The gauge algebras supported over them are not subject to any subtleties relating to the multi-component nature of Y_0 , and we mostly ignore them in what follows by keeping the exceptional curves blown-down, i.e. by maintaining $\hat{B} = \mathbb{F}_n$. In Appendix B.12 we briefly comment on them.

6.3.4 Restrictions on the local and global 7-brane content

The gauge algebra content at the endpoints of the infinite-distance limits that we study is analysed in two steps. First, we take a six-dimensional standpoint and determine the gauge algebras as read off from the central fiber Y_0 of the open-chain resolution $\rho : \mathcal{Y} \rightarrow D$ of the degeneration of Hirzebruch surfaces. Second, we consider any partial decompactifications that may occur along the limit, leading to gauge enhancements from the point of view of the asymptotic, higher-dimensional gauge theory.

The first of these points was addressed in Section 5.4. In the reducible variety Y_0 , individual gauge factors are associated to the global divisors that appear as components of the physical discriminant Δ_{phys} , and that in a horizontal model will be (multiples of) the classes just listed in Section 6.3.3. These divisors are obtained by consistently gluing the irreducible components of the restrictions $\{\Delta'_p\}_{0 \leq p \leq P}$ of the modified discriminant Δ' to the different base components $\{B^p\}_{0 \leq p \leq P}$. While the analysis in terms of the global divisors clarifies the complications arising in a componentwise study, the restrictions on the 7-brane content occurring in single components are still useful to consider, as they provide valuable information on the possible global 7-branes of the model. In this section, we comment on how this works for horizontal models.

The results can be succinctly summarised as follows: Those components at local strong coupling are not subject to any restrictions on their local 7-brane content. The components at local weak coupling can only present local 7-branes associated with Kodaira type I_m and I_m^* fibers. If a global 7-brane passes through various components it has to obey the most stringent of the individual local constraints found in them.

The effectiveness bounds (6.3.6b) imply that, as soon as a single component is at weak coupling, all intermediate components of the horizontal model must be as well. This leaves us with the cases with no codimension-zero singular elliptic fibers, those in which only the intermediate components are at weak coupling, and finally those in which the end-components also are, cf. the classification in Section 6.3.1.

6.3.4.1 Models with no components at weak coupling

When the generic elliptic fiber in all components $\{Y^p\}_{0 \leq p \leq P}$ is of Kodaira type I_0 , we see from (6.3.4b) and (6.3.5b) that the local 7-brane content in the intermediate components $\{Y^p\}_{1 \leq p \leq P-1}$ can only consist of vertical classes. This means that no global gauge enhancements can occur over the divisor classes $\{\mathcal{H}_\infty^p\}_{1 \leq p \leq P-1}$ or combinations containing them. The local 7-branes over the intermediate components can extend to global 7-branes in the divisor classes \mathcal{F} , \mathcal{H}_∞^P , or combinations of them. The global divisors \mathcal{H}_∞^0 , \mathcal{H}_0^P , and combinations involving them also can support gauge enhancements. Since no components are at weak coupling, all listed divisors can support any of the Kodaira type elliptic fibers, leading to the associated simply-laced ADE Lie algebras or, possibly, the non-simply-laced ones resulting from folding the corresponding Dynkin diagrams. Horizontal Type II.a models fall within this category.

6.3.4.2 Models with the intermediate components at weak coupling

For the intermediate components $\{Y^p\}_{1 \leq p \leq P-1}$ to be at weak coupling we need, at the very least, the single accidental cancellation structure (B.9.4) to hold, meaning that $f_p = -3h_p^2$, $g_p = 2h_p^3$ and $\Delta'_p = h_p^k \Delta''_p$, with $k \geq 2$ and $p \in \{1, \dots, P-1\}$. From (6.3.13) we read that

$$H_p = 4V_p \Rightarrow h_p = p_4([v : w]), \quad p \in \{1, \dots, P-1\}, \quad (6.3.41)$$

which is always reducible. The polynomials $\{h_p\}_{1 \leq p \leq P-1}$ must all be identical, since the local 7-branes need to consistently extend between components. None of the four roots of these polynomials may coincide in a horizontal model; this would lead to non-minimal component vanishing orders over a representative of the fiber class of the intermediate components and, as a consequence, the model would not be a single infinite-distance limit, see Definition 5.2.9. The structure (B.9.4) hence implies that we have four local Kodaira type D_m enhancements in the intermediate components, where m can also attain the values $m = 0, 1, 2$ and 3 . Additionally, we observe from (6.3.5b) that the intermediate components may also present Kodaira type I_m enhancements depending on the values of $\{n_p\}_{0 \leq p \leq P}$.

The end-components Y^0 and Y^P do not fulfil the structure (B.9.4), and their Weierstrass model is generic enough that the aforementioned local enhancements in the intermediate components generically extend without forcing a global enhancement.

Let us now list the types of singular elliptic fibers that can occur over global divisors in such a model. We only list a few divisor classes, with the understanding that divisor classes built as combinations of them are subject to the most stringent of the restrictions applying to their individual pieces. The global divisors \mathcal{H}_∞^0 and \mathcal{H}_0^P are fully contained in the Y^0 and Y^P component, respectively; since these components are not at weak coupling, no constraints apply, and they can support any of the Kodaira type elliptic fibers. The divisor classes \mathcal{F} and $\{\mathcal{H}_\infty^p\}_{1 \leq p \leq P}$ extend through the intermediate components, meaning that their associated global gauge factor must be compatible with the local weak coupling found in them (an exception occurs for horizontal models constructed over $\hat{B} = \mathbb{F}_0$, for which the \mathcal{H}_∞^P class is completely contained in the Y^P component and subject to the same considerations as \mathcal{H}_0^P). Hence, \mathcal{F} and \mathcal{H}_∞^P can only support A and D type singular elliptic fibers, while $\{\mathcal{H}_\infty^p\}_{1 \leq p \leq P-1}$ only allow for those of A type. The A type fibers of Kodaira type III and IV are also possible, as long as they suffer a local enhancement to Kodaira type I_m^* in the intermediate components. Horizontal Type III.a models fall within this category.

6.3.4.3 Models with the end-components at weak coupling

If, in addition to the intermediate components $\{Y^p\}_{1 \leq p \leq P-1}$, one of the two end-components $\{Y^p\}_{p=0,P}$ is also at weak coupling, the situation does not vary much with respect to the previous case. The degenerations still correspond to horizontal Type III.a models, and the gauge enhancements possible over the global divisors are essentially the ones previously listed. The differences arise for enhancements over the divisor classes \mathcal{H}_∞^0 or \mathcal{H}_0^P (also \mathcal{H}_∞^P if $\hat{B} = \mathbb{F}_0$), depending on which of the end-components is at weak coupling; these classes can only support A and D type singular elliptic fibers. The component that is not at weak coupling still prevents the forced local enhancements of the intermediate components from generically extending to a global enhancement.¹⁰

The situation changes once all components $\{Y^p\}_{0 \leq p \leq P}$ are at weak coupling, i.e. once we are dealing with a horizontal Type III.b model, which we saw in Section 6.3.2.3 can only occur when $\hat{B} = \mathbb{F}_n$ with $0 \leq n \leq 4$. Then, all components satisfy at least the single accidental cancellation

¹⁰This is different from the behaviour of the end-components at weak coupling in eight-dimensional models, which inevitably carry two Kodaira type I_m^* singularities [156, 157] that manifest from the global perspective. This is because 7-branes are points in the internal space in eight-dimensions, and therefore the relevant h_p polynomial always factorizes, similarly to how it occurs for the vertical classes in the intermediate components at weak coupling, with the difference that the points are fully contained in a component.

structure (B.9.4), and the global divisor

$$\mathcal{H} := \sum_{p=0}^P H_p - \begin{cases} 0, & 0 \leq n \leq 2, \\ S_p, & 3 \leq n \leq 4, \end{cases} \quad (6.3.42)$$

that we have defined as the gluing of the $\{H_p\}_{0 \leq p \leq P}$ with the non-Higgsable clusters subtracted, appears with physical vanishing orders

$$\text{ord}_{Y_0}(f_{\text{phys}}, g_{\text{phys}})_{\mathcal{H}} = (2, 3). \quad (6.3.43)$$

Taking into account (6.3.13), we see that

$$\mathcal{H} = (2T_0 + 4V_0) + \left(\sum_{p=1}^{P-1} 4V_p \right) + \begin{cases} 2T_P + 4V_P, & n = 0, \\ 2T_P + 2V_P, & n = 1, \\ 2T_P, & n = 2, \\ T_P + V_P, & n = 3, \\ T_P, & n = 4, \end{cases} \quad (6.3.44)$$

or, in terms of global divisors,

$$\mathcal{H} = 2\mathcal{H}_{\infty}^0 + \begin{cases} 2\mathcal{H}_{\infty}^P + 4\mathcal{F}, & n = 0, \\ 2\mathcal{H}_{\infty}^P + 2\mathcal{F}, & n = 1, \\ 2\mathcal{H}_{\infty}^P, & n = 2, \\ \mathcal{H}_{\infty}^P + \mathcal{F}, & n = 3, \\ \mathcal{H}_{\infty}^P, & n = 4, \end{cases} \quad (6.3.45)$$

meaning that we generically have a D type enhancement (or its folding) over a global mixed divisor. In models for which only single accidental cancellations occur

$$\text{ord}_{Y_0}(f_{\text{phys}}, g_{\text{phys}}, \Delta_{\text{phys}})_{\mathcal{H}} = (2, 3, 3) \quad (6.3.46)$$

are the generic physical vanishing orders, corresponding to D₁ type singular elliptic fibers. When higher accidental cancellations take place, this can be lowered to

$$\text{ord}_{Y_0}(f_{\text{phys}}, g_{\text{phys}}, \Delta_{\text{phys}})_{\mathcal{H}} = (2, 3, 2), \quad (6.3.47)$$

corresponding to D₀ type fibers, see the discussion in Appendix B.9. All gauge enhancements appearing in a horizontal Type III.b model are associated with Kodaira type I_m or I_m^{*} singular elliptic fibers.

In a horizontal Type II.b model we have a single component Y₀ for the central fiber of the resolved degeneration, which is at weak coupling. The generic elliptic fiber is of Kodaira type I_m, with I_{m'}^{*} fibers over a divisor in the class

$$H = 2h + (2+n)f - \begin{cases} 0, & 0 \leq n \leq 2, \\ h, & 3 \leq n \leq 4, \end{cases} \quad (6.3.48)$$

a I_{m''}^{*} non-Higgsable cluster over h when $\hat{B} = \mathbb{F}_n$ with $3 \leq n \leq 4$, and some additional I_{m'''} type fibers over curves.

Type	Split	Semi-split	Non-split
I_m	\mathfrak{su} -algebra (A)	—	\mathfrak{sp} -algebra (C)
I_0^*	\mathfrak{so} -algebra (D)	\mathfrak{so} -algebra (B)	\mathfrak{g}_2 -algebra (G)
$I_{m>0}^*$	\mathfrak{so} -algebra (D)	—	\mathfrak{so} -algebra (B)

Table 6.3.2: Gauge algebras associated to I_m and I_m^* fibers depending on the number of irreducible components of the monodromy cover.

6.3.5 Physical interpretation of the constraints

As we have just seen, the most notable effect of having codimension-zero $I_{n_p>0}$ singular elliptic fibers in a component is to restrict the local gauge enhancements in it to be associated with Kodaira type I_m or I_m^* singular elliptic fibers; this constraint affects in some form all global divisors traversing a component at weak coupling, and applies to all possible gauge enhancements in those models at global weak coupling.

In terms of the geometry of the elliptic fibration of the component at weak coupling, the restriction arises from the compatibility of the j -invariant of the generic elliptic fibers with the one found over the 7-brane loci. At weak coupling the generic elliptic fiber is such that $j(\tau) \rightarrow \infty$, a property that is shared by Kodaira type I_m and I_m^* fibers. From the point of view of the physics, the constraint stems from the fact that the exceptional gauge groups G_2 , F_4 , E_6 , E_7 and E_8 are non-perturbative in Type IIB, and therefore cannot appear in a component in which locally $g_s \rightarrow 0$.

While it is clear that F_4 , E_6 , E_7 and E_8 cannot appear if only Kodaira type I_m and I_m^* singular fibers are allowed, the same is not true for G_2 ; it can be produced by folding the D_4 Dynkin diagram associated to a I_0^* fiber, see Table 6.3.2. However, one can check that the monodromy cover in a component Y^p at weak coupling never allows for I_0^{*ns} fibers. If we have I_0^* fibers over a divisor $\mathcal{D} = \{p_{\mathcal{D}} = 0\}_{B^p}$, the single accidental cancellation structure (B.9.4) means that the defining polynomials will take the form

$$f_p = -3 (p_{\mathcal{D}} h'_p)^2, \quad g_p = 2 (p_{\mathcal{D}} h'_p)^3, \quad h'_p \in H^0(B^p, \mathcal{L}_p^{\otimes 2} - \mathcal{D}). \quad (6.3.49)$$

Then, the monodromy cover for the I_0^* fiber is

$$\psi^3 + \psi \left. \frac{f_p}{p_{\mathcal{D}}^2} \right|_{p_{\mathcal{D}}=0} + \left. \frac{g_p}{p_{\mathcal{D}}^3} \right|_{p_{\mathcal{D}}=0} = \left(\psi + 2 \left. h'_p \right|_{p_{\mathcal{D}}=0} \right) \left(\psi - \left. h'_p \right|_{p_{\mathcal{D}}=0} \right)^2, \quad (6.3.50)$$

and hence always at least semi-split. This ensures that a I_0^{*ns} fibers will never be supported on \mathcal{D} , in alignment with the considerations above.

The fact that horizontal global weak coupling limits can only be constructed over $\hat{B} = \mathbb{F}_n$ with $0 \leq n \leq 4$, as discussed in Section 6.3.2.3, can also be understood from a physical standpoint. Global weak coupling limits must have an interpretation as perturbative Type IIB orientifold compactifications; the models constructed over $\hat{B} = \mathbb{F}_n$ with $5 \leq n \leq 12$ present non-Higgsable clusters with gauge algebra \mathfrak{f}_4 , \mathfrak{e}_6 , \mathfrak{e}_7 or \mathfrak{e}_8 , see Table 6.3.1, and should therefore be incompatible with the global weak coupling limit.

While in a generic F-theory model with internal space $\pi : Y \rightarrow B$ we have that

$$\text{ord}_Y(f, g)_D = (2, 3) \Rightarrow \text{ord}_Y(\Delta)_D \geq 6 \quad (6.3.51)$$

and the D_m type singularities start therefore at D_4 , we have observed that in a component Y^P at weak coupling we have instead

$$\text{ord}_{Y^P}(f, g)_D = (2, 3) \Rightarrow \text{ord}_{Y^P}(\Delta)_D \geq 2, \quad (6.3.52)$$

meaning that D_0 , D_1 , D_2 and D_3 type singularities are also possible. This was observed already in [156, 157] for eight-dimensional models, and the explanation is the same: The D_m type singularities are interpreted as O7-planes with m mutually local 7-branes on top. While this is allowed in the strict weak coupling limit $g_s \rightarrow 0$ for any value of m , such configurations split up into mutually non-local branes if $0 \leq m \leq 3$ when g_s takes a non-zero value [202, 203].

6.3.6 Bounds on the vertical gauge rank

With the classification of Section 6.3.3 in mind, gauge algebra factors can be classified into horizontal and vertical if they are supported on the homonymous divisor classes, with gauge enhancements over mixed divisors arising from the Higgsing of these contributions. From the point of view of the heterotic dual theory, a correspondence that we review in Section 6.4.1, this distinction is also pertinent: Horizontal and vertical gauge factors on the F-theory side correspond to perturbative and non-perturbative gauge contributions, respectively, on the dual heterotic side.¹¹

Obtaining a rough bound for the rank of the horizontal gauge algebras is therefore direct from heterotic considerations, from where we see that

$$\text{rank}(\mathfrak{g}_{\text{hor}}) \leq 18. \quad (6.3.53)$$

This bound can be saturated in models at finite distance by tuning two lines of II^* fibers over representatives of the curves classes C_0 and C_∞ in $\hat{B} = \mathbb{F}_n$, and a line of IV fibers over a representative of C_∞ . In models at infinite distance the bound becomes more stringent, as we discuss later for the six-dimensional models under study, and was already observed in the analysis of eight-dimensional limits in [156, 157], and from the point of view of heterotic toroidal compactifications in [276].

Due to the non-perturbative nature (from a heterotic standpoint) of the vertical gauge algebras, obtaining bounds for them is less immediate. They can, however, be extracted from the geometry on the F-theory side and lead to bounds displayed in Table 6.3.3. Attempting to surpass said bounds sends us to infinite-distance in the moduli space, so they can be regarded as a measure of how much tuning of the vertical sector is possible at finite-distance.

To understand the origin of these bounds, we recall that in a Hirzebruch surface $\hat{B} = \mathbb{F}_n$ a curve C can have negative intersection product $C \cdot h$ with the $(-n)$ -curve h if and only if C contains h as a component, a fact that was already exploited in Section 6.3.2.3. For generic models this leads to the appearance of the non-Higgsable clusters of Table 6.3.1, or their appropriate enhancements if the component is at weak coupling. Suppose now that a vertical gauge factor

$$\text{ord}_{Y_0}(f_{\text{phys}}, g_{\text{phys}}, \Delta_{\text{phys}})_{\mathcal{F}} = (\alpha, \beta, \gamma) \quad (6.3.54)$$

has been tuned. The global divisor \mathcal{F} traverses all components, and in particular goes through the Y^P component, where we will have component vanishing orders

$$\text{ord}_{Y^P}(f_P, g_P, \Delta'_P)_{V_P} \geq (\alpha, \beta, \gamma). \quad (6.3.55)$$

¹¹The non-perturbative heterotic gauge sector is completely accounted for once the gauge algebra factors supported over the exceptional curves resulting from the resolution of codimension-two finite-distance non-minimal points are also considered.

We are focusing on the component Y^P because it is the one in which forced factorizations of S_P in Δ'_P will occur. Indeed, the vertical tuning favours this even further, since

$$V_P \cdot S_P = 1 \Rightarrow (\Delta'_P - \gamma V_P) \cdot S_P < \Delta'_P \cdot S_P. \quad (6.3.56)$$

As a consequence, a high enough vertical tuning will lead to a non-minimal enhancement over the curve S_P , limiting the vertical gauge rank that can be realized in the class of models.

Given a bound $\max(\text{rank}(\mathfrak{g}_{\text{ver}}))$ for the vertical gauge rank computed by an analysis along these lines, the geometry enforces the bound in a similar fashion to how it prevents certain global weak coupling limits. Consider a horizontal model whose open-chain resolution leads to $\{Y^p\}_{0 \leq p \leq P}$ components for the central fiber Y_0 of the degeneration. Tuning vertical gauge factors over $\mathcal{F} = \sum_{p=0}^P V_p$ leads, as we have just discussed, to forced gauge enhancements over S_P in the Y^P component. As long the vertical gauge factors are such that

$$\text{rank}(\mathfrak{g}_{\text{ver}}) \leq \max(\text{rank}(\mathfrak{g}_{\text{ver}})), \quad (6.3.57)$$

the component vanishing orders over S_P can be minimal.¹² Tuning a higher vertical enhancement such that

$$\text{rank}(\mathfrak{g}_{\text{ver}}) > \max(\text{rank}(\mathfrak{g}_{\text{ver}})) \quad (6.3.58)$$

is possible, but the component vanishing orders over S_P will then be non-minimal,¹³ meaning that (possibly after a base change) a new base blow-up must be performed in the resolution process of the horizontal model. The central fiber Y_0 then has $\{Y^q\}_{0 \leq q \leq Q}$ components, with $Q > P$. In the subset $\{Y^p\}_{0 \leq p \leq P} \subset \{Y^q\}_{0 \leq q \leq Q}$ of these (intuitively) corresponding to the “original” components, the local vertical gauge enhancements over representatives of $\sum_{p=0}^P V_p$ can exceed the vertical gauge rank bound due to the tuning. However, $\sum_{p=0}^P V_p$ no longer is the global vertical class, which after the new resolution process is given by $\mathcal{F} = \sum_{q=0}^Q V_q$. In the new end-component, the vertical gauge rank bound must be respected by the local vertical enhancements. Otherwise, the arguments above would apply, and we would have a non-minimal enhancement over S_P , at the very least, at the level of the component vanishing orders. This would mean that we would not have an open-chain resolution free of obscured infinite-distance limits. Hence, the attempted global vertical enhancement is rendered a local enhancement by the model shedding a new component in which the bound on the vertical gauge rank is respected. This discussion is summarised below in Figure 6.4.

While we have framed the discussion in terms of the horizontal models with a multi-component central fiber, similar bounds also apply to the six-dimensional F-theory models over the Hirzebruch surfaces at finite-distance. In fact, since for such models we have that

$$\mathcal{L}_{B_0} = h + 2f + (h + nf) = \mathcal{L}_P + (h + nf) \quad (6.3.59)$$

and $(h + nf) \cdot h = 0$, the resulting bounds are the same that hold for multi-component horizontal models in which no components of the central fiber are at weak coupling. This means that tuning

¹²Some vertical enhancement patterns can saturate the bound $\max(\text{rank}(\mathfrak{g}_{\text{ver}}))$, while others are less efficient in their expenditure of the available vertical classes, and lead to a non-minimal enhancement over S_P before the bound on the vertical gauge rank is reached.

¹³Given (6.3.5c), we see that some patterns of codimension-zero singular elliptic fibers subtract S_P divisor classes from Δ'_P . When this occurs, a vertical enhancement surpassing the bound leads to pathological vanishing orders over S_P ; as discussed in Section 6.3.2.3, these are removed via an appropriate base change, after which the need for additional base blow-ups in order to resolve the degeneration becomes evident.

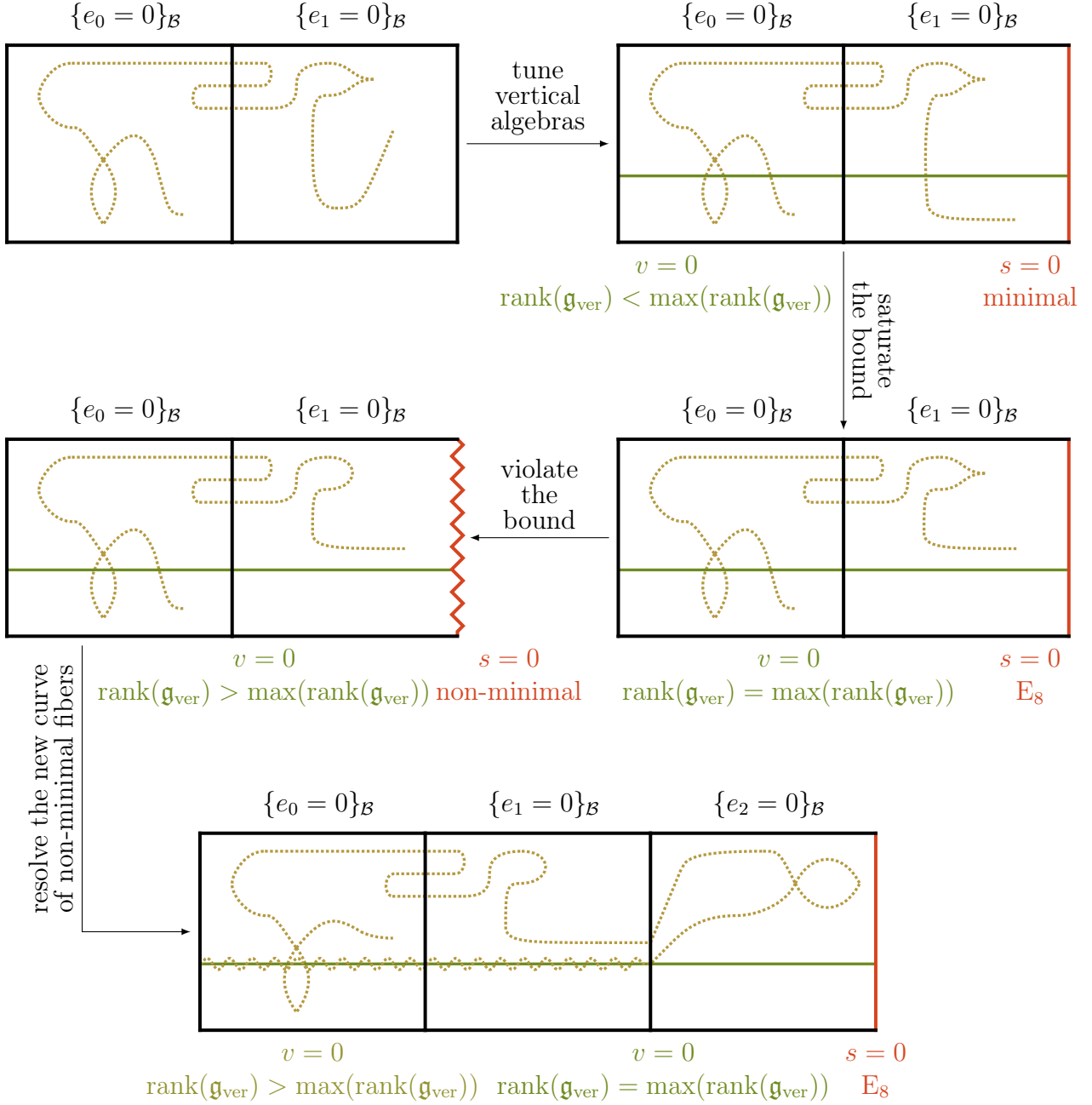


Figure 6.4: Tuning vertical algebras over representatives of the global divisor \mathcal{F} leads to forced enhancements over the S_P curve in the end-component. Eventually, the gauge factor supported on S_P corresponds to E_8 , meaning that further forced factorizations of S_P in Δ'_P will make it non-minimal. If we try to exceed the vertical gauge rank by a higher tuning over the representatives of \mathcal{F} , the model sheds a new component in which the bound is still satisfied, rendering the tuning a local enhancement. As a consequence, the bound is still respected from the global point of view that is used to assign the gauge algebras.

n	0	1	2	3	4	5	6	7	8	9	10	11	12
$\text{max}(\text{rank}(\mathfrak{g}_{\text{ver}}))$	18	17	16	16	10	9	8	8	4	2	1	0	0

Table 6.3.3: Bounds on the rank of the vertical gauge contribution in horizontal models, where n indicates the type of Hirzebruch surface $\hat{B} = \mathbb{F}_n$ over which the model is constructed.

too many vertical gauge factors in a Hirzebruch surface F-theory model leads to non-minimal elliptic curves over h , and therefore drives us to infinite distance in the moduli space.

Given that the mechanism enforcing the vertical gauge rank bounds is (6.3.56), it is clear that the bounds for models constructed over $\hat{B} = \mathbb{F}_n$ must become more stringent as we increase the value of n . In fact, for models constructed over $\hat{B} = \mathbb{F}_0$ the argument does not apply, since $h \cdot h = 0$. For these models, the distinction between horizontal and vertical divisors is arbitrary, since $\mathbb{F}_0 = \mathbb{P}_f^1 \times \mathbb{P}_b^1$; from the heterotic dual side, this corresponds to heterotic/heterotic duality [186, 187, 338]. Hence, the bound (6.3.53) also applies to the vertical gauge rank, and we have

$$\text{rank}(\mathfrak{g}_{\text{ver}}) \leq 18, \quad (6.3.60)$$

which applies to all horizontal models constructed over $\hat{B} = \mathbb{F}_n$ and is saturated for $\hat{B} = \mathbb{F}_0$.¹⁴

This bound can be refined by analysing the geometry in more detail. For example, for horizontal models in which no components are at weak coupling the bounds given in Table 6.3.3 apply, and we have checked in specific examples that they can be saturated. They are derived via the arguments given above, and we give an illustrative example of such a discussion in Section B.11.1. Once some components are at weak coupling, not all types of global gauge factors can be realised, as we elaborated on in Section 6.3.4. This makes the bounds on the vertical gauge rank become more stringent. For instance, for models constructed over $\hat{B} = \mathbb{F}_7$ the bound $\text{rank}(\mathfrak{g}_{\text{ver}}) \leq 8$ becomes $\text{rank}(\mathfrak{g}_{\text{ver}}) \leq 5$ as soon as one component is at weak coupling, see Section B.11.2. In addition to this effect, which depends solely on the existence of some components at weak coupling, the concrete pattern of codimension-zero singular elliptic fibers can reduce the maximal vertical gauge rank even further. For instance, consider again the models constructed over $\hat{B} = \mathbb{F}_7$. The bound $\text{rank}(\mathfrak{g}_{\text{ver}}) \leq 5$ can be saturated by tuning a vertical line of Kodaira type I_2^{*ns} fibers in a model with a $I_0 - I_1 - I_0$ pattern of codimension-zero singular elliptic fibers. The tuning of such a vertical gauge algebra forces an E_8 enhancement over the curve S_P . If the codimension-zero singular elliptic fibers appear instead in the pattern $I_0 - I_2 - I_0$, which can be achieved via a double cancellation structure according to the discussion in Section B.10.1, the number of local horizontal classes in Δ'_P is insufficient to realise an E_8 enhancement of the E_7 non-Higgsable cluster supported over S_P , meaning that any enhancement of it is non-minimal. This makes the vertical line of fibers saturating the bound $\text{rank}(\mathfrak{g}_{\text{ver}}) \leq 5$ not tunable in such a configuration.

6.4 Type II.a models as decompactifications with defects

Our interest in the degenerations $\hat{\rho} : \hat{\mathcal{Y}} \rightarrow D$ of elliptically fibered Calabi-Yau threefolds stems from the fact that they represent infinite-distance limits in the complex structure moduli space

¹⁴In a model constructed over $\hat{B} = \mathbb{F}_0$ and choosing to call the direction along which the splitting of the components occurs horizontal, the bound (6.3.53) becomes stricter in models at infinite distance, as we commented on above. The analogous vertical bound (6.3.60) remains, however, unaltered, since the vertical directions are “orthogonal” to the splitting of the components, and hence not really affected by it.

of six-dimensional F-theory. The central fiber Y_0 of the resolved degeneration $\rho : \mathcal{Y} \rightarrow D$ allows us to extract information about the asymptotic physics that these limits lead to. So far, we have mainly focused on two aspects: First, the possibility of realising global weak coupling limits, and second the gauge algebra content of the asymptotic models. Both facets of the problem were addressed in Section 6.3, with the discussion supported on the general analysis of the degenerations carried out in Chapter 5.

In determining the gauge algebra, we have thus far taken a six-dimensional standpoint. As we traverse an infinite distance in the moduli space, however, the theory may undergo a decompactification process that can lead to gauge enhancements as viewed from the perspective of the higher-dimensional theory. In fact, according to the Emergent String Conjecture [149], we expect the limits to have an interpretation either as decompactification or emergent string limits. In this section, we study how the information about the asymptotic physics extracted while insisting on the six-dimensional point of view reorganises itself once a more accurate picture for the endpoint of the limits is considered, and how the results fit with the Emergent String Conjecture. This was also the ultimate goal of the analogous systematic analysis in the moduli space of eight-dimensional F-theory carried out in [156, 157].

To this end, the single infinite-distance limit degenerations of Hirzebruch models that we focus on in the present chapter constitute an advantageous starting point for our survey for two reasons: F-theory compactified on an elliptically fibered Calabi-Yau threefold whose base is a Hirzebruch surface is dual to heterotic string theory compactified on a K3 surface. Additionally, horizontal degenerations of Hirzebruch models are a fiberwise generalisation of the degenerations of K3 surfaces studied in [156, 157], as we discussed in Section 6.3.1. This offers two complementary perspectives on the limits from which to extract the asymptotic physics. As we will explain, horizontal Type II.a limits are the perfect subclass to exploit this approach, and we focus on them in the remainder of this section.

We start in Section 6.4.1 by reviewing F-theory/heterotic duality and the conditions that need to be fulfilled in order to have explicit control over the corresponding duality map. In Section 6.4.2 we analyse the generic vertical slices of horizontal Type II.a models, which encode information about the bulk asymptotic physics. We focus first on studying the endpoints of horizontal Type II.a models constructed over $\hat{B} = \mathbb{F}_0$, providing a complete analysis in the so-called adiabatic regime and pointing out the challenges arising in a naive extension of these results away from it; the models constructed over $\hat{B} = \mathbb{F}_n$, whose asymptotic physics differs only slightly, are considered in Section 6.4.4. Our analysis also offers interesting new insights into the heterotic theory by itself. First, as we note in Section 6.4.5, non-minimal singularities of the heterotic K3 surface correspond to codimension-one infinite-distance degenerations on the F-theory side, after an appropriate base change has been performed. Furthermore, we comment on the role of vertical gauge algebras on the F-theory side as part of the non-perturbative heterotic gauge sector. This discussion is relegated to Appendix B.12.

6.4.1 F-theory/heterotic duality

F-theory/heterotic duality in six dimensions is a valuable tool to gain intuition about the asymptotic physics associated with the limits under study. In this section, we review how this duality works.¹⁵ Our focus is on the $E_8 \times E_8$ heterotic string, although the duality can also be taken to the $Spin(32)/\mathbb{Z}_2$ theory.

¹⁵A clear and succinct summary of the duality in 8D, 6D and 4D can also be found in [339].

In eight dimensions, F-theory compactified on a K3 surface is dual to heterotic string theory compactified on T_{het}^2 [89]. The F-theory side is defined by pure geometry, which is mapped to geometric, B-field and gauge bundle data on the heterotic side. If we demand the heterotic gauge group to be unbroken, i.e. we freeze the 16 Wilson line moduli at an appropriate point in the moduli space, the remaining complex structure and complexified Kähler modulus of T_{het}^2 can be very explicitly matched to the F-theory side, with the map between the two eight-dimensional theories constructed in [340–342].

The duality map becomes more subtle once we allow the heterotic gauge group to be broken, and hence need to also take into account the heterotic gauge bundle moduli. The data on both sides can be matched in a particular limit, which in the F-theory side is the stable degeneration limit of the K3 surface. On the heterotic side, this limit corresponds to the decompactification limit obtained by sending the area of T_{het}^2 to infinity. These are the Kulikov Type II.a decompactification limits studied in [156, 157] and reviewed in Section 6.2.1. The K3 surface $Y_{\hat{u} \neq 0}$ on the F-theory side degenerates into two log Calabi-Yau components $Y_0 = Y^0 \cup_{\mathcal{E}} Y^1$ glued along their boundaries, in this case an elliptic curve \mathcal{E} which is identified with the compactification space on the heterotic side. Each of the components $\{Y^p\}_{0 \leq p \leq 1}$ is a dP_9 surface. The data of the two E_8 heterotic bundles V_0 and V_1 is encoded in $\text{Def}(Y^0)$ and $\text{Def}(Y^1)$, respectively. One can intuitively think of this limit on the F-theory side as an elongation of the base \mathbb{P}^1 of the internal K3 surface separating the two poles of the sphere; the elongated \mathbb{P}^1 is then identified with the Hořava-Witten interval, with each of the poles associated with the information of one of the E_8 heterotic factors [186, 187]. Hence, the ten-dimensional heterotic dilaton is mapped to the volume of the base of the F-theory K3 surface measured in Type IIB string units

$$\mathcal{V}_{\mathbb{P}^1}^{\text{IIB}} \sim g_{\text{het}}. \quad (6.4.1)$$

The stable degeneration limit separates the Wilson line moduli information and ensures that the duals of the F-theory backgrounds are given by geometric compactifications of the heterotic string. Away from this boundary of the moduli space, the $O(\Lambda^{2,18})$ symmetry of the heterotic compactification on T_{het}^2 mixes the complex structure and complexified Kähler modulus of T_{het}^2 with the Wilson line moduli, making the heterotic compactification non-geometric. The connection between the two sides of the duality can still be made explicit when only a single Wilson line modulus is allowed to be non-zero, leading to an $E_7 \times E_8$ gauge symmetry [343–345].

This duality is the starting point to obtain a lower-dimensional duality as follows. Consider a theory A in D_A dimensions and a theory B in D_B dimensions that are dual to each other when compactified on the varieties X and Y , respectively, with dimensions $\dim(X) = D_A - d$ and $\dim(Y) = D_B - d$. Fibering the compactifications spaces over a common base B , the theories compactified on the total spaces

$$\begin{array}{ccc} X & \longrightarrow & \mathcal{X} \\ & & \downarrow \pi_A \\ & & B \end{array} \quad \text{and} \quad \begin{array}{ccc} Y & \longrightarrow & \mathcal{Y} \\ & & \downarrow \pi_B \\ & & B \end{array} \quad (6.4.2)$$

live in $d - \dim(B)$ dimensions. In a local patch, the fibrations can be trivialised to look like the product spaces $X \times \mathbb{R}^{\dim(B)}$ and $Y \times \mathbb{R}^{\dim(B)}$. If the parameters of the d -dimensional theories are varying slowly over B and the volumes exhibit the hierarchy $\mathcal{V}_B \gg \mathcal{V}_X$ and $\mathcal{V}_B \gg \mathcal{V}_Y$, a low-energy observer will not be able to locally distinguish between the theories A and B on the spaces $\mathcal{X} \times \mathbb{R}^{1,d-\dim(B)-1}$ and $\mathcal{Y} \times \mathbb{R}^{1,d-\dim(B)-1}$, respectively, and the theories on the spaces $X \times \mathbb{R}^{\dim(B)} \times \mathbb{R}^{1,d-\dim(B)-1}$ and $Y \times \mathbb{R}^{\dim(B)} \times \mathbb{R}^{1,d-\dim(B)-1}$. Since for the latter two the

d -dimensional duality applies, the low-energy observer can use it to translate from one description to the other. Given the slow variation of the d -dimensional parameters, it is reasonable to assume that the equivalence will remain valid globally as long as the low-energy observer suitably redefines the physical quantities while looping around B . This is a fiberwise application of the d -dimensional duality enabled by an adiabaticity assumption.¹⁶ Note that if there are loci in B over which the fiber degenerates, the compactification space will not look like a product variety in a neighbourhood around them, and the adiabaticity assumption hence fails. It is therefore reasonable to expect the physics new to $d - \dim(B)$ dimensions to be concentrated at these loci, as we will see in Section 6.4.3 is indeed the case.

In our context, this reasoning leads to the well-known duality between the heterotic string compactified on an elliptically fibered manifold X_d ,

$$\begin{array}{ccc} \mathcal{E} & \longrightarrow & X_d \\ & & \downarrow \pi_{\text{het}} \\ & & B_{d-1}, \end{array} \quad (6.4.3)$$

and F-theory compactified on a manifold Y_{d+1} fibered by elliptic K3 surfaces. The two fibrations

$$\begin{array}{ccc} \mathcal{E} & \longrightarrow & Y_{d+1} \\ & \downarrow \pi_{\text{ell}} & \text{and} \\ & & B_d \\ & & \text{K3} \longrightarrow Y_{d+1} \\ & & \downarrow \pi_{\text{K3}} \\ & & B_{d-1} \end{array} \quad (6.4.4)$$

are compatible in the sense that they fit into the diagram

$$\begin{array}{ccc} Y_{d+1} & \xrightarrow{\pi_{\text{ell}}} & B_d \\ \pi_{\text{K3}} \downarrow & & \downarrow \pi_{\mathbb{P}^1} \\ B_{d-1} & \xleftarrow{=} & B_{d-1} \end{array} \quad (6.4.5)$$

In particular, the base manifold B_d is, therefore, \mathbb{P}^1 -fibered itself.

When $d = 2$, the resulting lower-dimensional effective theories are six-dimensional, with the internal space on the F-theory side being an elliptically fibered Calabi-Yau threefold with base $B_2 = \mathbb{F}_n$, and the internal space on the heterotic side being a K3 surface that is an elliptic fibration over $B_1 = \mathbb{P}_b^1$. On the F-theory side, these are the types of compactifications whose complex structure infinite-distance limits we study, which therefore correspond to infinite-distance limits of heterotic string theory compactified on K3 upon taking the duality.

This six-dimensional duality was considered for the first time in [186, 187], with a comparison of the moduli spaces carried out in [190] by counting parameters on the two sides. The matching of the moduli spaces was made fully precise in the stable degeneration limit in [326, 347]. In this limit, the K3 fibers on the F-theory side undergo the stable degeneration limit discussed for the eight-dimensional duality above, i.e. they become Kulikov Type II.a models. The F-theory Calabi-Yau threefold splits into two log Calabi-Yau components $Y_0 = Y^0 \cup_{\text{K3}} Y^1$ glued along their boundaries, which are the K3 surface that is identified with the heterotic compactification

¹⁶Such a type of argument was used early on in the study of string dualities to establish connections between Type II and heterotic string theories [346].

space. This geometry corresponds to that of horizontal Type II.a models, in the language of Section 6.3.1, which are the relative version of the Kulikov Type II.a models found for the fiber, in accordance with the fiberwise construction of the duality. The data of the two E_8 heterotic bundles V_0 and V_1 is once again encoded in $\text{Def}(Y^0)$ and $\text{Def}(Y^1)$, respectively. Furthermore, we have the relation

$$\frac{\mathcal{V}_{\mathbb{P}_f^1}}{\mathcal{V}_{\mathbb{P}_b^1}} \sim (g_{\text{het}}^{\text{6D}})^2. \quad (6.4.6)$$

Note that when $B_2 = \mathbb{F}_0$, the two \mathbb{P}^1 factors present in the internal geometry on the F-theory side of the duality are on equal grounds. Exchanging them corresponds to heterotic/heterotic duality, which inverts the heterotic string coupling, as can be read from (6.4.6). Although the duality between F-theory and heterotic string theory is expected to hold in general, the precise map between the two is available only when we have the hierarchy of volumes

$$\mathcal{V}_{\mathbb{P}_b^1} \gg \mathcal{V}_{\text{K3}} \quad (\text{F-theory side}), \quad (6.4.7)$$

$$\mathcal{V}_{\mathbb{P}_b^1} \gg \mathcal{V}_{T_{\text{het}}^2} \quad (\text{heterotic side}), \quad (6.4.8)$$

which implements the adiabaticity of the fibrations¹⁷ on both sides, as is necessary for the fiberwise application of the eight-dimensional duality. Additionally, the volume of the heterotic elliptic curve $\mathcal{V}_{T_{\text{het}}^2} \rightarrow \infty$ as a consequence of the stable degeneration limit, and $\mathcal{V}_{\mathbb{P}_b^1} \gg \mathcal{V}_{\mathbb{P}_f^1}$ in order to be at weak heterotic coupling.

On the heterotic side, the E_8 bundles V_0 and V_1 are poly-stable, with

$$c_1(V_i) = 0 \pmod{2}, \quad i = 0, 1. \quad (6.4.9)$$

On the F-theory side, this maps to the usual condition that the total compactification space Y_0 must be a (possibly singular) Calabi-Yau manifold, even if the individual components after the stable degeneration are not. The integrated Bianchi identity on the heterotic side reads

$$c_2(V_0) + c_2(V_1) = c_2(\text{K3}) = 24, \quad (6.4.10)$$

which is fulfilled by a distribution of instanton numbers $c_2(V_{0,1}) = 12 \pm n$. On the F-theory side, the choice of how the heterotic instanton numbers are distributed corresponds to the choice of the Hirzebruch surface $\hat{B} = \mathbb{F}_n$ over which the horizontal Type II.a model is constructed. In our notation, the log Calabi-Yau component Y^1 corresponds to the gauge bundle V_1 with the smaller instanton number. As a result, it is this component that harbours the non-Higgsable cluster present when $n \geq 3$, i.e. when $c_2(V_1) < 10$.

The following point will be particularly important for our analysis: The heterotic gauge bundles are allowed to become singular by concentrating their curvature (or at least part of it) at a point, a situation in which the vector bundle would be more precisely described as a sheaf, with the aforementioned points of concentrated curvature being skyscraper sheaves. The subset of these that are point-like instantons with trivial holonomy contribute 1 unit each to $c_2(V_{\text{het}})$. Through a small instanton transition, a singular bundle contribution corresponding to a point-like instanton with trivial holonomy can be regarded as an NS5-brane or, in the language of heterotic M-theory, an M5-brane that can be separated from the Hořava-Witten walls and moved into the S^1/\mathbb{Z}_2 interval. This is allowed because a point-like instanton with

¹⁷In the precise formulation of the duality using vector bundles obtained via the spectral cover construction [326, 347], this guarantees the stability of said bundles.

trivial holonomy has 1 hypermultiplet parametrizing its position on the heterotic K3 surface, and 29 hypermultiplets parametrizing the deformations that would give finite volume to the curvature support. In the gravitational anomaly cancellation formula, we can trade the latter 29 hypermultiplets for 1 tensor, signalling that the configuration can be seen as an M5-brane with 1 hypermultiplet and 1 tensor multiplet in its worldvolume. Their scalars parametrize its position on the K3 surface and the Hořava-Witten interval, respectively [338, 348]. Having m such M5-branes modifies the integrated Bianchi identity to

$$c_2(V_1) + c_2(V_2) + m = c_2(\text{K3}) = 24. \quad (6.4.11)$$

We see that each brane contributes like 1 unit of instanton charge in this equation. Importantly, there can be additional types of singular gauge bundle contributions beyond point-like instantons with trivial holonomy. Apart from being interesting by themselves, these play a central role in our understanding of the gauge algebras on vertical divisors on the F-theory side. We describe them in more detail in Section B.12.2.

Trading a point-like instanton with trivial holonomy associated to one of the Hořava-Witten walls for an M5-brane, moving it to the opposite Hořava-Witten wall, and dissolving it back into gauge bundle changes the instanton number distribution between V_0 and V_1 . On the F-theory side, the point-like instantons with trivial holonomy that can be traded for the M5-branes correspond to codimension-two finite-distance non-minimal singularities. The possibility of blowing up the base in order to resolve them corresponds to moving the associated M5-branes through the Hořava-Witten interval; the distance to the Hořava-Witten walls is parametrized by a scalar in a tensor multiplet on the heterotic side, that on the F-theory side corresponds to the volume of the exceptional \mathbb{P}^1 curves introduced in the base blow-ups. Taking an M5-brane to the opposite Hořava-Witten wall and dissolving it into gauge bundle is identified with blowing up the base to produce an exceptional \mathbb{P}^1 and shrinking some other curve in order to recover a different Hirzebruch surface than the starting one. This coincides with the heterotic picture of redistributing the instanton numbers between V_0 and V_1 . The points in the moduli space in which the exceptional curves are kept contracted correspond to the origin of the tensor branch of the SCFTs associated with the codimension-two finite-distance non-minimal singularities, see [270] for a review.

6.4.2 Horizontal Type II.a models: generic vertical slices

The preceding discussion shows how useful it can be, when dealing with a relative model, to exploit our knowledge of the physics associated with the fibers as much as possible. As advanced in the introduction, this is the reason we focus on horizontal Type II.a models as the starting point of our analysis: We have just seen them naturally appear in the fiberwise extension of the eight-dimensional F-theory/heterotic duality, and they also are a relative version of the degenerations of K3 surfaces that were studied in detail in [156, 157]. In this spirit, we commence by analysing the physics associated with their vertical slices.

Horizontal Type II.a models with an open-chain resolution $\rho : \mathcal{Y} \rightarrow D$ were defined in Section 6.3.1 to be those whose generic vertical restriction $\sigma : \mathcal{Z} \rightarrow D$ is a Kulikov Type II.a model. In terms of the pattern of codimension-zero singular elliptic fibers, this is equivalent to demanding that no component is at weak coupling. Taking into consideration the expressions (6.3.5) for the restrictions $\{\Delta'_p\}_{0 \leq p \leq P}$ of the modified discriminant Δ' and the discussion on the local and global 7-brane content in Section 6.3.4, the intermediate components offer redundant information, and can be blown down to present the central fiber Y_0 as a two-component model. We assume in the remainder of the section that this has been done.

As in a Kulikov Type II.a model, the elliptic fiber of the central fiber Z_0 of the generic vertical restriction $\sigma : \mathcal{Z} \rightarrow D$ associated with a generic point $p_b \in \mathbb{P}_b^1$ degenerates over 12 points in each of the bases of the $\{Z^p\}_{0 \leq p \leq 1}$ components. This can be read from

$$\Delta_{\text{phys}} \cdot \mathcal{F} = 12 + 12, \quad (6.4.12)$$

where we recall the definition of the vertical class \mathcal{F} in (6.3.30). These degeneration points are given by the restriction of the horizontal (or mixed) global divisors in B_0 to the chosen generic vertical slice. Regarding $\sigma : \mathcal{Z} \rightarrow D$ as representing an infinite-distance limit in the complex structure moduli space of eight-dimensional F-theory, these are the two sets of 12 7-branes that furnish the two double loop algebras \hat{E}_9 sharing a common imaginary root and hence yielding the gauge algebra

$$G_\infty = (\hat{E}_9 \oplus \hat{E}_9) / \sim \quad (6.4.13)$$

as seen from the eight-dimensional standpoint; the algebra G_∞ is reinterpreted as

$$G_{10D} = E_8 \oplus E_8 \quad (6.4.14)$$

in the higher-dimensional theory that results from the limit, as we reviewed in Section 6.2, after the $U(1)_{KK}^2$ are reintegrated into the metric degrees of freedom. The positions of these two sets of 12 7-branes within their components is not relevant for the eight-dimensional asymptotic physics: They appear separated due to the resolution process employed to read off the physical information, but are to be taken as lumped together at the endpoint of the limit. Choosing a different generic point $p'_b \in \mathbb{P}_b^1$ to construct the generic vertical slice leads to a Kulikov Type II.a model whose only difference with the one just discussed is the position of the 7-branes within the components that they belong to. Therefore, the asymptotic physics of the associated eight-dimensional model is the same for all generic vertical slices of the horizontal Type II.a model. This is depicted in Figure 6.5.

There are 24 representatives of the vertical class \mathcal{F} (counted with multiplicity) that do not lead to a Kulikov Type II.a model presented in the resolved form used in [156, 157], as can be seen from

$$\Delta'_0 \cdot S_0 = \Delta'_1 \cdot T_1 = 24. \quad (6.4.15)$$

The way in which this can fail is either by one (or both) of the components of the vertical restriction presenting codimension-zero singular fibers, or by the eight-dimensional model exhibiting special fibers at the intersection of the components. We illustrated both situations in Figure 6.5. Under the adiabaticity assumption explained in Section 6.4.1, the heterotic dual theory is compactified on the elliptic K3 surface $Y^0 \cap Y^1$, with (6.4.15) corresponding to the 24 points over which the elliptic fiber must degenerate in such a surface. At these points the adiabaticity assumption fails, and we therefore expect purely six-dimensional features to arise, in alignment with the fiberwise argumentation. Since this only occurs over these isolated loci, the generic vertical slice of the horizontal Type II.a model will inform us about the bulk physics at the endpoint of the infinite-distance limit, while the points of failure of the adiabaticity assumption will relate to localised effects in the asymptotic theory, as we now argue in Section 6.4.3.

6.4.3 Horizontal Type II.a models over $\hat{B} = \mathbb{F}_0$

Horizontal Type II.a models constructed over $\hat{B} = \mathbb{F}_0$ constitute the most straightforward relative version of their eight-dimensional counterparts, due to the direct product nature of $\mathbb{F}_0 = \mathbb{P}_f^1 \times \mathbb{P}_b^1$.

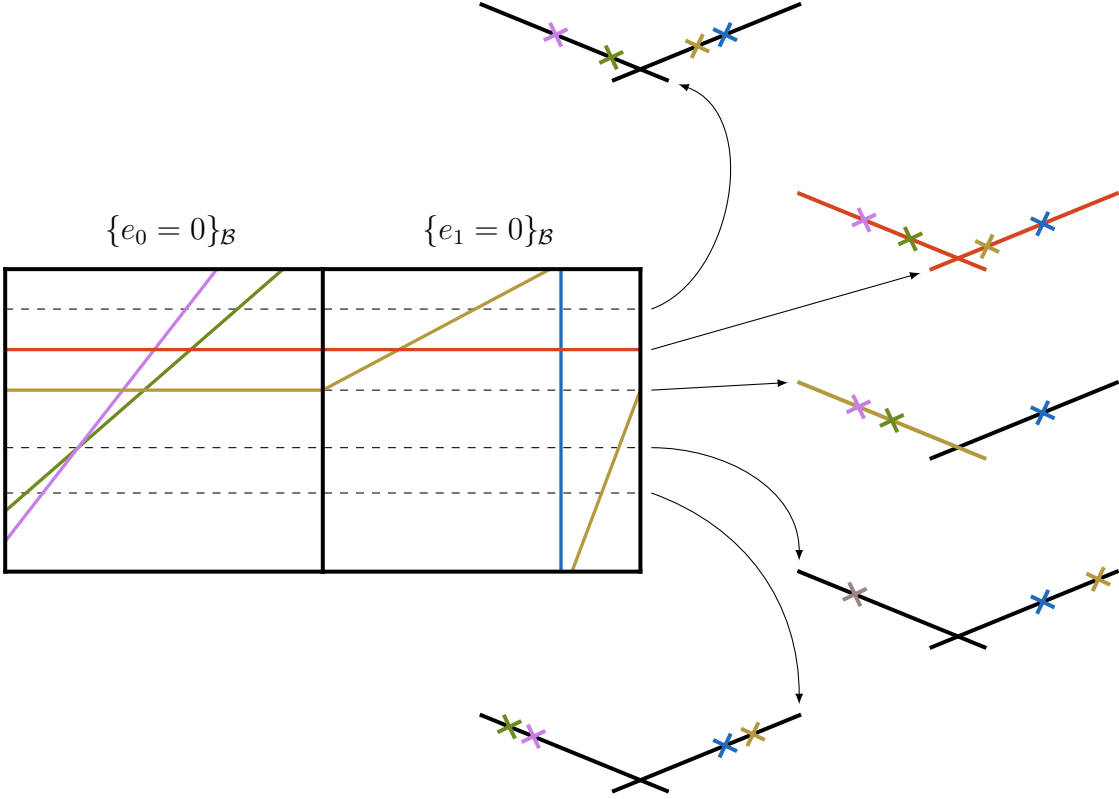


Figure 6.5: We schematically represent the base of the central fiber of a resolved horizontal Type II.a model constructed over $\hat{B} = \mathbb{F}_n$, with $n \geq 1$, on the left, and various vertical slices of it on the right. A reduced number of global 7-branes are depicted: two in the divisor class \mathcal{H}_∞^0 , one in \mathcal{H}_∞^1 , one in \mathcal{H}_0^1 and one in \mathcal{F} . The first, fourth and fifth vertical slices are generic and lead to Kulikov Type II.a models. This is not true for the second vertical slice, since it overlaps with the global 7-brane in the class \mathcal{F} in both components, and for the third vertical slice, since it overlaps with the global 7-brane in the class \mathcal{H}_∞^1 in the B^0 component.

Moreover, let us assume for now the structure

$$f = p_8^f([s : t], u)q_8^f([v : w], u), \quad (6.4.16a)$$

$$g = p_{12}^g([s : t], u)q_{12}^g([v : w], u), \quad (6.4.16b)$$

for the defining polynomials of the Weierstrass model of $\hat{\mathcal{Y}}$, which leads to central fibers Y_0 in which only the global divisor classes \mathcal{H}_∞^0 , \mathcal{H}_∞^1 , \mathcal{H}_0^1 and \mathcal{F} (defined in Section 6.3.3) can support gauge enhancements. This restricts our attention to the simplest possible horizontal Type II.a models, in which all generic vertical slices lead to, not only equivalent, but identical Kulikov Type II.a models. We now analyse these models in detail, relaxing the assumption (6.4.16) at the end of the section; the cases in which $\hat{B} = \mathbb{F}_n$ with $n \geq 1$ are treated in Section 6.4.4, and only differ slightly.

6.4.3.1 Analysis in the adiabatic regime: Decompactification with defects

In order to extract the asymptotic physics associated with horizontal Type II.a models, let us consider the adiabaticity assumption reviewed in Section 6.4.1 to hold. On the F-theory side, the hierarchy of volumes $\mathcal{V}_{\mathbb{P}_b^1} \gg \mathcal{V}_{K3}$ makes the fiberwise analysis of the geometry accurate, while

at the same time granting us explicit access to the heterotic dual models. We can then use the latter, in which the hierarchy of volumes $\mathcal{V}_{\mathbb{P}_b^1} \gg \mathcal{V}_{T_{\text{het}}^2}$ must hold, to confirm the findings on the F-theory side from a different perspective. The difficulties that arise in the interpretation of the F-theory model away from the adiabatic regime are discussed in Section 6.4.3.3.

Commencing on the F-theory side, we can analyse the horizontal Type II.a model by first taking vertical slices of the central fiber of the degeneration, and then completing the analysis by considering the horizontal slices as well.¹⁸

Consider the vertical slice of a horizontal Type II.a model associated with a generic point $p_b := [v_0 : w_0] \in \mathbb{P}_b^1$. Such slices were already studied in Section 6.4.2: they correspond to Kulikov Type II.a models with two sets of 12 7-branes, one in each of the $\{Z^p\}_{0 \leq p \leq 1}$ components of Z_0 . In a Kulikov Type II.a model, both components $\{Z^p\}_{0 \leq p \leq 1}$ have smooth codimension-zero elliptic fibers. Moreover, the resolution process of the degeneration $\hat{\rho} : \hat{\mathcal{Y}} \rightarrow D$ discussed in Chapter 5 ensures that no special fibers are found over the intersection $(B^0 \cap B^1)|_{[v:w]=p_b}$. As a consequence, no monodromy acts on the two 1-cycles $\sigma_i \in H_1(\mathcal{E}, \mathbb{Z})$, for $i = 1, 2$, of the elliptic fiber \mathcal{E} as we move around the base $B_0|_{[v:w]=p_b}$ of Z_0 . The geometry of $B_0|_{[v:w]=p_b}$ is that of two \mathbb{P}^1 curves intersecting over a point; a 1-cycle $\Sigma \in H_1(\mathbb{P}^1, \mathbb{Z})$ defined in either of the base components and encircling their intersection point can be deformed to the antipodal point, and is therefore trivial. However, fibering $\{\sigma_i\}_{i=1,2}$ over Σ leads to two non-trivial 2-cycles $\{\gamma_i\}_{i=1,2}$ in $H_2(Z_0, \mathbb{Z})$. Taking a string junctions perspective in the generic associated eight-dimensional model, this corresponds to the possibility of defining two non-trivial loop junctions encircling, in one base component, both the intersection point $(B^0 \cap B^1)|_{[v:w]=p_b}$ and one of the sets of 12 7-branes.¹⁹ In the generic associated eight-dimensional model, these loop junctions grant the double loop enhancement of the algebras coming from the two sets of 12 7-branes to (6.4.13), see [294]. The winding strings represented by the loop junctions become asymptotically massless because they are allowed to shrink to the point $(B^0 \cap B^1)|_{[v:w]=p_b}$ of the resolved geometry.²⁰ Alternatively, the calibrated volumes of the 2-cycles $\{\gamma_i\}_{i=1,2}$ vanish at the endpoint of the limit and, as a consequence, M2-branes wrapped on them lead to asymptotically massless particles; these are the particle states leading to the aforementioned enhancement [156, 157].

In those patches of Y_0 that only contain generic vertical slices, the preceding analysis extends locally. Moreover, and due to the adiabaticity assumption, the non-generic vertical slices are well separated and the parameters of the fibral models vary slowly over the base, making the range of validity of such a patch large. Hence, the 2-cycles $\{\gamma_i\}_{i=1,2}$ can be consistently defined over the generic points of \mathbb{P}_b^1 . As mentioned in Section 6.4.2, all generic vertical slices lead to associated eight-dimensional models whose asymptotic physics coincides. Altogether, a consistent picture arises over all of Y_0 but the measure zero set associated to the 24 non-generic points of \mathbb{P}_b^1 : M2-branes wrapping the local 2-cycles $\{\gamma_i\}_{i=1,2}$ generate two asymptotically massless towers of particles, signalling a partial decompactification that is to be overlaid with the partial decompactification resulting from enforcing the hierarchy of volumes necessary to situate the model in the adiabatic regime. This results, at least in the adiabatic regime, in a total decompactification to ten dimensions, as we will also argue from the dual heterotic side

¹⁸Mixed slices do not provide additional insights, as they essentially are an interpolating case between the previous two, and we therefore do not consider them.

¹⁹The two loop junctions under consideration have no asymptotic charge, which implies that their self-intersection is trivial. They are left invariant by the monodromy of the 12 7-branes that they encircle, and have non-vanishing charge in the junction lattice. This last fact prevents us from trivially contracting them, as this generates additional junctions through the Hanany-Witten effect.

²⁰In the unresolved central fiber the loop junctions can also shrink, since all 7-branes of one of the two sets of 12 are located at the same point to produce the non-minimal singularity.

below. The aforementioned towers also provide the necessary additional states to furnish the enhanced gauge algebras. Said enhancement affects, in each generic vertical slice, the gauge algebra stemming from the restriction of the horizontal 7-branes. Since this applies to almost all points of the internal space, we conclude that the gauge algebra factors obtained from the six-dimensional standpoint from global 7-branes in the divisor classes \mathcal{H}_∞^0 , \mathcal{H}_∞^1 and \mathcal{H}_0^1 , together with the asymptotically massless towers of particles, lead to the double loop algebra

$$G_\infty = \left(\hat{E}_9 \oplus \hat{E}_9 \right) / \sim, \quad (6.4.17)$$

which is reinterpreted from the point of view of the decompactified theory in ten dimensions as the bulk gauge algebra

$$G_{10D} = E_8 \times E_8. \quad (6.4.18)$$

The arguments used to construct the local 2-cycles $\{\gamma_i\}_{i=1,2}$ fail over the 24 non-generic points in \mathbb{P}_b^1 , and the two asymptotically massless towers associated to M2-branes wrapped on them are, consequently, furnished by non-BPS particles, since the 2-cycles trivialise from the global perspective. To see this, consider first the situation in which Y_0 presents an enhancement over a representative of \mathcal{F} whose (possibly covering) gauge algebra is in the D or E family. Then, the codimension-zero fibers in the $\{Z^p\}_{0 \leq p \leq P}$ components will be of the corresponding Kodaira type, and so will be the fibers over the intersection point $(B^0 \cap B^1)|_{[v:w]=p_b}$. The monodromy action²¹ induced by encircling this point leaves no 1-cycle in $H_1(\mathcal{E}, \mathbb{Z})$ invariant, and we therefore cannot consistently construct a 2-cycle in $H_2(Z_0, \mathbb{Z})$ by fibering 1-cycles over Σ . Alternatively, but using the language of string junctions, no monodromy invariant loop junction encircling $(B^0 \cap B^1)|_{[v:w]=p_b}$ can be defined. If, instead, all enhancements over representatives of \mathcal{F} are associated with elliptic fibers of Kodaira type I_m and hence in the A family, the monodromy action produced by looping around $(B^0 \cap B^1)|_{[v:w]=p_b}$ does leave one 1-cycle in $H_1(\mathcal{E}, \mathbb{Z})$ invariant, allowing for the consistent construction of a 2-cycle in $H_2(Z_0, \mathbb{Z})$. This was to be expected, since the restriction of a horizontal Type II.a model to a representative of \mathcal{F} supporting I_m fibers leads to a Kulikov Type III.b model. The global picture remains, however, unaltered: While in the restriction to each vertical line of I_m fibers these arguments can be used to claim that one of the local 2-cycles $\{\gamma_i\}_{i=1,2}$ survives, the collection of these vertical enhancements is mutually non-local. The surviving 2-cycle found over one of the vertical enhancements is hence incompatible with the one found over at least one of the others, since the invariant 1-cycle in $H_1(\mathcal{E}, \mathbb{Z})$ used in its construction is not invariant under the monodromy action induced by encircling the other vertical lines of I_m fibers. We conclude that, indeed, the local 2-cycles $\{\gamma_i\}_{i=1,2}$ cannot be defined globally.

We propose the following interpretation: Away from the non-generic vertical fibers, the theory asymptotically decompactifies to ten dimensions, with two KK towers from wrapped M2-branes along the locally defined vanishing 2-cycles (completed by the supergravity KK tower associated with the large base \mathbb{P}_b^1). The fact that these are not globally defined, and in particular cease to exist over the 24 non-generic vertical fibers means that the degrees of freedom localised there cannot form bound states with the KK towers. They therefore remain as six-dimensional defects in the asymptotically decompactifying bulk.

This picture is further supported by analysing the horizontal slices of the model. While vertical slices correspond to restrictions of Y_0 to representatives of \mathcal{F} , the number of horizontal curve classes that we can restrict to is greater. In a horizontal Type II.a model the irreducible possibilities are \mathcal{H}_∞^0 , \mathcal{H}_0^0 , \mathcal{H}_∞^1 and \mathcal{H}_0^1 , with the horizontal slice obtained by restricting to \mathcal{H}_0^0

²¹See [157] for the explicit matrix representation of the monodromy action, following the conventions of [294].

corresponding to the dual heterotic internal space in the adiabatic regime. However, since $B^0 \cong B^1 \cong \mathbb{F}_0$, these curve classes are linearly equivalent; the restricted models obtained from them have the same number

$$\Delta'_0 \cdot \mathcal{H}_\infty^0 = \Delta'_0 \cdot \mathcal{H}_0^0 = \Delta'_1 \cdot \mathcal{H}_\infty^1 = \Delta'_1 \cdot \mathcal{H}_0^1 = 24 \quad (6.4.19)$$

of 7-branes, and all lead to the same asymptotic picture. Generic horizontal slices correspond to the restriction of Y_0 to either a generic point $p_f \in \mathbb{P}_{f,0}^1$ or a generic point $p_f \in \mathbb{P}_{f,1}^1$. Their restricted geometry is that of a Kulikov Type I model, with base \mathbb{P}_b^1 , for which no asymptotically massless towers arise. Using the string junctions picture, this can be seen from the fact that a non-trivial loop junction encircling 12 of the 7-branes cannot shrink to a point, since there is no intersection point with a second base \mathbb{P}^1 curve containing the remaining branes, nor are the 12 7-branes lumped together to produce a non-minimal singularity. Hence, the gauge algebra factors arising from the restricted 7-branes do not enhance to gauge contributions that can be reinterpreted as bulk degrees of freedom in the decompactified theory, since the previous argument is common to all generic horizontal slices. Note that the 24 restricted branes stem from the intersections of the vertical classes in the discriminant with the horizontal curve used to slice the model. As a consequence, we can indeed conclude that the vertical gauge algebras supported over representatives of \mathcal{F} remain lower-dimensional, and are localised in the worldvolume of six-dimensional defects.

The collision of horizontal and vertical components of the physical discriminant Δ_{phys} can lead to codimension-two finite-distance non-minimal enhancements²² that can be resolved via a base blow-ups and the appropriate line bundle shifts. Since each exceptional curve arising from such a resolution procedure is completely contained in one of the two base components $\{B^p\}_{0 \leq p \leq 1}$, any local gauge enhancement supported on them is automatically a global gauge enhancement. Through the same arguments employed in the analysis of the vertical gauge algebra factors, we conclude that also these contributions remain lower-dimensional in the limit and are localised in the world-volume of six-dimensional defects present in the asymptotic model.

Summarising the discussion, horizontal Type II.a models in the adiabatic regime lead to a decompactification process from six to ten dimensions in which the horizontal 7-branes give rise to the bulk $G_{10D} = E_8 \times E_8$, and the stacks of vertical 7-branes produce six-dimensional defects whose worldvolume is populated by localised gauge degrees of freedom. We hence conclude that the six-dimensional theory does not simply decompactify to the vacuum in ten dimensions, but that we actually need to consider theories containing defects that break higher-dimensional Poincaré invariance.

Heterotic dual interpretation

Going now to the heterotic dual model, the complex structure limit corresponding to the stable degeneration limit on the F-theory side translates to the large volume limit $\mathcal{V}_{T_{\text{het}}^2} \rightarrow \infty$ of the heterotic elliptic fiber. In order to maintain the hierarchy of volumes $\mathcal{V}_{\mathbb{P}_b^1} \gg \mathcal{V}_{T_{\text{het}}^2}$ demanded by the adiabaticity assumption, we need to superimpose the large volume limit $\mathcal{V}_{\mathbb{P}_b^1} \rightarrow \infty$ in which the base of the heterotic K3 surface decompactifies faster than the elliptic fiber. Altogether, this implies a decompactification from six to ten dimensions.

The fiberwise application of the duality reviewed in Section 6.4.1 is valid away from the non-generic 24 points of \mathbb{P}_b^1 where adiabaticity fails. The generic vertical slice on the F-theory

²²Codimension-two infinite-distance non-minimal enhancements do not occur, by definition, in single infinite-distance limits, see Definition 5.2.9.

side, from which we extracted the information about the bulk physics at the endpoint of the limit, corresponds to the heterotic model away from the degeneration points of the elliptic fiber of the K3 surface.

Horizontal gauge enhancements on the F-theory side correspond to the perturbative gauge sector on the heterotic side.²³ The Higgsing of these perturbative contributions in six dimensions arises, in heterotic terms, from the non-trivial background field strength of the E_8 bundles defined over the internal space. As the theory undergoes the decompactification process, the bulk physics becomes indistinguishable from that of heterotic string theory on $\mathbb{R}^{1,9}$: the (non-singular) gauge bundle profiles are diluted, and the masses associated to the curvature of the internal space asymptote to zero. Note, however, that the decompactification process is a continuous one, meaning that the topology of spacetime is not changed by it; the loci over which the elliptic fiber of the K3 surface degenerates are still present. The supersymmetry breaking defects can nonetheless be placed infinitely far away from the bulk observer. Altogether, we indeed expect the full perturbative $E_8 \times E_8$ perturbative gauge group of the heterotic string to be restored in such a limit.²⁴ The asymptotically massless towers identified in the generic vertical slice of the horizontal Type II.a model correspond to the KK towers associated with the growing 1-cycles in $H_1(T_{\text{het}}^2, \mathbb{Z})$. Their non-BPS nature on the F-theory side was related to the failure of defining the local 2-cycles $\{\gamma_i\}_{i=1,2}$ over the non-generic points in \mathbb{P}_b^1 . Likewise, it is the non-mutually local degeneration of the heterotic elliptic fiber over these very same points that makes them 1-chains from a global perspective in the heterotic K3 surface, leading to the same conclusion. The metric $U(1)_{\text{KK}}$ factors in compactifications of string theory stem from the Killing vectors of the internal space. Since the heterotic K3 surface is a strict Calabi-Yau we do not have any continuous isometries, but as we take the limit, ensuring that the adiabaticity assumption is fulfilled, the local observer in the generic patch far away from the degeneration defects sees the continuous isometries of the torus fiber become symmetries of the internal space in a good approximation. These provide the $U(1)_{\text{KK}}^2$ factors enabling the double loop enhancement of the lower-dimensional algebra to G_∞ observed for the generic vertical slice on the F-theory side. The fact that this is only seen asymptotically in the adiabatic regime on the heterotic side corresponds to the fact that we are not demanding any special structure for the Mordell-Weil group of the internal space of the six-dimensional F-theory models.

To complete the heterotic picture of horizontal Type II.a models, we need to also take into account the vertical gauge enhancements appearing on the F-theory side of the duality, which form part of the non-perturbative gauge sector from a heterotic point of view (alongside the gauge algebras supported on the exceptional curves arising from the resolution of codimension-two finite-distance non-minimal singularities). As we discuss in more detail in Appendix B.12, such vertical gauge algebras, supported over representatives of \mathcal{F} , correspond to ADE singularities

²³Even though the distinction between horizontal and vertical divisors is arbitrary in a model constructed over $\hat{B} = \mathbb{F}_0$, a statement which is dual to heterotic/heterotic duality, a definite choice needs to be made when dealing with concrete scenarios. In this section, we have chosen to call horizontal the direction along which the curve of non-minimal elliptic fibers appears in \hat{B}_0 and, consequently, the enhancements found over representatives of the global divisor classes \mathcal{H}_∞^0 , \mathcal{H}_∞^1 and \mathcal{H}_0^1 correspond to the perturbative or bulk gauge algebra factors on the heterotic side of the duality.

²⁴Note that, although in six-dimensional models at finite distance we can achieve $\text{rank}(\mathfrak{g}_{\text{hor}}) = 18$ by tuning a line of Kodaira type II* fibers over the unique representative of h , another line of II* fibers over a representative of $h + nf$, and a third line of IV fibers over a different representative of $h + nf$, such an enhancement pattern is incompatible with tuning the necessary codimension-one non-minimal fibers necessary to achieve a horizontal Type II.a model. Once the latter structure is enforced, we can obtain at most $\text{rank}(\mathfrak{g}_{\text{hor}}) \leq 16$ from the six-dimensional standpoint before any asymptotic enhancements are taken into account. The geometry needs to enforce this in order to be compatible with the perturbative gauge group of the decompactified heterotic side.

of the heterotic K3 surface probed by point-like instantons. Heterotic ADE singularities do not lead to non-perturbative gauge algebra factors unless they are probed by a singular gauge bundle contribution [349]. As emphasised earlier, the decompactification process does not change the topology of the internal space, meaning that the ADE singularities are still present at the endpoint of the limit, nor can it dilute the singular gauge bundle contributions, for which the curvature is localised at points. Hence, the non-perturbative gauge factors arising from probed heterotic ADE singularities are unaffected by the infinite-distance limit. Due to their localised nature, they lead to six-dimensional defect gauge algebras in the asymptotic model, as was also observed from the F-theory standpoint. This is particularly clear when on the F-theory side the six-dimensional horizontal gauge algebra is the full unbroken perturbative heterotic gauge algebra $\mathfrak{g}_{\text{hor}} = \mathfrak{e}_8 \oplus \mathfrak{e}_8$: A vertical gauge algebra is then dual to a heterotic ADE singularity probed by point-like instantons with trivial holonomy [298], which can be traded for M5-branes via a small instanton transition. The six-dimensional defects surviving in the asymptotic model are then M5-branes located on top of the ADE singularities of the infinitely large heterotic K3 surface, see Section B.12.1. More generally, once we allow the horizontal gauge algebra to be broken $\mathfrak{g}_{\text{hor}} \leq \mathfrak{e}_8 \oplus \mathfrak{e}_8$, the heterotic ADE singularities can also be probed by point-like instantons with discrete holonomy. These singular gauge bundle contributions cannot be traded for M5-branes via small instanton transitions, and are associated to one of the Hořava-Witten walls, as we expand on in Section B.12.2. Due to their localised nature, they are also able to survive the infinite-distance limit, again leading to localised algebras living in six-dimensional defects. As explained in Section 5.4, only those local enhancements that patch up into global enhancements yielding a factorisation in Δ_{phys} lead to gauge algebra factors. Vertical gauge algebras are supported over divisors that traverse both base components of the resolved central fiber Y_0 , and such considerations are therefore relevant for them; in Appendix B.12 we comment on how this affects the non-perturbative heterotic sector and its relation to the distribution of instanton number between the two heterotic E_8 bundles.

6.4.3.2 Allowing for mixed enhancements

The structure (6.4.16) assumed for the defining polynomials of the Weierstrass model of $\hat{\mathcal{Y}}$ at the beginning of the section restricts us to horizontal Type II.a models over $\hat{B} = \mathbb{F}_0$ with only horizontal and vertical enhancements. We now relax it to allow for gauge algebras supported over mixed global divisors as well.

The maximal gauge rank in the class of models under study is

$$\text{rank}(\mathfrak{g}_{\text{hor}}) \leq 16, \quad \text{rank}(\mathfrak{g}_{\text{ver}}) \leq 18, \quad (6.4.20)$$

in the horizontal and vertical sectors, respectively.²⁵ The most efficient use of the divisor classes available in the discriminant in order to tune gauge algebra factors is to only engineer enhancements of these two types. This can be deduced from the fact that a mixed divisor factoring in the physical discriminant can be split into horizontal and vertical constituents through a finite-distance complex structure deformation. Such a splitting increases the total gauge rank of the model. As mentioned in Section 6.3.3, a gauge algebra factor supported on a

²⁵These bounds on the gauge algebra rank apply both from the six-dimensional point of view, before the enhancements associated to the asymptotically massless towers have been considered, and from the higher-dimensional perspective. Note that the gauge factors supported over the exceptional curves arising from the resolution of codimension-two finite-distance non-minimal singularities are not accounted for in these bounds. Such factors are ignored in this section, but we comment on them in Appendix B.12.

mixed divisor can therefore be seen as the result of Higgsing some horizontal and vertical gauge contributions.

Using the heterotic language, dropping the assumption (6.4.16) is hence equivalent to allowing for mixed Higgsings between the perturbative and non-perturbative sectors. Let us analyse this first from a six-dimensional perspective, and then fully consider the asymptotic physics. Given a mixed divisor \mathcal{D}_{mix} that supports a gauge algebra $\mathfrak{g}_{\text{mix}}$, consider the point

$$p_b^{\text{mix}} := \{e_1 = 0\}_{B^0} \cap \mathcal{D}_{\text{mix}}|_{B^0} = \{e_0 = 0\}_{B^1} \cap \mathcal{D}_{\text{mix}}|_{B^1} \quad (6.4.21)$$

at which \mathcal{D}_{mix} intersects $B^0 \cap B^1$. We can then, via a finite-distance tuning, split \mathcal{D}_{mix} into

$$\mathcal{D}_{\text{mix}} \longmapsto \sum_{i \in \mathcal{I}} \mathcal{D}_{\text{hor}}^i + \mathcal{D}_{\text{ver}}, \quad (6.4.22)$$

where \mathcal{D}_{ver} is the unique representative of \mathcal{F} passing through p_b^{mix} . In this model at finite distance from the original one, the collection of horizontal divisors $\{\mathcal{D}_{\text{hor}}^i\}_{i \in \mathcal{I}}$ and the vertical divisor \mathcal{D}_{ver} support the gauge algebras $\bigoplus_{i \in \mathcal{I}} \mathfrak{g}_{\text{hor}}^i$ and $\mathfrak{g}_{\text{ver}}$, respectively. While part of these gauge factors stem from the horizontal and vertical 7-branes that result from the splitting of \mathcal{D}_{mix} , these may not be the only contributions; for example, the original model prior to the finite-distance complex structure deformation may already present a gauge algebra supported on \mathcal{D}_{ver} , which is then further enhanced after the splitting of \mathcal{D}_{mix} .

Inverting the logic, we may consider that there is a horizontal Type II.a model constructed over $\hat{B} = \mathbb{F}_0$ and satisfying (6.4.16) that exhibits an original gauge algebra $\bigoplus_{i \in \mathcal{I}} \mathfrak{g}_{\text{hor}}^i \oplus \mathfrak{g}_{\text{ver}}$ supported over $\{\mathcal{D}_{\text{hor}}^i\}_{i \in \mathcal{I}}$ and \mathcal{D}_{ver} , and whose asymptotics physics we have already understood in Section 6.4.3.3. A fine-distance tuning, which does not interfere with the infinite-distance limit and that could also be implemented after the fact, recombines (at least part of) these 7-branes into \mathcal{D}_{mix} . This produces a Higgsing

$$\bigoplus_{i \in \mathcal{I}} \mathfrak{g}_{\text{hor}}^i \oplus \mathfrak{g}_{\text{ver}} \longmapsto \mathfrak{g}_{\text{mix}} \oplus \mathfrak{g}_{\text{hor}}^{\text{res}} \oplus \mathfrak{g}_{\text{ver}}^{\text{res}}, \quad (6.4.23)$$

where $\mathfrak{g}_{\text{hor}}^{\text{res}} \oplus \mathfrak{g}_{\text{ver}}^{\text{res}}$ accounts for the fact that not all 7-branes in the listed divisor classes need to recombine. The remaining ones lead to the residual horizontal and vertical gauge algebras. It may nonetheless occur that no, e.g., vertical gauge algebra remains after the recombination, as is represented in Figure 6.6.

Turning our attention to the asymptotic physics, we note that such a recombination process into a mixed divisor always requires vertical divisor classes. These are associated with the six-dimensional defects present in the decompactified theory, and therefore the Higgsing should be tied to them. Indeed, the generic vertical slices still lead to the same conclusions for the horizontal contribution to the gauge algebra, since the pertinent part of the discussion in Section 6.4.3.1 remains unaltered after the finite-distance deformation. After the recombination into a mixed divisor, a pair of branes in different base components of the associated generic eight-dimensional model can belong to the same global mixed divisor in the six-dimensional one, as shown in Figure 6.6 for the yellow 7-brane. Nonetheless, and according to the analysis of the generic vertical slices, they still contribute to a different factor of G_∞ each, with the two halves of the global 7-brane only joining at one of the 24 non-generic points in \mathbb{P}_b^1 . These union points play a role in the obstruction to globally defining the local 2-cycles $\{\gamma_i\}_{i=1,2}$, since they lead to special fibers at the intersection of the components in the corresponding vertical slice, and hence to the non-BPS nature of the particles furnishing the asymptotically massless towers.

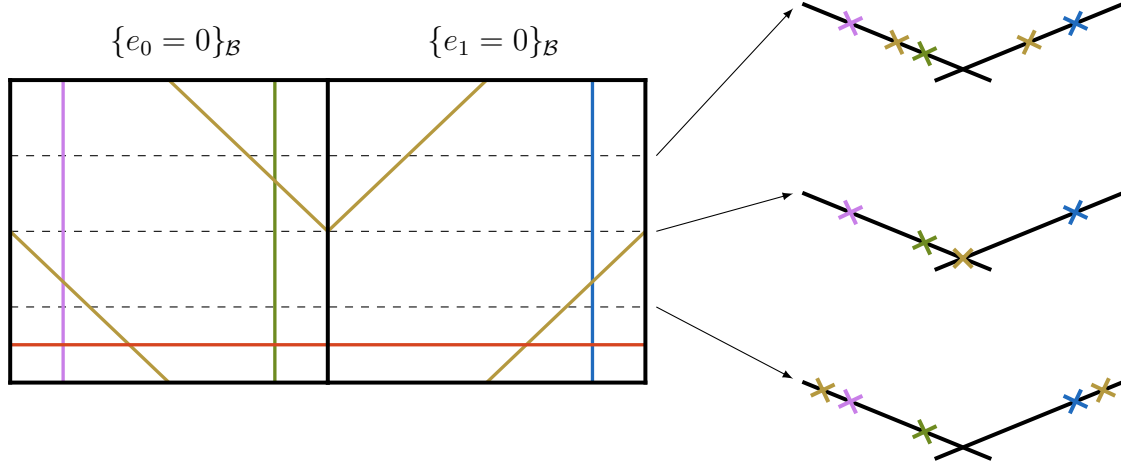


Figure 6.6: A schematic representation of the base of the central fiber of a resolved horizontal Type II.a model constructed over $\hat{B} = \mathbb{F}_0$ on the left, and various vertical slices of it on the right. We represent two horizontal 7-branes in the classes \mathcal{H}_∞^0 and \mathcal{H}_0^1 , respectively, a vertical 7-brane in the class \mathcal{F} , and a mixed 7-brane in the class $\mathcal{D}_{\text{mix}} = \mathcal{H}_\infty^0 + \mathcal{H}_0^1 + \mathcal{F}$. The first and the third vertical slices are generic, and lead to the same picture as in the unHiggsed model at finite distance. The second vertical slice has smooth codimension-zero elliptic fibers, but presents special fibers at the intersection of the components, signalling a complete Higgsing of the primordial vertical gauge algebra associated to the representative of \mathcal{F} intervening in the recombination process producing \mathcal{D}_{mix} .

We can understand the fact that the two halves of such a mixed 7-brane contribute to different factors of the perturbative heterotic gauge algebra as the dilution of the gauge bundle curvature during the decompactification process. This makes the masses associated with the Higgsing of the bulk gauge degrees of freedom asymptote to zero in the limit. The collection of non-generic vertical slices accounts both for those vertical gauge factors supported over representatives of \mathcal{F} unaffected by the recombination process, and for the residual vertical gauge algebras $\mathfrak{g}_{\text{ver}}^{\text{res}}$ resulting from a localised Higgsing of the primordial defect algebra $\mathfrak{g}_{\text{ver}}$. Such Higgsings can be complete, as represented in Figure 6.6. The fact that to produce such mixed enhancements the maximal vertical gauge rank needs to be reduced can be understood from the heterotic dual perspective as the need to deform some of the point-like instantons probing the heterotic ADE singularities into smooth gauge bundle contributions with structure group of positive dimension, as we revisit in Appendix B.12.

6.4.3.3 Away from the adiabatic regime

We now comment on the interpretation of the complex structure infinite-distance limit away from the strict adiabatic regime. Consider first the heterotic side of the duality and suppose, for simplicity of the argument, that the K3 surface is described by a smooth Weierstrass model. The Kähler volume of the K3 surface then takes the form

$$\mathcal{V}_{\text{K3}} = \frac{1}{2} \int_{\text{K3}} J^2 = \left(\mathcal{V}_{T_{\text{het}}^2} \right)^2 + \mathcal{V}_{T_{\text{het}}^2} \mathcal{V}_{\mathbb{P}_b^1}, \quad (6.4.24)$$

where $\mathcal{V}_{T_{\text{het}}^2}$ is the volume of the generic elliptic fiber. In the adiabatic regime, characterised by $\mathcal{V}_{\mathbb{P}_b^1} \gg \mathcal{V}_{T_{\text{het}}^2}$, the term quadratic in $\mathcal{V}_{T_{\text{het}}^2}$ is subleading, and the volume asymptotically factorises

as it would for a trivial fibration. In this regime, taking both $\mathcal{V}_{\mathbb{P}_b^1} \rightarrow \infty$ and $\mathcal{V}_{T_{\text{het}}^2} \rightarrow \infty$ such that $\mathcal{V}_{\mathbb{P}_b^1} \gg \mathcal{V}_{T_{\text{het}}^2}$ allows us to clearly distinguish between the Kaluza-Klein supergravity towers stemming from decompactification of the base \mathbb{P}_b^1 and the fiber T_{het}^2 . In fact, to the extent that the geometry of the elliptic fibration asymptotically behaves as it would in a trivial fibration, the fiber contributes two approximate Kaluza-Klein towers, each associated to one of the two local 1-cycles of its generic representative. This picture breaks down near the 24 degeneration loci of the fiber, which, however, are pushed to infinity in the adiabatic decompactification limit.

This behaviour is contrasted with the limit $\mathcal{V}_{T_{\text{het}}^2} \sim \lambda \mathcal{V}_{T_{\text{het}}^2}^0$ with $\lambda \rightarrow \infty$ and $\mathcal{V}_{T_{\text{het}}^2}^0$ constant, at finite $\mathcal{V}_{\mathbb{P}_b^1} = \mathcal{V}_{\mathbb{P}_b^1}^0$. In view of (6.4.24), the decompactification of the K3 surface can be interpreted as a homogenous rescaling of the K3 volume superimposed with a shrinking of the base \mathbb{P}_b^1 in the original, non-rescaled surface, i.e.

$$\mathcal{V}_{\text{K3}} \sim \lambda^2 \left[\left(\mathcal{V}_{T_{\text{het}}^2}^0 \right)^2 + \mathcal{V}_{T_{\text{het}}^2}^0 \frac{\mathcal{V}_{\mathbb{P}_b^1}^0}{\lambda} \right] =: \lambda^2 \mathcal{V}_{\text{K3}}^0, \quad \lambda \rightarrow \infty. \quad (6.4.25)$$

From the form of $\mathcal{V}_{\text{K3}}^0$, it is clear that the non-rescaled K3 surface approaches an orbifold point, where the (-2) -curve given by the zero-section of the elliptic fibration has shrunk; at the same rate as the orbifold point is reached, the total surface expands homogeneously. As a result, the non-adiabatic limit is still a total decompactification to ten dimensions, but the nature of the Kaluza-Klein towers differs from its counterpart in the adiabatic regime. In particular, the hierarchical split of the Kaluza-Klein towers into a tower from the expansion of the base and two asymptotically independent towers from the generic fiber breaks down. Rather, as we interpolate between the adiabatic and the non-adiabatic regimes at large overall volume, the supergravity towers reorganise in a complicated way. The fiber continues to contribute Kaluza-Klein tower(s), which, however, cannot be treated as two independent towers associated with local isometries along its generic representative.

This suggests that, similarly, the microscopic interpretation of the complex structure infinite-distance limit on the F-theory side must be modified away from the adiabatic regime. Note that, strictly speaking, the F-theory/heterotic duality dictionary in its form reviewed in Section 6.4.1 is valid only in the adiabatic limit, so that a priori special care must be applied in translating the heterotic interpretation of the limit to the F-theory side. Nonetheless, there are clear parallels. Away from the adiabatic regime, it is no longer possible to isolate the effect of the vertical fiber degenerations by sending them to infinity. Recall from the discussion in Section 6.4.3.1 that it is at these vertical degenerations that the local picture of asymptotically vanishing 2-cycles with the topology of a torus breaks down. Rather than a fibration of such local 2-cycles degenerating at isolated points that asymptotically move to infinity, it is more appropriate to view the complex structure degeneration as leading to vanishing 3-cycles: These arise by fiberizing the vanishing 2-chains over the 1-chains between pairs of points on \mathbb{P}_b^1 over which the singular vertical fibers are located. The geometric origin of the massless towers, which in the adiabatic regime arise from M2-branes wrapping the locally well-defined vanishing 2-cycles, is obscured by this. The benefit of the adiabatic limit, superimposed with the complex structure infinite-distance limit, is therefore to provide a clear geometric interpretation of the origin of the towers. In the strict large base limit, these are the two local towers from wrapped M2-branes in M-theory, dual to the two heterotic Kaluza-Klein towers from the adiabatically expanding fiber. The heterotic picture suggests that these two towers reorganise away from the adiabatic limit, but continue to signal a decompactification process also in F-theory. What is more challenging is to read off the end point of this decompactification limit, and in particular the dimensionality of the asymptotic

theory. It is natural to speculate that, as on the heterotic side, the decompactification is to a ten-dimensional theory with defect gauge sectors, but a quantitative underpinning of this conjecture is beyond the scope of this work.

6.4.4 Horizontal Type II.a models over $\hat{B} = \mathbb{F}_n$

Horizontal Type II.a models constructed over $\hat{B} = \mathbb{F}_n$, with $n \geq 1$, behave very similarly to the ones constructed over $\hat{B} = \mathbb{F}_0$ and just analysed in Section 6.4.3. We therefore only focus here on highlighting some of the differences, which mostly stem from the fact that now \mathcal{H}_∞^1 , defined in (6.3.39), is a mixed divisor.

Once $n \geq 1$, the two components $\{Y^p\}_{0 \leq p \leq 1}$ of the central fiber Y_0 no longer behave identically, as can be seen from the line bundles defining the component Weierstrass models,

$$\mathcal{L}_0 = S_0 + (2+n)V_0, \quad (6.4.26a)$$

$$\mathcal{L}_1 = S_1 + 2V_1. \quad (6.4.26b)$$

Since horizontal Type II.a models have smooth codimension-zero elliptic fibers, the $\{\Delta'_p\}_{0 \leq p \leq 1}$ are simply in the divisor class $\Delta'_p = 12\mathcal{L}_p$, cf. (6.3.5). On the heterotic dual side, this asymmetry corresponds to the uneven distribution of instanton numbers between the two E_8 bundles.

The Y^0 component, corresponding on the heterotic dual side to the E_8 bundle with instanton number $c_2(V_0) = 12 + n$, behaves mostly²⁶ like in the $\hat{B} = \mathbb{F}_0$ case. Its contribution to the six-dimensional horizontal gauge algebra fulfils $\text{rank}(\mathfrak{g}_{\text{hor}}^0) \leq 8$, and is saturated by tuning II^* fibers over a representative of \mathcal{H}_∞^0 . Such $\mathfrak{g}_{\text{hor}}^0 = \mathfrak{e}_8$ algebra can be Higgsed without affecting the vertical gauge algebra sector, although this still reduces the rank of the non-perturbative heterotic gauge sector, see Appendix B.12.

For the Y^1 component, which corresponds to the heterotic E_8 bundle with instanton number $c_2(V_1) = 12 - n$, the situation is different. Apart from the presence of non-Higgsable clusters for $n \geq 3$, which lie in Y^1 rather than Y^0 , another distinction with respect to the Y^0 component is how horizontal Higgsings affect the maximal vertical gauge rank that is possible, in addition to the effects on the non-perturbative sector already observed for the Y^0 component. The contribution of the Y^1 component to the six-dimensional horizontal gauge algebra fulfils $\text{rank}(\mathfrak{g}_{\text{hor}}^1) \leq 8$, and is saturated by tuning II^* fibers over the unique representative of \mathcal{H}_0^1 . Since the divisors in the class \mathcal{H}_∞^1 are now mixed, the $\mathfrak{g}_{\text{hor}}^1 = \mathfrak{e}_8$ algebra cannot be Higgsed without recombining \mathcal{H}_0^1 with a suitable number of copies of \mathcal{F} . As a consequence, the maximal vertical gauge rank is reduced, and the model can be seen as the Higgsing of one obtained by a finite-distance deformation, and with maximal primordial horizontal²⁷ and vertical gauge algebra factors, cf. Section 6.4.3.2.

For example, consider a horizontal Type II.a model constructed over $\hat{B} = \mathbb{F}_7$. According to Table 6.3.3, we have then $\text{rank}(\mathfrak{g}_{\text{ver}}) \leq 8$. The maximal horizontal and vertical gauge ranks can be obtained in a model with the gauge factors

$$\mathcal{H}_\infty^0 : E_8, \quad \mathcal{H}_0^1 : E_8, \quad \mathcal{F} : E_8. \quad (6.4.27)$$

²⁶The multiples of \mathcal{H}_∞^0 may now be irreducible, but this does not change the asymptotic physics.

²⁷While in the absence of a vertical enhancement the maximal horizontal gauge algebra rank can always be obtained by tuning $g_{\text{hor}} = \mathfrak{e}_8 \oplus \mathfrak{e}_8$, this is not always viable if we also want to realise the maximal vertical gauge rank simultaneously. For example, in horizontal Type II.a models constructed over $\hat{B} = \mathbb{F}_3$ we read from Table 6.3.3 that $\text{rank}(\mathfrak{g}_{\text{ver}}) \leq 16$. This can be achieved by tuning a global line of I_{12}^{*s} fibers over a representative of \mathcal{F} , corresponding to a vertical D_{16} algebra. Such a vertical tuning is incompatible with having $g_{\text{hor}} = \mathfrak{e}_8 \oplus \mathfrak{e}_8$, but the maximal horizontal gauge rank can still be obtained by tuning instead two horizontal lines of I_4^{*s} fibers, one over a representative of \mathcal{H}_∞^0 and another one over the unique representative of \mathcal{H}_0^1 , each corresponding to a horizontal D_8 algebra, i.e. we have instead $g_{\text{hor}} = \mathfrak{so}(16) \oplus \mathfrak{so}(16)$.

Due to the non-Higgsable cluster present in models constructed over $\hat{B} = \mathbb{F}_7$, see Table 6.3.1, the E_8 factor supported on \mathcal{H}_0^1 can be broken, at most, to an E_7 factor. To determine the maximal number α of representatives of the divisor class V_1 that can factorize in Δ'_1 consistent with this, we consider the residual discriminant $\Delta'_1 - 9S_1 - \alpha V_1$, and demand that it does not factor out an additional copy of S_1 (which would indicate an enhancement back to E_8). In particular, this implies that

$$(\Delta'_1 - 9S_1 - \alpha V_1) \cdot S_1 = 3 - \alpha \geq 0 \Leftrightarrow \alpha \leq 3, \quad (6.4.28)$$

and hence $\text{rank}(\mathfrak{g}_{\text{ver}}) \leq 1$ (saturated for Kodaira type III or type I₂ fibers along a representative of \mathcal{F} , and hence, in particular, along a representative of V_1) if we do not want the E_8 factor over \mathcal{H}_0^1 to be restored.²⁸ Therefore, Higgsing the horizontal gauge algebra in the Y^1 component leads to models in which the maximal enhancement, from the six-dimensional point of view, is

$$\mathcal{H}_\infty^0 : E_8, \quad \mathcal{H}_0^1 : E_7, \quad \mathcal{F} : A_1. \quad (6.4.29)$$

From the perspective of the asymptotic physics, the horizontal Higgsing is not that relevant, since the horizontal 7-branes will combine to produce the bulk G_{10D} algebra at the endpoint of the limit. The rank of the maximal defect algebra, however, is greatly reduced as a consequence of the preceding considerations.

Going to the adiabatic regime, we can understand this from a heterotic dual perspective. In the unHiggsed model in which the maximal horizontal gauge rank is realised, none of the instanton number budget $c_2(K3) = 24$ needs to be spent in order to break the perturbative gauge group. The instanton number can then, in particular, be accounted for by point-like instantons with trivial holonomy (which, indeed, leave the bulk gauge sector intact). These point-like instantons are hence available to be placed on top of the geometrical singularities of the heterotic K3, allowing for the manifestation of the maximal non-perturbative gauge algebra possible within the class of models. In order to break the perturbative gauge group, part of these point like instantons need to be smoothed out into a gauge bundle profile with structure group of positive dimension; while the geometrical singularity of the heterotic K3 surface is still present, fewer point-like instantons are able to probe it. This reduces the maximal possible rank of the non-perturbative gauge algebra. In the decompactification limit the gauge bundle curvature is diluted, and the masses associated with the Higgsing in the perturbative sector asymptote to zero, restoring the bulk gauge algebra. Point-like instantons are singular gauge bundle contributions, and hence do not dilute in the limit: The remaining non-perturbative gauge algebra is maintained in the limit, but its gauge rank is reduced with respect to the situation in which no point-like instantons are smoothed out and diluted.

The decompactified theories arising as the endpoints of infinite-distance limits represented by horizontal Type II.a models are qualitatively not that different from each other, but still can preserve some memory of the Hirzebruch surface $\hat{B} = \mathbb{F}_n$ employed in their construction. While point-like instantons with trivial holonomy are not associated with a given Hořava-Witten wall thanks to the possibility of trading them for M5-branes via a small instanton transition, the same is not true for point-like instantons with discrete holonomy. These are singular gauge bundle contributions that also survive the infinite-distance limit, but belong to one of the Hořava-Witten walls. Hence, their presence at the endpoint of the limit preserves some information on the distribution of instanton numbers between the two heterotic E_8 bundles or, in F-theory terms, the choice of Hirzebruch surface $\hat{B} = \mathbb{F}_n$. As a consequence, two distinct horizontal Type II.a models can either lead to the same asymptotic physics, or their endpoints

²⁸It can be shown that tuning a vertical line of I₃ type fibers also restores the E_8 factor over \mathcal{H}_0^1 .

require an additional finite-distance deformation and non-perturbative transition in order to be connected, see Appendix B.12.

6.4.5 Non-minimal singularities of the heterotic K3 surface

Minimal singular elliptic fibers in the heterotic K3 surface do not lead to non-perturbative gauge algebra factors unless they are probed by singular gauge bundle contributions, as we review at the beginning of Appendix B.12. This is due to α' -corrections having the effect of smoothing out their moduli space [349]. It would be conceivable that, in the same way that a minimal geometrical singularity is not enough to produce a non-perturbative gauge algebra factor, a non-minimal geometrical singularity could be brought to finite distance by similar effects. We argue that this is not the case, since non-minimal singularities of the heterotic K3 surface are equivalent to a codimension-one infinite-distance degeneration on the F-theory side of the duality.

In a resolved horizontal Type II.a model with central fiber $Y_0 = Y^0 \cup_{K3} Y^1$, the dual heterotic K3 surface is identified with $Y^0 \cap Y^1$. In terms of the Weierstrass model describing the family variety \mathcal{Y} of the resolved degeneration, a non-minimal singularity of the heterotic K3 surface arises if at a point $p \in B^0 \cap B^1$ the interface vanishing orders are

$$\text{ord}_{Y^0 \cap Y^1}(f_b|_{e_0=e_1=0}, g_b|_{e_0=e_1=0}, \Delta_b|_{e_0=e_1=0})_p \geq (4, 6, 12). \quad (6.4.30)$$

Earlier in our discussion, we have already considered what naively seem like worse degenerations in codimension-two over B_0 : Point-like instantons with trivial holonomy correspond to codimension-two finite-distance non-minimal points for which, at the very least, the component vanishing orders are non-minimal. In contrast, we are demanding in (6.4.30) only the interface vanishing order, i.e. the vanishing orders computed in a non-generic slice, to be non-minimal. Nonetheless, the fact that the non-generic slice corresponds to the heterotic K3 surface is quite relevant from the perspective of the F-theory geometry. A point with non-minimal interface vanishing orders on $B^0 \cap B^1$ corresponds to a (possibly obscured) infinite-distance limit, in the language of Chapter 5. In fact, tuning it takes us away from the single infinite-distance limit class of degenerations, see Section 5.4, since we are indeed overlaying an additional infinite-distance limit on top of the already existing one.

Succinctly summarising the discussion in Appendix B.3, such an obscured infinite-distance limit can be transformed into a codimension-one infinite-distance degeneration by performing a base change

$$\begin{aligned} \delta_k : D &\longrightarrow D \\ u &\longmapsto u^k \end{aligned} \quad (6.4.31)$$

with high enough branching degree. The equivalent degeneration obtained after the base change has a central fiber comprised of more than two components. The former point $p \in B^0 \cap B^1$ with non-minimal interface vanishing orders extends, after the base change, into a vertical line of non-minimal component vanishing orders traversing the intermediate components. By blowing the model down to one of said intermediate components, and possibly performing a second base change, we obtain a vertical codimension-one infinite-distance degeneration overlaid on top of the horizontal one that we started with.

To summarise, although tuning the non-minimal heterotic K3 singularity occurs in codimension-two in the original degeneration on the F-theory side, the required complex structure deformation is equivalent to tuning a codimension-one infinite-distance degeneration in a base changed model. We schematically depict this in Figure 6.7. Hence, we conclude that tuning

a non-minimal heterotic K3 singularity corresponds indeed to taking a complex structure infinite-distance limit.

6.5 Partial decompactification and weak coupling limits

After having analysed the asymptotic physics of horizontal Type II.a models in the adiabatic regime, we now move to the study of the remaining types of horizontal models, according to the classification of Section 6.3.1. We briefly comment on horizontal Type II.b models in Section 6.5.1, which simply are an instance of the Sen limit. Horizontal Type III.a models are analysed in Section 6.5.2; they lead, in the adiabatic regime, to a partial decompactification from six to nine dimensions, with the asymptotic theory containing localised defect algebras. We conclude by turning our attention to horizontal Type III.b models in Section 6.5.3. They are found to be a total decompactification from six to ten dimensions presenting, once again, localised defect algebras. In Section 6.5.3.1 we compare horizontal Type III.a and Type III.b models from the point of view of the perturbative Type IIB picture. Some comments on the degenerate K3 double covers that result when insisting on a Sen limit presentation of codimension-one infinite-distance degenerations are relegated to Appendix B.13.

6.5.1 Horizontal Type II.b models

Horizontal Type II.b models correspond to those degenerations $\hat{\rho} : \hat{\mathcal{Y}} \rightarrow D$ of Hirzebruch models in which the central fiber \hat{Y}_0 of the degeneration develops codimension-zero $I_{m>0}$ type fibers without presenting any infinite-distance non-minimal vanishing loci.²⁹ Hence, they are simply an infinite-distance weak coupling limit: the Sen limit [203] of six-dimensional F-theory models constructed over $\hat{B} = \mathbb{F}_n$. Their endpoint is an emergent string limit, the resulting theory corresponding to the perturbative Type IIB orientifold compactification to six-dimensions arising from the F-theory model at weak coupling. The constraints on the 7-brane content discussed in Sections 6.3.4 and 6.3.5 with the multi-component models in mind also apply here: only gauge enhancements associated with Kodaira type I_m and I_m^* fibers, except for I_0^{*ns} fibers, can be realised, in agreement with the perturbative Type IIB picture. The Sen limit has been extensively studied in the F-theory literature, see [185] for a review and references, and we do not comment further on it. With applications to the analysis of Type III.b models in mind, we review the concrete geometry relevant for the Sen limit of six-dimensional F-theory models having $B = \mathbb{F}_n$ as the base of their internal space in Section B.13.1.

6.5.2 Horizontal Type III.a models

Horizontal Type III.a models, as defined in Section 6.3.1, are those whose open-chain resolution $\rho : \mathcal{Y} \rightarrow D$ has generic vertical slices $\sigma : \mathcal{Z} \rightarrow D$ corresponding to Kulikov Type III.a models. Their central fiber is of the form $Y_0 = \bigcup_{p=0}^P Y^p$ with $P \geq 1$, and is characterised by having at least one component at weak coupling and at least one component at strong coupling, i.e. $n_p > 0$ for some $p \in \{0, \dots, P\}$ and $n_q = 0$ for some $p \neq q \in \{0, \dots, P\}$, expressing it in terms of the pattern of codimension-zero singular elliptic fibers. Given the effectiveness bounds (6.3.6), this

²⁹For this reason, we can simply refer to this class of degenerations as Type II.b models, since no horizontal, vertical or mixed non-minimal curve appears in \hat{B}_0 . We have nevertheless termed them horizontal Type II.b models because they are a relative version of Kulikov Type II.b models, and hence fit into the classification of Section 6.3.1.

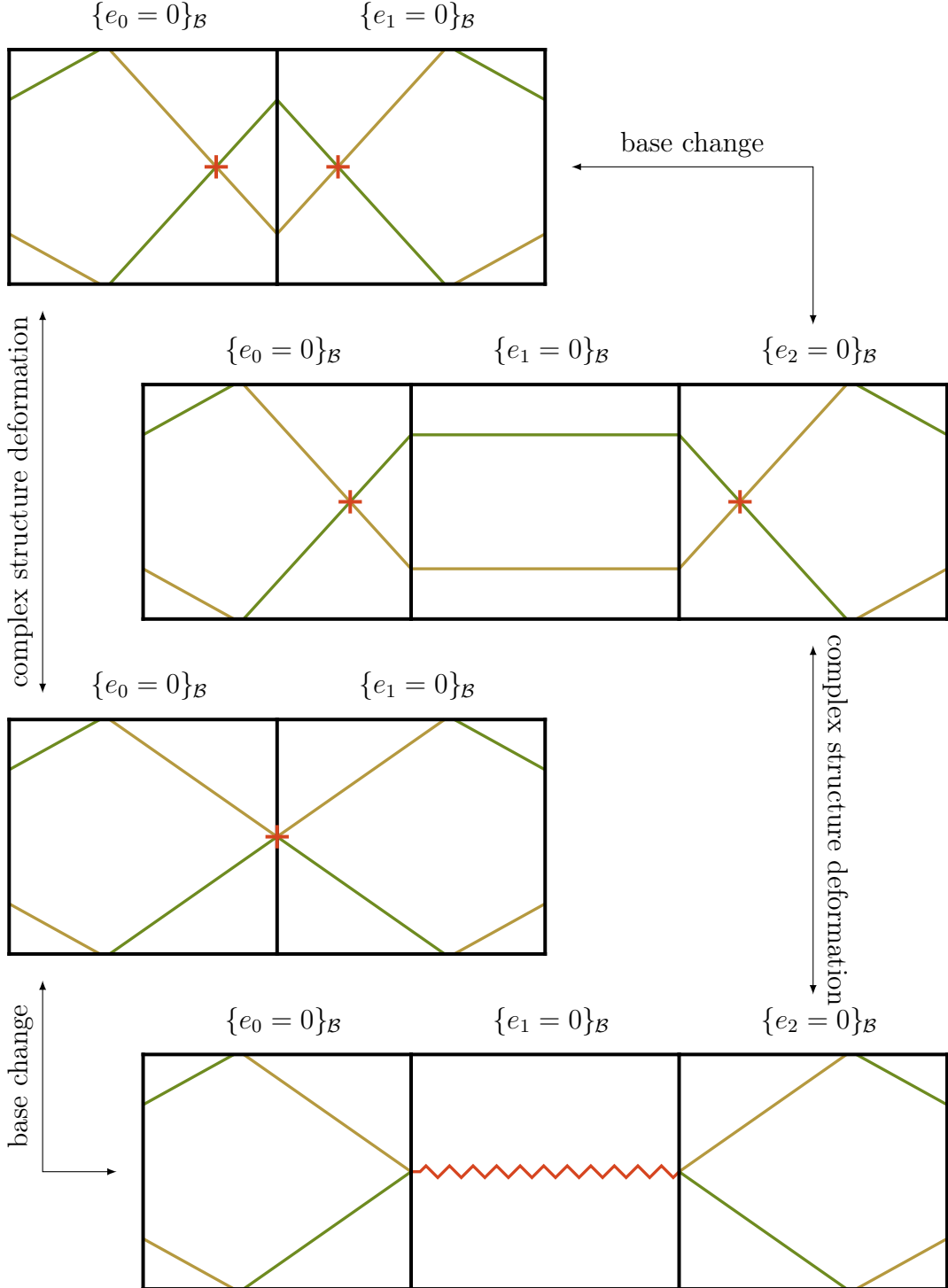


Figure 6.7: Base changing a horizontal Type II.a model has the effect of stretching the 24 points of intersection of the discriminant with $B^0 \cap B^1$ into local vertical branes. As a consequence, complex structure deformations moving these points of intersection and stacking them together are equivalent to local enhancements over the intermediate components. In the figure, we show how this makes moving finite-distance codimension-two non-minimal points to $B^0 \cap B^1$ lead to a local non-minimal codimension-one enhancement in the intermediate components of the equivalent model. Hence, tuning a non-minimal singularity of the heterotic K3 surface corresponds to a complex structure infinite-distance limit.

implies that all intermediate components must be at weak coupling, with at least one of the end-components at strong coupling. This last fact means that they do not correspond to global weak coupling limits and can hence be constructed quite generally without being subject to the types of constraints discussed in Section 6.3.2.3; comparisons to their geometrically reminiscent global weak coupling limit counterparts are drawn in Section 6.5.3.1.

Unlike horizontal Type II.a models, the heterotic dual of horizontal Type III.a models is more obscure. The geometry on the F-theory side is, however, well described by the preceding facts, and we can use it to perform a fiberwise extension of the asymptotic physics of the generic vertical slices in the adiabatic regime, in the same spirit as the discussion of Section 6.4.3. When $P = 1$ the models can be seen as a further deformation of a horizontal Type II.a model, and we can make some further comments from the heterotic dual perspective.

6.5.2.1 Generic vertical slices

Let us start by analysing the asymptotic physics of the would-be eight-dimensional F-theory models associated with the generic vertical slices of horizontal Type III.a models, to see how they paint a consistent picture that will later inform us about the bulk physics at the endpoint of the limit. We conclude the section by commenting on how this generic vertical slice point of view fails over certain loci, at which the purely six-dimensional features of the model will be concentrated, according to our experience from Section 6.4.

As mentioned earlier, horizontal Type III.a models contain components at weak coupling, which means that their discriminant Δ and their modified discriminant Δ' are no longer identical.³⁰ The information obtained from Δ concerns the pattern of codimension-zero singular elliptic fibers; for the generic vertical slice, the distribution of weak and strong coupling components is the same as in the full central fiber of the horizontal Type III.a model, as was explained in Section 6.3.1. The restrictions $\{\Delta'_p\}_{0 \leq p \leq P}$ of Δ' to the components, which are the same as the restrictions of Δ_{phys} , provide us with the information about the 7-brane content after the background value of the axio-dilaton has been subtracted. The number of 7-branes in the eight-dimensional model associated with the generic vertical slice, which stem from the restriction of horizontal and mixed branes to the chosen representative of \mathcal{F} , are

$$\Delta'_0 \cdot \mathcal{F}|_{E_0} = 12 + n_0 - n_1, \quad (6.5.1a)$$

$$\Delta'_p \cdot \mathcal{F}|_{E_p} = 2n_p - n_{p-1} - n_{p+1}, \quad p = 1, \dots, P-1, \quad (6.5.1b)$$

$$\Delta'_P \cdot \mathcal{F}|_{E_P} = 12 + n_P - n_{P-1}. \quad (6.5.1c)$$

Their total amount coincides with the number of 7-branes in a conventional F-theory model in eight dimensions

$$\Delta_{\text{phys}} \cdot \mathcal{F} = \sum_{p=0}^P \Delta'_p \cdot \mathcal{F}|_{E_p} = 24, \quad (6.5.2)$$

but their distribution is altered by the pattern of codimension-zero singular elliptic fibers. Not only that, but the types of 7-branes that can be found in each component also depend on said pattern, as was analysed from a six-dimensional standpoint in Section 6.3.4. By restricting the six-dimensional constraints on the (local) 7-brane content to the generic vertical

³⁰Let us recall that the modified discriminant Δ' is obtained from the discriminant Δ of the Weierstrass model of \mathcal{Y} after factoring out the components associated with the codimension-zero singular elliptic fibers in Y_0 , i.e. after subtracting the background value of the axio-dilaton. Δ_{phys} is then obtained as the restriction of Δ' to the base B_0 of Y_0 . See Chapter 5 for definitions and examples.

slice, we consistently reproduce the results found in [156, 157] for Kulikov Type III.a models: The intermediate components $\{Y^p\}_{1 \leq p \leq P-1}$ can only present singular elliptic fibers of A type supported over representatives of the classes $\{T_p\}_{1 \leq p \leq P-1}$ or multiples of them, which restrict to 7-branes of the corresponding type in the generic vertical slice. Those end-components $\{Y^p\}_{p=0,P}$ at local strong coupling can exhibit singular elliptic fibers of any of the Kodaira types, and this property descends to the 7-branes in the generic vertical slice. If an end-component $\{Y^p\}_{p=0,P}$ is at local weak coupling the defining polynomials of the Weierstrass model of Y^p must fulfil the accidental cancellation structure (B.9.4), meaning that $f_p = -3h_p^2$ and $g_p = 2h_p^3$. This leads to D type singular elliptic fibers supported over the (generically irreducible) divisor $\{h_p = 0\}_{B^p}$, which due to

$$\{h_0 = 0\}_{B^0} \cdot \mathcal{F}|_{E_0} = 2 \quad \text{or} \quad \{h_P = 0\}_{B^P} \cdot \mathcal{F}|_{E_P} = 2 \quad (6.5.3)$$

yield 2 singular elliptic fibers of D type in the generic vertical slice. Additionally, there may be A type singular elliptic fibers supported over representatives of T_0 or T_P and S_P , depending on the end-component under consideration, which restrict to the corresponding 7-brane type in the generic vertical slice. Altogether, this reproduces Table 3.2 of [156].

As the point $p_b \in \mathbb{P}_b^1$ over which the vertical slice is defined changes, the position of the 7-branes of the associated Kulikov Type III.a model move within their components. While their distribution among the various components has a tangible physical effect, their position within them is not relevant for the eight-dimensional asymptotic physics and, as a consequence, all generic vertical slices of a horizontal Type III.a model lead to a consistent picture: As we will argue in Section 6.5.2.2, the bulk physics of the asymptotic model resembles that of Kulikov Type III.a models, which we reviewed in Section 6.2.1. We provide a depiction of the central fiber of a horizontal Type III.a model and several global 7-branes within it, as well as a number of generic and non-generic vertical slices, in Figure 6.8.

There are non-generic representatives of \mathcal{F} that do not lead to this coherent interpretation: They are the loci over which the adiabaticity assumption must fail and where the six-dimensional features of the asymptotic physics will hence be concentrated at. Each pair of adjacent components Y^p and Y^{p+1} of the central fiber Y_0 intersects over a K3 surface. This can be seen from the fact that all interface curves $\{B^p \cap B^{p+1}\}_{0 \leq p \leq P-1}$ are \mathbb{P}^1 curves acting as the base of an elliptic fibration in which the elliptic fiber degenerates over a total of

$$\Delta|_{E_p} \cdot (E_p \cap E_{p+1}) = \Delta|_{E_{p+1}} \cdot (E_p \cap E_{p+1}) = 24, \quad p = 0, \dots, P-1, \quad (6.5.4)$$

points counted with multiplicity. Since the effectiveness bounds (6.3.6) force all intermediate components $\{Y^p\}_{1 \leq p \leq P-1}$ to be at local weak coupling, the interface K3 surfaces present Kodaira type I_m fibers in codimension-zero that are subject to additional A and D type enhancements over points. However, the number of intersections of the physical discriminant Δ_{phys} with the interface curves can differ from one to the other. Using that

$$\Delta'_p = \Delta|_{E_p} - \sum_{p=0}^P n_p E_p \Big|_{E_p}, \quad (6.5.5)$$

it can be computed to be

$$\Delta'_p \cdot S_p = 24 + n(n_{p+1} - n_p), \quad p = 0, \dots, P-1, \quad (6.5.6a)$$

$$\Delta'_p \cdot T_p = 24 + n(n_p - n_{p-1}), \quad p = 1, \dots, P, \quad (6.5.6b)$$

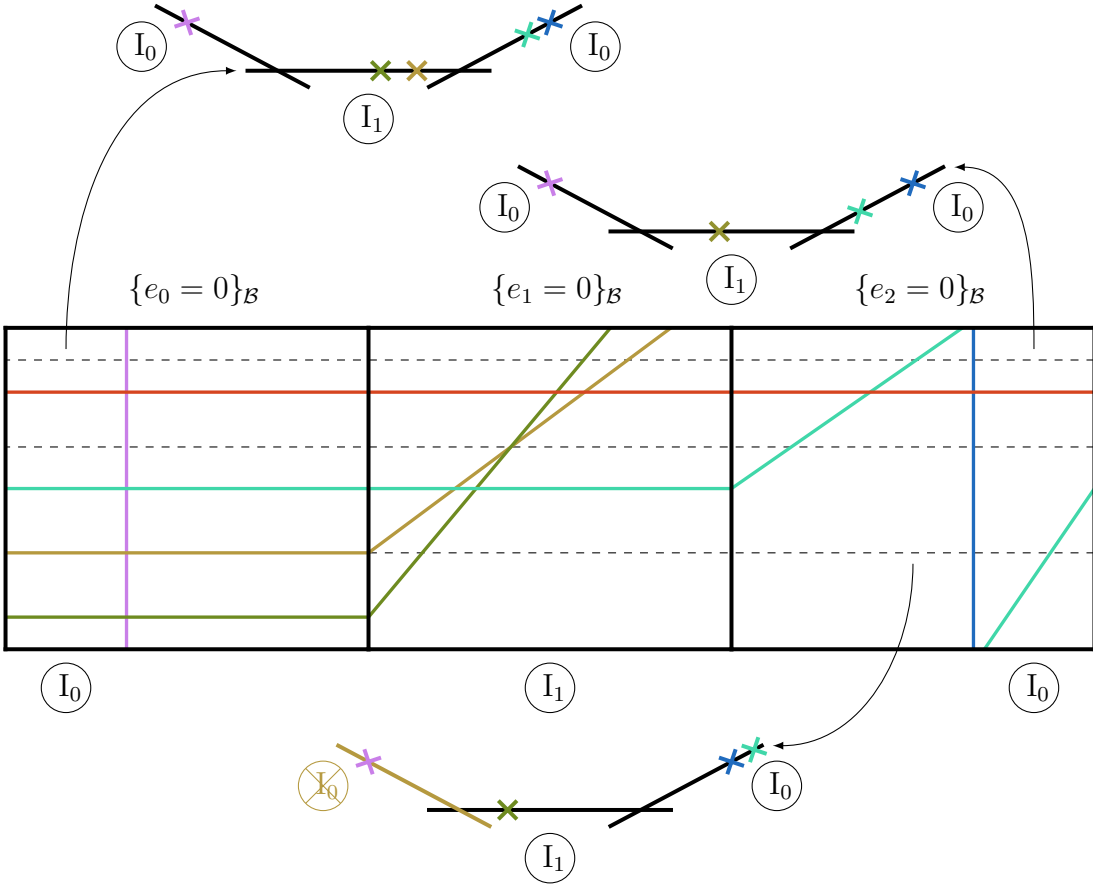


Figure 6.8: We schematically represent a reduced number of global 7-branes in the base of the central fiber of a resolved horizontal Type III.a model. The particular example depicted is constructed over $\hat{B} = \mathbb{F}_1$, and we see that the global 7-branes in the representatives of the class \mathcal{H}_∞^1 account for the difference in the number of intersection points of the discriminant with the curves $B^0 \cap B^1$ and $B^1 \cap B^2$. The two vertical restrictions shown above the central diagram are generic, while the third one, shown below it, is non-generic, since it overlaps with a global 7-brane in a representative of the class \mathcal{H}_∞^1 .

where in the first and the second line we compute it from the point of view of the B^p and the B^{p+1} component, respectively. Part of the effect of codimension-zero singular elliptic fibers is moving horizontal classes between the restrictions $\{\Delta'_p\}_{0 \leq p \leq P}$ of the modified discriminant; since in a component B^{p+1} a local 7-brane in the class T_{p+1} intersects the interface curve $B^p \cap B^{p+1}$, this results in the alteration of the intersection numbers observed above. The representatives of \mathcal{F} passing through these intersection points lead to non-generic vertical slices of the model.

6.5.2.2 Asymptotic physics in the adiabatic regime

In order to extract the asymptotic physics associated with horizontal Type III.a models we will follow the same strategy employed in the analysis of horizontal Type II.a models: We consider the hierarchy of volumes $\mathcal{V}_{\mathbb{P}_b^1} \gg \mathcal{V}_{K3}$ to hold, i.e. we study the models in the adiabatic regime. As explained in Section 6.4.3.3, taking the adiabatic limit makes the geometrical origin of the (dual) KK towers clear; away from this regime the towers that we will identify below still exist

and signal a decompactification limit, but they reorganise in a complicated manner, obscuring the unequivocal determination of the endpoint of such a process.

Given the many parallels with the analysis of Section 6.4.3, we keep the discussion more concise. In order to start with the simplest relative version of Kulikov Type III.a models, let us assume at first that the horizontal Type III.a models under consideration are constructed over $\hat{B} = \mathbb{F}_0$ and that their defining polynomials have the structure (6.4.16), i.e. only horizontal and vertical enhancements over representatives of the divisor classes $\{\mathcal{H}_\infty^p\}_{0 \leq p \leq P}$, \mathcal{H}_0^P and \mathcal{F} appear.

Consider the vertical slice of a horizontal Type III.a model associated with a generic point $p_b := [v_0 : w_0] \in \mathbb{P}_b^1$. Let us assume without loss of generality that the Y^0 component has smooth elliptic fibers in codimension-zero. In Section 6.4.3 the possibility of building the non-trivial shrinking 2-cycles $\{\gamma_i\}_{i=1,2}$ relied on the fact that the monodromy action on the two 1-cycles $\sigma_i \in H_1(\mathcal{E}, \mathbb{Z})$, for $i = 1, 2$, of the elliptic fiber \mathcal{E} when encircling $(B^0 \cap B^1)|_{[v:w]=p_b}$ was trivial. This is no longer true for the generic vertical slices of horizontal Type III.a models, but the monodromy action still leaves a 1-cycle $\sigma \in H_1(\mathcal{E}, \mathbb{Z})$ invariant, allowing for the construction a single non-trivial shrinking 2-cycle $\gamma \in H_2(Z_0, \mathbb{Z})$ on each such slice. Said monodromy action is the same in all generic vertical slices, meaning that the 2-cycle γ can be consistently defined in those patches of Y_0 consisting only of such vertical slices. In this way, we can define a local 2-cycle over the generic points of \mathbb{P}_b^1 . The M2-branes wrapping the shrinking local 2-cycle γ lead to a single tower of asymptotically massless particles, signalling a partial decompactification that is to be superimposed on top of the adiabatic limit. The non-BPS nature of these particles relates to the trivialisation of the local 2-cycle γ over the non-generic vertical slices. Note that, if both end-components $\{Y^p\}_{p=0,P}$ have smooth elliptic fibers in codimension-zero, the same construction can be performed on both ends of the open-chain; this still leads to a single local 2-cycle γ thanks to the mutual locality of the codimension-zero I_m fibers, which allows us to transport γ from one end-component to the other. Compared to the horizontal Type II.a models, we have lost one of the towers of asymptotically massless non-BPS particles associated with the isometries of the heterotic torus fiber. Hence, horizontal Type III.a limits in the adiabatic regime lead to a partial decompactification from six to nine dimensions.

Let us heuristically argue for this picture on the heterotic side of the duality by slightly abusing the dictionary reviewed in Section 6.4.1. To this end, let us focus on those horizontal Type III.a models for which $P = 1$, which most closely resemble horizontal Type II.a models in their two-component presentation. Starting with a resolved horizontal Type II.a model, the internal space on the heterotic side of the duality corresponds to the K3 surface $Y^0 \cap Y^1$, which undergoes a large volume limit both in the base $\mathcal{V}_{\mathbb{P}_b^1} \rightarrow \infty$ and in the fiber $\mathcal{V}_{T_{\text{het}}^2} \rightarrow \infty$ in a hierarchical way. Deforming the central fiber Y_0 such that it aligns with the geometry of a horizontal Type III.a model pushes one of its two components to local weak coupling. As a result, the K3 surface $Y^0 \cap Y^1$ develops Kodaira type I_m fibers in codimension-zero. This does not imply that the dual heterotic K3 surface itself develops Kodaira type I_m fibers in codimension-zero, but rather that the generic heterotic torus fiber also undergoes a large complex structure limit $U_{T_{\text{het}}^2} \rightarrow \infty$ that competes with the large volume limit $\mathcal{V}_{T_{\text{het}}^2} \rightarrow \infty$. In the actual horizontal Type III.a model the putative generic heterotic torus fiber undergoes both infinite-distance limits at the same time, resulting in a decompactification from six to nine dimensions, instead of to ten.

Returning to the F-theory discussion, we recall that the bulk physics of the asymptotic model is encapsulated in the patches of Y_0 containing only generic vertical slices. In the class of models under consideration, the 7-branes in the eight-dimensional model associated to the generic vertical slice stem from the restriction of global 7-branes in the divisor classes $\{\mathcal{H}_\infty^p\}_{0 \leq p \leq P}$ and \mathcal{H}_0^P . This set of 7-branes, together with the additional states provided by the tower of

asymptotically massless particles, enhance at the endpoint of the limit into a loop algebra, from the six-dimensional point of view. One factor of the asymptotic gauge algebra, which we will denote by H , is the gauge algebra associated to those horizontal 7-branes contained in the components at local weak coupling. These must therefore result from the A type branes in the intermediate components and, possibly, the A and D type branes in one of the end-components. In addition to this gauge algebra contribution, we will have one additional factor from each end-component at local weak coupling, consisting of the gauge algebra arising from taking together the set of horizontal 7-branes in the end-component under consideration, since the effect of the resolution process of the degeneration is to artificially separate them. All these factors are subject to a loop enhancement granted by the same imaginary root, as a consequence of the possibility of trivially transporting the local 2-cycle γ along the generic vertical slice of the central fiber of the open-chain resolution (without crossing the 7-branes in the end-components).³¹ If both end-components $\{Y^p\}_{p=0,P}$ are at local strong coupling, the resulting loop algebra is

$$G_\infty = \left(\hat{E}_{9-n_1} \oplus \hat{H} \oplus \hat{E}_{9-n_{P-1}} \right) / \sim, \quad (6.5.7)$$

and if only one end-component is at local strong coupling, we have instead

$$G_\infty = \left(\hat{E}_{9-n_p} \oplus \hat{H} \right) / \sim, \quad \text{with } p = 1, P-1. \quad (6.5.8)$$

From the point of view of the partially decompactified theory these are reinterpreted as the bulk gauge algebras

$$G_{9D} = E_{9-n_1} \oplus H \oplus E_{9-n_{P-1}}, \quad \text{or} \quad G_{9D} = E_{9-n_p} \oplus H, \quad \text{with } p = 1, P-1. \quad (6.5.9)$$

In the heuristic heterotic dual picture, the asymptotic enhancement to the loop algebra can be understood in terms of the metric $U(1)_{KK}$ factor associated with the continuous isometry along the torus radius that is becoming large in the limit. The perturbative heterotic gauge sector is mostly restored as the (non-singular) gauge bundle contributions dilute, but the part of them along the torus direction that remains small still have a tangible effect on the bulk algebra and are responsible for the partial Higgsing observed in the asymptotic model.³²

We now turn to the non-generic vertical slices of a horizontal Type III.a model. For $\hat{B} = \mathbb{F}_0$, and assuming first the structure (6.4.16), these are the global vertical 7-branes, which can be brought together in order to realise global vertical enhancements supported over representatives of \mathcal{F} . Taking horizontal slices of the model, the same arguments as in Section 6.4.3.1 imply that these gauge algebra contributions remain lower-dimensional at the endpoint of the limit, localised in the worldvolume of six-dimensional defects.

The redistribution of horizontal 7-branes among the components due to the presence of components at local weak coupling reduces the extent to which codimension-two finite-distance non-minimal points can be tuned. As a consequence, the total rank of the gauge algebra factors supported over the exceptional curves arising in the resolution of codimension-two non-minimal points decreases. Heuristically, we can understand this from the heterotic side as a by-product

³¹Using the string junctions picture, the loop enhancement by a common imaginary root is nicely explained for Kulikov Type III.a models in [276].

³²Similarly to how tuning the non-minimal singularities necessary to realise a horizontal Type II.a model tightens the six-dimensional horizontal gauge rank bound $\text{rank}(\mathfrak{g}_{\text{hor}}) \leq 18$ valid at finite-distance to the bound $\text{rank}(\mathfrak{g}_{\text{hor}}) \leq 16$, which matches the dual heterotic interpretation of a decompactification from six to ten dimensions, tuning a horizontal Type III.a models tightens it to $\text{rank}(\mathfrak{g}_{\text{hor}}) \leq 17$ instead, as would correspond for a heterotic dual interpretation as a decompactification from six to nine dimensions.

of the residual Higgsing: In order to realise it, part of the instanton number budget $c_2(\text{K3}) = 24$ needs to be spent on producing the non-trivial gauge bundle background necessary to realise it, and is therefore not available in order to produce singular gauge bundle contributions capable of probing the geometrical ADE singularities of the internal space. Hence, the bigger the residual Higgsing, the smaller the maximal non-perturbative gauge algebra that can be realised. Similarly, on the F-theory side, the more horizontal 7-branes are moved to the intermediate components, the smaller the vanishing orders that can be attained for the codimension-two non-minimal points and, consequently, the smaller the gauge algebra supported over exceptional curves. In addition, the bounds on the maximal rank of the vertical gauge algebra become stricter in the presence of local weak coupling components, as was explained in Section 6.3.6.

Relaxing the condition (6.4.16) amounts to allowing for mixed enhancements. Their interpretation is as in horizontal Type II.a models discussed in Section 6.4.3.2. Mixed enhancements result from a Higgsing between the perturbative and non-perturbative gauge sectors, using the heterotic language. The Higgsing effect of the perturbative sector is diluted in the limit while only the residual defect algebra survives in the asymptotic model.

Let us conclude our analysis of horizontal Type III.a models by considering those constructed over $\hat{B} = \mathbb{F}_n$, which only require a minor modification of the preceding discussion. The first effect of abandoning the direct product structure for the F-theory base space was already observed for horizontal Type II.a models in Section 6.4.4: While Higgsing the six-dimensional horizontal gauge algebra decreases the maximal rank that can be attained from the gauge sector supported over exceptional curves for all $\hat{B} = \mathbb{F}_n$, when $n \geq 1$ the rank of the vertical gauge algebra is also reduced, since \mathcal{F} classes are needed in order to realise the 7-brane recombinations necessary for the horizontal Higgsing. Once we move to horizontal Type III.a models a second, but related, effect occurs: The six-dimensional horizontal gauge algebra is partially Higgsed due to the redistribution of (local) horizontal 7-branes among the components. When $n \geq 1$, this entails part of the horizontal 7-branes that would have formed part of the maximal horizontal gauge algebra in the end-components recombining with a global vertical brane and moving to the intermediate components as mixed branes, which therefore decreases the maximal vertical gauge rank possible in the model (on top of the reduction of the gauge rank of the factors supported over exceptional curves, that was already mentioned for $\hat{B} = \mathbb{F}_0$ earlier). This effect was commented on from the geometrical point of view at the end of Section 6.3.6 using horizontal Type III.a models constructed over $\hat{B} = \mathbb{F}_7$ as an example.

6.5.3 Horizontal Type III.b models

Horizontal Type III.b models are those in which the generic vertical slice $\sigma : \mathcal{Z} \rightarrow D$ of their open-chain resolution $\rho : \mathcal{Y} \rightarrow D$ is a Kulikov Type III.b model. In terms of the pattern of codimension-zero singular elliptic fibers exhibited by their central fiber Y_0 , this class of models is characterised by having all components at local weak coupling, i.e. they are global weak coupling limits in which the Type IIB axio-dilaton is driven to infinity $\tau \rightarrow i\infty$.

As was discussed in Section 6.3.2.3, horizontal Type III.b models can only be constructed over $\hat{B} = \mathbb{F}_n$ with $0 \leq n \leq 4$, as can be argued either through their geometrical properties, or by realising that otherwise they would present non-Higgsable clusters supporting exceptional enhancements, which are incompatible with a perturbative Type IIB orientifold picture.

Moreover, the elliptic fibers found in codimension one and higher must be compatible with $j(\tau) \rightarrow \infty$, which imposes strict constraints on the local and global 7-brane content of these models, see Section 6.3.4. This restricts us to enhancements realising Kodaira type I_m and I_m^*

fibers. The geometry of horizontal Type III.b models also prevents a \mathfrak{g}_2 algebra, associated with I_0^{*ns} fibers, from being realised, by constraining the possible monodromy covers.

6.5.3.1 Type IIB orientifold picture

The central fiber Y_0 of a horizontal Type III.b model matches the structure of a horizontal Type III.a model except that both end-components $\{Y^p\}_{p=0,P}$ have been tuned to be at local weak coupling. Given the similarities between their geometries, it is worth spending a moment comparing them before we completely focus on horizontal Type III.b models.

Horizontal Type III.b models represent global weak coupling limits, and should therefore admit a description in terms of a Sen limit [203]. A global weak coupling F-theory model obtained by compactification on the elliptic fibration $\pi : Y \rightarrow B$ is interpreted as a Type IIB orientifold compactification, using the Sen limit language, in the following way: The internal space of the Type IIB theory is given by the Calabi-Yau double cover \check{B} of the base B . The branching locus of the double cover corresponds to the fixed loci of the orientifold involution, which are identified with the O7-planes in the Type IIB internal space. For six-dimensional F-theory models, the resulting double cover \check{B} is an elliptic K3 surface.

In order to bring a horizontal Type III.b model in this form, we can blow down its central fiber Y_0 to any of its components $\{Y^p\}_{0 \leq p \leq P}$. The central fiber \hat{Y}_0 of the resulting degeneration $\hat{\rho} : \hat{\mathcal{Y}} \rightarrow D$ will present, due the global weak coupling nature of horizontal Type III.b models, codimension-zero Kodaira type I_m fibers, and is therefore amenable to the Type IIB orientifold description just discussed above. However, since the blow-down has lead to an unresolved degeneration $\hat{\rho} : \hat{\mathcal{Y}} \rightarrow D$, this central fiber \hat{Y}_0 supports non-minimal elliptic fibers over some horizontal curves in the base. As a result, the Type IIB internal space \check{B} is an elliptic K3 surface that has undergone a Kulikov Type II.b degeneration, see Section B.13.2. A more detailed account of the process of blowing down the resolved degeneration and constructing the double cover of the base of the central fiber is given in Appendix B.13.

Note that, at least in terms of the geometrical double cover construction, the same Type IIB orientifold picture can be reached starting from a resolved horizontal Type III.a model. One distinction with the previous case is that horizontal Type III.a models contain at least one component at local strong coupling; the blow down process should be chosen such that the resulting \hat{Y}_0 corresponds to one of the components $\{Y^p\}_{0 \leq p \leq P}$ at local weak coupling.

In both instances, the end result for the Type IIB internal space is a degenerate elliptic K3 surface \check{B} of the type appearing as the central fiber of Kulikov Type II.b models. As we see in Section B.13.2, the degeneration of this K3 surface is directly tied to the codimension-one non-minimal loci appearing in the blown-down F-theory model; the latter, which correspond to the coalescence of O7-planes in the Type IIB interpretation, force a certain factorization structure for the branching locus of \check{B} . Moving O7-planes on top of each other usually involves strongly coupled dynamics, which competes with the global weak coupling limit. Depending on how they balance against each other, we end up with a horizontal Type III.a or Type III.b model. If the O7-planes are brought together too fast, the strongly coupled nature of the process prevails against the weak coupling limit, and we obtain a horizontal Type III.a model; the central fiber Y_0 of its open-chain resolution always presents at least one component at local strong coupling as a consequence of this. If the weak coupling limit is instead taken rapidly enough, the model can remain at global weak coupling, and we obtain a horizontal Type III.b model; all components of the central fiber Y_0 of its open-chain resolution are, for that reason, at local weak coupling. The additional level of tuning necessary to achieve this compared to a horizontal Type III.a

model ensures a careful balance between the weak coupling limit and the coalescence process of O7-planes in the Sen limit picture. The same logic underlies the related eight-dimensional F-theory degenerations [157].

From a perturbative Type IIB orientifold compactification perspective, the limits under consideration are fairly complicated. Starting from a generic Type IIB orientifold compactification on the K3 double cover, the internal space is subject to a Kulikov Type II.b degeneration at the same time as a limit in the string coupling g_{IIB} is taken. The shrinking transcendental 2-cycles of the internal space then lead to worldsheet and D-instanton corrections arising from strings wrapped on them. Their importance for the asymptotic physics of the infinite-distance limit depends on the precise way in which g_{IIB} scales along it. Potentially, the trajectories may even leave the regime of validity of the perturbative description. The analysis in F-theory automatically discriminates between the different possibilities through the resolution process of the degeneration of its internal space.

6.5.3.2 Generic vertical slices

As in the analysis of the other horizontal models, let us first study the eight-dimensional F-theory models associated with the generic vertical slices of horizontal Type III.b models. We can be brief because, as emphasised earlier, the geometry corresponds to a further tuning of horizontal Type III.a models analysed in Section 6.5.2.1.

The distribution of 7-branes in the eight-dimensional model associated with the generic vertical slice is still described by (6.5.1) and (6.5.2), with the only difference being that now $n_p > 0$ for all $p \in \{0, \dots, P\}$. The restrictions on the 7-brane types that can be found in its components descend again from the constraints on the (local) 7-brane content discussed for six-dimensional models in Section 6.3.4: All components can contain A type singular elliptic fibers, with the end-components $\{Y^p\}_{p=0,P}$ presenting in addition 2 singular elliptic fibers of D type each.

The non-generic representatives of \mathcal{F} are those passing through the intersection points of Δ_{phys} with the interface curves $\{B^p \cap B^{p+1}\}_{0 \leq p \leq P-1}$ over which the base components of the central fiber meet. The number of these intersection points varies from one pair of adjacent components to the other due to the redistribution of horizontal classes between the $\{\Delta'_p\}_{0 \leq p \leq P}$, and is given by (6.5.6).

6.5.3.3 Asymptotic physics in the adiabatic regime

We now analyse the asymptotic physics of horizontal Type III.b models in the adiabatic regime, i.e. by imposing the hierarchy of volumes $\mathcal{V}_{\mathbb{P}_b^1} \gg \mathcal{V}_{\text{K3}}$. First, we extract the bulk physics at the endpoint of the limit from the generic vertical slices of the model, to then examine the purely six-dimensional features associated with the loci over which the adiabaticity assumption fails.

Consider the vertical slice of a horizontal Type III.b model associated with a generic point $p_b := [v_0, w_0] \in \mathbb{P}_b^1$. All components of its central fiber have codimension-zero I_m fibers that are mutually local to each other, meaning that the 1-cycle $\sigma \in H_1(\mathcal{E}, \mathbb{Z})$ that collapses to produce the pinched torus fibers is the same in all components. Analogously to the discussion of Section 6.5.2.2, this leads to a shrinking 2-cycle $\gamma \in H_2(Z_0, \mathbb{Z})$ that can be extended to a shrinking local 2-cycle γ in the generic patches of Y_0 . The M2-branes wrapping γ lead to a single tower of asymptotically massless particles, which are non-BPS due to the trivialisation of γ over the non-generic vertical slices.

We can rephrase this in terms of the perturbative Type IIB orientifold interpretation of horizontal Type III.b models. The Type IIB internal space corresponds to a degenerate elliptic K3 surface of the type appearing as the endpoint of Kulikov Type II.b models, as mentioned above. Such a K3 surface has codimension-zero I_m fibers whose singularity type does, in addition, undergo A and D type enhancements over codimension-one loci in the base. Its elliptic fibration is also in the adiabatic regime thanks to the adiabaticity of the internal elliptic fibration of the F-theory model. The M2-branes wrapping the degenerate 1-cycle $\sigma \in H_1(\mathcal{E}, \mathbb{Z})$ present over the generic points of $p_b \in \mathbb{P}_b^1$ in the F-theory model lead to the non-BPS weakly coupled asymptotically tensionless fundamental string in the Type IIB picture. The M2-branes can not only wrap the local 1-cycle σ , but also the shrinking local 2-cycle γ , leading to the tower of asymptotically massless particles discussed earlier. In the Type IIB interpretation, this tower corresponds to the winding modes of the fundamental string wrapping the generic I_m fiber of the degenerate K3 surface. Since the geometrical scaling leading to the string and the particles to be asymptotically massless is the same, it is clear on dimensional grounds that the tower of asymptotically massless particles becomes light at a faster rate, such that horizontal Type III.b models do not represent emergent string limits. In addition to the tower of particles just discussed, there is a second one stemming from the torus direction that becomes large in the large complex structure limit of the generic elliptic fiber of the Type IIB internal K3 surface. Altogether, the adiabatic limit in conjunction with these two towers of asymptotically massless particles result in a total decompactification from six to ten dimensions.

As we have argued in the context of the other horizontal models, the global vertical enhancements remain lower-dimensional at the endpoint of the limit, and are localised in the worldvolume of six-dimensional defects of the decompactified theory. Due to the global weak coupling nature of horizontal Type III.b models, the types of gauge algebras that can appear are restricted to those associated with Kodaira type I_m or I_m^* fibers, except for I_0^{*ns} fibers that cannot be realised, see Sections 6.3.4 and 6.3.5.

Note that since the Type IIB internal K3 surface undergoes a Kulikov Type II.b degeneration, this leads to two shrinking 2-cycles $\{\gamma_i^{\text{IIB}}\}_{i=1,2}$ obtained from combining the vanishing 1-cycle of its generic elliptic fiber with the two 1-cycles of the elliptic curve corresponding to the double cover of \mathbb{P}_b^1 . By wrapping extended objects on these shrinking 2-cycles, we obtain $D3|_{\gamma_i^{\text{IIB}}}$ -strings and $F1|_{\gamma_i^{\text{IIB}}}$ - and $D1|_{\gamma_i^{\text{IIB}}}$ -instantons. The adiabatic limit makes these contributions irrelevant for the asymptotic physics. It would be interesting to understand if they play a prominent role away from the adiabatic regime, being an avatar of the complicated reorganisation of the towers of asymptotically massless particles observed in the M-/F-theory picture, or if the rapid weak coupling limit is still able to suppress them on its own.

6.6 Discussion and future directions

We have investigated a large class of complex structure degenerations that occur at infinite distance in the moduli space of F-theory compactified to six dimensions. While Chapter 5 focused on the geometric foundations, our goal here was to interpret the degenerations from the point of view of general quantum gravity expectations. The theories we have explored arise when the internal space develops non-Kodaira singularities in the elliptic fiber over curves on a Hirzebruch surface base. They correspond to certain infinite-distance limits in the non-perturbative open string moduli space, possibly superimposed with a weak coupling limit. As explained in the more general context of Chapter 5, to facilitate the systematics one can first focus on degenerations over non-intersecting curves, so-called single infinite-distance limits. This restricted class of

degenerations is possible only over special curves of genus zero, or over an anti-canonical divisor of the base. In this chapter we have analysed the first type of such models, which come in four classes as listed in Table 6.2.1. The bulk of this chapter is devoted to the horizontal models, while the remaining three cases are treated similarly, wherever possible, in Appendix B.14.

Horizontal models (as well as the related mixed (bi)sectional models in Table 6.2.1) arise from non-Kodaira singularities over sections of the Hirzebruch surface. As we have seen, this greatly facilitates the physics interpretation of the degenerations, at least in certain regimes of the moduli space where the base of the Hirzebruch surface is taken to be of asymptotically large volume. In such adiabatic limits, one can convincingly identify the towers of massless states that are expected in view of the Swampland Distance Conjecture [146] and its refinement, the Emergent String Conjecture [149]. These arise, in the language of M-theory, from M2-branes multi-wrapped along local 2-cycles of torus topology which exist away from isolated defects. This picture becomes more and more accurate as the location of the defects is pushed to infinity in the asymptotically adiabatic regime. The result is a relative version of the massless towers appearing in F-theory probing degenerations of K3 surfaces [156, 157]. As corroborated by the heterotic dual, the massless towers are interpreted as Kaluza-Klein towers signalling a decompactification limit. Since these are defined only away from isolated points on the base of the Hirzebruch surface, the latter play the role of six-dimensional (gauge) defects within an asymptotically nine or ten-dimensional bulk theory. In addition to these decompactification limits with lower-dimensional defects, some of the infinite distance limits (of Type II.b and III.b) have an interpretation as global weak coupling limits, again as in the eight-dimensional parent theories studied in [156, 157]. All this is in perfect agreement with the expectations of the Emergent String Conjecture [149]. The appearance of lower-dimensional defects in decompactification limits was observed before in a different context in [280].

The defect theories admit a particularly interesting interpretation from the dual heterotic point of view. They correspond to ADE type singularities on the heterotic K3 surface probed by point-like instantons of trivial or discrete holonomy. In the latter case there arise no tensor branch deformations. This matches the picture on the F-theory side of 7-branes wrapping the fiber of the Hirzebruch surface without being related to finite-distance non-minimal singularities. We have clarified some aspects of these non-perturbative gauge sectors in Appendix B.12.

Numerous open questions lend themselves for future investigations. Conceptually, the most important, but also most challenging, one is to establish a clear interpretation of the endpoints of the limits away from the adiabatic regime. When the defects no longer move to infinity, the limits are primarily characterised by the appearance of vanishing 3-cycles, while the role of the local 2-cycles becomes more obscure. We expect a reorganisation of the towers of asymptotically massless particles, but in such a way that eventually the limit is still a decompactification limit. As we explained, this picture is suggested by the behaviour on the heterotic dual side, at least if we can qualitatively trust the duality away from the adiabatic limit. Establishing such an interpretation would be important also as a way to tackle geometries in which no adiabatic limit can be taken, for instance the vertical degenerations. A related fruitful direction would be to put our findings in the context of the somewhat complementary approach to studying complex structure infinite-distance limits via asymptotic Hodge theory [252–254]. In this framework, the appearance of shrinking 3-cycles at infinite distance is established by studying monodromies around degeneration loci in the moduli space. In compactifications of Type IIB string theory to four dimensions, this makes manifest the appearance of towers of asymptotically massless states from wrapped D3-branes. Irrespective of the way in which the vanishing 3-cycles are deduced, more geometrically or more algebraically as in the Hodge theoretic approach, their role in relation

with the towers in six-dimensional F-theory, rather than four-dimensional Type IIB theory, is rather obscure. Our approach to demystify the situation was to take advantage of the adiabatic regime, where it is manifest that massless states arise from wrapped M2-branes on vanishing 2-chains, though these do not correspond to globally defined 2-cycles. To arrive at a satisfactory understanding of the limits in a more general context, without having to rely on adiabaticity, we will likely have to reconsider also the role of quantum effects as possible obstructions to certain directions in the moduli space. Indeed, both perturbative and non-perturbative quantum effects have the potential to affect infinite-distance limits in non-trivial ways, as studied in various frameworks [1, 153, 154].

At the level of systematics, we have focused on a subclass of the codimension-one single infinite-distance limits explored more generally in Chapter 5. Natural extensions would be to include also degenerations associated with non-minimal genus-one curves, or degenerations constructed over the complex projective plane, which lacks a fibration structure. One could also allow for codimension-one degenerations outside the single infinite-distance limit class by simultaneously engineering multiple complex structure degenerations, each of which would individually have served as a single infinite-distance limit, still within the framework of Chapter 5. Last but not least, infinite-distance limits can be associated with codimension-two non-Kodaira degenerations, which we have not explored systematically even at the purely geometric level. This state of affairs makes the complex structure degenerations of F-theory a remarkably rich field for future studies.

Part V

Peroratio

Chapter 7

Conclusions

This thesis focused on the analysis of general criteria which consistent theories of quantum gravity are expected to adhere to, according to the Swampland Conjectures. Such an exploration required studying the quantum geometry of non-perturbative string compactifications and its consequences for physics.

Quantum gravity is both a conceptual and practical desideratum of contemporary theoretical physics, as we argued in Chapter 1. String theory is a self-consistent theory of quantum gravity—and the remaining fundamental forces—from which we can extract quantitative conclusions under good technical control, making it invaluable in any exploration of quantum gravity. In Chapter 2 we reviewed the basic notions of string theory and string compactifications, the string duality web, and a formulation of the theory known as F-theory, which allows for the geometrization of physical problems—a Leitmotiv of the thesis.

A crucial feature of gravity, as opposed to other sectors of physics, is that its presence leads to UV/IR mixing; as a consequence, quantum gravity can and does, despite its UV nature, constrain low-energy gravitational EFTs. The set of those that can be consistently completed to a theory of quantum gravity, the Landscape, is enclaved within a much larger set of gravitational EFTs that seem consistent from effective reasoning, but break apart once their completion to quantum gravity is attempted: the Swampland. Chapter 3 reviewed the Swampland Program and some of its core Swampland Conjectures, with special emphasis on those that threaded the rest of the thesis: the Swampland Distance Conjecture and the Emergent String Conjecture.

The Swampland Distance Conjecture predicts that as we traverse an infinite-distance in the moduli space, an infinite tower of states becomes asymptotically massless at an exponential rate in the geodesic distance. The Emergent String Conjecture refines this statement by specifying that the tower must be furnished by Kaluza-Klein states, in which case the asymptotic physics corresponds to a decompactification, or by the excitations of a unique, weakly coupled, asymptotically tensionless critical string, signalling a transition to the duality frame determined by the emergent string. We challenged this conjecture by studying if membrane limits, i.e. those infinite-distance limits in which a membrane parametrically sits at the lightest scale, are possible. Moreover, we analysed the validity of the conjecture in the open string moduli space, a region of the moduli space less studied in this regard than its closed string counterpart.

The scrutiny of membrane limits was the subject of Chapter 4, based on the publication [1], where we concluded that membrane limits are obstructed in the quantum-corrected moduli space. Our analysis was divided in two parts. First, we studied how the consistency under dimensional reduction of the Emergent String Conjecture affects membrane limits. If the membrane that is parametrically leading along the limit yields a critical string upon circle reduction, one can show

that it must decouple from the Kaluza-Klein scale in the higher-dimensional theory, in order to avoid the existence of pathological string limits in the theory obtained by circle compactification. Second, we set out to test this behaviour without assuming the Emergent String Conjecture, by explicitly attempting to construct membrane limits in the hypermultiplet moduli space of five-dimensional M-theory. The choice of this setting was motivated by the fact that it is not a theory of strings, which on dimensional grounds tend to be parametrically leading with respect to membranes. Indeed, we were able to construct putative membrane limits in the classical hypermultiplet moduli space of the theory. However, as the trajectories corresponding to these classical membrane limits are traversed, M2-instanton corrections can be seen to become increasingly relevant. Through a chain of dualities— involving the formal identification of the hypermultiplet moduli space under study with that of four-dimensional Type IIA string theory and mirror symmetry to Type IIB—we were able to incorporate the effect of the M2-instantons. In the quantum-corrected hypermultiplet moduli space of five-dimensional M-theory, the putative membrane limits are deflected into decompactification limits. The membranes do indeed decouple from the lightest Kaluza-Klein scale along the limit, saturating, in fact, the minimal parametric separation between the two derived from the first part of the analysis. Hence, we found perfect agreement with the expectations from the Emergent String Conjecture.

Six-dimensional F-theory models in which the lower-dimensional Planck scale is finite have an elliptically fibered compact internal space. The position of the 7-branes of the model can be varied by moving in the non-perturbative open string moduli space of the theory, these trajectories corresponding from the F-theory perspective to complex structure deformations of the internal geometry. Interestingly, in spite of the compact nature of the space in which the 7-branes can move, these deformations can correspond to infinite-distance limits in the moduli space if a brane stack including a suitable set of mutually non-local $[p, q]$ 7-branes is brought together. The localised non-abelian gauge algebra arising when we move a collection of 7-branes on top of each other can be read off from the type of minimal singular elliptic fibers that the internal space develops along such a finite-distance degeneration. Likewise, infinite-distance limits in the complex structure moduli space of F-theory are associated to degenerations in which the endpoint of the limit exhibits non-minimal singular elliptic fibers. These do not allow for a crepant resolution in the fiber, like their minimal counterparts do, making their analysis more involved; models presenting this type of singularities are usually discarded in F-theory analysis. Understanding the geometry and physics of the infinite-distance non-minimal singularities of elliptic Calabi-Yau threefolds is therefore interesting both from an intrinsic F-theoretic point of view and from the perspective of the Swampland Program, more specifically in relation to the Emergent String Conjecture.

Chapter 5 was concerned with the systematic mathematical analysis of this problem, following the publication [2]. The infinite-distance limits under consideration can be described using the algebro-geometric language of degenerations. In order to later extract the asymptotic physics, it is convenient to present these infinite-distance complex structure degenerations in semi-stable form; we explicitly analysed how to do this through a series of modifications and base changes, in the context of the Semi-stable Reduction Theorem. The geometrical representative of the endpoint of the limit becomes, as a result of this resolution process, a union of log Calabi-Yau spaces glued together along their boundaries. We completely characterised the base geometry of these components and the line bundles that are defined over them. As an explicit example, we applied this machinery to a very general class of limits, namely the genus-zero single infinite-distance limit degenerations of Hirzebruch models. We concluded by explaining how to extract the gauge

algebra for F-theory probing such reducible asymptotic geometries from the notion of physical discriminant, also introduced during the chapter.

Building on these results, Chapter 6 studies the asymptotic physics associated with genus-zero single infinite-distance limit degenerations of Hirzebruch models, following the publication [3]. We concluded that a subclass of these degenerations result in decompactification limits that do not lead to the vacuum of the higher-dimensional theory, but rather force the presence of six-dimensional defects. We also found emergent string limits, whose endpoints are at global weak coupling. This last property depends on the pattern of codimension-zero singular elliptic fibers in the components of the model, and is hence fairly constrained; we determined the conditions that need to be met in the different classes of models in order for a global weak coupling limit to be possible. The results relied on an adiabatic limit that allowed us to gain further information on the asymptotically massless states from the structure of vanishing cycles. We complemented the study by taking the heterotic dual perspective whenever available. Our analysis showed agreement with the expectations set by the Emergent String Conjecture.

There are various directions in which these results could be expanded: studying non-minimal degenerations over representatives of the anti-canonical class in a similar level of detail, generalise the analysis to include those degenerations only exhibiting codimension-two infinite-distance non-minimal points, or interpreting the asymptotic physics away from the adiabatic regime, to name just a few. These were detailed at a more technical level in the relevant chapters.

More broadly, the non-trivial checks of the Emergent String Conjecture that we have carried out entailed computing the quantum-corrected geometry of the hypermultiplet moduli space, performing a systematic analysis of the infinite-distance semi-stable degenerations of Calabi-Yau threefolds, and translating all of these results into physics through M- and F-theory. The subtle and fruitful interplay between physics and mathematics, familiar from string theory and theoretical physics at large, also manifests itself as we explore the asymptotic regions of the moduli space. It will be interesting to see how this and other forms of argumentation converge together in the Swampland Program to establish the general properties of quantum gravity on firm ground.

Appendices

Appendix A

Addenda to Part III

The material collected in this appendix complements the discussion of Chapter 4.

A.1 KK scale in A-F1-limits

In this appendix, we comment on the correct identification of the KK scale in the A-F1-limit of Section 4.5.1. As claimed there, the KK scale is set by the modes coming from the shrinking S^3 , which is not the fastest growing cycle and in fact is shrinking along the limit. To understand this, we first emphasize that the truly meaningful scalings are the quantum-corrected ones, since in the A-F1-limit the distinction between classical and quantum-corrected trajectories is arbitrary.¹ The rate at which all possible KK modes become light is uniform after taking the corrected trajectories into account. Indeed, deep enough along the limit eventually $z_{\text{IIA}}^a \sim \text{const.}$, and therefore we can directly write

$$\left(\frac{M_{\text{KK}}}{M_{\text{Pl}}^{\text{4D}}}\right)^2 = \frac{1}{(\mathcal{V}_{\text{3-cycle}}^{\text{IIA}})^{\frac{2}{3}}} \left(\frac{M'_s}{M_{\text{Pl}}^{\text{4D}}}\right)^2 \xrightarrow{\text{QC}} 1 \cdot \frac{1}{\chi'} \sim \frac{1}{\lambda^3}, \quad (\text{A.1.1})$$

without reference to the specific 3-cycle considered.

However, at least for the classical A-F1-limit, we find some additional KK towers with scaling

$$\left(\frac{M_{\text{KK},\gamma^\alpha}}{M_{\text{Pl}}^{\text{4D}}}\right)^2 = \frac{1}{(\mathcal{V}_{\gamma^\alpha}^{\text{IIA}})^{\frac{2}{3}}} \left(\frac{M'_s}{M_{\text{Pl}}^{\text{4D}}}\right)^2 \sim \frac{1}{\lambda^{2-\frac{\alpha}{3}}}, \quad (\text{A.1.2})$$

where $\alpha = 0, 1, 2, 3$. The case with $\alpha = 3$ corresponds to the S^3 tower highlighted above, but, for example, the putative KK tower associated with the growing T^3 ($\alpha = 0$) becomes light faster than any other scale in the problem. This cannot be true, as no such phenomenon occurs in the mirror dual Type IIB limit, i.e. in the classical F1-limit.

To resolve this puzzle, recall that we are using the SYZ fibration structure and the LCS behaviour of the periods in order to extract the scalings for the classical limits. This works well in the limit of large S^3 base, but soon becomes invalid for a trajectory like the one taken in the A-F1-limit. Luckily, mapping the quantum-corrected F1-limit to the mirror side is still possible thanks to the simplicity provided by the freezing of the Kähler coordinates on the Type IIB side.

In spite of this, taking the classical limit precisely neglects these subtleties and exploits the LCS results beyond their regime of applicability. This is the origin of the pathological behaviour

¹See Footnote 8.

that is removed after taking the pertinent corrections into account. From this point of view, we might want to still argue why a tower like the one corresponding to the growing T^3 from the SYZ fibration should not be there even before exiting the regime of validity of the LCS approximation. A heuristic way to see this is to consider mirror symmetry as T-duality on the SYZ torus. This duality maps the T^3 KK tower observed on the Type IIA side to string winding states along the dual SYZ torus fiber. If present, these light winding states would also endanger the classical F1-limit. However, on the IIB side it is clear that the winding states are not there as asymptotically light particles since the Calabi-Yau exhibits a non-trivial fibration structure rather than being a direct product $T^3 \times S^3$. The degenerations of the T^3 fiber trivialise the homology class of the S^1 factors inside the T^3 as elements of $H_1(Y, \mathbb{Z})$, giving a non-zero mass term to the naive winding states. As a consequence, the KK modes on the Type IIA side must also be absent, or at least they cannot become asymptotically massless. This expected behaviour is confirmed by numerical computation of the eigenvalues of the scalar Laplace operator on the Dwork family ($\sum_i X_i^5 + \psi \prod_i X_i$) of quintic threefolds [350–352]. The towers corresponding to $\alpha = 1, 2$ would correspond to cycles that are partially inside the T^3 fiber and degenerate in a similar fashion. Therefore, in the limits in which the manifold is shrinking from the Type IIB perspective, we only take into account the S^3 KK modes for the classical analysis on the Type IIA side.

Appendix B

Addenda to Part IV

The material collected in this appendix complements the discussion of Chapters 5 and 6.

B.1 Six-dimensional F-theory bases

In this appendix, we review the base spaces that can occur for elliptic Calabi-Yau threefolds, given by [311]

1. $B = \mathbb{P}^2$, the complex projective plane;
2. $B = \mathbb{F}_n$, the Hirzebruch surfaces with $0 \leq n \leq 12$; and
3. $\text{Bl}(\mathbb{P}^2)$ and $\text{Bl}(\mathbb{F}_n)$, arbitrary blow-ups of the previous two.

While the first two possibilities are very concrete, the third case encompasses a wealth of geometries, due to the many ways in which a surface can be blown up. The complex projective plane \mathbb{P}^2 and the Hirzebruch surfaces \mathbb{F}_n with $n \neq 1$ are the minimal surfaces obtained by repeated application of Castelnuovo's contraction theorem in the class of surfaces that can be F-theory bases, hence their simplicity.

After first reviewing well-known properties of \mathbb{P}^2 and \mathbb{F}_n , we recall some basics of the blow-ups of algebraic surfaces at points and apply these facts to blow-ups of \mathbb{P}^2 and Hirzebruch surfaces. The material of this appendix also serves as a preparation for Appendix B.2, where the genus-zero base curves that can support non-minimal singular elliptic fibers are analysed.

B.1.1 \mathbb{P}^2 and \mathbb{F}_n

The complex projective plane \mathbb{P}^2 can be described using the coordinates $[z_1 : z_2 : z_3]$ homogenous under the \mathbb{C}^* -action. \mathbb{P}^2 is a toric variety with fan $\Sigma_{\mathbb{P}^2}$ given by the edges

$$z_1 = (1, 0), \quad z_2 = (0, 1), \quad z_3 = (-1, -1), \quad (\text{B.1.1})$$

in the lattice

$$N := \langle (1, 0), (0, 1) \rangle_{\mathbb{Z}}. \quad (\text{B.1.2})$$

Its Picard group is

$$\text{Pic}(\mathbb{P}^2) = \langle H \rangle_{\mathbb{Z}}, \quad (\text{B.1.3})$$

where H denotes the hyperplane class, with self-intersection

$$H \cdot H = 1. \quad (\text{B.1.4})$$

The anticanonical class of \mathbb{P}^2 is given by

$$\overline{K}_{\mathbb{P}^2} = 3H. \quad (\text{B.1.5})$$

Next, we centre our attention on \mathbb{F}_n , that is used as the base in most of our explicit examples. A Hirzebruch surface is a \mathbb{P}^1 -bundle obtained from the projectivization of rank 2 vector bundles over \mathbb{P}^1 , which can always be written as

$$\mathbb{F}_n := \mathbb{P}(\pi : \mathcal{O}_{\mathbb{P}^1} \oplus \mathcal{O}_{\mathbb{P}^1}(n) \longrightarrow \mathbb{P}^1). \quad (\text{B.1.6})$$

We can take $n \geq 0$, since $\mathbb{F}_n \simeq \mathbb{F}_{-n}$ due to the invariance of the projectivization of a bundle under twists by Abelian line bundles. The Picard group of \mathbb{F}_n is

$$\text{Pic}(\mathbb{F}_n) = \langle h, f \rangle_{\mathbb{Z}}, \quad (\text{B.1.7})$$

where h is the class of the zero section and f is the class of a fiber. Their intersection products are given by

$$h \cdot h = -n, \quad h \cdot f = 1, \quad f \cdot f = 0. \quad (\text{B.1.8})$$

Apart from the $(-n)$ -curve h coming from the sub-bundle $\mathcal{O}_{\mathbb{P}^1}$, there exists another independent section associated with the sub-bundle $\mathcal{O}_{\mathbb{P}^1}(n)$. This is the $(+n)$ -curve, which we will denote by C_{∞} (using then also the notation $C_0 := h$). Unlike the rigid curve C_0 , the curve C_{∞} moves in an n -dimensional linear system, with any two representatives meeting in n points. Using the linear equivalence

$$C_{\infty} = h + nf, \quad (\text{B.1.9})$$

we obtain the intersection products

$$C_{\infty} \cdot C_{\infty} = n, \quad C_{\infty} \cdot C_0 = 0, \quad C_{\infty} \cdot f = 1. \quad (\text{B.1.10})$$

The anticanonical class of the Hirzebruch surface \mathbb{F}_n is

$$\overline{K}_{\mathbb{F}_n} = 2h + (2+n)f. \quad (\text{B.1.11})$$

Let us denote the fibral \mathbb{P}^1 by \mathbb{P}_f^1 and the base one by \mathbb{P}_b^1 . We then introduce the homogeneous coordinates $[s : t]$ for \mathbb{P}_f^1 and $[v : w]$ for \mathbb{P}_b^1 , with weights

	s	t	v	w
$\mathbb{C}_{\lambda_1}^*$	1	1	0	0
$\mathbb{C}_{\lambda_2}^*$	0	n	1	1

(B.1.12)

under the two \mathbb{C}^* -actions of \mathbb{F}_n . Given a set of polynomials $\{f_1, \dots, f_r\}$, let us refer to the vanishing locus of (the ideal generated by) them simply by $\{f_1 = \dots = f_r = 0\}$. With this notation, the coordinate divisors correspond to

$$S := \{s = 0\} = C_0, \quad T := \{t = 0\} = C_{\infty}, \quad V := \{v = 0\} = f = \{w = 0\} =: W. \quad (\text{B.1.13})$$

\mathbb{F}_n is a toric variety with fan $\Sigma_{\mathbb{F}_n}$ given by the edges

$$v = (1, 0), \quad t = (0, 1), \quad w = (-1, -n), \quad s = (0, -1), \quad (\text{B.1.14})$$

in the lattice

$$N := \langle (1, 0), (0, 1) \rangle_{\mathbb{Z}}. \quad (\text{B.1.15})$$

All other possible base surfaces are blow-ups of \mathbb{F}_n . The ways in which we can blow-up a Hirzebruch surface are numerous, and we relegate a discussion of the resulting geometries and those properties of them relevant to our analysis to Section B.1.3. Note that, although \mathbb{F}_n itself is toric, its blow-ups are not (in general) toric varieties. Additionally, some blow-ups may lead to surfaces with a non-effective anticanonical class, which would not constitute a valid six-dimensional F-theory base and should therefore be discarded.

Out of the non-trivial F-theory bases, the Hirzebruch surfaces \mathbb{F}_n correspond to F-theory models with $n_T = 1$ tensors. The models over $\text{Bl}(\mathbb{F}_n)$, containing $n_T > 1$ tensors, are closely related to those over \mathbb{F}_n . Namely, blowing down the exceptional divisors of $\text{Bl}(\mathbb{F}_n)$ leads to a Weierstrass model over \mathbb{F}_n with codimension-two finite-distance vanishing orders. This operation physically corresponds to going to the origin of the tensor branch, which takes us a finite distance away in moduli space from the original model. The presence of this type of singularities signals the existence of a strongly coupled six-dimensional SCFT sector, see [270] for a review.

Finally, the Weierstrass models over \mathbb{P}^2 correspond to F-theory models with $n_T = 0$ tensors. If they present at least one finite-distance non-minimal codimension-two singularity, we can blow it up in order to turn them into Weierstrass models over \mathbb{F}_1 , by virtue of the isomorphism $\text{Bl}_1(\mathbb{P}^2) = \text{dP}_1 \cong \mathbb{F}_1$. In the absence of such a singularity, tuning one would correspond to traversing a finite distance in moduli space. The geometrical connection between models over \mathbb{F}_1 and models over \mathbb{P}^2 means that their physics from the point of view of F-theory is also related, with an E-string wrapping the exceptional curve becoming light during the transition from the former set of models to the latter.

The connectedness of the six-dimensional F-theory moduli space under tensionless string transitions mirrors the mathematical minimal surface program. Obtaining a minimal model for a smooth surface by repeated application of Castelnuovo's contraction theorem corresponds in F-theory to moving to the origin of the tensor branch.

Returning to the degenerations of six-dimensional F-theory models discussed in Section 5.2.1, assume that \hat{B} in $\hat{\mathcal{B}} = \hat{B} \times D$ is not a minimal surface. If C is a (-1) -curve in \hat{B} such that $\pi_{\hat{B}}^*(C)$ exhibits infinite-distance non-minimal vanishing orders, the degeneration obtained by contracting C to a point in \hat{B} (hence $\pi_{\hat{B}}^*(C)$ to a curve in $\hat{\mathcal{B}}$) will present codimension-two infinite-distance non-minimal fibral singularities, beyond the codimension-two finite-distance non-minimal fibral singularities usually associated to the contraction of such a curve. This does not mean that codimension-one and codimension-two degenerations can always be connected in this way, since there exist models over the minimal model of the surface presenting the codimension-two non-minimal fibral singularities in the absence of the finite-distance ones.

In the explicit examples that we analyse both here and in Chapter 6 the birational transformations necessary to arrive at the resolved degeneration $\rho : \mathcal{Y} \rightarrow D$ clearly commute with the blow-ups needed to remove the finite-distance non-minimal fibral singularities; we therefore keep them unresolved in order to simplify the exposition. The discussion is nonetheless maintained general throughout, and the tools we provide apply to any of the allowed six-dimensional F-theory bases.

B.1.2 Blow-ups of algebraic surfaces

Given an algebraic surface B , we can blow it up with centre a point $p \in B$ by a local procedure to yield the blown up surface \hat{B} . This operation usually appears in the context of the resolution of singularities, but it can also be applied to smooth varieties. In this section, we recall how this blow-up process works in order to set the notation for the rest of the discussion. The properties of blow-ups, both for surfaces and varieties of other dimensionalities, are covered in most algebraic geometry textbooks, see e.g. [193, 353–355]. Before we start, let us already make some notational remarks.

Remark B.1.1. Let B be an algebraic surface, that we will assume throughout to be smooth. When we speak of a curve $C \subset B$, we will always mean an effective divisor in B . The Picard group of B will be referred to as $\text{Pic}(B)$, while we will use the notation $\text{NS}(B)$ for the Néron-Severi group. We will denote the effective cone of divisors by $\text{Eff}(B)$, and its closure, the pseudoeffective cone, by $\overline{\text{Eff}}(B)$. Since we are working with surfaces, the effective cone and the Mori cone, also known as the cone of curves, are coinciding notions.

We will make extensive use of the following two results for irreducible curves on surfaces.

Proposition B.1.2. *Let B be an algebraic surface, and let $C \subset B$ be an irreducible curve. The intersection product $C \cdot C'$, where $C' \subset B$ is an arbitrary curve, is negative if and only if C' contains C as a component and $C \cdot C < 0$.*

Proposition B.1.3 (Adjunction formula). *Let C be a smooth, irreducible curve on an algebraic surface B , and denote its genus by $g(C)$. Then, we have the identity*

$$C \cdot (\overline{K}_M - C) = 2 - 2g(C). \quad (\text{B.1.16})$$

Next, we review the definition of the blow-up of a surface with centre a point, and its associated exceptional divisor, as well as the concepts of strict and total transforms of the curves in the original surface.

Definition B.1.4. Let B be an algebraic surface and $p \in B$ a point. Then, there exists a surface \hat{B} and a morphism $\pi : \hat{B} \rightarrow B$, which are unique up to isomorphism, such that

1. the restriction of π to $\pi^{-1}(M \setminus \{p\})$ is an isomorphism onto $M \setminus \{p\}$; and
2. $\pi^{-1}(p) =: E$ is isomorphic to \mathbb{P}^1 .

We call π the blow-up of M with centre p , and E the exceptional divisor of the blow-up.

Lemma B.1.5. *Let $C \subset B$ be an irreducible curve that passes through p with multiplicity m . The closure of $\pi^{-1}(C - p)$ in \hat{B} is an irreducible curve $\hat{C} \subset \hat{B}$ satisfying*

$$\pi^*(C) = \hat{C} + mE. \quad (\text{B.1.17})$$

We call \hat{C} the strict transform of C and $\pi^*(C)$ the proper or total transform of C .

Corollary B.1.6. *With the same hypotheses, $\hat{C} \cdot_{\hat{B}} E = m$.*

The next result characterizes many of the properties of the blown up surface \hat{B} in terms of the analogous ones for the original surface B .

Proposition B.1.7. *Let B be an algebraic surface, $\pi : \hat{B} \rightarrow B$ the blow-up of B at a point $p \in B$, and $E \subset \hat{B}$ the exceptional divisor of the blow-up.*

1. *There is an isomorphism*

$$\begin{aligned} \sim: \text{Pic}(B) \oplus \mathbb{Z} &\longrightarrow \text{Pic}(\hat{B}) \\ (D, n) &\longmapsto \pi^*(D) + nE. \end{aligned} \quad (\text{B.1.18})$$

2. *Let D, D' be divisors on B . Then*

$$\pi^*(D) \cdot_{\hat{B}} \pi^*(D') = D \cdot_B D', \quad E \cdot_{\hat{B}} \pi^*(D) = 0, \quad E \cdot_{\hat{B}} E = -1. \quad (\text{B.1.19})$$

3. $\text{NS}(\hat{B}) \cong \text{NS}(B) \oplus \langle E \rangle_{\mathbb{Z}}$.

4. $K_{\hat{B}} = \pi^*(K_B) + E$.

B.1.3 Arbitrary blow-ups of \mathbb{P}^2 and \mathbb{F}_n

By blowing up points in \mathbb{P}^2 and \mathbb{F}_n (with $0 \leq n \leq 12$) we can produce a plethora of surfaces that can act as F-theory bases, due to the many ways in which we can choose the positions of the blow-up centres.

The simplest such blow-ups are the so-called del Pezzo surfaces dP_k (the two-dimensional Fano varieties), obtained by blowing up \mathbb{P}^2 in up to 8 points in general position, which we denote by $\text{Bl}_k(\mathbb{P}^2)$. If one blows up \mathbb{P}^2 at $k \geq 9$ points in general position, the Mori cone is no longer finitely generated, despite the finite generation of $\text{NS}(\text{Bl}_k(\mathbb{P}^2)) \cong \text{Pic}(\text{Bl}_k(\mathbb{P}^2))$. A lot of information on blow-ups of \mathbb{P}^2 at generic points as well as the generators of the Mori cones of the del Pezzo surfaces can be found in [356].

But instead of choosing points in general position on the original surface, we can make other choices. For example, we may blow up a point in an exceptional divisor resulting from a previous blow-up. In what follows, we would like to analyse what these choices are and extract those features of these arbitrary blow-ups of \mathbb{P}^2 and \mathbb{F}_n that are relevant for our analysis.

The first thing to be noted is that we can simply worry about the arbitrary blow-ups of \mathbb{F}_n , since this encompasses the arbitrary blow-ups of \mathbb{P}^2 as well. This is due to the well-known fact that the blow-up of \mathbb{P}^2 at one point is $dP_1 \cong \mathbb{F}_1$, and therefore any further blow-ups can be regarded as blow-ups of \mathbb{F}_1 .

In order to analyse the possible blow-ups we can perform, let us blow up the surfaces one point at a time. That is, for a surface that we have obtained by blowing up K points we have the maps

$$\pi : \hat{B}_K \xrightarrow{\pi_K} \hat{B}_{K-1} \xrightarrow{\pi_{K-1}} \cdots \xrightarrow{\pi_2} \hat{B}_1 \xrightarrow{\pi_1} B, \quad \pi = \pi_1 \circ \cdots \circ \pi_K. \quad (\text{B.1.20})$$

After i blow-ups have been performed, we have the choice of where to locate the point p_{i+1} that will be blown up, leading to different ‘‘blow-up paths’’ that we can take.

In order to illustrate this, let us take the first few blow-ups of \mathbb{P}^2 as an example, summarizing the discussion in Figure B.1. For the first blow-up, we can only choose an arbitrary point. In the next step we can choose to blow-up a point in $\hat{B}_1 \setminus E_1$, a generic point in the exceptional divisor E_1 , or the point in which E_1 intersects the original surface. This leads to different surfaces, as can be seen from their anticanonical class, which we compute in Section B.1.3.2. Let us choose

the intermediate option. Now we have the choice of blowing up a point in $\hat{B}_2 \setminus (E_1 \cup E_2)$, a generic point in the (strict transform of) the first exceptional divisor E_1 , a generic point in the second exceptional divisor E_2 , or one of the two points of intersection that exist. In this way, the blow-up paths quickly branch. Note that, as shown in Figure B.1, two different blow-up paths can lead to the same surface; for example, the order in which we blow up general points in the original surface is not relevant.

The discussion above actually illustrates all the possible choices that we have at each step of the blow-up process, namely:

- (A) we can blow up a point in the original surface,
- (B) we can blow up a generic point in the (strict transforms of) an exceptional divisor,
- (C) we can blow up a point of intersection between the (strict transforms of) two exceptional divisors, or
- (D) we can blow up a point of intersection between the original surface and (the strict transform of) an exceptional divisor.

What we would like to do now is to analyse how, starting from \mathbb{P}^2 or \mathbb{F}_n , an arbitrary sequence of these individual blow-ups affects the anticanonical class of the surface and its intersection ring. This information will be used, in Appendix B.2, to restrict the genus of the smooth, irreducible curves over which non-minimal elliptic fibers of the type studied in the body of the work can be realized.

B.1.3.1 Basis and notation for $\text{Bl}(\mathbb{P}^2)$ and $\text{Bl}(\mathbb{F}_n)$

The surfaces from which we start the blow-up process are \mathbb{P}^2 and \mathbb{F}_n . For \mathbb{P}^2 , we will denote the hyperplane class by H , which then forms a basis for both the Picard group and the effective cone

$$\mathbb{P}^2 : \quad \text{Pic}(\mathbb{P}^2) = \langle H \rangle_{\mathbb{Z}}, \quad \overline{\text{Eff}}(\mathbb{P}^2) = \langle H \rangle_{\mathbb{R}_{\geq 0}}. \quad (\text{B.1.21})$$

For \mathbb{F}_n , we use the notation introduced in Section B.1.1, i.e. we denote by h the section given by the $(-n)$ -curve and by f the fiber class, having then

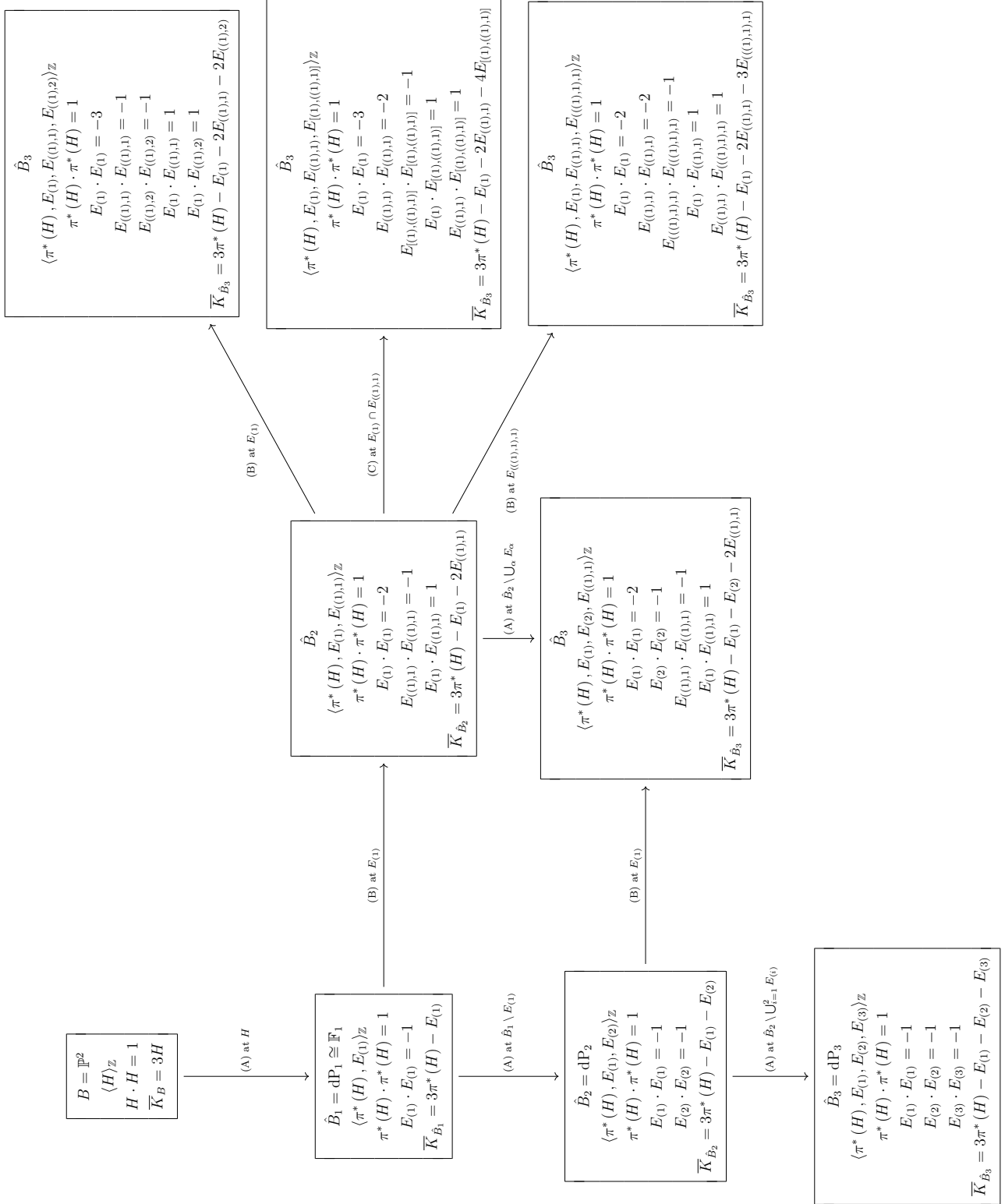
$$\mathbb{F}_n : \quad \text{Pic}(\mathbb{F}_n) = \langle h, f \rangle_{\mathbb{Z}}, \quad \overline{\text{Eff}}(\mathbb{F}_n) = \langle h, f \rangle_{\mathbb{R}_{\geq 0}}. \quad (\text{B.1.22})$$

Let us collectively denote the elements of these bases by $\{D_i\}_{i \in \mathcal{I}}$, with $\{D_1\} = \{H\}$ for \mathbb{P}^2 and $\{D_1, D_2\} = \{h, f\}$ for \mathbb{F}_n .

After each blow-up $\pi_i : \hat{B}_i \rightarrow \hat{B}_{i-1}$ in (B.1.20) we have a new exceptional irreducible divisor E_i . The collection of total transforms of the exceptional divisors stemming from the previous blow-ups $\{\pi_{i-1}^* \circ \dots \circ \pi_1^*(E_j)\}_{1 \leq j \leq i-1}$ may no longer be comprised of irreducible divisors. This will occur if some points in the exceptional divisors were blown up, in which case the total and strict transforms differ. To avoid confusion, we will always express the quantities at each step of the blow-up process in terms of the strict transforms of the exceptional divisors, which we will simply denote by $\{E_1, \dots, E_i\}$, dropping the hats.

Due to Proposition B.1.7, we know that at each step of the process a basis for the Picard group is given by

$$\begin{aligned} \text{Pic}(\hat{B}_i) &= \langle \pi_{i-1}^* \circ \dots \circ \pi_1^*(D_j), \pi_i^*(E_1), \dots, \pi_i^*(E_{i-1}), E_i \rangle_{\mathbb{Z}} \\ &= \langle \pi_{i-1}^* \circ \dots \circ \pi_1^*(D_j), E_1, \dots, E_i \rangle_{\mathbb{Z}}, \end{aligned} \quad (\text{B.1.23})$$



where in the last line we have used the fact that $\pi_i^*(E_j)$ and E_j differ by factors of E_i . Applying this inductively to the bases listed above, we can, after blowing-up K points in \mathbb{P}^2 or \mathbb{F}_n , choose as basis for the Picard group

$$\text{Pic}(\hat{B}_K) = \langle \pi^*(D_j), E_1, \dots, E_K \rangle_{\mathbb{Z}}. \quad (\text{B.1.24})$$

These elements will not give a basis of the effective cone, the computation of which can be complicated [357]. It will nonetheless be true that

$$\langle \pi^*(D_j), E_1, \dots, E_K \rangle_{\mathbb{Z}} \subset \overline{\text{Eff}}(\hat{B}_K). \quad (\text{B.1.25})$$

For our purposes using this basis is enough. We will express the quantities of interest to us using the total transforms of the original divisors $\{D_i\}_{i \in \mathcal{I}}$, which have trivial intersection with the $\{E_j\}_{1 \leq j \leq i}$ at each step. This makes the blow-up type (D) effectively type (B) from the computational point of view that matters in this section, since the properties of the classes $\{D_i\}_{i \in \mathcal{I}}$ that we employ in the Picard basis remain unaffected by it. We therefore omit this type of blow-up in the remainder of the section.

B.1.3.2 Anticanonical class after an arbitrary blow-up

The change in the anticanonical class of the surface after each blow-up $\pi_i : \hat{B}_i \rightarrow \hat{B}_{i-1}$ in (B.1.20) is given in Proposition B.1.7. We only need to compose these changes along the blow-up path. If at each step we have

$$\overline{K}_{\hat{B}_i} = \pi_i^* \left(\overline{K}_{\hat{B}_{i-1}} \right) - E_i, \quad (\text{B.1.26})$$

the final anticanonical class after the K blow-ups will be

$$\overline{K}_{\hat{B}_K} = \pi^* \left(\overline{K}_B \right) - \sum_{i=1}^{K-2} \pi_K^* \circ \dots \circ \pi_{i+1}^* (E_i) - \pi_K^* (E_{K-1}) - E_K. \quad (\text{B.1.27})$$

Expressing this in terms of the basis (B.1.24) we have

$$\overline{K}_{\hat{B}_K} = \pi^* \left(\overline{K}_B \right) - \sum_{i=1}^K d_i E_i, \quad d_i \in \mathbb{Z}_{\geq 0}, \quad (\text{B.1.28})$$

where the d_i are known as the discrepancies.¹

Characterizing the value of the discrepancies d_i is simple for the type of blow-ups that we are considering, i.e. those centred at smooth points of a surface. Let us do so by introducing a notation for the (strict transforms of) the exceptional divisors that we find useful, since it informs us about the “blow-up history” of said divisor. In the following paragraph, we denote by $\pi : \hat{B} \rightarrow B$ the composition of all the blow-ups performed until that point in the discussion, and $\rho : \hat{B} \rightarrow \hat{B}_{\text{old}}$ the last blow-up performed.

We start by considering all the blow-ups of type (A), i.e. the blow-ups of points in the original surface. Say that we perform k said blow-ups. These will be characterized by specifying a collection $\{p_i\}_{1 \leq i \leq k}$ of points in B . Any order in which we perform these blow-ups leads to the

¹Negative discrepancies do appear in the resolution process of log terminal and log canonical singularities, but here we are blowing up smooth points.

same resulting surface, and we can therefore perform all such blow-ups in one step, leading to a collection $\{E_i\}_{1 \leq i \leq k}$ of exceptional divisors and a blown up surface \hat{B} with anticanonical class

$$\bar{K}_{\hat{B}} = \pi^*(\bar{K}_B) - \sum_{i=1}^k d_i E_i, \quad d_i = 1, \quad \forall i = 1, \dots, k. \quad (\text{B.1.29})$$

We have performed all desired blow-ups of type (A). At this point of the blow-up process, there are no intersection points between the exceptional divisors, such that the only possibility is to perform a blow-up of type (B), i.e. blowing up a point in one of the exceptional divisors. Say that we choose a collection of generic points $\{p_{(\alpha,i)}\}_{1 \leq i \leq k_\alpha}$ in the exceptional divisor $E_\alpha \in \{E_i\}_{1 \leq i \leq k}$. Performing the blow-up of these points, we have that

$$\rho^*(E_\alpha) = E_\alpha + \sum_{i=1}^{k_\alpha} E_{(\alpha,i)}, \quad (\text{B.1.30})$$

leading to the anticanonical class

$$\bar{K}_{\hat{B}} = \pi^*(\bar{K}_B) - \sum_{i=1}^k d_i E_i - \sum_{i=1}^{k_\alpha} d_{(\alpha,i)} E_{(\alpha,i)}, \quad \begin{aligned} d_i &= 1, & \forall i &= 1, \dots, k, \\ d_{(\alpha,j)} &= d_j + 1, & \forall j &= 1, \dots, k_\alpha. \end{aligned} \quad (\text{B.1.31})$$

The discrepancies $\{d_{(\alpha,i)}\}_{1 \leq i \leq k_\alpha}$ of the exceptional divisors $\{E_{(\alpha,i)}\}_{1 \leq i \leq k_\alpha}$ have increased by one with respect to the d_α of E_α , owing to the fact that they are one level deeper in the blow-up chain. Let us continue by considering for now only blow-ups of type (B). We can choose now to blow-up a collection of generic points in $\{p_{(\beta,i)}\}_{1 \leq i \leq k_\beta}$ in an exceptional divisor $E_{\beta \neq \alpha} \in \{E_i\}_{1 \leq i \leq k}$. This would lead to a collection of exceptional divisors $\{E_{(\beta,i)}\}_{1 \leq i \leq k_\beta}$ at the second level in the blow-up chain, and appearing in the anticanonical class with discrepancies $d_{(\beta,i)} = 2, \forall i = 1, \dots, k_\beta$. Alternatively, and still within the blow-ups of type (B), we could blow-up a collection of generic points $\{p_{((\alpha,i),j)}\}_{1 \leq j \leq k_{(\alpha,i)}}$ in the exceptional divisor $E_{(\alpha,i)} \in \{E_{(\alpha,j)}\}_{0 \leq j \leq k_\alpha}$. This would lead to the exceptional divisors $\{E_{((\alpha,i),j)}\}_{1 \leq j \leq k_{(\alpha,i)}}$ at the third level in the blow-up chain, and appearing in the anticanonical class with discrepancies $d_{((\alpha,i),j)} = 3, \forall j = 1, \dots, k_{(\alpha,i)}$. Using this notation, in which the subindex of an exceptional divisor consists of parentheses with the left entry designating the divisor whose points are blown-up and the right entry listing the new exceptional divisors arising from said blow-up, and renaming the divisors in the first level to $\{E_{(i)}\}_{1 \leq i \leq k}$, the anticanonical class resulting from an arbitrary number of blow-ups of type (A) and (B) is

$$\bar{K}_{\hat{B}} = \pi^*(K_B) - \sum_{\alpha} d_{\alpha} E_{\alpha}, \quad d_{\alpha} = \text{level of the exceptional divisor} \geq 1. \quad (\text{B.1.32})$$

The subindex notation contains the “blow-up history” of a given exceptional divisor, and the level can be computed by simply counting the number of parentheses pairs in the subindex.

Finally, we need to consider the possibility of performing blow-ups of type (C), i.e. blowing up the intersection point of two exceptional divisors. Let E_α and E_β be two exceptional divisors with intersection product $E_\alpha \cdot E_\beta = 1$. Blowing up their intersection point, and denoting the resulting exceptional divisor by $E_{[\alpha,\beta]}$, we have that

$$\rho^*(E_\alpha) = E_\alpha + E_{[\alpha,\beta]}, \quad (\text{B.1.33a})$$

$$\rho^*(E_\beta) = E_\beta + E_{[\alpha,\beta]}, \quad (\text{B.1.33b})$$

leading to the anticanonical class

$$\overline{K}_{\hat{B}} = \pi^*(K_B) - \sum_{\alpha} d_{\alpha} E_{\alpha} - d_{[\alpha, \beta]} E_{[\alpha, \beta]}, \quad \begin{aligned} d_{\alpha} &= \text{level of the exceptional divisor ,} \\ d_{[\alpha, \beta]} &= 1 + d_{\alpha} + d_{\beta}. \end{aligned} \quad (\text{B.1.34})$$

On generic points of the resulting divisor $E_{[\alpha, \beta]}$ one can then perform blow-ups of type (B) or, alternatively, one can perform blow-ups of type (C) at the intersection points of $E_{[\alpha, \beta]}$ with E_{α} and E_{β} . The discrepancies of divisors arising from blow-ups of type (C) are one unit higher than the sum of the discrepancies of their parent divisors, as we see above.

One can then keep iterating blow-ups of type (B) and (C) until the desired arbitrary blow-up \hat{B} of B has been reached. Using the subindex notation that we have introduced, the anticanonical class is

$$\overline{K}_{\hat{B}} = \pi^*(K_B) - \sum_{\alpha} d_{\alpha} E_{\alpha}, \quad d_{\alpha} \geq 1, \quad (\text{B.1.35})$$

where the subindex α contains the ‘‘blow-up history’’ of the exceptional divisor E_{α} . To compute the value of the discrepancy, we keep adding one unit per pair of outer parentheses in α until we are done, or we encounter a pair of square brackets. These contribute by the discrepancy value assigned to their two entries plus one. Using this notation we can write branching blow-up diagrams like the one represented in Figure B.1 and directly obtain the anticanonical class in our desired basis.

Let us give an example using \mathbb{P}^2 as the starting point. Blow it up at a point $p_{(1)}$, giving the exceptional divisor $E_{(1)}$. Continue by blowing up a generic point $p_{((1),1)}$ in $E_{(1)}$, producing the exceptional divisor $E_{((1),1)}$. Then, blow up the intersection point of the two exceptional divisors to produce $E_{[(1),((1),1)]}$. Finally, blow-up a generic point $p_{([(1),((1),1)],1)}$ in $E_{[(1),((1),1)]}$ to produce the exceptional divisor $E_{([(1),((1),1)],1)}$. Altogether, this leads to the exceptional divisors

$$E_{(1)} \longleftrightarrow d_{(1)} = 1, \quad (\text{B.1.36a})$$

$$E_{((1),1)} \longleftrightarrow d_{((1),1)} = 2, \quad (\text{B.1.36b})$$

$$E_{[(1),((1),1)]} \longleftrightarrow d_{[(1),((1),1)]} = 4, \quad (\text{B.1.36c})$$

$$E_{([(1),((1),1)],1)} \longleftrightarrow d_{([(1),((1),1)],1)} = 5, \quad (\text{B.1.36d})$$

meaning that the anticanonical class in our basis of choice is

$$\overline{K}_{\hat{B}} = \pi^*(\overline{K}_{\mathbb{P}^2}) - E_{(1)} - 2E_{((1),1)} - 4E_{[(1),((1),1)]} - 5E_{([(1),((1),1)],1)}. \quad (\text{B.1.37})$$

An arbitrary blow-up of $B = \mathbb{P}^2$ or $B = \mathbb{F}_n$ may lead to a surface \hat{B} with non-effective anticanonical class $\overline{K}_{\hat{B}}$, meaning that the global holomorphic sections necessary to construct the F-theory Weierstrass model are not available. These cases are therefore to be discarded in our analysis; in what follows, we implicitly assume that we are choosing blow-up paths that lead to surfaces with an effective anticanonical class.

B.1.3.3 Intersection ring after an arbitrary blow-up

The intersection product between the elements of the Picard basis (B.1.24) can be directly computed from Lemma B.1.5, Corollary B.1.6 and Proposition B.1.7. At the start of the process, we have the Picard basis $\{D_i\}_{i \in \mathcal{I}}$, with known intersection products

$$\mathbb{P}^2 : \quad H \cdot H = 1, \quad (\text{B.1.38a})$$

$$\mathbb{F}_n : \quad h \cdot h = -n, \quad f \cdot f = 0, \quad h \cdot f = 1. \quad (\text{B.1.38b})$$

Since we work with the total transforms of these divisors, their intersections remain the same after the blow-up process, and we therefore omit it in what follows.

Let us perform the blow-up process, following the same steps taken in the discussion of the anticanonical class. First, we perform all desired blow-ups of type (A). This leads to the Picard basis $\{D_i\}_{i \in \mathcal{I}} \cup \{E_i\}_{1 \leq i \leq k}$, with the intersection products

$$\pi^*(D_i) \cdot E_j = 0, \quad E_i \cdot E_j = -\delta_{ij}. \quad (\text{B.1.39})$$

Performing now blow-ups of type (B) over points in a divisor $E_\alpha \in \{E_i\}_{0 \leq i \leq k}$ leads to the intersection products

$$\left. \begin{array}{l} \pi^*(D_i) \cdot E_j = 0 \\ E_i \cdot E_j = -\delta_{ij} \end{array} \right\} \longrightarrow \left\{ \begin{array}{l} \pi^*(D_i) \cdot E_\beta = 0 \\ E_i \cdot E_j = -\delta_{ij} (1 + \delta_{\alpha i} k_\alpha) \\ E_{(\alpha, i)} \cdot E_{(\alpha, j)} = -\delta_{ij} \\ E_\alpha \cdot E_{(\alpha, i)} = 1 \\ E_{i \neq \alpha} \cdot E_{(\alpha, j)} = 0 \end{array} \right., \quad (\text{B.1.40})$$

where E_β stands for any of the $\{E_i\}_{1 \leq i \leq k}$ and $\{E_{(\alpha, i)}\}_{1 \leq i \leq k_\alpha}$. Of the old intersection products, only the self-intersection $E_\alpha \cdot E_\alpha$ is modified, owing to the local nature of the blow-up process. More generally, if we perform blow-ups of type (B) on generic points in a divisor E_α , producing the exceptional divisors $\{E_{(\alpha, i)}\}_{0 \leq i \leq k_\alpha}$, the new intersection products are

$$\left. \begin{array}{l} D_{\text{old}} \cdot D'_{\text{old}} = \dots \\ E_\alpha \cdot E_\alpha = -r_\alpha \\ D_{\text{old}} \cdot E_\alpha = \dots \end{array} \right\} \longrightarrow \left\{ \begin{array}{l} \rho^*(D_{\text{old}}) \cdot \rho^*(D'_{\text{old}}) = D_{\text{old}} \cdot D'_{\text{old}} \\ E_\alpha \cdot E_\alpha = -r_\alpha - k_\alpha \\ E_{(\alpha, i)} \cdot E_{(\alpha, j)} = -\delta_{ij} \\ E_\alpha \cdot E_{(\alpha, i)} = 1 \\ \rho^*(D_{\text{old}}) \cdot E_\alpha = D_{\text{old}} \cdot E_\alpha \\ \rho^*(D_{\text{old}}) \cdot E_{(\alpha, i)} = 0 \end{array} \right., \quad (\text{B.1.41})$$

where D_{old} stands for the divisors in \hat{B}_{old} , with the exception of E_α . The final type of blow-up we need to consider is that of type (C). Take two exceptional divisors E_α and E_β , with intersection product $E_\alpha \cdot E_\beta = 1$, and blow up their point of intersection to produce a new exceptional divisor $E_{[\alpha, \beta]}$. Then, the new intersection products are

$$\left. \begin{array}{l} D_{\text{old}} \cdot D'_{\text{old}} = \dots \\ E_\alpha \cdot E_\alpha = -r_\alpha \\ E_\beta \cdot E_\beta = -r_\beta \\ E_\alpha \cdot E_\beta = 1 \\ D_{\text{old}} \cdot E_\alpha = \dots \\ D_{\text{old}} \cdot E_\beta = \dots \end{array} \right\} \longrightarrow \left\{ \begin{array}{l} \rho^*(D_{\text{old}}) \cdot \rho^*(D'_{\text{old}}) = D_{\text{old}} \cdot D'_{\text{old}} \\ E_\alpha \cdot E_\alpha = -r_\alpha - 1 \\ E_\beta \cdot E_\beta = -r_\beta - 1 \\ E_{[\alpha, \beta]} \cdot E_{[\alpha, \beta]} = -1 \\ E_\alpha \cdot E_\beta = 0 \\ E_\alpha \cdot E_{[\alpha, \beta]} = 1 \\ E_\beta \cdot E_{[\alpha, \beta]} = 1 \\ \rho^*(D_{\text{old}}) \cdot E_\alpha = D_{\text{old}} \cdot E_\alpha \\ \rho^*(D_{\text{old}}) \cdot E_\beta = D_{\text{old}} \cdot E_\beta \\ \rho^*(D_{\text{old}}) \cdot E_{[\alpha, \beta]} = 0 \end{array} \right., \quad (\text{B.1.42})$$

where D_{old} stands for the divisors in \hat{B}_{old} , with the exceptions of E_α and E_β .

Using these rules, it is easy to keep track of the intersection products of interest to us as we follow the branching blow-up paths leading from B to the blown up surface \hat{B} , as exemplified in Figure B.1.

B.2 Restricting the genus of non-minimal curves

In this appendix we prove Proposition 5.2.7 of Section 5.2.3, which restricts the genus of the curves that can support non-minimal elliptic fibers. We will compute, via adjunction, the genus of such curves on general blow-ups of \mathbb{P}^2 and \mathbb{F}_n . The properties of the anticanonical class and the intersection pairing of divisors in arbitrary blow-ups of \mathbb{P}^2 and \mathbb{F}_n , as reviewed in Section B.1.3, then yield the restrictions on the genus as stated in Proposition 5.2.7.

As a final preparation, let us gather a couple of auxiliary results that we will invoke during the argument. First, we need a property of the effective divisors expressed in the Picard basis (B.1.24).

Proposition B.2.1. *Let \hat{B} be an arbitrary blow-up of $B = \mathbb{P}^2$ or $B = \mathbb{F}_n$, and D an effective divisor in \hat{B} . Expressing D in terms of the Picard basis (B.1.24), i.e. writing it as*

$$D = \sum_{i \in \mathcal{I}} a_i \pi^*(D_i) + \sum_{\alpha} c_{\alpha} E_{\alpha}, \quad (\text{B.2.1})$$

the total transforms $\{\pi^(D_i)\}_{i \in \mathcal{I}}$ always appear with non-negative coefficients $a_i \in \mathbb{Z}_{\geq 0}, \forall i \in \mathcal{I}$.*

Proof. Expressing D in terms of the Picard basis (B.1.24) we have

$$D = \sum_{i \in \mathcal{I}} a_i \pi^*(D_i) + \sum_{\alpha} c_{\alpha} E_{\alpha}. \quad (\text{B.2.2})$$

If D is a reducible effective divisor, it will be a positive linear combination of irreducible effective divisors. Hence, if we prove that $a_i \in \mathbb{Z}_{\geq 0}, \forall i \in \mathcal{I}$ for all irreducible effective divisors, the same result follows for all effective divisors. Moreover, the result is true for the collection of irreducible effective divisors $\{E_{\alpha}\}_{\alpha \in A}$. Let us therefore assume in what follows that D is an irreducible effective divisor distinct from the $\{E_{\alpha}\}_{\alpha \in A}$. We will first prove the result assuming that only k blow-ups of type (A) have been performed, and then generalize it to include arbitrary blow-ups.

After k blow-ups of type (A), we can write the divisor D as

$$D = \sum_{i \in \mathcal{I}} a_i \pi^*(D_i) + \sum_{i=1}^k c_i E_i. \quad (\text{B.2.3})$$

Using Proposition B.1.2, we see that, since D and the $\{E_i\}_{0 \leq i \leq k}$ are irreducible

$$D \cdot E_i = -c_i \geq 0 \Rightarrow c_i \leq 0, \quad \forall i = 1, \dots, k. \quad (\text{B.2.4})$$

Let us now treat the blow-ups of \mathbb{P}^2 and \mathbb{F}_n separately.

- Blow-ups $\text{Bl}(\mathbb{P}^2)$: Assume that $a < 0$. Making the signs explicit, we have

$$D = -a^+ \pi^*(H) - \sum_{i=1}^k c_i^+ E_i, \quad a^+, c_i^+ \geq 0. \quad (\text{B.2.5})$$

From the effective cone inclusion (B.1.25), we see that

$$D \in \overline{\text{Eff}}(\text{Bl}(\mathbb{P}^2)) \Rightarrow -a^+ \pi^*(H) \in \overline{\text{Eff}}(\text{Bl}(\mathbb{P}^2)). \quad (\text{B.2.6})$$

But we know that $a^+ \pi^*(H) \in \overline{\text{Eff}}(\text{Bl}(\mathbb{P}^2))$. Since the effective cone is salient and $a^+ \pi^*(H)$ is not trivial, $-a^+ \pi^*(H)$ cannot be contained in $\overline{\text{Eff}}(\text{Bl}(\mathbb{P}^2))$. Hence, $a \geq 0$.

- Blow-ups $\text{Bl}(\mathbb{F}_n)$: We separate this case into various subcases.

- Assume that $a, b \leq 0$. Making the signs explicit, we have

$$D = -a^+ \pi^*(h) - b^+ \pi^*(f) - \sum_{i=1}^k c_i^+ E_i, \quad a^+, b^+, c_i^+ \geq 0. \quad (\text{B.2.7})$$

From the effective cone inclusion (B.1.25), we obtain

$$D \in \overline{\text{Eff}}(\text{Bl}(\mathbb{P}^2)) \Rightarrow -a^+ \pi^*(h) - b^+ \pi^*(f) \in \overline{\text{Eff}}(\text{Bl}(\mathbb{P}^2)). \quad (\text{B.2.8})$$

Since $a^+ \pi^*(h) + b^+ \pi^*(f) \in \overline{\text{Eff}}(\text{Bl}(\mathbb{P}^2))$, either $a = b = 0$, or we enter in contradiction with the fact that the effective cone is salient. But when $a = b = 0$, we have a negative linear combination of the $\{E_i\}_{0 \leq i \leq k}$. Using again the fact that the effective cone is salient and positive linear combinations of the $\{E_i\}_{0 \leq i \leq k}$ are contained in it, we conclude that $a, b \leq 0$ is not possible unless D is trivial.

- Assume that $a \geq 0$ and $b < 0$. Making the signs explicit, we have

$$D = a^+ \pi^*(h) - b^+ \pi^*(f) - \sum_{i=1}^k c_i^+ E_i, \quad a^+, b^+, c_i^+ \geq 0. \quad (\text{B.2.9})$$

We now would like to exploit the negative self-intersection property of $\pi^*(h)$. Since $h \subset \mathbb{F}_n$ has a unique representative, no representative of $\pi^*(h)$ will be irreducible if a point in $h \subset \mathbb{F}_n$ has been blown up. We work instead with the strict transform \hat{h} of h , which we know is irreducible and related to the total transform by a negative contribution of exceptional divisors

$$\hat{h} = \pi^*(h) - \sum_{i=1}^{k_h} c_i^h E_i \Rightarrow \hat{h} \cdot \hat{h} \leq h \cdot h = -n, \quad c_i^h \geq 0. \quad (\text{B.2.10})$$

Using then Proposition B.1.2, we obtain the constraint

$$D \cdot \hat{h} = -a^+ n - b^+ - \sum_{i=1}^{k_h} c_i^h c_i^+ \geq 0, \quad a^+, b^+, c_i^h, c_i^+ \geq 0, \quad (\text{B.2.11})$$

since $D \neq \hat{h}$. Insisting on $a \geq 0$, this only has a chance of being positive if $b > 0$.

- Assume that $a < 0$ and $b \geq 0$. Making the signs explicit, we have

$$D = -a^+ \pi^*(h) + b^+ \pi^*(f) - \sum_{i=1}^k c_i^+ E_i, \quad a^+, b^+, c_i^+ \geq 0. \quad (\text{B.2.12})$$

We can always find a representative of $f \subset \mathbb{F}_n$ that is not affected by the blow-ups. Its total/strict transform $\pi^*(f)$ is then irreducible, and we have, using Proposition B.1.2, that

$$D \cdot \pi^*(f) = -a^+ \geq 0, \quad a^+ > 0, \quad (\text{B.2.13})$$

since $D \neq \pi^*(f)$. We conclude that $a > 0$.

Taken together, we see that $a, b \geq 0$.

To obtain the desired result, we now need to show that the above arguments still hold when we allow for blow-ups of types (B) and (C). The only points that are slightly affected when we allow for further blow-ups are the proof of the negativity of the c_α coefficients and the constraint coming from the intersection product $D \cdot \hat{h}$.

First, consider that we allow for arbitrary blow-ups of type (A) and (B). We then have a collection of exceptional divisors $\{E_\alpha\}_{\alpha \in A}$. Let us highlight among them those that arose from the type (A) blow-ups $\{E_{(i)}\}_{0 \leq i \leq k} \subset \{E_\alpha\}_{\alpha \in A}$. The intersection product with D of one of these divisors is then

$$D \cdot E_i = -(1 + k_i)c_{(i)} + \sum_{j=1}^{k_i} c_{((i),j)} \geq 0, \quad (\text{B.2.14})$$

$$D \cdot E_{(\alpha,i)} = -(1 + k_{(\alpha,i)}) + c_\alpha + \sum_{j=1}^{k_{(\alpha,i)}} c_{((\alpha,i),j)} \geq 0. \quad (\text{B.2.15})$$

By summing all the inequalities obtained from the intersection products of D with a given divisor E_α and all the other exceptional divisors that stem from the sequence of type (B) blow-ups of points in E_α , we obtain the inequality

$$-c_\alpha + c_{\substack{\text{parent} \\ \text{divisor}}} \geq 0, \quad (\text{B.2.16})$$

where by parent divisor we mean the divisor where the point that was blown-up in order to generate E_α is located, assuming that for the $\{E_{(i)}\}_{0 \leq i \leq k}$ we take $c_{\substack{\text{parent} \\ \text{divisor}}} = 0$. Using these inequalities iteratively level by level, we obtain

$$c_\alpha \leq 0, \quad \alpha \in A. \quad (\text{B.2.17})$$

Given two divisors E_α and E_β , we can allow now for a blow-up of type (C) over their intersection point $E_\alpha \cap E_\beta$. This modifies two of the already considered inequalities, leading to

$$D \cdot E_\alpha \geq 0 \longrightarrow \text{old terms} - c_\alpha - c_\beta + c_{[\alpha,\beta]} \geq 0, \quad (\text{B.2.18})$$

$$D \cdot E_\beta \geq 0 \longrightarrow \text{old terms} - c_\beta - c_\alpha + c_{[\alpha,\beta]} \geq 0. \quad (\text{B.2.19})$$

On top of this, we obtain the new inequality

$$D \cdot E_{[\alpha,\beta]} = -c_{[\alpha,\beta]} + c_\alpha + c_\beta. \quad (\text{B.2.20})$$

We see that we can use it to cancel the new terms in the old inequalities, in such a way that the arguments above apply and $c_{\gamma \neq [\alpha,\beta]} \leq 0, \forall \gamma \in A$, from where it then follows that also $c_{[\alpha,\beta]} \leq 0$. Allowing then for further blow-ups of type (B) over $E_{[\alpha,\beta]}$ reproduces the form of the inequalities

studied above, and more blow-ups of type (C) only result in modifications like the one just discussed. Hence, we can conclude that

$$c_\alpha \leq 0, \quad \alpha \in A. \quad (\text{B.2.21})$$

for an arbitrary combination of types (A), (B) and (C) blow-ups.

Let us now move to the analysis of how the intersection product $D \cdot \hat{h}$ changes. Let us recall that, after performing k blow-ups of type (A), out of which k_h were of points located in h , we have

$$D \cdot \hat{h} = -a^+ n - b^+ - \sum_{i=1}^{k_h} c_i^h c_i^+ \geq 0, \quad a^+, b^+, c_i^h, c_i^+ \geq 0. \quad (\text{B.2.22})$$

Although above we did not specify it, the c_i^h are $c_i^h = 1$, since we are blowing up points with multiplicity one. Let us now perform arbitrary blow-ups of type (B) and (C), with the exception of those type (C) blow-ups involving the points $\{\hat{h} \cap E_i\}_{0 \leq i \leq k_h}$, and call the composition of these new blow-ups $\rho : \hat{B}_2 \rightarrow \hat{B}_1$, with the original blow-up being $\pi : \hat{B}_1 \rightarrow B$. We have that

$$\rho^* \left(\pi^*(h) - \sum_{i=1}^{k_h} E_i \right) = \hat{h}, \quad (\text{B.2.23})$$

where \hat{h} now stands for the strict transform under the composition of all the blow-ups. Expressing D in terms of the total transforms under the last set of blow-ups, we have

$$\begin{aligned} D &= a^+ \rho^*(\pi^*(h)) - b^+ \rho^*(\pi^*(f)) - \sum_{i=1}^k c_i E_i - \sum_{\rho \in P} c_\rho E_\rho \\ &= \rho^* \left(a^+ \pi^*(h) - b^+ \pi^*(f) - \sum_{i=1}^k c_i E_i \right) - \sum_{\rho \in P} c'_\rho E_\rho, \end{aligned} \quad (\text{B.2.24})$$

where the $\{E_\rho\}_{\rho \in P}$ are the exceptional divisors arising from the last set of blow-ups. It is then clear that no change in the expression $D \cdot \hat{h}$ occurs. The situation is different when we blow-up one of the points $\{\hat{h} \cap E_i\}_{0 \leq i \leq k_h}$. Say that we blow-up the point $\hat{h} \cap E_i$, producing the exceptional divisor $E_{[\hat{h}, i]}$. Then,

$$\rho^* \left(\pi^*(h) - \sum_{i=1}^{k_h} E_i \right) = \hat{h} + E_{[\hat{h}, i]}. \quad (\text{B.2.25})$$

Expressing D again in terms of the total transforms under the last set of blow-ups and separating the term containing $E_{[\hat{h}, i]}$, we have

$$\begin{aligned} D &= a^+ \rho^*(\pi^*(h)) - b^+ \rho^*(\pi^*(f)) - \sum_{i=1}^k c_i E_i - \sum_{\rho \in P'} c_\rho E_\rho - c_{[\hat{h}, i]} E_{[\hat{h}, i]} \\ &= \rho^* \left(a^+ \pi^*(h) - b^+ \pi^*(f) - \sum_{i=1}^k c_i E_i \right) - \sum_{\rho \in P'} c'_\rho E_\rho - (c_{[\hat{h}, i]} - c_i) E_{[\hat{h}, i]}. \end{aligned} \quad (\text{B.2.26})$$

The intersection product is then modified to

$$D \cdot \hat{h} = -a^+ n - b^+ - c_{[\hat{h}, i]} + c_i - \sum_{j=1}^{k_h} c_j E_j, \quad (\text{B.2.27})$$

but this does not affect the arguments used above. Further blow-ups of type (B) and (C) can be treated in the way just described, and therefore the discussion does generalize to an arbitrary combination of them. \square

The classes of the irreducible curves C over which we find Kodaira singularities in six-dimensional F-theory models are contained in the discriminant, meaning that they are effective divisors satisfying $C \leq \Delta = 12\bar{K}_B$. It may, in general, be false that they satisfy $C \leq \bar{K}_B$. If C supports non-minimal singularities, then it is further constrained.

Proposition B.2.2. *Let Y be the Weierstrass model Calabi-Yau threefold with base B having effective anticanonical class \bar{K}_B , and $C \subset B$ a smooth irreducible curve in the base supporting non-minimal singular fibers. Then, $C \leq \bar{K}_B$.*

Proof. If C supports non-minimal fibers, the vanishing orders over it must satisfy

$$\text{ord}_Y(f, g)_C \geq (4, 6), \quad (\text{B.2.28})$$

which in turn implies

$$\left. \begin{aligned} 4C &\leq F = 4\bar{K}_B \\ 6C &\leq G = 6\bar{K}_B \end{aligned} \right\} \Rightarrow C \leq \bar{K}_B. \quad (\text{B.2.29})$$

\square

We can now restrict the genus of an irreducible curve supporting non-minimal fibers in a six-dimensional F-theory model, i.e. prove Proposition 5.2.7, whose precise statement we recall.

Proposition 5.2.7. *Let Y be an elliptically fibered Calabi-Yau threefold with base \hat{B} , where \hat{B} is one of the allowed six-dimensional F-theory bases. Let $C \subset \hat{B}$ be a smooth irreducible curve of genus $g(C)$ supporting non-minimal singular fibers. Then, $g(C) \leq 1$, and $g(C) = 1$ if and only if $C = \bar{K}_{\hat{B}}$.*

Proof. Let us consider a smooth, irreducible curve C in an arbitrary blow-up of \mathbb{P}^2 or \mathbb{F}_n . Using the Picard basis (B.1.24), we can express the class of C as

$$\hat{B} = \text{Bl}(\mathbb{P}^2) : \quad C = a\pi^*(H) + \sum_{\alpha} c_{\alpha}E_{\alpha}, \quad (\text{B.2.30a})$$

$$\hat{B} = \text{Bl}(\mathbb{F}_n) : \quad C = a\pi^*(h) + b\pi^*(f) + \sum_{\alpha} c_{\alpha}E_{\alpha}. \quad (\text{B.2.30b})$$

Using the same basis, the anticanonical class of the base B is

$$\bar{K}_{\hat{B}} = \pi^*(K_B) - \sum_{\alpha} d_{\alpha}E_{\alpha}, \quad d_{\alpha} \geq 0, \quad (\text{B.2.31})$$

see Section B.1.3.2. The cases in which the base is $B = \mathbb{P}^2$ or $B = \mathbb{F}_n$ are recovered by setting $c_{\alpha} = d_{\alpha} = 0$ throughout the argument.

Invoking Proposition B.1.3, we see that the genus of C is given by

$$g(C) = \frac{C \cdot C - C \cdot \bar{K}_{\hat{B}}}{2} + 1. \quad (\text{B.2.32})$$

The implication $C = \overline{K}_B \Rightarrow g(C) = 1$ is then immediate. An irreducible curve C satisfies

$$g(C) \leq 1 \Leftrightarrow C \cdot C \leq C \cdot \overline{K}_B. \quad (\text{B.2.33})$$

We would therefore like to prove that there exists no smooth irreducible curve C supporting non-minimal fibers and satisfying $C \cdot C > C \cdot \overline{K}_B$ at the same time.

If we have only performed k blow-ups of type (A), the inequality $C \cdot C \geq C \cdot \overline{K}_B$ reads

$$\sum_{i \in \mathcal{I}} a_i \pi^*(D_i) \cdot \sum_{j \in \mathcal{J}} a_j \pi^*(D_j) - \sum_{i=1}^k c_i^2 \geq \sum_{i \in \mathcal{I}} a_i \pi^*(D_i) \cdot \pi^*(\overline{K}_B) + \sum_{i=1}^k c_i d_i. \quad (\text{B.2.34})$$

We can define the functions

$$h(c_i)_{(\text{A})\text{-blow-up}} := \sum_{i=1}^k c_i^2 + c_i, \quad (\text{B.2.35})$$

$$f(a_i)_B := \sum_{i \in \mathcal{I}} a_i \pi^*(D_i) \cdot \sum_{j \in \mathcal{J}} a_j \pi^*(D_j) - \sum_{i \in \mathcal{I}} a_i \pi^*(D_i) \cdot \pi^*(\overline{K}_B), \quad (\text{B.2.36})$$

where we have used that $d_i = 1, \forall i = 1, \dots, k$, to express it as

$$f(a_i)_B \geq h(c_i)_{(\text{A})\text{-blow-up}}. \quad (\text{B.2.37})$$

The function $f(a_i)_B$ only involves total transforms of the divisors $\{D_i\}_{i \in \mathcal{I}}$ of B , which have trivial intersection with the rest of divisors in the Picard basis (B.1.24). This implies that, even after allowing for an arbitrary blow-up, the function $f(a_i)_B$ will not change. The same is not true for $h(c_i)_{(\text{A})\text{-blow-up}}$, and we need to determine its most general form. Taking into account the form of the intersection ring (B.1.41), we can see that the additional terms contributing to $C \cdot C \geq C \cdot \overline{K}_B$ after blowing up k_α generic points in an exceptional divisor E_α , i.e. by a blow-up of type (B), are

$$\dots - k_\alpha c_\alpha^2 + 2 \sum_{i=1}^{k_\alpha} c_\alpha c_{(\alpha,i)} - \sum_{i=1}^{k_\alpha} c_{(\alpha,i)}^2 \geq \dots - k_\alpha c_\alpha d_\alpha + \sum_{i=1}^{k_\alpha} c_{(\alpha,i)} d_{(\alpha,i)}. \quad (\text{B.2.38})$$

Hence, allowing for blow-ups both of type (A) and (B) the r.h.s. of the inequality needs to be

$$h(c_i)_{(\text{AB})\text{-blow-up}} = h(c_i)_{(\text{A})\text{-blow-up}} + \sum_{\substack{\text{divisors } E_\alpha \\ \text{where } k_\alpha \\ \text{generic points} \\ \text{were blown up}}} \sum_{i=1}^{k_\alpha} [(c_\alpha^2 - c_\alpha) - 2c_\alpha c_{(\alpha,i)} + (c_{(\alpha,i)}^2 + c_{(\alpha,i)})], \quad (\text{B.2.39})$$

where we have used that $d_{(\alpha,i)} = d_\alpha + 1$ to simplify the expression. The terms added to $C \cdot C \geq C \cdot \overline{K}_B$ by a blow-up of type (C) can be computed to be

$$\begin{aligned} \dots - c_\alpha^2 - c_\beta^2 - 2c_\alpha c_\beta + 2c_\alpha c_{[\alpha,\beta]} + 2c_\beta c_{[\alpha,\beta]} - c_{[\alpha,\beta]}^2 &\geq \dots + c_\alpha d_\alpha + c_\beta d_\beta + c_\alpha d_\beta + c_\beta d_\alpha \\ &\quad - c_\alpha d_{[\alpha,\beta]} - c_\beta d_{[\alpha,\beta]} - d_\alpha c_{[\alpha,\beta]} - d_\beta c_{[\alpha,\beta]} \\ &\quad + c_{[\alpha,\beta]} d_{[\alpha,\beta]} \end{aligned} \quad (\text{B.2.40})$$

using the intersection ring (B.1.42). This leads to the r.h.s. of the inequality being

$$h(c_i)_{(\text{ABC})\text{-blow-up}} = h(c_i)_{(\text{AB})\text{-blow-up}} + \sum_{\substack{\text{pairs } E_\alpha, E_\beta \\ \text{whose intersection} \\ \text{point was} \\ \text{blown up}}} (c_\alpha + c_\beta - c_{[\alpha, \beta]}) (c_\alpha + c_\beta - c_{[\alpha, \beta]} - 1) , \quad (\text{B.2.41})$$

where we have used $d_{[\alpha, \beta]} = d_\alpha + d_\beta + 1$ to cancel terms. Further blow-ups of type (B) or (C) just add more terms of the form computed above. Therefore, for a general blow-up of B we have

$$C \cdot C \geq C \cdot \bar{K}_B \Leftrightarrow f(a_i)_B \geq h(c_i)_{\text{blow-up}} , \quad (\text{B.2.42})$$

with the definitions

$$h(c_i)_{\text{blow-up}} := \sum_{i=1}^k p_1(c_i) + \sum_{\substack{\text{divisors } E_\alpha \\ \text{where } k_\alpha \\ \text{generic points} \\ \text{were blown up}}} \sum_{i=1}^{k_\alpha} p_2(c_\alpha, c_{(\alpha, i)})_i + \sum_{\substack{\text{pairs } E_\alpha, E_\beta \\ \text{whose intersection} \\ \text{point was} \\ \text{blown up}}} p_3(c_\alpha, c_\beta, c_{[\alpha, \beta]}) , \quad (\text{B.2.43})$$

$$f(a_i)_B := \sum_{i \in \mathcal{I}} a_i \pi^*(D_i) \cdot \sum_{j \in \mathcal{J}} a_j \pi^*(D_j) - \sum_{i \in \mathcal{I}} a_i \pi^*(D_i) \cdot \pi^*(\bar{K}_B) , \quad (\text{B.2.44})$$

where

$$p_1(c_i) := (c_i^2 + c_i) , \quad (\text{B.2.45})$$

$$p_2(c_\alpha, c_{(\alpha, i)})_i := (c_\alpha^2 - c_\alpha) - 2c_\alpha c_{(\alpha, i)} + (c_{(\alpha, i)}^2 + c_{(\alpha, i)}) , \quad (\text{B.2.46})$$

$$p_3(c_\alpha, c_\beta, c_{[\alpha, \beta]}) := (c_\alpha + c_\beta - c_{[\alpha, \beta]}) (c_\alpha + c_\beta - c_{[\alpha, \beta]} - 1) . \quad (\text{B.2.47})$$

Let us first use these expressions to prove that, with the hypotheses of the proposition, the strict version of the inequality (B.2.42) cannot be satisfied. The anticanonical classes of \mathbb{P}^2 and \mathbb{F}_n are

$$\bar{K}_{\mathbb{P}^2} = 3H , \quad \bar{K}_{\mathbb{F}_n} = 2h + (2+n)f . \quad (\text{B.2.48})$$

Computing the form of $f(a_i)_B$ for blow-ups of these two surfaces we obtain

$$f(a)_{\mathbb{P}^2} = a^2 - 3a , \quad (\text{B.2.49})$$

$$f(a, b)_{\mathbb{F}_n} = 2ab - a^2n - 2a - 2b + an . \quad (\text{B.2.50})$$

From Proposition B.2.1 and Proposition B.2.2 we obtain the constraints

$$\mathbb{P}^2 : \quad 0 \leq a \leq 3 , \quad (\text{B.2.51})$$

$$\mathbb{F}_n : \quad 0 \leq a \leq 2 , \quad 0 \leq b \leq 2+n . \quad (\text{B.2.52})$$

This leads to the values

$$f(0)_{\mathbb{P}^2} = 0 \leq 0 , \quad (\text{B.2.53a})$$

$$f(1)_{\mathbb{P}^2} = -2 \leq 0 , \quad (\text{B.2.53b})$$

$$f(2)_{\mathbb{P}^2} = -2 \leq 0 , \quad (\text{B.2.53c})$$

$$f(3)_{\mathbb{P}^2} = 0 \leq 0 , \quad (\text{B.2.53d})$$

and

$$f(0, b)_{\mathbb{F}_n} = -2b \leq 0, \quad (\text{B.2.54a})$$

$$f(1, b)_{\mathbb{F}_n} = -2 \leq 0, \quad (\text{B.2.54b})$$

$$f(2, b)_{\mathbb{F}_n} = -4 + 2(b - n) \leq 0. \quad (\text{B.2.54c})$$

Therefore, for $B = \mathbb{P}^2$ and $B = \mathbb{F}_n$ we have that $f(a_i)_B \leq 0$ for the allowed values of the a_i coefficients. On the other hand,

$$p_1(c_i) \geq 0, \quad p_2(c_\alpha, c_{(\alpha, i)})_i \geq 0, \quad p_3(c_\alpha, c_\beta, c_{[\alpha, \beta]}) \geq 0, \quad c_i, c_\alpha, c_\beta, c_{(\alpha, i)}, c_{[\alpha, \beta]} \in \mathbb{Z}. \quad (\text{B.2.55})$$

We hence conclude that

$$C \cdot C > C \cdot \overline{K}_B^\omega \Leftrightarrow 0 \geq f(a_i)_B > h(c_i)_{\text{blow-up}} \geq 0, \quad (\text{B.2.56})$$

which is not possible, meaning that $g(C) \leq 1$.

Above we have seen that $C = \overline{K}_B^\omega$ immediately implies $g(C) = 1$. To conclude, let us prove the converse statement. We have that

$$g(C) = 1 \Leftrightarrow C \cdot C = C \cdot \overline{K}_B^\omega \Leftrightarrow f(a_i)_B = h(c_i)_{\text{blow-up}} = 0. \quad (\text{B.2.57})$$

From (B.2.53) and (B.2.54) we see that this can occur, regarding $f(a_i)_B$, only for

$$\mathbb{P}^2 : \quad a = 0 \quad \text{or} \quad a = 3, \quad (\text{B.2.58})$$

$$\mathbb{F}_n : \quad a = 0, b = 0 \quad \text{or} \quad a = 2, b = 2 + n. \quad (\text{B.2.59})$$

Since all the terms in $h(c_i)_{\text{blow-up}}$ are positive, they must vanish separately, leading to

$$(c_i^2 + c_i) = 0 \Leftrightarrow c_i = -1 \quad \text{or} \quad c_i = 0, \quad (\text{B.2.60})$$

$$(c_\alpha^2 - c_\alpha) - 2c_\alpha c_{(\alpha, i)} + (c_{(\alpha, i)}^2 + c_{(\alpha, i)}) = 0 \Leftrightarrow c_{(\alpha, i)} = c_\alpha \quad \text{or} \quad c_{(\alpha, i)} = -1 + c_\alpha, \quad (\text{B.2.61})$$

$$(c_\alpha + c_\beta - c_{[\alpha, \beta]}) (c_\alpha + c_\beta - c_{[\alpha, \beta]} - 1) = 0 \Leftrightarrow c_{[\alpha, \beta]} = c_\alpha + c_\beta \quad \text{or} \quad c_{[\alpha, \beta]} = -1 + c_\alpha + c_\beta. \quad (\text{B.2.62})$$

The solutions (B.2.60) are non-positive, which makes the solutions (B.2.61) non-positive as well. This then implies that the solutions (B.2.62) are also non-negative. Assume now that we choose as solution of $f(a_i)_B = 0$ either

$$\mathbb{P}^2 : \quad a = 0, \quad \text{or} \quad \mathbb{F}_n : \quad a = 0, b = 0. \quad (\text{B.2.63})$$

Then C would be a non-negative sum of the $\{E_\alpha\}_{\alpha \in A}$. Since positive sums of the $\{E_\alpha\}_{\alpha \in A}$ are in the effective cone, and said cone is salient, a negative linear combination of the $\{E_\alpha\}_{\alpha \in A}$ must be either trivial or not effective. Hence, we must discard these solutions and are restricted to

$$\mathbb{P}^2 : \quad a = 3, \quad \text{or} \quad \mathbb{F}_n : \quad a = 2, b = 2 + n. \quad (\text{B.2.64})$$

Proposition B.2.2 implies that

$$c_\alpha \leq -d_\alpha \leq -1, \quad \forall \alpha \in A. \quad (\text{B.2.65})$$

Using this constraint successively for (B.2.60), (B.2.61) and (B.2.62) leads to

$$c_\alpha = -d_\alpha, \quad \forall \alpha \in A, \quad (\text{B.2.66})$$

which in turn implies $C = \overline{K}_B^\omega$. □

Remark B.2.3. For \mathbb{F}_n this can be seen directly by examining the list of curves in Proposition 5.3.1.

Remark B.2.4. The case $g(C) = 1 \Leftrightarrow C = \overline{K}_{\hat{B}}$ can only be realized if the anticanonical class does not have reducible generic representatives. This is what limits it to the complex projective plane \mathbb{P}^2 , the Hirzebruch surfaces without non-Higgsable clusters (i.e. \mathbb{F}_n with $0 \leq n \leq 2$), and blow-ups of these.

Note, however, that not every blow-up will preserve the property of the generic representative of \overline{K}_B being irreducible. To exemplify this, take the blow-up of \mathbb{P}^2 at four points. If the points are in general position, we obtain $\text{Bl}_4(\mathbb{P}^2) = \text{dP}_4 \cong \text{Bl}_3(\mathbb{F}_1)$. Since the points are in general position, a representative of the hyperplane class H of \mathbb{P}^2 can pass through at most two of them, and the effective cone is generated by

$$\overline{\text{Eff}}(\text{dP}_4) = \langle \hat{H}_{ij} := \pi^*(H) - E_i - E_j, E_k \rangle_{\mathbb{Z}_{\geq 0}}, \quad 1 \leq i < j \leq 4, \quad 1 \leq k \leq 4. \quad (\text{B.2.67})$$

The anticanonical class

$$\overline{K}_{\text{dP}_4} = 3\pi^*(H) - \sum_{k=1}^4 E_k \quad (\text{B.2.68})$$

is generically irreducible, with intersection products

$$\hat{H}_{ij} \cdot \overline{K}_{\text{dP}_4} = 1, \quad E_k \cdot \overline{K}_{\text{dP}_4} = 1, \quad 1 \leq i < j \leq 4, \quad 1 \leq k \leq 4. \quad (\text{B.2.69})$$

If instead we choose the points to be in the special position in which they are aligned, there exists a representative of the hyperplane class H of \mathbb{P}^2 that passes through all of them, which means that its strict transform is the irreducible effective divisor

$$\hat{H} = \pi^*(H) - \sum_{k=1}^4 E_k, \quad (\text{B.2.70})$$

whose intersection product with the anticanonical class is

$$\hat{H} \cdot \overline{K}_{\text{Bl}(\mathbb{P}^2)} = -1. \quad (\text{B.2.71})$$

From Proposition B.1.2 we see that $\overline{K}_{\text{Bl}(\mathbb{P}^2)}$ will be reducible, containing an \hat{H} component, and therefore the $g(C) = 1$ case cannot be realized using this base.

B.3 Obscured infinite-distance limits

In this appendix we address the phenomenon of obscured infinite-distance limits. Recall from Section 5.2.2 that there can arise situations in which the family vanishing orders of the defining polynomials of the Weierstrass model are minimal over a codimension-one curve in the base of a component of the central fiber, while the component vanishing orders are non-minimal. This can occur over a curve $C \subset \hat{B}_0 = \{u = 0\}_{\hat{B}}$ in the central fiber $\pi : \hat{Y}_0 \rightarrow \hat{B}_0$ of a degeneration $\hat{\rho} : \hat{\mathcal{Y}} \rightarrow D$ in which $\hat{\mathcal{Y}}$ presents no non-minimal singular elliptic fibers,

$$\text{minimal} \sim \text{ord}_{\hat{\mathcal{Y}}}(f, g)_C \leq \text{ord}_{\hat{Y}_0}(f|_{u=0}, g|_{u=0})_C \sim \text{non-minimal}, \quad (\text{B.3.1})$$

or over a curve $C \subset B^p = \{e_p = 0\}_{\mathcal{B}}$ in a component $\pi_p : Y^p \rightarrow B^p$ of the multi-component central fiber of a resolved degeneration $\rho : \mathcal{Y} \rightarrow \mathcal{B}$ obtained as explained in Section 5.2.2.1,

$$\text{minimal} \sim \text{ord}_{\mathcal{Y}}(f_b, g_b)_C \leq \text{ord}_{Y^p}(f_b|_{e_p=0}, g_b|_{e_p=0})_C \sim \text{non-minimal}. \quad (\text{B.3.2})$$

This phenomenon arises because, for such a model, the slice $\pi : \hat{Y}_0 \rightarrow \hat{B}_0$ (or $\pi_p : Y^p \rightarrow B^p$) of the model $\Pi_{\text{ell}} : \hat{\mathcal{Y}} \rightarrow \hat{\mathcal{B}}$ (or $\Pi_{\text{ell}} : \mathcal{Y} \rightarrow \mathcal{B}$) used to compute the component vanishing orders is non-generic. However, because of the interpretation of the degeneration as a family of six-dimensional F-theory models limiting to the one described by the central fiber, we are forced to give special consideration to these non-generic slices of the family variety. We will refer to degenerations presenting this feature as having an obscured infinite-distance limit, since (at least part of) their infinite-distance non-minimal nature is not directly apparent when looking at the elliptic fibers of the family variety.

The problem with such a degeneration is that the F-theory model given by the geometrical representative \hat{Y}_0 of the central fiber of the degeneration presents non-minimal singular elliptic fibers over a curve, that need to be removed. However, since the family variety $\hat{\Pi}_{\text{ell}} : \hat{\mathcal{Y}} \rightarrow \hat{\mathcal{B}}$ is minimal over the same curve, the total transform divisors \tilde{F} , \tilde{G} and $\tilde{\Delta}$ under a base blow-up map do not contain enough components of the exceptional divisor E to allow for a line bundle shift. Insisting on such a line bundle shift would make the shifted divisors F , G and Δ not effective. Hence, the resolution process described in Section 5.2.2.1 and consisting of iterative base blow-ups followed by line bundle shifts in order to preserve the Calabi-Yau condition is not possible.

As mentioned above, the mismatch between the family and component vanishing orders occurs because the slice of the family variety containing the elliptic fibration over the component is not generic, i.e. it intersects the discriminant of the family variety with higher multiplicity than the generic slice does, yielding a subvariety with worse singular elliptic fibers. In order to equate the two notions of vanishing orders, we need to find an equivalent degeneration in which the slice giving the component is the generic slice. This can be achieved by incorporating base changes into the resolution process, as we now describe.

If, of the two cases described above, we find the obscured infinite-distance limit over a curve $C \subset B^p$ in a component of the central fiber Y_0 of the resolved degeneration $\rho : \mathcal{Y} \rightarrow D$, we start by blowing down to said component to obtain a degeneration $\hat{\rho} : \hat{\mathcal{Y}} \rightarrow D$ in which $\hat{\mathcal{B}} = B \times D$. In the other case, this is already the starting point. The triviality of the divisor class D means that we can add copies of it to the defining holomorphic line bundle $\hat{\mathcal{L}}$ of the Weierstrass model without affecting the Calabi-Yau condition or, in more practical terms, that the coordinate u can appear with arbitrary degree in the monomials of f , g and Δ . We are therefore allowed to perform the base change

$$\begin{aligned} \delta_k : D &\longrightarrow D \\ u &\longmapsto u^k, \end{aligned} \tag{B.3.3}$$

which for high enough k makes the $\{u = 0\}_{\hat{\mathcal{B}}}$ slice no longer tangent to the discriminant of the family variety. Then, $\{u = 0\}_{\hat{\mathcal{B}}}$ becomes the generic slice of $\hat{\Pi}_{\text{ell}} : \hat{\mathcal{Y}} \rightarrow \hat{\mathcal{B}}$ and we have

$$\text{ord}_{\hat{\mathcal{Y}}}(f, g)_C = \text{ord}_{Y_0}(f|_{u=0}, g|_{u=0})_C \sim \text{non-minimal}, \tag{B.3.4}$$

allowing us to blow-up the family variety along C and carry out the line bundle shift to recover the Calabi-Yau condition. If we obtained $\hat{\rho} : \hat{\mathcal{Y}} \rightarrow D$ by blowing down $\rho : \mathcal{Y} \rightarrow D$, we will have additional curves of non-minimal fibers that need to be resolved; due to the base change this will require more blow-ups than it originally did, increasing the number of components of the central fiber of the resolved degeneration not only along the new blow-up centre, but also along the original ones. This process can be repeated until all obscure infinite-distance limits have been removed.

This type of base change was already important in the analysis of infinite-distance limits in the complex structure moduli space of eight-dimensional F-theory in [156, 157]. Indeed, although

not discussed as explicitly, the vanishing orders of the defining polynomials of a Weierstrass model in [156, 157] over a point in the family base were understood as the maximal vanishing orders that could be obtained after a base change over said point. In the more general context of the semi-stable reduction theorem [308], a base change may need to be performed before a given degeneration admits a semi-stable modification, as we further discuss in Section 5.2.2.3. In our more restrictive setup, in which we consider degenerations of elliptic fibrations with a section, the obscure infinite-distance limits are one avatar of this need for base changes, that manifests itself very explicitly through the non-genericity of the $\{u = 0\}_{\hat{\mathcal{B}}}$ slice.

Before we conclude the section, let explore a couple of illustrative examples of obscured infinite-distance limits, the first one for a degeneration of elliptic K3 surfaces (for which the above discussion proceeds analogously but in one dimension lower), and the second one for a degeneration of elliptic fibrations over a Hirzebruch surface. In the former we present a family variety in which all the fibers are minimal but an obscured infinite-distance limit is present, while in the latter the obscured infinite-distance limit appears in the exceptional component arising from the blow-up along a curve of non-minimal singularities in the original component.

Example B.3.1. We can already give a simple example of an obscured infinite-distance limit in the context of [156, 157]. Consider a degeneration of elliptic K3 surfaces given by a Weierstrass model over $\mathcal{B} = \mathbb{P}^1 \times D$ with defining polynomials of the form

$$f = s^4 p_4^0([s : t]) + \sum_{i=1}^4 u^i p_8^i([s : t], u^i), \quad (\text{B.3.5a})$$

$$g = s^6 p_6^0([s : t]) + \sum_{i=1}^6 u^i p_8^i([s : t], u^i), \quad (\text{B.3.5b})$$

$$\Delta = s^{12} p_{12}^0([s : t]) + \sum_{i=1}^{12} u^i p_{24}^i([s : t], u^i), \quad (\text{B.3.5c})$$

where the $p_*^i([s : t], u^i)$ polynomials in f and g are generic. The family and component vanishing orders over $\{s = u = 0\}_{\mathcal{B}}$ are

$$(1, 1, 2) = \text{ord}_{\hat{\mathcal{Y}}}(f, g, \Delta)_{s=u=0} \leq \text{ord}_{\hat{Y}_0}(f|_{u=0}, g|_{u=0}, \Delta|_{u=0})_{s=u=0} = (4, 6, 12). \quad (\text{B.3.6})$$

Working in the patch $([s : t], u)$, the family vanishing orders can be computed by restricting $\hat{\mathcal{B}}$ to the line $\mathcal{W} := \{(s, u) = (\mu a, \mu b)\}_{\hat{\mathcal{B}}}$ with a generic choice for the coefficients a and b . The component vanishing orders correspond to the choice $b = 0$, which can be seen to be the only choice intersecting Δ at $\{s = u = 0\}_{\mathcal{B}} = \{\mu = 0\}_{\mathcal{W}}$ with higher multiplicity than the rest of the lines. This is represented in Figure B.2a. After a base change

$$\begin{aligned} \delta_6 : D &\longrightarrow D \\ u &\longmapsto u^6, \end{aligned} \quad (\text{B.3.7})$$

we obtain

$$(4, 6, 12) = \text{ord}_{\hat{\mathcal{Y}}}(f, g, \Delta)_{s=u=0} \leq \text{ord}_{\hat{Y}_0}(f|_{u=0}, g|_{u=0}, \Delta|_{u=0})_{s=u=0} = (4, 6, 12), \quad (\text{B.3.8})$$

and the choice $b = 0$ becomes generic, which can be seen by computing the intersection multiplicity or pictorially by looking at the progression of the intersection shown in Figure B.2 as we increase the branching degree of the base change. Hence, the model can be resolved by blowing up $\hat{\mathcal{B}}$ along $\{s = u = 0\}_{\mathcal{B}}$ and shifting the line bundle afterwards, leading to a two-component central fiber.

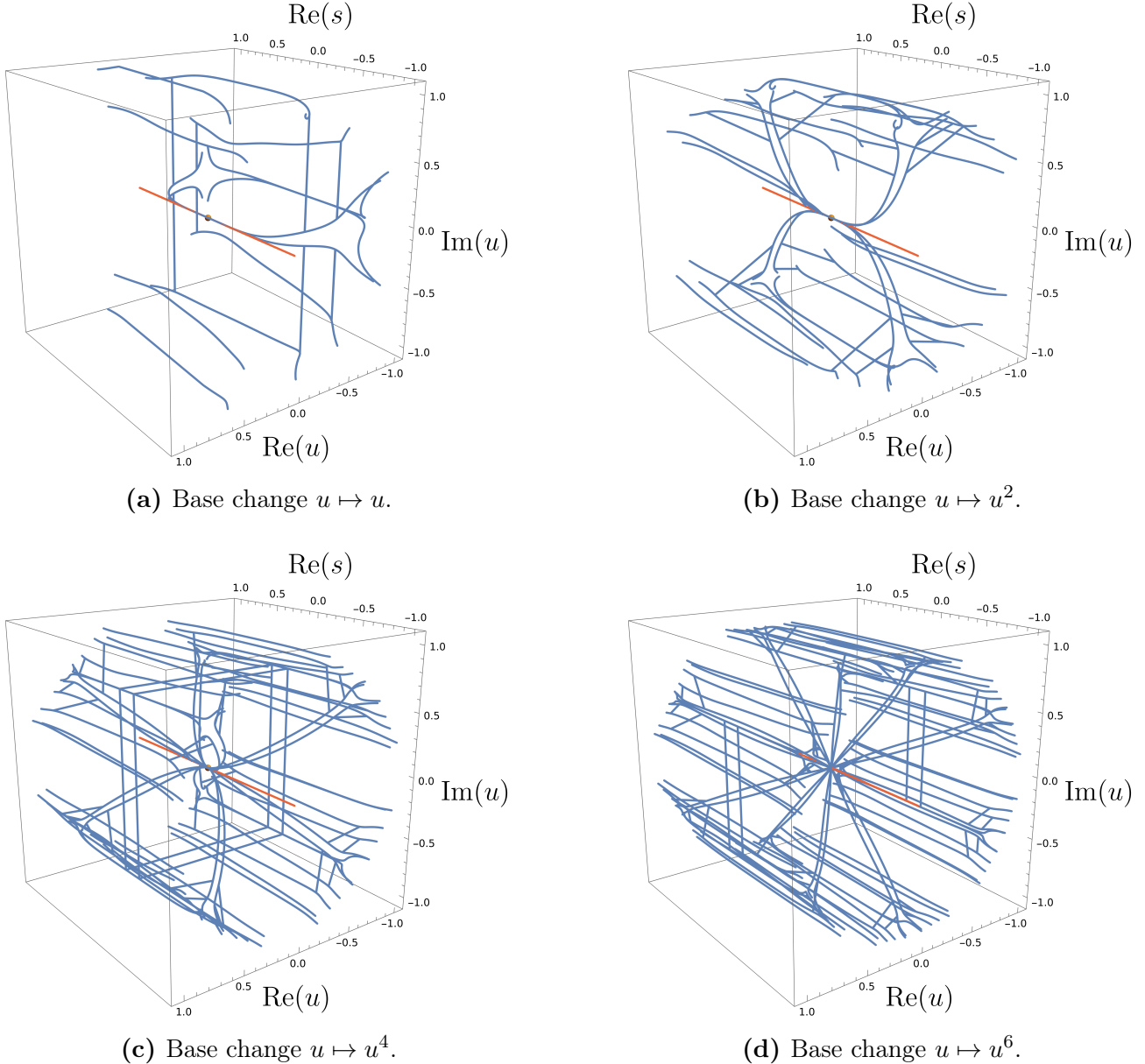


Figure B.2: (Real) three-dimensional cut $\Delta|_{\text{Im}(s)=0}$ of the discriminant (B.3.5c) for a particular, but generic, choice of coefficients in the patch $([s : 1], u)$. The locus $\{u = 0\}_B$ is shown in red. We observe that its tangent intersection with the discriminant becomes transverse for a base change with high enough branching degree.

Example B.3.2. Consider the Weierstrass model

$$f = s^2 t^4 v^4 (s^2 v^4 + s^2 v^2 w^2 + s^2 w^4 + t^2 u^2 v^4) , \quad (\text{B.3.9a})$$

$$g = s^4 t^5 v^4 (s^3 w^8 + s^2 t v^4 w^4 + s^2 t v^2 w^6 + t^3 u^2 v^8 + t^3 u^2 v^2 w^6) , \quad (\text{B.3.9b})$$

$$\Delta = s^6 t^{10} v^8 p_{8,16}([s : t], [v : w], u) , \quad (\text{B.3.9c})$$

defining an elliptically fibered variety $\hat{\mathcal{Y}}$ over the base $\hat{\mathcal{B}} = \mathbb{F}_0 \times D$ and supporting non-minimal singular fibers over the curve $\mathcal{S} \cap \mathcal{U}$ with

$$\text{ord}_{\hat{\mathcal{Y}}}(f, g, \Delta)_{s=u=0} = (4, 6, 12) . \quad (\text{B.3.10})$$

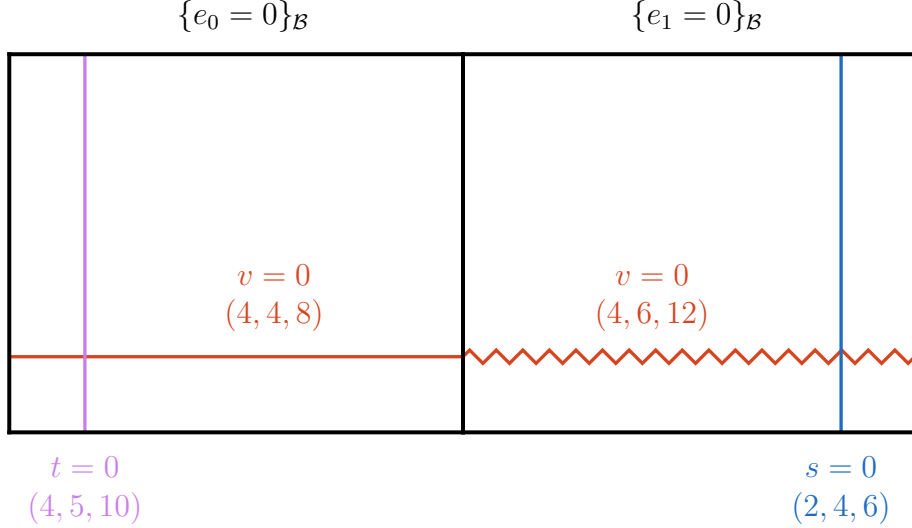


Figure B.3: Restrictions Δ'_0 and Δ'_1 of the (modified) discriminant for Example B.3.2, with the residual discriminant omitted for clarity. The printed vanishing orders correspond to the component vanishing orders in each component. We observe an obscured infinite-distance limit in the B^1 component.

The family vanishing orders over all the other codimension-one loci are minimal, and over the codimension-two loci are either minimal or finite-distance non-minimal. The same is true for the component vanishing orders. Hence, at first sight, we seem not to have any obscured infinite-distance limits lurking in this model. Performing a (toric) blow-up of $\hat{\mathcal{B}}$ along $\mathcal{S} \cap \mathcal{U}$ we obtain the defining polynomials

$$f_b = s^2 t^4 v^4 (e_0^2 t^2 v^4 + s^2 v^4 + s^2 v^2 w^2 + s^2 w^4) , \quad (\text{B.3.11a})$$

$$g_b = s^4 t^5 v^4 (e_1 s^3 w^8 + e_0^2 t^3 v^8 + e_0^2 t^3 v^2 w^6 + s^2 t v^4 w^4 + s^2 t v^2 w^6) , \quad (\text{B.3.11b})$$

$$\Delta_b = s^6 t^{10} v^8 p_{8,16,6}([s:t], [v:w], [s:e_0:e_1]) , \quad (\text{B.3.11c})$$

with Stanley-Resiner ideal

$$\mathcal{I}_{\mathcal{B}} = \langle st, vw, se_0, te_1 \rangle \quad (\text{B.3.12})$$

giving the Weierstrass model $\Pi_{\text{ell}} : \mathcal{Y} \rightarrow \mathcal{B}$ of the resolved degeneration $\rho : \mathcal{Y} \rightarrow D$. While all the family vanishing orders of the resolved model can be seen to be minimal in codimension-one, and minimal or finite-distance non-minimal in codimension-two, we have an obscured infinite-distance limit in the exceptional component arising from the blow-up, as can be seen from

$$(4, 5, 10) = \text{ord}_{\mathcal{Y}}(f_b, g_b, \Delta_b)_{v=u=0} \leq \text{ord}_{Y^1} (f|_{e_1=0}, g|_{e_1=0}, \Delta|_{e_1=0})_{v=u=0} (4, 6, 12) . \quad (\text{B.3.13})$$

Applying the procedure described above, we blow the model down to the Y^1 component and perform the base change

$$\begin{aligned} \delta_6 : D &\longrightarrow D \\ u &\longmapsto u^6 , \end{aligned} \quad (\text{B.3.14})$$

after which we read over the curves $\mathcal{T} \cap \mathcal{U}$ and $\mathcal{V} \cap \mathcal{U}$ the non-minimal family vanishing orders

$$\text{ord}_{\hat{\mathcal{Y}}}(f, g, \Delta)_{t=u=0} = (4, 6, 12) , \quad (\text{B.3.15a})$$

$$\text{ord}_{\hat{\mathcal{Y}}}(f, g, \Delta)_{v=u=0} = (4, 6, 12) , \quad (\text{B.3.15b})$$

i.e. the obscured infinite-distance limit is now apparent at the level of the family variety. Blowing up and performing the necessary line bundle shifts successively along the curves $\mathcal{V} \cap \mathcal{U}$, $\mathcal{T} \cap E_0$ and $\mathcal{T} \cap E_1$ leads to the Weierstrass model $\Pi_{\text{ell}} : \mathcal{Y} \rightarrow \mathcal{B}$ given by the defining polynomials²

$$f_b = s^2 t^4 v^4 (e_1^4 s^2 v^4 + e_1^2 s^2 v^2 w^2 + e_1^4 e_2^2 e_3^4 t^2 v^4 + s^2 w^4) , \quad (\text{B.3.18a})$$

$$g_b = s^4 t^5 v^4 (e_0^2 e_2 s^3 w^8 + e_1^2 s^2 t v^4 w^4 + e_1^6 e_2^2 e_3^4 t^3 v^8 + e_2^2 e_3^4 t^3 v^2 w^6 + s^2 t v^2 w^6) , \quad (\text{B.3.18b})$$

$$\Delta_b = s^6 t^{10} v^8 p_{8,16,4,2,2}([s : t], [v : w], [v : e_0 : e_1], [t : e_0 : e_2], [t : e_2 : e_3]) , \quad (\text{B.3.18c})$$

together with the Stanley-Reisner ideal

$$\mathcal{I}_{\mathcal{B}} = \langle st, e_2 s, e_3 s, e_0 t, e_2 t, v w, e_0 v, e_2 v, e_3 v, e_1 w, e_0 e_3 \rangle . \quad (\text{B.3.19})$$

One can check that no infinite-distance non-minimal singularities are found at the level of the family variety, its restriction to the components or its restriction to the intersections of components; the base change has indeed allowed us to obtain a resolved degeneration $\rho : \mathcal{Y} \rightarrow \mathcal{B}$ free of obscured infinite-distance limits.

While the family and component vanishing orders did not allow us to detect the presence of the obscured infinite-distance limit, the unresolved degeneration (B.3.9) already hints at its existence. To see how, let us plot the restriction $\Delta_b|_{B_0}$ of (B.3.11c), which we do in Figure B.4. The component of $\Delta_b|_{E_1}$ responsible for the obscured infinite-distance limit intersects the curve over which the base components intersect at the point $\{e_0 = e_1 = v = 0\}_{\mathcal{B}}$. The component vanishing orders for this point computed from both sides disagree, having

$$(4, 5, 10) = \text{ord}_{Y^0}(f_b|_{e_0}, g_b|_{e_0}, \Delta_b|_{e_0})_{e_0=e_1=v=0} \neq \text{ord}_{Y^1}(f_b|_{e_1}, g_b|_{e_1}, \Delta_b|_{e_1})_{e_0=e_1=v=0} = (4, 6, 12) . \quad (\text{B.3.20})$$

What agrees are the vanishing orders found when we restrict the model to the intersection of the two components from either side, i.e. the interface vanishing orders

$$\text{ord}_{Y^0 \cap Y^1}(f_b|_{e_0=e_1=0}, g_b|_{e_0=e_1=0}, \Delta_b|_{e_0=e_1=0})_{e_0=e_1=v=0} = (4, 6, 12) . \quad (\text{B.3.21})$$

We see that the curve $E_0 \cap E_1$ shaded in grey in Figure B.4 is the generic slice from the point of view of the B^1 component, while it is non-generic from the B^0 side, explaining the discrepancy.

At the end of Section 5.2.2.2, we mentioned that these interface vanishing orders can be directly computed in the unresolved degeneration. Since the point on the interface curve with

²Blowing up in a different order gives the same defining polynomials f_b , g_b and Δ_b , but a different Stanley-Reisner ideal. For example, we could have performed the blow-ups along the curves $\mathcal{T} \cap \mathcal{U}$, $\mathcal{T} \cap E_1$ and $\mathcal{V} \cap E_3$, obtaining the Stanley-Reisner ideal

$$\mathcal{I}_{\mathcal{B}} = \langle st, e_1 s, e_2 s, e_0 t, e_1 t, e_3 t, v w, e_0 v, e_3 w, e_0 e_2, e_2 e_3 \rangle . \quad (\text{B.3.16})$$

While with this resolution no infinite-distance non-minimal family vanishing orders are found, we still have the infinite-distance non-minimal component vanishing orders

$$\text{ord}_{Y^1}(f_b|_{e_1=0}, g_b|_{e_1=0}, \Delta_b|_{e_1=0})_{e_1=v=0} = (4, 6, 12) . \quad (\text{B.3.17})$$

These are not problematic, since they can be removed by performing the flop $\{e_1 = v = 0\}_{\mathcal{B}} \leftrightarrow \{e_2 = e_3 = 0\}_{\mathcal{B}}$, which constitutes a valid modification of the degeneration. The resulting \mathcal{B} is, however, singular. Its singularity can be removed by performing the flop $\{e_2 = v = 0\}_{\mathcal{B}} \leftrightarrow \{e_3 = t = 0\}_{\mathcal{B}}$, at which point we obtain the resolution given by (B.3.19) up to a relabelling of the exceptional components. The fact that the two resolutions are related by some flops is expected, see Remark B.4.1. In the body of the text we have chosen the resolution process that directly gives the geometrical representative for the central fiber of the degeneration with the most favourable properties, in order to simplify the discussion.

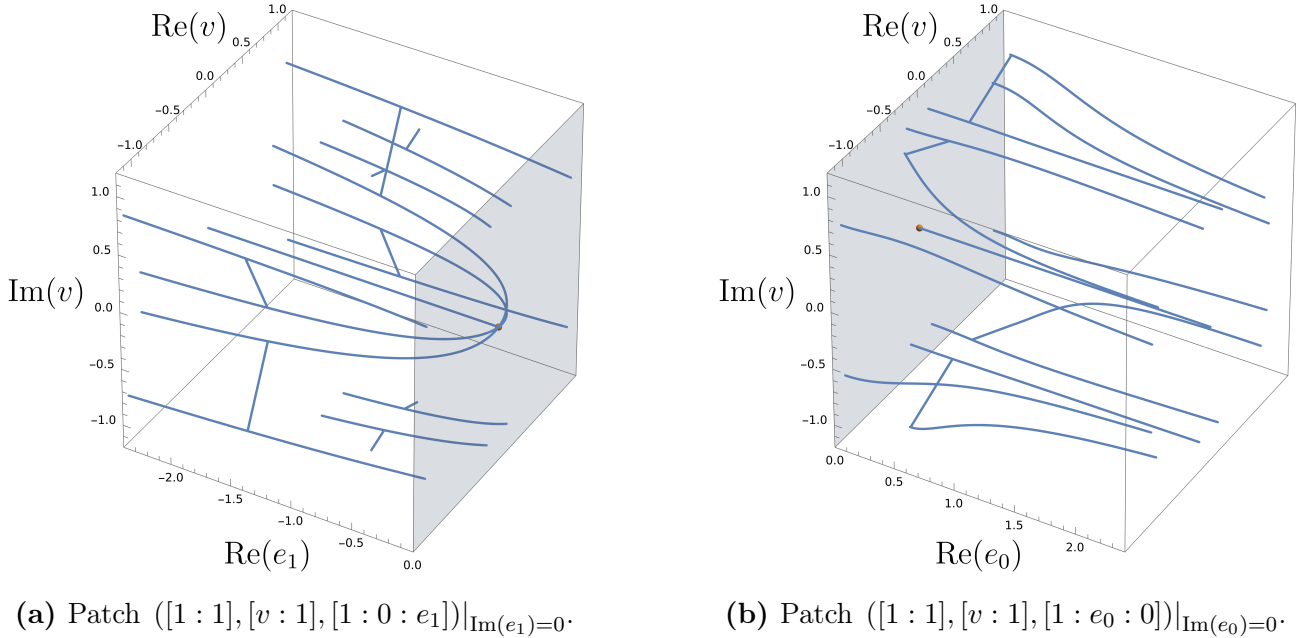


Figure B.4: Plot of the restriction $\Delta|_{B_0}$ of the discriminant (B.3.11c). The intersections of the discriminant with the interface curve $E_0 \cap E_1 \subset B_0 \subset \mathcal{B}$ need to agree from both sides. This implies that the point $\{e_0 = e_1 = v = 0\}_{\mathcal{B}}$ is to be non-minimal in the B^0 component if we compute the vanishing orders of the defining polynomials along the (in this case non-generic) curve $E_0 \cap E_1$, i.e. if we compute the interface vanishing orders.

non-minimal interface vanishing orders is so tightly related to the obscured infinite-distance limit, this gives us a way to detect it even before starting to blow-up the base. Namely, a point with non-minimal interface vanishing orders, but minimal family vanishing orders, on top of a curve supporting non-minimal elliptic fibers at the level of the family variety signals the presence of an obscured infinite-distance limit in the exceptional components arising from the base blow-ups centred at the aforementioned non-minimal curve.

In the example under scrutiny, we can indeed obtain the interface vanishing orders (B.3.21) directly from (B.3.9). To achieve this, recognize that, if we denote the blow-up map leading to (B.3.11) by $\pi : \mathcal{B} \rightarrow \hat{\mathcal{B}}$ we have for this model that

$$\pi_*(F_0) = F|_{\mathcal{U}} - 4(\mathcal{S} \cap \mathcal{U}), \quad (\text{B.3.22a})$$

$$\pi_*(G_0) = G|_{\mathcal{U}} - 6(\mathcal{S} \cap \mathcal{U}), \quad (\text{B.3.22b})$$

$$\pi_*(\Delta_0) = \Delta|_{\mathcal{U}} - 12(\mathcal{S} \cap \mathcal{U}), \quad (\text{B.3.22c})$$

see (B.5.2). We obtain then the interface vanishing orders (B.3.21) by computing

$$\text{ord}_{\pi^*(\mathcal{S} \cap \mathcal{U})} \left(\frac{f}{s^4} \Big|_{u=s=0}, \frac{g}{s^6} \Big|_{u=s=0}, \frac{\Delta}{s^{12}} \Big|_{u=s=0} \right)_{v=0} = (4, 6, 12), \quad (\text{B.3.23})$$

and therefore the obscured infinite-distance limit could have indeed been detected³ at the start of the discussion.

³Performing the base change $u \mapsto u^2$ directly in the original model (B.3.9) allows us to blow-up and line bundle shift along the curves $\mathcal{S} \cap \mathcal{U}$, $\mathcal{S} \cap E_1$ and $\mathcal{V} \cap E_2$. After this resolution, no infinite-distance non-minimal family vanishing orders are found, but the infinite-distance non-minimal component vanishing orders

$$\text{ord}_{Y^1}(f_b|_{e_1=0}, g_b|_{e_1=0}, \Delta_b|_{e_1=0})_{e_1=v=0} = (4, 6, 12) \quad (\text{B.3.24})$$

A variation of what we have just observed in Example B.3.2 would be given by a model in which the interface curve between the two components presents a point with non-minimal interface vanishing orders, but no codimension-one (obscured or conventional) infinite-distance limits are observed in either of the two components. This also corresponds, in fact, to a form of obscured infinite-distance limit in codimension-one. Upon performing a base change, blowing up the base to arrive at the resolve degeneration leads to more than two-components for its central fiber, and in the ones arising from the intermediate blow-ups we will exhibit an obscured infinite-distance limit of the form described earlier in the section. This special type of obscured infinite-distance limits and their interpretation in the heterotic dual models (whenever these are available) are discussed in greater length in Section 6.4.5.

The signature of obscured infinite-distance limits as points with non-minimal interface vanishing orders on top of the blow-up centres of the original degeneration will be relevant later on in Appendix B.5.

B.4 Resolution trees

In this appendix, we generalise the discussion of Section 5.2.4 beyond the class of single infinite-distance limits and their open-chain resolutions. First, we will prove and exemplify Proposition 5.2.19, which identifies the components of more general infinite-distance limits as Hirzebruch surfaces or suitable blow-ups thereof, which form a resolution tree rather than an open chain. Then we characterise the Weierstrass models over the components of these resolutions.

B.4.1 Geometry of the components

Let us use the same notation as in Section 5.2.4. In order to determine the geometry of the $\{B^p\}_{0 \leq p \leq P}$ components in the resolution of a general degeneration, we need to produce the analogue of Proposition 5.2.13 after dropping the assumption of vanishing intersection among the $\{C_p\}_{1 \leq p \leq P}$ curves. This results in the following proposition.

Proposition 5.2.19. *Let $\hat{\mathcal{B}}$ be the base family variety of a genus-zero degeneration $\hat{\rho} : \hat{\mathcal{Y}} \rightarrow D$, and $\text{Bl}_{p-1}(\hat{\mathcal{B}})$ be the result of $p-1$ blow-ups of $\hat{\mathcal{B}}$. Let $C_p \subset B^i$ be a smooth irreducible curve over which $\text{Bl}_{p-1}(\hat{\mathcal{Y}})$ presents non-minimal singular fibers. Then, the exceptional component $B^p = E_p$ arising from the blow-up of $\text{Bl}_{p-1}(\hat{\mathcal{B}})$ along C_p is the Hirzebruch surface*

$$B^p = \mathbb{F}_{|n_p|}, \quad n_p := C_p \cdot_{B^i} C_p + \sum_{\substack{q=0 \\ q \neq i}}^{p-1} E_q|_{E_i} \cdot_{B^i} C_p. \quad (5.2.113)$$

Moreover, define the set of components $\{B^q\}_{q \in \mathcal{I}}$ to be comprised by those elements in $\{B^q\}_{0 \leq q \leq p-1}$ such that

$$\text{codim}_{B^i} \left(E_q|_{E_i} \cdot_{B^i} C_p \right) = 2. \quad (5.2.114)$$

After the blow-up along C_p , the old components $\{B^q\}_{q \in \mathcal{I}}$ must be substituted for their blow-ups $\{\text{Bl}_{E_q|_{E_i} \cdot_{B^i} C_p}(B^q)\}_{q \in \mathcal{I}}$.

are still present. These can be removed through the flop $\{e_1 = v = 0\}_{\mathcal{B}} \leftrightarrow \{e_0 = e_3 = 0\}_{\mathcal{B}}$, that leads, however, to a singular \mathcal{B} .

Proof. The proof of Proposition 5.2.12 applies until we reach the computation of $\mathcal{N}_{E_i/\text{Bl}_{p-1}(\hat{B})}$, which needs to be modified. In the more general situation, we have that

$$\mathcal{N}_{E_i/\text{Bl}_{p-1}(\hat{B})} = \mathcal{O}_{\text{Bl}_{p-1}(\hat{B})}(E_i) \Big|_{E_i} = E_i \cdot_{\text{Bl}_{p-1}(\hat{B})} E_i = - \sum_{\substack{q=0 \\ q \neq i}}^{p-1} E_i \cdot_{\text{Bl}_{p-1}(\hat{B})} E_q = - \sum_{\substack{q=0 \\ q \neq i}}^{p-1} E_q|_{E_i}, \quad (\text{B.4.1})$$

leading to

$$\mathcal{N}_{B^i/\text{Bl}_{p-1}(\hat{B})} \Big|_{C_p} = \mathcal{O}_{\mathbb{P}^1}(-m_p), \quad m_p := \sum_{\substack{q=0 \\ q \neq i}}^{p-1} E_q|_{E_i} \cdot_{B^i} C_p. \quad (\text{B.4.2})$$

Altogether, we find

$$E_p = \mathbb{P}(\mathcal{O}_{\mathbb{P}^1} \oplus \mathcal{O}_{\mathbb{P}^1}(|n_p|)) = \mathbb{F}_{|n_p|}, \quad n_p := C_p \cdot_{B^i} C_p + \sum_{\substack{q=0 \\ q \neq i}}^{p-1} E_q|_{E_i} \cdot_{B^i} C_p. \quad (\text{B.4.3})$$

Consider now a fixed component B^q . Since C_p is an irreducible curve, if

$$\text{codim}_{B^i} \left(E_q|_{E_i} \cdot_{B^i} C_p \right) = 1, \quad (\text{B.4.4})$$

we have that $C_p \subset E_q|_{E_i}$, and therefore the blow-up centre $C_p \subset B^q$. Then

$$\pi^*(E_q) = E_q + E_p, \quad (\text{B.4.5})$$

and with our notation B^q represents the strict transform of the former B^p after the blow-up $\pi_p : \text{Bl}_p(\hat{\mathcal{B}}) \rightarrow \text{Bl}_{p-1}(\hat{\mathcal{B}})$. Hence, the surface to which B^q refers has not changed. If instead

$$\text{codim}_{B^i} \left(E_q|_{E_i} \cdot_{B^i} C_p \right) = 1, \quad (\text{B.4.6})$$

only a set of points of the blow-up centre sits in B^q . The blow-up $\pi_p : \text{Bl}_p(\hat{\mathcal{B}}) \rightarrow \text{Bl}_{p-1}(\hat{\mathcal{B}})$ then induces a surface blow-up $\pi_{p,q} : \text{Bl}_{E_q|_{E_i} \cdot_{B^i} C_p}(B^q) \rightarrow B^q$ along the points $E_q|_{E_i} \cdot_{B^i} C_p \subset B^q$, and we relabel the irreducible component to be $B^q := \text{Bl}_{E_q|_{E_i} \cdot_{B^i} C_p}(B^q)$. \square

Remark B.4.1. Consider a set of intersecting curves of non-minimal singular fibers contained in a given base component. The order in which we blow-up the base family variety along them matters for the resulting geometry, as the last exceptional component will be a Hirzebruch surface, while the rest will be blow-ups thereof. Since any order in which we perform the blow-ups is a valid modification of the original degeneration, all the resulting geometrical representatives of the central fiber correspond to the same limit. In fact, they are related to each other by flopping the exceptional curves arising over the intersection points of the blow-up centres.

Let us see how this geometry is realized in some concrete examples. We start with a model in which the base of the central fiber of the degeneration contains two curves of non-minimal singular fibers intersecting at a point and leading to a three-component central fiber for the resolved family variety, focusing on how the two possible blow-up orders are related by a flop.

Example B.4.2. Consider the Weierstrass model describing an elliptically fibered variety $\hat{\mathcal{Y}}$ over the base $\hat{\mathcal{B}} = \mathbb{F}_3 \times D$ given by

$$f = s^4 t^4 v^4 (uv^4 + uw^4 + v^4 + v^2 w^2 + w^4) , \quad (\text{B.4.7a})$$

$$g = s^5 t^5 v^5 (s^2 uv^{10} + s^2 uw^{10} + s^2 v^{10} + stvw^6 + t^2 uw^4) , \quad (\text{B.4.7b})$$

$$\Delta = s^{10} t^{10} v^{10} p_{4,20}([s:t], [v:w:t], u) . \quad (\text{B.4.7c})$$

It supports non-minimal singular fibers over the curves $\mathcal{S} \cap \mathcal{U}$ and $\mathcal{V} \cap \mathcal{U}$, as can be seen from

$$\text{ord}_{\hat{\mathcal{Y}}}(f, g, \Delta)_{s=u=0} = (4, 6, 12) , \quad (\text{B.4.8a})$$

$$\text{ord}_{\hat{\mathcal{Y}}}(f, g, \Delta)_{v=u=0} = (4, 6, 12) . \quad (\text{B.4.8b})$$

Since the example is amenable to a toric treatment, we will display the information about the geometry of the different components in terms of their toric fan, in order to be more concise. The starting toric fan describing $\hat{\mathcal{B}} = \mathbb{F}_3 \times D$ is

$$v = (1, 0, 0) , \quad t = (0, 1, 0) , \quad w = (-1, -n, 0) , \quad s = (0, -1, 0) , \quad u = (0, 0, 1) , \quad (\text{B.4.9})$$

in the lattice

$$N := \mathbb{Z}\langle(1, 0, 0), (0, 1, 0), (0, 0, 1)\rangle . \quad (\text{B.4.10})$$

Performing the two (toric) blow-ups along these curves together with the appropriate line bundle shifts, we arrive at

$$f_b = s^4 t^4 v^4 (e_0 e_s e_v^5 v^4 + e_0 e_s e_v w^4 + e_v^4 v^4 + e_v^2 v^2 w^2 + w^4) , \quad (\text{B.4.11a})$$

$$g_b = s^5 t^5 v^5 (e_0 e_s^2 e_v^{10} s^2 v^{10} + e_0 e_s^2 s^2 w^{10} + e_0 t^2 w^4 + e_s e_v^9 s^2 v^{10} + stvw^6) , \quad (\text{B.4.11b})$$

$$\Delta_b = s^{10} t^{10} v^{10} p_{4,20,2,2}([s:t], [v:w:t], [s:e_0, e_s], [v:e_0, e_v]) , \quad (\text{B.4.11c})$$

where we have denoted the exceptional coordinates by e_s and e_v to keep track of their origin. Blowing up first along $\mathcal{S} \cap \mathcal{U}$ and then along $\mathcal{V} \cap E_0$ or vice versa only affects the resulting Stanley-Reisner ideal, yielding

$$\mathcal{I}_{\mathcal{B}}^{sv} = \langle st, vw, se_0, te_s, ve_0, we_v, se_v \rangle , \quad (\text{B.4.12})$$

$$\mathcal{I}_{\mathcal{B}}^{vs} = \langle st, vw, ve_0, we_v, se_0, te_s, ve_s \rangle , \quad (\text{B.4.13})$$

respectively, meaning that the resulting toric fans $\Sigma_{\mathcal{B}}^{sv}$ and $\Sigma_{\mathcal{B}}^{vs}$ only differ by some 2-cones. $\mathcal{I}_{\mathcal{B}}^{sv}$ and $\mathcal{I}_{\mathcal{B}}^{vs}$ are therefore related to each other, as can be seen by comparing the fans in Figure B.5, by flopping the curves $\{v = e_s = 0\} \leftrightarrow \{s = e_v = 0\}$ in the base family variety \mathcal{B} , as we commented on in Remark B.4.1. In both cases, we observe that there no longer are infinite-distance non-minimal singularities present.

Let us now focus on the geometry of the components obtained by first blowing up along $\mathcal{S} \cap \mathcal{U}$ and then along $\mathcal{V} \cap E_0$. The three components $\{B^0, B^s, B^v\}$ of B_0 are also toric varieties, and their toric fans can be obtained from $\Sigma_{\mathcal{B}}^{sv}$ by computing the orbit closure of the edges $\{e_0, e_s, e_v\}$. The results are shown in Figure B.6. The toric computation tells us that the base components of the central fiber correspond to the surfaces

$$B^0 = \mathbb{F}_3 , \quad B^s = \text{Bl}_1(\mathbb{F}_3) , \quad B^v = \mathbb{F}_1 . \quad (\text{B.4.14})$$

We now compare these with the expectations from Proposition 5.2.19. The two blow-up centres are contained in $\hat{B}_0 = \mathbb{F}_3$, and therefore the component B^0 is just its strict transform. To

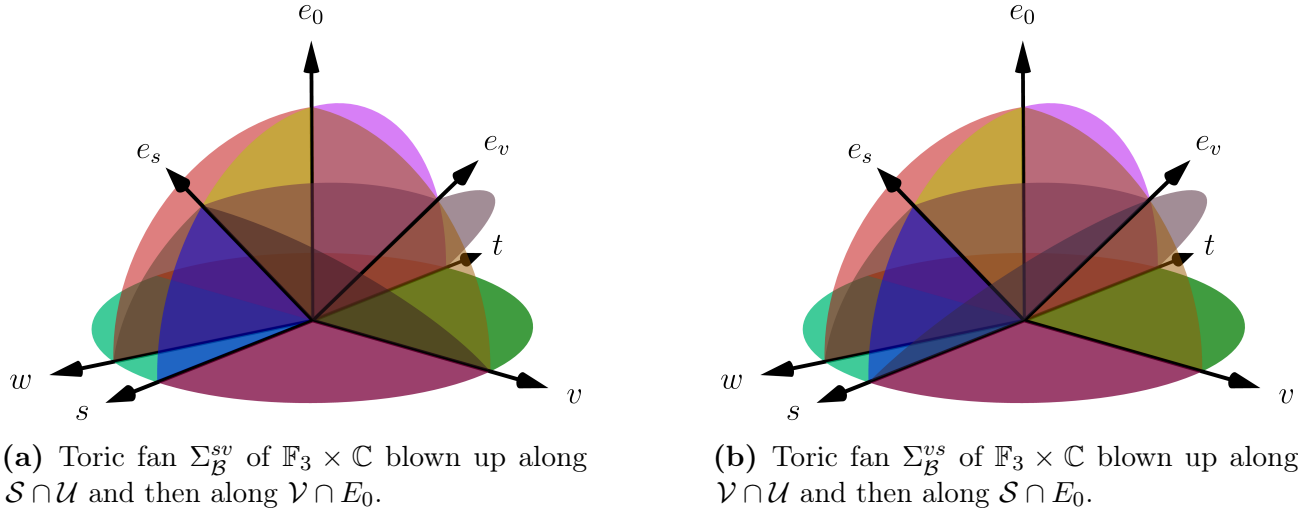


Figure B.5: Toric fans associated to the two possible blow-up orders. They are related to each other by exchanging the 2-cones (v, e_s) and (s, e_v) , i.e. flopping the corresponding curves.

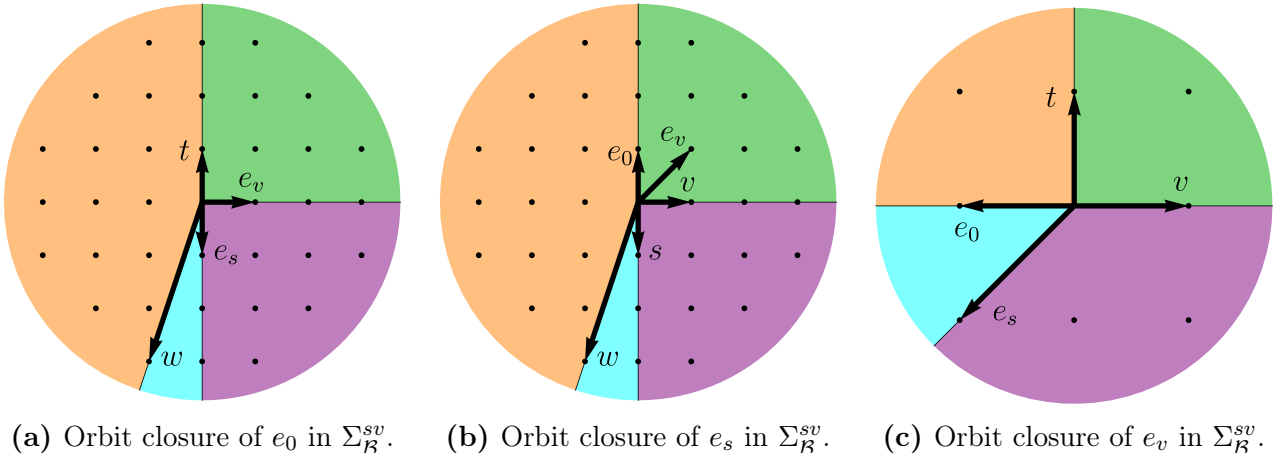


Figure B.6: Geometry of the components of \mathcal{B} obtained from $\hat{\mathcal{B}}$ by first blowing up along $\mathcal{S} \cap \mathcal{U}$ and then along $\mathcal{V} \cap E_0$.

obtain the other two components, we first label the blow-up centre in order, i.e. $C_1 = \mathcal{S} \cap \mathcal{U}$ and $C_2 = \mathcal{V} \cap E_0$. The two curves intersect at one point, namely at

$$C_1 \cap C_2 = \mathcal{S} \cap \mathcal{V} \cap \mathcal{U}' = \{s = v = u = 0\}. \quad (\text{B.4.15})$$

The first blow-up produces

$$B^s = \mathbb{F}_{|C_1 \cdot \hat{\mathcal{B}}_0 C_1|} = \mathbb{F}_3. \quad (\text{B.4.16})$$

The second blow-up produces

$$B^v = \mathbb{F}_{|C_2 \cdot B^s C_2 + E_s|_{E_0 \cdot B^s C_2}} = \mathbb{F}_{|C_2 \cdot B^s C_2 + C_1 \cdot B^s C_2|} = \mathbb{F}_1, \quad (\text{B.4.17})$$

and the former component B^s must be blown-up at the point $\{s = v = 0\}_{E_s}$, yielding the surface $B^s = \text{Bl}_1(\mathbb{F}_3)$. This agrees with the toric computation.

Consider now the case in which we blow up first along $\mathcal{V} \cap \mathcal{U}$ and then along $\mathcal{S} \cap E_0$. The toric fans obtained from the orbit closure of the edges $\{e_0, e_s, e_v\}$ in Σ_B^{vs} are depicted in Figure B.7.

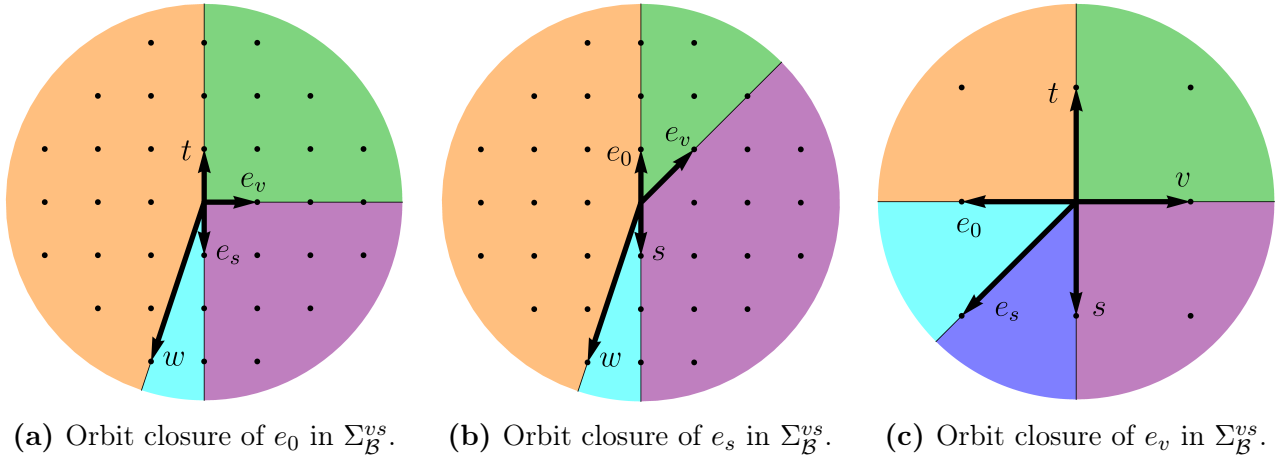


Figure B.7: Geometry of the components of \mathcal{B} , obtained from $\hat{\mathcal{B}}$ by first blowing up along $\mathcal{V} \cap \mathcal{U}$ and then along $\mathcal{S} \cap E_0$.

We identify the surfaces corresponding to the base components of the central fiber to be

$$B^0 = \mathbb{F}_3, \quad B^s = \mathbb{F}_2, \quad B^v = \text{Bl}_1(\mathbb{F}_1). \quad (\text{B.4.18})$$

Again, B^0 is simply the strict transform of $\hat{B}_0 = \mathbb{F}_3$, since the latter contains both blow-up centres. We compare with Proposition 5.2.19, now labelling the curves $C_1 = \mathcal{V} \cap \mathcal{U}$ and $C_2 = \mathcal{S} \cap E_0$, in agreement with the new blow-up order. From the first blow-up we obtain

$$B^v = \mathbb{F}_{|C_1 \cdot \hat{B}_0 C_1|} = \mathbb{F}_0. \quad (\text{B.4.19})$$

The second blow-up produces

$$B^s = \mathbb{F}_{|C_2 \cdot B^0 C_2 + E_v|_{E_0 \cdot B^0 C_2}} = \mathbb{F}_{|C_2 \cdot B^0 C_2 + C_1 \cdot B^0 C_2|} = \mathbb{F}_2, \quad (\text{B.4.20})$$

and also blows-up the former component B^s at the point $\{s = v = 0\}_{E_v}$, leading to $B^v = \text{Bl}_1(\mathbb{F}_0)$, in agreement with the toric computation.

The effect of the flop $\{v = e_s = 0\} \leftrightarrow \{s = e_v = 0\}$ connecting the two base family varieties of the resolved degeneration can be seen at the level of components in Figures B.6 and B.7, which only differ by the addition or subtraction of certain edges to the toric fans of B^s and B^v .

At each step in the previous example, only the centres of the already performed blow-ups were relevant in order to determine the geometry of the new components. More generally, two components need not intersect along a blow-up centre, which is why (5.2.113) cannot be expressed only in terms of the curves $\{C_p\}_{1 \leq p \leq P}$. This is showcased in the next example, in which we also see that the geometry of the original component \hat{B}_0 can be affected by the blow-up process as well, the end product not always simply corresponding to the original type of surface.

Example B.4.3. Consider the Weierstrass model

$$f = t^3 (s^5 u^3 v^9 + s^4 t u^4 w^8 + s^4 t v^8 + s^4 t v^4 w^4 + t^5 w^4), \quad (\text{B.4.21a})$$

$$g = t^4 (s^8 u^6 v^{14} + s^8 u^6 v^4 w^{10} + s^6 t^2 u^6 w^{12} + s^6 t^2 v^{12} + s^6 t^2 v^6 w^6 + t^8 w^6), \quad (\text{B.4.21b})$$

$$\Delta = t^8 p_{16,28}([s : t], [v : w : t], u), \quad (\text{B.4.21c})$$

defining an elliptically fibered variety $\hat{\mathcal{Y}}$ over the base $\hat{\mathcal{B}} = \mathbb{F}_1 \times D$ and supporting non-minimal singular fibers over the curve $\mathcal{T} \cap \mathcal{U}$, as can be seen from

$$\text{ord}_{\hat{\mathcal{Y}}}(f, g, \Delta)_{t=u=0} = (4, 6, 12). \quad (\text{B.4.22})$$

One possible sequence of blow-ups leading to the resolved degeneration $\rho: \mathcal{Y} \rightarrow D$ is

$$\pi_1: \text{Bl}_1(\hat{\mathcal{B}}) \rightarrow \hat{\mathcal{B}}, \quad \text{along } C_1 = \mathcal{T} \cap \mathcal{U}, \quad (\text{B.4.23a})$$

$$\pi_2: \text{Bl}_2(\hat{\mathcal{B}}) \rightarrow \text{Bl}_1(\hat{\mathcal{B}}), \quad \text{along } C_2 = \mathcal{V} \cap E_1, \quad (\text{B.4.23b})$$

$$\pi_3: \text{Bl}_3(\hat{\mathcal{B}}) \rightarrow \text{Bl}_2(\hat{\mathcal{B}}), \quad \text{along } C_3 = \mathcal{T} \cap E_1, \quad (\text{B.4.23c})$$

$$\pi_4: \text{Bl}_4(\hat{\mathcal{B}}) \rightarrow \text{Bl}_3(\hat{\mathcal{B}}), \quad \text{along } C_4 = \mathcal{T} \cap E_3, \quad (\text{B.4.23d})$$

$$\pi_5: \mathcal{B} \rightarrow \text{Bl}_4(\hat{\mathcal{B}}), \quad \text{along } C_5 = \mathcal{T} \cap E_2. \quad (\text{B.4.23e})$$

This produces the defining polynomials of the blown up Weierstrass model

$$f_b = t^3 (e_0^3 e_1^2 e_2^7 e_3 e_5^6 s^5 v^9 + e_2^4 e_5^4 s^4 t v^8 + e_0^4 e_1^4 e_3^4 e_4^4 s^4 t w^8 + e_1^4 e_3^8 e_5^4 e_4^{12} t^5 w^4 + s^4 t v^4 w^4), \quad (\text{B.4.24a})$$

$$g_b = t^4 (e_0^6 e_1^4 e_2^{12} e_3^2 e_5^{10} s^8 v^{14} + e_0^6 e_1^4 e_2^2 e_3^2 s^8 v^4 w^{10} + e_2^6 e_5^6 s^6 t^2 v^{12} + e_0^6 e_1^6 e_3^6 e_4^6 s^6 t^2 w^{12} + e_1^6 e_3^{12} e_5^6 e_4^{18} t^8 w^6 + s^6 t^2 v^6 w^6), \quad (\text{B.4.24b})$$

$$\Delta_b = t^8 p_{16,28,4,12,4,4,4}(s, t, v, w, e_0, e_1, e_2, e_3, e_4, e_5), \quad (\text{B.4.24c})$$

with the subscripts in $p_{16,28,4,12,4,4,4}(s, t, v, w, e_0, e_1, e_2, e_3, e_4, e_5)$ referring to the homogeneous degrees in the coordinates $[s : t]$, $[v : w : t]$, $[t : e_0 : e_1]$, $[v : e_1 : e_2]$, $[t : e_1 : e_3]$, $[t : e_3 : e_4]$ and $[t : e_2 : e_5]$, respectively. The resulting Stanley-Reisner ideal is

$$\begin{aligned} \mathcal{I} = \langle & st, e_1 s, e_2 s, e_3 s, e_4 s, e_5 s, e_0 t, e_1 t, e_2 t, e_3 t, v w, \\ & e_1 v, e_3 v, e_4 v, e_2 w, e_5 w, e_0 e_3, e_0 e_4, e_0 e_5, e_1 e_4, e_1 e_5, e_3 e_5 \rangle. \end{aligned} \quad (\text{B.4.25})$$

By repeated application of Proposition 5.2.19, we can compute the surfaces that correspond to the $\{B^p\}_{0 \leq p \leq 5}$ base components of the central fiber Y^0 of $\rho: \mathcal{Y} \rightarrow D$. We summarize the result of the blow-up process, step by step, in Figure B.8. The starting point is $B^0 = \mathbb{F}_1$, from which we obtain the surface $B^1 = \mathbb{F}_1$ by blowing up along C_1 , which is the class of the $(+1)$ -curve of B^0 . The next blow-up is along C_2 , in the fiber class of B^1 . Due to its intersection point with $E_0|_{E_1} = C_1 \subset B^1$, we obtain $B^2 = \mathbb{F}_1$ and the zeroth component must be blown-up once to become $B^0 = \text{Bl}_1(\mathbb{F}_1)$. We continue by blowing up along C_3 , in the class of the $(+1)$ -curve of B^1 and with an intersection point with $E_2|_{E_0} = C_2 \subset B^1$, leading to $B^3 = \mathbb{F}_2$ and prompting us to substitute the second component by $B^2 = \text{Bl}_1(\mathbb{F}_1)$. The components B^2 and B^3 meet along a curve that is in the fiber class in B^3 and the exceptional curve of the surface blow-up in B^2 , which is compatible since

$$\begin{aligned} E_2|_{E_3} \cdot_{B^3} E_2|_{E_3} &= E_2 \cdot_{\text{Bl}_3(\hat{\mathcal{B}})} E_2 \cdot_{\text{Bl}_3(\hat{\mathcal{B}})} E_3 = E_2 \cdot_{\text{Bl}_3(\hat{\mathcal{B}})} \left(- \sum_{\substack{q=0 \\ q \neq 2}}^3 E_q \right) \cdot_{\text{Bl}_3(\hat{\mathcal{B}})} E_3 \\ &= - E_3|_{E_2} \cdot_{B^2} E_3|_{E_2} - 1. \end{aligned} \quad (\text{B.4.26})$$

This curve is not one of the blow-up centres, i.e. it is not in the set $\{C_p\}_{1 \leq p \leq 5}$. It affects the next blow-up, however, since it intersects C_4 , which is in the class of the $(+2)$ -curve of B^3 , leading to

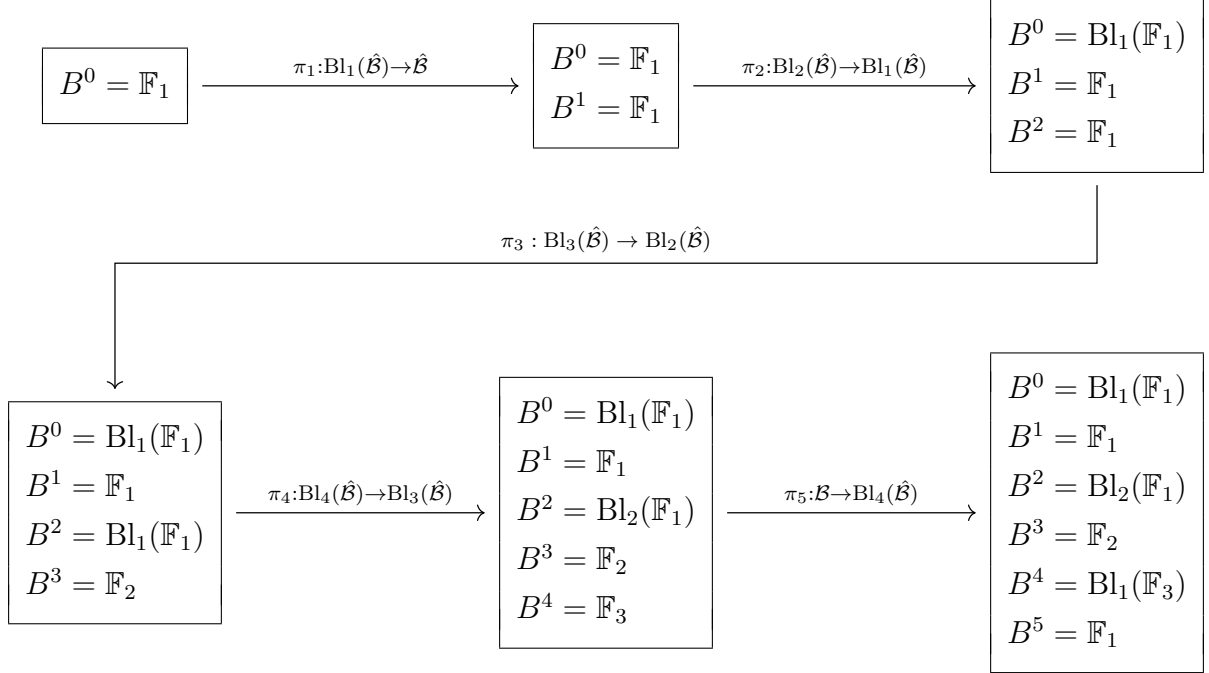


Figure B.8: Components $\{B^p\}_{0 \leq p \leq 5}$ of B_0 arising from the blow-up sequence (B.4.23).

the component $B^4 = \mathbb{F}_3$ and requiring the substitution of the second component by $B^2 = \text{Bl}_2(\mathbb{F}_2)$. The final blow-up is along the curve C_5 , which is the strict transform of the representative of the fiber class of B^2 that has been blown-up twice, and therefore $C_5 \cdot_{B^2} C_5 = -2$. Together with the intersection point with $E_4|_{E_2} = C_4 \subset B^2$, this yields the component $B^5 = \mathbb{F}_1$ and the surface blow-up $B^4 = \text{Bl}_1(\mathbb{F}_3)$.

An alternative modification of the degeneration $\hat{\rho} : \hat{\mathcal{Y}} \rightarrow D$ is given by the sequence of blow-ups

$$\check{\pi}_1 : \text{Bl}_1(\hat{\mathcal{B}}) \rightarrow \hat{\mathcal{B}}, \quad \text{along } \check{C}_1 = \mathcal{T} \cap \mathcal{U}, \quad (\text{B.4.27a})$$

$$\check{\pi}_2 : \text{Bl}_2(\hat{\mathcal{B}}) \rightarrow \text{Bl}_1(\hat{\mathcal{B}}), \quad \text{along } \check{C}_2 = \mathcal{T} \cap \check{E}_1, \quad (\text{B.4.27b})$$

$$\check{\pi}_3 : \text{Bl}_3(\hat{\mathcal{B}}) \rightarrow \text{Bl}_2(\hat{\mathcal{B}}), \quad \text{along } \check{C}_3 = \mathcal{T} \cap \check{E}_2, \quad (\text{B.4.27c})$$

$$\check{\pi}_4 : \text{Bl}_4(\hat{\mathcal{B}}) \rightarrow \text{Bl}_3(\hat{\mathcal{B}}), \quad \text{along } \check{C}_4 = \mathcal{V} \cap \check{E}_1, \quad (\text{B.4.27d})$$

$$\check{\pi}_5 : \check{\mathcal{B}} \rightarrow \text{Bl}_4(\hat{\mathcal{B}}), \quad \text{along } \check{C}_5 = \mathcal{V} \cap \check{E}_2. \quad (\text{B.4.27e})$$

The resulting Stanley-Reisner ideal is

$$\check{\mathcal{I}} = \langle st, \check{e}_1s, \check{e}_2s, \check{e}_3s, \check{e}_4s, \check{e}_5s, \check{e}_0t, \check{e}_1t, \check{e}_2t, \check{e}_4t, \check{e}_5t, \\ vw, \check{e}_1v, \check{e}_2v, \check{e}_4w, \check{e}_5w, \check{e}_0\check{e}_2, \check{e}_0\check{e}_3, \check{e}_0\check{e}_5, \check{e}_1\check{e}_3, \check{e}_1\check{e}_5, \check{e}_3\check{e}_4 \rangle. \quad (\text{B.4.28})$$

The components resulting from the two blow-up sequences considered can be related to each other by identifying the homogeneous coordinates

$$\{e_0, e_1, e_2, e_3, e_4, e_5\} \longleftrightarrow \{\check{e}_0, \check{e}_1, \check{e}_3, \check{e}_4, \check{e}_2, \check{e}_5\}, \quad (\text{B.4.29})$$

from which we can see that \mathcal{B} and $\check{\mathcal{B}}$ are connected by performing the flops

$$\{t = e_5 = 0\}_{\mathcal{B}} \longleftrightarrow \{v = \check{e}_3 = 0\}_{\check{\mathcal{B}}}, \quad (\text{B.4.30a})$$

$$\{e_2 = e_4 = 0\}_{\mathcal{B}} \longleftrightarrow \{\check{e}_2 = \check{e}_5 = 0\}_{\check{\mathcal{B}}}, \quad (\text{B.4.30b})$$

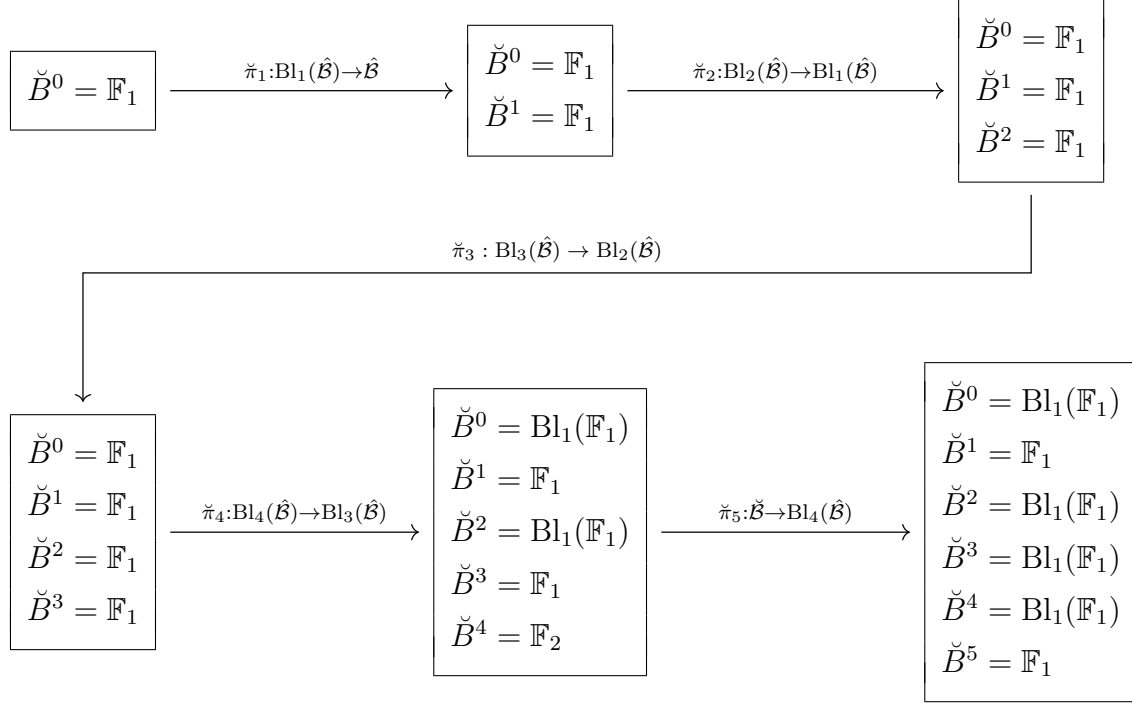


Figure B.9: Components $\{\check{B}^p\}_{0 \leq p \leq 5}$ of \check{B}_0 arising from the blow-up sequence (B.4.27).

The base components for the central fiber of the resolved degeneration $\check{\rho} : \check{\mathcal{Y}} \rightarrow D$ are collected, step by step, in Figure B.9. We do not detail this blow-up sequence further.

B.4.2 Line bundles

Adapting now the discussion of Section 5.2.5 to the general case, let us compute the holomorphic line bundles associated to the Weierstrass models describing the components of the central fiber of a resolved degeneration.

Proposition B.4.4. *Let $\{B^p\}_{0 \leq p \leq P}$ be the base components of the central fiber Y_0 of the modification $\rho : \mathcal{Y} \rightarrow D$ giving the resolution of a degeneration $\hat{\rho} : \hat{\mathcal{Y}} \rightarrow D$. Then, the holomorphic line bundles $\{\mathcal{L}_p\}_{0 \leq p \leq P} := \{\mathcal{L}_{B^p}\}_{0 \leq p \leq P}$ defining the Weierstrass models over the $\{B^p\}_{0 \leq p \leq P}$ are*

$$\mathcal{L}_p = \overline{K}_{B^p} - \sum_{\substack{q=0 \\ q \neq p}}^P E_q|_{E_p} , \quad 0 \leq p \leq P . \quad (\text{B.4.31})$$

Proof. Since the $\{E_p\}_{0 \leq p \leq P}$ and \mathcal{B} are smooth, we obtain from the adjunction formula

$$\mathcal{L}_p = \overline{K}_{B^p} + E_p|_{E_p} = \overline{K}_{B^p} - \sum_{\substack{q=0 \\ q \neq p}}^P E_q|_{E_p} , \quad 0 \leq p \leq P . \quad (\text{B.4.32})$$

□

We see that, as occurred for single infinite-distance limits, the component Weierstrass models $\pi_p : Y^p \rightarrow B^p$ are not describing Calabi-Yau varieties, since $\mathcal{L}_p \neq \overline{K}_{B^p}$. Rather, the pairs

$$\left(Y^p, \pi^* \left(\sum_{\substack{q=0 \\ q \neq p}}^P E_q|_{E_p} \right) \right), \quad 0 \leq p \leq P \quad (\text{B.4.33})$$

are log Calabi-Yau spaces, with their union $Y_0 = \bigcup_{p=0}^P Y^p$ along the boundaries yielding a Calabi-Yau variety.

Using the modified discriminant of Definition 5.2.16, the component by component analysis of a model is performed working with the polynomials $\{f_p, g_p, \Delta'_p\}_{0 \leq p \leq P}$. Let us collect their associated divisor classes.

Proposition B.4.5. *Let $\{B^p\}_{0 \leq p \leq P}$ be the base components of the central fiber Y_0 of the modification $\rho : \mathcal{Y} \rightarrow D$ giving the resolution of a degeneration $\hat{\rho} : \hat{\mathcal{Y}} \rightarrow D$, and let*

$$\text{ord}_{\mathcal{Y}}(f_b, g_b, \Delta_b)_{E_p} = (0, 0, n_p), \quad 0 \leq p \leq P, \quad (\text{B.4.34})$$

be the vanishing orders associated to the codimension-zero singular fibers in said components. The (modified) divisor classes associated to the Weierstrass models in the components are

$$F_p = 4\overline{K}_{B^p} - \sum_{q \neq p} 4E_q|_{E_p}, \quad G_p = 6\overline{K}_{B^p} - \sum_{q \neq p} 6E_q|_{E_p}, \quad (\text{B.4.35a})$$

$$\Delta'_p = 12\overline{K}_{B^p} + \sum_{q \neq p} (n_q - 12)E_q|_{E_p}, \quad (\text{B.4.35b})$$

for $0 \leq p \leq P$.

Proof. It follows from Proposition B.4.4 and Definition 5.2.16. \square

We complete the examples of Section B.4.1 in order to illustrate the above discussion.

Example B.4.6. Continuing with Example B.4.2, we see from (B.4.11) that the components of the central fiber of the resolved degeneration $\{Y^0, Y^s, Y^v\}$ are smooth in codimension-zero, i.e.

$$\text{ord}_{\mathcal{Y}}(f_b, g_b, \Delta_b)_{E_0} = (0, 0, 0), \quad (\text{B.4.36a})$$

$$\text{ord}_{\mathcal{Y}}(f_b, g_b, \Delta_b)_{E_s} = (0, 0, 0), \quad (\text{B.4.36b})$$

$$\text{ord}_{\mathcal{Y}}(f_b, g_b, \Delta_b)_{E_v} = (0, 0, 0). \quad (\text{B.4.36c})$$

Using Proposition B.4.5, we determine for the blow-up order $C_1 = \mathcal{S} \cap \mathcal{U}$ and $C_2 = \mathcal{V} \cap E_0$ the holomorphic line bundles associated to the Weierstrass models in the components to be

$$\mathcal{L}_0 = S_0 + 4V_0, \quad (\text{B.4.37a})$$

$$\mathcal{L}_s = S_s + 2V_s + C_E^1, \quad (\text{B.4.37b})$$

$$\mathcal{L}_v = S_v + 2V_v, \quad (\text{B.4.37c})$$

where we have denoted by C_E^1 the exceptional curve in $B^s = \text{Bl}_1(\mathbb{F}_3)$. If, instead, we consider the blow-up order $C_1 = \mathcal{V} \cap \mathcal{U}$ and $C_2 = \mathcal{S} \cap E_0$, we have the holomorphic line bundles

$$\mathcal{L}_0 = S_0 + 4V_0, \quad (\text{B.4.38a})$$

$$\mathcal{L}_s = S_s + V_s, \quad (\text{B.4.38b})$$

$$\mathcal{L}_v = 2S_v + V_v. \quad (\text{B.4.38c})$$

Although the line bundle defining the Weierstrass model $\rho : \mathcal{Y} \rightarrow D$ is the same independently of which of the two blow-up orders is chosen, the same is not true for the component line bundles, since they are affected by higher codimension effects in \mathcal{B} like the flop of curves. In the absence of codimension-zero singularities, the divisor classes associated to the defining polynomials and the modified discriminant of the component Weierstrass models are simply $F_p = 4\mathcal{L}_p$, $G_p = 6\mathcal{L}_p$ and $\Delta'_p = 12\mathcal{L}_p$ for $p \in \{0, s, v\}$. Indeed, the restrictions of the polynomials $\{f_b, g_b, \Delta'_b\}$ to the B^0 component,

$$f_0 = s^4 t^4 v^4 (e_v^2 v^2 - e_v v w + w^2) (e_v^2 v^2 + e_v v w + w^2) , \quad (\text{B.4.39a})$$

$$g_0 = s^6 t^5 v^6 (e_s e_v^9 s v^9 + t w^6) , \quad (\text{B.4.39b})$$

$$\begin{aligned} \Delta'_0 = & s^{12} t^{10} v^{12} (27 e_s^2 e_v^{18} s^2 v^{18} + 54 e_s e_v^9 s t v^9 w^6 + 4 e_v^{12} t^2 v^{12} + 12 e_v^{10} t^2 v^{10} w^2 \\ & + 24 e_v^8 t^2 v^8 w^4 + 28 e_v^6 t^2 v^6 w^6 + 24 e_v^4 t^2 v^4 w^8 + 12 e_v^2 t^2 v^2 w^{10} + 31 t^2 w^{12}) , \end{aligned} \quad (\text{B.4.39c})$$

to the B^s component,

$$f_s = s^4 t^4 v^4 (e_v^2 v^2 - e_v v w + w^2) (e_v^2 v^2 + e_v v w + w^2) , \quad (\text{B.4.40a})$$

$$g_s = s^5 t^6 v^5 w^4 (e_0 t + s v w^2) , \quad (\text{B.4.40b})$$

$$\begin{aligned} \Delta'_s = & s^{10} t^{12} v^{10} (54 e_0 s t v w^{10} + 27 e_0^2 t^2 w^8 + 4 e_v^{12} s^2 v^{14} + 12 e_v^{10} s^2 v^{12} w^2 + 24 e_v^8 s^2 v^{10} w^4 \\ & + 28 e_v^6 s^2 v^8 w^6 + 24 e_v^4 s^2 v^6 w^8 + 12 e_v^2 s^2 v^4 w^{10} + 31 s^2 v^2 w^{12}) , \end{aligned} \quad (\text{B.4.40c})$$

and to the B^v component

$$f_v = s^4 t^4 v^4 w^4 , \quad (\text{B.4.41a})$$

$$g_v = s^5 t^5 v^5 w^4 (e_0 e_s^2 s^2 w^6 + e_0 t^2 + s t v w^2) , \quad (\text{B.4.41b})$$

$$\begin{aligned} \Delta'_v = & s^{10} t^{10} v^{10} w^8 (27 e_0^2 e_s^4 s^4 w^{12} + 54 e_0 e_s^2 s^3 t v w^8 + 54 e_0^2 e_s^2 s^2 t^2 w^6 + 54 e_0 s t^3 v w^2 \\ & + 27 e_0^2 t^4 + 31 s^2 t^2 v^2 w^4) \end{aligned} \quad (\text{B.4.41c})$$

are sections of the appropriate line bundles. Here, we have not used the available \mathbb{C}^* -actions to fix the redundant coordinates to one in order to provide expressions valid for both blow-up orders.

Example B.4.7. For completeness, let us also compute the line bundles over the base components in Example B.4.3. We observe from (B.4.11) that the $\{Y^p\}_{0 \leq p \leq 5}$ are smooth in codimension-zero, since

$$\text{ord}_Y(f_b, g_b, \Delta_b)_{E_0} = (0, 0, 0) , \quad 0 \leq p \leq 5 . \quad (\text{B.4.42})$$

This means that, for both sequences of blow-ups, the divisor classes associated to the defining polynomials and the modified discriminant on the component Weierstrass models are just appropriate multiples of \mathcal{L}_p (or $\check{\mathcal{L}}_p$) for $0 \leq p \leq 5$. We compute said line bundles using (B.4.31). For the sequence of blow-ups (B.4.23) we find

$$\mathcal{L}_0 = \overline{K}_{\text{Bl}_1(\mathbb{F}_1)} - E_1|_{E_0} - E_2|_{E_0} = S_0 + 2V_0 + C_E^1 , \quad (\text{B.4.43a})$$

$$\mathcal{L}_1 = \overline{K}_{\mathbb{F}_1} - E_0|_{E_1} - E_2|_{E_1} - E_3|_{E_1} = V_0 , \quad (\text{B.4.43b})$$

$$\mathcal{L}_2 = \overline{K}_{\text{Bl}_2(\mathbb{F}_1)} - E_0|_{E_2} - E_1|_{E_2} - E_3|_{E_2} - E_4|_{E_2} - E_5|_{E_2} = S_2 + V_2 + 2C_E^1 + 3C_E^2 , \quad (\text{B.4.43c})$$

$$\mathcal{L}_3 = \overline{K}_{\mathbb{F}_2} - E_1|_{E_3} - E_2|_{E_3} - E_4|_{E_3} = V_3 , \quad (\text{B.4.43d})$$

$$\mathcal{L}_4 = \overline{K}_{\text{Bl}_1(\mathbb{F}_3)} - E_2|_{E_4} - E_3|_{E_4} - E_5|_{E_4} = S_4 + 4V_4 + 3C_E^1 , \quad (\text{B.4.43e})$$

$$\mathcal{L}_5 = \overline{K}_{\mathbb{F}_1} - E_2|_{E_5} - E_4|_{E_5} = S_5 + 2V_5 , \quad (\text{B.4.43f})$$

while for the sequence of blow-ups (B.4.27) we obtain instead

$$\check{\mathcal{L}}_0 = \overline{K}_{\text{Bl}_1(\mathbb{F}_1)} - E_1|_{E_0} - E_4|_{E_0} = S_0 + 2V_0 + C_E^1, \quad (\text{B.4.44a})$$

$$\check{\mathcal{L}}_1 = \overline{K}_{\mathbb{F}_1} - E_0|_{E_1} - E_2|_{E_1} - E_4|_{E_1} = V_1, \quad (\text{B.4.44b})$$

$$\check{\mathcal{L}}_2 = \overline{K}_{\text{Bl}_1(\mathbb{F}_1)} - E_1|_{E_2} - E_3|_{E_2} - E_4|_{E_2} - E_5|_{E_2} = V_2 + C_E^1, \quad (\text{B.4.44c})$$

$$\check{\mathcal{L}}_3 = \overline{K}_{\text{Bl}_1(\mathbb{F}_1)} - E_2|_{E_3} - E_5|_{E_3} = S_3 + 3V_3 + 3C_E^1, \quad (\text{B.4.44d})$$

$$\check{\mathcal{L}}_4 = \overline{K}_{\text{Bl}_1(\mathbb{F}_1)} - E_0|_{E_4} - E_1|_{E_4} - E_2|_{E_4} - E_5|_{E_4} = S_4 + V_4 + 2C_E^1, \quad (\text{B.4.44e})$$

$$\check{\mathcal{L}}_5 = \overline{K}_{\mathbb{F}_1} - E_2|_{E_5} - E_3|_{E_5} - E_4|_{E_5} = V_5. \quad (\text{B.4.44f})$$

Above, we have denoted the exceptional curves of the surface blow-ups by C_E^\bullet . One can easily check that the restrictions to the components of the polynomials (B.4.11) are indeed sections of powers of the listed line bundles.

B.5 Single infinite-distance limits and their resolutions

In Section 5.2.3 we stated that single infinite-distance limit degenerations in the sense of Definition 5.2.9 lead to open-chain resolutions. In this appendix we provide the proof for this central result.

We start by recalling the notion of a single infinite-distance limit degeneration.

Definition 5.2.9 (Single infinite-distance limits). Let $\hat{\rho} : \hat{\mathcal{Y}} \rightarrow D$ be a degeneration of the type described in Section 5.2.1 such that there is a collection of curves $\hat{\mathcal{C}}_r := \{\mathcal{C}_i \cap \mathcal{U}\}_{1 \leq i \leq r}$ in $\hat{\mathcal{B}}$ with non-minimal component vanishing orders. We call the degeneration a single infinite-distance limit if

- (i) $(\mathcal{C}_i \cap \mathcal{U}) \cdot_{\hat{\mathcal{B}}} (\mathcal{C}_j \cap \mathcal{U}) = 0$ for all $1 \leq i < j \leq r$,
- (ii) no point in the $\{\mathcal{C}_i \cap \mathcal{U}\}_{1 \leq i \leq r}$ curves has non-minimal interface vanishing orders, and
- (iii) no point in $\hat{\mathcal{B}} \setminus (\bigcup_{i=1}^r \mathcal{C}_i \cap \mathcal{U})$ presents infinite-distance non-minimal component vanishing orders.

The role of each of these conditions in enforcing the open-chain resolution structure is intuitively clear. Let us analyse them in turn.

First, suppose that two curves supporting non-minimal elliptic fibers in the family variety intersect each other. Then, the exceptional components arising from blowing up along these curves will also intersect each other, on top of intersecting the strict transform of the component that contained these curves of non-minimal elliptic fibers. Hence, the components cannot intersect as in an open-chain resolution. This is prevented by Condition (i) in Definition 5.2.9. Note that here we have referred to curves with non-minimal family vanishing orders, while Definition 5.2.9 is concerned with curves presenting non-minimal component vanishing orders; since the former implies the latter, Condition (i) is still in effect.

However, we could conceive of having a third curve of non-minimal singular elliptic fibers in $\hat{\mathcal{B}}_0$ that does not intersect the others. This would mean that B^0 would intersect more than two components, which cannot happen for a component in an open-chain resolution. The situation just described is not prevented, a priori, by Condition (i) in Definition 5.2.9. Nonetheless, we argue in Appendix B.6 that this cannot occur in a Calabi-Yau Weierstrass model whose base is

one of the allowed six-dimensional F-theory bases. Namely, the following happens if we attempt to tune such a model.

Proposition B.5.1. *Let $\hat{\rho} : \hat{\mathcal{Y}} \rightarrow D$ be a degeneration of the type described in Section 5.2.2.1 such that there is a collection of curves $\hat{\mathcal{C}}_r := \{\mathcal{C}_i \cap \mathcal{U}\}_{1 \leq i \leq r}$ in $\hat{\mathcal{B}} = B \times D$ with non-minimal component vanishing orders. If $r \geq 3$, then at least two of these curves intersect.*

Next, we may worry that, starting from curves of non-minimal fibers in \hat{B}_0 that seem like they would lead to an open-chain resolution, we might encounter a curve with non-minimal (possibly only component) vanishing orders in an exceptional component arising in the blow-up sequence, and whose resolution (possibly after base change) would destroy the open-chain structure. This is what can be observed in Example B.3.2, where we also see that Condition (ii) in Definition 5.2.9 allows us to detect this. Indeed, this is true in general.

Lemma B.5.2. *Let $\rho : \mathcal{Y} \rightarrow D$ be an open-chain resolution of a degeneration $\hat{\rho} : \hat{\mathcal{Y}} \rightarrow D$. If a component Y^p , with $p \neq 0$, of the open-chain $Y_0 = \bigcup_{p=0}^P Y^p$ contains a curve $C_p \subset B^p$ presenting non-minimal component vanishing orders, and this curve is not an end-curve of the open-chain, then one of the blow-up centres in B^0 contains a point with non-minimal interface vanishing orders.*

Proof. First, let us note that because we are dealing with an open-chain resolution, all components B^p , with $p \neq 0$, are Hirzebruch surfaces \mathbb{F}_{n_p} due to Proposition 5.2.12. C_p cannot be one of the curves over which the components intersect, see the comments in Section 5.2.2.3. We can distinguish two cases depending on the component in which C_p is contained, which we discuss in turn.

- (1) If C_p is contained in an intermediate component B^p of the base central fiber, we know from (5.2.92) that F_p and G_p only contain fiber classes. Hence, $C_p \sim V_p$, and since $S_p \cdot V_p = T_p \cdot V_p = 1$, this makes a point in each of the component interfaces have non-minimal interface vanishing orders. This needs to be realized from the other side of the interface as well. If $B^0 \cap B^p \neq \emptyset$, we have obtained the desired result. If, on the other hand, $B^0 \cap B^p = \emptyset$, take the chain of components connecting B^0 and B^p , which (possibly after relabelling) we can take to be $B^0 - B^1 - \dots - B^{p-1} - B^p$. The intermediate components $\{B^q\}_{1 \leq q \leq p-1}$ also have F_q and G_q consisting only of fiber classes, and therefore the only way to have consistent interface vanishing orders throughout is for the non-minimal curve C_p to extend through all $B^0 - B^1 - \dots - B^{p-1} - B^p$, at which point we can take B^p to be B^1 and reduce to the previous situation.
- (2) If C_p is contained in an end-component B^p , we are assuming that it is distinct from the end-curve of the component. Since the end-curve of B^p is the only curve class in \mathcal{L}_p that does not intersect the interface with the adjacent component, C_p must intersect it. This makes a point at the interface curve have non-minimal vanishing orders. The adjacent component is either B^0 or an intermediate component; either way, the arguments given earlier apply, and we reach the desired result.

□

Condition (iii) in Definition 5.2.9 rules out the presence of codimension-two points in B^0 with infinite-distance non-minimal component vanishing orders. These points cannot appear in the other components either, unless they are located over a non-minimal curve, as we now argue.

Lemma B.5.3. *Let $\rho : \mathcal{Y} \rightarrow D$ be an open-chain resolution of a degeneration $\hat{\rho} : \hat{\mathcal{Y}} \rightarrow D$. No component Y^p , with $p \neq 0$, of the open-chain $Y_0 = \bigcup_{p=0}^P Y^p$ can contain a point in B^p with infinite-distance non-minimal component vanishing orders that is not located over a curve with non-minimal component vanishing orders.*

Proof. Over the base components apart from B^0 , we recall from (5.2.92) that the defining holomorphic line bundle of the Weierstrass model is

$$\mathcal{L}_p = 2V_p, \quad \text{if } B^p \text{ is an intermediate component,} \quad (\text{B.5.1a})$$

$$\mathcal{L}_p = S_p + 2V_p \quad \text{or} \quad \mathcal{L}_p = T_p + 2V_p, \quad \text{if } B^p \text{ is an end-component.} \quad (\text{B.5.1b})$$

When B^p is an intermediate component, this implies that $F_p = 8V_p$ and $G_p = 12V_p$. Since $V_p \cdot V_p = 0$, there can be no codimension-two enhancements. When B^p is an end-component, we can try to tune high codimension-two vanishing orders by forcing F_p , G_p and Δ_p to self-intersect many times over a point. Once we fix said point, there is a unique representative of V_p that passes through it, let us call it \check{V}_p . If said point lies over the unique representative of S_p , both curves would need to support non-minimal vanishing orders in order for the point to support infinite-distance non-minimal vanishing orders. Assume instead that it is over a representative of T_p , and that we have tuned a factor of $\alpha \check{V}_p$ and of $\beta \check{V}_p$ over F_p and G_p respectively. Since $(F_p - \alpha \check{V}_p) \cdot \check{V}_p = 4$ and $(G_p - \beta \check{V}_p) \cdot \check{V}_p = 6$, the best component vanishing orders that we can tune over the point are $(4 + \alpha, 6 + \beta) < (8, 12)$ unless the tuning of \check{V}_p is non-minimal. \square

Finally, after resolving a single infinite-distance limit degeneration $\hat{\rho} : \hat{\mathcal{Y}} \rightarrow D$ and obtaining an open-chain resolution $\rho : \mathcal{Y} \rightarrow D$ free of obscured infinite-distance limits, we may fear that a different modification of $\check{\rho} : \check{\mathcal{Y}} \rightarrow D$ could lead, upon applying the procedures explained in Section 5.2.2, to a resolution that does not have the open-chain structure. This can also be discarded.

Lemma B.5.4. *Let $\rho : \mathcal{Y} \rightarrow D$ be an open-chain resolution of a degeneration $\hat{\rho} : \hat{\mathcal{Y}} \rightarrow D$. If a combination of base changes and modifications allows us to obtain a resolution $\check{\rho} : \check{\mathcal{Y}} \rightarrow D$ that does not have an open-chain structure, then $\rho : \mathcal{Y} \rightarrow D$ contained an obscured infinite-distance limit that did not occur over one of the end-curves of the open-chain.*

Proof. The modifications respecting the elliptic fibration of the family variety are of the type explained in Section 5.2.2.1, i.e. a combination of base blow-ups and blow-downs followed by line bundle shifts in order to restore the Calabi-Yau condition, see the comments in Section 5.2.2.3. By themselves, these do not change the open-chain nature of the obtained resolutions. The base change can lead to the need for blow-ups along additional curves, potentially spoiling the open-chain structure if they are not end-curves of the open-chain. Saying that this occurs is equivalent to saying that an obscured infinite-distance limit exists over a curve besides the end-curves of the open-chain, see Appendix B.3. \square

We can now integrate the results given above into the statement that single infinite-distance limit degenerations lead to open-chain resolutions.

Proposition B.5.5. *Let $\hat{\rho} : \hat{\mathcal{Y}} \rightarrow D$ be a single infinite-distance limit degeneration. Its resolved modifications $\rho : \mathcal{Y} \rightarrow \mathcal{B}$, obtained as explained in Section 5.2.2, are open-chain resolutions.*

Proof. We have three possibilities for $\rho : \mathcal{Y} \rightarrow D$. Either the resolution is

- (1) an open-chain resolution free of obscured infinite-distance limits, or

- (2) an open-chain resolution containing obscured infinite-distance limits, or
- (3) is not an open-chain resolution.

If we are in Case (1), we are done, since by Lemma B.5.4 any sequence of base changes and modifications of $\hat{\rho} : \hat{\mathcal{Y}} \rightarrow D$ preserving the elliptic fibration will also lead to resolutions falling under Case (1).

Let us now consider Case (2). This case can be subdivided into the following subcases, depending on how the obscured infinite-distance limit arises.

- (2.a) There is an obscured infinite-distance limit over a curve C in B^0 : Denoting the composition of base blow-ups by $\pi : \mathcal{B} \rightarrow \hat{\mathcal{B}}$, one can see using the relations (5.2.42) and (5.2.44) that for an open-chain resolution

$$\pi_*(F_0) = F|_{\mathcal{U}} - \sum_{i=1}^r 4C_r, \quad (\text{B.5.2a})$$

$$\pi_*(G_0) = G|_{\mathcal{U}} - \sum_{i=1}^r 6C_r, \quad (\text{B.5.2b})$$

where $\{C_i\}_{0 \leq i \leq r}$ is the collection of curves over which B^0 intersects other components. This relation is still true if a base change is performed, since we are considering the restrictions $F|_{\mathcal{U}}$ and $G|_{\mathcal{U}}$. As a consequence, the component vanishing orders over C in \hat{B}_0 are also non-minimal. By assumption, C will not intersect any of the other curves with non-minimal component vanishing orders. A high enough base change will make the fibers over C non-minimal singular elliptic fibers of $\hat{\mathcal{Y}}$, at which point we can resolve over the curve C as well to obtain a modification $\check{\rho} : \check{\mathcal{Y}} \rightarrow D$, which we categorize again. We can repeat this process until Case (2.a) is no longer realized.

- (2.b) There is an obscured infinite-distance limit over a curve in B^p , with $p \neq 0$: Invoking Lemma B.5.2, we see that either Condition (ii) of Definition 5.2.9 is violated, leading to a contradiction, or the obscured infinite-distance limit would not destroy the open-chain structure if manifest at the family level (i.e. it is found over an end-curve of the open-chain). In the latter case, we make the obscured infinite-distance limit apparent at the family level as explained in Appendix B.3, and resolve to obtain the modification $\check{\rho} : \check{\mathcal{Y}} \rightarrow D$, to which we apply the proposition again.
- (2.c) There is a point with non-minimal interface vanishing orders in one of the intersection curves $B^p \cap B^q$: Given the fact that the intermediate components of an open-chain resolution are Hirzebruch surfaces in which F_p and G_p consist only of fiber classes, see (5.2.92), this case reduces to Case (2.a) unless we are dealing with a two-component resolution. But due to (B.5.2) that would imply that Condition (ii) of Definition 5.2.9 is once again violated, leading to a contradiction.
- (2.d) There is a point with infinite-distance non-minimal component vanishing orders in one of the components B^p : From Lemma B.5.3, we know that this can only occur in B^0 , but due to (B.5.2) this implies that Condition (iii) of Definition 5.2.9 is violated.

Finally, consider Case (3). Start by partially blowing down $\rho : \mathcal{Y} \rightarrow D$ until an open-chain structure for the (now partial) resolution $\check{\rho} : \check{\mathcal{Y}} \rightarrow D$ is obtained. The blow-down leads to

non-minimal family vanishing orders along the former blow-up centre, which in particular means non-minimal component vanishing orders along the same loci. The components that we have to blow-down in order to reach the open-chain structure can be of the following types.

- (3.a) A component B^p arising from a blow-up along a curve C : Note that this curve cannot be one of the end-curves of an end-component, since their blow-up would not destroy the open-chain structure, and we would therefore not have blown the associated component down. This means that the curve can be either in
 - the strict transform B^0 of the original component \hat{B}_0 , in which case the fact that blowing it up destroys the open-chain structure means that it intersects one of the other blow-up centres in \hat{B}^0 , violating Condition (i) of Definition 5.2.9, and therefore leading to a contradiction; or in
 - an intermediate or end-component of the chain, in which case Lemma B.5.2 implies a violation of Condition (ii) of Definition 5.2.9 and, hence, a contradiction again.
- (3.b) A component arising from a blow-up along an isolated⁴ codimension-two infinite-distance non-minimal point: The blow-down of this component leads to a point with non-minimal component vanishing orders that, due to Lemma B.5.3, must be located in the strict transform of the original component. Then, due to (B.5.2), this implies that Condition (iii) of Definition 5.2.9 is violated.

□

Hence, as we had claimed, single infinite-distance limit degenerations will indeed lead to open-chain resolutions, and the results of Section 5.2.4 and Section 5.2.5 for the latter apply, in particular, to the former.

B.6 Restricting star degenerations

Degenerations with an open-chain resolution, see Definition 5.2.10, have a multi-component central fiber for their base family manifold whose structure consists of a distinguished component (the strict transform of the original base component of the central fiber of the unresolved degeneration) to which one or two strings of Hirzebruch surface components intersecting in a chain are attached. This is represented in Figure 5.2.

Suppose now that there exists a degeneration in which the original base component contains more than two mutually non-intersecting curves of non-minimal elliptic fibers. Given Proposition 5.2.13, this would lead to a resolution with a similar structure, but in which more than two strings of Hirzebruch surfaces are attached to the strict transform of the original base component, resembling a star-shaped resolution, rather than an open-chain one.

In this appendix, we argue that such star-shaped resolutions cannot occur for degenerations of Calabi-Yau Weierstrass models constructed over one of the allowed six-dimensional F-theory bases (as reviewed in Section 5.2.1) if their star resolution is to be free of obscured infinite-distance limits. While one can try to tune more than two mutually non-intersecting curves of non-minimal elliptic fibers, the structure of the Weierstrass model always forces some additional curves that intersect the originally tuned non-minimal curves to also factorize non-minimally. If the non-minimal nature of these additional curves is apparent at the level of the family vanishing

⁴Meaning that it does not sit on top of a curve with non-minimal family vanishing orders.

orders, we will not obtain a star resolution; in the cases in which the non-minimal nature of these curves only manifests itself at the level of the component vanishing orders, the obtained star resolution will contain obscured infinite-distance limits.

We proceed with this discussion as part of the characterization of single infinite-distance limits done in Appendix B.5. Since non-minimal vanishing orders along a curve imply, in particular, non-minimal component vanishing orders along the same curve, we perform the study at the level of the central fiber of the starting degeneration. The analysis is carried out inductively, proving it first for Calabi-Yau Weierstrass models constructed over $\hat{B}_0 = \mathbb{P}^2$ or $\hat{B}_0 = \mathbb{F}_n$, and arguing in steps that it generalizes to models constructed over the arbitrary blow-ups $\hat{B}_0 = \text{Bl}(\mathbb{F}_n)$, following the same path as in Section B.1.3. The final claim is the following.

Proposition B.5.1. *Let $\hat{\rho} : \hat{\mathcal{Y}} \rightarrow D$ be a degeneration of the type described in Section 5.2.2.1 such that there is a collection of curves $\hat{\mathcal{C}}_r := \{C_i \cap \mathcal{U}\}_{1 \leq i \leq r}$ in $\hat{\mathcal{B}} = B \times D$ with non-minimal component vanishing orders. If $r \geq 3$, then at least two of these curves intersect.*

B.6.1 Models constructed over \mathbb{P}^2 or \mathbb{F}_n

The claim of Proposition B.5.1 can readily be proven for models constructed over $\hat{B}_0 = \mathbb{P}^2$ or $\hat{B}_0 = \mathbb{F}_n$ by directly solving for all the curves that can be simultaneously tuned to be non-minimal without mutually intersecting each other.

Proposition B.6.1. *Let $\pi : Y \rightarrow B$ be a Calabi-Yau Weierstrass model over $B = \mathbb{P}^2$ or $B = \mathbb{F}_n$ in which a set of curves $\mathcal{C}_r := \{C_i\}_{1 \leq i \leq r}$ in B supports non-minimal elliptic fibers. If $r \geq 3$, then $C_i \cdot C_j \neq 0$ for some $1 \leq i < j \leq r$. In fact, the only collections of mutually non-intersecting curves on non-minimal elliptic fibers over these surfaces are*

- $\mathcal{C}_1 = \{H\}$, $\mathcal{C}_1 = \{2H\}$ or $\mathcal{C}_1 = \{3H\}$ for $B = \mathbb{P}^2$; or
- $\mathcal{C}_1 = \{C\}$, with C one of the curves listed in Table 5.3.1, or $\mathcal{C}_2 = \{C_0, C_\infty\}$ for \mathbb{F}_n .

Proof. When $B = \mathbb{P}^2$, it is clear that this is the case, since all curves in \mathbb{P}^2 intersect each other and only the curves listed fulfil $C \leq \bar{K}_{\mathbb{P}^2}$, see Proposition B.2.2.

For $B = \mathbb{F}_n$, Proposition 5.3.1 (with the refinements of Section 5.3.4.1) provides the list of all non-minimal curves C that can be tuned without forcing a second non-minimal curve to factorize, which therefore are the only valid elements of \mathcal{C}_r when $r = 1$. Assume now that we have at least two curves of non-minimal elliptic fibers. Two irreducible curves

$$C_1 = ah + bf, \quad a \geq 0, \quad b \geq 0, \quad (\text{B.6.1a})$$

$$C_2 = ch + df, \quad c \geq 0, \quad d \geq 0, \quad (\text{B.6.1b})$$

fulfil the conditions

$$\left. \begin{aligned} C_1 \cdot C_2 &= 0 \\ C_1 + C_2 &\leq \bar{K}_{\mathbb{F}_n} \end{aligned} \right\} \Leftrightarrow \left\{ \begin{aligned} C_1 &= C_2 = f, \\ C_1 &= h, \quad C_2 = h + nf, \end{aligned} \right. \quad (\text{B.6.2})$$

where we have used Proposition B.2.2. The first case leads to

$$F - 8f = 4C_0 + 4C_\infty, \quad (\text{B.6.3a})$$

$$G - 12f = 6C_0 + 6C_\infty, \quad (\text{B.6.3b})$$

where we see that no curves with trivial intersection with C_1 and C_2 can be tuned to be non-minimal. Moreover, due to Proposition B.1.2, we need to demand that $n = 0$ to avoid non-minimal elliptic fibers over C_0 , at which point saying $C_1 = C_2 = f$ or $C_1 = C_0$ and $C_2 = C_\infty$ is merely a matter of convention. The second case leads to

$$F - 8f = 8f, \quad (\text{B.6.4a})$$

$$G - 12f = 12f, \quad (\text{B.6.4b})$$

where n can be $0 \leq n \leq 12$ and we see that no further non-minimal curves with trivial intersection with C_1 and C_2 can be tuned. \square

B.6.2 Models constructed over $\text{Bl}(\mathbb{F}_n)$ of type (A)

Beyond $\hat{B}_0 = \mathbb{P}^2$ and $\hat{B}_0 = \mathbb{F}_n$, six-dimensional F-theory also allows us to construct models over arbitrary blow-ups $\hat{B}_0 = \text{Bl}(\mathbb{F}_n)$, of which we recall that $\hat{B}_0 = \text{Bl}(\mathbb{P}^2)$ is a particular case. As we saw in Section B.1.3, the collection of possible base surfaces is huge, and we therefore cannot tackle them individually.

Instead, let us work inductively by exploiting the fact that we know the result to be true for $\hat{B}_0 = \mathbb{P}^2$ and $\hat{B}_0 = \mathbb{F}_n$ from Proposition B.6.1, and that the remaining candidate surfaces are constructed by successive blow-ups of these. To this end, we need to analyse how the blow-up of a point may increase our prospects of violating the claim of Proposition B.5.1. Since the blow-up operation is a local one, the candidate set of curves $\hat{\mathcal{C}}_r$ must at least contain one curve affected by the blow-up in some way, as otherwise its pushforward would be a valid set of mutually non-intersecting non-minimal curves in the blown down surface.

Lemma B.6.2. *Let $\pi_{\text{ell}} : Y \rightarrow B$ be a Calabi-Yau Weierstrass model over a smooth surface B in which a set of smooth irreducible curves $\mathcal{C}_r := \{C_i\}_{1 \leq i \leq r}$ in B supports non-minimal elliptic fibers and such that if $r \geq 3$, then $C_i \cdot C_j \neq 0$ for some $1 \leq i < j \leq r$. Let $\pi : \hat{B} \rightarrow B$ be the blow-up of B at a point $p \in B$ and $\hat{\pi}_{\text{ell}} : \hat{Y} \rightarrow \hat{B}$ a Calabi-Yau Weierstrass model constructed over it. A collection $\hat{\mathcal{C}}_r = \{C_r\}_{1 \leq i \leq r}$ of irreducible curves in \hat{B} supporting non-minimal elliptic fibers and with $r \geq 3$ has $C_i \cdot C_j \neq 0$ for some $1 \leq i < j \leq r$ unless $E \in \hat{\mathcal{C}}_r$ or $C'_p \in \hat{\mathcal{C}}_r$, where E is the exceptional divisor of the blow-up and C'_p is the strict transform of a curve $C_p \subset B$ passing through $p \in B$.*

Proof. The defining holomorphic line bundles $\hat{\mathcal{L}}$ and \mathcal{L} of the Calabi-Yau Weierstrass models $\hat{\pi}_{\text{ell}} : \hat{Y} \rightarrow \hat{B}$ and $\pi_{\text{ell}} : Y \rightarrow B$ are related by

$$\hat{\mathcal{L}} = \overline{K}_{\hat{B}} = \pi^* \overline{K}_B - E = \pi^* \mathcal{L} - E. \quad (\text{B.6.5})$$

Consider a collection $\hat{\mathcal{C}}_r = \{C_i\}_{1 \leq i \leq r}$ of mutually non-intersecting irreducible curves in \hat{B} . Assume that the elements in $\hat{\mathcal{C}}_r$ are all total/strict transforms of curves in B not passing through the blow-up centre $p \in B$. If $\sum_{i=1}^r C_i \leq \overline{K}_{\hat{B}}$, the collection of curves can simultaneously support non-minimal elliptic fibers, according to Proposition B.2.2. Since they are chosen to be mutually non-intersecting, this is a valid set $\hat{\mathcal{C}}_r$ unless

$$\hat{F}_{\text{res}} := \hat{F} - \sum_{i=1}^r 4C_i, \quad \hat{G}_{\text{res}} := \hat{G} - \sum_{i=1}^r 6C_i, \quad (\text{B.6.6})$$

are reducible and forcing an $(r+1)$ -th curve C_{r+1} to factorize non-minimally, i.e. the divisors \hat{F}_{res} and \hat{G}_{res} contain components $4C_{r+1}$ and $6C_{r+1}$ respectively. Then, either C_{r+1} intersects

one of the curves in $\hat{\mathcal{C}}_r$, in which case the original set was not valid, or we are forced to have a bigger set $\hat{\mathcal{C}}_{r+1}$ of mutually non-intersecting smooth irreducible curves of non-minimal fibers. Continuing in this way, we end up either discovering that we started with a bad candidate set, or with a collection $\hat{\mathcal{C}}_{r'}$ of mutually non-intersecting curves in \hat{B} supporting non-minimal fibers and with $r' \geq 3$. The non-minimal factorization process stops when

$$\left(\hat{G}_{\text{res}} - 5C \right) \cdot C \geq 0, \quad \forall C \subset \hat{B} \quad \text{with} \quad C \cdot C < 0, \quad (\text{B.6.7})$$

see Proposition B.1.2. If due to these forced factorizations the set $\hat{\mathcal{C}}_{r'}$ is now such that $E \in \hat{\mathcal{C}}_{r'}$ or $C'_p \in \hat{\mathcal{C}}_{r'}$, we are done. Otherwise, consider the set of curves $\mathcal{C}_{r'}$ in B given by the pushforward of the elements in $\hat{\mathcal{C}}_{r'}$. The set $\mathcal{C}_{r'}$ still consists of r' distinct mutually non-intersecting curves in B , given the assumptions on $\hat{\mathcal{C}}_{r'}$. Moreover, they can simultaneously support non-minimal elliptic fibers, since our assumptions on $\hat{\mathcal{C}}_r$ in conjunction with (B.6.5) imply

$$\sum_{i=1}^r C_i \leq \bar{K}_{\hat{B}} \Rightarrow \sum_{i=1}^r \pi_* C_i \leq \bar{K}_B. \quad (\text{B.6.8})$$

In addition, if C is the strict transform of a curve in B passing through $p \in B$ with multiplicity m , we have with our assumptions for $\hat{\mathcal{C}}_{r'}$ that

$$\left(\hat{G} - \sum_{i=1}^r 6C_i - 5C \right) \cdot_{\hat{B}} C = \left(G - \sum_{i=1}^r 6\pi_* C_i - 5\pi_* C \right) \cdot_B \pi_* C - m, \quad (\text{B.6.9})$$

meaning that (B.6.7) implies that no forced non-minimal factorizations occur in B upon tuning $\mathcal{C}_{r'}$ to support non-minimal elliptic fibers. Hence, $\mathcal{C}_{r'}$ is a set of mutually non-intersecting curves of non-minimal elliptic fibers in B with $r' \geq 3$, leading to a contradiction. \square

In Section B.1.3 we listed a possible way to classify the types of blow-ups that we can take of a surface. We commence our iterative study of Proposition B.5.1 by considering first models constructed over the $\hat{B}_0 = \text{Bl}(\mathbb{F}_n)$ obtained by a succession of type (A) blow-ups.

Type (A) blow-ups of a surface B are those in which we choose a collection of points $\{p_i\}_{1 \leq i \leq n_p}$ in B and blow them up, rather than allowing blow-ups at points of the exceptional divisors as well. This means that the blow-up maps commute, and the order in which we take the points is not relevant.

Since a Hirzebruch surface \mathbb{F}_n is a \mathbb{P}^1 -bundle over \mathbb{P}^1 , we can subdivide type (A) blow-ups into those in which the blow-up centre touches the base, and those in which it does not. In order to introduce the notation that we will use below, let us be rather explicit about the types of divisors fitting into $\bar{K}_{\text{Bl}(\mathbb{F}_n)}$ that we can encounter in $\hat{B}_0 = \text{Bl}(\mathbb{F}_n)$ after the composition of a series of type (A) blow-ups.

First, note that the case $\hat{B}_0 = \text{Bl}(\mathbb{F}_0)$ is slightly different in this regard, since the starting geometry is $\mathbb{F}_0 = \mathbb{P}^1 \times \mathbb{P}^1$. This means that what we call fiber and section is arbitrary, and that $C_0 = C_\infty$; we have no rigid curve with negative self-intersection in the starting surface. The curves in the original surface \mathbb{F}_0 will be denoted using the notation introduced in Section B.1.1. To refer to the strict transforms of curves in \mathbb{F}_n under the composition of all blow-up maps we will use primes, when the curve passes through a blow-up centre and hence its total and strict transform differ, and tildes, when the curve does not pass through a blow-up centre and its total and strict transform coincide. Exceptional divisors will always be denoted without a prime, as in Section B.1.3, referring to their strict transform under the composition of all posterior blow-up

maps. Occasionally, we will indicate in square brackets some of the blow-up centres associated with the strict transform or exceptional divisor, to avoid ambiguities. With this notation, the curves that we need to consider are:

- \tilde{C}_0 , the strict transform of a representative of C_0 not passing through any $p \in \{p_i\}_{0 \leq i \leq n_p}$;
- \tilde{f} , the strict transform of a representative of f not passing through any $p \in \{p_i\}_{0 \leq i \leq n_p}$;
- $C'_{0,i}[p_j, \neg p_k]$, the strict transform of a representative of C_0 passing through the blow-up centre $p_j \in \{p_i\}_{1 \leq i \leq n_p}$, not passing through the blow-up centre $p_k \in \{p_i\}_{1 \leq i \leq n_p}$, and in which a total of i points have been blown up;
- $f'_i[p_j, \neg p_k]$, the strict transform of a representative of f passing through the blow-up centre $p_j \in \{p_i\}_{1 \leq i \leq n_p}$, not passing through the blow-up centre $p_k \in \{p_i\}_{1 \leq i \leq n_p}$, and in which a total of i points have been blown up; and
- E_i , the exceptional divisor associated to the blow-up with centre $p_i \in \{p_i\}_{1 \leq i \leq n_p}$.

Not every type (A) blow-up of \mathbb{F}_0 leads to a base $\hat{B}_0 = \text{Bl}(\mathbb{F}_0)$ with effective anticanonical class $\overline{K}_{\text{Bl}(\mathbb{F}_0)}$. Recalling from Section B.1.3.2 that after a composition of type (A) blow-ups we have the anticanonical class (B.1.29), or written with our current notation

$$\overline{K}_{\text{Bl}(\mathbb{F}_0)} = 2\tilde{C}_0 + 2\tilde{f} - \sum_{i=1}^{n_p} E_i, \quad (\text{B.6.10})$$

we see that blowing up more than four points in general position leads to a non-effective anticanonical class. It is possible to blow up more than four points, but some of them must lie on the same representative of C_0 of f . Due to Proposition B.2.2, the situation is even more stringent when it comes to tuning exceptional divisors to be non-minimal, since, e.g., tuning E_i and E_j to be non-minimal means that if a third E_k is tuned to be non-minimal it must stem from the blow-up of a point in the same representative of C_0 or f that gave rise to either E_i or E_j .

Moving now to the cases $\hat{B}_0 = \text{Bl}(\mathbb{F}_n)$, with $1 \leq n \leq 12$, we can distinguish those blow-ups associated to points $p \in \{p_i\}_{1 \leq i \leq n_p}$ such that $p \in C_0$ from those in which $p \notin C_0$. Let us denote the total number of the former type of blow-ups by n_0 and the associated blow-up centres by $\{p_i\}_{i \in \mathcal{N}_0} \subset \{p_i\}_{1 \leq i \leq n_p}$, and the total number of the latter by n_∞^{tot} and the associated blow-up centres by $\{p_i\}_{i \in \mathcal{N}_\infty} \subset \{p_i\}_{1 \leq i \leq n_p}$, such that $n_p = n_0 + n_\infty^{\text{tot}}$. Each point $p \notin C_0$ sits in a unique representative of f . It will be convenient to define a quantity $n_\infty \leq n_\infty^{\text{tot}}$ counting the number of distinct f representatives affected by the n_∞^{tot} blow-ups at points $p \notin C_0$. Occasionally, we will need to refer to all the blow-up centres associated with a strict transform C' , which we will do by $p\{C'\}$. We will use a notation similar to the one employed in the $\hat{B}_0 = \text{Bl}(\mathbb{F}_0)$ case. With this notation, the curves that we need to consider are:

- \tilde{C}_∞ , the strict transform of a representative of C_∞ not passing through any $p \in \{p_i\}_{0 \leq i \leq n_p}$;
- \tilde{f} , the strict transform of a representative of f not passing through any $p \in \{p_i\}_{0 \leq i \leq n_p}$;
- C'_0 , the strict transform of the unique representative of C'_0 , in which a total of n_0 points have been blown up;

- $C'_{\infty,i}[p_j, \neg p_k]$: the strict transform of a representative of C_∞ passing through the blow-up centre $p_j \in \{p_i\}_{1 \leq i \leq n_p}$, not passing through the blow-up centre $p_k \in \{p_i\}_{1 \leq i \leq n_p}$, and in which a total of i points have been blown up;
- $f'_{0,i}$ the strict transform of a representative of f passing through a blow-up centre $p \in C_0$, and in which a total of i points have been blown up;
- $f'_{\infty,i}[p_j, \neg p_k]$ the strict transform of a representative of f passing through the blow-up centre $p_j \in \{p_i\}_{1 \leq i \leq n_p}$, not passing through the blow-up centre $p_k \in \{p_i\}_{1 \leq i \leq n_p}$, and in which a total of i points $p \notin C_0$ have been blown up;
- $f'_{0/\infty,i}[p_j, \neg p_k]$ the strict transform of a representative of f passing through the blow-up centre $p_j \in \{p_i\}_{1 \leq i \leq n_p}$, not passing through the blow-up centre $p_k \in \{p_i\}_{1 \leq i \leq n_p}$, and in which a total of $i - 1$ points $p \notin C_0$ and a point $p \in C_0$ have been blown up;
- E_i^0 : the exceptional divisor associated to a blow-up with centre $p \in C_0$; and
- $E_i^\infty[C'_j, \neg C'_k]$: the exceptional divisor associated to a blow-up with centre $p \notin C_0$, with the pushforwards of C'_j and C'_k passing and not passing through p , respectively.

The cases $f'_{0,i}$ and $f'_{0/\infty,i}[p_j, \neg p_k]$ are essentially the same, but it is contextually useful to use this notation, as the latter expression will mean that the point of intersection of the fiber class representative from which $f'_{0/\infty,i}[p_j, \neg p_k]$ stems with the particular representative of C_∞ whose strict transform is relevant at that point in the discussion has been blown up. Every so often we will write $C'_1[p\{C'_2\}]$; this does not mean that the pushforward of $C'_1[p\{C'_2\}]$ passes through all points $p\{C'_2\}$, but rather that any points of intersection between the pushforwards of the two curves have been blown up. Sporadically, we will drop the square brackets after first introducing a curve, if the subindices are enough to distinguish it in the subsequent context.

As occurred for the $\hat{B}_0 = \text{Bl}(\mathbb{F}_0)$ case, not every type (A) blow-up of \mathbb{F}_n , with $1 \leq n \leq 12$, leads to a base $\hat{B}_0 = \text{Bl}(\mathbb{F}_n)$ with effective anticanonical class $\overline{K}_{\text{Bl}(\mathbb{F}_n)}$. Writing (B.1.29) with our current notation we have

$$\overline{K}_{\text{Bl}(\mathbb{F}_n)} = 2\tilde{C}_0 + (2+n)\tilde{f} - \sum_{i=1}^{n_p} E_i = 2C'_0 + (2+n)\tilde{f} + \sum_{i \in \mathcal{N}_0} E_i^0 - \sum_{i \in \mathcal{N}_\infty} E_i^\infty. \quad (\text{B.6.11})$$

The $\{E_i^0\}_{i \in \mathcal{N}_0}$ do not pose a threat to the effectiveness of the anticanonical class $\overline{K}_{\text{Bl}(\mathbb{F}_n)}$. Since C_0 has a unique representative, whose total transform gives

$$\tilde{C}_0 = C'_0 + \sum_{i \in \mathcal{N}_0} E_i^0, \quad (\text{B.6.12})$$

and this class appears twice in $\overline{K}_{\text{Bl}(\mathbb{F}_n)}$, we have that $E_i^0 \leq \overline{K}_B$ for all $i \in \mathcal{N}_0$, and can tune them to support non-minimal fibers according to Proposition B.2.2. The $\{E_i^\infty\}_{i \in \mathcal{N}_\infty}$, on the other hand, are related to particular representatives of f , meaning that we have

$$\tilde{f} = f'_{\infty,i} + \sum_{\substack{i \in \mathcal{N}_0 \text{ s.t.} \\ p_i \in p\{f'_{\infty,i}\}}} E_i^\infty = f'_{\infty,i'} + \sum_{\substack{i' \in \mathcal{N}_0 \text{ s.t.} \\ p_{i'} \in p\{f'_{\infty,i'}\}}} E_{i'}^\infty. \quad (\text{B.6.13})$$

Hence, we need to have at least n_∞ representatives of \tilde{f} available in $\overline{K}_{\text{Bl}(\mathbb{F}_n)}$ for it to still be effective after the blow-up process, from where we obtain the effectiveness bound

$$n_\infty \leq n + 2. \quad (\text{B.6.14})$$

This bound is just to have $\overline{K}_{\text{Bl}(\mathbb{F}_n)}$ be effective, but if we want to tune an exceptional divisor E_i^∞ to be non-minimal we need in addition $E_i^\infty \leq \overline{K}_{\text{Bl}(\mathbb{F}_n)}$ to comply with Proposition B.2.2. Denoting by m the number of elements in $\{E_i^\infty\}_{i \in \mathcal{N}_\infty}$ stemming from different fiber class representatives that we want to tune non-minimally, the effectiveness bound becomes

$$n_\infty + m \leq n + 2. \quad (\text{B.6.15})$$

Although we have just seen that the number of blow-ups n_0 over points $p \in C_0$ is not restricted by requiring the effectiveness of $\overline{K}_{\text{Bl}(\mathbb{F}_n)}$, if we blow C_0 up at too many points the self-intersection of C'_0 becomes so negative that a non-minimal non-Higgsable cluster appears for $\text{Bl}(\mathbb{F}_n)$. This would mean that any degeneration of elliptic Calabi-Yau threefolds fibered over $\hat{B}_0 = \text{Bl}(\mathbb{F}_n)$ would present, at least at the level of the component vanishing orders, non-minimal singularities over all $u \in D$, and not only over the central fiber. In order to avoid this, we also need to demand

$$n + n_0 \leq 12. \quad (\text{B.6.16})$$

The divisor classes listed above are not the only ones over which we can tune non-minimal elliptic fibers in $\text{Bl}(\mathbb{F}_n)$. The rest, however, are obtained as combinations of these, and are a less efficient use of the divisor classes available in $\overline{K}_{\text{Bl}(\mathbb{F}_n)}$ (if our aim is to find a candidate triplet of curves violating Proposition B.5.1), meaning that they will intersect more curves and force more factorizations of the residual defining polynomials. Hence, we need to search for candidate triplets among the divisors listed earlier, which we now do.

Proposition B.6.3. *Let $\pi : Y \rightarrow B$ be a Calabi-Yau Weierstrass model over B , where $B = \text{Bl}(\mathbb{F}_n)$ is the surface obtained by choosing a collection of points in \mathbb{F}_n and blowing them up. Let $\mathcal{C}_r := \{C_i\}_{1 \leq i \leq r}$ be a set of curves in B that support non-minimal elliptic fibers. If $r \geq 3$, then $C_i \cdot C_j \neq 0$ for some $1 \leq i < j \leq r$.*

Proof. Let us work by induction, with the base case provided by Proposition B.6.1. Assume that the result holds for Calabi-Yau Weierstrass models constructed over $B = \text{Bl}_k(\mathbb{F}_n)$, obtained as the blow-up of \mathbb{F}_n with centre at the points $\{p_i\}_{1 \leq i \leq k}$, where $k := n_p = n_0 + n_\infty^{\text{tot}}$. Consider now the Calabi-Yau Weierstrass models constructed over $\hat{B} = \text{Bl}_{k+1}(\mathbb{F}_n)$, obtained by a further blow-up with a $(k+1)$ -th point p_{k+1} in \mathbb{F}_n as centre, such that $\hat{n}_p = n_0 + n_\infty^{\text{tot}} + 1$. We can distinguish the three cases $n = 0$, $n \geq 1$ with $p_{k+1} \in C_0$, and $n \geq 1$ with $p_{k+1} \notin C_0$, that we treat separately.

To avoid any ambiguity, let us clarify that below n_0 , n_∞ and n_∞^{tot} refer to the B surface, and do not count the $(k+1)$ -th blow-up. When we write a strict transform in \hat{B} like, e.g., $f'_{\infty,i}$, the subindex i refers to all the blow-ups affecting the representative of f that $f'_{\infty,i}$ stems from, including the $(k+1)$ -th blow-up if appropriate.

(1) $n = 0$: According to Lemma B.6.2, we need to consider the candidate triplets $\{E_{k+1}, \cdot, \cdot\}$, $\{C'_{0,i}(p_{k+1}), \cdot, \cdot\}$ and $\{f'_i(p_{k+1}), \cdot, \cdot\}$. In fact, when $n = 0$, the choice of what we call section and fiber is arbitrary, and therefore the second and the third candidate triplets are analogous. Hence, we only address the first.

(1.a) $\{E_{k+1}, \cdot, \cdot\}$: E_{k+1} intersects the total transforms $C'_{0,i}[p_{k+1}]$ and $f'_i[p_{k+1}]$, which discards them as candidates to complete the triplet. We need to analyse the following candidates for triplet completion: \tilde{C}_0 , $C'_{0,i}[\neg p_{k+1}]$, \tilde{f} , $f'_i[\neg p_{k+1}]$ and E_i .

- (1.a.i) $\{E_{k+1}, \tilde{C}_0, \cdot\}$: After tuning these two divisors to be non-minimal, the residual \hat{G} divisor is

$$\hat{G}_{\text{res}} = 6\tilde{C}_0 + 12\tilde{f} - \sum_{i=1}^{n_p} 6E_i - 12E_{k+1}. \quad (\text{B.6.17})$$

Since

$$(\hat{G}_{\text{res}} - \alpha f'_i[p_{k+1}]) \cdot f'_i[p_{k+1}] = -(6 - \alpha)i \quad (\text{B.6.18})$$

and $i \geq 1$, we see that $f'_i[p_{k+1}]$ factorizes non-minimally, with $f'_i[p_{k+1}] \cdot E_{k+1} = 1$.

- (1.a.ii) $\{E_{k+1}, C'_{0,i}[\neg p_{k+1}], \cdot\}$: In this case the residual \hat{G} divisor after the tuning is

$$\hat{G} = 12\tilde{C}_{0,i} + 12\tilde{f} - \sum_{i=1}^{n_p} 6E_i - 6E_{k+1} - 6C'_{0,i}[\neg p_{k+1}]. \quad (\text{B.6.19})$$

We can distinguish two subcases:

- if the intersection point $f'_j[p_{k+1}] \cap C'_{0,i}[\neg p_{k+1}] =: p$ in \mathbb{F}_0 has not been blown-up, we have

$$(G_{\text{res}} - \alpha f'_j[p_{k+1}]) \cdot f'_j[p_{k+1}] = -(6 - \alpha)j, \quad (\text{B.6.20})$$

with $j \geq 1$, such that $f'_j[p_{k+1}]$ factorizes non-minimally; and

- if the intersection point of $f'_j[p_{k+1}]$ and $C'_{0,i}[\neg p_{k+1}]$ in \mathbb{F}_0 has been blown-up, we have instead

$$(G_{\text{res}} - \alpha f'_j[p_{k+1}]) \cdot f'_j[p_{k+1}] = 6 - (6 - \alpha)j, \quad (\text{B.6.21})$$

with $j \geq 2$. This means that at least $3f'_j[p_{k+1}]$ will factorize, implying, in turn, that due to

$$(G_{\text{res}} - 3f'_j[p_{k+1}] - \alpha E_l[p]) = -3 + \alpha, \quad (\text{B.6.22})$$

at least $3E_l[p]$ will factorize. Then

$$(G_{\text{res}} - 3f'_j[p_{k+1}] - 3E_l[p] - \alpha f'_j[p_{k+1}]) \cdot f'_j[p_{k+1}] = 3 - (3 - \alpha)i, \quad (\text{B.6.23})$$

with $j \geq 2$, leading to an additional factorization of at least $3f'_j[p_{k+1}]$. Since

$$(G_{\text{res}} - 5f'_j[p_{k+1}] - 3E_l[p] - \alpha E_l) = -2 + \alpha, \quad (\text{B.6.24})$$

at least $2E_l[p]$ further factorize, which finally leads to

$$(G_{\text{res}} - 5f'_j[p_{k+1}] - 5E_l[p]) \cdot f'_j[p_{k+1}] = 1 - j, \quad (\text{B.6.25})$$

with $j \geq 2$, meaning that $f'_j[p_{k+1}]$ factorizes non-minimally.

In both cases $f'_j[p_{k+1}] \cdot E_{k+1} = 1$.

- (1.a.iii) $\{E_{k+1}, \tilde{f}, \cdot\}$: This case is analogous to Case (1.a.i), with the roles of $\{\tilde{C}_0, f'_i[p_{k+1}]\}$ and $\{\tilde{f}, C'_{0,i}[\neg p_{k+1}]\}$ exchanged.

- (1.a.iv) $\{E_{k+1}, f'_i[p_{k+1}], \cdot\}$: This case is analogous to Case (1.a.ii), after exchanging the roles of $\{C'_{0,i}[\neg p_{k+1}], f'_i[p_{k+1}]\}$ and $\{f'_i[\neg p_{k+1}], C'_{0,j}[p_{k+1}]\}$.

- (1.a.v) $\{E_{k+1}, E_j, \cdot\}$: The residual \hat{G} divisor after tuning these two divisors to be non-minimal is

$$\hat{G}_{\text{res}} = 12\tilde{C}_0 + 12\tilde{f} - \sum_{i=1}^{n_p} 6E_i - 6E_j - 12E_{k+1}. \quad (\text{B.6.26})$$

We can distinguish two subcases:

- if E_{k+1} and E_j are associated to the blow-ups of the same C_0 representative (or f , for which the same argument would apply), then

$$\left(\hat{G}_{\text{res}} - \alpha C'_{0,i}[p_{k+1}, p_j] \right) \cdot C'_{0,i}[p_{k+1}, p_j] = -(6 - \alpha)i, \quad (\text{B.6.27})$$

with $i \geq 2$, yielding a non-minimal factorization of $C'_{0,i}[p_{k+1}, p_j]$; and

- if E_{k+1} and E_j are not associated to the blow-ups of a common C_0 or f representative, in which case the residual \hat{G}_{res} discriminant can be rewritten as

$$\hat{G}_{\text{res}} = 12C'_{0,i}[p_{k+1}] + 12f'_l[p_j] + \sum_r 6E_r[C'_{0,i}[p_{k+1}]] + \sum_s 6E_s[f'_l[p_j]], \quad (\text{B.6.28})$$

from where we see that the only possible non-minimal effective tunings that can be performed of divisors not intersecting E_{k+1} and E_j are those involving another exceptional divisor E_m . It must be, however, related to either the blow-ups of the pushforward of $C'_{0,i}[p_{k+1}]$, or to the blow-ups of the pushforward of $f'_l[p_j]$, which amounts again to the previous case.

- (1.b) $\{C'_{0,i}[p_{k+1}], \cdot, \cdot\}$: $C'_{0,i}[p_{k+1}]$ intersects E_{k+1} and the other exceptional divisors associated with the blow-ups of the pushforward of $C'_{0,j}[p_{k+1}]$, as well as the strict transforms $f'_j[\neg p_{k+1}]$. We need to consider the following candidates for triplet completion: \tilde{C}_0 , $C'_{0,j}[\neg p_{k+1}]$, $f'_j[p_{k+1}]$ and $E_j[C'_{0,i}[p_{k+1}]]$.

- (1.b.i) $\{C'_{0,i}[p_{k+1}], \tilde{C}_0, \cdot\}$: Tuning these two divisors to be non-minimal leaves us with

$$\hat{G}_{\text{res}} = 6\tilde{C}_0 + 12\tilde{f} - \sum_{i=1}^{n_p} 6E_i - 6E_{k+1} - 6C'_{0,i}. \quad (\text{B.6.29})$$

Since

$$\left(\hat{G}_{\text{res}} - \alpha f'_l[p_{k+1}] \right) \cdot f'_l[p_{k+1}] = -(6 - \alpha)l, \quad (\text{B.6.30})$$

with $l \geq 1$, $f'_l[p_{k+1}]$ factorizes non-minimally, with $f'_l[p_{k+1}] \cdot \tilde{C}_{0,i} = 1$.

- (1.b.ii) $\{C'_{0,i}[p_{k+1}], C'_{0,j}[\neg p_{k+1}], \cdot\}$: After tuning these two divisors to be non-minimal, we have

$$\hat{G}_{\text{res}} = 12\tilde{f} - \sum_r 6E_r[\neg C'_{0,i}[p_{k+1}], \neg C'_{0,j}[\neg p_{k+1}]]. \quad (\text{B.6.31})$$

There are two types of divisors that do not intersect $C'_{0,i}[p_{k+1}]$ and $C'_{0,j}[\neg p_{k+1}]$ that can be tuned effectively:

- we can tune an exceptional divisor $E_r[\neg C'_{0,i}[p_{k+1}], \neg C'_{0,j}[\neg p_{k+1}]]$, which would lead us to Case (1.a.ii); or

- assuming that the pushforward of $f'_l[p_{k+1}]$ intersects the pushforward of $C'_{0,j}[\neg p_{k+1}]$ at a point p_j that has been blown-up, we can tune the strict transform $f'_l[p_{k+1}, p_j]$. However, this leads to the residual \hat{G}_{res} divisor

$$\begin{aligned}\hat{G}_{\text{res}} = 6\tilde{f} - \sum_{r'} 6E_{r'}[\neg C'_{0,i}[p_{k+1}], \neg C'_{0,j}[\neg p_{k+1}], \neg f'_l[p_{k+1}, p_j]] \\ + 6E_{k+1}[p_{k+1}] + 6E_j[p_j].\end{aligned}\quad (\text{B.6.32})$$

Then $E_{k+1}[p_{k+1}]$ and $E_j[p_j]$ factorize non-minimally, with the intersections $C'_{0,i}[p_{k+1}] \cdot E_{k+1}[p_{k+1}] = 1$ and $C'_{0,j}[\neg p_{k+1}] \cdot E_j[p_j] = 1$.

- (1.b.iii) $\{C'_{0,i}[p_{k+1}], f'_{0,j}[p_{k+1}], \cdot\}$: After tuning these two divisors to be non-minimal, the residual \hat{G}_{res} divisor is

$$\hat{G}_{\text{res}} = 6\tilde{C}_0 + 6\tilde{f} - \sum_r 6E_r[\neg C'_{0,i}[p_{k+1}], \neg f'_{0,j}[p_{k+1}]] + 6E_{k+1}, \quad (\text{B.6.33})$$

from which we see that E_{k+1} factorizes non-minimally, with $C'_{0,i}[p_{k+1}] \cdot E_{k+1} = 1$ and $f'_{0,j}[p_{k+1}] \cdot E_{k+1} = 1$.

- (1.b.iv) $\{C'_{0,i}[p_{k+1}], E_j[\neg p_{k+1}], \cdot\}$: This is analogous to Case (1.a.ii).

- (2) $n \geq 1$ with $p_{k+1} \in C_0$: According to Lemma B.6.2, we need to consider the candidate triplets $\{E_{k+1}^0, \cdot, \cdot\}$, $\{C'_0[p_{k+1}], \cdot, \cdot\}$ and $\{f'_{0,i}[p_{k+1}], \cdot, \cdot\}$.

- (2.a) $\{E_{k+1}^0, \cdot, \cdot\}$: After tuning E_{k+1}^0 to be non-minimal, the residual \hat{G} divisor is

$$\hat{G}_{\text{res}} = 12\tilde{C}_0 + (12 + 6n)\tilde{f} - \sum_{i \in \mathcal{N}_0} 6E_i^0 - \sum_{i \in \mathcal{N}_\infty} 6E_i^\infty - 12E_{k+1}^0, \quad (\text{B.6.34})$$

for which we have

$$(\hat{G}_{\text{res}} - \alpha C'_0) \cdot C'_0 = -(6 - \alpha)(n - n_0). \quad (\text{B.6.35})$$

Since $n \geq 1$, this implies that C'_0 factorizes non-minimally, with $C'_0 \cdot E_{k+1}^0 = 1$.

- (2.b) $\{C'_0, \cdot, \cdot\}$: C'_0 intersects the strict transforms \tilde{f} , $f'_{\infty,i}$ and the exceptional divisors E_i^0 . The possible triplet completions to be considered are: \tilde{C}_∞ , $C'_{\infty,j}$, $f'_{0,j}$ and E_j^∞ .

- (2.b.i) $\{C'_{0,i}, \tilde{C}_\infty, \cdot\}$: After tuning these two divisors to be non-minimal, the residual \hat{G} divisor is

$$\hat{G}_{\text{res}} = (12 + 6n)\tilde{f} - \sum_{i \in \mathcal{N}_\infty} 6E_i^\infty, \quad (\text{B.6.36})$$

from which we see that the strict transforms $f'_{\infty,j}$ factorize non-minimally, with $f'_{\infty,j} \cdot C'_0 = 1$.

- (2.b.ii) $\{C'_0, C'_{\infty,i}, \cdot\}$: The residual \hat{G} divisor is in this occasion

$$\hat{G}_{\text{res}} = 12\tilde{C}_0 + (12 + 6n)\tilde{f} - \sum_{i=1}^{n_p} E_i - 6E_{k+1}^0 - 6C'_0 - 6C'_{\infty,i}. \quad (\text{B.6.37})$$

Given the divisors that intersect C'_0 , listed above, and the fact that $f'_{0,j}[\neg C'_{\infty,i}]$ and $E_l^\infty[C'_{\infty,i}]$ intersect $C'_{\infty,i}$, the only two types of divisors that we can effectively tune non-minimally are the strict transform of a vertical line $f'_0[C'_{\infty,i}]$, or an exceptional divisor $E_l^\infty[\neg C'_{\infty,i}]$. However, we see that

- due to the intersection

$$\left(\hat{G}_{\text{res}} - 6f'_{0,j}[\neg C'_{\infty,i}] - \alpha E_l^0[f'_{0,j}[\neg C'_{\infty,i}]] \right) \cdot E_l^0[f'_{0,j}[\neg C'_{\infty,i}]] = -6 + \alpha, \quad (\text{B.6.38})$$

$E_l^0[f'_{0,j}[\neg C'_{\infty,i}]]$ factorizes non-minimally, with $E_l^0[f'_{0,j}[\neg C'_{\infty,i}]] \cdot C'_{0,i} = 1$; and

- due to the intersection

$$\left(\hat{G}_{\text{res}} - 6E_l^\infty[\neg C'_{\infty,i}, f'_{(0/\infty,m)}] - \alpha f'_{(0/\infty,m)} \right) \cdot f'_{(0/\infty,m)} = -(6 - \alpha)m, \quad (\text{B.6.39})$$

with $m \geq 1$, $f'_{(0/\infty,m)}$ factorizes non-minimally, and $f'_{(0/\infty,m)} \cdot E_l^\infty = 1$.

- (2.c) $\{f'_{0,i}[p_{k+1}], \cdot, \cdot\}$: $f'_{0,i}$ intersects \tilde{C}_∞ , $C'_{\infty,j}$ and E_{k+1}^0 . The possible triplet completions that we need to consider are: C'_0 , \tilde{f} , $f'_{0,j}[\neg p_{k+1}]$, $f'_{\infty,j}[\neg p_{k+1}]$, E_i^0 and E_i^∞ .
- (2.c.i) $\{f'_{0,i}[p_{k+1}], C'_0, \cdot\}$: After tuning these two divisors to be non-minimal, the residual \hat{G} divisor is

$$\hat{G}_{\text{res}} = 6C'_0 + (12 + 6n)\tilde{f} - \sum_{i \in \mathcal{N}_\infty} 6E_i^\infty - 6f'_{0,i}[p_{k+1}]. \quad (\text{B.6.40})$$

Given the intersection

$$\left(\hat{G}_{\text{res}} - \alpha E_{k+1}^0 \right) \cdot E_{k+1}^0 = -6 + \alpha, \quad (\text{B.6.41})$$

we see that E_{k+1}^0 factorizes non-minimally, with $E_{k+1}^0 \cdot f'_{0,i}[p_{k+1}] = 1$.

- (2.c.ii) $\{f'_{0,i}[p_{k+1}], \tilde{f}, \cdot\}$: The residual \hat{G} divisor is

$$\hat{G}_{\text{res}} = 12\tilde{C}_0 + (12 + 6n)\tilde{f} - \sum_{i=1}^{n_p} 6E_i - 6E_{k+1}^0 - 6f'_{0,i}[p_{k+1}] - 6\tilde{f}. \quad (\text{B.6.42})$$

This leads to

$$\left(\hat{G}_{\text{res}} - \alpha C'_0 \right) \cdot C'_0 = -6(n + n_0), \quad (\text{B.6.43})$$

with $n \geq 1$ and $n_0 \geq 1$, meaning that C'_0 factorizes non-minimally. This implies

$$\left(\hat{G}_{\text{res}} - 6C'_0 - \alpha E_{k+1}^0 \right) \cdot E_{k+1}^0 = -6 + \alpha, \quad (\text{B.6.44})$$

yielding a non-minimal factorization of E_{k+1}^0 , with $E_{k+1}^0 \cdot f'_{0,i}[p_{k+1}] = 1$.

- (2.c.iii) $\{f'_{0,i}[p_{k+1}], f'_{0,j}[\neg p_{k+1}], \cdot\}$: The residual \hat{G} divisor is

$$\hat{G}_{\text{res}} = 12\tilde{C}_0 + (12 + 6n)\tilde{f} - \sum_{i=1}^{n_p} 6E_i - 6E_{k+1}^0 - 6f'_{0,i}[p_{k+1}] - 6f'_{0,j}[\neg p_{k+1}]. \quad (\text{B.6.45})$$

The intersection

$$\left(\hat{G}_{\text{res}} - \alpha C'_0 \right) \cdot C'_0 = 6 - (6 - \alpha)(n + n_0), \quad (\text{B.6.46})$$

with $n \geq 1$ and $n_0 \geq 1$, means that at least $3C'_0$ factorize. Then

$$\left(\hat{G}_{\text{res}} - 3C'_0 - \alpha E_{k+1}^0 \right) \cdot E_{k+1}^0 = -3 + \alpha, \quad (\text{B.6.47})$$

leading to at least $3E_{k+1}^0$ factorizing. This, in turn, implies that

$$\left(\hat{G}_{\text{res}} - 3C'_0 - 3E_{k+1}^0 - \alpha C'_0\right) \cdot C'_0 = 3 - (3 - \alpha)(n + n_0), \quad (\text{B.6.48})$$

yielding an additional factorization of at least $2C'_0$. Then

$$\left(\hat{G}_{\text{res}} - 5C'_0 - 3E_{k+1}^0 - \alpha E_{k+1}^0\right) \cdot E_{k+1}^0 = -2 + \alpha, \quad (\text{B.6.49})$$

forces an additional factorization of at least $2E_{k+1}^0$. From these, we obtain

$$\left(\hat{G}_{\text{res}} - 5C'_0 - 5E_{k+1}^0 - \alpha C'_0\right) \cdot C'_0 = -(1 - \alpha)(n + n_0) + 1, \quad (\text{B.6.50})$$

leading to an additional factorization of at least C'_0 . Finally, this yields

$$\left(\hat{G}_{\text{res}} - 6C'_0 - 5E_{k+1}^0 - \alpha E_{k+1}^0\right) \cdot E_{k+1}^0 = -1 + \alpha, \quad (\text{B.6.51})$$

meaning that E_{k+1}^0 factorizes non-minimally, with $E_{k+1}^0 \cdot f'_{0,i}[p_{k+1}] = 1$.

- (2.c.iv) $\{f'_{0,i}[p_{k+1}], f'_{\infty,j}[\neg p_{k+1}], \cdot\}$: This case is analogous to Case (2.c.ii).
- (2.c.v) $\{f'_{0,i}[p_{k+1}], E_j^0, \cdot\}$: This case is analogous to Case (2.c.ii).
- (2.c.vi) $\{f'_{0,i}[p_{k+1}], E_j^\infty, \cdot\}$: Since we have discarded all the other cases, the only possible remaining triplet completion is $\{f'_{0,i}[p_{k+1}], E_j^\infty, E_l^\infty\}$, where E_l^∞ may be associated to a blow-up of the same representative of f as E_j^∞ , or a different one. The residual \hat{G} divisor after tuning these three divisors to be non-minimal is

$$\hat{G}_{\text{res}} = 12\tilde{C}_0 + (12 + 6n)\tilde{f} - \sum_{i=1}^{n_p} E_i - 6E_{k+1}^0 - 6f'_{0,i}[p_{k+1}] - 6E_j^\infty - 6E_l^\infty. \quad (\text{B.6.52})$$

Then, we have that

- if E_j^∞ and E_l^∞ stem from the blow-up of two different representatives of f , the factorization process is analogous to that of Case (2.c.iii); while
- if E_j^∞ and E_l^∞ stem from the blow-up of the same representative of f , call its strict transform $f'_{0/\infty,m}$, we have instead

$$\left(\hat{G}_{\text{res}} - \alpha f'_{0/\infty,m}\right) \cdot f'_{0/\infty,m} = -(6 - \alpha)m, \quad (\text{B.6.53})$$

leading to a non-minimal factorization of $f'_{0/\infty,m}$, with $f'_{0/\infty,m} \cdot E_j^\infty = 1$ and $f'_{0/\infty,m} \cdot E_l^\infty = 1$.

- (3) $n \geq 1$ with $p \notin C_0$: According to Lemma B.6.2, we need to consider the candidate triplets $\{E_{k+1}^\infty, \cdot, \cdot\}$, $\{C'_{\infty,i}, \cdot, \cdot\}$, $\{f'_{\infty,i}[p_{k+1}], \cdot, \cdot\}$ and $\{f'_{0/\infty,i}[p_{k+1}], \cdot, \cdot\}$.
- (3.a) $\{E_{k+1}^\infty, \cdot, \cdot\}$: E_{k+1}^∞ intersects the strict transforms of $\tilde{C}_\infty[p_{k+1}]$ and $f[p_{k+1}]$ representatives. We need to consider the following candidates for triplet completion: C'_0 , \tilde{C}_∞ , $C'_{\infty,i}[\neg p_{k+1}]$, \tilde{f} , $f'_{\infty,i}[\neg p_{k+1}]$, $f'_{0,i}$, $f'_{0/\infty,i}[\neg p_{k+1}]$, E_i^0 and E_i^∞ .

- (3.a.i) $\{E_{k+1}^\infty, C'_0, \cdot\}$: After tuning these two divisors to be non-minimal, the residual \hat{G} divisor is

$$\hat{G}_{\text{res}} = 6\tilde{C}_0 + (12 + 6n)\tilde{f} - \sum_{i \in \mathcal{N}_\infty} E_i^\infty - 12E_{k+1}^\infty. \quad (\text{B.6.54})$$

Let us denote the intersection point of the representative $f[p_{k+1}]$ of f with C_0 as $f[p_{k+1}] \cap C_0 =: p_j$. We need to distinguish two subcases:

- if p_j has not been blown up, we have the intersection

$$\left(\hat{G}_{\text{res}} - \alpha f'_{\infty,i}[p_{k+1}] \right) \cdot f'_{\infty,i}[p_{k+1}] = -(6 - \alpha)i, \quad (\text{B.6.55})$$

where $i \geq 1$, and as a consequence $f'_{\infty,i}[p_{k+1}]$ factorizes non-minimally, with $f'_{\infty,i}[p_{k+1}] \cdot E_{k+1}^\infty = 1$;

- if p_j has been blown up, we have instead

$$\left(\hat{G}_{\text{res}} - \alpha f'_{0/\infty,i}[p_{k+1}] \right) \cdot f'_{0/\infty,i}[p_{k+1}] = 6 - (6 - \alpha)i, \quad (\text{B.6.56})$$

with $i \geq 2$, leading to the cascade of factorizations

$$\begin{aligned} \hat{G}_{\text{res}} &\longrightarrow \hat{G}_{\text{res}} - 3f'_{0/\infty,i}[p_{k+1}] \\ &\longrightarrow \hat{G}_{\text{res}} - 3f'_{0/\infty,i}[p_{k+1}] - 3E_l^0[p_j] \\ &\longrightarrow \hat{G}_{\text{res}} - 5f'_{0/\infty,i}[p_{k+1}] - 3E_l^0[p_j] \\ &\longrightarrow \hat{G}_{\text{res}} - 5f'_{0/\infty,i}[p_{k+1}] - 5E_l^0[p_j] \\ &\longrightarrow \hat{G}_{\text{res}} - 6f'_{0/\infty,i}[p_{k+1}] - 5E_l^0[p_j], \end{aligned} \quad (\text{B.6.57})$$

such that $f'_{0/\infty,i}[p_{k+1}]$ factorizes non-minimally, with $f'_{0/\infty,i}[p_{k+1}] \cdot E_{k+1}^\infty = 1$.

After the various explicit examples given above, we have been more succinct here, only indicating the cascade of factorizations that occurs, without printing all the relevant intersection products. We will often do this in what follows.

- (3.a.ii) $\{E_{k+1}^\infty, \tilde{C}_\infty, \cdot\}$: This case is analogous to Case (3.a.i).

- (3.a.iii) $\{E_{k+1}^\infty, C'_{\infty,i}[\neg p_{k+1}], \cdot\}$: This case is analogous to Case (3.a.i).

- (3.a.iv) $\{E_{k+1}^\infty, \tilde{f}, \cdot\}$: The following candidate divisors are still possible triplet completions: \tilde{f} , $f'_{\infty,i}[\neg p_{k+1}]$, $f'_{0,i}$, $f'_{0/\infty,i}[\neg p_{k+1}]$, E_l^0 and E_i^∞ .

- $\{E_{k+1}^\infty, \tilde{f}, \tilde{f}\}$ and $\{E_{k+1}^\infty, \tilde{f}, f'_{\infty,i}[\neg p_{k+1}]\}$ lead to the intersection

$$\left(\hat{G}_{\text{res}} - \alpha C'_0 \right) \cdot C'_0 = -(6 - \alpha)(n + n_0), \quad (\text{B.6.58})$$

with $n \geq 1$. This means that C'_0 factorizes non-minimally, with $C'_0 \cdot \tilde{f} = 1$ and $C'_0 \cdot f'_{\infty,i}[\neg p_{k+1}] = 1$.

- $\{E_{k+1}^\infty, \tilde{f}, f'_{0,i}\}$, $\{E_{k+1}^\infty, \tilde{f}, f'_{0/\infty,i}[\neg p_{k+1}]\}$ and $\{E_{k+1}^\infty, \tilde{f}, E_l^0\}$ all imply that $n \geq 1$ and $n_0 \geq 1$.

Assume first that the intersection point of the representative $f[p_{k+1}]$ of f and C_0 was not blown-up, i.e. that we have $f'_{\infty,j}[p_{k+1}]$. The intersection

$$\left(\hat{G}_{\text{res}} - \alpha C'_0 \right) \cdot C'_0 = 6 - (6 - \alpha)(n + n_0) \quad (\text{B.6.59})$$

leads to a factorization of at least $3C'_0$. Then,

$$\left(\hat{G}_{\text{res}} - 3C'_0 - \alpha f'_{\infty,j}[p_{k+1}] \right) \cdot f'_{\infty,j}[p_{k+1}] = 3 - (6 - \alpha)j, \quad (\text{B.6.60})$$

with $j \geq 1$. This leads to a factorization of at least $3f'_{\infty,j}[p_{k+1}]$. This means, in turn, that

$$\left(\hat{G}_{\text{res}} - 3C'_0 - 3f'_{\infty,j}[p_{k+1}] - \alpha C'_0 \right) \cdot C'_0 = 3 - (3 - \alpha)(n + n_0), \quad (\text{B.6.61})$$

forcing an additional factorization of at least $2C'_0$. Then

$$\left(\hat{G}_{\text{res}} - 5C'_0 - 3f'_{\infty,j}[p_{k+1}] - \alpha f'_{\infty,j}[p_{k+1}] \right) \cdot f'_{\infty,j}[p_{k+1}] = 1 - (3 - \alpha)j, \quad (\text{B.6.62})$$

leading to a further factorization of at least $2f'_{\infty,j}[p_{k+1}]$. Finally, since

$$\left(\hat{G}_{\text{res}} - 5C'_0 - 5f'_{\infty,i}[p_{k+1}] - \alpha C'_0 \right) \cdot C'_0 = 1 - (1 - \alpha)(n + n_0), \quad (\text{B.6.63})$$

C'_0 factorizes non-minimally, with $C'_0 \cdot \tilde{f} = 1$.

Assume instead that the intersection point of the representative $f[p_{k+1}]$ of f and C_0 was blown-up, i.e. that we have $f'_{0/\infty,j}[p_{k+1}]$. In the case at hand, we observe that $n \geq 1$, $n_0 \geq 2$ and $j \geq 2$. Then,

$$\begin{aligned} \hat{G}_{\text{res}} &\longrightarrow \hat{G}_{\text{res}} - 4C'_0 - 3f'_{0/\infty,j}[p_{k+1}] \\ &\longrightarrow \hat{G}_{\text{res}} - 4C'_0 - 3f'_{0/\infty,j}[p_{k+1}] - E_l^0[p_{k+1}] \\ &\longrightarrow \hat{G}_{\text{res}} - 5C'_0 - 4f'_{0/\infty,j}[p_{k+1}] - E_l^0[p_{k+1}] \\ &\longrightarrow \hat{G}_{\text{res}} - 5C'_0 - 4f'_{0/\infty,j}[p_{k+1}] - 3E_l^0[p_{k+1}] \\ &\longrightarrow \hat{G}_{\text{res}} - 6C'_0 - 5f'_{0/\infty,j}[p_{k+1}] - 3E_l^0[p_{k+1}], \end{aligned} \quad (\text{B.6.64})$$

with $C'_0 \cdot \tilde{f} = 1$.

- $\{E_{k+1}^\infty, \tilde{f}, E_i^\infty\}$: This case works analogously to the previous one, but starting from $n \geq 2$ and $n_0 \geq 0$.
- (3.a.v) $\{E_{k+1}^\infty, f'_{\infty,i}[\neg p_{k+1}], \cdot\}$: This case is analogous to Case (3.a.iv).
- (3.a.vi) $\{E_{k+1}^\infty, f'_{0,i}, \cdot\}$: The following divisors still need to be considered as valid triplet completions: $f'_{0,j}$, $f'_{0/\infty,j}[\neg p_{k+1}]$, E_i^0 and E_i^∞ .

- $\{E_{k+1}^\infty, f'_{0,i}, f'_{0,j}\}$, $\{E_{k+1}^\infty, f'_{0,i}, f'_{0/\infty,j}[\neg p_{k+1}]\}$ and $\{E_{k+1}^\infty, f'_{0,i}, E_j^0\}$ all imply that $n \geq 1$ and $n_0 \geq 2$.

Assume first that the intersection point of the representative $f[p_{k+1}]$ of f and C_0 was not blown-up, i.e. that we have $f'_{\infty,l}[p_{k+1}]$. Under this assumption, we have the cascade of factorizations

$$\begin{aligned} \hat{G}_{\text{res}} &\longrightarrow \hat{G}_{\text{res}} - 2C'_0 \\ &\longrightarrow \hat{G}_{\text{res}} - 2C'_0 - 2f'_{\infty,l}[p_{k+1}] \\ &\longrightarrow \hat{G}_{\text{res}} - 3C'_0 - 2f'_{\infty,l}[p_{k+1}] \\ &\longrightarrow \hat{G}_{\text{res}} - 3C'_0 - 3f'_{\infty,l}[p_{k+1}] \end{aligned}$$

$$\begin{aligned}
&\longrightarrow \hat{G}_{\text{res}} - 3C'_0 - 3f'_{\infty,l}[p_{k+1}] - 3E_m^0[C'_0, f'_{0,i}] \\
&\longrightarrow \hat{G}_{\text{res}} - 4C'_0 - 3f'_{\infty,l}[p_{k+1}] - 3E_m^0[C'_0, f'_{0,i}] \\
&\longrightarrow \hat{G}_{\text{res}} - 4C'_0 - 4f'_{\infty,l}[p_{k+1}] - 4E_m^0[C'_0, f'_{0,i}] \\
&\longrightarrow \hat{G}_{\text{res}} - 5C'_0 - 4f'_{\infty,l}[p_{k+1}] - 4E_m^0[C'_0, f'_{0,i}] \\
&\longrightarrow \hat{G}_{\text{res}} - 5C'_0 - 5f'_{\infty,l}[p_{k+1}] - 5E_m^0[C'_0, f'_{0,i}] \\
&\longrightarrow \hat{G}_{\text{res}} - 6C'_0 - 5f'_{\infty,l}[p_{k+1}] - 5E_m^0[C'_0, f'_{0,i}] \\
&\longrightarrow \hat{G}_{\text{res}} - 6C'_0 - 6f'_{\infty,l}[p_{k+1}] - 6E_m^0[C'_0, f'_{0,i}],
\end{aligned} \tag{B.6.65}$$

with $f'_{\infty,l}[p_{k+1}] \cdot E_{k+1}^\infty = 1$ and $E_m^0[C'_0, f'_{0,i}] \cdot f'_{0,i} = 1$.

Assume first that the intersection point of the representative $f[p_{k+1}]$ of f and C_0 was blown-up, i.e. that we have $f'_{0/\infty,l}[p_{k+1}]$. This implies that $n \geq 1$, $n_0 \geq 3$ and $l \geq 2$. This leads to the cascade of factorizations

$$\begin{aligned}
\hat{G}_{\text{res}} &\longrightarrow \hat{G}_{\text{res}} - 3C'_0 - 3f'_{0/\infty,l}[p_{k+1}] \\
&\longrightarrow \hat{G}_{\text{res}} - 3C'_0 - 3f'_{0/\infty,l}[p_{k+1}] - 3E_m^0[C'_0, f'_{0,i}] \\
&\longrightarrow \hat{G}_{\text{res}} - 4C'_0 - 3f'_{0/\infty,l}[p_{k+1}] - 3E_m^0[C'_0, f'_{0,i}] \\
&\longrightarrow \hat{G}_{\text{res}} - 4C'_0 - 3f'_{0/\infty,l}[p_{k+1}] - 4E_m^0[C'_0, f'_{0,i}] \\
&\longrightarrow \hat{G}_{\text{res}} - 4C'_0 - 3f'_{0/\infty,l}[p_{k+1}] - 4E_m^0[C'_0, f'_{0,i}] - E_n^0[C'_0, f'_{0/\infty,l}[p_{k+1}]] \\
&\longrightarrow \hat{G}_{\text{res}} - 5C'_0 - 4f'_{0/\infty,l}[p_{k+1}] - 4E_m^0[C'_0, f'_{0,i}] - E_n^0[C'_0, f'_{0/\infty,l}[p_{k+1}]] \\
&\longrightarrow \hat{G}_{\text{res}} - 5C'_0 - 4f'_{0/\infty,l}[p_{k+1}] - 5E_m^0[C'_0, f'_{0,i}] - 3E_n^0[C'_0, f'_{0/\infty,l}[p_{k+1}]] \\
&\longrightarrow \hat{G}_{\text{res}} - 5C'_0 - 5f'_{0/\infty,l}[p_{k+1}] - 5E_m^0[C'_0, f'_{0,i}] - 3E_n^0[C'_0, f'_{0/\infty,l}[p_{k+1}]] \\
&\longrightarrow \hat{G}_{\text{res}} - 5C'_0 - 5f'_{0/\infty,l}[p_{k+1}] - 5E_m^0[C'_0, f'_{0,i}] - 4E_n^0[C'_0, f'_{0/\infty,l}[p_{k+1}]] \\
&\longrightarrow \hat{G}_{\text{res}} - 6C'_0 - 6f'_{0/\infty,l}[p_{k+1}] - 5E_m^0[C'_0, f'_{0,i}] - 4E_n^0[C'_0, f'_{0/\infty,l}[p_{k+1}]],
\end{aligned} \tag{B.6.66}$$

with $f'_{0/\infty,l}[p_{k+1}] \cdot E_{k+1}^\infty = 1$.

- (3.a.vii) $\{E_{k+1}^\infty, f'_{0/\infty,j}[\neg p_{k+1}], \bullet\}$: This case is analogous to Case (3.a.vi).
- (3.a.viii) $\{E_{k+1}^\infty, E_i^0, \bullet\}$: Tuning these two divisors to be non-minimal leaves us with the residual \hat{G} divisor

$$\hat{G}_{\text{res}} = 12\tilde{C}_0 + (12 + 6n)\tilde{f} - \sum_{i=1}^{n_p} E_i - 12E_{k+1}^\infty - 6E_i^0, \tag{B.6.67}$$

which yields the intersection

$$\left(\hat{G}_{\text{res}} - \alpha C'_0 \right) \cdot C'_0 = -(6 - \alpha)(n + n_0). \tag{B.6.68}$$

This leads to a non-minimal factorization of C'_0 , with $C'_0 \cdot E_i^0 = 1$

- (3.a.ix) $\{E_{k+1}^\infty, E_i^\infty, \bullet\}$: The only candidate for triplet completion left is a third E_j^∞ . Tuning $\{E_{k+1}^\infty, E_i^\infty, E_j^\infty\}$ gives the residual \hat{G} divisor

$$\hat{G}_{\text{res}} = 12\tilde{C}_0 + (12 + 6n)\tilde{f} - \sum_{i=1}^{n_p} E_i - 12E_{k+1}^\infty - 6E_i^\infty - 6E_j^\infty. \tag{B.6.69}$$

We now need to distinguish two subcases depending on the existing relation among these exceptional divisors.

- If at least two of E_{k+1}^∞ , E_i^∞ and E_j^∞ stem from blow-ups of the same representative of f (say $f[p_{k+1}, p_i]$, for concreteness), we have

$$\left(\hat{G}_{\text{res}} - \alpha f[p_{k+1}, p_i] \right) \cdot f[p_{k+1}, p_i] \leq -(6 - \alpha)j, \quad (\text{B.6.70})$$

yielding a non-minimal factorization of $f[p_{k+1}, p_i]$, with $f[p_{k+1}, p_i] \cdot E_{k+1} = 1$.

- If E_{k+1}^∞ , E_i^∞ and E_j^∞ each stem from the blow-up of a different representative of f , we need to have $n \geq 4$ to satisfy the effectiveness bounds. We now need to distinguish the cases in which the intersection points of said representatives of f with C_0 have not been blown-up, and those in which they have. We consider the two extreme cases, in which none or all of them have been blown-up, with the intermediate cases leading to hybrids of the factorization cascades presented below.

Assume first that none of the intersection points of the three relevant representatives of f with C_0 have been blown-up. We then have

$$\begin{aligned} \hat{G}_{\text{res}} &\longrightarrow \hat{G}_{\text{res}} - 3C'_0 \\ &\longrightarrow \hat{G}_{\text{res}} - 3C'_0 - 3f'_{\infty,l}[p_{k+1}] - 3f'_{\infty,m}[p_i] - 3f'_{\infty,n}[p_j] \\ &\longrightarrow \hat{G}_{\text{res}} - 6C'_0 - 3f'_{\infty,l}[p_{k+1}] - 3f'_{\infty,m}[p_i] - 3f'_{\infty,n}[p_j] \\ &\longrightarrow \hat{G}_{\text{res}} - 6C'_0 - 6f'_{\infty,l}[p_{k+1}] - 6f'_{\infty,m}[p_i] - 6f'_{\infty,n}[p_j], \end{aligned} \quad (\text{B.6.71})$$

with $f'_{\infty,l}[p_{k+1}] \cdot E_{k+1}^\infty = 1$, etc.

Assume now that the intersection points of the three relevant representatives of f with C_0 have been blown-up. This not only entails $n \geq 4$, but also $n_0 \geq 3$. We then have

$$\begin{aligned} \hat{G}_{\text{res}} &\longrightarrow \hat{G}_{\text{res}} - 5C'_0 - 3f'_{0/\infty,l}[p_{k+1}] - 3f'_{0/\infty,m}[p_i] - 3f'_{0/\infty,n}[p_j] \\ &\longrightarrow \hat{G}_{\text{res}} - 5C'_0 - 3f'_{0/\infty,l}[p_{k+1}] - 3f'_{0/\infty,m}[p_i] - 3f'_{0/\infty,n}[p_j] \\ &\quad - 2E_{k+1}^0 - 2E_i^0 - 2E_j^0 \\ &\longrightarrow \hat{G}_{\text{res}} - 7C'_0 - 4f'_{0/\infty,l}[p_{k+1}] - 4f'_{0/\infty,m}[p_i] - 4f'_{0/\infty,n}[p_j] \\ &\quad - 2E_{k+1}^0 - 2E_i^0 - 2E_j^0 \\ &\longrightarrow \hat{G}_{\text{res}} - 7C'_0 - 4f'_{0/\infty,l}[p_{k+1}] - 4f'_{0/\infty,m}[p_i] - 4f'_{0/\infty,n}[p_j] \\ &\quad - 5E_{k+1}^0 - 5E_i^0 - 5E_j^0 \\ &\longrightarrow \hat{G}_{\text{res}} - 9C'_0 - 7f'_{0/\infty,l}[p_{k+1}] - 7f'_{0/\infty,m}[p_i] - 7f'_{0/\infty,n}[p_j] \\ &\quad - 5E_{k+1}^0 - 5E_i^0 - 5E_j^0, \end{aligned} \quad (\text{B.6.72})$$

with $f'_{0/\infty,l}[p_{k+1}] \cdot E_{k+1}^\infty = 1$, etc.

- (3.b) $\{C'_{\infty,i}[p_{k+1}], \cdot, \cdot\}$: $C'_{\infty,i}[p_{k+1}]$ intersects the strict transforms \tilde{C}_∞ , $\tilde{C}_\infty[\neg p\{C'_{\infty,i}[p_{k+1}]\}]$, \tilde{f} , $f'_{\infty,j}[\neg p\{C'_{\infty,i}[p_{k+1}]\}]$, $f'_{0,j}[\neg p\{C'_{\infty,i}[p_{k+1}]\}]$, $f'_{0/\infty,j}[\neg p\{C'_{\infty,i}[p_{k+1}]\}]$, and the exceptional divisors $E_j^\infty[C'_{\infty,i}[p_{k+1}]]$. We need to consider as candidates for triplet completion: C'_0 , $f'_{\infty,j}[p\{C'_{\infty,i}[p_{k+1}]\}]$, $f'_{0/\infty,j}[p\{C'_{\infty,i}[p_{k+1}]\}]$, E_j^0 and $E_j^\infty[\neg C'_{\infty,i}[p_{k+1}]]$.

- (3.b.i) $\{C'_{\infty,i}[p_{k+1}], C'_0, \cdot\}$: The only possible triplet completions not intersecting the curves $C'_{\infty,i}[p_{k+1}]$ or C'_0 are $f'_{0/\infty,j}[p_{k+1}]$ and $E_j^\infty[\neg C'_{\infty,i}[p_{k+1}]]$.
- Tuning $\{C'_{\infty,i}[p_{k+1}], C'_0, f'_{0/\infty,j}[p\{C'_{\infty,i}[p_{k+1}]\}]\}$ leads to

$$\left(\hat{G}_{\text{res}} - \alpha E_l^0[f'_{0/\infty,j}[p\{C'_{\infty,i}[p_{k+1}]\}]] \right) \cdot E_l^0[f'_{0/\infty,j}[p\{C'_{\infty,i}[p_{k+1}]\}]] = -6 + \alpha, \quad (\text{B.6.73})$$

meaning that $E_l^0[f'_{0/\infty,j}[p\{C'_{\infty,i}[p_{k+1}]\}]]$ factorizes non-minimally with the intersection $E_l^0[f'_{0/\infty,j}[p\{C'_{\infty,i}[p_{k+1}]\}]] \cdot C'_0 = 1$.

- Tuning $\{C'_{\infty,i}[p_{k+1}], C'_0, E_j^\infty[\neg C'_{\infty,i}[p_{k+1}]]\}$ is analogous to Case (3.a.i).

- (3.b.ii) $\{C'_{\infty,i}[p_{k+1}], f'_{\infty,j}[p_{k+1}], \cdot\}$: This leads to the intersection

$$\left(\hat{G}_{\text{res}} - \alpha E_{k+1}^\infty \right) \cdot E_{k+1}^\infty = -6 + \alpha, \quad (\text{B.6.74})$$

making E_{k+1}^∞ factorize non-minimally, with $E_{k+1}^\infty \cdot f'_{\infty,j}[p_{k+1}] = 1$.

- (3.b.iii) $\{C'_{\infty,i}[p_{k+1}], f'_{0/\infty,j}[p_{k+1}], \cdot\}$: This case is analogous to Case (3.b.ii).

- (3.b.iv) $\{C'_{\infty,i}[p_{k+1}], E_j^0, \cdot\}$: Consider the representative $f[p_j]$ of f passing through the blow-up centre from which E_j^0 stems. Depending on if the intersection point of $f[p_j]$ with $C'_{\infty,i}[p_{k+1}]$ has been blown-up or not, we distinguish two cases.

Assume first that it has not been blown-up. We then have

$$\left(\hat{G}_{\text{res}} - \alpha f'_{0,l}[p_j] \right) \cdot f'_{0,l}[p_j] = -(6 - \alpha)l \quad (\text{B.6.75})$$

with $l \geq 1$, leading to $f'_{0,l}[p_j]$ factorizing non-minimally with $f'_{0,l}[p_j] \cdot E_j^0 = 1$. Assume now that it has been blown-up. Then, the cascade of factorizations

$$\begin{aligned} \hat{G}_{\text{res}} &\longrightarrow \hat{G}_{\text{res}} - 3f'_{0/\infty,l}[p_j] \\ &\longrightarrow \hat{G}_{\text{res}} - 3f'_{0/\infty,l}[p_j] - 3E_m^\infty[f'_{0/\infty,l}[p_j]] \\ &\longrightarrow \hat{G}_{\text{res}} - 5f'_{0/\infty,l}[p_j] - 3E_m^\infty[f'_{0/\infty,l}[p_j]] \\ &\longrightarrow \hat{G}_{\text{res}} - 5f'_{0/\infty,l}[p_j] - 5E_m^\infty[f'_{0/\infty,l}[p_j]] \\ &\longrightarrow \hat{G}_{\text{res}} - 6f'_{0/\infty,l}[p_j] - 5E_m^\infty[f'_{0/\infty,l}[p_j]] \end{aligned} \quad (\text{B.6.76})$$

makes $f'_{0/\infty,l}[p_j]$ factorize non-minimally, with $f'_{0/\infty,l}[p_j] \cdot E_j^0 = 1$.

- (3.b.v) $\{C'_{\infty,i}[p_{k+1}], E_i^\infty[\neg C'_{\infty,i}[p_{k+1}]], \cdot\}$: This case is analogous to Case (3.a.iii).

- (3.c) $\{f'_{\infty,i}[p_{k+1}], \cdot, \cdot\}$: $f'_{\infty,i}[p_{k+1}]$ intersects $C'_0, \tilde{C}_\infty, C'_{\infty,j}[\neg p\{f'_{\infty,i}[p_{k+1}]\}]$ and the exceptional divisor E_{k+1}^∞ . We need to study the factorizations forced by the following triplet completion candidates: $C'_{\infty,j}[p\{f'_{\infty,i}[p_{k+1}]\}], \tilde{f}, f'_{0,j}[\neg p_{k+1}], f'_{\infty,j}[\neg p_{k+1}], f'_{0/\infty,j}[\neg p_{k+1}], E_j^0$ and $E_j^\infty[\neg p\{f'_{\infty,i}[p_{k+1}]\}]$.

- (3.c.i) $\{f'_{\infty,i}[p_{k+1}], C'_{\infty,j}[p\{f'_{\infty,i}[p_{k+1}]\}], \cdot\}$: This leads to the intersection

$$\left(\hat{G}_{\text{res}} - \alpha E_l^\infty[f'_{\infty,i}, C'_{\infty,j}] \right) \cdot E_l^\infty[f'_{\infty,i}, C'_{\infty,j}] = -6 + \alpha, \quad (\text{B.6.77})$$

meaning that $E_l^\infty[f'_{\infty,i}, C'_{\infty,j}]$ factorizes non-minimally, while having the intersections $E_l^\infty[f'_{\infty,i}, C'_{\infty,j}] \cdot f'_{\infty,i}[p_{k+1}] = 1$ and $E_l^\infty[f'_{\infty,i}, C'_{\infty,j}] \cdot C'_{\infty,j}[p\{f'_{\infty,i}[p_{k+1}]\}] = 1$.

(3.c.ii) $\{f'_{\infty,i}[p_{k+1}], \tilde{f}, \bullet\}$: Due to the intersection

$$\left(\hat{G}_{\text{res}} - \alpha C'_0 \right) \cdot C'_0 = -(6 - \alpha)(n + n_0), \quad (\text{B.6.78})$$

we have a non-minimal factorization of C'_0 , with $C'_0 \cdot f'_{\infty,i}[p_{k+1}] = 1$.

(3.c.iii) $\{f'_{\infty,i}[p_{k+1}], f'_{0,j}[\neg p_{k+1}], \bullet\}$: This tuning leads to the cascade of factorizations

$$\begin{aligned} \hat{G}_{\text{res}} &\longrightarrow \hat{G}_{\text{res}} - 3C'_0 \\ &\longrightarrow \hat{G}_{\text{res}} - 3C'_0 - 3E_l^0[f'_{0,j}] \\ &\longrightarrow \hat{G}_{\text{res}} - 5C'_0 - 3E_l^0[f'_{0,j}] \\ &\longrightarrow \hat{G}_{\text{res}} - 5C'_0 - 5E_l^0[f'_{0,j}] \\ &\longrightarrow \hat{G}_{\text{res}} - 6C'_0 - 5E_l^0[f'_{0,j}], \end{aligned} \quad (\text{B.6.79})$$

with C'_0 factorizing non-minimally and $C'_0 \cdot f'_{\infty,i}[p_{k+1}] = 1$.

(3.c.iv) $\{f'_{\infty,i}[p_{k+1}], f'_{\infty,j}[\neg p_{k+1}], \bullet\}$: This case is analogous to Case (3.c.ii).

(3.c.v) $\{f'_{\infty,i}[p_{k+1}], f'_{0/\infty,j}[\neg p_{k+1}], \bullet\}$: This case is analogous to Case (3.c.iii).

(3.c.vi) $\{f'_{\infty,i}[p_{k+1}], E_i^0, \bullet\}$: This leads to the intersection

$$\left(\hat{G}_{\text{res}} - \alpha C'_0 \right) \cdot C'_0 = -(6 - \alpha)(n + n_0), \quad (\text{B.6.80})$$

from which we see that C'_0 factorizes non-minimally, with $C'_0 \cdot E_i^0 = 1$.

(3.c.vii) $\{f'_{\infty,i}[p_{k+1}], E_j^\infty[\neg p\{f'_{\infty,i}[p_{k+1}]\}], \bullet\}$: This case is analogous to Case (3.a.iv).

(3.d) $\{f'_{0/\infty,i}[p_{k+1}], \bullet, \bullet\}$: $f'_{0/\infty,i}[p_{k+1}]$ intersects \tilde{C}_∞ , $C'_{\infty,j}[\neg p\{f'_{0/\infty,i}[p_{k+1}]\}]$ and the exceptional divisor E_{k+1}^∞ . We need to study the factorizations forced by the following candidates for triplet completion: C'_0 , $C'_{\infty,j}[p\{f'_{0/\infty,i}[p_{k+1}]\}]$, \tilde{f} , $f'_{0,j}[\neg p_{k+1}]$, $f'_{\infty,j}[\neg p_{k+1}]$, $E_j^0[\neg f'_{0/\infty,i}[p_{k+1}]]$ and $E_j^\infty[\neg p\{f'_{0/\infty,i}[p_{k+1}]\}]$.

(3.d.i) $\{f'_{0/\infty,i}[p_{k+1}], C'_0, \bullet\}$: Let us denote the intersection points of the pushforwards $f[p_{k+1}] \cap C_0 =: p_j$. Tuning these divisors to be non-minimal leads

$$\left(\hat{G}_{\text{res}} - \alpha E_l^0[p_j] \right) \cdot E_l^0[p_j] = -6 + \alpha, \quad (\text{B.6.81})$$

from which we see that $E_l^0[p_j]$ factorizes non-minimally, with the intersections $E_l^0[p_j] \cdot f'_{0/\infty,i}[p_{k+1}] = 1$ and $E_l^0[p_j] \cdot C'_0 = 1$.

(3.d.ii) $\{f'_{0/\infty,i}[p_{k+1}], C'_{\infty,j}[p\{f'_{0/\infty,i}[p_{k+1}]\}], \bullet\}$: This case is analogous to Case (3.c.i).

(3.d.iii) $\{f'_{0/\infty,i}[p_{k+1}], \tilde{f}, \bullet\}$: This leads to the cascade of factorizations

$$\begin{aligned} \hat{G}_{\text{res}} &\longrightarrow \hat{G}_{\text{res}} - 3C'_0 \\ &\longrightarrow \hat{G}_{\text{res}} - 3C'_0 - 3E_j^0[f'_{0/\infty,i}[p_{k+1}]] \\ &\longrightarrow \hat{G}_{\text{res}} - 5C'_0 - 3E_j^0[f'_{0/\infty,i}[p_{k+1}]] \\ &\longrightarrow \hat{G}_{\text{res}} - 5C'_0 - 5E_j^0[f'_{0/\infty,i}[p_{k+1}]] \\ &\longrightarrow \hat{G}_{\text{res}} - 6C'_0 - 5E_j^0[f'_{0/\infty,i}[p_{k+1}]] \\ &\longrightarrow \hat{G}_{\text{res}} - 6C'_0 - 6E_j^0[f'_{0/\infty,i}[p_{k+1}]], \end{aligned} \quad (\text{B.6.82})$$

such that $E_j^0[f'_{0/\infty,i}[p_{k+1}]]$ factorizes non-minimally with the intersection product $E_j^0[f'_{0/\infty,i}[p_{k+1}]] \cdot f'_{0/\infty,i}[p_{k+1}] = 1$.

(3.d.iv) $\{f'_{0/\infty,i}[p_{k+1}], f'_{0,j}[\neg p_{k+1}], \cdot\}$: This leads to the cascade of factorizations

$$\begin{aligned}
\hat{G}_{\text{res}} &\longrightarrow \hat{G}_{\text{res}} - 2C'_0 \\
&\longrightarrow \hat{G}_{\text{res}} - 2C'_0 - 2E_l^0[f'_{0/\infty,i}[p_{k+1}]] - 2E_m^0[f'_{0,j}[\neg p_{k+1}]] \\
&\longrightarrow \hat{G}_{\text{res}} - 4C'_0 - 2E_l^0[f'_{0/\infty,i}[p_{k+1}]] - 2E_m^0[f'_{0,j}[\neg p_{k+1}]] \\
&\longrightarrow \hat{G}_{\text{res}} - 4C'_0 - 4E_l^0[f'_{0/\infty,i}[p_{k+1}]] - 4E_m^0[f'_{0,j}[\neg p_{k+1}]] \\
&\longrightarrow \hat{G}_{\text{res}} - 5C'_0 - 4E_l^0[f'_{0/\infty,i}[p_{k+1}]] - 4E_m^0[f'_{0,j}[\neg p_{k+1}]] \\
&\longrightarrow \hat{G}_{\text{res}} - 5C'_0 - 5E_l^0[f'_{0/\infty,i}[p_{k+1}]] - 5E_m^0[f'_{0,j}[\neg p_{k+1}]] \\
&\longrightarrow \hat{G}_{\text{res}} - 6C'_0 - 5E_l^0[f'_{0/\infty,i}[p_{k+1}]] - 5E_m^0[f'_{0,j}[\neg p_{k+1}]] \\
&\longrightarrow \hat{G}_{\text{res}} - 6C'_0 - 6E_l^0[f'_{0/\infty,i}[p_{k+1}]] - 6E_m^0[f'_{0,j}[\neg p_{k+1}]] ,
\end{aligned} \tag{B.6.83}$$

from where we see that $E_l^0[f'_{0/\infty,i}[p_{k+1}]]$ and $E_m^0[f'_{0,j}[\neg p_{k+1}]]$ non-minimally factorize, with $E_l^0[f'_{0/\infty,i}[p_{k+1}]] \cdot f'_{0/\infty,i}[p_{k+1}] = 1$ and $E_m^0[f'_{0,j}[\neg p_{k+1}]] \cdot f'_{0,j}[\neg p_{k+1}] = 1$.

(3.d.v) $\{f'_{0/\infty,i}[p_{k+1}], f'_{\infty,j}[\neg p_{k+1}], \cdot\}$: This case is analogous to Case (3.d.iii).

(3.d.vi) $\{f'_{0/\infty,i}[p_{k+1}], f'_{0/\infty,j}[\neg p_{k+1}], \cdot\}$: This case is analogous to Case (3.d.iv).

(3.d.vii) $\{f'_{0/\infty,i}[p_{k+1}], E_j^0[\neg f'_{0/\infty,i}[p_{k+1}]], \cdot\}$: Tuning these divisors to be non-minimal leads to the cascade of factorizations

$$\begin{aligned}
\hat{G}_{\text{res}} &\longrightarrow \hat{G}_{\text{res}} - 4C'_0 \\
&\longrightarrow \hat{G}_{\text{res}} - 4C'_0 - 4f'_{0/(\infty),l}[E_j^0[\neg f'_{0/\infty,i}[p_{k+1}]]] \\
&\longrightarrow \hat{G}_{\text{res}} - 5C'_0 - 4f'_{0/(\infty),l}[E_j^0[\neg f'_{0/\infty,i}[p_{k+1}]]] \\
&\longrightarrow \hat{G}_{\text{res}} - 5C'_0 - 5f'_{0/(\infty),l}[E_j^0[\neg f'_{0/\infty,i}[p_{k+1}]]] \\
&\longrightarrow \hat{G}_{\text{res}} - 6C'_0 - 5f'_{0/(\infty),l}[E_j^0[\neg f'_{0/\infty,i}[p_{k+1}]]] ,
\end{aligned} \tag{B.6.84}$$

from where we see that C'_0 factorizes non-minimally, with the intersection product $C'_0 \cdot E_j^0[\neg f'_{0/\infty,i}[p_{k+1}]] = 1$.

(3.d.viii) $\{f'_{0/\infty,i}[p_{k+1}], E_j^\infty[\neg p\{f'_{0/\infty,i}[p_{k+1}]\}], \cdot\}$: This case is analogous to Case (3.d.vii).

□

B.6.3 Models constructed over the remaining $\text{Bl}(\mathbb{F}_n)$

With Proposition B.6.1 and Proposition B.6.3 at hand, we have established the result of Proposition B.5.1 for Calabi-Yau Weierstrass models over $\hat{B}_0 = \mathbb{P}^2$, $\hat{B}_0 = \mathbb{F}_n$, and their type (A) blow-ups. Proceeding in the same fashion, one can extend the result to the $\hat{B}_0 = \text{Bl}(\mathbb{F}_n)$ surfaces obtained by also including type (B), (C) and (D) blow-ups. Since this is not a very enlightening discussion, we choose instead to comment on some features of these additional cases and give two detailed examples showing that the prospects of finding a triplet of curves violating Proposition B.5.1 are not improved by performing these types of blow-ups.

B.6.3.1 Type (B) blow-ups

Let us start by considering also type (B) blow-ups. i.e. the ones performed over generic points of exceptional divisors, away from the intersections of these with other divisors.

We recall from Section B.1.3.2, that after performing type (A) and (B) blow-ups the anticanonical class of the surface is given by (B.1.32), which we can write

$$\overline{K}_{\hat{B}} = 2\tilde{C}_0 + (2+n)\tilde{f} - \sum_{\alpha} d_{\alpha} E_{\alpha}, \quad d_{\alpha} = \text{level of the exceptional divisor} \geq 1. \quad (\text{B.6.85})$$

The discrepancies of the exceptional divisors grow the deeper they are located within a chain of type (B) blow-ups. However, in the analogues of the linear equivalences (B.6.12) and (B.6.13) all exceptional divisors appear with coefficient one, given that type (B) divisors only affect a single exceptional divisor at a time. As a consequence, the effectiveness bounds become more stringent as we perform further type (B) blow-ups.

To give a first example of this, consider the surfaces $\hat{B}_0 = \text{Bl}(\mathbb{F}_0)$ in which we have performed a single type (A) blow-up, giving rise to an exceptional divisor on which we then perform type (B) blow-ups. It is then clear that for the anticanonical class $\overline{K}_{\hat{B}_0}$ to be effective we need

$$\max_{\alpha} (d_{\alpha}) \leq 4. \quad (\text{B.6.86})$$

Both this bound and the ones we will discuss below are not modified by the number of points blown up in a given exceptional divisor; the only relevant aspect is the mismatch between the discrepancies and the appearance of the exceptional divisors in the strict transforms of the \tilde{C}_0 and \tilde{f} representatives. If we have a second chain of type (B) blow-ups on the exceptional divisor of a type (A) blow-up of a generic point in the original surface, we obtain

$$\max_{\alpha_1} (d_{\alpha_1}^1) + \max_{\alpha_2} (d_{\alpha_2}^2) \leq 4. \quad (\text{B.6.87})$$

Since we are assuming these to be chains of type (B) blow-ups we have $d_{\alpha}^i \geq 2$ for $i = 1, 2$, concluding that two type (B) chains in general position are the best we can do. The situation can be improved by performing the type (B) blow-ups over exceptional divisor arising from type (A) blow-ups with centre at points on the same representatives of C_0 of f . In this way, we can achieve at most four type (B) chains going up to level two.

Moving to the surfaces $\hat{B}_0 = \text{Bl}(\mathbb{F}_n)$, with $1 \leq n \leq 12$, we can argue in the same fashion that

$$\sum_{i=1}^{n_0} \left(\max_{\alpha_i} d_{\alpha_i}^i - 2 \right) \theta \left(\max_{\alpha_i} d_{\alpha_i}^i - 2 \right) + \sum_{i=1}^{n_{\infty}} \max_{\alpha_i} d_{\alpha_i}^i \leq n + 2 \quad (\text{B.6.88})$$

for $\overline{K}_{\hat{B}_0}$ to be effective. The first term is shifted to account for the fact that C_0 has a unique representative, whose total transform \tilde{C}_0 can account for discrepancies of up to two units. The Heaviside function prevents this term from giving negative contributions.

The bounds given above ensure that $\overline{K}_{\hat{B}_0}$ is effective after the blow-up, but tuning an exceptional divisor E_i to be non-minimal requires $E_i \leq \overline{K}_{\hat{B}_0}$, according to Proposition B.2.2. Hence, the l.h.s. of (B.6.88) must be increased by one unit if we want to tune any exceptional divisor related to a type (A) blow-up at $p \in C_0$, and one unit for each exceptional divisor related to a type (A) blow-up at $p \notin C_0$ on distinct representatives of f , cf. (B.6.15).

Carefully taking these bounds into account is relevant in order to discard some candidate triplets when generalizing the results of Proposition B.6.3 to include type (B) blow-ups. In this regard, we can also note that, due to Lemma B.6.2, we only need to take into account at each step candidate triplets $\{E_{p+1}, \cdot, \cdot\}$, where E_{p+1} is the exceptional divisor arising from the last type (B) blow-up. The candidate triplets including the strict transform of the exceptional divisor

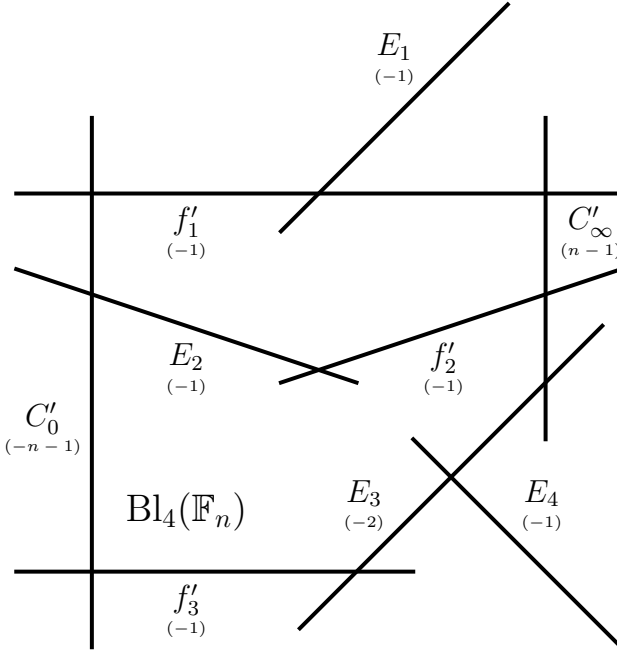


Figure B.10: Surface $\hat{B}_0 = \text{Bl}_4(\mathbb{F}_n)$ obtained by performing three type (A) and one type (B) blow-ups on the Hirzebruch surface \mathbb{F}_n . The self-intersection of the depicted curves is shown below their names in parentheses.

E_p that E_{p+1} is stemming from behave in the same way as they did in the blown down surface and do not need to be checked again. One can see that tuning E_{p+1} to be non-minimal can trigger a non-minimal factorization of E_p if the level of E_{p+1} is too high. This does not occur in the example that we now analyse, but a factorization of various copies of E_p can already be observed for a rather short sequence of type (B) blow-ups.

Example B.6.4. Consider a Hirzebruch surface \mathbb{F}_n in which three type (A) blow-ups have been performed, $n_0 = 1$ at a point $p \in C_0$ with exceptional divisor E_1 , and $n_{\infty} = n_{\infty}^{\text{tot}} = 2$ at two points $p \notin C_0$ in distinct representatives of the fiber class f with exceptional divisors E_2 and E_3 . Perform then a further blow-up of type (B) on the exceptional divisor E_3 to arrive at the six-dimensional F-theory base $\hat{B}_0 = \text{Bl}_4(\mathbb{F}_n)$. The intersection properties of the strict transforms of the curves affected by the successive blow-ups are represented in Figure B.10.

The anticanonical class $\bar{K}_{\hat{B}_0}$ after the blow-ups can be written as

$$\bar{K}_{\hat{B}_0} = 2\tilde{C}_0 + (2+n)\tilde{f} - E_1 - E_2 - E_3 - 2E_4. \quad (\text{B.6.89})$$

It is useful to recall that we have the linear equivalences

$$\tilde{C}_0 = C'_0 + E_2, \quad (\text{B.6.90a})$$

$$\tilde{f} = f'_1 + E_1, \quad (\text{B.6.90b})$$

$$\tilde{f} = f'_2 + E_2, \quad (\text{B.6.90c})$$

$$\tilde{f} = f'_3 + E_3 + E_4, \quad (\text{B.6.90d})$$

from where we see that we need $n \geq 1$ for $\bar{K}_{\hat{B}_0}$ to be effective, as can be read in (B.6.88). The type (B) blow-up opens the possibility of a $\{E_4, \cdot, \cdot\}$ triplet perhaps violating Proposition B.5.1.

Let us explore this possibility by first tuning E_4 to be non-minimal, which leads to the \hat{G} divisor

$$\hat{G} = (6E_4) + \left[12\tilde{C}_0 + (12 + 6n)\tilde{f} - 6E_1 - 6E_2 - 6E_3 - 18E_4 \right], \quad (\text{B.6.91})$$

where in parentheses we are showing the factorized curves and in square brackets the class of \hat{G}_{res} . This tuning increases the effectiveness bound to $n \geq 2$. Tuning E_4 to be non-minimal forces additional factorizations. We can see from

$$(\hat{G}_{\text{res}} - \alpha E_3) \cdot E_3 = -6 + 2\alpha, \quad (\text{B.6.92a})$$

$$(\hat{G}_{\text{res}} - \alpha C'_0) \cdot C'_0 = 12 - (6 - \alpha)(n + n_0), \quad (\text{B.6.92b})$$

where $n_0 = 1$, that we have a factorization of at least $3E_3$ and $2C'_0$, leading to

$$\hat{G} = (6E_4) + (3E_3) + (2C'_0) + \left[6\tilde{C}_0 + 4C'_0 + (12 + 6n)\tilde{f} - 6E_1 - 9E_3 - 18E_4 \right]. \quad (\text{B.6.93})$$

We can now consider the candidates for triplet completion, which in this case are C'_0 , \tilde{C}_∞ , C'_∞ , \tilde{f} , f'_1 , f'_2 , f'_3 , E_1 and E_2 . Let us list how all of them lead to E_3 factorizing non-minimally, with $E_3 \cdot E_4 = 1$.

- (1) $\{E_4, C'_0, \cdot\}$: A cascade of factorizations occurs between f'_3 and E_3 , ultimately leading to E_3 factorizing non-minimally.
- (2) $\{E_4, \tilde{C}_\infty, \cdot\}$: This case is analogous to Case (1).
- (3) $\{E_4, C'_\infty, \cdot\}$: This directly leads to E_3 factorizing non-minimally.
- (4) $\{E_4, \tilde{f}, \cdot\}$: This triggers a cascade of C'_0 , f'_3 and E_3 factorizations, leading in the end to E_3 factorizing non-minimally.
- (5) $\{E_4, f'_1, \cdot\}$: This case is analogous to Case (4).
- (6) $\{E_4, f'_3, \cdot\}$: This case is analogous to Case (3).
- (7) $\{E_4, E_2, \cdot\}$: This case is analogous to Case (4).
- (8) $\{E_4, E_1, \cdot\}$: This tuning modifies the effectiveness bound to $n \geq 3$ and triggers a cascade of C'_0 , f'_1 , f'_3 and E_3 factorizations making E_3 non-minimal.
- (9) $\{E_4, f'_2, \cdot\}$: Tuning these two divisors to be non-minimal is possible without any non-minimal factorizations being forced, but the previous analysis leaves no candidates left to complete the triplet.

B.6.3.2 Type (C) and (D) blow-ups

The discussion proceeds similarly for surfaces $\hat{B}_0 = \text{Bl}(\mathbb{F}_n)$ obtained by also allowing for type (C) and (D) blow-ups, with the effectiveness constraints becoming even more stringent for these cases. We only provide an illustrative example for this class of models, to avoid repeating a discussion analogous to the one above.

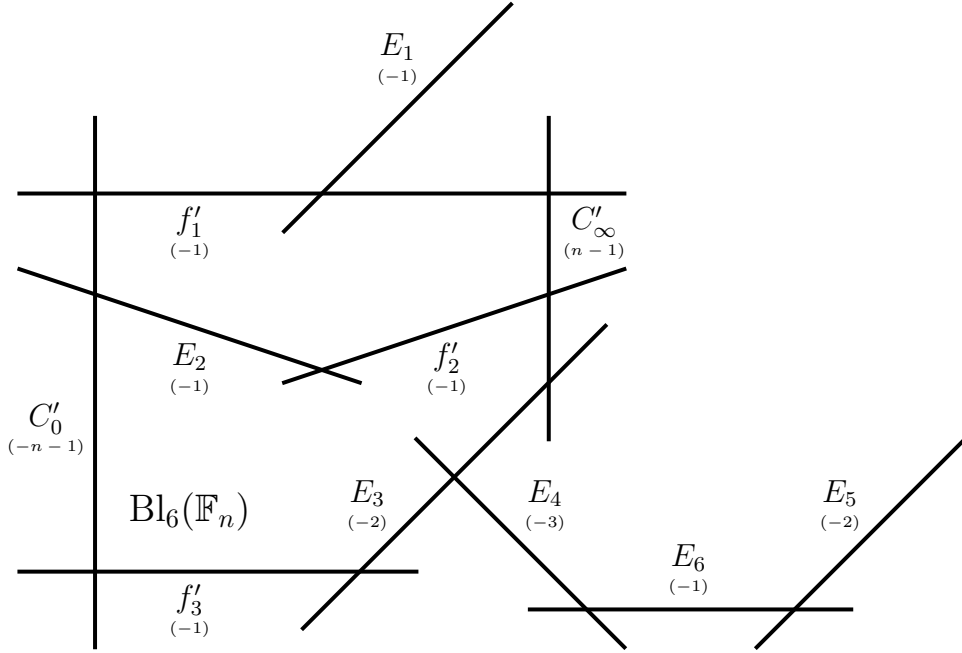


Figure B.11: Surface $\hat{B}_0 = \text{Bl}_6(\mathbb{F}_n)$ obtained by performing three type (A), two type (B) and one type (C) blow-ups on the Hirzebruch surface \mathbb{F}_n . The self-intersection of the depicted curves is shown below their names in parentheses.

Example B.6.5. Consider the blown up Hirzebruch surface $\text{Bl}_4(\mathbb{F}_n)$ of Example B.6.4 and perform an additional type (B) blow-up on E_4 , with exceptional divisor E_5 , and a type (C) blow-up at the intersection point $E_4 \cap E_5$. This leads to the six-dimensional F-theory base $\hat{B}_0 = \text{Bl}_6(\mathbb{F}_n)$, that we represent in Figure B.11.

The anticanonical class $\overline{K}_{\hat{B}_0}$ after the blow-ups can be written as

$$\overline{K}_{\hat{B}_0} = 2\tilde{C}_0 + (2+n)\tilde{f} - E_1 - E_2 - E_3 - 2E_4 - 3E_5 - 6E_6. \quad (\text{B.6.94})$$

Keeping in mind the linear equivalences

$$\tilde{C}_0 = C'_0 + E_2, \quad (\text{B.6.95a})$$

$$\tilde{f} = f'_1 + E_1, \quad (\text{B.6.95b})$$

$$\tilde{f} = f'_2 + E_2, \quad (\text{B.6.95c})$$

$$\tilde{f} = f'_3 + E_3 + E_4 + E_5 + 2E_6 \quad (\text{B.6.95d})$$

we see that the effectiveness bound is $n \geq 2$. The surface has non-Higgsable clusters, such that without any further tuning we already have

$$\hat{G} = (2C'_0) + (2E_3) + (3E_4) + \left[6\tilde{C}_0 + 4C'_0 + (12+6n)\tilde{f} - 6E_1 - 8E_3 - 15E_4 - 18E_5 - 36E_6 \right]. \quad (\text{B.6.96})$$

After the type (C) blow-up, Lemma B.6.2 tells us that we need to consider the candidate triplets $\{E_4, \cdot, \cdot\}$, $\{E_5, \cdot, \cdot\}$ and $\{E_6, \cdot, \cdot\}$, which we do in turn.

- (1) $\{E_4, \cdot, \cdot\}$: The analysis of these types of triplets is the same that was performed during the study of Example B.6.4, with the exception of the new candidate triplet $\{E_4, E_5, \cdot\}$. Tuning these two divisors directly forces E_6 to factorize non-minimally, with $E_4 \cdot E_6 = E_5 \cdot E_6 = 1$.

- (2) $\{E_5, \cdot, \cdot\}$: Tuning E_5 to be non-minimal forces some additional factorizations in \hat{G} , leading to the residual \hat{G}_{res} divisor

$$\begin{aligned} \hat{G} = & (3C'_0) + (2E_3) + (4E_4) + (6E_5) + (4E_6) \\ & + \left[6\tilde{C}_0 + 3C'_0 + (12 + 6n)\tilde{f} - 6E_1 - 8E_3 - 16E_4 - 24E_5 - 40E_6 \right]. \end{aligned} \quad (\text{B.6.97})$$

We can now consider the candidates for triplet completion, which in this case are C'_0 , \tilde{C}_∞ , C'_∞ , \tilde{f} , f'_1 , f'_2 , f'_3 , E_1 , E_2 and E_3 , since we have already considered $\{E_5, E_4, \cdot\}$ above in Case (1). With the exception of $\{E_5, f'_2, \cdot\}$, the tuning of all these pairs leads to a cascade of factorizations ultimately making E_6 factorize non-minimally, with $E_6 \cdot E_5 = 1$. In the case of the pair $\{E_5, E_1, \cdot\}$ we need to take into account during the analysis that the effectiveness bound is modified to $n \geq 4$ to allow for the tuning. Although the pair $\{E_5, f'_2, \cdot\}$ can be tuned to be non-minimal without additional non-minimal factorizations, there is no candidate left in order to complete the triplet.

- (3) $\{E_6, \cdot, \cdot\}$: Tuning E_6 to be non-minimal forces some additional factorizations in \hat{G} , leading to the residual \hat{G}_{res} divisor

$$\begin{aligned} \hat{G} = & (3C'_0) + (3E_3) + (5E_4) + (3E_5) + (6E_6) \\ & + \left[6\tilde{C}_0 + 3C'_0 + (12 + 6n)\tilde{f} - 6E_1 - 9E_3 - 17E_4 - 21E_5 - 42E_6 \right]. \end{aligned} \quad (\text{B.6.98})$$

We can now consider the candidates for triplet completion, which are still C'_0 , \tilde{C}_∞ , C'_∞ , \tilde{f} , f'_1 , f'_2 , f'_3 , E_1 , E_2 and E_3 . Similarly to the previous case, tuning these pairs to be non-minimal forces a cascade of factorizations leading to E_4 factorizing non-minimally, with $E_4 \cdot E_6 = 1$. In the analysis of the pair $\{E_6, E_1, \cdot\}$ we need to take into account that the effectiveness bound becomes $n \geq 4$ for the tuning to be possible.

B.7 Blowing down vertical components

While in horizontal models the open-chain resolution can be directly blown down to a component different from B^0 , this is not possible in vertical models; for such models one needs to flop some curves before carrying out the blow-down.⁵ This affects, in particular, the explicit method to remove horizontal and vertical Class 5 models discussed in [309] and some of the manipulations entering the discussion of obscured infinite-distance limits in Appendix B.3, since these may entail blowing down vertical components.

Let us consider a single infinite-distance limit degeneration $\hat{\rho} : \hat{\mathcal{Y}} \rightarrow D$ of vertical type and assume that $\hat{B}_0 = \mathbb{F}_n$ with $n > 0$, to avoid the horizontal case for which the problem does not arise. If we were able to perform a blow-down directly to a component B^p , with $p = 1, \dots, P$, of the open-chain resolution, we would lose information about the degree n of the line bundle $\mathcal{O}_{\mathbb{P}^1}(n)$ intervening in the construction of the original base component $\hat{B}_0 = \mathbb{F}_n$. Instead, the geometry forces us to flop curves until the component to which we blow down has also the Hirzebruch surface \mathbb{F}_n as its base.

This can be seen very directly from the toric diagrams used in Section 5.3 to describe $\hat{\mathcal{B}}$ and the result of blowing it up \mathcal{B} . Consider first a horizontal model whose base $\hat{\mathcal{B}}$ has been blown-up leading to the toric fans described in Section 5.3.2 and portrayed, in a two-component example,

⁵See, e.g., [358] for some classical results regarding the issue of contracting divisors.

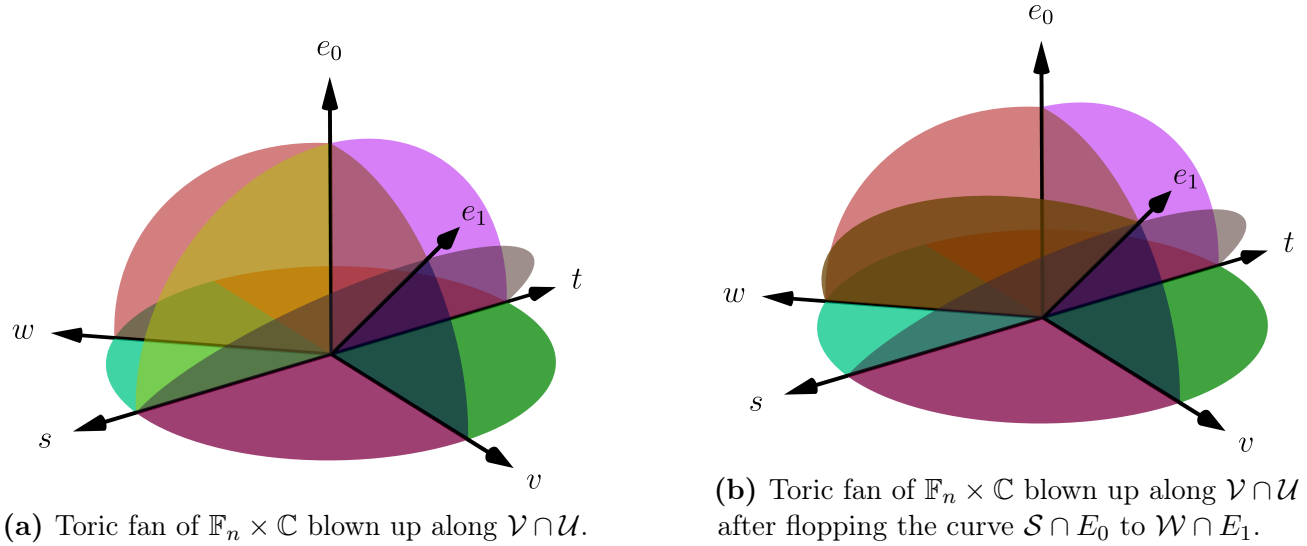


Figure B.12: Toric fans associated with a vertical model.

in Figure 5.4b. Blowing down back to B^0 is clearly possible, since this just gives us the original model back. Consider instead that we want to blow down to an B^p component besides B^0 . For concreteness, let us focus on the two-component example and consider, hence, the blow-down to the component B^1 given by the map

$$\sigma : \mathcal{B} \longrightarrow \text{Bd}_{E_0}(\mathcal{B}), \quad (\text{B.7.1})$$

that contracts the E_0 divisor in \mathcal{B} . Let us denote the 1-skeleton of the fan Σ_X of a toric variety X by $\Sigma(1)_X$. We observe that the 1-skeleton $\Sigma(1)_{\text{Bd}_{E_0}(\mathcal{B})} := \Sigma(1)_{\mathcal{B}} \setminus \{e_0\}$ can be completed into a fan in a unique way, the resulting variety being $\text{Bd}_{E_0}(\mathcal{B})$, whose fan we denote $\Sigma_{\text{Bd}_{E_0}(\mathcal{B})}$. The 1-skeleton $\Sigma(1)_{\mathcal{B}}$ can also only be completed into a fan in a unique way, yielding indeed $\Sigma_{\mathcal{B}}$. The fan $\Sigma_{\mathcal{B}}$ is a refinement of $\Sigma_{\text{Bd}_{E_0}(\mathcal{B})}$, in which the 3-cone spanned by (t, w, e_1) is subdivided by introducing the edge e_0 and the appropriate 2-cones.

Going through the same procedure for a vertical model, we see that the situation is different. Let us consider a vertical model whose base $\hat{\mathcal{B}}$ has been blown-up until the resolved base \mathcal{B} with the toric fan described in Section 5.3.3 was obtained, that we plot for a two-component example in Figure B.12a. As above, we discuss the geometry for the concrete case of a two-component model, but the results hold in general for a model with $P + 1$ components. The 1-skeleton $\Sigma(1)_{\text{Bd}_{E_0}(\mathcal{B})} := \Sigma(1)_{\mathcal{B}} \setminus \{e_0\}$ can only be completed into a fan $\Sigma_{\text{Bd}_{e_0}(\mathcal{B})}$ in a unique way, giving the toric variety $\text{Bd}_{e_0}(\mathcal{B})$, in which the B^0 component has been blown-down. This is not true for the 1-skeleton $\Sigma(1)_{\mathcal{B}}$; it can be completed into a fan in 3 different ways, that we now list. They differ in how the edges s, w, e_0 and e_1 are integrated into higher dimensional cones. Let us therefore focus on this aspect of the fan.

- (1) The first possibility is to take the 3-cone spanned by (s, w, e_0, e_1) and the 2-cones given by its faces in order to define the fan. This leads to a singular toric variety $\text{Sing}(\mathcal{B})$. The other fans that can be constructed from $\Sigma(1)_{\mathcal{B}}$, which are the ones of interest to us, are obtained by subdividing the 3-cone (s, w, e_0, e_1) through the addition of a new 2-cone or curve, which can be done in two ways.
- (2) We can subdivide the 3-cone (s, w, e_0, e_1) by adding the curve (s, e_0) . The resulting toric variety is smooth and corresponds to \mathcal{B} , whose fan $\Sigma_{\mathcal{B}}$ is represented in Figure B.12a for a

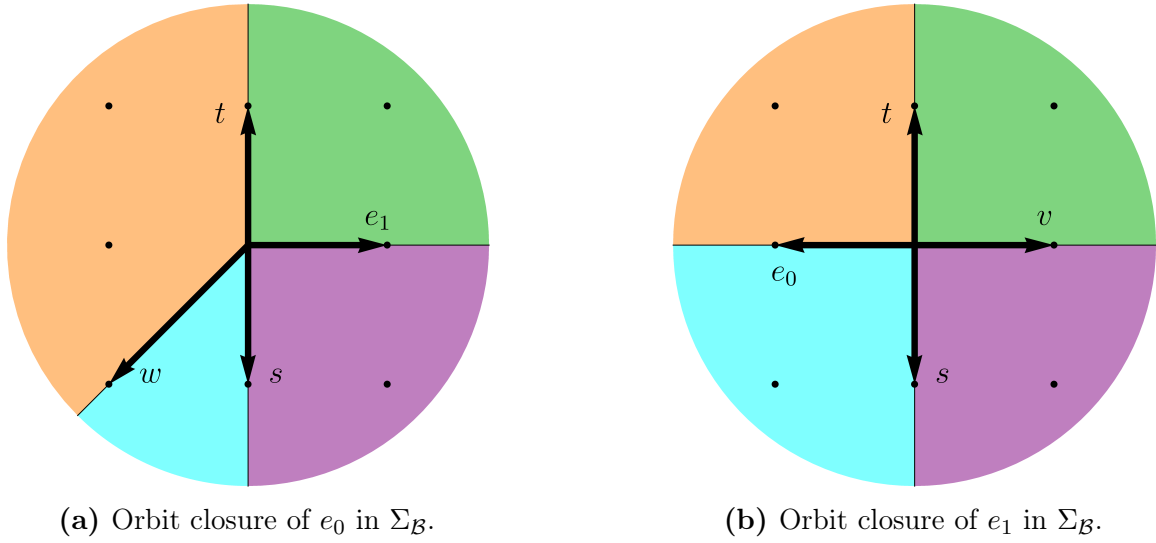


Figure B.13: Geometry of the components of \mathcal{B} , resulting from the blow-up process.

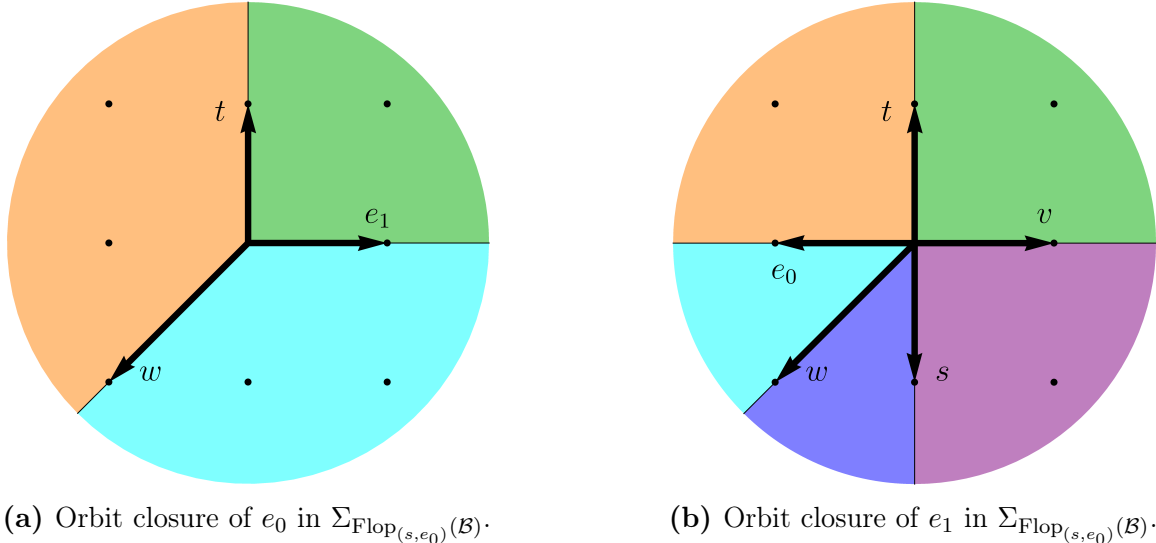


Figure B.14: Geometry of the components of $\text{Flop}_{(s,e_0)}(\mathcal{B})$, obtained from \mathcal{B} by floppping the (s, e_0) curve into the (w, e_1) curve.

model constructed over \mathbb{F}_1 . This toric fan is the one that is obtained from the blow-up process of $\hat{\mathcal{B}}$ described in Section 5.3.3. Computing the orbit-closure of e_0 and e_1 we obtain the $B^0 = \mathbb{F}_n$ and $B^1 = \mathbb{F}_0$ components, respectively, whose fans we represent in Figure B.13.

- (3) Alternatively, we can subdivide the 3-cone (s, w, e_0, e_1) by adding the curve (w, e_1) . This yields a toric variety that we denote by $\text{Flop}_{(s,e_0)}(\mathcal{B})$, and whose fan $\Sigma_{\text{Flop}_{(s,e_0)}(\mathcal{B})}$ is represented in Figure B.12b for a model constructed over \mathbb{F}_1 . $\text{Flop}_{(s,e_0)}(\mathcal{B})$ is smooth when $n = 1$, and singular when $n \geq 2$. This toric fan naturally results from taking the fan $\Sigma_{\text{Bd}_{e_0}(\mathcal{B})}$ and refining it by subdividing its (t, w, e_1) 3-cone through the addition of the e_0 edge and the appropriate 2- and 3-cones. Computing the orbit closure of e_0 and e_1 leads to \mathbb{P}_{11n}^2 and $\text{Bl}^1(\mathbb{F}_0)$ components, respectively, with the fans given in Figure B.14.

The fan $\Sigma_{\text{Flop}_{(s,e_0)}(\mathcal{B})}$ is a refinement of the fan $\Sigma_{\text{Bd}_{E_0}(\mathcal{B})}$, corresponding to restoring the B^0 component. The fan $\Sigma_{\mathcal{B}}$ is the result of blowing up $\hat{\mathcal{B}}$, but is not a refinement of $\Sigma_{\text{Bd}_{E_0}(\mathcal{B})}$. $\Sigma_{\mathcal{B}}$ and $\Sigma_{\text{Flop}_{(s,e_0)}(\mathcal{B})}$ are connected by flopping the curve (s, e_0) into the curve (w, e_1) . This shows that blowing down the B^0 component entails performing such a flop first. The effect of the flop is also apparent in the components. The component B^0 is originally \mathbb{F}_n , but we contract the $(-n)$ -curve turning it into \mathbb{P}_{11n}^2 . Meanwhile, the component B^1 , with F_0 geometry, acquires a new curve, which corresponds to a (weighted, for $n \geq 2$) blow-up by the addition of the edge $(-1, -n)$. Blowing then the B^0 component down removes the $(-1, 0)$ edge out of the fan of the B^1 component, leaving us with an \mathbb{F}_n surface.

As mentioned earlier, although the discussion has focused on a vertical two-component model, the same results apply for any vertical model in which we try to blow down the strict transform of \mathcal{U} , i.e. the B^0 component with \mathbb{F}_n geometry, since the blow-up and blow-down operations are local. The components $B^p = \mathbb{F}_0$, where $p = 1, \dots, P$, can always be blown down without the need to perform a flop first.

B.8 Polynomial factorization in rings with zero divisors

The physical defining polynomials f_{phys} , g_{phys} and Δ_{phys} studied in Section 5.4.3 are elements of the ring with zero divisors $S_{\mathcal{B}}/I_{\tilde{\mathcal{U}}}$. This strays away from the context of integral domains, in which the factorization of polynomials is most commonly studied. The more general question of the factorization of polynomials in commutative rings with unity and zero divisors has been studied in the mathematical literature, see, e.g., the non-comprehensive list of references [359–362]. Here we only review some of the differences that arise with respect to the factorization theory in integral domains, referring to the literature for an in-depth analysis.

Following [360–362], in a unital commutative ring there are three different notions of associate elements, that can be used to define four different notions of irreducible element.

Definition B.8.1. Let R be a commutative ring with unity and let $a, b \in R$. Then:

1. a and b are associates, written $a \sim b$, if $\langle a \rangle = \langle b \rangle$;
2. a and b are strong associates, written $a \approx b$, if $a = ub$ for some unit u ;
3. a and b are very strong associates, written $a \cong b$, if $a \sim b$ and either $a = b = 0$ or $a \neq 0$ and $a = rb$ implies that r is a unit.

Definition B.8.2. Let R be a commutative ring and $a \in R$ a non-unit. Then:

1. a is irreducible if $a = bc \Rightarrow a \sim b$ or $a \sim c$;
2. a is strongly irreducible if $a = bc \Rightarrow a \approx b$ or $a \approx c$;
3. a is m -irreducible if (a) is maximal among the proper principal ideals;
4. a is very strongly irreducible if $a = bc \Rightarrow a \cong b$ or $a \cong c$.

With these definitions, the implications

$$\begin{array}{c}
 \text{prime} \\
 \Downarrow \\
 \text{very strongly irreducible} \implies m\text{-irreducible} \implies \text{strongly irreducible} \implies \text{irreducible}
 \end{array} \tag{B.8.1}$$

are satisfied for non-zero non-unit elements of the ring. In an integral domain, the implications in the bottom line reverse, and the four notions of irreducibility coincide. In a GCD domain, the vertical implication reverses as well.

Each of the notions of irreducibility listed above leads to a different notion of atomicity, the property of being able to express each non-zero non-unit element of R as a finite product of irreducible elements. Namely, a unital commutative ring R can be atomic, strongly atomic, m -atomic or very strongly atomic, see [360] for a detailed analysis. For example, unital commutative rings satisfying the ascending chain condition on principal ideals are atomic, which means that Noetherian rings like $S_{\mathcal{B}}/I_{\tilde{\mathcal{U}}}$ are, in particular, atomic.

B.9 Discriminant in the weakly coupled components

The form that the discriminant takes in a component Y^p that is at weak string coupling, i.e. one that presents codimension-zero fibers of Kodaira type $I_{n_p > 0}$, is more constrained than in a strongly coupled component. To address this in the explicit global coordinate description that we employ while analysing horizontal and vertical models, let us rewrite the defining polynomials of the Weierstrass model of the family variety \mathcal{Y} as

$$f = e_p^{l_p} \check{f}_p + f_p, \quad (\text{B.9.1a})$$

$$g = e_p^{m_p} \check{g}_p + g_p, \quad (\text{B.9.1b})$$

$$\Delta = e_p^{s_p} \check{\Delta}_p + \Delta_p. \quad (\text{B.9.1c})$$

We have to consider various ways in which the codimension-zero $I_{n_p > 0}$ fibers can arise, each demanding more tuning than the previous one.

- (1) Single accidental cancellation: In order for the generic elliptic fiber over B^p to be of Kodaira type $I_{n_p > 0}$, we need Δ_p to vanish. Plugging (B.9.1a) and (B.9.1b) into

$$\Delta = 4f^3 + 27g^2, \quad (\text{B.9.2})$$

we obtain

$$\Delta = (4f_p^3 + 27g_p^2) + 12f_p e_p^{l_p} (\check{f}_p f_p + e_p^{l_p} \check{f}_p^2) + 54e_p^{m_p} g_p \check{g}_p + (4e_p^{3l_p} \check{f}_p^3 + 27e^{2m_p} \check{g}_p^2). \quad (\text{B.9.3})$$

The necessary accidental cancellation for Δ_p to vanish occurs when⁶

$$f_p = -3h_p^2, \quad g_p = 2h_p^3, \quad h_p \in H^0(B^p, \mathcal{L}_p^{\otimes 2}), \quad (\text{B.9.4})$$

and assuming this structure leads to

$$\Delta = 108h_p^4 e_p^{l_p} \check{f}_p - 36h_p^2 e_p^{2l_p} \check{f}_p^2 + 108h_p^3 e_p^{m_p} \check{g}_p + 4e_p^{3l_p} \check{f}_p^3 + 27e^{2m_p} \check{g}_p^2. \quad (\text{B.9.5})$$

Unless further cancellations take place, we have $n_p = s_p = \min(l_p, m_p)$, and

$$\check{\Delta}_p|_{E_p} = 108h_p^3 (e_p^{l_p - n_p} \check{f}_p h_p + e_p^{m_p - n_p} \check{g}_p)|_{e_p=0} = h_p^k \Delta_p'', \quad k \geq 3. \quad (\text{B.9.6})$$

⁶In this section, we are considering the coordinate divisors $E_p = \{e_p = 0\}_{\mathcal{B}}$, but we could carry out the discussion for more general divisors $\mathcal{D} = \{p_{\mathcal{D}} = 0\}_{\mathcal{B}}$ (working locally, if necessary). Then, the single accidental cancellation in the discriminant can occur not only when the structure (B.9.4) is realised, but also when we have $4f_{\mathcal{D}}^3 + 27g_{\mathcal{D}}^2 = p_{\mathcal{D}}^{\delta_{\mathcal{D}}} q_{\mathcal{D}}$ with $\delta_{\mathcal{D}} \geq 1$. It is clear that when $p_{\mathcal{D}} = e_p$ this second type of accidental cancellation cannot occur, and we therefore neglect it in the remainder of the section. We also use the structure of accidental cancellations in the derivation of the vertical gauge rank bounds for horizontal models printed in Section 6.3.6 and further discussed in Appendix B.11, where the second possibility needs to and has been taken into account.

- (2) Double accidental cancellation: Additional cancellations can occur when (B.9.4) is satisfied and $l_p = m_p =: r_s$, in which case

$$\Delta = 108h_p^3 e_p^{r_p} (h_p \check{f}_p + \check{g}_p) - 36h_p^2 e_p^{2r_p} \check{f}_p^2 + 4e_p^{3r_p} \check{f}_p^3 + 27e_p^{2r_p} \check{g}_p^2. \quad (\text{B.9.7})$$

We can then have the structure

$$h_p \check{f}_p + \check{g}_p = e_p^{\rho_p} q_p, \quad \rho_p \geq 1, \quad (\text{B.9.8})$$

leading to

$$\Delta = 108h_p^3 e_p^{r_p + \rho_p} q_p - 36h_p^2 e_p^{2r_p} \check{f}_p^2 + 4e_p^{3r_p} \check{f}_p^3 + 27e_p^{2r_p} \check{g}_p^2. \quad (\text{B.9.9})$$

A particular subcase is the one realised when $q_p = 0$, to which we assign $\rho_p = \infty$. The resulting component discriminant $\check{\Delta}_p|_{E_p}$ depends on the value of $r_p + \rho_p$. We assume below that no additional cancellations take place.

- (2.a) If $r_p + \rho_p < 2r_p$, we have that $n_p = r_p + \rho_p \geq 2$, and the restriction $\check{\Delta}_p|_{E_p}$ is given by

$$\check{\Delta}_p|_{E_p} = 108h_p^3 q_p|_{e_p=0}. \quad (\text{B.9.10})$$

- (2.b) If $r_p + \rho_p = 2r_p$, we obtain $n_p = 2r_p \geq 2$, and the restriction $\check{\Delta}_p|_{E_p}$ is

$$\check{\Delta}_p|_{E_p} = 9h_p^2 (12h_p q_p - \check{f}_p^2)|_{e_p=0}. \quad (\text{B.9.11})$$

- (2.c) If $r_p + \rho_p > 2r_p$, we still obtain $n_p = 2r_p \geq 2$, and the restriction $\check{\Delta}_p|_{E_p}$ is now

$$\check{\Delta}_p|_{E_p} = -9h_p^2 \check{f}_p^2|_{e_p=0}. \quad (\text{B.9.12})$$

The last two cases can give $k = 2$.

- (3) Triple accidental cancellation: If the conditions (B.9.4) and (B.9.8) are satisfied, and also $r_p = \rho_p = l_p = m_p =: t_p$, the discriminant can be expressed as

$$\Delta = 9h_p^2 e_p^{2t_p} (12h_p q_p - \check{f}_p^2) + 2\check{f}_p e_p^{3t_p} (2\check{f}_p^2 - 27h_p q_p) + 27e_p^{4t_p} q_p^2. \quad (\text{B.9.13})$$

We see that additional cancellations can occur if we have the structure

$$12h_p q_p - \check{f}_p^2 = e_p^\sigma \check{q}_p, \quad \sigma_p \geq 1, \quad (\text{B.9.14})$$

leading to

$$\Delta = 9h_p^2 e_p^{2t_p + \sigma_p} \check{q}_p - 6h_p e_p^{3t_p} q_p \check{f}_p - 4e_p^{3t_p + \sigma_p} \check{f}_p \check{q}_p + 27e_p^{4t_p} q_p^2. \quad (\text{B.9.15})$$

Again, to the particular subcase $\check{q}_p = 0$ we assign $\sigma_p = \infty$. The form of the component discriminant $\check{\Delta}_p|_{E_p}$ depends on the value of $2t_p + \sigma_p$. Below, we assume that no additional cancellations take place.

- (3.a) If $2t_p + \sigma_p < 3t_p$, we have that $n_p = 2t_p + \sigma_p \geq 3$, and the restriction $\check{\Delta}_p|_{E_p}$ is

$$\check{\Delta}_p|_{E_p} = 9h_p^2 \check{q}_p|_{e_p=0}. \quad (\text{B.9.16})$$

(3.b) If $2t_p + \sigma_p = 3t_p$, we obtain $n_p = 3t_p \geq 3$, and $\check{\Delta}_p|_{E_p}$ is

$$\check{\Delta}_p|_{E_p} = h_p (9h_p \check{q}_p - 6q_p \check{f}_p)|_{e_p=0}. \quad (\text{B.9.17})$$

(3.c) If $2t_p + \sigma_p > 3t_p$, then $n_p = 2t_p + \sigma_p \geq 3$, and $\check{\Delta}_p|_{E_p}$ is

$$\check{\Delta}_p|_{E_p} = -6h_p q_p \check{f}_p|_{e_p=0} = 0. \quad (\text{B.9.18})$$

These cases also lead to $k \geq 2$. To see these for the last two of them, note that (B.9.14) implies that

$$\check{f}_p^2|_{e_p=0} = 12h_p q_p|_{e_p=0} \Rightarrow q_p|_{e_p=0} = h_p q''_p|_{e_p=0}, \quad (\text{B.9.19})$$

where we have used that the generic $h_p = h_p|_{e_p=0}$ polynomial is not a perfect square.

- (4) Quadruple accidental cancellation: If the conditions (B.9.4), (B.9.8) and (B.9.14) are satisfied, and also $t_p = r_p = \rho_p = l_p = m_p$ and $2t_p + \sigma_p = 3t_p$, additional cancellations can occur if we have the structure

$$9h_p \check{q}_p - 6q_p \check{f}_p = e^{\tau_p} \check{q}_p, \quad \tau_p \geq 1. \quad (\text{B.9.20})$$

The analysis of this and further accidental cancellation structures would proceed along the same lines as that of the cases previously studied, and we do not perform it explicitly.

To summarise, the component discriminant $\check{\Delta}_p|_{E_p}$ after tuning codimension-zero Kodaira type $\text{I}_{n_p > 0}$ fibers in the Y^p components takes the form

$$\check{\Delta}_p|_{E_p} = h_p^k \Delta_p'', \quad k \geq 2. \quad (\text{B.9.21})$$

The minimal value of $k = 2$ is associated with the appearance of type D_0 singularities, see the discussion in Section 6.3.4, explaining why we cannot go lower. Note that the object $\check{\Delta}_p|_{E_p}$ considered in this section is different from the restriction Δ'_p of the modified discriminant Δ' to the component. The two objects are related by

$$\check{\Delta}_p = e_0^{n_0} e_1^{n_1} \cdots \overset{p}{\check{\wedge}} e_{P-1}^{n_{P-1}} e_P^{n_P} \Delta' \Rightarrow \check{\Delta}_p|_{E_p} = e_0^{n_0} e_1^{n_1} \cdots \overset{p}{\check{\wedge}} e_{P-1}^{n_{P-1}} e_P^{n_P} \Delta'_p. \quad (\text{B.9.22})$$

B.10 Bounds on $|n_p - n_{p+1}|$

Beyond the effectiveness bounds for the pattern of codimension-zero singular elliptic fibers in the central fiber of horizontal and vertical models derived in Sections B.14.1.1 and 6.3.2.1, respectively, one can obtain tighter constraints by studying the resolution structure taking us from the original degeneration $\hat{\rho} : \hat{\mathcal{Y}} \rightarrow D$ to its open-chain resolution $\rho : \mathcal{Y} \rightarrow D$. Such bounds were presented in Section 6.3.2.2 for horizontal models; here, we give the technical arguments on which they are sustained and also discuss them for vertical models in Section B.10.2. They vary slightly depending on how tuned the accidental cancellations giving rise to the weakly coupled components are, see Appendix B.9. We focus on obtaining bounds that apply when the single or double accidental cancellation structure is realised.

B.10.1 Horizontal models

We start by deriving the tighter bounds on $|n_p - n_{p+1}|$ that were printed in Section 6.3.2.2. It turns out that the inequalities are asymmetric, depending on if we consider $n_p - n_{p+1}$, for $p \in \{0, \dots, P-1\}$, or $n_p - n_{p-1}$, for $p \in \{1, \dots, P\}$. We treat each case in turn.

Tighter bounds on $n_p - n_{p+1}$

Consider a component Y^p , with $p \in \{0, \dots, P-1\}$, of the central fiber Y_0 of a resolved horizontal model $\rho : \mathcal{Y} \rightarrow D$ and tune over it codimension-zero $I_{n_p > 0}$ fibers. This entails enforcing, at least, the single accidental cancellation structure (B.9.4). To achieve this, certain powers of the exceptional coordinate e_p must factorize in some terms of the defining polynomials, which we then write as

$$f - f_p = e_p^{l_p} \check{f}, \quad (\text{B.10.1a})$$

$$g - g_p = e_p^{m_p} \check{g}. \quad (\text{B.10.1b})$$

But the powers with which the exceptional coordinates $\{e_p\}_{0 \leq p \leq P}$ appear in the monomials of f and g are not arbitrary. Leaving a more detailed analysis of this aspect for [309], it suffices for now to note how individual monomials in f and g are affected by the resolution process of a horizontal model.

Consider, without loss of generality, that we are dealing with a horizontal model in which $\hat{\mathcal{C}}_1 = \{h\}$. We then have that the resolution process acts on the monomials like

$$u^{\mu_{i,0}} s^i t^{8-i} v^j w^{(8+4n)-(8-i)n-j} \subset f \mapsto \prod_{p=0}^P e_p^{\mu_{i,p}} s^i t^{8-i} v^j w^{(8+4n)-(8-i)n-j} \subset f, \quad (\text{B.10.2a})$$

$$u^{\nu_{i,0}} s^i t^{12-i} v^j w^{(12+6n)-(12-i)n-j} \subset g \mapsto \prod_{p=0}^P e_p^{\nu_{i,p}} s^i t^{12-i} v^j w^{(12+6n)-(12-i)n-j} \subset g, \quad (\text{B.10.2b})$$

where

$$\mu_{i,p} := \mu_{i,0} + p(i-4), \quad (\text{B.10.3a})$$

$$\nu_{j,p} := \nu_{j,0} + p(j-6). \quad (\text{B.10.3b})$$

The slopes of these linear functions are determined by the power with which s appears in the monomial under consideration. Since f and g are global holomorphic sections of the line bundles $F = 4\bar{K}_{\hat{\mathcal{B}}}$ and $G = 6\bar{K}_{\hat{\mathcal{B}}}$, respectively, with

$$\bar{K}_{\hat{\mathcal{B}}} = 2\mathcal{S} + (2+n)\mathcal{V}, \quad (\text{B.10.4})$$

we have that

$$0 \leq i \leq 8, \quad (\text{B.10.5a})$$

$$0 \leq j \leq 12. \quad (\text{B.10.5b})$$

The factorization (B.10.1) implies that

$$\mu_{i,p} \geq l_p, \quad \nu_{j,p} \geq m_p, \quad (\text{B.10.6})$$

for all monomials in $f - f_p$ and $g - g_p$. Defining

$$(\alpha, \beta) := \text{ord}_{\mathcal{Y}}(f, g)_{s=0}, \quad (\text{B.10.7})$$

we get then from (B.10.3) and (B.10.6) the bounds

$$\mu_{i,p+1} \geq \mu_{i,p} - (4 - i) \geq l_p - \max_{i' \in \{\alpha, \dots, 8\}} (4 - i') \geq l_p - (4 - \alpha), \quad \forall i \in \{\alpha, \dots, 8\}, \quad (\text{B.10.8a})$$

$$\nu_{j,p+1} \geq \nu_{j,p} - (6 - j) \geq m_p - \max_{j' \in \{\beta, \dots, 12\}} (6 - j') \geq m_p - (6 - \beta), \quad \forall j \in \{\beta, \dots, 12\}, \quad (\text{B.10.8b})$$

which apply to the aforementioned monomials. This means that there is a further factorization

$$f = e_p^{l_p} e_{p+1}^{\tilde{\mu}_{p+1}} \check{f}'_p + f_p, \quad (\text{B.10.9a})$$

$$g = e_p^{l_p} e_{p+1}^{\tilde{\nu}_{p+1}} \check{g}'_p + g_p, \quad (\text{B.10.9b})$$

where we have introduced

$$\tilde{\mu}_{p+1} := \min \mu_{i,p+1}, \quad \tilde{\mu}_{p+1} \geq l_p - (4 - \alpha), \quad \tilde{\mu}_{p+1} \geq 0, \quad (\text{B.10.10a})$$

$$\tilde{\nu}_{p+1} := \min \nu_{i,p+1}, \quad \tilde{\nu}_{p+1} \geq m_p - (6 - \beta), \quad \tilde{\nu}_{p+1} \geq 0 \quad (\text{B.10.10b})$$

with the minimum is taken over all monomials in $f - f_p$ and $g - g_p$, respectively.

Assume now that the single accidental cancellation structure (B.9.4) is satisfied in the Y^p component, without additional cancellations taking place. The form of the discriminant is then (B.9.5), from which one can see that

$$n_{p+1} \geq \min(\tilde{\mu}_{p+1}, \tilde{\nu}_{p+1}) = \min(l_p - (4 - \alpha), m_p - (6 - \beta)) = n_p - \max(4 - \alpha, 6 - \beta). \quad (\text{B.10.11})$$

Hence, for a single accidental cancellation structure in Y^p we have that

$$n_p - n_{p+1} \leq \max(4 - \alpha, 6 - \beta), \quad p \in \{0, \dots, P - 1\}. \quad (\text{B.10.12})$$

Allow now for a double accidental cancellation to occur in Y^p , i.e. assume that (B.9.4) and (B.9.8) are satisfied while $l_p = m_p =: r_p$. Let us rewrite (B.9.8) as

$$h_p \check{f}_p + \check{g}_p = e_p^{\rho_p} e_p^{\rho_{p+1}} q'_p, \quad \rho_p \geq 1, \quad \rho_{p+1} \geq 0. \quad (\text{B.10.13})$$

By definition, h_p contains no powers of e_p , and the monomials in \check{f}_p and \check{g}_p are those fulfilling (B.10.6), which have been divided by $e_p^{-r_p}$. Once the necessary cancellations to produce the r.h.s. take place, only those monomials whose provenance can be traced back to monomials in $f - f_p$ and $g - g_p$ satisfying

$$\mu_{i,p} \geq r_p + \rho_p, \quad \nu_{j,p} \geq r_p + \rho_p, \quad (\text{B.10.14})$$

survive, from which we conclude that

$$\rho_{p+1} \geq \min(r_p + \rho_p - (4 - \alpha), r_p + \rho_p - (6 - \beta)) = r_p + \rho_p - \max(4 - \alpha, 6 - \beta). \quad (\text{B.10.15})$$

Moreover, we see from (B.10.13) and the fact that h_p contains no overall powers of e_{p+1} (since these would lead to special fibers at the intersection of the components, see Section 5.4.6), that for the cancellations on the l.h.s. to be possible the lowest power of e_{p+1} appearing in both

terms must be the same and smaller than ρ_{p+1} , i.e. $\tilde{\mu}_{p+1} = \tilde{\nu}_{p+1} < \rho_{p+1}$. Additionally, the double accidental cancellation cases discussed in Appendix B.9 showed that

$$n_p = \begin{cases} r_p + \rho_p, & \text{if } r_p + \rho_p < 2r_p \Rightarrow 2r_p > r_p + \rho_p = n_p, \\ 2r_p, & \text{if } r_p + \rho_p \geq 2r_p \Rightarrow r_p + \rho_p \geq 2r_p = n_p, \end{cases} \quad (\text{B.10.16})$$

and hence the bounds

$$r_p + \rho_p \geq n_p, \quad 2r_p \geq n_p, \quad (\text{B.10.17})$$

are always satisfied. From the resulting form (B.9.9) of the discriminant, we observe that

$$n_{p+1} \geq \min(\rho_{p+1}, 2 \min(\tilde{\mu}_{p+1}, \tilde{\nu}_{p+1})) . \quad (\text{B.10.18})$$

We then distinguish two cases:

- If $\min(\rho_{p+1}, 2 \min(\tilde{\mu}_{p+1}, \tilde{\nu}_{p+1})) = \rho_{p+1}$, the inequalities given above result in

$$n_{p+1} \geq \rho_{p+1} \geq n_p - \max(4 - \alpha, 6 - \beta) \Leftrightarrow n_p - n_{p+1} \leq \max(4 - \alpha, 6 - \beta) . \quad (\text{B.10.19})$$

- If $\min(\rho_{p+1}, 2 \min(\tilde{\mu}_{p+1}, \tilde{\nu}_{p+1})) = 2 \min(\tilde{\mu}_{p+1}, \tilde{\nu}_{p+1})$, we have instead

$$\left. \begin{array}{l} n_{p+1} \geq 2\tilde{\mu}_{p+1} \geq n_p - 2(4 - \alpha) \\ n_{p+1} \geq 2\tilde{\nu}_{p+1} \geq n_p - 2(6 - \beta) \end{array} \right\} \Leftrightarrow n_p - n_{p+1} \leq 2 \min(4 - \alpha, 6 - \beta) , \quad (\text{B.10.20})$$

where we have used (B.10.10).

Altogether, for a double accidental cancellation structure in Y^p we have the bound

$$n_p - n_{p+1} \leq \max(\max(4 - \alpha, 6 - \beta), 2 \min(4 - \alpha, 6 - \beta)) , \quad p \in \{0, \dots, P - 1\} , \quad (\text{B.10.21})$$

which is laxer than the one found for the single accidental cancellation structure.

For the generic model with a given pattern $I_{n_0} - \dots - I_{n_p}$ of codimension-zero singular elliptic fibers in Y_0 obtained through single and double accidental cancellations, we therefore have

$$n_p - n_{p+1} \leq \begin{cases} 8, & 0 \leq n \leq 2, \\ 4, & 3 \leq n \leq 4, \\ 2, & 5 \leq n \leq 8, \\ 1, & 9 \leq n \leq 12, \end{cases} \quad p = 0, \dots, P - 1 , \quad (\text{B.10.22})$$

where we have used the values of α and β associated with the non-Higgsable clusters listed in Table 6.3.1. It would be interesting to know if the bounds can be relaxed to match the effectiveness bounds of Section 6.3.2.1 by allowing further accidental cancellations to occur as discussed in Appendix B.9.

Tighter bounds on $n_p - n_{p-1}$

The same type of arguments can be used to derive bounds in the opposite direction. The starting inequalities that we need to consider now are the analogues of (B.10.8), namely

$$\mu_{i,p-1} \geq \mu_{i,p} + (4 - i) \geq l_p + \min_{i' \in \{\alpha, \dots, 8\}} (4 - i') \geq l_p - 4 , \quad \forall i \in \{\alpha, \dots, 8\} , \quad (\text{B.10.23a})$$

$$\nu_{j,p-1} \geq \nu_{j,p} + (6 - j) \geq m_p + \min_{j' \in \{\beta, \dots, 12\}} (6 - j') \geq m_p - 6 , \quad \forall j \in \{\beta, \dots, 12\} . \quad (\text{B.10.23b})$$

These have the same form as (B.10.8) with $(\alpha, \beta) = (0, 0)$. Hence, the resulting inequalities for the single and double accidental cancellation structures are (B.10.12) and (B.10.21) particularised for this value, which combined result in

$$n_p - n_{p-1} \leq 8, \quad p = 1, \dots, P. \quad (\text{B.10.24})$$

The reason we do not find different bounds depending on the Hirzebruch surface $\hat{B} = \mathbb{F}_n$ over which the model is constructed, is that the inequalities in this direction involve the linear functions $\mu_{i,p}$ and $\nu_{j,p}$ with the highest slopes, whose presence in a generic model is unaffected by the existence of non-Higgsable clusters. In the preceding discussion, it was the linear functions with the smallest slopes that set the bounds.

B.10.2 Vertical models

The tighter bounds on $|n_p - n_{p+1}|$ for vertical models are obtained in an analogous way to the ones applying to horizontal models. Hence, we keep the discussion brief and only point out the differences with respect to the preceding case and the final result.

Tighter bounds on $n_p - n_{p+1}$ and $n_p - n_{p-1}$

The main difference with respect to the horizontal case is that in the equations (B.10.3) the variables i and j now refer to the power with which, without loss of generality, v appears in the monomial under consideration. Hence, we have to substitute (B.10.5) for

$$0 \leq i \leq 8 + 4n, \quad (\text{B.10.25})$$

$$0 \leq j \leq 12 + 6n, \quad (\text{B.10.26})$$

where we observe that only the upper bounds are different. The bounds (B.10.22) on $n_p - n_{p+1}$, with $p \in \{0, \dots, P-1\}$, for horizontal models were set by the linear functions $\mu_{i,p}$ and $\nu_{j,p}$ of smallest slope, and therefore remain valid for vertical models, i.e. we have again

$$n_p - n_{p+1} \leq \begin{cases} 8, & 0 \leq n \leq 2, \\ 4, & 3 \leq n \leq 4, \\ 2, & 5 \leq n \leq 8, \\ 1, & 9 \leq n \leq 12, \end{cases} \quad p = 0, \dots, P-1. \quad (\text{B.10.27})$$

The bounds (B.10.24) on $n_p - n_{p+1}$, with $p \in \{1, \dots, P\}$, for horizontal models were determined by the linear functions $\mu_{i,p}$ and $\nu_{j,p}$ of highest slope, instead. Since in vertical models these functions can be steeper according to (B.10.26), we find, *mutatis mutandis*, that

$$n_p - n_{p-1} \leq 2(4 + 4n). \quad (\text{B.10.28})$$

Both sets of constraints apply to vertical models presenting the single and double accidental cancellation structures.

B.11 Bounds on the vertical gauge rank

In Section 6.3.6, we argued that the rank of the gauge factors supported over representatives of the global divisor \mathcal{F} cannot be arbitrarily high in a horizontal model, with the obvious bound

$$\text{rank}(\mathfrak{g}_{\text{ver}}) \leq 18 \quad (\text{B.11.1})$$

coming from heterotic/heterotic duality. This bound can be improved by analysing the geometry more carefully, which in horizontal models with no components at weak coupling leads to the bounds given in Table 6.3.3. To illustrate the process, we derive the bound for horizontal models constructed over $\hat{B} = \mathbb{F}_8$ with no components at weak coupling in Section B.11.1. In the presence of components at weak coupling, the bounds can become more stringent; we exemplify this in Section B.11.2 by deriving a new bound for horizontal models constructed over $\hat{B} = \mathbb{F}_7$ with codimension-zero singular elliptic fibers that is stricter than the one printed in Table 6.3.3.

B.11.1 $\hat{B} = \mathbb{F}_8$ with no components at weak coupling

According to Table 6.3.3, for horizontal models constructed over $\hat{B} = \mathbb{F}_8$ with no components at weak coupling the vertical gauge rank is subject to the constraint

$$\text{rank}(\mathfrak{g}_{\text{ver}}) \leq 4. \quad (\text{B.11.2})$$

Let us derive this result.

The starting point is the rough bound (B.11.1) derived from heterotic/heterotic duality considerations. An improved rough bound can be obtained by estimating how many vertical classes can be factorised before we encounter a curve of non-minimal fibers. In a resolved horizontal model constructed over $\hat{B} = \mathbb{F}_8$, the Y^P component of the central fiber Y_0 contains a non-Higgsable cluster with component vanishing orders

$$\text{ord}_{Y^P}(f_P, g_P, \Delta'_P)_{s=0} = (3, 5, 9), \quad (\text{B.11.3})$$

see Table 6.3.1. Such a line of singular elliptic fibers can remain of Kodaira type III*, enhance to Kodaira type II* or become non-minimal. It is then clear that for this class of models⁷

$$\text{ord}_{Y^P}(\Delta'_P)_{s=0} \leq 10. \quad (\text{B.11.4})$$

Particularizing the discriminant (6.3.5c) to the case in which no component is at weak coupling, we obtain

$$\Delta'_P = 12S_P + 24V_P. \quad (\text{B.11.5})$$

After a given number of tunings involving S_P and V_P classes, the residual discriminant will not be forced to contain an S_P component as long as

$$(\Delta'_P - \alpha V_P - \beta S_P) \cdot S_P \geq 0 \Leftrightarrow n(\beta - 12) + 24 \geq \alpha. \quad (\text{B.11.6})$$

Using then (B.11.4) and particularizing to $\hat{B} = \mathbb{F}_8$, we obtain that the number α of V_P classes that can be factorised in the discriminant must be

$$\alpha \leq 8, \quad (\text{B.11.7})$$

if we want to avoid non-minimal component vanishing orders over S_P . With a budget of $8V_P$ vertical classes in Δ'_P to be distributed over the local vertical gauge enhancements in the Y^P component, and hence a maximum of $8\mathcal{F}$ classes in Δ_{phys} , we can simply list the a priori possible combinations of vertical enhancements. In Table B.11.1 we do this for the subset of them that use all available $8V_P$ classes and that therefore are the best candidates to give the highest vertical gauge rank, in principle. Going through this list and assigning an optimistic naive rank to each

⁷If the enhancement over S_P is of I_m or I_m^* type, the inequality no longer holds.

Vanishing orders	Naive rank	Result of the analysis
(2, 3, 8)	$D_6 \sim 6$	$(2, 3, 7) \sim B_4 \sim 4$
$(2, 3, 6) + (0, 0, 2)$	$D_4 + A_1 \sim 5$	$(2, 3, 6) \sim G_2 \sim 2$
$(1, 2, 3) + (1, 2, 3) + (0, 0, 2)$	$A_1 + A_1 + A_1 \sim 3$	$(1, 2, 3) + (1, 2, 3) \sim A_1 + A_1 \sim 2$
$(1, 2, 3) + (0, 0, 5)$	$A_1 + A_4 \sim 5$	$(1, 2, 3) + (0, 0, 2) \sim A_1 + A_1 \sim 2$
$(1, 2, 3) + (0, 0, 3) + (0, 0, 2)$	$A_1 + A_2 + A_1 \sim 4$	$(1, 2, 3) + (0, 0, 1) + (0, 0, 1) \sim A_1 \sim 1$
(0, 0, 8)	$A_7 \sim 7$	$(0, 0, 4) \lesssim A_3 \sim 3$
$(0, 0, 6) + (0, 0, 2)$	$A_5 + A_1 \sim 6$	$(0, 0, 3) + (0, 0, 1) \lesssim A_2 \sim 2$
$(0, 0, 5) + (0, 0, 3)$	$A_4 + A_2 \sim 6$	$(0, 0, 3) + (0, 0, 1) \lesssim A_2 \sim 2$
$(0, 0, 4) + (0, 0, 4)$	$A_3 + A_3 \sim 6$	$(0, 0, 2) + (0, 0, 2) \lesssim A_1 + A_1 \sim 2$
$(0, 0, 4) + (0, 0, 2) + (0, 0, 2)$	$A_3 + A_1 + A_1 \sim 5$	$(0, 0, 2) + (0, 0, 1) + (0, 0, 1) \lesssim A_1 \sim 1$
$(0, 0, 3) + (0, 0, 3) + (0, 0, 2)$	$A_2 + A_2 + A_1 \sim 5$	$(0, 0, 2) + (0, 0, 1) + (0, 0, 1) \lesssim A_1 \sim 1$
$(2, 2, 4) + (2, 2, 4)$	$A_2 + A_2 \sim 4$	$(2, 2, 4) + (2, 2, 4) \sim A_1 + A_1 \sim 2$

Table B.11.1: A priori possible maximal vertical gauge ranks over \mathbb{F}_8 .

enhancement, i.e. assuming that it is possible and that the associated monodromy cover is split, we obtain a new rough bound for the vertical gauge rank in this class of models, namely

$$\text{rank}(\mathfrak{g}_{\text{ver}}) \leq 7, \quad (\text{B.11.8})$$

that is much tighter than (B.11.1).

In order to improve on this result and obtain a bound that can actually be saturated, we need to analyse the viability of the possible patterns of vertical enhancements, which we now do case by case.

- I_m series: Let us start by considering the case of a single vertical line of I_m fibers in the Y^P component obtained through a single accidental cancellation. Let us assume without loss of generality that the tuning occurs over the representative of V_P given by $\{v = 0\}_{B^P}$. We then must have

$$f_P = v^{l_v} \check{f}_P^v + f_P^v, \quad (\text{B.11.9a})$$

$$g_P = v^{m_v} \check{g}_P^v + g_P^v, \quad (\text{B.11.9b})$$

with

$$f_P^v = -3h_v^2, \quad g_P^v = 2h_v^3. \quad (\text{B.11.10})$$

Since

$$H_v = 2S_P + 4V_P \Rightarrow h_v \propto s^2, \quad (\text{B.11.11})$$

the obstruction granting minimal component vanishing orders over S_P must come from \check{f}_P^v and \check{g}_P^v . Taking into account the non-Higgsable cluster, these are in the curve classes

$$\check{F}_P^v = (3S_P) + [S_P + (8 - l_v)V_P], \quad (\text{B.11.12a})$$

$$\check{G}_P^v = (5S_P) + [S_P + (12 - m_v)V_P]. \quad (\text{B.11.12b})$$

As a consequence, \check{f}_P^v/s^3 and \check{g}_P^v/s^5 are irreducible if $l_v \leq 0$ and $m_v \leq 4$, respectively. It follows that the best we can obtain through a single accidental cancellation structure is I_4 fibers. The associated monodromy cover in the Y^P component is always split⁸

$$\psi + \frac{9g_P}{2f_P} \Big|_{v=0} = \psi - 3h_v|_{v=0} = \psi - s^2w^4 = (\psi + sw^2)(\psi - sw^2) = 0, \quad (\text{B.11.13})$$

leading to $\text{rank}(\mathfrak{g}_{\text{ver}}) \leq 3$ from this pattern of enhancements.

Obtaining a higher cancellation structure demands that $l_v = m_v \geq 1$, see Appendix B.9, and cannot therefore not be realised in these models, since it would lead to non-minimal component vanishing orders above S_P .

Finally, we may consider tuning various lines of vertical I_m fibers, each of them obtained through a single accidental cancellation structure. Considering for example tuning two, the same arguments given above lead, *mutatis mutandis*, to $l_1 + l_2 \leq 0$ and $m_1 + m_2 \leq 4$. This is less efficient and leads to lower vertical gauge ranks than what can be obtained with a single vertical I_m tuning.

- $I_m^* + I_{m'}$ series: This case encompasses both the situation in which the lines of vertical I_m^* and $I_{m'}$ fibers are separated, as well as the one in which the latter are brought on top of the former to produce a higher I_m^* enhancement.

Start by tuning a line of vertical I_0^* fibers, which can be located without loss of generality over $\{v = 0\}_{B^P}$. This enhances the non-Higgsable cluster to

$$\text{ord}_{Y^P}(f_P, g_P, \Delta'_P)_{s=0} = (4, 5, 10). \quad (\text{B.11.14})$$

As a consequence, the only obstruction to having non-minimal component vanishing orders over S_P comes from g_P . Consider tuning an additional I_m type vertical line of fibers over $C = \{p_C = 0\}_{B^P}$. Writing g_P as

$$g_P = p_C^{m_C} \check{g}_P^C + g_P^C, \quad (\text{B.11.15})$$

and noting that

$$\check{G}_P^C = (5S_P) + [S_P + (12 - 3 - m_1)V_P], \quad (\text{B.11.16})$$

we see that $m_C \leq 1$ and at most we can obtain I_1 fibers through a single accidental cancellation, which by themselves do not lead to an increase in the vertical gauge rank. Hence, we need to analyse the cases in which we have

$$\text{ord}_{Y^P}(f_P, g_P, \Delta'_P)_{v=0} = (2, 3, 6) \quad \text{or} \quad (2, 3, 7). \quad (\text{B.11.17})$$

For the first of these, the monodromy cover in the component is non-split,

$$\psi^3 + \psi \left(\frac{f_P}{v^2} \right) \Big|_{v=0} + \left(\frac{g_P}{v^3} \right) \Big|_{v=0} = \psi^3 + \psi s^4 w^6 + s^5 (sw^9 + e_{P-1} w) = 0, \quad (\text{B.11.18})$$

⁸To determine the gauge rank for the global vertical enhancement we would need to analyse the monodromy cover in all components, see Section 5.4.4. We do not do so because, even if it were globally split, the obtained rank would be surpassed by the one obtained from other series below and therefore not inform us about the bound.

leading to I_0^{*ns} fibers. This folding of the algebra affects the global enhancement over \mathcal{F} , and we therefore have an associated \mathfrak{g}_2 algebra.

For the second case, we have instead the monodromy cover

$$\psi^2 + \frac{1}{4} \left(\frac{\Delta'_P}{v^7} \right) \left(\frac{2vf_P}{9g_P} \right)^3 \Big|_{v=0} = 0. \quad (\text{B.11.19})$$

Since $m_C = 1$, the structure of Δ'_P must be

$$\Delta'_P = vh_C^k \Delta''_P, \quad k \geq 3. \quad (\text{B.11.20})$$

The divisor class of Δ''_P is then

$$\Delta''_P = [(10 - 2k)S_P] + [2S_P + (24 - 1 - 4k)V_P]. \quad (\text{B.11.21})$$

The first term in the preceding expression corresponds to the part of the enhanced non-Higgsable cluster that is not accounted for by the h_C^k factor. If $k \geq 4$, the second term is generically reducible, factorising $2S_P$, and since $h_C \propto s^2$ we obtain $\Delta'_P \propto s^{2k} s^{10-2k+2} = s^{12}$, i.e. to non-minimal component vanishing orders over S_P . The monodromy cover for the remaining case $k = 3$ takes the form

$$\frac{1}{4} \left(\frac{\Delta'_P}{v^7} \right) \left(\frac{2vf_P}{9g_P} \right)^3 \Big|_{v=0} = \left(-\frac{1}{108} \frac{1}{v^3} \Delta''_P \right) \Big|_{v=0}. \quad (\text{B.11.22})$$

Given that

$$\Delta''_P - 3V_P \sim 5S_P + T_P, \quad (\text{B.11.23})$$

we therefore generically have

$$\psi^2 - \frac{1}{108} s^5 p_{1,8}([s : t], [v : w]) = 0. \quad (\text{B.11.24})$$

Forcing the monodromy to be split would require tuning the t term in $p_{1,8}([s : t], [v : w])$ to be zero, but this is the term preventing the non-minimal enhancement over S_P . Therefore, we have a I_1^{*ns} fiber, associated with the gauge algebra B_4 . We have realised such a model in an explicit example, meaning that $\text{rank}(\mathfrak{g}_{\text{ver}}) = 4$ is possible; hence, those candidate patterns of vertical tunings that do not surpass this rank in the following series do not need to be analysed explicitly for the determination of the bound.

- $\text{III} + I_m$ series: The only candidate in this series that could surpass the putative bound of $\text{rank}(\mathfrak{g}_{\text{ver}}) \leq 4$ is $\text{III} + I_5$, but we have noted earlier that tuning I_5 type vertical lines is not even possible in the absence of the III enhancement. It can be seen, through arguments analogous to the ones employed above, that we can at best have

$$(1, 2, 3) + (0, 0, 2) \sim A_1 + A_1, \quad (\text{B.11.25})$$

or

$$(1, 2, 3) + (1, 2, 3) \sim A_1 + A_1, \quad (\text{B.11.26})$$

after which no additional vertical tunings are possible. Both of these are well below the putative bound.

- IV series: It can be checked that all vertical enhancement patterns involving a line of IV fibers lie below the putative bound of $\text{rank}(\mathfrak{g}_{\text{ver}}) \leq 4$. One of these patterns, namely having IV + IV, can in principle saturate the bound. However, the vertical tuning enhances the non-Higgsable cluster to

$$\text{ord}_{Y^P}(f_P, g_P, \Delta'_P)_{s=0} = (4, 5, 10), \quad (\text{B.11.27})$$

which means that g_P must contain a $p_{1,8}([s:t], [v:w])$ factor whose t term cannot vanish if we want to avoid a non-minimal enhancement over S_P . This makes the monodromy cover for both lines of IV fibers take the form

$$\psi^2 - \frac{g}{w^2} \Big|_{w=0} = \psi^2 - s^5 p_{1,8}([s:t], [v:w]) (q_{0,1}([s:t], [v:w]))^2 = 0, \quad (\text{B.11.28})$$

which is always non-split, meaning that at best we can achieve $A_1 + A_1$ with this pattern.

Altogether, we have obtained an explicit example that reaches $\text{rank}(\mathfrak{g}_{\text{ver}}) = 4$, and checked that those candidates that could in principle surpass this value either cannot be tuned, or have non-split monodromy cover that reduce their rank. We conclude that, for a horizontal model constructed over $\hat{B} = \mathbb{F}_8$ with no components at weak coupling, the bound on the vertical gauge rank is

$$\text{rank}(\mathfrak{g}_{\text{ver}}) \leq 4. \quad (\text{B.11.29})$$

B.11.2 $\hat{B} = \mathbb{F}_7$ with components at weak coupling

Once we allow some components to have codimension-zero Kodaira type $I_{n_p > 0}$ elliptic fibers, the bounds on the vertical gauge rank computed above can, and indeed in most cases do, become stricter. The reason for this is the restriction on the types of enhancements that can occur over components with $I_{n_p > 0}$ codimension-zero fibers, which, as we explained in Section 6.3.4, must be compatible with the local weak coupling. This means that, focusing on those types of singular fibers associated to a non-trivial gauge algebra, the global vertical enhancements can only be of Kodaira type III, IV, I_m or I_m^* if at least one component is at weak coupling; in a global weak coupling limit only the latter two can be realised. If the bound given in Table 6.3.3 for the models without codimension-zero singular fibers cannot be saturated using only these types of enhancements, the presence of the components at weak coupling will correspondingly decrease the possible maximal vertical gauge rank. Note that, due to the non-generic nature of the Weierstrass models that support such codimension-zero singular fibers, it may be that even if enhancements of these types can saturate the bound in the generic case, they are no longer viable in models with components at weak coupling.

The bounds given in Table 6.3.3 can still be saturated for horizontal models constructed over $\hat{B} = \mathbb{F}_n$, with $8 \leq n \leq 12$, even when there are components at weak coupling. We take instead those horizontal models constructed over $\hat{B} = \mathbb{F}_7$ to illustrate the reduction in the possible vertical gauge rank. We will assume in the derivation below that the end component Y^P is not at weak coupling, since this is less constraining than the alternative, which would likely lead to a stronger bound. According to Table 6.3.3, in the absence of codimension-zero $I_{n_p > 0}$ fibers we have

$$\text{rank}(\mathfrak{g}_{\text{ver}}) \leq 8. \quad (\text{B.11.30})$$

This bound can most easily be saturated by tuning a vertical line of II^* fibers; this is one type of enhancement that is no longer possible over \mathcal{F} once we have even a single component at weak coupling.

Vanishing orders	Naive rank	Result of the analysis
$(0, 0, 10)$	$A_9 \sim 9$	$(0, 0, 5) \lesssim A_4 \sim 4$
$(1, 2, 3) + (0, 0, 7)$	$A_1 + A_6 \sim 7$	$(1, 2, 3) + (0, 0, 3) \lesssim A_1 + A_2 \sim 3$
$(2, 2, 4) + (0, 0, 6)$	$A_2 + A_5 \sim 7$	$(2, 2, 4) + (0, 0, 3) \lesssim A_2 + A_2 \sim 4$
$(1, 2, 3) + (1, 2, 3) + (1, 2, 3)$	$A_1 + A_1 + A_1 \sim 3$	$(1, 2, 3) + (1, 2, 3) \sim A_1 + A_1 \sim 2$
$(1, 2, 3) + (2, 2, 4) + (0, 0, 3)$	$A_1 + A_2 + A_2 \sim 5$	$(1, 2, 3) + (2, 2, 4) + (0, 0, 1) \lesssim A_1 + A_2 \sim 3$
$(2, 2, 4) + (2, 2, 4) + (0, 0, 2)$	$A_2 + A_2 + A_1 \sim 4$	$(2, 2, 4) + (2, 2, 4) + (0, 0, 1) \lesssim A_2 + A_2 \sim 4$
$(2, 3, 10)$	$D_8 \sim 8$	$(2, 3, 8) \sim B_5 \sim 5$
$(2, 3, 6) + (0, 0, 4)$	$D_4 + A_3 \sim 7$	$(2, 3, 6) + (0, 0, 2) \lesssim D_4 + A_1 \sim 5$
$(2, 3, 6) + (1, 2, 3)$	$D_4 + A_1 \sim 5$	$(2, 3, 6) + (1, 2, 3) \lesssim D_4 + A_1 \sim 5$
$(2, 3, 6) + (2, 2, 4)$	$D_4 + A_2 \sim 6$	$(2, 3, 6) + (2, 2, 4) \lesssim D_4 + A_1 \sim 5$

Table B.11.2: Possible maximal vertical gauge ranks over \mathbb{F}_7 in the presence of codimension-zero $I_{n_p > 0}$ fibers over the intermediate components.

We keep the discussion brief, since the analysis follows the same lines as the one in the previous section. The non-Higgsable in the Y^P component of the central fiber Y_0 of a resolved horizontal model constructed over $\hat{B} = \mathbb{F}_8$ is

$$\text{ord}_{Y^P}(f_P, g_P, \Delta'_P)_{s=0} = (3, 5, 9), \quad (\text{B.11.31})$$

see Table 6.3.1. Hence, (B.11.4) and (B.11.6) still apply, and we have a budget of at most $10V_P$ vertical classes in Δ'_P to be distributed over the local vertical enhancements in the Y^P component, a fact that is mirrored globally for the \mathcal{F} class in Δ_{phys} . The subset of a priori possible vertical enhancement patterns that both use these $10V_P$ available classes and are compatible with some components being at weak coupling are listed in Table B.11.2.

Let us now do a detailed analysis, case by case.

- I_m series: Considering first the case of a single vertical line of I_m fibers, the same argument of Section B.11.1 leads in this case to $l_v \leq 1$ and $m_v \leq 5$ for \check{f}_P^v/s^3 and \check{g}_P^v/s^5 to be irreducible, respectively. This means that, if the I_m fibers are tuned through a single accidental cancellation structure, we can obtain up to Kodaira type I_5 . The tuning is less efficient in terms of obtained rank if we try to obtain various lines of I_m fibers.⁹

For a double accidental cancellation to be possible, we need $l_v = m_v =: r_v$, which means that $r_v \leq 1$ and, as a consequence, we can at best obtain a vertical line of I_2 fibers through this type of tuning.

Higher accidental cancellation structures cannot be realised in this class of models. These build on top of each other, and therefore the first one to be considered is that of triple accidental cancellations. We use the same notation as in Appendix B.9, slightly adapted. From (B.9.8) we see that, since $h_P^v \propto s^2$, we must have $\check{f}_P^v \propto s^3$ at most; otherwise, the terms in \check{g}_P^v proportional to s^5 or smaller would need to be set to zero for the accidental

⁹It could occur that a single vertical line of I_m fibers is forced, for high m , to be non-split, its rank being then surpassed by various independent tunings that, although naively would lead to a smaller rank, allow for a split monodromy cover. This cannot be the case here, since the vertical I_m singularities turn out to be split for horizontal models constructed over $\hat{B} = \mathbb{F}_7$.

cancellations to be possible, which would lead to a non-minimal enhancement over S_P . In fact, we see from that the presence of the non-Higgsable cluster means that

$$\left. \begin{aligned} h_P^v &\propto s^2 \\ \check{f}_P^v &\propto s^3 \\ \check{g}_P^v &\propto s^5 \end{aligned} \right\} \Rightarrow q_P^v \propto s^5. \quad (\text{B.11.32})$$

In the triple accidental cancellation structure (B.9.14) this means that the first term is $h_P^v q_P^v \propto s^7$, while the second is $\check{f}_P^v \propto s^6$ and cannot go higher, meaning that the cancellation cannot occur.

- III series: Tuning a vertical III + III enhancement is possible without producing non-minimal fibers over S_P , while adding a third III forces $4S_P$ and $6S_P$ to factorise in F_P and G_P , respectively. The result is below the rank that could be achieved with the vertical line of I_m fibers. After tuning III + III we see, arguing as we did above, that we can additionally have a single accidental cancellation producing a line of vertical I_1 fibers, which does not increase the obtained rank.
- III + IV series: Tuning a vertical III + IV leads to the residual divisors

$$F_P - V_P - 2V_P = 4S_P + 5V_P, \quad (\text{B.11.33a})$$

$$G_P - 2V_P - 2V_P = 5S_P + (S_P + 8V_P), \quad (\text{B.11.33b})$$

from which we see that no non-abelian gauge algebra involving a factorisation of V_P classes in F_P and G_P can be tuned without leading to a non-minimal enhancement over S_P . It is possible to tune an additional vertical line of I_1 fibers, which does not, however, increase the rank. This means that, even if the IV singularities have a split monodromy cover, we have $\text{rank}(\mathfrak{g}_{\text{ver}}) \leq 3$ in this series.

- IV series: Arguing analogously, we observe that we can tune a vertical IV + IV, with room left only for an accidental cancellation yielding an additional vertical line of I_1 fibers. Even if both IV singularities are split, we obtain at most $\text{rank}(\mathfrak{g}_{\text{ver}}) \leq 4$ in this series, which is below the maximal vertical gauge rank that we will achieve below.
- III + $I_{m'}$ series: Tuning a single vertical line of III fibers still leaves room to tune a single accidental cancellation up to a vertical line of Kodaira type I_3 fibers which, even if split, would yield at most $\text{rank}(\mathfrak{g}_{\text{ver}}) \leq 3$ in this series.
- IV + I_m series: Similarly to the previous case, we can tune a vertical line of IV fibers and, additionally, a single accidental cancellation up to a vertical line of Kodaira type I_3 fibers. This leads, at best, to $\text{rank}(\mathfrak{g}_{\text{ver}}) \leq 4$ in this series.
- $I_m^* + I_{m'}$ series: Tuning a vertical line of I_0^* fibers leaves enough room for accidental cancellations to occur, with

$$\check{f}_P^v = (3S_P) + [S_P + (8 - 2 - l_v)V_P], \quad (\text{B.11.34a})$$

$$\check{g}_P^v = (5S_P) + [S_P + (12 - 3 - m_v)V_P]. \quad (\text{B.11.34b})$$

This means that only the single accidental cancellation structure can be realised, with $m_v \leq 2$, leaving as possible vertical enhancement patterns

$$(2, 3, 8) \lesssim D_6, \quad (B.11.35)$$

$$(2, 3, 7) + (0, 0, 1) \lesssim B_5, \quad (B.11.36)$$

$$(2, 3, 6) + (0, 0, 2) \lesssim D_4 + A_1. \quad (B.11.37)$$

Out of these tunings I_2^* reaches the highest possible vertical rank in the series, even if it is non-split. To determine whether it can be split or not, we first look at the monodromy cover in the Y^P component. For $m_v = 2$, we see that the only term preventing a non-minimal enhancement over S_P is the t term in the factor $p_{1,7}([s : e_{P-1}], [v : w]) = S_P + 7V_P$ in g_P . The monodromy cover in the component is

$$\psi^2 + \left(\frac{\Delta'_P}{v^7} \right) \left(\frac{2vf_P}{9g_P} \right)^2 \Big|_{v=0} = 0, \quad (B.11.38)$$

which will be non-split due to the presence of that very same term. We have explicitly constructed such an enhancement in a horizontal model constructed over $\hat{B} = \mathbb{F}_7$ with a $I_0 - I_1 - I_0$ pattern of codimension-zero singular elliptic fibers.

- $I_m^* + \text{III}$ series: It is possible to tune a vertical $I_m^* + \text{III}$, with no room left for further non-abelian vertical enhancements. This would give, at best, $D_4 + A_1$, which would not improve the vertical gauge rank found above.
- $I_m^* + \text{IV}$ series: Tuning a vertical $I_m^* + \text{IV}$ is possible, with no further vertical lines of singular fibers possible. In principle, this can surpass the rank obtained above if both singularities are split, giving $D_4 + A_2$. The tuning leads to

$$F_P = (2V_P) + (2V_P) + (4S_P) + [4V_P], \quad (B.11.39)$$

$$G_P = (3V_P) + (2V_P) + (5S_P) + [S_P + 7V_P], \quad (B.11.40)$$

where we see that having non-minimal fibers over S_P is only prevented by the t term in the factor $p_{1,7}([s : t], [v : w]) = S_P + 7V_P$ in g_P . This factor cannot be set to zero, and it makes the monodromy cover of the IV enhancement in the B^P component, which has the form

$$\psi^2 - \left(\frac{g_P}{v^2} \right) \Big|_{v=0} = 0, \quad (B.11.41)$$

non-split. This implies that the enhancement is then at most $D_4 + A_1$, and we do not need to analyse the case further.

We conclude that, in the presence of components at weak coupling, the vertical gauge rank in horizontal models constructed over $\hat{B} = \mathbb{F}_7$ must satisfy

$$\text{rank}(\mathfrak{g}_{\text{ver}}) \leq 5. \quad (B.11.42)$$

The highest possible vertical gauge rank has decreases with respect to the one that can be achieved in the absence of codimension-zero singular elliptic fibers, shown in Table 6.3.3.

B.12 Defect algebras in the heterotic dual

Motivated by the goal to understand the vertical gauge algebras as defects in the decompactification limits, we use this appendix to elaborate on their interpretation as non-perturbative gauge algebra factors in the heterotic dual. Among these factors, those not related to a tensor branch transition originate from point-like instantons with discrete holonomy probing geometric singularities on the heterotic K3 surface [199]. These are also known as fractional point-like instantons. As a novel point, we emphasise in Section B.12.2 the relevance of the distribution of such point-like instantons between the two Hořava-Witten walls for realising the non-perturbative gauge algebra. This is to be contrasted with the behaviour of point-like instantons with trivial holonomy, which we discuss in Section B.12.1. The natural appearance of heterotic ADE singularities probed by fractional point-like instantons in the analysis of the asymptotic physics of codimension-one infinite-distance degenerations of F-theory models has recently sparked interest in a detailed local analysis of the Higgs branch of the associated LSTs [363–368].

Heterotic string theory compactified on a K3 surface with ADE singularities was analysed by Witten in [349]. Interestingly, such singularities behave rather differently from how they do in M-theory or Type IIA string theory.

As is well known, an ADE singularity in the internal space of M-theory or Type IIA string theory signals a gauge enhancement of ADE type. The exceptional \mathbb{P}^1 curves shrinking to zero volume at the corresponding point in moduli space have an intersection matrix reproducing the Cartan matrix of the underlying ADE Lie algebra. The M2-branes wrapping these exceptional curves lead to a series of massless particles that furnish the non-abelian gauge algebra. This is precisely how such algebras arise in the F-theory limit of M-theory.¹⁰

The conclusion of [349] is that the heterotic string theory near an ADE singularity does not exhibit a corresponding non-perturbative gauge algebra unless it is probed by small instantons. The analysis proceeds by considering heterotic string theory in the absence of small instantons, which makes it tractable in the framework of conformal field theory. The appearance of gauge algebras like the ones discussed is associated to singularities in the moduli space of the theory, which are a possible signal of non-perturbative physics. Working at string tree level, [349] analyses the moduli space of the theory, finding that it should be smooth once α' -corrections are taken into account,¹¹ and therefore concluding that no non-perturbative gauge algebra arises.¹²

The situation changes if the ADE singularity is probed by a small instanton. This can be heuristically understood by looking at the classical equation of motion for the ten-dimensional dilaton [349], which can be schematically written as

$$\Delta^2 \phi = \text{tr } F_{ij} F^{ij} - \text{tr } R_{ij} R^{ij}. \quad (\text{B.12.1})$$

Here F_{ij} is the curvature of the heterotic gauge bundle and R_{ij} is the Ricci tensor of the internal space. A small instanton is a skyscraper sheaf, i.e. a singular gauge bundle in which all the curvature has been concentrated at a point. Such a configuration hence locally drives the dilaton to strong coupling. It is, therefore, not surprising that in the presence of small instantons probing the ADE singularity non-perturbative features become manifest. In their absence, the

¹⁰To be fully precise, the resulting algebra may not be of ADE type after folding by a monodromy action.

¹¹More concretely, [349] proposes that the moduli space for heterotic string theory near an ADE singularity of type G is the space of vacua of a minimal supersymmetric 3D $\mathcal{N} = 4$ gauge theory with gauge group G .

¹²The analysis of [349] holds both for $E_8 \times E_8$ and $\text{Spin}(32)/\mathbb{Z}_2$ heterotic string theory, since it is performed at string tree level and the two theories are distinguished by the fluctuations around the $F = 0$ background appearing once string loops are included.

geometric curvature associated with the ADE singularity works in the opposite direction, driving the dilaton towards small coupling, and hence preventing non-perturbative effects from arising.

The F-theory/heterotic duality, reviewed in Section 6.4.1, allows us to establish a connection between horizontal Type II.a models in the adiabatic regime and their controlled heterotic duals. This was done in Section 6.4: The gauge algebras localised at the six-dimensional defects within the decompactified theory have a heterotic dual interpretation in terms of ADE singularities of the internal K3 surface probed by small instantons, which we have just discussed above. Since these defect algebras are an important feature of the asymptotic physics of horizontal Type II.a models, it is worth revisiting them in some more detail from the point of view of F-theory/heterotic duality.

Let us recall that, according to this duality, the heterotic K3 surface can be identified with the intersection $Y^0 \cap Y^1$ of the components of the central fiber Y_0 of the resolved horizontal Type II.a model. The 24 singular elliptic fibers of the heterotic K3, counted with multiplicity, correspond to the 24 non-generic vertical slices on the F-theory side, i.e. to the intersection points

$$\Delta'_0 \cdot S_0 = \Delta'_1 \cdot T_1 = 24. \quad (\text{B.12.2})$$

The defining polynomials f_b , g_b and Δ_b of the Weierstrass model of the resolved family variety \mathcal{Y} of the horizontal Type II.a model contain the information about the elliptically fibered heterotic K3 surface. Namely, the defining polynomials of its Weierstrass model are

$$f_{K3} := f_b|_{e_0=e_1=0}, \quad g_{K3} := g_b|_{e_0=e_1=0}, \quad \Delta_{K3} := \Delta_b|_{e_0=e_1=0}. \quad (\text{B.12.3})$$

As a consequence, the types of ADE singularities present in the heterotic K3 surface can be read off from the Kodaira-Néron classification of singular elliptic fibers using the interface vanishing orders on the F-theory side. As pointed out in Section 5.2.2.2, the same information can be obtained directly from the unresolved horizontal Type II.a model. Denoting the base blow-up map involved in the open-chain resolution process by $\pi : \mathcal{B} \rightarrow \hat{\mathcal{B}}$, we have that

$$\pi_*(F_0) = F|_{\mathcal{U}} - 4(\mathcal{S} \cap \mathcal{U}), \quad (\text{B.12.4a})$$

$$\pi_*(G_0) = G|_{\mathcal{U}} - 6(\mathcal{S} \cap \mathcal{U}), \quad (\text{B.12.4b})$$

$$\pi_*(\Delta_0) = \Delta|_{\mathcal{U}} - 12(\mathcal{S} \cap \mathcal{U}), \quad (\text{B.12.4c})$$

and as a consequence

$$\text{ord}_{Y^0 \cap Y^1}(f_{K3}, g_{K3}, \Delta_{K3})_{\mathcal{Z}} = \text{ord}_{\pi^*(\mathcal{S} \cap \mathcal{U})} \left(\frac{f}{s^4} \Big|_{u=s=0}, \frac{g}{s^6} \Big|_{u=s=0}, \frac{\Delta}{s^{12}} \Big|_{u=s=0} \right)_{\mathcal{Z}}. \quad (\text{B.12.5})$$

To put it differently, the complete information on the heterotic K3 surface at the endpoint of the limit is contained in the coefficients in f , g and Δ (the defining polynomials of the Weierstrass model of the unresolved family variety $\hat{\mathcal{Y}}$) of the terms of middle homogeneous degree in the coordinates of \mathbb{P}_f^1 and independent on the coordinate of D . The remaining terms independent of the coordinate of D encode information on the heterotic gauge bundles at the endpoint of the limit [187].

In horizontal Type II.a limits in the adiabatic regime, the heterotic K3 surface decompactifies. Since this is a continuous process, the topology of the internal space is not changed by it, and the degeneration loci of the elliptic fiber are still present. A local patch around one such locus is equivalent to heterotic string theory on $\mathbb{C}^2/\Gamma_g \times \mathbb{R}^{1,5}$, where $\Gamma_g \hookrightarrow \text{SU}(2)$ is a finite subgroup of $\text{SU}(2)$ related to the singularity of the K3 surface via the McKay correspondence. In studies

oriented towards understanding 6D SCFTs, this is the local picture usually taken, see [270] for a review.

Heterotic ADE singularities in the presence of small instantons were studied in [298], assuming that the perturbative $E_8 \times E_8$ heterotic gauge group is unbroken, by using the duality to the F-theory side in the stable degeneration limit. We revisit and refine this discussion in Section B.12.1, considering the case in which the heterotic bulk gauge group is Higgsed, from a six-dimensional standpoint, in Section B.12.2. The situation in which enough ADE singularities of the heterotic K3 surface coalesce as to produce a non-minimal point was explored in Section 6.4.5.

B.12.1 Unbroken horizontal $E_8 \times E_8$ gauge algebra

Consider the subclass of horizontal Type II.a models constructed over the Hirzebruch surface $\hat{B} = \mathbb{F}_n$ in which, from the six-dimensional standpoint, the horizontal gauge algebra is

$$\mathfrak{g}_{\text{hor}} = \mathfrak{e}_8 \oplus \mathfrak{e}_8, \quad (\text{B.12.6})$$

obtained by supporting the gauge factors

$$\mathcal{H}_\infty^0 : E_8, \quad \mathcal{H}_0^1 : E_8. \quad (\text{B.12.7})$$

The divisor classes associated with the defining polynomials of the Weierstrass model of the components $\{Y^p\}_{0 \leq p \leq 1}$ are

$$F_0 = 4T_0 + F_0^{\text{res}}, \quad F_0^{\text{res}} := 8V_0, \quad (\text{B.12.8a})$$

$$G_0 = 5T_0 + G_0^{\text{res}}, \quad G_0^{\text{res}} := T_0 + 12V_0, \quad (\text{B.12.8b})$$

$$\Delta'_0 = 10T_0 + \Delta_0^{\text{res}}, \quad \Delta_0^{\text{res}} := 2T_0 + 24V_0, \quad (\text{B.12.8c})$$

in the B^0 component, and

$$F_1 = 4S_1 + F_1^{\text{res}}, \quad F_1^{\text{res}} := 8V_1 \quad (\text{B.12.9a})$$

$$G_1 = 5S_1 + G_1^{\text{res}}, \quad G_1^{\text{res}} := S_1 + 12V_1 \quad (\text{B.12.9b})$$

$$\Delta'_1 = 10S_1 + \Delta_1^{\text{res}}, \quad \Delta_1^{\text{res}} := 2S_1 + 24V_1 \quad (\text{B.12.9c})$$

in the B^1 component. In such a model we have the linear equivalence $\Delta_p^{\text{res}} = 2G_p^{\text{res}}$, for $p = 0, 1$, but also the identity of sets

$$\Delta_0^{\text{res}} \cap T_0 = G_0^{\text{res}} \cap T_0, \quad \Delta_1^{\text{res}} \cap S_1 = G_1^{\text{res}} \cap S_1. \quad (\text{B.12.10})$$

This can be directly seen from the polynomials whose vanishing loci describe the concrete divisor representatives associated with the model. Hence, the

$$G_0^{\text{res}} \cdot T_0 = 12 + n \quad \text{intersections in } B^0 \quad (\text{B.12.11a})$$

$$\text{and } G_1^{\text{res}} \cdot S_1 = 12 - n \quad \text{intersections in } B^1 \quad (\text{B.12.11b})$$

of $G_{\text{phys}}^{\text{res}}$ with the two horizontal lines of II^* fibers correspond, in a sufficiently generic model, to that many distinct nodes of $\Delta_{\text{phys}}^{\text{res}}$; their collision with the representatives of \mathcal{H}_∞^0 and \mathcal{H}_0^1 supporting the horizontal gauge enhancements leads to a series of codimension-two finite-distance non-minimal points.

As explained in [298], these codimension-two finite-distance non-minimal points correspond on the heterotic side to point-like instantons with trivial holonomy. Such singular gauge bundle

contributions do indeed preserve the unbroken perturbative heterotic gauge group, as expected from the F-theory side. Since they each contribute one unit of instanton charge to the integrated Bianchi identity, their distribution among the two heterotic E_8 bundles must agree with the instanton number splitting $c_2(V_{0,1}) = 12 \pm n$. This matches the assignment found in (B.12.11). Point-like instantons with trivial holonomy can be traded, through small instanton transitions, for M5-branes moving in the Hořava-Witten interval. Their position in S^1/\mathbb{Z}_2 corresponds to the volume of the exceptional \mathbb{P}^1 curves appearing on the F-theory side when the codimension-two finite-distance non-minimal points are resolved, as we already reviewed in Section 6.4.1. Of special relevance to our current discussion is the 1 hypermultiplet parametrising the position of a point-like instanton on the heterotic K3 surface. It is unaffected by small instanton transitions, and therefore plays the same role if we wish to take the M5-brane perspective. Consider the position within the \mathbb{P}_b^1 base of the heterotic K3 surface of a point-like instanton with trivial holonomy, corresponding to a certain node of $\Delta_{\text{phys}}^{\text{res}}$ on the F-theory side; it can be mapped to the position of said node within the representative of \mathcal{H}_∞^0 or \mathcal{H}_0^1 supporting the E_8 gauge factor associated with the heterotic gauge bundle to which the point-like instanton belongs. The freedom to move the position of the nodes of $\Delta_{\text{phys}}^{\text{res}}$ through a finite-distance complex structure deformation on the F-theory side allows us to arrange for the point-like instantons to probe or not probe the ADE singularities of the heterotic K3 surface. This is important for the manifestation of non-perturbative physics, as highlighted at the beginning of the section.

Let us start by considering heterotic K3 singularities not probed by singular gauge bundle contributions of any kind. According to the heterotic analysis of [349], such singularities should not lead to a non-perturbative gauge algebra contribution. As explained earlier, the Weierstrass model of the heterotic K3 surface is given by the defining polynomials f_{K3} , g_{K3} and Δ_{K3} ; on the F-theory side they encapsulate information on how the divisors F_{phys} , G_{phys} and Δ_{phys} intersect the interface curve $B^0 \cap B^1$. By making this intersection tangent, it is possible to increase the interface vanishing orders without increasing the component vanishing orders associated with the representative of f passing through the intersection point in B^0 and B^1 . This means that a heterotic ADE singularity can be tuned over a point of $B^0 \cap B^1$ without producing a codimension-one vertical enhancement on the F-theory side,¹³ and while maintaining the positions of the codimension-two finite-distance non-minimal points in \mathbb{P}_b^1 away from the position of the heterotic K3 singularity. Such a situation is depicted in the upper half of Figure B.15.

Through a finite-distance deformation of the model, we can alter the position of the point-like instantons in \mathbb{P}_b^1 to place them on top of the heterotic ADE singularity. On the F-theory side, one moves one of the codimension-two finite-distance non-minimal points occurring over the E_8 branes at \mathcal{H}_∞^0 and \mathcal{H}_0^1 to align it with the interface ADE singularity. This forces two copies of the representative of the fiber class f passing through that point to factorise in Δ'_0 or Δ'_1 , respectively.¹⁴ This leads to a local vertical enhancement that closes the gap between the

¹³Notice the similarities with the discussion on obscured infinite-distance limits carried out in Appendix B.3 and revisited in a concrete scenario in Section 6.4.5. The difference between the two situations stems from the fact that the base change revealing the obscured infinite-distance limit at the level of the family vanishing orders now, since the interface vanishing orders are minimal, merely has the effect of producing a minimal local gauge enhancement in the intermediate components of the central fiber of the base-changed model. Since such a local gauge enhancement does not extend into a global gauge enhancement, there is no gauge algebra associated with it. This was to be expected, since the base-changed degeneration is physically equivalent to the original one.

¹⁴The divisors $\{F_p^{\text{res}}\}_{0 \leq p \leq P}$ consist purely of vertical classes, which makes their interface vanishing orders at the heterotic K3 singularity agree with the component vanishing orders over the vertical line passing through it. The divisors $\{G_p^{\text{res}}\}_{0 \leq p \leq P}$ have intersection $G_p^{\text{res}} \cdot f = 1$, for $p = 0, 1$, which for the representative of f passing through the heterotic K3 singularity is already accounted for by said point. As explained in [298], moving a point-like instanton to lie on the same representative of f would lead to a second point of intersection, a contradiction that

interface vanishing orders corresponding to the heterotic ADE singularity and the component vanishing orders associated with the representative of f passing through it, but only in the component to which the codimension-two finite-distance non-minimal point that was aligned with it belongs to. We depict the result of such a finite-distance deformation in the lower half of Figure B.15. Hence, we learn from the F-theory side that it is not only important that the heterotic K3 singularity is probed by point-like instantons; the heterotic E_8 bundle to which they belong determines which half of the F-theory dual model realises a local vertical enhancement. This raises the question of what happens when the singularity is probed asymmetrically.

From the heterotic point of view, it is clear that the non-perturbative gauge algebra should only depend on the number of point-like instantons with trivial holonomy probing the heterotic ADE singularity. This is because, through a small instanton transition, we can trade them for M5-branes located in the Hořava-Witten interval, at which point they no longer belong to one of the two heterotic E_8 bundles and the notion of asymmetric probing loses its meaning.

The same conclusion holds on the F-theory side: As we now explain, the notion of asymmetrically probing a heterotic ADE singularity by point-like instantons with trivial holonomy is an artefact of the resolved degeneration. Even if the stable degeneration limit is necessary to have control over the heterotic dual model, let us for a moment entertain the possibility of studying the codimension-two finite-distance non-minimal singularities in a conventional six-dimensional F-theory model in which the base is an irreducible surface $B = \mathbb{F}_n$. After performing a base blow-up leading to $\hat{B} = \text{Bl}_1(\mathbb{F}_n)$, the base geometry is agnostic to its origin as the blow-up of $B = \mathbb{F}_n$ or, say, $B' = \mathbb{F}_{n-1}$. This can be easily seen from the toric fans of these three surfaces.¹⁵ This reflects the fact that, once we consider \hat{B} as the base of the F-theory model, we have moved the M5-brane into the Hořava-Witten interval in the putative heterotic dual, and the F-theory geometry no longer knows the initial distribution of instanton number between the two heterotic E_8 bundles. The effect of the stable degeneration limit is to separate the information pertaining to the two heterotic E_8 bundles, which for the reducible central fiber $Y_0 = Y^0 \cup_{K3} Y^1$ is encoded in $\text{Def}(Y^0)$ and $\text{Def}(Y^1)$, respectively. The blow-up of the reducible base surface B_0 with centre a codimension-two finite-distance non-minimal point is now different depending on whether this point is located on B^0 or on B^1 : Even after moving into the tensor branch, there is a clear notion of the heterotic E_8 bundle to which the M5-brane belongs, namely the one associated to the component in which the exceptional curve is located. In this sense, asymmetrically probing heterotic ADE singularities by point-like instantons with trivial holonomy has a definite meaning, but the resulting physics should not depend on this notion.

Indeed, the non-perturbative heterotic gauge sector corresponds on the F-theory side to the collection of gauge algebra factors supported both on the exceptional curves arising from the resolution of codimension-two finite-distance non-minimal points and on global vertical divisors. The former are always contained within a component, while the latter traverse the whole base geometry. This means that a discrepancy between vertical local and global gauge enhancements can occur. This discrepancy corresponds to the heterotic ADE singularity being asymmetrically probed by (k_0, k_1) point-like instantons with trivial holonomy. The vertical gauge algebra that manifests is the same one appearing if the heterotic ADE singularity is symmetrically probed by $k := \min(k_0, k_1)$ point-like instantons with trivial holonomy. The additional point-like instantons

the geometry resolves by making G_0^{res} or G_1^{res} , depending on the component under consideration, reducible with a copy of the relevant f representative factoring out. Altogether, this means that moving a point-like instanton on top of the heterotic K3 singularity leads to a local vertical $(1, 1, 2)$ enhancement. This process continues as we probe the ADE singularity with point-like instantons until the interface and component vanishing orders are equal in the component under consideration, at which point the previous arguments no longer apply.

¹⁵This is nicely discussed in Section 3 of [369].

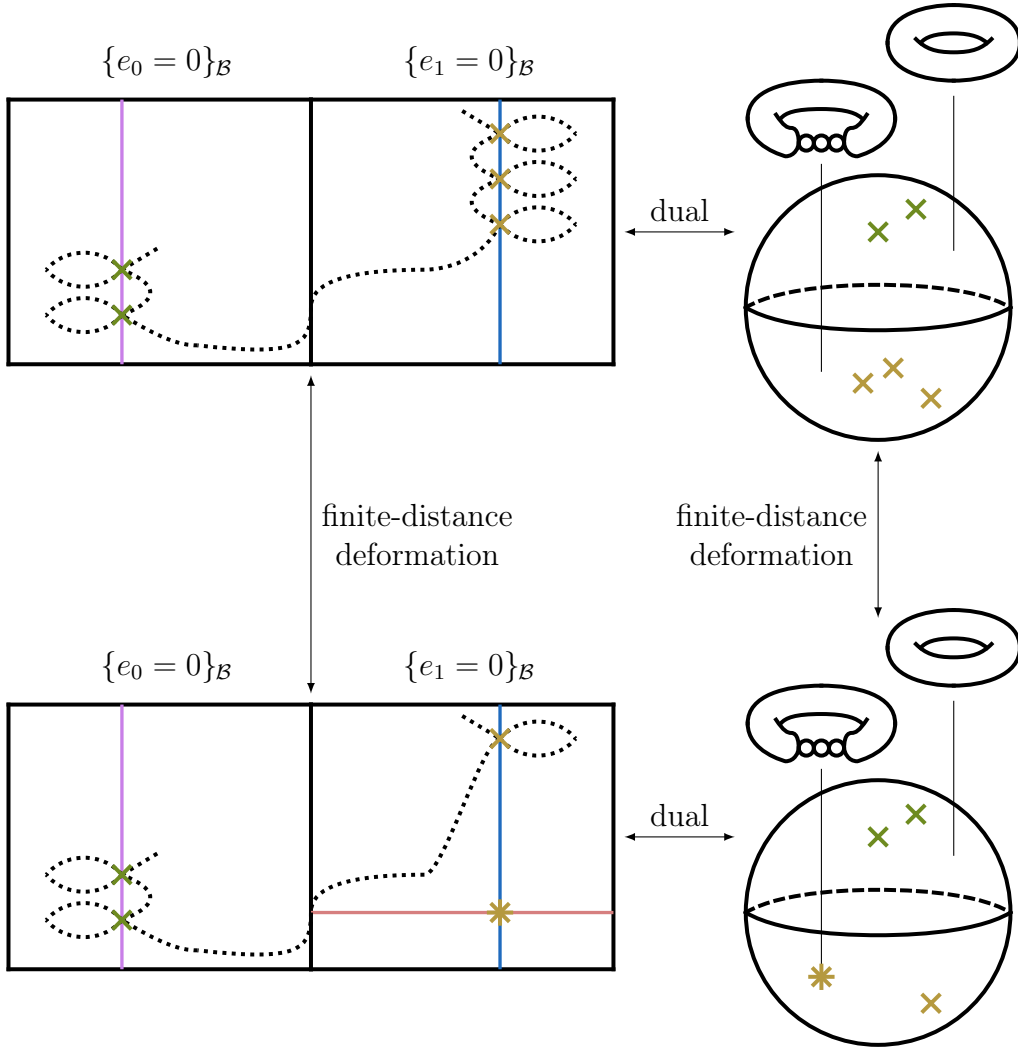


Figure B.15: In the upper-left part of the figure, we schematically represent a horizontal Type II.a model in which Δ_{phys} tangentially intersects the interface curve $B^0 \cap B^1$. This corresponds on the heterotic side to an ADE singularity not probed by point-like instantons with trivial holonomy, depicted in the upper-right corner. Through a finite-distance deformation, part of the point-like instantons can be moved on top of the ADE singularity, as shown in the lower-right corner. The dual situation in F-theory is depicted in the lower-left corner, where moving the codimension-two finite-distance non-minimal points to align with the interface singularity forces local vertical enhancements in the corresponding components. To produce a global vertical enhancement, it is necessary to align such non-minimal points in the two components or, using the heterotic dual language, the ADE singularity must be probed symmetrically by point-like instantons with trivial holonomy associated with both heterotic E_8 bundles.

on one side enhance the non-perturbative gauge factors supported over the exceptional curves. The vertical gauge algebra is singled out among the collection of non-perturbative gauge factors by the resolution process of the degeneration, and the total non-perturbative gauge algebra associated to the heterotic ADE singularity is simply that corresponding to $k_0 + k_1$ point-like instantons with trivial holonomy probing it, irrespectively of their distribution. The bounds on

the vertical gauge rank given in Table 6.3.3 affect the vertical gauge algebras,¹⁶ not the complete non-perturbative sector.

To give a concrete example, consider a horizontal Type II.a model constructed over $\hat{B} = \mathbb{F}_{10}$. The maximal vertical gauge algebra that can be realised in such a model is of rank($\mathfrak{g}_{\text{ver}}$) = 1, which can be for example obtained from a vertical line of Kodaira type III fibers. We then have, in terms of the physical vanishing orders, a (1, 2, 3) enhancement over a representative of \mathcal{F} , whose collision with the (4, 5, 10) enhancements supported over a representative of \mathcal{H}_∞^0 and the unique representative of \mathcal{H}_0^1 , respectively, produces two (5, 7, 14) points. This corresponds to a heterotic \mathbb{C}/\mathbb{Z}_2 singularity probed by $(k_0, k_1) = (2, 2)$ point-like instantons with trivial holonomy. Resolving the codimension-two finite-distance non-minimal points leads to no additional non-perturbative gauge factors. Consider now a horizontal Type II.a model constructed over $\hat{B} = \mathbb{F}_{11}$, where such a vertical gauge algebra is not possible, see Table 6.3.3. However, we can still tune a local vertical gauge enhancement in B^0 with (1, 3, 3) vanishing orders extending as residual discriminant into B^1 . It collides with the (4, 5, 10) enhancement supported over a representative of \mathcal{H}_∞^0 to produce a (5, 9, 15) point. The exceptional curve arising from the resolution of such a codimension-two finite-distance non-minimal point supports Kodaira type III fibers and, because it is fully contained within B^0 , it leads to a global gauge enhancement. This corresponds to a heterotic $\mathbb{C}^2/\mathbb{Z}_2$ singularity probed by $(k_0, k_1) = (4, 0)$ point-like instantons with trivial holonomy. Hence, we conclude that both models lead to the same asymptotic physics, namely that of the HE string in the presence of a $\mathbb{C}^2/\mathbb{Z}_2$ singularity with two M5-branes on top. The special role played by the vertical gauge algebra is an artefact of the resolution of the degeneration, and only the total number of M5-branes probing a heterotic ADE singularity is relevant in order to determine the non-perturbative gauge algebra associated with it. This agrees with the common lore applied in the context of studying six-dimensional SCFTs.

At any rate, and as explained in Section 5.4, employing the physical vanishing orders in the resolved horizontal Type II.a model is important in order to correctly determine the gauge algebra contributions, and in particular to determine the vertical gauge algebra and hence the non-perturbative heterotic gauge sector. A heterotic ADE singularity can be completely asymmetrically probed by point-like instantons with trivial holonomy, e.g. a heterotic E_8 singularity probed by $(k_0, k_1) = (0, 10)$ such instantons, not leading to a vertical gauge enhancement at all. The vertical line of fibers prior to the degeneration is also not indicative of the vertical gauge algebra found at the endpoint of the limit, since the physical vanishing orders found over a vertical locus may be bigger than the family vanishing orders over it (meaning that the finite-distance enhancement occurs at the same time that the infinite-distance limit is taken).¹⁷

¹⁶One can use the fact that symmetrically probing a heterotic ADE singularity is only possible up to a certain extent in horizontal Type II.a models constructed over $\hat{B} = \mathbb{F}_n$, due to the distribution of instanton numbers $c_2(V_{0,1}) = 12 \pm n$, to derive rough bounds on the rank of the vertical gauge algebra. To this end, simply equate each unit of instanton number to a local vertical (1, 1, 2) enhancement in the corresponding component. For most $\hat{B} = \mathbb{F}_n$ the bounds naively derived in this way are not as tight as the ones provided in Table 6.3.3, since they do not take into consideration the possibility of a monodromy action reducing the rank. In some select cases, namely for horizontal Type II.a models constructed over $\hat{B} = \mathbb{F}_3$ and $\hat{B} = \mathbb{F}_1$, the naive bounds derived in this fashion are, in fact, tighter than the ones printed in Table 6.3.3. The reason for this is that in this section we are considering the horizontal gauge algebra to be an unbroken $\mathfrak{g}_{\text{hor}} = \mathfrak{e}_8 \oplus \mathfrak{e}_8$, which is incompatible with the maximal vertical gauge rank possible in the models constructed over these Hirzebruch surfaces, cf. Footnote 27.

¹⁷These last two facts contrast with some comments made in [298], without this discrepancy altering the picture put forward in that work due to the preceding discussion in this section.

B.12.2 Broken horizontal $E_8 \times E_8$ gauge algebra

Above, we have discussed the non-perturbative heterotic gauge algebras associated with heterotic ADE singularities probed by point-like instantons with trivial holonomy. These are not the only singular gauge bundle contributions that can probe such singularities: The non-perturbative gauge algebras can also arise if the heterotic ADE singularity is probed by point-like instantons with discrete holonomy, a situation that we now describe.

In models with unbroken horizontal gauge algebra $\mathfrak{g}_{\text{hor}} = \mathfrak{e}_8 \oplus \mathfrak{e}_8$, any collision of the component residual discriminant $\{\Delta_p^{\text{res}}\}_{0 \leq p \leq 1}$ with the representatives of \mathcal{H}_∞^0 and \mathcal{H}_0^1 supporting it is always non-minimal. This is what allows us to perform a base blow-up, followed by an appropriate line bundle shift, in order to resolve the codimension-two finite-distance non-minimal points. These points are identified with point-like instantons with trivial holonomy, and the resolution procedure moves us to the interior of the tensor branch by separating M5-branes from the Hořava-Witten walls.

If $\mathfrak{g}_{\text{hor}} \neq \mathfrak{e}_8 \oplus \mathfrak{e}_8$, however, not all collisions of the residual discriminant with the horizontal divisors supporting it need to be non-minimal. This means that we can tune vertical gauge algebras without producing codimension-two finite-distance non-minimal points. This is most clear if we only tune a vertical gauge algebra small enough that the model presents no such points whatsoever. Point-like instantons with trivial holonomy are then absent, since they can always be subject to a small instantons transition, which on the F-theory side is tied to the codimension-two finite-distance non-minimal points, as reviewed above. From a heterotic standpoint, this seems reasonable, since point-like instantons with trivial holonomy leave the perturbative gauge group intact and must be deformed into a gauge bundle profile in order to break it. Such deformations are parametrised by the 29 hypermultiplets that must be traded by 1 tensor in the gravitational anomaly cancellation formula in order to realise a small instanton transition, that is hence obstructed after the deformation.

This raises the question of how the vertical gauge algebra associated to the heterotic K3 singularity arises from the heterotic point of view. While on the F-theory side of the duality a model as the one just described clearly shows a vertical gauge algebra factor, we know from the review of [349] at the beginning of this section that the corresponding ADE singularity of the heterotic K3 surface should be probed a some kind of singular gauge bundle contributions,¹⁸ a role played until this moment by the now absent point-like instantons with trivial holonomy.

An alternative source of concentrated gauge bundle curvature are point-like instantons with discrete holonomy. Let us briefly review them on the heterotic side of the duality. In a compactification of $E_8 \times E_8$ heterotic string theory on the internal space X we have the two poly-stable E_8 bundles

$$\pi_i : V_i \longrightarrow X, \quad i = 0, 1, \quad (\text{B.12.12})$$

with structure groups $H_i \subset E_8$. The gauge group G_i associated to each gauge bundle V_i in the lower-dimensional theory is given by the centralizer (commutant) $C_{E_8}(H_i)$ of the structure group $H_i \subset E_8$. A point-like instanton corresponds to a skyscraper sheaf, a singular gauge bundle in which all curvature has been concentrated at a point, while having a flat connection at infinity. Hence, they generate a discrete holonomy around their location, associated to those loops that are non-contractible once the support of the point-like instanton has been excised from the

¹⁸Horizontal Type II.a limits correspond to a (possibly partial) decompactification process, which dilutes the gauge bundle curvature. Since non-perturbative gauge factors associated with a heterotic K3 singularity are of local nature, it seems intuitive that they should not disappear along the decompactification process. Hence, if their manifestation depends on having a gauge configuration probing the singularity, said configuration should indeed be singular, which heuristically aligns with [349].

space,¹⁹ while their curvature contribution to the holonomy vanishes. The discrete holonomy that a point-like instanton can exhibit depends on the fundamental group of a neighbourhood around with the location of the instanton excised [370]. Over smooth points of the heterotic K3 surface we hence have (after a retraction) $\pi_1(S^3) = 0$, and the discrete holonomy must be trivial. Hence, over generic points of the heterotic K3 only point-like instantons with trivial holonomy are supported. If the instanton is located at a heterotic \mathbb{C}^2/Γ_g singularity we have instead $\pi_1(S^3/\Gamma_g) \cong \Gamma_g$, and the discrete holonomy H'_i of the point-like instanton can be any subgroup of Γ_g , where i labels from which of the heterotic E_8 bundles the point-like instanton stems or, equivalently, to which Hořava-Witten wall it is associated with. The corresponding E_8 gauge factor is broken by the presence of a point-like instanton to $C_{E_8}(H'_i)$. Due to the discrete nature of H'_i , a configuration with only point-like instantons will either leave $E_8 \times E_8$ unbroken or break it into a non-simply connected subgroup, which on the F-theory side corresponds to non-trivial torsion subgroup of the Mordell-Weil group [199].

In the absence of codimension-two finite-distance non-minimal points, and hence, using the heterotic language, of point-like instantons with trivial holonomy, the vertical gauge algebras must therefore correspond to heterotic ADE singularities probed by point-like instantons with discrete holonomy. The latter class of point-like instantons cannot be traded for M5-branes via small instanton transitions due to the lack of enough available deformation moduli to be traded for a tensor in the gravitational anomaly cancellation formula. This means that they are stuck at the Hořava-Witten walls, which aligns with the absence of Kähler moduli associated with exceptional curves on the F-theory side. Moreover, while the position of point-like instantons with trivial holonomy within the K3 surface could be tuned freely by moving the associated codimension-two finite-distance non-minimal points within \mathbb{P}_b^1 , the ones with discrete holonomy are associated to the vertical line. This is in agreement with the fact that they are stuck at the heterotic \mathbb{C}^2/Γ_g singularity allowing them to be realised. Such instantons were explicitly studied in [199], finding that they are associated to codimension-two minimal enhancement points corresponding to the hypermultiplet matter that populates the representations allowed by the non-simply connected gauge groups; furthermore, they contribute fractionally to the instanton number budget $c_2(K3) = 24$.

By turning on local curvature in a neighbourhood around a heterotic ADE singularity a point-like instanton with discrete holonomy can be continuously deformed into a gauge bundle contribution with structure group of positive dimension, while preserving the point-like instanton at its core. Such a configuration would be able to probe the heterotic ADE singularities without necessarily enforcing a non-simply connected gauge group to arise, which would explain why on the F-theory side we can tune vertical gauge algebras without enforcing a particular non-trivial torsion subgroup of the Mordell-Weil group. At the endpoint of a horizontal Type II.a limit the singular gauge bundle part of such a configuration is not diluted away, hence still allowing the non-perturbative gauge algebra to manifest. Away from the six-dimensional defects the bulk gauge group is restored due to the arguments given in Section 6.4.3. An observer concerned with the six-dimensional theory living on a defect, and hence placed on top of it, sees the bulk gauge group as a flavour group that is partially broken due to the discrete holonomy of the surviving point-like instanton. This local picture is the one taken in the analyses of the Higgs branch of heterotic LSTs [363–368].

Since a point-like instanton with discrete holonomy is associated to one of the Hořava-Witten walls, it is meaningful to probe heterotic ADE singularities asymmetrically. In the absence of codimension-two finite-distance non-minimal points no gauge factors can be supported over

¹⁹K3 surfaces are simply connected, and hence these are the only non-contractible loops to be considered.

exceptional curves. The non-perturbative heterotic gauge sector hence entirely corresponds to the vertical gauge algebra. Given a representative of \mathcal{F} , tuning a local enhancement over $\mathcal{F}|_{B^i}$ is associated with $\text{Def}(Y^i)$, and hence with point-like instantons in the V_i heterotic gauge bundle. To produce the vertical gauge enhancement one must symmetrically probe the heterotic ADE singularity, which ensures that the local gauge enhancements on both components lead to a global gauge enhancement factorising in Δ_{phys} . This aspect is nicely captured by the resolved horizontal Type II.a models. Due to these considerations, the asymptotic physics associated with a heterotic ADE singularity does in general not only depend on the total instanton number of the singular gauge bundle contributions probing it, but also on their distribution within the Hořava-Witten walls. In this regard, the point-like instantons with trivial holonomy are special due to their equivalence to M5-branes in the Hořava-Witten interval, as discussed in the previous section. By contrast, moving a point-like instanton with discrete holonomy from one Hořava-Witten wall to the other would entail an additional finite-distance deformation of the model; after bringing it together with other fractional point-like instantons, this turns the fractional instantons into a full instanton with trivial holonomy.

Let us consider a concrete example. In the following discussion, the horizontal gauge algebra is kept small enough so that no codimension-two finite-distance non-minimal points arise. Hence, we only have to account for fractional point-like instantons. Consider tuning a global vertical $(1, 2, 3)$ enhancement, which does lead to an $\mathfrak{su}(2)$ gauge algebra from the F-theory perspective. This is dual to a heterotic $\mathbb{C}^2/\mathbb{Z}_2$ singularity probed by some singular gauge bundle contribution. Each local vertical $(1, 2, 3)$ enhancement acting as one half of the global one is independent of the other half. It must therefore concentrate by itself a certain amount of instanton charge, denoted by c_{III} for concreteness, at the $\mathbb{C}^2/\mathbb{Z}_2$ point. On the F-theory side, we can enhance the interface vanishing orders of said point to produce a heterotic $\mathbb{C}^2/2D_4$ singularity, by making the residual discriminant pass through it tangentially. Since this does not change the global vertical $(1, 2, 3)$ enhancement, the gauge algebra is unaffected. On the heterotic, side this corresponds to bringing some of the I_1 singular elliptic fibers, at which no instanton charge is concentrated, on top of the original orbifold point. This leads to a $\mathbb{C}^2/2D_4$ singularity symmetrically probed by $c_{\text{III}} + c_{\text{III}}$ instanton charge and hence, still, to an $\mathfrak{su}(2)$ gauge algebra. Alternatively, we can start by tuning two local vertical $(1, 2, 3)$ lines in, for example, the B^0 component that do not extend into global vertical enhancements. In such a case, there arises no vertical gauge group factor. This produces two heterotic $\mathbb{C}^2/\mathbb{Z}_2$ singularities, each probed by $c_{\text{III}} + 0$ instanton charge. Bringing these two local vertical enhancements together produces a single local vertical $(2, 3, 6)$ line on the F-theory side, which does not extend into a global vertical enhancement and therefore has no associated gauge algebra. On the heterotic side, this corresponds to bringing together the two $\mathbb{C}^2/\mathbb{Z}_2$ points alongside the instanton charge concentrated at them, which results in a heterotic $\mathbb{C}^2/2D_4$ singularity probed by $2c_{\text{III}} + 0$ instanton charge, but not leading to any gauge algebra, according to the F-theory analysis.

B.13 Type IIB orientifold picture of Type III.b models

Since Type III.b models represent global weak coupling limits, their endpoints can be described as Type IIB orientifold compactifications in the context of the Sen limit [203]. In this language, the Type IIB internal space on which we place the O7-planes is the Calabi-Yau double cover \check{B} of the base B of the F-theory elliptic fibration. The branching points of the double cover correspond to the fixed loci of the orientifold involution, and hence to the position of the O7-planes in the

Type IIB compactification. For six-dimensional models with minimal supersymmetry, \check{B} is a K3 surface.

To interpret the endpoint of an, e.g. horizontal, Type III.b degeneration $\rho : \mathcal{Y} \rightarrow D$ as a Sen limit we can blow down the model such that the new central fiber corresponds to the former component Y^p . This can be accomplished via the coordinate substitutions

$$e_p \mapsto u, \quad e_{q \neq p} \mapsto 1, \quad p, q \in \{0, \dots, P\}, \quad (\text{B.13.1})$$

in the defining polynomials f_b , g_b and Δ_b of the family fourfold \mathcal{Y} . Since all components of the central fiber Y_0 of $\rho : \mathcal{Y} \rightarrow D$ have codimension-zero I_m fibers, the central fiber \hat{Y}_0 of the blown-down degeneration $\hat{\rho} : \hat{\mathcal{Y}} \rightarrow D$ does as well.²⁰ This means that, irrespective of the choice Y^p of component that we make, the family variety of the blown-down degeneration has defining polynomials of the form

$$f = e_p^{l_p} \check{f}_p + f_p \mapsto f = u^{l_p} \check{f} - 3h^2, \quad (\text{B.13.2a})$$

$$g = e_p^{m_p} \check{g}_p + g_p \mapsto g = u^{m_p} \check{g} + 2h^3, \quad (\text{B.13.2b})$$

with $h \in H^0 \left(\mathbb{F}_n, \overline{K}_{\mathbb{F}_n}^{\otimes 2} \right)$, see Appendix B.9. The divisor defined by the vanishing locus $\{h = 0\}_{\hat{B}_0}$ corresponds to the branching locus of the double cover of \hat{B}_0 , i.e. the fixed locus of the orientifold involution of the Type IIB model. The irreducible components of $\{h = 0\}_{\hat{B}_0}$ hence correspond to the O7-planes. The parameter u implements the Sen limit, with $u \rightarrow 0$ bringing us (at least in global weak coupling limits) to the perturbative regime.

Before analysing the particular features of the Type IIB orientifolds obtained as the endpoints of Type III.b models, it is convenient to explicitly discuss the geometry related to the Sen limits of generic six-dimensional F-theory models with $B = \mathbb{F}_n$ acting as their base.

B.13.1 Sen limit in six-dimensional F-theory models

We are interested in understanding the geometric degeneration undergone by the K3 double covers \check{B} of the bases B of six-dimensional F-theory models explicitly. For concreteness, and since it is the case of interest for what follows, we center our attention on $B = \mathbb{F}_n$ with $0 \leq n \leq 4$. We briefly comment on the other possible B geometries at the end.

Let us start by discussing the relevant geometry in eight-dimensional F-theory models. In this context, the base of the internal elliptic fibration must be $B = \mathbb{P}^1$ with Calabi-Yau double $\check{B} = T^2$. The explicit description of this double cover naturally arises when taking the Sen limit of such an F-theory model. Consider the defining polynomials

$$f = u^l \check{f} - 3h^2, \quad (\text{B.13.3})$$

$$g = u^m \check{g} + 2h^3 \quad (\text{B.13.4})$$

for the Weierstrass model of the internal space $\pi : Y \rightarrow B$, where $h \in H^0 \left(\mathbb{P}^1, \overline{K}_{\mathbb{P}^1}^{\otimes 2} \right)$ and $u \rightarrow 0$ implements the weak coupling limit. The Calabi-Yau double cover of $\mathbb{P}_{[s:t]}^1$ is obtained by enlarging the set of homogeneous coordinates of B by ξ and considering the hypersurface

$$\check{B} : \quad \{P_{\check{B}} = 0\}_{\mathbb{P}_{112}^2}, \quad P_{\check{B}} := \xi^2 - h([s:t]). \quad (\text{B.13.5})$$

²⁰Alternatively, we can start with a Type III.a model and blow down to one of the components at local weak coupling. This is used in the comparison of horizontal Type III.a and Type III.b models in Section 6.5.3.1.

The ambient space must then be \mathbb{P}_{112}^2 with homogeneous coordinates $[s : t : \xi]$, such that the defining polynomial $P_{\check{B}}$ is homogeneous under the \mathbb{C}^* -action. The new variable ξ appears quadratically in $P_{\check{B}}$. For every point $[s_0 : t_0]$ in $\mathbb{P}_{[s:t]}^1$ we therefore obtain two points, counted with multiplicity, in $\{P_{\check{B}} = 0\}_{\mathbb{P}_{112}^2}$. This yields the desired double cover. The ramification points of the cover are given by the roots of h . Since $\overline{K}_{\mathbb{P}^1} = 2H$, where H is the hyperplane class, $h = h_4([s : t])$ is a degree four polynomial, and the double cover has four such ramification points, counted with multiplicity. Since $P_{\check{B}}$ is of homogeneous degree four, we have a non-generic quadric $\mathbb{P}_{112}^2[4]$ in which the linear terms in ξ have been set to zero. Quadrics $\mathbb{P}_{112}^2[4]$ are elliptic curves, and therefore we have obtained a double cover of \mathbb{P}^1 by T^2 branched at four points. Summarising, the Sen limit of eight-dimensional F-theory models naturally yields a branched cover

$$\pi : \{P_{\check{B}} = 0\}_{\mathbb{P}_{112}^2} \cong T^2 \longrightarrow \mathbb{P}^1 \quad (\text{B.13.6})$$

in which the algebraic extension of the function fields is of degree 2. The cover is in particular an (Abelian) Galois cover in which $G = \mathbb{Z}/2\mathbb{Z} \in \text{Aut}(T^2)$ with $T^2/G \cong \mathbb{P}^1$, and the stabilisers are $\text{Stab}_G(x) = \mathbb{Z}/2\mathbb{Z}$ for those $x \in \{P_{\check{B}} = 0\}_{\mathbb{P}_{112}^2}$ such that $h(x) = 0$, and $\text{Stab}_G(x) = 0$ elsewhere, giving the desired orientifold picture.

Consider now the same construction for a six-dimensional F-theory model whose base is $B = \mathbb{F}_n$, with $0 \leq n \leq 4$. This should lead to a K3 double cover \check{B} . The fact that \check{B} is Calabi-Yau can easily be seen in the smooth case. Namely, consider the dominating morphism of smooth surfaces

$$\check{\pi} : \check{B} \longrightarrow B \quad (\text{B.13.7})$$

given by the double cover. If we denote the ramification divisor by $R \subset \check{B}$, the canonical divisors of \check{B} and B are related by (Theorem 5.5 of [371])

$$K_{\check{B}} = \pi^* K_B + R. \quad (\text{B.13.8})$$

Since the ramification index is 2 for all components of R , we have that $2R = \pi^*(\{h = 0\}_B)$. Using then that we are taking $\{h = 0\}_B \sim 2\overline{K}_B$, we obtain

$$2K_{\check{B}} = 2\pi^* K_B + 2R = \pi^*(2K_B + 2\overline{K}_B) = 0. \quad (\text{B.13.9})$$

The fact that it is concretely a K3 surface, as the physics demands, we will see explicitly below without assuming smoothness.

To obtain a global description of \check{B} , enlarge the set of homogeneous coordinates of $B = \mathbb{F}_n$ by ξ and consider the hypersurface

$$\check{B} : \quad \{P_{\check{B}} = 0\}_X, \quad P_{\check{B}} := \xi^2 - h([s : t], [v : w : t]). \quad (\text{B.13.10})$$

In order to make $\mathbb{P}_{\check{B}}$ homogeneous under the \mathbb{C}^* -actions, the ambient space must be

$$\begin{aligned} X &:= (\mathbb{C}^5 \setminus Z) / \mathbb{C}_{\lambda_1}^* \times \mathbb{C}_{\lambda_2}^*, \quad \mathbb{C}_{\lambda_1}^* : (s, t, v, w, \xi) \mapsto (\lambda_1^1 s, \lambda_1^1 t, v, w, \lambda_1^2 \xi), \\ Z &:= \{s = t = \xi = 0\} \cup \{t = v = w = \xi = 0\} \quad \mathbb{C}_{\lambda_2}^* : (s, t, v, w, \xi) \mapsto (s, \lambda_2^n t, \lambda_2^1 v, \lambda_2^1 w, \lambda_2^{2+n} \xi). \end{aligned} \quad (\text{B.13.11})$$

Since $h \in H^0(\mathbb{F}_n, \overline{K}_{\mathbb{F}_n}^{\otimes 2})$, it is a polynomial of homogeneous degrees 4 and $4 + 2n$ under the two \mathbb{C}^* -actions, i.e. $h = h_{4,4+2n}([s : t], [v : w : t])$.

The F-theory base $B = \mathbb{F}_n$ is a \mathbb{P}_f^1 -fibration over the base $\mathbb{P}_b^1 = \mathbb{P}_{[v:w]}^1$,

$$\pi_{\mathbb{F}_n} : B \longrightarrow \mathbb{P}_b^1, \quad (\text{B.13.12})$$

with a section C_0 (and another independent section C_∞). Its double cover \check{B} constructed above is a genus one fibration over the same base \mathbb{P}_b^1 . It is given by the flat surjective morphism

$$\begin{aligned}\pi_{\check{B}} : \{P_{\check{B}} = 0\}_X &= \check{B} \longrightarrow \mathbb{P}_b^1 \\ (s, t, v, w, \xi) &\longmapsto (v, w),\end{aligned}\tag{B.13.13}$$

with $\pi_{\check{B}} = \pi_{\mathbb{F}_n} \circ \check{\pi}$. The generic fiber of $\pi_{\check{B}}$ over a generic point $p_0 = [v_0 : w_0] \in \mathbb{P}_b^1$ is given by

$$\pi_{\check{B}}^{-1}([v_0 : w_0]) = \{P_{\check{B}} = 0\}_X \cap \{[v : w] = [v_0 : w_0]\}_X = \{\xi^2 - h_{4,4+2n}([s : t], [v_0 : w_0 : t]) = 0\}_{X_0},\tag{B.13.14}$$

with

$$X_0 = X \cap \{[v : w] = [v_0 : w_0]\} = \mathbb{P}_{112}^2.\tag{B.13.15}$$

Therefore,

$$\pi_{\check{B}}^{-1}([v_0 : w_0]) = \{\xi^2 - h_4^0([s : t]) = 0\}_{\mathbb{P}_{112}^2} = \mathbb{P}_{112}^2[4]\tag{B.13.16}$$

is an elliptic curve, that can degenerate over codimension-one loci in \mathbb{P}_b^1 . We use the super- and subscripts 0 to mark the dependence of the concrete objects on the choice of generic point p_0 . This merely shows the intuitive result that the generic fiber of $\pi_{\check{B}}$ is the T^2 double cover of the \mathbb{P}_f^1 fiber of $\pi_{\mathbb{F}_n}$. Note that the section of the $\pi_{\mathbb{F}_n}$ fibration does not in general lift to a section of $\pi_{\check{B}}$. The geometry that we have found for \check{B} is that of a Calabi-Yau $\mathbb{P}_{112}^2[4]$ -fibration over \mathbb{P}_b^1 , which is indeed known to not have a section in general, but a bisection. In our construction, said bisection corresponds to the double cover $\pi_{\check{B}}^{-1}(\mathbb{P}_b^1)$ of the base of B . This type of fibration has been extensively studied in the context of F-theory compactified on genus-one fibrations in relation with the appearance of discrete abelian gauge groups, see [185] for a review and references. We now proceed to outline its geometry, referring the reader to the previous sources for more detail.

As we have just determined, \check{B} is a $\mathbb{P}_{112}^2[4]$ -fibration over \mathbb{P}_b^1 . The most general $\mathbb{P}_{112}^2[4]$ curve is described by the vanishing locus of the polynomial

$$P = b_\xi \xi^2 + b_0 s^2 \xi + b_1 s t \xi + b_2 t^2 \xi + c_0 s^4 + c_1 s^3 t + c_2 s^2 t^2 + c_3 s t^3 + c_4 t^4.\tag{B.13.17}$$

By taking the b_i and c_i to be sections of a base \tilde{B} we obtain a $\mathbb{P}_{112}^2[4]$ -fibration over \mathbb{P}_b^1 . Considering the special case in which $b_\xi = 1$, the total space of the fibration is Calabi-Yau if

$$\begin{aligned}b_0 &\sim \beta, & b_1 &\sim \overline{K}_{\tilde{B}}, & b_2 &\sim -\beta + 2\overline{K}_{\tilde{B}}, \\ c_0 &\sim 2\beta, & c_1 &\sim \beta + \overline{K}_{\tilde{B}}, & c_2 &\sim 2\overline{K}_{\tilde{B}}, & c_3 &\sim -\beta + 3\overline{K}_{\tilde{B}}, & c_4 &\sim -2\beta + 4\overline{K}_{\tilde{B}},\end{aligned}\tag{B.13.18}$$

where β is some divisor class in \tilde{B} such that all the above classes are effective. Such a generic model admits no rational section and contains smooth I_2 fibers. Upon tuning $c_4 = 0$ (or $c_0 = 0$) the model develops a conifold singularity at

$$\{s = 0\}_{\tilde{B}} \cap \{\xi = 0\}_{\tilde{B}} \cap \{b_2 = 0\}_{\tilde{B}} \cap \{c_3 = 0\}_{\tilde{B}}\tag{B.13.19}$$

and admits a holomorphic and a rational section.

Specialising this to the construction of the double cover \check{B} , the hypersurface that we consider in the fiber ambient space \mathbb{P}_{112}^2 is defined by the polynomial

$$P_{\check{B}} = \xi^2 - h_{4,4+2n}([s : t], [v : w : t]).\tag{B.13.20}$$

We observe that there are no linear terms in ξ , meaning that for the double cover

$$b_0 = b_1 = b_2 = 0. \quad (\text{B.13.21})$$

The section c_0 is the coefficient of the s^4 term in $P_{\tilde{B}}$, which can be isolated by setting $t = 0$. Since $T \cdot \{h = 0\}_{\mathbb{F}_n} = 4 + 2n$, we have that

$$c_0 = -h_{4,4+2n}([1:0], [v:w:0]) = p_{4+2n}^0([v:w]) = (2+n)\bar{K}_{\tilde{B}}, \quad (\text{B.13.22})$$

with $\tilde{B} = \mathbb{P}_b^1$. Therefore,

$$\beta = \frac{(2+n)}{2}\bar{K}_{\tilde{B}} = (2+n)H. \quad (\text{B.13.23})$$

For the remaining c_i one obtains

$$c_0 = (4+2n)H, \quad c_1 = (4+n)H, \quad c_2 = 4H, \quad c_3 = (4-n)H, \quad c_4 = (4-2n)H, \quad (\text{B.13.24})$$

such that the Calabi-Yau condition (B.13.18) is met. Note that for the cases of interest $n = 3$ and $n = 4$ the class c_4 does not cease to be effective, but rather becomes $c_4 = 0$ due to the non-Higgsable clusters forcing the factorisation $h = sh'$ in those models constructed over these Hirzebruch surfaces. This also means that, for these two geometries, the double cover \check{B} always is an elliptic fibration. In the models that we work with, and due to the fact that the $b_i = 0$, the codimension-two locus

$$C_I : \{b_2 = 0\}_{\tilde{B}} \cap \{c_3 = 0\}_{\tilde{B}} \quad (\text{B.13.25})$$

of the conifold singularities that develop upon tuning $c_4 = 0$ becomes the codimension-one locus

$$C_I : \{c_3 = 0\}_{\tilde{B}}. \quad (\text{B.13.26})$$

The $\mathbb{P}_{112}^2[4]$ -fibration has an associated Weierstrass model, which can be obtained by defining the sections

$$\begin{aligned} e_0 &= -c_0 + \frac{1}{4}b_0^2, & e_1 &= -c_1 + \frac{1}{2}b_0b_1 \\ e_2 &= -c_2 + \frac{1}{2}b_0b_2 + \frac{1}{4}b_1^2, & e_3 &= -c_3 + \frac{1}{2}b_1b_2, & e_4 &= -c_4 + \frac{1}{4}b_2^2, \end{aligned} \quad (\text{B.13.27})$$

and taking the defining polynomials to be

$$f_{J(\check{B})} = e_1e_3 - \frac{1}{3}e_2^2 - 4e_0e_4, \quad (\text{B.13.28})$$

$$g_{J(\check{B})} = -e_0e_3^2 + \frac{1}{3}e_1e_2e_3 - \frac{2}{27}e_2^3 + \frac{8}{3}e_0e_2e_4 - e_1^2e_4. \quad (\text{B.13.29})$$

If the $\mathbb{P}_{112}^2[4]$ -fibration has a section then it is birationally equivalent to this Weierstrass model. Particularizing this to $b_i = 0$ and $\tilde{B} = \mathbb{P}_b^1$, as in the double cover \check{B} , we find that

$$F \sim 8H = 4\bar{K}_{\mathbb{P}_b^1}, \quad G = 12H = 6\bar{K}_{\mathbb{P}_b^1} \Rightarrow \Delta = 24H = 12\bar{K}_{\mathbb{P}_b^1}, \quad (\text{B.13.30})$$

as corresponds to a K3 Weierstrass model. Further tuning $c_4 = 0$ results in the Weierstrass model supporting singular I_2 fibers in codimension-one over $\{c_3 = 0\}_{\tilde{B}}$. The total space of a Weierstrass model has ordinary quadratic singularities at the location of I_2 singularities,

i.e. conifold singularities; the aforementioned I_2 singularities over $\{c_3 = 0\}_{\tilde{B}}$ are the conifold singularities found over the same locus in \tilde{B} for the $\mathbb{P}_{112}^2[4]$ -fibration.

The Weierstrass model obtained in this way is the Jacobian of the double cover \tilde{B} . Every Calabi-Yau surface Y with a genus-one fibration over a base B

$$\pi : Y \longrightarrow B \quad (\text{B.13.31})$$

has an associated Calabi-Yau surface $J(Y)$ that is elliptically fibered over the same base

$$\pi_J : J(Y) \longrightarrow B, \quad (\text{B.13.32})$$

known as the Jacobian of the fibration. The multivalued $\tau(b)$, $b \in B$, functions, $\text{SL}(2, \mathbb{Z})$ representations, and discriminant subvarieties $\Delta \subseteq B$ are identical for the two fibrations π and π_J [188]. The total spaces Y and $J(Y)$, however, do present some differences. For example, a $\mathbb{P}_{112}^2[4]$ -fibration like the ones discussed above may have I_2 fibers that do not lead to a singularity of the total space of the fibration; this is not possible in a Weierstrass model, and they are therefore contracted into singular I_2 fibers in the Jacobian.²¹ The analysis of the relation between F-theory models on Y and $J(Y)$ was started in [188]. While strictly speaking we are interested in the F-theory model on Y , due to the shared properties between both spaces, we can use the Weierstrass model of $J(Y)$ to read off the non-minimal loci of Y , which is all the information that we intend to extract.

Before studying the concrete K3 surfaces \tilde{B} that arise as the double covers of the endpoints of horizontal Type III.b limits, let us note a few geometrical facts about the K3 double covers arising for the Sen limit of generic six-dimensional F-theory models with $B = \mathbb{F}_n$ as their base. First, recall that if \tilde{B} and B are two complex projective surfaces with B smooth, and there is a double cover $\tilde{\pi} : \tilde{B} \rightarrow B$ with branching locus $\{h = 0\}_B \subset B$, then \tilde{B} is smooth if and only if $\{h = 0\}_B$ is smooth, since \tilde{B} can only have singularities over the singular points of $\{h = 0\}_B$. Given that $B = \mathbb{F}_n$ is smooth, we are in the conditions in which this applies. Since $h \in H^0\left(\mathbb{F}_n, \overline{K}_{\mathbb{F}_n}^{\otimes 2}\right)$, no factorizations occur for a generic h when $n = 0, 1, 2$, while

$$h = sh', \quad n = 3, 4, \quad \text{with} \quad h' \sim 3S + (4 + 2n)V, \quad (\text{B.13.33})$$

generically. Thus, we expect the K3 double cover of \mathbb{F}_n obtained by taking the Sen limit of a generic F-theory model whose internal space has base $B = \mathbb{F}_n$ with $n = 0, 1, 2$ to be smooth. The same expectation holds for $n = 4$, since in spite of the factorization of $h = sh'$, we have that $S \cdot \{h' = 0\}_B = 0$. The same is not true when $n = 3$, since $S \cdot \{h' = 0\}_B = 1$ leading to a transverse intersection of the two components of $\{h = 0\}_B$; we therefore expect a singularity in the K3 double cover of $B = \mathbb{F}_3$ obtained from the Sen limit of the generic F-theory model whose internal space has this Hirzebruch surface as its base. Taking into account that the non-Higgsable cluster $(2, 2, 4)$ over $S \subset B$ enhances to at least $(2, 3, 5)$ by taking the Sen limit, this is the quadric cone singularity associated to orthogonal groups expected from the analysis of the Donagi-Wijnholt limit of Tate models [332] performed in [333], and that is avoided by the particularities of the intersection theory of the base in the case of $B = \mathbb{F}_4$. The singular K3 double cover \tilde{B} of $B = \mathbb{F}_3$ admits a crepant resolution, compatible with the orientifold involution, to a smooth K3 surface $\text{Bl}(\tilde{B})$ that is the double cover of the blow-up $\text{Bl}(B)$ of the Hirzebruch surface along the self-intersection locus of $\{h = 0\}_B$.

²¹The Jacobian $J(Y)$ of an (even non-singular) genus-one fibered Calabi-Yau threefold Y typically presents \mathbb{Q} -factorial terminal singularities [188].

The physics of the Sen limit of F-theory compactified on $\pi : Y \rightarrow B$ with $B = \mathbb{F}_n$ beautifully captures in this way the mathematics of K3 double covers of Hirzebruch surfaces. The smooth quotients of K3 surfaces by finite abelian groups have been analysed in the mathematics literature, see the seminal works of Nikulin [335–337] and more recent studies on the subject [372, 373]. Restricting our attention to $B = \mathbb{P}^2$ and $B = \mathbb{F}_n$ the following holds.

Theorem B.13.1. *Let X be a smooth K3 surface and G be a finite subgroup of $\text{Aut}(X)$ such that X/G is smooth. There exist birational morphisms $f : X/G \rightarrow \mathbb{P}^2$ and $f : X/G \rightarrow \mathbb{F}_n$ for $n = 0, 1, 2, 3, 4, 6, 8, 12$. Moreover, the group G is one in the lists \mathcal{AG}_∞ or \mathcal{AG}_n , respectively.*

The complete lists \mathcal{AG}_∞ and \mathcal{AG}_n can be consulted in [373]. Since we are interested in double covers of the F-theory base, the group that is relevant for us is $G = \mathbb{Z}/2\mathbb{Z}$. Since

$$\mathbb{Z}/2\mathbb{Z} \in \mathcal{AG}_\infty \cap \mathcal{AG}_0 \cap \mathcal{AG}_1 \cap \mathcal{AG}_2 \cap \mathcal{AG}_4, \quad (\text{B.13.34})$$

while

$$\mathbb{Z}/2\mathbb{Z} \notin \mathcal{AG}_3 \cup \mathcal{AG}_6 \cup \mathcal{AG}_8 \cup \mathcal{AG}_{12}, \quad (\text{B.13.35})$$

we see that smooth K3 double covers of \mathbb{F}_n only exist for $n = 0, 1, 2, 4$. The K3 double cover of \mathbb{F}_3 must always be singular, but can be crepantly resolved into a smooth K3 double cover of the blow-up of \mathbb{F}_3 , as explained above. F-theory captures this as a codimension-two finite-distance singularity, an SCFT point, located at the intersection point $S \cdot \{h' = 0\}_B = 1$. The tensor branch of the SCFT interpolates between the singular and the smooth K3 double covers.

B.13.2 K3 double covers and horizontal Type III.b limits

Since the Weierstrass model (B.13.2) is obtained by blowing down a horizontal Type III.b model, in addition to the codimension-zero I_m fibers we must also find some non-minimal curves in the base \hat{B}_0 of the central fiber \hat{Y}_0 of the blown-down degeneration. These will correspond to $\mathcal{S} \cap \mathcal{U}$, $\mathcal{T} \cap \mathcal{U}$ and $\mathcal{S} \cap \mathcal{U}$, or $\mathcal{T} \cap \mathcal{U}$ depending on if we have blown down to the Y^0 , $Y^p \in \{Y^q\}_{1 \leq q \leq P-1}$, or Y^P component. Let us assume, without loss of generality, that we have blown down to the Y^0 component.

After blowing down to the Y^0 component, we must have codimension-zero I_m fibers at the endpoint of the limit, implying the structure (B.13.2) for the Weierstrass model of the blown-down degeneration, and non-minimal fibers over the curve $\mathcal{S} \cap \mathcal{U}$. The latter means that the h polynomial cannot be generic, but rather must factorize like

$$h = s^2 h', \quad h' \sim 2S + (4 + 2n)V. \quad (\text{B.13.36})$$

Constructing the K3 double cover of \hat{B}_0 as explained in Section B.13.1, we find that $c_3 = c_4 = 0$, in addition to $b_i = 0$. Since $c_4 = 0$, the $\mathbb{P}_{112}^2[4]$ -fibration does admit a section.²² Given the fact that also $c_3 = 0$, the defining polynomials of the Weierstrass model describing the Jacobian $J(\check{B})$ are

$$f_{J(\check{B})} = -3h_{J(\check{B})}^2, \quad g_{J(\check{B})} = 2h_{J(\check{B})}^3 \quad \text{with} \quad h_{J(\check{B})} = \frac{1}{3}c_2, \quad (\text{B.13.37})$$

where $h_{J(\check{B})}$ is a generic polynomial of homogeneous degree 4 in $[v : w]$. Hence, it has codimension-zero I_m fibers in codimension-zero. Moreover, we find no codimension-one non-minimal singularities due to the genericity of $h_{J(\check{B})}$. Hence, both $J(\check{B})$ and its birational equivalent \check{B} correspond to the central fiber of a Kulikov Type II.b model.

²²Blowing down to the Y^P component would mean that $c_0 = 0$ instead, while blowing down to an intermediate component $\{Y^p\}_{1 \leq p \leq P-1}$ means that $c_0 = c_4 = 0$. Hence, we have a section in all cases.

B.13.3 K3 double covers and vertical Type III.b limits

We can perform the same analysis for vertical Type III.b models. After blowing down to the Y^0 component, the curve $\mathcal{V} \cap \mathcal{U}$ will support non-minimal elliptic fibers. This means that the h polynomial must factorize like

$$h = v^2 h', \quad h' \sim 4S + (2 + 2n)V. \quad (\text{B.13.38})$$

For the K3 double cover of \hat{B}_0 this implies that, in addition to $b_i = 0$, we also have

$$h = v^2 h' \Rightarrow c_i = v^2 c'_i, \quad i = 0, 1, 2, 3, 4. \quad (\text{B.13.39})$$

which leads to

$$e_i \sim c_i \propto v^2, \quad i = 0, 1, 2, 3, 4. \quad (\text{B.13.40})$$

As a consequence of the schematic form of $f_{J(\check{B})}$ and $g_{J(\check{B})}$

$$f \sim e_i^2, \quad g \sim e_i^3, \quad (\text{B.13.41})$$

we encounter the non-minimal vanishing orders

$$\text{ord}_{J(\check{B})} \left(f_{J(\check{B})}, g_{J(\check{B})}, \Delta_{J(\check{B})} \right)_{v=0} = (4, 6, 12). \quad (\text{B.13.42})$$

The reason for the printed vanishing order for $\Delta_{J(\check{B})}$ is that, after the factorization of v^2 has been taken into account in h , the remainder polynomial h' is generic in a generic vertical Type III.b model. Hence, no accidental cancellation increasing this vanishing order should occur generically. The resulting K3 double cover is the endpoint of a codimension-one degeneration of K3 surfaces. For the generic vertical Type III.b model, we expect it to correspond to the endpoint of a Kulikov Type II.a model, since producing codimension-zero $I_{m>0}$ fibers would entail additional tuning.

B.14 Vertical and mixed (bi)section degenerations

Genus-zero single infinite-distance limit degenerations of Hirzebruch models can be classified into the Cases A to D, see Table 6.2.1. In Sections 6.3 to 6.5 we have analysed the general properties of the horizontal models (Case A), and studied the associated asymptotic physics in the adiabatic regime. We now turn our attention to the remaining types of geometries. We first comment on the vertical models (Case B) in Section B.14.1. After discussing some of their general properties, we point out why the strategy employed in the study of horizontal models is not effective for vertical models. We conclude by analysing mixed section (Case C) and mixed bisection models (Case D) in Sections B.14.2 and B.14.3, respectively, where we study some of their general properties and extract their asymptotic physics in the adiabatic regime by extrapolating the lessons learnt during the study of horizontal models.

B.14.1 Vertical models (Case B)

Among the genus-zero single infinite-distance limit degenerations of Hirzebruch models, the vertical models (Case B) are possibly the hardest to analyse in terms of their asymptotic physics. Since they are the degenerations ‘‘orthogonal’’ to the horizontal models, the strategy used to study the latter in the adiabatic regime no longer applies, as we elaborate on at the end of this

brief section. At the same time, they would be particularly interesting to understand because they represent the F-theory duals to certain infinite-distance limits of the heterotic K3 surface, see Section 6.4.5. For completeness, we therefore collect some of their basic properties, like the constraints on the possible patterns of codimension-zero singular elliptic fibers in Section B.14.1.1, the restrictions on the existence of global weak coupling limits in Section B.14.1.2, and their generic horizontal slices in Section B.14.1.3.

B.14.1.1 Effectiveness bounds

The most immediate constraint on the pattern $I_{n_0} - \dots - I_{n_P}$ of codimension-zero singular elliptic fibers of the central fiber Y_0 of a vertical model is obtained from demanding the divisor classes of the restrictions $\{\Delta'_p\}_{0 \leq p \leq P}$ of the modified discriminant Δ' , see Table 6.2.1, to be effective. This results in the bounds

$$n_0 \geq n_1 - 12 - 12n, \quad (\text{B.14.1a})$$

$$n_p \geq \frac{n_{p-1} + n_{p+1}}{2}, \quad p = 1, \dots, P-1, \quad (\text{B.14.1b})$$

$$n_P \geq n_{P-1} - 12, \quad (\text{B.14.1c})$$

where $n_p \in \mathbb{Z}_{\geq 0}$ for all $p \in \{0, \dots, P\}$. As an immediate consequence, once at least one component is at local weak coupling all the intermediate components $\{Y^p\}_{1 \leq p \leq P-1}$ must be at local weak coupling as well.

As discussed in Section 6.3.2.2 and Section B.10.1 for horizontal models, we can obtain tighter bounds for $|n_p - n_{p+1}|$, with $p \in \{0, \dots, P-1\}$, depending on the type of accidental cancellation structure used to tune the pattern $I_{n_0} - \dots - I_{n_P}$. We provide the analogous results for vertical models in Section B.10.2.

B.14.1.2 Restrictions on global weak coupling limits

In global weak coupling limits all components of Y_0 have codimension-zero $I_{n>0}$ fibers. Such models are highly tuned to fulfil the accidental cancellation structure discussed in Appendix B.9, leading to strong constraints. For example, we found in Section 6.3.2.3 that horizontal global weak coupling limits can only be constructed over the Hirzebruch surfaces $\hat{B} = \mathbb{F}_n$ with $0 \leq n \leq 4$. In this section, we carry out the same analysis for vertical models, finding that they are even more constrained, namely, vertical global weak coupling limits can only be constructed over $\hat{B} = \mathbb{F}_n$ with $0 \leq n \leq 2$.

In the open-chain resolution of a vertical model all components $B^p = \mathbb{F}_0$ for $p \in \{1, \dots, P\}$, see Table 6.2.1. Hence, we must focus on the $B^0 = \mathbb{F}_n$ component to analyse forced factorisations of curves with negative self-intersection in the discriminant. In a global weak coupling limit, this component must, at the very least, satisfy the single accidental cancellation structure (B.9.4), with

$$h_0 \in H^0(B^0, \mathcal{L}_0^{\otimes 2}) \Rightarrow H_0 = 2\mathcal{L}_0 = 4S_0 + (2 + 2n)W_0. \quad (\text{B.14.2})$$

Given the intersection numbers

$$H_0 \cdot S_0 < 0 \Leftrightarrow n \geq 2, \quad (\text{B.14.3})$$

$$(H_0 - S_0) \cdot S_0 < 0 \Leftrightarrow n \geq 3, \quad (\text{B.14.4})$$

the polynomial h_0 must factorize like

$$h_0 \propto \begin{cases} s, & n = 2, \\ s^2, & n \geq 3. \end{cases} \quad (\text{B.14.5})$$

From the structure of f_0 , g_0 and Δ'_0 we see that the minimal vanishing orders over S_0 are

$$\text{ord}_{Y^0}(f_0, g_0, \Delta'_0)_{s=0} \geq \begin{cases} (2, 3, k + \alpha), & n = 2, \\ (4, 6, 2k + \alpha), & n \geq 3, \end{cases} \quad (\text{B.14.6})$$

where α accounts for additional factorisations forced by the reducibility of

$$\Delta''_0 := \Delta'_0 - kH_0. \quad (\text{B.14.7})$$

Its value can be computed by considering the intersection numbers of the classes Δ''_0 and S_0 . The class $\Delta''_0 - \alpha S_0$ will still contain S_0 components as long as

$$(\Delta''_0 - \alpha S_0) \cdot S_0 < 0 \Leftrightarrow \alpha < \frac{2k + (n_1 - n_0) - 12}{n} + 12 - 2k. \quad (\text{B.14.8})$$

Therefore, the final value of α is

$$\alpha = \max \left\{ \left\lceil \frac{2k + (n_1 - n_0) - 12}{n} + 12 - 2k \right\rceil, 0 \right\}. \quad (\text{B.14.9})$$

Unlike for horizontal models, we see that α depends not only on n and k , but also on $n_0 - n_1$. Let us analyse the possibility of tuning vertical models corresponding to global weak coupling limits depending on the type of Hirzebruch surface $\hat{B} = \mathbb{F}_n$ over which they are constructed.

Models with $3 \leq n \leq 12$ Vertical models constructed over these Hirzebruch surfaces have components vanishing orders in the Y^0 component

$$\text{ord}_{Y^0}(f_0, g_0)_{s=0} = (4, 6). \quad (\text{B.14.10})$$

Hence, tuning this component to be at local weak coupling forces (at the very least) an obscured infinite-distance limit over S_0 . This actually takes us away from the single infinite-distance limit class of degenerations that we are focusing on in this chapter. At any rate, the model demands an additional resolution process that will lead to new components at local strong coupling. We therefore conclude that vertical global weak coupling limits are not possible in models constructed over $\hat{B} = \mathbb{F}_n$, with $3 \leq n \leq 12$. Note that the non-minimal component vanishing orders over $\{s = 0\}_{B^0}$ may be of the (naively) pathological type, see the comments in Section 6.3.2.3.

Models with $n = 2$ Models constructed over this Hirzebruch surface can indeed be global weak coupling limits. The necessary tuning to achieve this forces an enhancement in the Y^0 component over the S_0 curve, with component vanishing orders

$$\text{ord}_{Y^0}(f_0, g_0, \Delta'_0)_{s=0} \geq (2, 3, k + \alpha), \quad k \geq 2. \quad (\text{B.14.11})$$

The minimal values of

$$\text{ord}_{Y^0}(f_0, g_0, \Delta'_0)_{s=0} \geq (2, 3, 2) \quad (\text{B.14.12})$$

can be attained, but this requires at least a double accidental cancellation structure, see (B.14.9), Appendix B.9 and the bounds discussed in Section B.10.1.

Models with $\mathbf{n} = 1$ Global weak coupling limits can also be realised in those vertical models constructed over $\hat{B} = \mathbb{F}_1$. The necessary tuning leads in the Y^0 component to the local enhancement

$$\text{ord}_{Y^0}(f_0, g_0, \Delta'_0)_{s=0} \geq (0, 0, \max(n_1 - n_0, 0)), \quad (\text{B.14.13})$$

over the S_0 curve.

Models with $\mathbf{n} = 0$ Vertical models constructed over $\hat{B} = \mathbb{F}_0$ can correspond to global weak coupling limits, without any forced enhancements tied to the necessary tuning, since we generically have

$$\text{ord}_{Y^0}(f_0, g_0, \Delta'_0)_{s=0} = (0, 0, 0). \quad (\text{B.14.14})$$

This was necessary for consistency with the results of Section 6.3.2.3, since over $\hat{B} = \mathbb{F}_0$ there is no geometrical distinction between horizontal and vertical models.

B.14.1.3 Generic horizontal slices

The generic vertical slices of horizontal models played a prominent role in their study, first for their classification in Section 6.3.1 and later in the analysis of their asymptotic physics in Sections 6.4 and 6.5. The analogue for vertical models would be to study their generic horizontal slices.

In the base components $B^p = \mathbb{F}_0$, where $p = 1, \dots, P$, there is no distinction between horizontal and vertical directions. Hence, the slicing behaves like for horizontal models. In the Y^0 component, however, we do now not have a canonical choice for extending the slice from the other components. Consider first the horizontal slice by the distinguished curve

$$\mathcal{H}_0 := \sum_{p=0}^P S_p = \mathcal{S}|_{\tilde{U}}. \quad (\text{B.14.15})$$

This leads to an associated eight-dimensional model with

$$\Delta'_0 \cdot \mathcal{H}_0|_{E_0} = 12 - 12n + n_0 - n_1, \quad (\text{B.14.16a})$$

$$\Delta'_p \cdot \mathcal{H}_0|_{E_p} = 2n_p - n_{p-1} - n_{p+1}, \quad p = 1, \dots, P-1 \quad (\text{B.14.16b})$$

$$\Delta'_P \cdot \mathcal{H}_0|_{E_P} = 12 + n_P - n_{P-1}. \quad (\text{B.14.16c})$$

7-branes in each component. We could also consider taking horizontal slices restricting to generic representatives of

$$\mathcal{H}_\infty := \sum_{p=0}^P T_p = \mathcal{T}|_{\tilde{U}}, \quad (\text{B.14.17})$$

which leads to the same results with the exception of

$$\Delta'_0 \cdot \mathcal{H}_\infty|_{E_0} = \Delta'_0 \cdot \mathcal{H}_0|_{E_0} + 24n. \quad (\text{B.14.18})$$

Recombining vertical classes into the divisor used to take the horizontal slice also changes these intersection numbers by multiples of 12. Hence, all generic horizontal slices (where by generic we mean that they do not overlap with components of Δ_{phys} or pass through its intersections with the interface curves between components), lead to the same types of eight-dimensional models that were found in the analysis of horizontal models, with the only difference that they may

differ by some sets of 12 7-branes. Because these sets of additional 12 7-branes appearing in the horizontal slices produce a combined trivial monodromy action, a common picture for the generic horizontal slices can still be concocted. Vertical models can therefore still be classified by inheriting the classification of Kulikov models from their generic vertical slices. In that classification, the K3 double covers associated with vertical Type III.b models are the endpoints of, generically, Kulikov Type II.a models, see Section B.13.3.

However, we can no longer trust an analysis of the asymptotic physics using these slices and then the orthogonal ones, which would simply put the strategy applied to the horizontal models upside-down. The fiberwise analysis of horizontal models relied on the adiabaticity assumption, which was particularly useful thanks to the degeneration forcing the Hirzebruch surface to split along the fibral curve \mathbb{P}_f^1 . The adiabatic limit separated, as a consequence, the defects in the orthogonal slices responsible for trivialising the local 2-cycles apart. In vertical models the Hirzebruch surface splits along the base curve \mathbb{P}_b^1 , and the same approach is no longer possible. Understanding how the towers of asymptotically massless particles reorganise away from the adiabatic regime already for the simpler horizontal models would shed light also on the vertical models. This would be particularly interesting because, stretching the F-theory/heterotic duality reviewed in Section 6.4.1, they are dual to a non-minimal degeneration along the non-perturbative heterotic sector.

B.14.2 Mixed section models (Case C)

Mixed section models, Case C in Table 6.2.1, behave very similarly to horizontal models because the non-minimal curve

$$C = h + (n + \alpha)f, \quad \text{where} \quad \begin{cases} \alpha = 1, & \text{with } n \leq 6, \\ \alpha = 2, & \text{with } n = 0, \end{cases} \quad (\text{B.14.19})$$

is also a section.

B.14.2.1 Effectiveness bounds

We can constrain the pattern $I_{n_0} - \cdots - I_{n_P}$ of codimension-zero singular elliptic fibers of the central fiber Y_0 of a mixed section model by demanding that the divisor classes of the restrictions $\{\Delta'_p\}_{0 \leq p \leq P}$ of the modified discriminant Δ' , printed in Table 6.2.1, are effective. This leads to the bounds

$$n_0 \geq n_1 - 12, \quad (\text{B.14.20a})$$

$$n_p \geq \frac{n_{p-1} + n_{p+1}}{2}, \quad p = 1, \dots, P-1, \quad (\text{B.14.20b})$$

$$n_P \geq n_{P-1} - 12, \quad (\text{B.14.20c})$$

from their horizontal part, and

$$n_{p-1} - n_p \leq \frac{24}{n + 2\alpha}, \quad p = 1, \dots, P-1, \quad n_{P-1} - n_P \leq \frac{24 - 12\alpha}{n + \alpha}, \quad (\text{B.14.21})$$

from their vertical part, where $n_p \in \mathbb{Z}_{\geq 0}$ for all $p \in \{0, \dots, P\}$.

Comparing with the effectiveness bounds obtained for horizontal models in Section 6.3.2.1, we observe that those obtained from the horizontal part are identical; this owes to the fact that

the non-minimal curve C is still a section. Similarly, the bounds derived from the vertical part for the differences $n_{p-1} - n_p$, with $p \in \{1, \dots, P-1\}$, also coincide with the ones obtained for a horizontal model constructed over $\hat{B} = \mathbb{F}_{n+2\alpha}$, which can be understood from the structure of the central fiber Y_0 displayed in Table 6.2.1.

B.14.2.2 Restrictions on global weak coupling limits

Tuning a global weak coupling limit in a mixed section model may induce new non-minimal curves and hence new components at local strong coupling. We now analyse the resulting constraints on the models.

Consider the end-component $B^P = \mathbb{F}_n$, containing the curve S_P with negative self-intersection $S_P \cdot S_P = -n$; one can check that the other components do not lead to additional constraints. Note that, if components of this curve factorize, we do not only destroy the global weak coupling limit, but also exit the single infinite-distance degeneration class of models. This is due to the non-trivial intersection $C' \cdot S_P = \alpha$ between the new non-minimal curve S_P and the strict transform C' of the original non-minimal curve C . Any local description of the component Y^P in terms of local coordinates will necessarily lead to the accidental cancellation structure (B.9.4), and we can therefore exploit the fact that

$$F_P = 2H_P, \quad G_P = 3H_P, \quad H_P = 2\mathcal{L}_P. \quad (\text{B.14.22})$$

When $n = 0$, the intersection product $S_P \cdot S_P = 0$ and, as a consequence, no forced factorization of S_P will occur. We conclude that mixed section models corresponding to global weak coupling limits are possible when $\alpha = 1, 2$ and $n = 0$.

This leaves us with the cases $\alpha = 1$, with $1 \leq n \leq 6$, to be analysed. From Table 6.2.1 we read that in these cases

$$H_P = 2S_P + 2V_P. \quad (\text{B.14.23})$$

In view of the intersection products

$$H \cdot S_P < 0 \Leftrightarrow n \geq 2, \quad (\text{B.14.24})$$

$$(H - S_P) \cdot S_P < 0 \Leftrightarrow n \geq 3, \quad (\text{B.14.25})$$

we find that

$$\text{ord}_{Y^P}(f_P, g_P, \Delta'_P)_{S_P} \geq \begin{cases} (2, 3, k + \alpha), & n = 2, \\ (4, 6, 2k + \alpha), & n \geq 3, \end{cases} \quad (\text{B.14.26})$$

where α accounts for additional factors of S_P forced by the reducibility

$$\Delta''_P := \Delta'_P - kH_P. \quad (\text{B.14.27})$$

From the intersection product

$$(\Delta''_P - \alpha S_P) \cdot S_P < 0 \Leftrightarrow \alpha < \frac{2k - (n_P - n_{P-1}) - 12}{n} + 12 - 2k. \quad (\text{B.14.28})$$

we conclude that

$$\alpha = \max \left\{ \left\lceil \frac{2k - (n_P - n_{P-1}) - 12}{n} + 12 - 2k \right\rceil, 0 \right\}. \quad (\text{B.14.29})$$

As occurred for vertical models, the final value of α not only depends on n and k , but also on the difference $n_P - n_{P-1}$.

Models with $3 \leq n \leq 12$ A mixed section model constructed over these Hirzebruch surfaces cannot correspond to a global weak coupling limit. Trying to force the geometry to present all components at local weak forces the curve S_P in B^P to factorise with component vanishing orders

$$\text{ord}_{Y^P}(f_P, g_P) \geq (4, 6), \quad (\text{B.14.30})$$

bringing us out of the mixed section model class due to the non-trivial intersection $C' \cdot S_P = \alpha$.

Models with $n = 2$ We can construct mixed section global weak coupling limits in models constructed over $\hat{B} = \mathbb{F}_2$. This forces a D type local enhancement over the curve S_P in B^P , as implied by (B.14.26).

Models with $n = 1$ Mixed section models constructed over $\hat{B} = \mathbb{F}_1$ also allow for global weak coupling limits. The geometry forces a local I_m type enhancement over S_P in B^P , with vanishing orders

$$\text{ord}_{Y^P}(f_P, g_P, \Delta'_P)_{S_P} \geq (0, 0, \max(n_{P-1} - n_P, 0)), \quad (\text{B.14.31})$$

where $n_{P-1} - n_P \leq 6$ due to (B.14.21).

Models with $n = 0$ Mixed section global weak coupling limits are also allowed in models constructed over $\hat{B} = \mathbb{F}_0$, with no local enhancement enforced by the tuning.

B.14.2.3 Generic vertical slices

In mixed section models, the global vertical divisor in B_0 is defined in the same way as for horizontal models, namely

$$\mathcal{F} := \sum_{p=0}^P V_p. \quad (\text{B.14.32})$$

We see from Table 6.2.1 that the eight-dimensional models obtained by taking generic vertical slices are identical to the ones appearing as the generic vertical slices of horizontal models, presenting the distribution of 7-branes

$$\Delta'_0 \cdot \mathcal{F}|_{E_0} = 12 + n_0 - n_1, \quad (\text{B.14.33a})$$

$$\Delta'_p \cdot \mathcal{F}|_{E_p} = 2n_p - n_{p-1} - n_{p+1}, \quad p = 1, \dots, P-1, \quad (\text{B.14.33b})$$

$$\Delta'_P \cdot \mathcal{F}|_{E_P} = 12 + n_P - n_{P-1}. \quad (\text{B.14.33c})$$

Mixed section models can then be classified according to the Kulikov model type of their generic vertical slice.

Those representatives of \mathcal{F} passing through the intersection points of Δ_{phys} with the interface curves between component do not lead to generic vertical slices. The number of said points of intersection at each interface is

$$\Delta'_p \cdot S_p = 24 + (n + 2\alpha)(n_{p+1} - n_p), \quad p = 0, \dots, P-1, \quad (\text{B.14.34a})$$

$$\Delta'_p \cdot T_p = 24 + (n + 2\alpha)(n_p - n_{p-1}), \quad p = 1, \dots, P-1, \quad (\text{B.14.34b})$$

$$\Delta'_P \cdot C = 24 + (n + 2\alpha)(n_P - n_{P-1}). \quad (\text{B.14.34c})$$

B.14.2.4 Fiberwise analysis in the adiabatic regime

Mixed section models behave very similarly to horizontal models due to the fact that the non-minimal curve C in \hat{B}_0 is also a section. Their generic vertical slices are identical to those found for horizontal models. Moreover, since the local 2-cycles defined over such slices are trivialised over the non-generic vertical slices, and these can be pushed far away from each other by demanding the hierarchy of volumes $\mathcal{V}_{\mathbb{P}_b^1} \gg \mathcal{V}_{K3}$ characteristic of the adiabatic limit, we can perform a fiberwise analysis of the asymptotic physics of mixed section models in the adiabatic regime.

The bulk physics of the asymptotic model is extracted from the generic vertical slices, extending their local analysis to the generic patches of Y_0 , as was done in Sections 6.4 and 6.5. Since their generic vertical slices are identical, mixed section Type II.a, Type III.a and Type III.b models have the same asymptotic bulk physics as their horizontal counterparts.

The vertical gauge algebras in mixed section models lead to localised algebras living in the worldvolume of six-dimensional defects present in the decompactified theories. It is clear from their geometry that the gauge rank supported over vertical divisors or the exceptional curves in the fiber is smaller than in their horizontal counterparts. This is intuitively clear from the way in which mixed section models are constructed: The would-be non-minimal curves of a horizontal model are recombined with vertical classes and made non-minimal in order to arrive at a mixed section model. Hence, tuning a codimension-one degeneration along the curve C uses up part of the divisor classes that would be associated with the localised defect algebra sector in the horizontal model.

B.14.3 Mixed bisection models (Case D)

The final class of models correspond to a codimension-one degeneration along the bisection

$$C = 2h + bf \quad \text{with} \quad (n, b) = (0, 1), (1, 2). \quad (\text{B.14.35})$$

For this reason, their behaviour shows many parallels to that of horizontal and mixed section models.

B.14.3.1 Effectiveness bounds

The constraints on the pattern $I_{n_0} - \dots - I_{n_P}$ of codimension-zero singular elliptic fibers of Y_0 are given by the bounds

$$n_0 \geq n_1 - 12, \quad (\text{B.14.36a})$$

$$n_p \geq \frac{n_{p-1} + n_{p+1}}{2}, \quad p = 1, \dots, P-1, \quad (\text{B.14.36b})$$

$$n_P \geq n_{P-1}, \quad (\text{B.14.36c})$$

together with

$$n_{p-1} - n_p \leq 6, \quad p = 1, \dots, P-1, \quad n_{P-1} - n_P \leq \frac{12}{n+1}, \quad (\text{B.14.37})$$

where $n_p \in \mathbb{Z}_{\geq 0}$ for all $p \in \{0, \dots, P\}$.

Note that this time, the bounds (B.14.36) imply that, once a single component has codimension-zero I_m fibers, all $\{Y^p\}_{1 \leq p \leq P}$ components must do as well. This is different from the other of

models, for which this effect occurs only for the intermediate components $\{Y^p\}_{1 \leq p \leq P-1}$. It will become intuitively clear why the end-component Y^P behaves like an intermediate component once we analyse the generic vertical slices of the model in Section B.14.3.3.

B.14.3.2 Restrictions on global weak coupling limits

To constrain the possible global weak coupling limits we analyse the effects of tuning the Y^P component to be at local weak coupling; one can check that the other components do not lead to additional constraints. Any description of the component B^P in terms of local coordinates will necessarily lead to, at least, the accidental cancellation structure (B.9.4), and therefore

$$F_P = 2H_P, \quad G_P = 3H_P, \quad H_P = 2\mathcal{L}_P. \quad (\text{B.14.38})$$

From Table 6.2.1 we see that $H_P = 2V_P$ and, therefore, we encounter no forced factorization leading to a non-minimal curve in B^P as a consequence of tuning the codimension-zero I_{n_P} fibers over the component. This is not too surprising since the bisection degenerations are possible only over Hirzebruch surfaces \mathbb{F}_n for $n = 0, 1$.

B.14.3.3 Generic vertical slices

Let us consider the generic vertical slices of a mixed bisection model. The non-minimal curve C in \hat{B}_0 is a bisection, as can be seen from $C \cdot f = 2$. In the open-chain resolution of the model, this curve acts as the interface curve $E_P|_{E_{P-1}}$ between the B^{P-1} and B^P base components. This implies that, in the base B_0 of the central fiber Y_0 of the resolved degeneration, the global vertical divisors are

$$\mathcal{F} := \sum_{p=0}^{P-1} 2V_p + V_P. \quad (\text{B.14.39})$$

Consider now the eight-dimensional model associated with the vertical slice cut by a generic representative of this class. In the Y^P component, we are taking a single local vertical cut, leading to one elliptic surface. In the components $\{Y^p\}_{0 \leq p \leq P-1}$, however, we obtain two distinct (due to the generic choice of the representative) local vertical cuts, leading to two elliptic surfaces per component. All these elliptic surfaces intersect their neighbour over an elliptic curve, and their bases intersect in an open chain. Computing the 7-brane content of the eight-dimensional model associated with the generic vertical slice, we find

$$\Delta'_0 \cdot \mathcal{F}|_{E_0} = (12 + n_0 - n_1) + (12 + n_0 - n_1), \quad (\text{B.14.40a})$$

$$\Delta'_p \cdot \mathcal{F}|_{E_p} = (2n_p - n_{p-1} - n_{p+1}) + (2n_p - n_{p-1} - n_{p+1}), \quad p = 1, \dots, P-1 \quad (\text{B.14.40b})$$

$$\Delta'_P \cdot \mathcal{F}|_{E_P} = 2n_P - n_{P-1} - n_{P-1}. \quad (\text{B.14.40c})$$

where in the products $\Delta'_p \cdot \mathcal{F}|_{E_p}$ with $p \in \{0, \dots, P-1\}$ each term in parentheses corresponds to one of the two local vertical slices. Hence, the generic vertical slice corresponds to the one of a codimension-one degeneration along a section of the Hirzebruch surface, is in a horizontal or a mixed section model, whose resolution leads to a $(2P+1)$ -component central fiber, but that has been “folded” in the Y^P component to fit into the $(P+1)$ -component central fiber of the Case D model.

This explains why the effectiveness bounds (B.14.36) imply that, in the presence of at least a single component at local weak coupling, all components $\{Y^p\}_{1 \leq p \leq P}$ must be at local weak coupling as well: The vertical slice of the end-component Y^P leads to an intermediate

component of the generic vertical slice, for which this effect is in place. In order for the pattern $I_{n_0} - \dots - I_{n_P}$ of codimension-zero singular elliptic fiber to match between the central fiber of the six-dimensional model and its generic vertical slice the aforementioned implication must indeed hold. Hence, the end-component Y^P behaves in many regards like an intermediate component. Notice as well that the holomorphic line bundle \mathcal{L}_P associated with the Weierstrass model of the elliptic fibration $\pi_P : Y^P \rightarrow B^P$ is purely vertical, as occurs for the intermediate components of horizontal or mixed section models.

We can then classify mixed bisectional models in the same way as the other models under consideration, i.e. by inheriting the classification of Kulikov models from its generic vertical fiber. Due to the “folded” nature of such a generic vertical fiber, notice that only those Kulikov Type III.a models with both components at local strong coupling can arise from the restriction of a mixed bisectional model.

The non-generic vertical slices are those associated with the representatives of \mathcal{F} passing through the intersection points of Δ_{phys} with the interface curve over which the base components intersect. Counting the number of intersection points at each interface, we find

$$\Delta'_p \cdot S_p = 24 + 4(n_{p+1} - n_p), \quad p = 0, \dots, P-1, \quad (\text{B.14.41a})$$

$$\Delta'_p \cdot T_p = 24 + 4(n_p - n_{p-1}), \quad p = 1, \dots, P-1, \quad (\text{B.14.41b})$$

$$\Delta'_P \cdot \mathcal{C} = 24 + 4(n_P - n_{P-1}). \quad (\text{B.14.41c})$$

B.14.3.4 Fiberwise analysis in the adiabatic regime

Since the curve C in \hat{B}_0 is a bisection, the resulting models behave very similarly to horizontal and mixed section models also with respect to the adiabatic limit. The hierarchy of volumes $\mathcal{V}_{\mathbb{P}_b^1} \gg \mathcal{V}_{K3}$ separates the non-generic vertical slices, making a fiberwise analysis possible in the adiabatic regime.

The bulk physics at the endpoint of the limit is encoded in the generic vertical slice, as we have seen already for various models. As explained above, the generic vertical slices are identical to the ones obtained for horizontal and mixed section models. Hence, the bulk physics of Case D Type II.a, Type III.a and Type III.b models will behave as in their horizontal and mixed section model counterparts.

Vertical gauge algebras lead to localised algebras in the worldvolume of six-dimensional defects of the decompactified theory. As for mixed section degenerations, the expenditure of vertical classes in the tuning of a Case D model reduces the maximal gauge rank that can be attained for the defect algebras in the limit with respect to horizontal models. This is most clearly seen by the reduction in the number of local vertical classes in Δ'_P .

Acknowledgements

Science is a human endeavour; during my doctoral studies I have had the luck to cross worldlines not only with excellent scientists, but with remarkable human beings. It is with great pleasure that I use the lines below to express my gratitude to them.

First and foremost, I would like to thank my supervisor Timo Weigand for generously sharing his expertise, time and intuition with me. In contrast with the inherently fluid and dynamic nature of research, his guidance and support have remained a constant. I have greatly enjoyed discussing with and learning from him. For the joy that working and growing under his mentorship has been, I have nothing but the deepest gratitude.

I would also like to thank Alexander Westphal for many discussions, revolving around physics and beyond, which were as enlightening and informative as they were entertaining; I very much value all these interactions. Likewise, I want to also express my appreciation to Vicente Cortés and Craig Lawrie for insightful discussions.

It has been a pleasure to collaborate with Ralph Blumenhagen, Daniel Kläwer, Christian Kneifl, Seung-Joo Lee, Andriana Makridou and Lorenz Schlechter during my doctoral studies; I have learnt a lot from all of them. Special thanks to Seung-Joo Lee for countless hours of stimulating discussions and for such a pleasant collaboration.

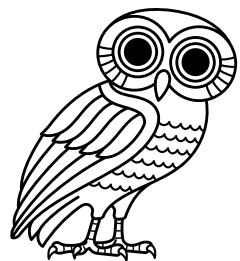
Understanding why my time in Hamburg has been so enjoyable would be difficult without mentioning the past and present members of the group; in addition to insightful conversations about physics, we have shared so much more. For such an unforgettable time, I must thank Florent Baume, César Fierro Cota, Mateo Galdeano Solans, Veronica Guidetti, Daniel Kläwer, Stefano Lanza, Craig Lawrie, Jacob Leedom, Lorenzo Mansi, Alessandro Mininno, Margherita Putti, Nicole Righi and Paul Veltman. I wish you all the best. I must also mention Alain, Alessio, Carlo, Davide, Deniz, Felix, Gabriele, Kateryna, Paula and Sara, who contribute to the vivid atmosphere of the institute.

Furthermore, I will fondly remember the moments spent in the company of Alejandro, Andrés, Cósima, Daniel, David, Deniz, Isabela, Julia, Mateo and Paula. You are such a cheerful group.

Por último, me gustaría agradecer a mi familia su continuado apoyo. Aun en la distancia, su confianza me motiva hoy como lo hizo ayer.

Porque aun sin querer columbro siempre, al través de cada moneda recibida, la faz curtida y sudorosa del campesino, quien, en definitiva, sufraga nuestros lujos académicos y científicos.

— Santiago Ramón y Cajal, *El mundo visto a los 80 años*



Bibliography

- [1] R. Álvarez-García, D. Kläwer and T. Weigand, *Membrane limits in quantum gravity*, *Phys. Rev. D* **105** (2022) 066024 [[2112.09136](#)].
- [2] R. Álvarez-García, S.-J. Lee and T. Weigand, *Non-minimal Elliptic Threefolds at Infinite Distance I: Log Calabi-Yau Resolutions*, [2310.07761](#).
- [3] R. Álvarez-García, S.-J. Lee and T. Weigand, *Non-minimal Elliptic Threefolds at Infinite Distance II: Asymptotic Physics*, [2312.11611](#).
- [4] R. Álvarez-García, R. Blumenhagen, C. Kneissl, A. Makridou and L. Schlechter, *Swampland conjectures for an almost topological gravity theory*, *Phys. Lett. B* **825** (2022) 136861 [[2107.07546](#)].
- [5] R. Álvarez-García and L. Schlechter, *Analytic periods via twisted symmetric squares*, *JHEP* **07** (2022) 024 [[2110.02962](#)].
- [6] L.E. Ibañez and A.M. Uranga, *String theory and particle physics: An introduction to string phenomenology*, Cambridge University Press (2012).
- [7] F. Marchesano, G. Shiu and T. Weigand, *The Standard Model from String Theory: What Have We Learned?*, [2401.01939](#).
- [8] J.D. Bekenstein, *Black holes and entropy*, *Phys. Rev. D* **7** (1973) 2333.
- [9] J.D. Bekenstein, *Generalized second law of thermodynamics in black-hole physics*, *Phys. Rev. D* **9** (1974) 3292.
- [10] S.W. Hawking, *Black hole explosions*, *Nature* **248** (1974) 30.
- [11] S.W. Hawking, *Particle Creation by Black Holes*, *Commun. Math. Phys.* **43** (1975) 199.
- [12] D. Rickles and C.M. DeWitt, *The Role of Gravitation in Physics: Report from the 1957 Chapel Hill Conference*, Max-Planck-Gesellschaft zur Förderung der Wissenschaften (2011).
- [13] R. Feynman, F. Morinigo, W. Wagner and B. Hatfield, *Feynman Lectures On Gravitation*, Frontiers in Physics Series, Avalon Publishing (1995).
- [14] Y. Aharonov and D. Rohrlich, *How to observe a quantum wave*, in *Quantum Paradoxes*, pp. 211–224, John Wiley & Sons, Ltd (2005), DOI.
- [15] K. Eppley and E. Hannah, *The necessity of quantizing the gravitational field*, *Foundations of Physics* **7** (1977) 51.

- [16] J. Mattingly, *Why Eppley and Hannah's thought experiment fails*, *Phys. Rev. D* **73** (2006) 064025 [[gr-qc/0601127](#)].
- [17] W.G. Unruh, *Steps towards a quantum theory of gravity*, Adam Hilger Limited, United Kingdom (1984).
- [18] D. Rickles, *Quantum gravity: A primer for philosophers*, in *The Ashgate Companion to Contemporary Philosophy of Physics*, pp. 262–366, Routledge (2008).
- [19] J. Martin, *Everything You Always Wanted To Know About The Cosmological Constant Problem (But Were Afraid To Ask)*, *Comptes Rendus Physique* **13** (2012) 566 [[1205.3365](#)].
- [20] SUPERNOVA COSMOLOGY PROJECT collaboration, *Measurements of Ω and Λ from 42 high redshift supernovae*, *Astrophys. J.* **517** (1999) 565 [[astro-ph/9812133](#)].
- [21] SUPERNOVA SEARCH TEAM collaboration, *Observational evidence from supernovae for an accelerating universe and a cosmological constant*, *Astron. J.* **116** (1998) 1009 [[astro-ph/9805201](#)].
- [22] PLANCK collaboration, *Planck 2018 results. VI. Cosmological parameters*, *Astron. Astrophys.* **641** (2020) A6 [[1807.06209](#)].
- [23] V. Mukhanov, *Physical Foundations of Cosmology*, Cambridge University Press, Oxford (2005), 10.1017/CBO9780511790553.
- [24] D. Baumann, *Cosmology*, Cambridge University Press (7, 2022), 10.1017/9781108937092.
- [25] D. Rickles, *Covered with Deep Mist*, Oxford University Press (3, 2020).
- [26] A. Einstein, *Näherungsweise Integration der Feldgleichungen der Gravitation*, *Sitzungsberichte der Königlich Preußischen Akademie der Wissenschaften* (1916) 688.
- [27] G. Gor'kavik, *The First Steps of Quantum Gravity and the Planck Values*, *Studies in the History of General Relativity* (1992) 364.
- [28] W. Heisenberg and W. Pauli, *Zur Quantendynamik der Wellenfelder*, *Z. Phys.* **56** (1929) 1.
- [29] M.D. Schwartz, *Quantum Field Theory and the Standard Model*, Cambridge University Press (3, 2014).
- [30] G. 't Hooft and M.J.G. Veltman, *One loop divergencies in the theory of gravitation*, *Ann. Inst. H. Poincaré Phys. Theor. A* **20** (1974) 69.
- [31] M.H. Goroff and A. Sagnotti, *Quantum gravity at two loops*, *Phys. Lett. B* **160** (1985) 81.
- [32] B.S. DeWitt, *Quantum Field Theory in Curved Spacetime*, *Phys. Rept.* **19** (1975) 295.
- [33] V. Mukhanov and S. Winitzki, *Introduction to Quantum Effects in Gravity*, Cambridge University Press (6, 2007).
- [34] C.P. Burgess, *Introduction to Effective Field Theory*, Cambridge University Press (12, 2020), 10.1017/9781139048040.
- [35] P.A.M. Dirac, *The Cosmological constants*, *Nature* **139** (1937) 323.

- [36] P.A.M. Dirac, *New basis for cosmology*, *Proc. Roy. Soc. Lond. A* **165** (1938) 199.
- [37] G. 't Hooft, *Naturalness, chiral symmetry, and spontaneous chiral symmetry breaking*, *NATO Sci. Ser. B* **59** (1980) 135.
- [38] J.F. Donoghue, *Leading quantum correction to the Newtonian potential*, *Phys. Rev. Lett.* **72** (1994) 2996 [[gr-qc/9310024](#)].
- [39] J.F. Donoghue, *Introduction to the effective field theory description of gravity*, in *Advanced School on Effective Theories*, 6, 1995 [[gr-qc/9512024](#)].
- [40] M.R. Douglas and N.A. Nekrasov, *Noncommutative field theory*, *Rev. Mod. Phys.* **73** (2001) 977 [[hep-th/0106048](#)].
- [41] N. Craig, *Naturalness: past, present, and future*, *Eur. Phys. J. C* **83** (2023) 825 [[2205.05708](#)].
- [42] HIRES collaboration, *Detection of a cosmic ray with measured energy well beyond the expected spectral cutoff due to cosmic microwave radiation*, *Astrophys. J.* **441** (1995) 144 [[astro-ph/9410067](#)].
- [43] TELESCOPE ARRAY collaboration, *An extremely energetic cosmic ray observed by a surface detector array*, *Science* **382** (2023) abo5095 [[2311.14231](#)].
- [44] T. Rothman and S. Boughn, *Can gravitons be detected?*, *Found. Phys.* **36** (2006) 1801 [[gr-qc/0601043](#)].
- [45] F. Dyson, *Is a graviton detectable?*, *Int. J. Mod. Phys. A* **28** (2013) 1330041.
- [46] D. Carney, V. Domcke and N.L. Rodd, *Graviton detection and the quantization of gravity*, *Phys. Rev. D* **109** (2024) 044009 [[2308.12988](#)].
- [47] L.M. Krauss and F. Wilczek, *Using Cosmology to Establish the Quantization of Gravity*, *Phys. Rev. D* **89** (2014) 047501 [[1309.5343](#)].
- [48] J. Martin and V. Vennin, *Quantum Discord of Cosmic Inflation: Can we Show that CMB Anisotropies are of Quantum-Mechanical Origin?*, *Phys. Rev. D* **93** (2016) 023505 [[1510.04038](#)].
- [49] M. Parikh, F. Wilczek and G. Zahariade, *Signatures of the quantization of gravity at gravitational wave detectors*, *Phys. Rev. D* **104** (2021) 046021 [[2010.08208](#)].
- [50] J. Maldacena, *A model with cosmological Bell inequalities*, *Fortsch. Phys.* **64** (2016) 10 [[1508.01082](#)].
- [51] D. Green and R.A. Porto, *Signals of a Quantum Universe*, *Phys. Rev. Lett.* **124** (2020) 251302 [[2001.09149](#)].
- [52] D. Carney, P.C.E. Stamp and J.M. Taylor, *Tabletop experiments for quantum gravity: a user's manual*, *Class. Quant. Grav.* **36** (2019) 034001 [[1807.11494](#)].
- [53] M.B. Green, J.H. Schwarz and E. Witten, *Superstring Theory Vol. 1: 25th Anniversary Edition*, Cambridge Monographs on Mathematical Physics, Cambridge University Press (11, 2012), 10.1017/CBO9781139248563.

- [54] M.B. Green, J.H. Schwarz and E. Witten, *Superstring Theory Vol. 2: 25th Anniversary Edition*, Cambridge Monographs on Mathematical Physics, Cambridge University Press (11, 2012), 10.1017/CBO9781139248570.
- [55] J. Polchinski, *String theory. Vol. 1: An introduction to the bosonic string*, Cambridge Monographs on Mathematical Physics, Cambridge University Press (12, 2007), 10.1017/CBO9780511816079.
- [56] J. Polchinski, *String theory. Vol. 2: Superstring theory and beyond*, Cambridge Monographs on Mathematical Physics, Cambridge University Press (12, 2007), 10.1017/CBO9780511618123.
- [57] R. Blumenhagen, D. Lüst and S. Theisen, *Basic concepts of string theory*, Theoretical and Mathematical Physics, Springer, Heidelberg, Germany (2013), 10.1007/978-3-642-29497-6.
- [58] A. Strominger and C. Vafa, *Microscopic origin of the Bekenstein-Hawking entropy*, *Phys. Lett. B* **379** (1996) 99 [[hep-th/9601029](#)].
- [59] A. Sen, *Universality of the tachyon potential*, *JHEP* **12** (1999) 027 [[hep-th/9911116](#)].
- [60] M. Schnabl, *Analytic solution for tachyon condensation in open string field theory*, *Adv. Theor. Math. Phys.* **10** (2006) 433 [[hep-th/0511286](#)].
- [61] L.J. Dixon and J.A. Harvey, *String Theories in Ten-Dimensions Without Space-Time Supersymmetry*, *Nucl. Phys. B* **274** (1986) 93.
- [62] H. Kawai, D.C. Lewellen and S.H.H. Tye, *Classification of Closed Fermionic String Models*, *Phys. Rev. D* **34** (1986) 3794.
- [63] S. Elitzur and A. Giveon, *Connection Between Spectra of Nonsupersymmetric Heterotic String Models*, *Phys. Lett. B* **189** (1987) 52.
- [64] L. Alvarez-Gaume, P.H. Ginsparg, G.W. Moore and C. Vafa, *An $O(16) \times O(16)$ Heterotic String*, *Phys. Lett. B* **171** (1986) 155.
- [65] S. Sugimoto, *Anomaly cancellations in type I D-9 - anti-D-9 system and the $USp(32)$ string theory*, *Prog. Theor. Phys.* **102** (1999) 685 [[hep-th/9905159](#)].
- [66] A. Sagnotti, *Some properties of open string theories*, in *International Workshop on Supersymmetry and Unification of Fundamental Interactions (SUSY 95)*, pp. 473–484, 9, 1995 [[hep-th/9509080](#)].
- [67] A. Sagnotti, *Surprises in open string perturbation theory*, *Nucl. Phys. B Proc. Suppl.* **56** (1997) 332 [[hep-th/9702093](#)].
- [68] K.R. Dienes, *Modular invariance, finiteness, and misaligned supersymmetry: New constraints on the numbers of physical string states*, *Nucl. Phys. B* **429** (1994) 533 [[hep-th/9402006](#)].
- [69] N. Cribiori, S. Parameswaran, F. Tonioni and T. Wräse, *Misaligned Supersymmetry and Open Strings*, *JHEP* **04** (2021) 099 [[2012.04677](#)].

- [70] S. Abel, K.R. Dienes and E. Mavroudi, *Towards a nonsupersymmetric string phenomenology*, *Phys. Rev. D* **91** (2015) 126014 [[1502.03087](#)].
- [71] B. Fraiman, M. Graña, H. Parra De Freitas and S. Sethi, *Non-Supersymmetric Heterotic Strings on a Circle*, [2307.13745](#).
- [72] I. Basile, A. Debray, M. Delgado and M. Montero, *Global anomalies & bordism of non-supersymmetric strings*, *JHEP* **02** (2024) 092 [[2310.06895](#)].
- [73] D. Rickles, *A brief history of string theory: From dual models to M-theory*, The frontiers collection, Springer, Heidelberg, Germany (2014), 10.1007/978-3-642-45128-7.
- [74] G. Veneziano, *Construction of a crossing-symmetric, Regge behaved amplitude for linearly rising trajectories*, *Nuovo Cim. A* **57** (1968) 190.
- [75] A. Neveu and J. Scherk, *Connection between Yang-Mills fields and dual models*, *Nucl. Phys. B* **36** (1972) 155.
- [76] J. Scherk and J.H. Schwarz, *Dual Models for Nonhadrons*, *Nucl. Phys. B* **81** (1974) 118.
- [77] M.B. Green and J.H. Schwarz, *Anomaly Cancellation in Supersymmetric D=10 Gauge Theory and Superstring Theory*, *Phys. Lett. B* **149** (1984) 117.
- [78] D.J. Gross, J.A. Harvey, E.J. Martinec and R. Rohm, *Heterotic String Theory. 1. The Free Heterotic String*, *Nucl. Phys. B* **256** (1985) 253.
- [79] D.J. Gross, J.A. Harvey, E.J. Martinec and R. Rohm, *Heterotic String Theory. 2. The Interacting Heterotic String*, *Nucl. Phys. B* **267** (1986) 75.
- [80] P. Candelas, G.T. Horowitz, A. Strominger and E. Witten, *Vacuum configurations for superstrings*, *Nucl. Phys. B* **258** (1985) 46.
- [81] K. Kikkawa and M. Yamasaki, *Casimir Effects in Superstring Theories*, *Phys. Lett. B* **149** (1984) 357.
- [82] A. Font, L.E. Ibanez, D. Lust and F. Quevedo, *Strong-weak coupling duality and nonperturbative effects in string theory*, *Phys. Lett. B* **249** (1990) 35.
- [83] W. Lerche, C. Vafa and N.P. Warner, *Chiral Rings in N=2 Superconformal Theories*, *Nucl. Phys. B* **324** (1989) 427.
- [84] B.R. Greene and M.R. Plesser, *Duality in Calabi-Yau Moduli Space*, *Nucl. Phys. B* **338** (1990) 15.
- [85] P. Candelas, M. Lynker and R. Schimmrigk, *Calabi-Yau Manifolds in Weighted \mathbb{P}_4* , *Nucl. Phys. B* **341** (1990) 383.
- [86] P. Candelas, X.C. De La Ossa, P.S. Green and L. Parkes, *A Pair of Calabi-Yau manifolds as an exactly soluble superconformal theory*, *Nucl. Phys. B* **359** (1991) 21.
- [87] J. Polchinski, *Dirichlet Branes and Ramond-Ramond charges*, *Phys. Rev. Lett.* **75** (1995) 4724 [[hep-th/9510017](#)].

- [88] E. Witten, *String theory dynamics in various dimensions*, *Nucl. Phys. B* **443** (1995) 85 [[hep-th/9503124](#)].
- [89] C. Vafa, *Evidence for F theory*, *Nucl. Phys. B* **469** (1996) 403 [[hep-th/9602022](#)].
- [90] J.M. Maldacena, *The Large N limit of superconformal field theories and supergravity*, *Adv. Theor. Math. Phys.* **2** (1998) 231 [[hep-th/9711200](#)].
- [91] J. Polchinski and A. Strominger, *New vacua for type II string theory*, *Phys. Lett. B* **388** (1996) 736 [[hep-th/9510227](#)].
- [92] J. Michelson, *Compactifications of type IIB strings to four-dimensions with nontrivial classical potential*, *Nucl. Phys. B* **495** (1997) 127 [[hep-th/9610151](#)].
- [93] T.R. Taylor and C. Vafa, *R R flux on Calabi-Yau and partial supersymmetry breaking*, *Phys. Lett. B* **474** (2000) 130 [[hep-th/9912152](#)].
- [94] M.R. Douglas, *The Statistics of string/M theory vacua*, *JHEP* **05** (2003) 046 [[hep-th/0303194](#)].
- [95] S. Kachru, R. Kallosh, A.D. Linde and S.P. Trivedi, *De Sitter vacua in string theory*, *Phys. Rev. D* **68** (2003) 046005 [[hep-th/0301240](#)].
- [96] V. Balasubramanian, P. Berglund, J.P. Conlon and F. Quevedo, *Systematics of moduli stabilisation in Calabi-Yau flux compactifications*, *JHEP* **03** (2005) 007 [[hep-th/0502058](#)].
- [97] J.P. Conlon, F. Quevedo and K. Suruliz, *Large-volume flux compactifications: Moduli spectrum and D3/D7 soft supersymmetry breaking*, *JHEP* **08** (2005) 007 [[hep-th/0505076](#)].
- [98] C. Beasley, J.J. Heckman and C. Vafa, *GUTs and Exceptional Branes in F-theory - I*, *JHEP* **01** (2009) 058 [[0802.3391](#)].
- [99] C. Beasley, J.J. Heckman and C. Vafa, *GUTs and Exceptional Branes in F-theory - II: Experimental Predictions*, *JHEP* **01** (2009) 059 [[0806.0102](#)].
- [100] R. Donagi and M. Wijnholt, *Breaking GUT Groups in F-Theory*, *Adv. Theor. Math. Phys.* **15** (2011) 1523 [[0808.2223](#)].
- [101] R. Donagi and M. Wijnholt, *Model Building with F-Theory*, *Adv. Theor. Math. Phys.* **15** (2011) 1237 [[0802.2969](#)].
- [102] C. Vafa, *The String landscape and the swampland*, [hep-th/0509212](#).
- [103] E. Bergshoeff, E. Sezgin and P.K. Townsend, *Supermembranes and Eleven-Dimensional Supergravity*, *Phys. Lett. B* **189** (1987) 75.
- [104] M.J. Duff and K.S. Stelle, *Multimembrane solutions of D = 11 supergravity*, *Phys. Lett. B* **253** (1991) 113.
- [105] M.J. Duff, P.S. Howe, T. Inami and K.S. Stelle, *Superstrings in D=10 from Supermembranes in D=11*, *Phys. Lett. B* **191** (1987) 70.

- [106] C.M. Hull and P.K. Townsend, *Unity of superstring dualities*, *Nucl. Phys. B* **438** (1995) 109 [[hep-th/9410167](#)].
- [107] P.K. Townsend, *The eleven-dimensional supermembrane revisited*, *Phys. Lett. B* **350** (1995) 184 [[hep-th/9501068](#)].
- [108] R. Blumenhagen, M. Cvetic, P. Langacker and G. Shiu, *Toward realistic intersecting D-brane models*, *Ann. Rev. Nucl. Part. Sci.* **55** (2005) 71 [[hep-th/0502005](#)].
- [109] M. Graña, *Flux compactifications in string theory: A Comprehensive review*, *Phys. Rept.* **423** (2006) 91 [[hep-th/0509003](#)].
- [110] R. Blumenhagen, B. Kors, D. Lust and S. Stieberger, *Four-dimensional String Compactifications with D-Branes, Orientifolds and Fluxes*, *Phys. Rept.* **445** (2007) 1 [[hep-th/0610327](#)].
- [111] M. Ammon and J. Erdmenger, *Gauge/gravity duality: Foundations and applications*, Cambridge University Press, Cambridge (4, 2015), 10.1017/CBO9780511846373.
- [112] E. Plauschinn, *Non-geometric backgrounds in string theory*, *Phys. Rept.* **798** (2019) 1 [[1811.11203](#)].
- [113] S. Hellerman and I. Swanson, *Charting the landscape of supercritical string theory*, *Phys. Rev. Lett.* **99** (2007) 171601 [[0705.0980](#)].
- [114] N. Marcus, *A Tour through $N=2$ strings*, in *International Workshop on String Theory, Quantum Gravity and the Unification of Fundamental Interactions*, 11, 1992 [[hep-th/9211059](#)].
- [115] H. Erbin, *String Field Theory: A Modern Introduction*, vol. 980 of *Lecture Notes in Physics*, Springer Nature Switzerland AG (2021), 10.1007/978-3-030-65321-7.
- [116] T. Banks, W. Fischler, S.H. Shenker and L. Susskind, *M theory as a matrix model: A Conjecture*, *Phys. Rev. D* **55** (1997) 5112 [[hep-th/9610043](#)].
- [117] L. Susskind, *Another conjecture about M (atrix) theory*, [hep-th/9704080](#).
- [118] W. Taylor, *M (atrix) Theory: Matrix Quantum Mechanics as a Fundamental Theory*, *Rev. Mod. Phys.* **73** (2001) 419 [[hep-th/0101126](#)].
- [119] R. Dijkgraaf, E.P. Verlinde and H.L. Verlinde, *Matrix string theory*, *Nucl. Phys. B* **500** (1997) 43 [[hep-th/9703030](#)].
- [120] E.J. Martinec, *Matrix models and 2D string theory*, in *NATO Advanced Study Institute: Marie Curie Training Course: Applications of Random Matrices in Physics*, pp. 403–457, 10, 2004 [[hep-th/0410136](#)].
- [121] M.J. Dolan, S. Krippendorf and F. Quevedo, *Towards a Systematic Construction of Realistic D-brane Models on a del Pezzo Singularity*, *JHEP* **10** (2011) 024 [[1106.6039](#)].
- [122] P. Candelas, A.M. Dale, C.A. Lutken and R. Schimmrigk, *Complete Intersection Calabi-Yau Manifolds*, *Nucl. Phys. B* **298** (1988) 493.

- [123] M. Kreuzer and H. Skarke, *Reflexive polyhedra, weights and toric Calabi-Yau fibrations*, *Rev. Math. Phys.* **14** (2002) 343 [[math/0001106](#)].
- [124] M. Kreuzer and H. Skarke, *Complete classification of reflexive polyhedra in four-dimensions*, *Adv. Theor. Math. Phys.* **4** (2000) 1209 [[hep-th/0002240](#)].
- [125] S.B. Giddings, S. Kachru and J. Polchinski, *Hierarchies from fluxes in string compactifications*, *Phys. Rev. D* **66** (2002) 106006 [[hep-th/0105097](#)].
- [126] S. Ashok and M.R. Douglas, *Counting flux vacua*, *JHEP* **01** (2004) 060 [[hep-th/0307049](#)].
- [127] J. Halverson, C. Long and B. Sung, *Algorithmic universality in F-theory compactifications*, *Phys. Rev. D* **96** (2017) 126006 [[1706.02299](#)].
- [128] W. Taylor and Y.-N. Wang, *The F-theory geometry with most flux vacua*, *JHEP* **12** (2015) 164 [[1511.03209](#)].
- [129] F. Ruehle, *Data science applications to string theory*, *Phys. Rept.* **839** (2020) 1.
- [130] R.H. Brandenberger and C. Vafa, *Superstrings in the Early Universe*, *Nucl. Phys. B* **316** (1989) 391.
- [131] A.D. Linde, *Eternally Existing Selfreproducing Chaotic Inflationary Universe*, *Phys. Lett. B* **175** (1986) 395.
- [132] D. Baumann and L. McAllister, *Inflation and String Theory*, Cambridge Monographs on Mathematical Physics, Cambridge University Press (5, 2015), 10.1017/CBO9781316105733, [[1404.2601](#)].
- [133] U.H. Danielsson and T. Van Riet, *What if string theory has no de Sitter vacua?*, *Int. J. Mod. Phys. D* **27** (2018) 1830007 [[1804.01120](#)].
- [134] G. Obied, H. Ooguri, L. Spodyneiko and C. Vafa, *De Sitter Space and the Swampland*, [1806.08362](#).
- [135] H. Ooguri, E. Palti, G. Shiu and C. Vafa, *Distance and de Sitter Conjectures on the Swampland*, *Phys. Lett. B* **788** (2019) 180 [[1810.05506](#)].
- [136] A. Bedroya and C. Vafa, *Trans-Planckian Censorship and the Swampland*, *JHEP* **09** (2020) 123 [[1909.11063](#)].
- [137] T.D. Brennan, F. Carta and C. Vafa, *The String Landscape, the Swampland, and the Missing Corner*, *PoS TASI2017* (2017) 015 [[1711.00864](#)].
- [138] E. Palti, *The Swampland: Introduction and Review*, *Fortsch. Phys.* **67** (2019) 1900037 [[1903.06239](#)].
- [139] M. van Beest, J. Calderón-Infante, D. Mirfendereski and I. Valenzuela, *Lectures on the Swampland Program in String Compactifications*, *Phys. Rept.* **989** (2022) 1 [[2102.01111](#)].
- [140] M. Graña and A. Herráez, *The Swampland Conjectures: A Bridge from Quantum Gravity to Particle Physics*, *Universe* **7** (2021) 273 [[2107.00087](#)].

- [141] N.B. Agmon, A. Bedroya, M.J. Kang and C. Vafa, *Lectures on the string landscape and the Swampland*, 2212.06187.
- [142] A. Adams, O. DeWolfe and W. Taylor, *String universality in ten dimensions*, *Phys. Rev. Lett.* **105** (2010) 071601 [1006.1352].
- [143] H.-C. Kim, G. Shiu and C. Vafa, *Branes and the Swampland*, *Phys. Rev. D* **100** (2019) 066006 [1905.08261].
- [144] M. Montero and C. Vafa, *Cobordism Conjecture, Anomalies, and the String Lamppost Principle*, *JHEP* **01** (2021) 063 [2008.11729].
- [145] N. Arkani-Hamed, L. Motl, A. Nicolis and C. Vafa, *The String landscape, black holes and gravity as the weakest force*, *JHEP* **06** (2007) 060 [hep-th/0601001].
- [146] H. Ooguri and C. Vafa, *On the Geometry of the String Landscape and the Swampland*, *Nucl. Phys. B* **766** (2007) 21 [hep-th/0605264].
- [147] T. Banks and L.J. Dixon, *Constraints on String Vacua with Space-Time Supersymmetry*, *Nucl. Phys. B* **307** (1988) 93.
- [148] T. Banks and N. Seiberg, *Symmetries and Strings in Field Theory and Gravity*, *Phys. Rev. D* **83** (2011) 084019 [1011.5120].
- [149] S.-J. Lee, W. Lerche and T. Weigand, *Emergent strings from infinite distance limits*, *JHEP* **02** (2022) 190 [1910.01135].
- [150] BICEP2 collaboration, *Detection of B-Mode Polarization at Degree Angular Scales by BICEP2*, *Phys. Rev. Lett.* **112** (2014) 241101 [1403.3985].
- [151] D.H. Lyth, *What would we learn by detecting a gravitational wave signal in the cosmic microwave background anisotropy?*, *Phys. Rev. Lett.* **78** (1997) 1861 [hep-ph/9606387].
- [152] BICEP2, PLANCK collaboration, *Joint Analysis of BICEP2/KeckArray and Planck Data*, *Phys. Rev. Lett.* **114** (2015) 101301 [1502.00612].
- [153] D. Klaewer, S.-J. Lee, T. Weigand and M. Wiesner, *Quantum corrections in 4d $N = 1$ infinite distance limits and the weak gravity conjecture*, *JHEP* **03** (2021) 252 [2011.00024].
- [154] F. Marchesano and M. Wiesner, *Instantons and infinite distances*, *JHEP* **08** (2019) 088 [1904.04848].
- [155] F. Baume, F. Marchesano and M. Wiesner, *Instanton Corrections and Emergent Strings*, *JHEP* **04** (2020) 174 [1912.02218].
- [156] S.-J. Lee and T. Weigand, *Elliptic K3 surfaces at infinite complex structure and their refined Kulikov models*, *JHEP* **09** (2022) 143 [2112.07682].
- [157] S.-J. Lee, W. Lerche and T. Weigand, *Physics of infinite complex structure limits in eight dimensions*, *JHEP* **06** (2022) 042 [2112.08385].
- [158] T. Kaluza, *Zum Unitätsproblem der Physik*, *Sitzungsber. Preuss. Akad. Wiss. Berlin (Math. Phys.)* **1921** (1921) 966 [1803.08616].

- [159] O. Klein, *Quantum Theory and Five-Dimensional Theory of Relativity. (In German and English)*, *Z. Phys.* **37** (1926) 895.
- [160] M.R. Douglas and S. Kachru, *Flux compactification*, *Rev. Mod. Phys.* **79** (2007) 733 [[hep-th/0610102](#)].
- [161] T. Hubsch, *Calabi-Yau manifolds: A Bestiary for physicists*, World Scientific, Singapore (1994).
- [162] S. Kachru, A. Tripathy and M. Zimet, *K3 metrics from little string theory*, [1810.10540](#).
- [163] S. Kachru, A. Tripathy and M. Zimet, *K3 metrics*, [2006.02435](#).
- [164] L.B. Anderson, J. Gray and M. Larfors, *Lectures on Numerical and Machine Learning Methods for Approximating Ricci-flat Calabi-Yau Metrics*, [2312.17125](#).
- [165] B. Andreas and D. Hernandez Ruiperez, *Fourier Mukai transforms and applications to string theory*, [math/0412328](#).
- [166] R. Blumenhagen and E. Plauschinn, *Introduction to conformal field theory: with applications to String theory*, vol. 779, Springer, Berlin, Germany (2009), [10.1007/978-3-642-00450-6](#).
- [167] K. Hori, S. Katz, A. Klemm, R. Pandharipande, R. Thomas, C. Vafa et al., *Mirror symmetry*, vol. 1 of *Clay mathematics monographs*, AMS, Providence, USA (2003).
- [168] S. Alexandrov, *Twistor Approach to String Compactifications: a Review*, *Phys. Rept.* **522** (2013) 1 [[1111.2892](#)].
- [169] S. Alexandrov, J. Manschot, D. Persson and B. Pioline, *Quantum hypermultiplet moduli spaces in $N=2$ string vacua: a review*, *Proc. Symp. Pure Math.* **90** (2015) 181 [[1304.0766](#)].
- [170] D. Robles-Llana, F. Saueressig, U. Theis and S. Vandoren, *Membrane instantons from mirror symmetry*, *Commun. Num. Theor. Phys.* **1** (2007) 681 [[0707.0838](#)].
- [171] A. Strominger, S.-T. Yau and E. Zaslow, *Mirror symmetry is T duality*, *Nucl. Phys. B* **479** (1996) 243 [[hep-th/9606040](#)].
- [172] P.S. Aspinwall, T. Bridgeland, A. Craw, M.R. Douglas, A. Kapustin, G.W. Moore et al., *Dirichlet branes and mirror symmetry*, vol. 4 of *Clay Mathematics Monographs*, AMS, Providence, RI (2009).
- [173] M. Gross, *Mirror symmetry and the strominger-yau-zaslow conjecture*, *arXiv preprint arXiv:1212.4220* (2012) .
- [174] T. Pantev and E. Sharpe, *Duality group actions on fermions*, *JHEP* **11** (2016) 171 [[1609.00011](#)].
- [175] Y. Tachikawa and K. Yonekura, *Why are fractional charges of orientifolds compatible with Dirac quantization?*, *SciPost Phys.* **7** (2019) 058 [[1805.02772](#)].
- [176] M. Dierigl, J.J. Heckman, M. Montero and E. Torres, *IIB string theory explored: Reflection 7-branes*, *Phys. Rev. D* **107** (2023) 086015 [[2212.05077](#)].

- [177] A. Debray, M. Dierigl, J.J. Heckman and M. Montero, *The Chronicles of IIBordia: Dualities, Bordisms, and the Swampland*, 2302.00007.
- [178] M. Dierigl, J.J. Heckman, M. Montero and E. Torres, *R7-branes as charge conjugation operators*, *Phys. Rev. D* **109** (2024) 046004 [2305.05689].
- [179] E. Bergshoeff, J. Hartong, T. Ortin and D. Roest, *IIB seven-branes revisited*, *J. Phys. Conf. Ser.* **66** (2007) 012054.
- [180] S. Cecotti, *Introduction to String Theory*, vol. 9783031365300, Springer (10, 2023), 10.1007/978-3-031-36530-0.
- [181] D.R. Morrison, *TASI lectures on compactification and duality*, in *Theoretical Advanced Study Institute in Elementary Particle Physics (TASI 99): Strings, Branes, and Gravity*, pp. 653–719, 1999 [[hep-th/0411120](#)].
- [182] F. Denef, *Lectures on constructing string vacua*, *Les Houches* **87** (2008) 483 [[0803.1194](#)].
- [183] T. Weigand, *Lectures on F-theory compactifications and model building*, *Class. Quant. Grav.* **27** (2010) 214004 [[1009.3497](#)].
- [184] R. Blumenhagen, *Basics of F-theory from the Type IIB Perspective*, *Fortsch. Phys.* **58** (2010) 820 [[1002.2836](#)].
- [185] T. Weigand, *F-theory*, *PoS TASI2017* (2018) 016 [[1806.01854](#)].
- [186] D.R. Morrison and C. Vafa, *Compactifications of F theory on Calabi-Yau threefolds. 1.*, *Nucl. Phys. B* **473** (1996) 74 [[hep-th/9602114](#)].
- [187] D.R. Morrison and C. Vafa, *Compactifications of F theory on Calabi-Yau threefolds. 2.*, *Nucl. Phys. B* **476** (1996) 437 [[hep-th/9603161](#)].
- [188] V. Braun and D.R. Morrison, *F-theory on Genus-One Fibrations*, *JHEP* **08** (2014) 132 [[1401.7844](#)].
- [189] J. Tate, *Algorithm for determining the type of a singular fiber in an elliptic pencil*, in *Modular Functions of One Variable IV*, B.J. Birch and W. Kuyk, eds., (Berlin, Heidelberg), pp. 33–52, Springer Berlin Heidelberg, 1975.
- [190] M. Bershadsky, K.A. Intriligator, S. Kachru, D.R. Morrison, V. Sadov and C. Vafa, *Geometric singularities and enhanced gauge symmetries*, *Nucl. Phys. B* **481** (1996) 215 [[hep-th/9605200](#)].
- [191] S. Katz, D.R. Morrison, S. Schafer-Nameki and J. Sully, *Tate's algorithm and F-theory*, *JHEP* **08** (2011) 094 [[1106.3854](#)].
- [192] A. Grassi and D.R. Morrison, *Anomalies and the Euler characteristic of elliptic Calabi-Yau threefolds*, *Commun. Num. Theor. Phys.* **6** (2012) 51 [[1109.0042](#)].
- [193] P. Griffiths and J. Harris, *Principles of Algebraic Geometry*, Wiley Classics Library, Wiley (2014).

- [194] T. Shioda, *On elliptic modular surfaces*, *Journal of The Mathematical Society of Japan* **24** (1972) 20.
- [195] J. Tate, *Algebraic cycles and poles of zeta functions*, *Arithmetic algebraic geometry* (1965) 93.
- [196] J. Tate, *On the conjectures of Birch and Swinnerton-Dyer and a geometric analog*, in *Séminaire Bourbaki : Années 1964/65-1965/66, Exposés 277-312*, no. 9 in Séminaire Bourbaki, pp. 415–440, Société Mathématique de France (1966).
- [197] R. Wazir, *Arithmetic on elliptic threefolds*, *Compositio Mathematica* **140** (2004) 567.
- [198] P.S. Aspinwall, S.H. Katz and D.R. Morrison, *Lie groups, Calabi-Yau threefolds, and F theory*, *Adv. Theor. Math. Phys.* **4** (2000) 95 [[hep-th/0002012](#)].
- [199] P.S. Aspinwall and D.R. Morrison, *Nonsimply connected gauge groups and rational points on elliptic curves*, *JHEP* **07** (1998) 012 [[hep-th/9805206](#)].
- [200] T.W. Grimm and T. Weigand, *On Abelian Gauge Symmetries and Proton Decay in Global F-theory GUTs*, *Phys. Rev. D* **82** (2010) 086009 [[1006.0226](#)].
- [201] C. Mayrhofer, D.R. Morrison, O. Till and T. Weigand, *Mordell-Weil Torsion and the Global Structure of Gauge Groups in F-theory*, *JHEP* **10** (2014) 016 [[1405.3656](#)].
- [202] A. Sen, *F theory and orientifolds*, *Nucl. Phys. B* **475** (1996) 562 [[hep-th/9605150](#)].
- [203] A. Sen, *Orientifold limit of F theory vacua*, *Phys. Rev. D* **55** (1997) R7345 [[hep-th/9702165](#)].
- [204] S.H. Katz and C. Vafa, *Matter from geometry*, *Nucl. Phys. B* **497** (1997) 146 [[hep-th/9606086](#)].
- [205] A. Grassi and D.R. Morrison, *Group representations and the Euler characteristic of elliptically fibered Calabi-Yau threefolds*, [math/0005196](#).
- [206] A. Grassi and T. Weigand, *On topological invariants of algebraic threefolds with (\mathbb{Q} -factorial) singularities*, [1804.02424](#).
- [207] P. Arras, A. Grassi and T. Weigand, *Terminal Singularities, Milnor Numbers, and Matter in F-theory*, *J. Geom. Phys.* **123** (2018) 71 [[1612.05646](#)].
- [208] M. Cvetič and L. Lin, *TASI Lectures on Abelian and Discrete Symmetries in F-theory*, *PoS TASI2017* (2018) 020 [[1809.00012](#)].
- [209] M. Montero, G. Shiu and P. Soler, *The Weak Gravity Conjecture in three dimensions*, *JHEP* **10** (2016) 159 [[1606.08438](#)].
- [210] D. Gaiotto, A. Kapustin, N. Seiberg and B. Willett, *Generalized Global Symmetries*, *JHEP* **02** (2015) 172 [[1412.5148](#)].
- [211] B. Heidenreich, J. McNamara, M. Montero, M. Reece, T. Rudelius and I. Valenzuela, *Chern-Weil global symmetries and how quantum gravity avoids them*, *JHEP* **11** (2021) 053 [[2012.00009](#)].

- [212] B. Heidenreich, J. McNamara, M. Montero, M. Reece, T. Rudelius and I. Valenzuela, *Non-invertible global symmetries and completeness of the spectrum*, *JHEP* **09** (2021) 203 [2104.07036].
- [213] L. Susskind, *Trouble for remnants*, [hep-th/9501106](#).
- [214] D. Harlow and H. Ooguri, *Symmetries in quantum field theory and quantum gravity*, *Commun. Math. Phys.* **383** (2021) 1669 [1810.05338].
- [215] D. Harlow and H. Ooguri, *Constraints on Symmetries from Holography*, *Phys. Rev. Lett.* **122** (2019) 191601 [1810.05337].
- [216] J. McNamara and C. Vafa, *Cobordism Classes and the Swampland*, [1909.10355](#).
- [217] E. Palti, *A Brief Introduction to the Weak Gravity Conjecture*, *LHEP* **2020** (2020) 176.
- [218] D. Harlow, B. Heidenreich, M. Reece and T. Rudelius, *Weak gravity conjecture*, *Rev. Mod. Phys.* **95** (2023) 035003 [2201.08380].
- [219] B. Heidenreich, M. Reece and T. Rudelius, *Sharpening the Weak Gravity Conjecture with Dimensional Reduction*, *JHEP* **02** (2016) 140 [1509.06374].
- [220] B. Heidenreich, M. Reece and T. Rudelius, *Evidence for a sublattice weak gravity conjecture*, *JHEP* **08** (2017) 025 [1606.08437].
- [221] B. Heidenreich, M. Reece and T. Rudelius, *Repulsive Forces and the Weak Gravity Conjecture*, *JHEP* **10** (2019) 055 [1906.02206].
- [222] S. Andriolo, D. Junghans, T. Noumi and G. Shiu, *A Tower Weak Gravity Conjecture from Infrared Consistency*, *Fortsch. Phys.* **66** (2018) 1800020 [1802.04287].
- [223] C.F. Cota, A. Mininno, T. Weigand and M. Wiesner, *The asymptotic Weak Gravity Conjecture for open strings*, *JHEP* **11** (2022) 058 [2208.00009].
- [224] C.F. Cota, A. Mininno, T. Weigand and M. Wiesner, *The asymptotic weak gravity conjecture in M-theory*, *JHEP* **08** (2023) 057 [2212.09758].
- [225] C.F. Cota, A. Mininno, T. Weigand and M. Wiesner, *The Minimal Weak Gravity Conjecture*, [2312.04619](#).
- [226] T. Rudelius, *Constraints on Axion Inflation from the Weak Gravity Conjecture*, *JCAP* **09** (2015) 020 [1503.00795].
- [227] M. Montero, A.M. Uranga and I. Valenzuela, *Transplanckian axions!?*, *JHEP* **08** (2015) 032 [1503.03886].
- [228] J. Brown, W. Cottrell, G. Shiu and P. Soler, *Fencing in the Swampland: Quantum Gravity Constraints on Large Field Inflation*, *JHEP* **10** (2015) 023 [1503.04783].
- [229] A. Hebecker, P. Mangat, F. Rompineve and L.T. Witkowski, *Winding out of the Swamp: Evading the Weak Gravity Conjecture with F-term Winding Inflation?*, *Phys. Lett. B* **748** (2015) 455 [1503.07912].

- [230] T. Crisford and J.E. Santos, *Violating the Weak Cosmic Censorship Conjecture in Four-Dimensional Anti-de Sitter Space*, *Phys. Rev. Lett.* **118** (2017) 181101 [[1702.05490](#)].
- [231] P. Saraswat, *Weak gravity conjecture and effective field theory*, *Phys. Rev. D* **95** (2017) 025013 [[1608.06951](#)].
- [232] L.E. Ibanez and M. Montero, *A Note on the WGC, Effective Field Theory and Clockwork within String Theory*, *JHEP* **02** (2018) 057 [[1709.02392](#)].
- [233] G. Dvali, *Black Holes and Large N Species Solution to the Hierarchy Problem*, *Fortsch. Phys.* **58** (2010) 528 [[0706.2050](#)].
- [234] G. Dvali and D. Lust, *Evaporation of Microscopic Black Holes in String Theory and the Bound on Species*, *Fortsch. Phys.* **58** (2010) 505 [[0912.3167](#)].
- [235] G. Dvali and C. Gomez, *Species and Strings*, [1004.3744](#).
- [236] G. Dvali, C. Gomez and D. Lust, *Black Hole Quantum Mechanics in the Presence of Species*, *Fortsch. Phys.* **61** (2013) 768 [[1206.2365](#)].
- [237] D. van de Heisteeg, C. Vafa and M. Wiesner, *Bounds on Species Scale and the Distance Conjecture*, [2303.13580](#).
- [238] D. van de Heisteeg, C. Vafa, M. Wiesner and D.H. Wu, *Species Scale in Diverse Dimensions*, [2310.07213](#).
- [239] N. Cribiori, D. Lüst and G. Staudt, *Black hole entropy and moduli-dependent species scale*, *Phys. Lett. B* **844** (2023) 138113 [[2212.10286](#)].
- [240] N. Cribiori, D. Lust and C. Montella, *Species entropy and thermodynamics*, *JHEP* **10** (2023) 059 [[2305.10489](#)].
- [241] N. Cribiori and D. Lüst, *A Note on Modular Invariant Species Scale and Potentials*, *Fortsch. Phys.* **71** (2023) 2300150 [[2306.08673](#)].
- [242] I. Basile, N. Cribiori, D. Lust and C. Montella, *Minimal Black Holes and Species Thermodynamics*, [2401.06851](#).
- [243] F. Baume and E. Palti, *Backreacted Axion Field Ranges in String Theory*, *JHEP* **08** (2016) 043 [[1602.06517](#)].
- [244] D. Klaewer and E. Palti, *Super-Planckian Spatial Field Variations and Quantum Gravity*, *JHEP* **01** (2017) 088 [[1610.00010](#)].
- [245] R. Blumenhagen, D. Kläwer, L. Schlechter and F. Wolf, *The Refined Swampland Distance Conjecture in Calabi-Yau Moduli Spaces*, *JHEP* **06** (2018) 052 [[1803.04989](#)].
- [246] A. Joshi and A. Klemm, *Swampland Distance Conjecture for One-Parameter Calabi-Yau Threefolds*, *JHEP* **08** (2019) 086 [[1903.00596](#)].
- [247] D. Erkinger and J. Knapp, *Refined swampland distance conjecture and exotic hybrid Calabi-Yaus*, *JHEP* **07** (2019) 029 [[1905.05225](#)].

- [248] D. Kläwer, *Modular curves and the refined distance conjecture*, *JHEP* **12** (2021) 088 [[2108.00021](#)].
- [249] J. Calderón-Infante, A.M. Uranga and I. Valenzuela, *The Convex Hull Swampland Distance Conjecture and Bounds on Non-geodesics*, *JHEP* **03** (2021) 299 [[2012.00034](#)].
- [250] S. Hosono, A. Klemm, S. Theisen and S.-T. Yau, *Mirror symmetry, mirror map and applications to Calabi-Yau hypersurfaces*, *Commun. Math. Phys.* **167** (1995) 301 [[hep-th/9308122](#)].
- [251] S. Hosono, A. Klemm, S. Theisen and S.-T. Yau, *Mirror symmetry, mirror map and applications to complete intersection Calabi-Yau spaces*, *Nucl. Phys. B* **433** (1995) 501 [[hep-th/9406055](#)].
- [252] T.W. Grimm, E. Palti and I. Valenzuela, *Infinite Distances in Field Space and Massless Towers of States*, *JHEP* **08** (2018) 143 [[1802.08264](#)].
- [253] T.W. Grimm, C. Li and E. Palti, *Infinite Distance Networks in Field Space and Charge Orbits*, *JHEP* **03** (2019) 016 [[1811.02571](#)].
- [254] T.W. Grimm, C. Li and I. Valenzuela, *Asymptotic Flux Compactifications and the Swampland*, *JHEP* **06** (2020) 009 [[1910.09549](#)].
- [255] M. Etheredge, B. Heidenreich, S. Kaya, Y. Qiu and T. Rudelius, *Sharpening the Distance Conjecture in diverse dimensions*, *JHEP* **12** (2022) 114 [[2206.04063](#)].
- [256] N. Gendler and I. Valenzuela, *Merging the weak gravity and distance conjectures using BPS extremal black holes*, *JHEP* **01** (2021) 176 [[2004.10768](#)].
- [257] D. Lüst, E. Palti and C. Vafa, *AdS and the Swampland*, *Phys. Lett. B* **797** (2019) 134867 [[1906.05225](#)].
- [258] O. DeWolfe, A. Giryavets, S. Kachru and W. Taylor, *Type IIA moduli stabilization*, *JHEP* **07** (2005) 066 [[hep-th/0505160](#)].
- [259] J. McOrist and S. Sethi, *M-theory and Type IIA Flux Compactifications*, *JHEP* **12** (2012) 122 [[1208.0261](#)].
- [260] D. Junghans, *O-Plane Backreaction and Scale Separation in Type IIA Flux Vacua*, *Fortsch. Phys.* **68** (2020) 2000040 [[2003.06274](#)].
- [261] F. Marchesano, E. Palti, J. Quirant and A. Tomasiello, *On supersymmetric AdS_4 orientifold vacua*, *JHEP* **08** (2020) 087 [[2003.13578](#)].
- [262] N. Cribiori, D. Junghans, V. Van Hemelryck, T. Van Riet and T. Wräse, *Scale-separated AdS_4 vacua of IIA orientifolds and M-theory*, *Phys. Rev. D* **104** (2021) 126014 [[2107.00019](#)].
- [263] F. Apers, M. Montero, T. Van Riet and T. Wräse, *Comments on classical AdS flux vacua with scale separation*, *JHEP* **05** (2022) 167 [[2202.00682](#)].
- [264] F. Baume and J. Calderón Infante, *Tackling the SDC in AdS with CFTs*, *JHEP* **08** (2021) 057 [[2011.03583](#)].

- [265] E. Perlmutter, L. Rastelli, C. Vafa and I. Valenzuela, *A CFT distance conjecture*, *JHEP* **10** (2021) 070 [[2011.10040](#)].
- [266] F. Baume and J. Calderón-Infante, *On higher-spin points and infinite distances in conformal manifolds*, *JHEP* **12** (2023) 163 [[2305.05693](#)].
- [267] M. Reece, *Photon Masses in the Landscape and the Swampland*, *JHEP* **07** (2019) 181 [[1808.09966](#)].
- [268] R. Blumenhagen, *Large Field Inflation/Quintessence and the Refined Swampland Distance Conjecture*, *PoS CORFU2017* (2018) 175 [[1804.10504](#)].
- [269] M. Scalisi and I. Valenzuela, *Swampland distance conjecture, inflation and α -attractors*, *JHEP* **08** (2019) 160 [[1812.07558](#)].
- [270] J.J. Heckman and T. Rudelius, *Top Down Approach to 6D SCFTs*, *J. Phys. A* **52** (2019) 093001 [[1805.06467](#)].
- [271] S.-J. Lee, W. Lerche and T. Weigand, *Tensionless Strings and the Weak Gravity Conjecture*, *JHEP* **10** (2018) 164 [[1808.05958](#)].
- [272] S.-J. Lee, W. Lerche and T. Weigand, *Emergent strings, duality and weak coupling limits for two-form fields*, *JHEP* **02** (2022) 096 [[1904.06344](#)].
- [273] T. Rudelius, *Gopakumar-Vafa Invariants and the Emergent String Conjecture*, [2309.10024](#).
- [274] F. Xu, *On TCS G_2 manifolds and 4D emergent strings*, *JHEP* **10** (2020) 045 [[2006.02350](#)].
- [275] S.-J. Lee, W. Lerche and T. Weigand, *Modular Fluxes, Elliptic Genera, and Weak Gravity Conjectures in Four Dimensions*, *JHEP* **08** (2019) 104 [[1901.08065](#)].
- [276] V. Collazuol, M. Graña, A. Herráez and H. Parra De Freitas, *Affine algebras at infinite distance limits in the Heterotic String*, *JHEP* **07** (2023) 036 [[2210.13471](#)].
- [277] V. Collazuol and I.V. Melnikov, *A twist at infinite distance in the CHL string*, [2402.01606](#).
- [278] I. Basile, *Emergent Strings at an Infinite Distance with Broken Supersymmetry*, *Astronomy* **2** (2023) 206 [[2201.08851](#)].
- [279] T. Rudelius, *Revisiting the refined Distance Conjecture*, *JHEP* **09** (2023) 130 [[2303.12103](#)].
- [280] M. Etheredge, B. Heidenreich, J. McNamara, T. Rudelius, I. Ruiz and I. Valenzuela, *Running Decompactification, Sliding Towers, and the Distance Conjecture*, [2306.16440](#).
- [281] B. Heidenreich, M. Reece and T. Rudelius, *Weak Gravity Strongly Constrains Large-Field Axion Inflation*, *JHEP* **12** (2015) 108 [[1506.03447](#)].
- [282] S. Cremonini, C.R.T. Jones, J.T. Liu, B. McPeak and Y. Tang, *NUT charge weak gravity conjecture from dimensional reduction*, *Phys. Rev. D* **103** (2021) 106011 [[2011.06083](#)].

- [283] T. Rudelius, *Dimensional reduction and (Anti) de Sitter bounds*, *JHEP* **08** (2021) 041 [[2101.11617](#)].
- [284] A.C. Cadavid, A. Ceresole, R. D'Auria and S. Ferrara, *Eleven-dimensional supergravity compactified on Calabi-Yau threefolds*, *Phys. Lett. B* **357** (1995) 76 [[hep-th/9506144](#)].
- [285] N. Lambert, *M-Branes: Lessons from M2's and Hopes for M5's*, *Fortsch. Phys.* **67** (2019) 1910011 [[1903.02825](#)].
- [286] S. Alexandrov and S. Banerjee, *Hypermultiplet metric and D-instantons*, *JHEP* **02** (2015) 176 [[1412.8182](#)].
- [287] V. Cortés and I. Tulli, *Quaternionic Kähler metrics associated to special Kähler manifolds with mutually local variations of BPS structures*, [2105.09011](#).
- [288] B. Pioline and D. Persson, *The Automorphic NS5-brane*, *Commun. Num. Theor. Phys.* **3** (2009) 697 [[0902.3274](#)].
- [289] D. Robles-Llana, M. Rocek, F. Saueressig, U. Theis and S. Vandoren, *Nonperturbative corrections to 4D string theory effective actions from $SL(2, \mathbb{Z})$ duality and supersymmetry*, *Phys. Rev. Lett.* **98** (2007) 211602 [[hep-th/0612027](#)].
- [290] R. Bohm, H. Gunther, C. Herrmann and J. Louis, *Compactification of type IIB string theory on Calabi-Yau threefolds*, *Nucl. Phys. B* **569** (2000) 229 [[hep-th/9908007](#)].
- [291] S. Alexandrov and F. Saueressig, *Quantum mirror symmetry and twistors*, *JHEP* **09** (2009) 108 [[0906.3743](#)].
- [292] S. Alexandrov and B. Pioline, *S-duality in Twistor Space*, *JHEP* **08** (2012) 112 [[1206.1341](#)].
- [293] S. Alexandrov and S. Banerjee, *Modularity, quaternion-Kähler spaces, and mirror symmetry*, *J. Math. Phys.* **54** (2013) 102301 [[1306.1837](#)].
- [294] O. DeWolfe and B. Zwiebach, *String junctions for arbitrary Lie algebra representations*, *Nucl. Phys. B* **541** (1999) 509 [[hep-th/9804210](#)].
- [295] O. DeWolfe, T. Hauer, A. Iqbal and B. Zwiebach, *Uncovering infinite symmetries on $[p, q]$ 7-branes: Kac-Moody algebras and beyond*, *Adv. Theor. Math. Phys.* **3** (1999) 1835 [[hep-th/9812209](#)].
- [296] O. DeWolfe, T. Hauer, A. Iqbal and B. Zwiebach, *Uncovering the symmetries on $[p, q]$ seven-branes: Beyond the Kodaira classification*, *Adv. Theor. Math. Phys.* **3** (1999) 1785 [[hep-th/9812028](#)].
- [297] R. Donagi, S. Katz and M. Wijnholt, *Weak Coupling, Degeneration and Log Calabi-Yau Spaces*, *Pure Appl. Math. Quart.* **09** (2013) 665 [[1212.0553](#)].
- [298] P.S. Aspinwall and D.R. Morrison, *Point-like instantons on K3 orbifolds*, *Nucl. Phys. B* **503** (1997) 533 [[hep-th/9705104](#)].
- [299] A. Clingher and J.W. Morgan, *Mathematics underlying the F-theory/Heterotic string duality in eight-dimensions*, *Commun. Math. Phys.* **254** (2005) 513 [[math/0308106](#)].

- [300] V. Kulikov, *Degenerations of K3 surfaces and Enriques surfaces*, *Mathematics of the USSR-Izvestiya* **11** (1977) 957.
- [301] U. Persson, *On degenerations of algebraic surfaces*, no. 189 in *Memoirs of the American Mathematical Society*, American Mathematical Society, Providence (1977).
- [302] R. Friedman and D.R. Morrison, *The Birational Geometry of Degenerations*, vol. 29 of *Progress in Mathematics*, Birkhäuser Boston, MA (1983).
- [303] V. Alexeev, A. Brunyate and P. Engel, *Compactifications of moduli of elliptic K3 surfaces: stable pair and toroidal*, 2002.07127.
- [304] A. Brunyate, *A modular compactification of the space of elliptic K3 surfaces*, 2015.
- [305] K. Ascher and D. Bejleri, *Compact moduli of elliptic K3 surfaces*, 1902.10686.
- [306] Y. Odaka and Y. Oshima, *Collapsing K3 surfaces, Tropical geometry and Moduli compactifications of Satake, Morgan-Shalen type*, 1810.07685.
- [307] Y. Odaka, *PL density invariant for type II degenerating K3 surfaces, Moduli compactification and hyperKahler metrics*, 2010.00416.
- [308] G. Kempf, F. Knudsen, D. Mumford and B. Saint-Donat, *Toroidal Embeddings 1*, Lecture Notes in Mathematics, Springer-Verlag Berlin, Heidelberg (1973).
- [309] R. Álvarez-García, S.-J. Lee and T. Weigand, to appear.
- [310] V. Collazuol, M. Graña and A. Herráez, *E_9 symmetry in the heterotic string on S^1 and the weak gravity conjecture*, *JHEP* **06** (2022) 083 [2203.01341].
- [311] A. Grassi, *On minimal models of elliptic threefolds*, *Mathematische Annalen* **290** (1991) 287.
- [312] R. Miranda, *Smooth models for elliptic threefolds*, *Progress in Mathematics* **29** (1983) 85.
- [313] R. Miranda and U. di Pisa. Dipartimento di matematica, *The Basic Theory of Elliptic Surfaces: Notes of Lectures*, Dottorato di ricerca in matematica / Università di Pisa, Dipartimento di Matematica, ETS Editrice (1989).
- [314] M. Esole and S.-T. Yau, *Small resolutions of $SU(5)$ -models in F-theory*, *Adv. Theor. Math. Phys.* **17** (2013) 1195 [1107.0733].
- [315] M. Esole, J. Fullwood and S.-T. Yau, *D_5 elliptic fibrations: non-Kodaira fibers and new orientifold limits of F-theory*, *Commun. Num. Theor. Phys.* **09** (2015) 583 [1110.6177].
- [316] S.L. Cacciatori, A. Cattaneo and B. Geemen, *A new CY elliptic fibration and tadpole cancellation*, *JHEP* **10** (2011) 031 [1107.3589].
- [317] A. Cattaneo, *Crepant resolutions of Weierstrass threefolds and non-Kodaira fibres*, 1307.7997.
- [318] D. Huybrechts, *Lectures on K3 Surfaces*, Cambridge Studies in Advanced Mathematics, Cambridge University Press (2016), 10.1017/CBO9781316594193.

- [319] V. Kulikov, *On modifications of degenerations of surfaces with $\kappa = 0$* , *Mathematics of the USSR-Izvestiya* **17** (1981) 339.
- [320] U. Persson and H. Pinkham, *Degeneration of surfaces with trivial canonical bundle*, *Annals of Mathematics* **113** (1981) 45.
- [321] J. Włodarczyk, *Toroidal varieties and the weak factorization theorem*, *Inventiones mathematicae* **154** (2003) 223.
- [322] D. Abramovich, K. Karu, K. Matsuki and J. Włodarczyk, *Torification and factorization of birational maps*, *Journal of the American Mathematical Society* **15** (2002) 531.
- [323] J. Włodarczyk, *Simple constructive weak factorization*, *Algebraic geometry — Seattle 2005. Part 2* (2009) 957.
- [324] D.R. Morrison and W. Taylor, *Classifying bases for 6D F-theory models*, *Central Eur. J. Phys.* **10** (2012) 1072 [[1201.1943](#)].
- [325] M.F. Atiyah, *Vector bundles over an elliptic curve*, *Proceedings of the London Mathematical Society* **s3-7** (1957) 414.
- [326] R. Friedman, J. Morgan and E. Witten, *Vector bundles and F-theory*, *Commun. Math. Phys.* **187** (1997) 679 [[hep-th/9701162](#)].
- [327] D. Cox, J. Little and H. Schenck, *Toric Varieties*, Graduate studies in mathematics, American Mathematical Society (2011).
- [328] D.A. Cox, *Erratum to “The Homogeneous Coordinate Ring of a Toric Variety”, along with the original paper*, *arXiv e-prints* (1992) alg [[alg-geom/9210008](#)].
- [329] E.J. Elizondo, K. Kurano and K.-i. Watanabe, *The total coordinate ring of a normal projective variety*, *arXiv Mathematics e-prints* (2003) math/0305354 [[math/0305354](#)].
- [330] T. Hungerford, *Algebra*, Graduate Texts in Mathematics, Springer New York (1974).
- [331] A. Font, A. Herráez and L.E. Ibáñez, *The Swampland Distance Conjecture and Towers of Tensionless Branes*, *JHEP* **08** (2019) 044 [[1904.05379](#)].
- [332] R. Donagi and M. Wijnholt, *Higgs Bundles and UV Completion in F-Theory*, *Commun. Math. Phys.* **326** (2014) 287 [[0904.1218](#)].
- [333] M. Esole and R. Savelli, *Tate Form and Weak Coupling Limits in F-theory*, *JHEP* **06** (2013) 027 [[1209.1633](#)].
- [334] A.P. Braun, S. Gerigk, A. Hebecker and H. Triendl, *D7-Brane Moduli vs. F-Theory Cycles in Elliptically Fibred Threefolds*, *Nucl. Phys. B* **836** (2010) 1 [[0912.1596](#)].
- [335] V.V. Nikulin, *On factor groups of the automorphism groups of hyperbolic forms modulo subgroups generated by 2-reflections*, in *Doklady Akademii Nauk*, vol. 248, pp. 1307–1309, Russian Academy of Sciences, 1979.
- [336] V.V. Nikulin, *Quotient-groups of groups of automorphisms of hyperbolic forms of subgroups generated by 2-reflections*, in *Dokl. Akad. Nauk SSSR*, vol. 248, pp. 1307–1309, 1979.

- [337] V.V. Nikulin, *Discrete reflection groups in lobachevsky spaces and algebraic surfaces*, in *Proceedings of the International Congress of Mathematicians*, vol. 1, pp. 654–671, Citeseer, 1986.
- [338] M.J. Duff, R. Minasian and E. Witten, *Evidence for heterotic/heterotic duality*, *Nucl. Phys. B* **465** (1996) 413 [[hep-th/9601036](#)].
- [339] L.B. Anderson and W. Taylor, *Geometric constraints in dual F-theory and heterotic string compactifications*, *JHEP* **08** (2014) 025 [[1405.2074](#)].
- [340] G. Lopes Cardoso, G. Curio, D. Lust and T. Mohaupt, *On the duality between the heterotic string and F theory in eight-dimensions*, *Phys. Lett. B* **389** (1996) 479 [[hep-th/9609111](#)].
- [341] W. Lerche and S. Stieberger, *Prepotential, mirror map and F-theory on K3*, *Adv. Theor. Math. Phys.* **2** (1998) 1105 [[hep-th/9804176](#)].
- [342] S. Tetsuji, *Kummer sandwich theorem of certain elliptic K3 surfaces*, *Proceedings of the Japan Academy, Series A, Mathematical Sciences* **82** (2006) 137 .
- [343] A. Malmendier and D.R. Morrison, *K3 surfaces, modular forms, and non-geometric heterotic compactifications*, *Lett. Math. Phys.* **105** (2015) 1085 [[1406.4873](#)].
- [344] J. Gu and H. Jockers, *Nongeometric F-theory–heterotic duality*, *Phys. Rev. D* **91** (2015) 086007 [[1412.5739](#)].
- [345] I. García-Etxebarria, D. Lust, S. Massai and C. Mayrhofer, *Ubiquity of non-geometry in heterotic compactifications*, *JHEP* **03** (2017) 046 [[1611.10291](#)].
- [346] C. Vafa and E. Witten, *Dual string pairs with $N=1$ and $N=2$ supersymmetry in four-dimensions*, *Nucl. Phys. B Proc. Suppl.* **46** (1996) 225 [[hep-th/9507050](#)].
- [347] R. Friedman, J.W. Morgan and E. Witten, *Vector bundles over elliptic fibrations*, [alg-geom/9709029](#).
- [348] O.J. Ganor and A. Hanany, *Small $E(8)$ instantons and tensionless noncritical strings*, *Nucl. Phys. B* **474** (1996) 122 [[hep-th/9602120](#)].
- [349] E. Witten, *Heterotic string conformal field theory and A-D-E singularities*, *JHEP* **02** (2000) 025 [[hep-th/9909229](#)].
- [350] V. Braun, T. Breidze, M.R. Douglas and B.A. Ovrut, *Eigenvalues and Eigenfunctions of the Scalar Laplace Operator on Calabi-Yau Manifolds*, *JHEP* **07** (2008) 120 [[0805.3689](#)].
- [351] A. Ashmore, *Eigenvalues and eigenforms on Calabi-Yau threefolds*, [2011.13929](#).
- [352] A. Ashmore and F. Ruehle, *Moduli-dependent KK towers and the swampland distance conjecture on the quintic Calabi-Yau manifold*, *Phys. Rev. D* **103** (2021) 106028 [[2103.07472](#)].
- [353] R. Hartshorne, *Algebraic Geometry*, Graduate Texts in Mathematics, Springer (1977).

- [354] A. Beauville, *Complex Algebraic Surfaces*, London Mathematical Society Student Texts, Cambridge University Press, 2 ed. (1996), 10.1017/CBO9780511623936.
- [355] R. Lazarsfeld, *Positivity in Algebraic Geometry I: Classical Setting: Line Bundles and Linear Series*, *Ergebnisse der Mathematik und ihrer Grenzgebiete. 3. Folge A Series of Modern Surveys in Mathematics*, Springer (2004).
- [356] J.A. Rosoff, *Effective divisor classes and blowings-up of \mathbf{P}^2* , *Pacific Journal of Mathematics* **89** (1980) 419.
- [357] W. Taylor and Y.-N. Wang, *Non-toric bases for elliptic Calabi–Yau threefolds and 6D F-theory vacua*, *Adv. Theor. Math. Phys.* **21** (2017) 1063 [1504.07689].
- [358] M. Artin, *Algebraization of Formal Moduli: II. Existence of Modifications*, *Annals of Mathematics* **91** (1970) 88.
- [359] S. Galovich and M. Goldberg, *Unique factorization rings with zero divisors*, *Mathematics Magazine* **51** (1978) 276 [<https://doi.org/10.1080/0025570X.1978.11976729>].
- [360] D. Anderson and S. Valdes-Leon, *Factorization in Commutative Rings with Zero Divisors*, *Rocky Mountain Journal of Mathematics* **26** (1996) 439.
- [361] D. Anderson and S. Chun, *Irreducible elements in commutative rings with zero-divisors*, *Houston Journal of Mathematics* **37** (2011) 741.
- [362] S. Chun and D. Anderson, *Irreducible elements in commutative rings with zero-divisors, II*, *Houston Journal of Mathematics* **39** (2013) 741.
- [363] M. Del Zotto, M. Liu and P.-K. Oehlmann, *Back to heterotic strings on ALE spaces. Part I. Instantons, 2-groups and T-duality*, *JHEP* **01** (2023) 176 [2209.10551].
- [364] M. Del Zotto, M. Liu and P.-K. Oehlmann, *Back to Heterotic Strings on ALE Spaces: Part II – Geometry of T-dual Little Strings*, 2212.05311.
- [365] M. Del Zotto, M. Fazzi and S. Giri, *The Higgs branch of Heterotic ALE instantons*, 2307.11087.
- [366] H. Ahmed, P.-K. Oehlmann and F. Ruehle, *T-Duality and Flavor Symmetries in Little String Theories*, 2311.02168.
- [367] M. Del Zotto, M. Liu and P.-K. Oehlmann, *6D Heterotic Little String Theories and F-theory Geometry: An Introduction*, 2303.13502.
- [368] C. Lawrie and L. Mansi, *The Higgs Branch of Heterotic LSTs: Hasse Diagrams and Generalized Symmetries*, 2312.05306.
- [369] A.P. Braun, C.R. Brodie, A. Lukas and F. Ruehle, *NS5-Branes and Line Bundles in Heterotic/F-Theory Duality*, *Phys. Rev. D* **98** (2018) 126004 [1803.06190].
- [370] P.S. Aspinwall, *Point-like instantons and the $Spin(32)/Z(2)$ heterotic string*, *Nucl. Phys. B* **496** (1997) 149 [[hep-th/9612108](https://arxiv.org/abs/hep-th/9612108)].

- [371] S. Iitaka, *Algebraic Geometry*, Graduate Texts in Mathematics, Springer New York, NY (1982).
- [372] T. Hayashi, *Non-symplectic automorphisms of order 3, 4, and 6 of K3 surfaces with smooth quotient*, *Communications in Algebra* **51** (2023) 596 [<https://doi.org/10.1080/00927872.2022.2107210>].
- [373] T. Hayashi, *Finite abelian groups of K3 surfaces with smooth quotient*, *Chinese Annals of Mathematics, Series B* **44** (2023) 99.